

University of Glasgow



INVESTIGATIONS OF THE THERMAL STABILITY AND
DEGRADATION MECHANISMS OF SEVERAL
POLYMER-ADDITIVE AND COPOLYMER-ADDITIVE
SYSTEMS

by

MUSARRAT HALIMA MOHAMMED B.Sc.

A THESIS FOR THE DEGREE OF
DOCTOR OF PHILOSOPHY

Supervisor: Dr. I.C. McNeill

Faculty of Science
Chemistry Department
University of Glasgow

AUGUST 1993

© MUSARRAT HALIMA MOHAMMED

ProQuest Number: 13834108

All rights reserved

INFORMATION TO ALL USERS

The quality of this reproduction is dependent upon the quality of the copy submitted.

In the unlikely event that the author did not send a complete manuscript and there are missing pages, these will be noted. Also, if material had to be removed, a note will indicate the deletion.



ProQuest 13834108

Published by ProQuest LLC (2019). Copyright of the Dissertation is held by the Author.

All rights reserved.

This work is protected against unauthorized copying under Title 17, United States Code
Microform Edition © ProQuest LLC.

ProQuest LLC.
789 East Eisenhower Parkway
P.O. Box 1346
Ann Arbor, MI 48106 – 1346

Thesis
9638
copy 1



To my parents who have waited
patiently for this production.

ACKNOWLEDGEMENTS

The work described in this thesis was carried out in the Department of Physical Chemistry at the University of Glasgow during the period November 1989 to September 1992.

I would like to express my sincere gratitude to my supervisor Dr. I.C. McNeill for his advice, guidance, encouragement and patience throughout the course of this research.

I wish to thank sincerely my industrial supervisor Dr. K. Wilkinson and his assistant Dr. N. Davidson for the helpful discussions and advice provided during this work.

I acknowledge with gratitude the assistance given by the members of the academic staff especially Dr. W.J. Cole for help with the Gas Chromatography and GC-MS. I also extend my thanks to all the members of the technical staff who have contributed in various ways: G. McCulloch, W. McCormack, T. Ritchie and J. Gorman are particularly acknowledged. Many thanks are also given to all the colleagues in the Polymer Research Group, particularly G. Seeley, for invaluable assistance.

I am also grateful to all the member of my family for their support, encouragement and patience during the period of this study.

Finally, I am obliged to BP Chemicals Limited for the research scholarship during the tenure of which this work was carried out.

CONTENTS

| | | Page |
|------------------|---|-----------|
| | SUMMARY | vii |
| CHAPTER 1 | INTRODUCTION | 1 |
| 1.1. | POLYMER DEGRADATION | 1 |
| 1.1.1. | Introduction | 1 |
| 1.1.2. | Classification of Thermal Degradation Reactions | 3 |
| 1.2. | DEGRADATION OF POLYMERS IN THE PRESENCE OF ADDITIVES | 4 |
| 1.2.1. | Fire-Retardant Compounds | 5 |
| 1.2.1.1. | <i>A general Introduction</i> | 5 |
| 1.3. | OBJECTIVE OF THIS RESEARCH | 12 |
| CHAPTER 2 | EXPERIMENTAL TECHNIQUES OF THERMAL DEGRADATION AND METHODS OF ANALYSIS | 13 |
| 2.1. | INTRODUCTION | 13 |
| 2.2. | THERMAL DEGRADATION TECHNIQUES | 13 |
| 2.2.1. | Thermogravimetry | 13 |
| 2.2.2. | Differential Scanning Calorimetry (DSC) | 14 |
| 2.2.3. | Thermal Volatilisation Analysis (TVA) | 15 |
| 2.2.4. | "Sealed Tube" Degradation | 20 |
| 2.3. | SUBAMBIENT TVA (SATVA) | 21 |
| 2.4. | ANALYSIS OF DEGRADATION PRODUCTS | 22 |
| 2.5. | ANALYTICAL TECHNIQUES USED IN THIS RESEARCH WORK | 23 |
| 2.5.1 | Infrared Spectroscopy | 23 |
| 2.5.2. | Elemental Analysis | 24 |
| 2.5.3. | Nuclear Magnetic resonance Spectroscopy (NMR) | 24 |
| 2.5.4. | Mass Spectrometry | 24 |
| 2.5.5. | Gas Chromatography | 24 |

| | | |
|------------|---|----|
| 2.5.6. | Gas Chromatography-Mass Spectrometry (GC-MS) | 25 |
| 2.5.7. | Electron Microscopy | 25 |
| 2.6. | BLEND PREPARATION | 25 |
| | | |
| CHAPTER 3 | ETHYLENE AND ETHYL ACRYLATE COPOLYMER | 26 |
| 3.1. | INTRODUCTION | 26 |
| 3.2. | THERMAL DEGRADATION OF LOW DENSITY POLYETHYLENE (LDPE) | 26 |
| 3.2.1. | Introduction | 26 |
| 3.3. | EXPERIMENTAL | 28 |
| 3.2.1. | Preparation and Purification of PEA | 28 |
| 3.3.2. | Source of LDPE and EEA Copolymer | 28 |
| 3.3.3. | Microanalysis | 28 |
| 3.3.4. | Infrared Spectra | 29 |
| 3.3.5. | ^1H NMR Spectra | 29 |
| 3.3.6. | Thermal Decomposition of PEA, LDPE and EEA Copolymer | 34 |
| 3.3.6.1. | <i>Thermogravimetry (TG)</i> | 34 |
| 3.3.6.1.1. | <i>TG-DTG Under Nitrogen</i> | 34 |
| 3.3.6.1.2. | <i>TG-DTG Under Air</i> | 35 |
| 3.3.6.2. | <i>Differential Scanning Calorimetry (DSC)</i> | 35 |
| 3.3.6.3. | <i>Thermal Volatilisation Analysis (TVA) and SATVA</i> <i>Separation of Condensable Degradation Products</i> | 41 |
| 3.3.6.3.1. | <i>PEA</i> | 41 |
| 3.3.6.3.2. | <i>LDPE</i> | 49 |
| 3.3.6.3.3. | <i>EEA Copolymer</i> | 49 |
| 3.3.7. | Thermal Degradation of PEA at Lower Temperature | 63 |
| 3.4. | DISCUSSION | 64 |
| 3.5. | MECHANISMS OF FORMATION OF DEGRADATION PRODUCTS FROM POLYOLEFINS | 65 |
| 3.5.1. | Mechanism of Formation of Degradation Products from PEA | 65 |

| | | |
|------------------|---|------------|
| 3.5.2. | Mechanism of Formation of Degradation Products from LDPE | 67 |
| 3.5.3. | Mechanism of Formation of Degradation Products from EEA Copolymer | 69 |
| 3.6. | CONCLUSIONS | 73 |
| CHAPTER 4 | DEGRADATION OF SILICONE POLYMERS | 75 |
| 4.1. | Introduction | 75 |
| 4.2. | PHYSICAL PROPERTIES OF SILICON AND ITS COMPOUNDS | 79 |
| 4.3. | THERMAL DEGRADATION OF POLYDIMETHYLSILOXANE | 82 |
| 4.4. | EXPERIMENTAL | 85 |
| 4.4.1. | Thermal Analysis of Polydimethylsiloxane | 85 |
| 4.4.1.1. | <i>Thermogravimetry (TG)</i> | 85 |
| 4.4.1.2. | <i>Differential Scanning Calorimetry (DSC)</i> | 89 |
| 4.4.1.3. | <i>Thermal Volatilisation Analysis (TVA)</i> | 92 |
| 4.4.1.4. | <i>SATVA Separation of Condensable Degradation Products</i> | 93 |
| 4.5. | DISCUSSION | 103 |
| 4.6. | CONCLUSIONS | 105 |
| CHAPTER 5 | BLENDS OF POLYOLEFINS AND INORGANIC FILLERS | 107 |
| 5.1. | INTRODUCTION | 107 |
| 5.2 | EXPERIMENTAL | 108 |
| 5.2.1. | Preparation and Composition of Blends | 108 |
| 5.2.2. | Thermal Analysis of Polyolefins and Inorganic Fillers | 109 |
| 5.2.2.1. | <i>Thermogravimetry</i> | 109 |
| 5.2.2.1.1. | <i>TG-DTG Under Nitrogen</i> | 109 |
| 5.2.2.1.1.1. | <i>Blend of LDPE and CaCO₃</i> | 109 |

| | | |
|------------------|---|------------|
| 5.2.2.1.1.2. | <i>Blend of PEA and CaCO₃</i> | 109 |
| 5.2.2.1.1.3. | <i>Blends of EEA Copolymer and CaCO₃</i> | 112 |
| 5.2.2.1.1.4. | <i>Blends of EEA Copolymer and Other Inorganic Fillers</i> | 113 |
| 5.2.2.1.2. | <i>TG-DTG Under Air</i> | 114 |
| 5.2.2.2. | <i>Differential Scanning Calorimetry (DSC)</i> | 115 |
| 5.2.2.3. | <i>Thermal Volatilisation Analysis (TVA) and SATVA Separation of Condensable Degradation Products</i> | 127 |
| 5.2.2.3.1. | <i>Blend of LDPE and CaCO₃</i> | 127 |
| 5.2.2.3.2. | <i>Blend of PEA and CaCO₃</i> | 127 |
| 5.2.2.3.3. | <i>Blends EEA Copolymer and CaCO₃</i> | 132 |
| 5.2.2.3.4. | <i>Blend EEA Copolymer and CaCO₃ Heated up to 600°C</i> | 134 |
| 5.2.2.3.5. | <i>Blends EEA Copolymer and CaCO₃ 400°C</i> | 134 |
| 5.2.2.3.6. | <i>Blends EEA Copolymer and Other Inorganic Fillers</i> | 142 |
| 5.3. | DISCUSSION | 154 |
| 5.4. | CONCLUSIONS | 162 |
| CHAPTER 6 | BLENDS OF POLYOLEFINS AND POLYDIMETHYLSILOXANE | 163 |
| 6.1. | INTRODUCTION | 163 |
| 6.2 | EXPERIMENTAL | 163 |
| 6.2.1. | Preparation and Composition of Blends | 163 |
| 6.2.2. | Thermal Analysis of PDMS with Additives | 164 |
| 6.3. | RESULTS | 164 |
| 6.3.1. | Thermogravimetry | 164 |
| 6.3.1.1. | <i>TG-DTG Under Nitrogen</i> | 164 |
| 6.3.1.1.1. | <i>Blends of LDPE and PDMS</i> | 164 |
| 6.3.1.1.2. | <i>Blends of PEA and PDMS</i> | 165 |
| 6.3.1.1.3. | <i>Blends of EEA Copolymer and PDMS</i> | 165 |
| 6.3.1.2. | <i>TG-DTG Under Air</i> | 165 |
| 6.3.2. | Differential Scanning Calorimetry (DSC) | 170 |

| | | |
|------------------|---|------------|
| 6.3.3. | Thermal Volatilisation Analysis (TVA) and SATVA Separation of Condensable Degradation Products | 171 |
| 6.3.3.1. | <i>Blend of LDPE and PDMS</i> | 171 |
| 6.3.3.2. | <i>Blend of PEA and PDMS</i> | 174 |
| 6.3.3.3. | <i>Blends of EEA Copolymer and PDMS</i> | 178 |
| 6.4. | DISCUSSION | 189 |
| 6.5. | CONCLUSIONS | 198 |
| CHAPTER 7 | BLENDS OF POLYDIMETHYLSILOXANE AND ADDITIVES | 200 |
| 7.1. | INTRODUCTION | 200 |
| 7.2 | EXPERIMENTAL | 202 |
| 7.2.1. | Preparation and Composition of Blends | 202 |
| 7.2.2. | Thermal Analysis of PDMS with Additives | 204 |
| 7.3. | RESULTS AND DISCUSSION | 205 |
| 7.3.1. | Electron Microscopy | 205 |
| 7.3.2. | Thermogravimetry | 205 |
| 7.3.2.1. | <i>TG-DTG Under Nitrogen</i> | 205 |
| 7.3.2.1.1. | <i>Blends of PDMS and CaCO₃</i> | 205 |
| 7.3.2.1.2. | <i>Blends of PDMS and MgCO₃</i> | 208 |
| 7.3.2.1.3. | <i>Blends of PDMS and Metal Hydroxides</i> | 208 |
| 7.3.2.1.4. | <i>Blends of PDMS and Metal Oxides</i> | 209 |
| 7.3.2.1.5. | <i>Blends of PDMS and Other Additives</i> | 209 |
| 7.3.2.2. | <i>TG-DTG Under Air</i> | 210 |
| 7.3.3. | Differential Scanning Calorimetry (DSC) | 236 |
| 7.3.4. | Thermal Volatilisation Analysis (TVA) and SATVA Separation of Condensable Degradation Products | 240 |
| 7.3.3.1. | <i>Blends of PDMS and CaCO₃</i> | 240 |
| 7.3.3.2. | <i>ELECTRON MICROSCOPY</i> | 251 |

| | | |
|------------------|--|------------|
| 7.3.3.3. | <i>Blends of Siloxane Polymer with Different Type and Particle sized CaCO₃</i> | 258 |
| 7.3.3.4. | <i>Blend of PDMS with Trimethyl End groups and CaCO₃</i> | 262 |
| 7.3.3.5. | <i>Blend of PDMS and MgCO₃</i> | 264 |
| 7.3.3.6. | <i>Blends of PDMS and Metal Hydroxides</i> | 270 |
| 7.3.3.7. | <i>Blends of PDMS and Metal Oxides</i> | 282 |
| 7.3.3.8. | <i>Blends of Siloxane Polymer and Other Additives</i> | 291 |
| 7.5. | MECHANISMS OF FORMATION OF DEGRADATION PRODUCTS FROM BLENDS OF PDMS WITH ADDITIVES | 320 |
| 7.6. | CONCLUSIONS | 326 |
| CHAPTER 8 | BLENDS OF POLYOLEFINS, POLYDIMETHYLSILOXANE AND INORGANIC FILLER | 329 |
| 8.1 | INTRODUCTION | 329 |
| 8.2. | EXPERIMENTAL | 329 |
| 8.2.1. | Preparation and Composition of Blends | 329 |
| 8.2.2. | Analysis of Blends of Polyolefins with PDMS and CaCO ₃ | 330 |
| 8.3. | RESULTS AND DISCUSSION | 331 |
| 8.3.1. | Thermogravimetry | 331 |
| 8.3.1.1. | <i>TG-DTG Under Nitrogen</i> | 331 |
| 8.3.1.2. | <i>TG-DTG Under Air</i> | 332 |
| 8.3.2. | Thermal Volatilisation Analysis (TVA) and SATVA Separation of Condensable Degradation Products | 345 |
| 8.3.2.1. | <i>Blend of LDPE, PDMS and CaCO₃</i> | 345 |
| 8.3.2.2. | <i>Blend of PEA, PDMS and CaCO₃</i> | 346 |
| 8.3.2.3. | <i>Blends of EEA Copolymer, PDMS and CaCO₃</i> | 347 |
| 8.4. | CONCLUSIONS | 353 |
| | REFERENCES | 354 |

SUMMARY

An ever increasing demand for the synthetic polymers and the fire hazards associated with these polymers requires some knowledge of the processes occurring in a fire situation and how these hazards could be at least minimised. Chapter 1 deals with some of the processes which could occur during controlled thermal decomposition of polymer systems. There is a brief account of the type of fire retardants, degradation in their presence and how fire retardants can work. Since traditional halogenated fire retardants have been proved health hazard, there are brief notes on the non-halogenated fire retardants which are found to be effective. This chapter also includes the aim of the present work.

Chapter 2 summarises the apparatus and experimental techniques employed in this research. The first section describes the thermal analysis techniques while the second summarises analytical methods used to identify the degradation products.

Characterisation and thermal degradations of low density polyethylene (LDPE), poly(ethyl acrylate) (PEA) and ethylene ethyl acrylate (EEA) copolymer are discussed in Chapter 3. EEA copolymer is found to be more stable than PEA but less stable than LDPE. Thermal decomposition of EEA copolymer is found to be initiated at weak points and the degradation products to be mainly the sum of degradation products from LDPE and PEA. The systems are found to be more stable in an inert atmosphere than in air because oxidation results in the formation of groups such as hydroperoxides which lead to in the formation of ketones and peracids at lower temperatures.

Chapter 4 gives a brief account of the history of silicones, their industrial applications and physical properties of silicon and its compounds. This chapter also describes the work carried out on thermal degradation of silicone polymers by other research workers. Finally, thermal degradation of polydimethylsiloxane (PDMS) with different end groups is described. The main degradation products are found to be cyclic siloxane oligomers, with cyclic hexamethylsiloxane being the major product. The degradation products are formed by Si-O bond rupture but the mechanism of

degradation depends on the chain end groups. It is also found that PDMS is more stable in air than in an inert atmosphere.

In Chapter 5, the thermal degradation of polyolefins in the presence of coated CaCO_3 is described. EEA copolymer is also considered with $\text{Mg}(\text{OH})_2$, $\text{Al}(\text{OH})_3$, MgO , TiO_2 and different sized (coated and uncoated) CaCO_3 . It is found that calcium carbonate does not stabilise LDPE. CaCO_3 interacts with polyolefins if polar groups are introduced by copolymerisation. The mechanism for the formation of some degradation products changes. It is observed that stabilisation of blends of EEA copolymer with metal hydroxides depends on the endothermic decomposition of metal hydroxides while $\text{Mg}(\text{OH})_2$ also interacts with the ester groups and stabilises the copolymer, hence changes the mechanism of the degradation products. Most fillers prevent the formation of acids by forming ionic salts with the acid groups introduced during the decomposition of ethyl acrylate. TiO_2 stabilises the copolymer initially but the degradation products are similar to those from the pure copolymer although some degradation routes are more favoured than the others. Stabilisation of EEA copolymer increases in air in the presence of CaCO_3 since the filler possibly reacts with the acidic groups produced due to the oxidative attack and stabilises the system.

The thermal degradation of blends of polyolefins with high molecular weight vinyl end grouped PDMS is discussed in Chapter 6. All blends form high levels of insoluble rubbery residues due to crosslinking introduced by radical reactions between the components. It is observed that quantity of residue and stabilisation of polyolefins with polar groups increases with increasing percentage content of PDMS. It has been found that initial stabilisation of PDMS with LDPE is only shown in dynamic nitrogen atmosphere while PDMS is stabilised under all conditions with other systems. Decomposition of PDMS in such systems occurs after the decomposition of the organic polymer. The mechanism of degradation changes and new siloxane products are formed resulting mainly from the radical reactions between the components or as a result of radical centres introduced into PDMS chains.

The influence of various inorganic fillers and some other additives on the thermal degradation of PDMS is investigated in Chapter 7. It was observed that fillers and additives interact with PDMS (with either end group) and result in great stabilisation of the polymer. The interaction of the components results in the formation of rubbery,

insoluble residues while in most cases a bubble is also formed. The fillers also contribute in stabilisation by acting as heat sinks, therefore increasing their percentage content results in increasing the stability of the polymer. Basic inorganic fillers result in the Si-C bond scission near the point of filler-polymer interaction due to the electron-withdrawing effects caused by interaction. This results in the formation of new compounds, but the main degradation products from all blends are still cyclic siloxane oligomers. It is also found that stabilisation of the polymer is influenced by the particle size, type and surface treatment of the filler. Fillers with smaller particle size and highly surface treated for better dispersion, show most stabilisation. It is found that heating of cyclic siloxane oligomers in the presence of fillers, especially in a closed system, results in the polymerisation of these compounds so it is difficult to estimate the true quantity of degradation products at any given temperature. It has also been found that the overall effect for most blends represents more stabilisation in air than in inert atmosphere.

In Chapter 8 the thermal degradation of polyolefins with PDMS and CaCO_3 is investigated. It is found that all polyolefins tested are stabilised mainly due to interactions with PDMS.

CHAPTER 1

INTRODUCTION

Synthetic polymers in the form of rubbers, plastics and fibres have been used in practically every possible aspect of life since the mid twentieth century and in many applications they have partially or completely replaced the usual cellulosic materials and metals. Their usage has been a major contribution to the wealth and comfort of modern society. However, most synthetic polymers are basically hydrocarbon-based, and therefore are flammable.

For certain applications, e.g. rocket propellants, the ability to undergo combustion is an essential requirement, but for the large majority of purposes for which polymers are used, flammability is a serious disadvantage and severely limits their commercial applications. These fires not only destroy property but also result in the loss of human life, even in quite small fires. This is mostly caused by the physiological effects of the fire gases, causing lack of visibility due to the dense smoke, intoxication due to toxic fumes and suffocation due to exhaustion of oxygen^{1, 2}.

The Home Office report 'Fire risks of new materials', published in 1978³ drew attention to the fact that the nature of many domestic fires has changed and that now there is a rapid growth of fire and greater smoke generation which is the cause of considerable loss of life. This is largely due to the increased usage and fire hazards of synthetic polymers. Governments are now introducing strict regulations about the limits of flammability of materials of construction.

As a consequence, intensive studies have been carried out into developing flame retardance and fire retarded polymers, although much research is still required to understand fully the complex processes which occur in both the gaseous and condensed phases. Controlled polymer degradation plays a major contribution in understanding the chemical and physical properties.

1.1. POLYMER DEGRADATION

1.1.1. Introduction

Polymer degradation⁴⁻¹³, in general, describes various processes which may occur in everyday use of the material at any time, depending on the particular environment and

its applications. Ultraviolet and visible radiation combined with oxidation by atmospheric oxygen play a large part in the natural weathering and deterioration of the polymeric material. Heat, mechanical stress, chemicals and bacteria also are the cause of polymer degradation. Degradation of a polymer may occur while the polymer is synthesised, processed or fabricated.

Generally, polymer degradation is considered as an unfavourable process which should be prevented since it results in the deterioration of the characteristic properties of the polymer. However, polymer degradation is not always a disadvantage as in many cases it is encouraged. There are various applications for which polymer degradation is important, for example in the medical field in biodegradable sutures in surgery and for the controlled release of drugs¹⁴.

These degradation processes are very complex but thermally-induced degradation studies can explain the behaviour of polymers under conditions of high temperature, or other modifying influences. Degradation mechanisms can be established when these processes are understood, which may thus enable existing polymers to be stabilised in a logical way and new polymers to be synthesised to meet new or existing requirements.

Polymer degradation can also be used to recover monomer. For example, almost 100% recovery of methyl methacrylate from poly(methyl methacrylate) through depolymerisation is possible¹⁵. It is important in such cases to find the optimum conditions for efficient reaction. Polymer degradation is also used to prepare carbon fibres by heating polyacrylonitrile fibres to temperatures above 1500°C in an inert atmosphere.

Studies of thermal degradation of polymers can also help to characterise their structures by providing information on the sequence and arrangement of the repeated units and side-groups in the polymer or copolymer chain. It can also provide information on the nature of the chain ends, crosslinks between chains and the strength of the various bonds within the macromolecule. The kinetics of the degradation reactions and the effects of sample environment on the rates and products of degradation can also be studied.

Throughout this thesis the term "polymer degradation" is used to describe all reactions of polymers taking place under thermal conditions whether there is a net decrease in molecular weight or not.

1.1.2. Classification of Thermal Degradation Reactions

Polymer degradation reactions can be classified according to the main factors responsible for the degradation e.g. photo-, thermal, biological, radiation, chemical or mechanical degradation, but in this work only the processes taking place during controlled thermal degradation have been investigated.

Many different kinds of degradation reactions may be induced thermally in polymers but they can normally be divided into two distinct classes¹²:

- (i) depolymerisation
- (ii) substituent reactions.

Depolymerisation, also known as main chain scission, can be divided further into radical depolymerisation and non-radical depolymerisation. Depolymerisation is characterised by the cleavage of the main polymer backbone resulting in the formation of macroradicals or short chain fragments of different lengths so that at any intermediate stage the products are similar to the parent material in the sense that the monomer units are still distinguishable. The final product may be monomer as from poly(methyl methacrylate) or volatile chain fragments like the range of short chain alkanes and alkenes from polyethylene. These are examples of radical depolymerisation reactions. New type of end groups may or may not appear, depending upon the nature of the chain-scission processes. Many depolymerisation reactions do not involve radicals. Polyesters, polysiloxanes and polyurethanes which are important as commercial materials undergo such depolymerisation.

Substituent reactions involve the modification or total elimination of the substituents attached to the backbone of the polymer. These reactions occur as dominating processes in polymer systems in which they can be initiated at temperatures lower than that at which main chain scission takes place. In these types of reactions, the chain structure may not be broken but the chemical nature of the repeat unit in the polymer is changed. Typical examples are the elimination of hydrogen chloride from poly(vinyl chloride) and cyclisation of polyacrylonitrile^{16, 17}. These reactions mostly produce small volatile products which are chemically unlike the monomer. This is not true with polyacrylonitrile, however, which begins to discolour at 150°C, due to conjugation arising from the polymerisation of sequences of the neighbouring nitrile groups without liberating any products.

1.2. DEGRADATION OF POLYMERS IN THE PRESENCE OF ADDITIVES

The chemical and physical properties of polymeric materials can be modified by adding suitable chemicals^{18, 19} which may affect the various stages of the burning process in a number of different ways. Other methods can occasionally also be used to control the rates of these stages hence alter the flammability of the polymer. However, there is no such additive which would impart total protection from flammability and the main aim is to reach specified levels of performance as laid down by a wide range of standards and legislation.

Additional restrictions now have to be taken into account because of the severely threatening hazards of the fire as mentioned earlier on. These hazards were previously underestimated or neglected.

There is a wide range of fire retardants (FRs) which can be divided into two broad classes: inorganic fillers and organic compounds. The latter can be sometimes further sub-divided into additive FRs and reactive FRs. Additive FRs are simply mechanically mixed with the polymer, usually during processing, although they can also be coated on the external surface of the polymer to form a suitable protective barrier. Reactive FRs are chemically linked to the polymer chain in some way and form part of the polymeric structure. This type of fire-retarded polymer is produced either by modification of the polymer to make it thermally very stable so that its initial breakdown is prevented, or by copolymerisation¹².

Stabilisation through modification is the simplest way of making a polymer fire-retarded. Thermally stable polymers have been developed in the past for special applications²⁰⁻²⁵ but these materials are not easy to process and also do not possess many of the properties required for the wide range of applications. They are also very expensive to produce therefore as the industry point of view not profitable to process.

The most widely used approaches for fire-retardant systems depend on the use of additives and inorganic fillers because these systems are more flexible and of general application. Also they are useful as the initial approach for guiding the selection of chemical structures for permanent introduction into the polymer.

Reactive FRs have advantages over additive FRs as they cannot be lost by evaporation, since a lot of additives are considerably volatile, or by leaching with water or other solvents during the useful life of the polymer. They are also not subject to hydrolysis and are available to protect the polymer whenever required in the fire situation since they will be released in the polymer simultaneously with the

decomposition of the polymer. Reactive FRs, however, need to be introduced at a much earlier stage of manufacturing and once incorporated, form a permanent part of the polymer structure. Therefore, they are much more likely to affect the chemical stability of the polymer.

The introduction of additive FRs is the simplest way of making an organic polymer less flammable because the additives can be incorporated during the final stage of production of the finished material. The decomposition or volatilisation temperature of an additive, however, must be carefully matched to that of the polymer so that it is available when the polymer decomposes.

Whatever is used, the main objective is to decrease the fuel available to the fire; to absorb heat from the flame; to reduce flame propagation; and to prevent flame reaching the polymeric material by interposing charred or intumescent matter. However, for the purpose of this general introduction the degradation of polymer-additive system is reviewed in general as fire-retardant compounds mainly for polyolefins.

1.2.1. Fire-Retardant Compounds

1.2.1.1. A General Introduction

The various commercially available fire-retardants function through a number of different mechanisms. In order to understand these processes, it is necessary to have some knowledge and understanding of the events which occur during the combustion of a polymer. Polymers do not burn, it is the flammable volatile products of degradation which do so, evolving large amounts of heat which causes further degradation and eventually to fire. Thus the combustion of a polymer or of any solid material, can be described by two consecutive chemical processes, decomposition and combustion. Decomposition is normally an endothermic reaction which occurs when the solid polymer is heated and combustible products are evolved, possibly with a non-volatile residue or char which is sometimes called the pre-flame or cool-flame zone. These flammable degradation products then mix with oxygen and enter the flame zone and sustain combustion to form combustion products with simultaneous evolution of heat. Some of this heat transfers back to the polymer surface and initiates further degradation thus yielding more combustible products. These series of events occurring are known as the combustion cycle and can be represented as in the Figure 1.

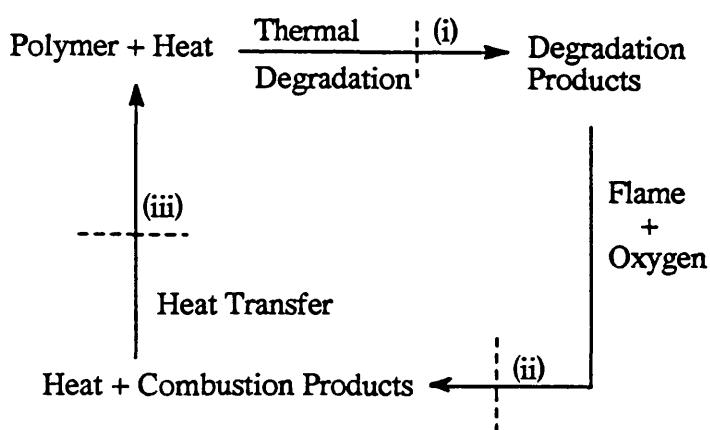


Figure 1: Diagrammatic representation of combustion cycle²⁶.

It is clear that this cycle must be prevented to occur, at least at one or more of the points (i), (ii) and (iii) to make a polymer fire-retardant^{9, 18, 19}. This can be achieved by:

(i) modifying the thermal decomposition of the polymer to produce less flammable degradation products thus reducing the amount of fuel supplied to the flame

(ii) reducing the amount of air to the flame

(iii) reducing the supply of heat from the flame back to the decomposing polymer

The most obvious stage which can be affected by an additive is the initial thermal decomposition of the polymer to give less combustible gaseous products. This can be done by altering the breakdown of the polymer in such a way that either the nature or the rate of the evolution of the gaseous decomposition products is changed.

The mechanisms by which FRs can act are:

Flame reactive products: inhibit the propagating chemical reactions which occur in the flame. In this case a flame retardant acts simply by chemical termination in the condensed phase of the free-radical chains by which thermal decomposition of the polymer takes place. This is commonly known as radical quenching and organo-halogen compounds are often used with a synergist, especially antimony oxide, for this purpose.

Gas blanketing: keeps the flammable degradation products and oxygen apart, or at least dilutes the mixture.

Cooling: removes energy from the flame.

Char forming: creates a barrier on the solid polymer/degradation products to interrupt the escape of volatile degradation products.

Intumescent materials: create a thermal barrier between the flame and the solid polymer to reduce further degradation.

Melt modification: burning can be reduced by encouraging the polymer to melt and flow away from the flame.

Many, if not most flame retardants appear to be capable of functioning simultaneously by several different mechanisms, often depending on the nature of the organic polymer, flame retardant and the presence of other materials, particularly synergists. Thus it is difficult to associate a commercial fire retardant with a particular classification by mechanism. It is therefore practical to describe flame retardants according to chemical types with reference to the mechanisms by which they can operate²⁷⁻³⁴.

Flame retardants may be used in combinations and their effects may be additive, synergistic or occasionally antagonistic (smaller than additive effect). Synergism (when the combined effect of two or more fire retardants is greater than the sum of the individual fire-retardant effects) is important in formulating to accomplish maximum cost-effectiveness or minimum adverse effect on physical properties of the polymer.

The major flame-retardant additives have always been six elements from Groups III, V, and VII of the Periodic Table^{35, 36}. These six elements particularly associated with the fire retardance with polymers are boron and aluminium (Group III), phosphorus and antimony (Group V) and chlorine and bromine (Group VII). In addition, nitrogen (Group V), which is present in significant degree in some natural and synthetic polymers, confers some degree of flame retardance. Silicon (Group IV) compounds are also now proved to be effective flame retardants^{37, 38}. Other elements and their compounds are found to be less effective, although certain compounds of barium and zinc, tin, molybdenum, and sulphur are useful flame retardants in some polymers.

However, due to the awareness of regulations regarding flammability, flame spread, toxic emissions and smoke density, the overall fire hazards associated with halogen-based systems which are among the most widely used and effective fire retardants at the present time are being re-examined. This has attracted research interest towards designing and finding alternative materials for some of the above mentioned fire-retardants. Investigations of non-halogenated additives such as $\text{Al}(\text{OH})_3$, $\text{Mg}(\text{OH})_2$ and others for use in composites with thermoplastics such as polyethylene (PE), polypropylene (PP) and ethylene vinyl acetate (EVA) copolymers are becoming very common^{39, 40}. Fillers when present in considerable quantities act as heat sinks as a result

of their heat capacity and conduct heat away from the polymers. As a result polymers may not reach at their significant decomposition temperatures.

The most important inorganic FR at present is alumina trihydrate (ATH), $\text{Al}_2\text{O}_3 \cdot 3\text{H}_2\text{O}$. This hydrated salt, containing some 35% by weight of water, is added as a filler and the mechanism of flame retardance consists apparently of physical dilution of the polymer which provides lower amounts of combustion gases on decomposition, the filler itself acting as a heat sink. Its thermal decomposition occurs in stages between 230°C and 350°C . The strongly endothermic reaction removes heat from the decomposing polymer (acts as heat sink) while the water vapour cools the flame and dilutes flammable gases. It has no direct effect on the free radical mechanisms in the flame. The other product of decomposition, alumina (Al_2O_3), contributes bulk to the char barrier and protects the underlying polymer. Alumina itself has for long been used as a filler both to modify the physical properties and in certain applications to reduce the effective cost of the synthetic polymers.

ATH is used at high loading levels, usually in products where fire retardancy and physical properties are not critical. As a filler it also has the effect of diluting the amount of flammable polymer available for combustion in a given volume. One of the basic drawbacks with ATH when it comes to thermoplastics is its limitation to processing temperatures under 200°C . However, developments in surface coatings have resulted in ATH grades that can be compounded into polypropylene without problems from thermal decomposition at temperatures up to 215°C . The coating is a silane-based coupling agent that improves heat transfer through the polymer/ATH melt thus avoiding local hot-spots that could result in decomposition. However, mechanical properties are still found to be a problem.

Aluminium hydroxide is also a widely used fire retardant in polymers, in terms of tonnage. Like ATH, it is a low cost product and requires very high levels of addition, 60% wt or more, to be effective. This therefore limits its use to polymers and applications that tolerate levels of 50-200 parts per hundred parts of resin. Aluminium hydroxide decomposes between $180\text{-}200^\circ\text{C}$ with release of water vapour.



The mechanism of action is similar to that of ATH but its low decomposition temperature limits its usage since it can only be incorporated to polymers which are processed below 180°C . Furthermore, under slow heat-up conditions, particularly in the

case of thin sections, water would possibly be lost before decomposition of polymer occurs.

Magnesium hydroxide $Mg(OH)_2$ is an alternative since it has greater thermal stability and releases its bound water at about $340^\circ C$. This can overcome some of the disadvantages of aluminium hydroxide. However, suitable grades are not as readily available and again high loadings are required. The effects of different types of magnesium hydroxide with different particle and crystallite sizes and different degree of agglomeration have been studied⁴¹ with polypropylene. It was found that at least 57% by weight of filler made the composite non-flammable but at the same time reduced its impact and tensile yield strengths considerably. It has also been noticed that filler with less agglomeration and with crystallite size in the range of about $2\mu m$ gives better mechanical properties for the composite. Magnesium hydroxide coated with about 3% sodium stearate is found to give an increased melt flow and impact strength to the composite as compared with uncoated. The mechanism of flame retardance is similar to that of aluminium hydroxide.

Although ATH has proved itself in many systems, to achieve suitable performance in polyolefins high loading levels are required, which can present difficulties in processing and end-product use. ATH particles do not readily couple to or disperse in polyolefin resins, which could lead a finished product with poor mechanical properties. Union Carbide has produced an organosilicon material (named Ucarsil, UC) which they claim can make possible ATH loadings as high as 70% without affecting the performance of the product. UC fire retardant additives act by improving coupling and dispersion in polyolefin resins and this makes the high loadings possible. These new materials thus make easier the use of ATH in the formation of polyolefin building products such as electrical conduit, wire insulation and jacketing and wall partitions with improved fire safety. PE flame retarded with ATH together with UC show greatly reduced levels of smoke compared with PVC and halogen-retarded PE and better physical properties than conventional ATH/PE systems. This new finding will satisfy the strict demands placed on some of the applications such as on wire and cable constructions.

UC is one of the five new materials fabricated as a result of combining silicone and non-silicone technologies, in the form of additives, compounds and composite tapes (mica and glass united by silicone binder resin), each fulfilling specific criteria for satisfying established or expected safety standards⁴². One of these other materials is also like UC, an extension of traditional silicone technology while the other three are predominantly non-silicone materials.

The silicone-based fire retardant system contains a combination of reactive silicone polymers, a linear silicone fluid or gum and a silicone resin which is soluble in the fluid, plus a metal soap. While a wide variety of metal soaps may be used, it has been reported that so far magnesium stearate demonstrates the best performance. Silicones in combination with other ingredients can be used to flame retard crosslinked polyolefins including polyethylene for wire and cable applications^{37, 38, 43}.

In a fire this new silicone mixture, specially tailored for thermoplastics, functions synergistically with the magnesium stearate to produce a hard, slightly intumescent char that insulates the remaining substrate from heat and prevents spread by eliminating dripping. Its effectiveness is pronounced in the most severe flame tests and only a little help is needed from decabromodiphenyloxide (DBDPO) and ATH to pass the tests. Bromine from the DBDPO is held mostly in the char and therefore is not discharged as a gaseous product, a conclusion supported by toxic gas analysis.

It has been shown that the silicone retardant alone raises the oxygen index to 23 volume %, while addition of DBDPO moves it to 27 volume % and better still on addition of ATH with DBDPO it moves to 30 volume %, ATH functioning as described before.

In addition to the three key ingredients, other special purpose ingredients may be added to enhance specific properties including flame retardancy. These formulations, however, do not achieve good flame retardance in uncrosslinked polyolefins.

The second product type in this group are siloxane polyimide copolymers produced by the combination of a high temperature thermoplastic polyimide with the thermally stable polydimethylsiloxane through copolymerisation. These non-halogen, flame retardant materials are said to offer the possibility for the whole new family of flame retardant products. Product data established for one thermoplastic formulation in this silicone-polyimide group has shown excellent flame, smoke and electrical properties. Since it is a non-halogen material, the decomposition by-products of combustion do not contain toxic and corrosive HCl or HF gases.

Silicone rubber foam is another area of silicone technology, designed specifically for electrical insulation, vibration damping and acoustical material with distinct flame retardancy characteristics which is finding increasing applications. It is particularly useful as a flame retardant cable valley and penetration seals in electric installations in building construction, offering the advantages of light weight, simple, direct insulation and improved flame retardancy over solid sealant materials. The greater retardancy of the silicone foam can be graphically illustrated by comparison with polyurethane foam. The

polyurethane foam is destroyed within seconds when burned vertically, while the silicone foam exhibits practically no propagation. Fire retardancy of silicone rubber foam was dramatically demonstrated in 1985 with a NASA/FAA test crash of a Boeing 720 aircraft. The entire plane cabin was destroyed in a two hour blaze while all cameras and audio recording equipment protected with silicone foam and rigid epoxy survived. The film and sound footage recording the occurrences inside the plane were unharmed.

Thin glass-mica tape united by silicone binder resin offers premium performance for high temperature wire and cable insulation systems. With silicone only 10% of the construction, the flame, smoke and toxicant levels approach non-detectable in virtually all cases.

Crosslinked polyethylene (PE) and ethylenepropylene rubber (EPR) have been commonly used as industrial polymers and most of the cure processes, especially for PE, involve chemical crosslinking in the rubber state using peroxide. However, additional benefits could be achieved by involving the grafting of an organofunctional silane onto the polymer chain followed by its condensation reaction in the presence of moisture and catalyst. One of the benefits is the increased stability of the polymers towards oxidation⁴⁴⁻⁴⁶.

Synergistic combinations of fire-retardants are becoming increasingly important as a method of modifying and extending polymer properties to satisfy commercial requirements. It has been known for several years that small amounts of lead compounds and silicone gum when blended into low-density crosslinked polyethylene act as a synergistic fire retardant. Large amounts of halogenated compounds were needed in past to achieve similar levels of fire resistance in polyethylene⁴⁷. Another advantage of this new fire retardant is that since it is non-halogenated, it would not produce toxic and corrosive gases on decomposition.

The demand for low-smoke, halogen-free flame retardants has also resulted in another flame retardant called Spinflam⁴⁸. Spinflam has been designed for use with PE, PP, and polyurethane (PU). The active component is said to be an oligomeric nitrogen and phosphorus compound developed by Montedison, initially for in-house use in Himont's PP. Nitrogen content varies according to grade from 16 to 18%, while the phosphorus content lies between 20 and 22%. It is claimed to work by producing a tough, carbon foamed char which hinders oxygen diffusion and heat transmission to the burning polymer. Smoke and toxic and corrosive fume emissions are said to be much less than with typical halogenated FRs.

Another halogen-free fire retardant system called Plasoat LSOH, based on nitrogen compounds and other compounds, has been designed for PP. This material is said to form a protective char between the plastic and the flame when ignited. It is claimed that the char is self-extinguishing and gives out a very low density smoke for a brief period.

1.3. OBJECTIVE OF THIS RESEARCH

Recently it has become a fundamental interest of the plastics industry to investigate the fire hazards of polymers and find methods of reducing these by means of fire retardant additives, particularly those which do not produce smoke and corrosive and toxic gases. However, the degradation processes of polymers are very complex and difficult to understand particularly when these degradation processes occur in oxygen. Therefore, there is a need first to understand these degradation processes occurring in the absence of oxygen. The comparison between the polymer degradation data and burning behaviour in model conditions could provide the basic understanding of the mechanisms of fire retardance processes occurring. The effects of the chemical structure of the polymer on its thermal behaviour can be best understood by the thermal degradation of the polymer system under vacuum conditions. The objective of this project is to study the interaction of some fire retardant systems, particularly inorganic fillers with certain polyolefins and polydimethylsiloxane. The research concentrates on the investigation of the thermal decomposition of the components separately and in mixtures with polymers, under vacuum. The purpose is a detailed analysis of volatile degradation products of components examined separately and together, changes in the involatile residue, both physical and chemical, and thermal stability of the polymer-additive systems. This investigation is carried out in order to gain an insight into the fundamental processes and thus mechanisms that operate when polymer-additive systems are subjected to high temperature. The same systems were also studied under nitrogen and air at atmospheric pressure by thermogravimetry for comparison.

CHAPTER 2

EXPERIMENTAL TECHNIQUES OF THERMAL DEGRADATION AND METHODS OF ANALYSIS

2.1. INTRODUCTION

Earlier work carried out on the thermal degradation of polymers by various research workers has shown that the mechanisms of thermal degradation are complex and result in the formation of products with different characteristics. Degradation products may be volatile at the degradation temperature but condense at or below ambient temperature or may be too volatile to be condensable at liquid nitrogen temperature (-196°C). There is also the possibility of reactions occurring within the samples being degraded, resulting in structural changes without producing any volatile materials.

All these different kinds of reactions taking place, resulting in a wide range of mechanisms and products, can usually only be fully understood if more than one thermal analysis technique has been applied, especially techniques which give information on the nature of the degradation products. This chapter outlines the various techniques applied in this research. Thermal Volatilisation Analysis (TVA) is considered especially important since it is one of the most flexible techniques described which allows study of all of the products of degradation by MS, GC-MS, NMR IR and UV spectroscopy, electron microscopy, GLC, TLC and HPLC, depending on the nature of the products and apparatus available.

2.2. THERMAL DEGRADATION TECHNIQUES

2.2.1. Thermogravimetry

Thermogravimetry (TG), unlike TVA, displays the total weight loss of a sample on heating either as a function of time or temperature under programmed heating.

Thermogravimetric experiments, for the purpose of this work, were carried out using a Du Pont model 951 Thermogravimetric Analyser coupled with a model 990 Thermal Analyser. This system in addition to weight measurement, records simultaneously the derivative of the weight loss (DTG curve). Samples (5-10 mg unless

indicated otherwise) were heated in an aluminium sample holder at 10°C / min under a dynamic nitrogen or air flow of 50ml / min from ambient to 650°C. The temperature-measuring thermocouple was placed 1.0 mm from the top of the sample holder.

Throughout this thesis, the temperature at which weight loss is first detected is termed T_{onset} while the point when weight loss begins to fall sharply is termed $T_{\text{threshold}}$ (Fig. 2.1). The temperature for maximum ratio of weight loss T_{max} corresponds to the maximum in the DTG curve while T_{50} represents the temperature at which 50% of the sample weight is lost. The behaviour of each blend predicted, assuming no interaction between the components, has been calculated from the TG curves of the components and their relative amounts. These calculated TG curves are shown for each blend in subsequent chapters.

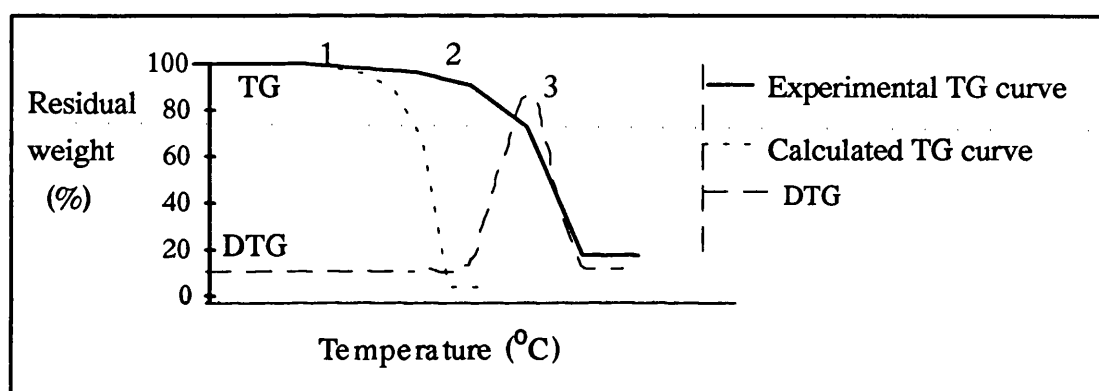


Fig. 2.1. TG and DTG curves showing definitions of (1) T_{onset} , (2) $T_{\text{threshold}}$ and (3) T_{max} .

2.2.2. Differential Scanning Calorimetry (DSC)

Differential scanning calorimetry involves the heating of a sample and an inert reference simultaneously at a programmed heating rate. If the material undergoes any physical (e.g. melting or transition from one crystalline form to another) or chemical change then heat is either absorbed or evolved. This energy change of the sample would result in a difference of temperature between the sample and the reference. The DSC apparatus is designed such that it keeps both at the same programmed temperature by the addition of heat to the cooler component. The energy required to keep the colder component at the same temperature as the other, is recorded as a function of time. Endothermic reaction results if the sample is the cooler component since extra energy is required to keep the sample at the same temperature as the reference while reverse is

true for the exothermic reaction. A DSC trace is in fact a plot of dH/dT versus time, where H is the amount of heat supplied in a given time. Total amount of energy transferred can be calculated from the area under the curve.

The instrument used for this work was a Stanton Redcroft TG-DSC 780 Differential Scanning Calorimeter. All analyses were carried out in a dynamic atmosphere of nitrogen at a flow rate of 50ml/min from room temperature to 650°C using 7-10mg samples. The inert reference used was similar to that which was used in the investigated blend as filler. A typical DSC curve is shown in Fig. 2.2.

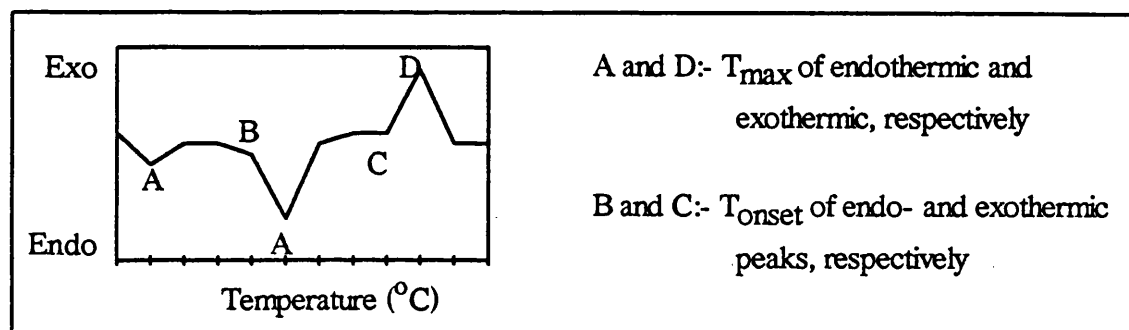
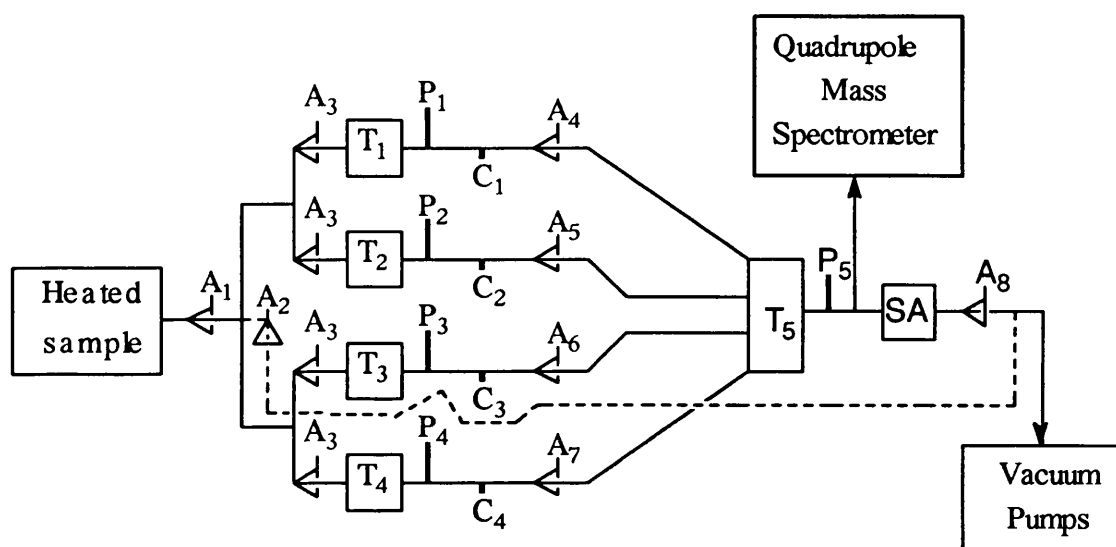


Fig 2.2. Typical DSC curve.

2.2.3. Thermal Volatilisation Analysis

Thermal volatilisation analysis (TVA) is a thermoanalytical technique developed and devised in this department which has been the subject of a number of publications⁴⁹⁻⁵⁶ and is now a well established technique of thermal analysis.

The technique measures (as a function of time or temperature) the small pressure increase developed due to the volatile degradation products in a continuously evacuated system during the degradation of a polymer sample which is heated either under linear programmed heating or isothermally. The degradation products could be either gases, liquids or solids at room temperature and atmospheric pressure. The pressure change which is measured by a Pirani gauge is related to the rate of volatilisation of degradation products. The TVA trace obtained resembles a derivative TG curve but it only records the evolution of volatile products which do not condense before reaching the gauge. A Schematic layout of this arrangement along with subambient TVA (SATVA) is shown in Fig. 2.3.



A_1 - A_8 :- Stopcocks; T_1 - T_5 :- Cold traps (0°C , -45°C , -75°C , -100°C , -196°C)
 C_1 - C_4 :-Sample receiving tubes or IR gas cells; P_1 - P_5 :- Pirani gauges;
 SA:- U-shaped subambient trap surrounded by 2.5 mm glass beads contained in a Pyrex glass vessel.
 -----:- Section of the system used during the isolation of products by SATVA and closed during the degradation by stopcock A_2

Fig. 2.3. Parallel Limb TVA and SATVA system.

The system was evacuated such that the Pirani gauges are initially at zero response (high vacuum, ie. 10^{-5} - 10^{-6} mm Hg). The polymer sample was then heated on a base of a Pyrex glass tube, 12" long with a diameter of 1.5" , if degradation was carried out below 500°C , in a Perkin Elmer F11 oven coupled with a linear temperature programmer which allowed the sample to be heated from the room temperature to a maximum temperature of 500°C at heating rates from 1°C to $40^\circ\text{C}/\text{min}$. The heating assembly is shown in Fig. 2.4 (a). Degradations at higher temperatures (500 - 700°C) were carried out in a silica boat inserted inside a 14" long silica tube with a diameter of 0.7" inserted in an NEF 2-1 60A Air Exchange Furnace. The sample in this case was heated horizontally as shown in the Fig. 2.4 (b). Both ovens could be used isothermally but in this research ovens were used almost entirely in programmed mode, using a heating rate of $10^\circ\text{C}/\text{min}$.

Oven temperatures were measured using a chromel-alumel thermocouple, fixed externally near the base of the degradation tube and having a 0°C (ice in water) reference. The thermocouple and Pirani gauges were joined to an interface connected to a BBC micro computer. The interface scales the voltage outputs from the thermocouple

and Pirani gauges to a suitable level for the analogue to digital converter in the BBC computer. A program then samples the voltages and stores the data for subsequent graphical presentation. This data acquisition system was designed in the department as an undergraduate research project by S.W. Mackay under the supervision of Dr. I.C. McNeill and Dr. J.K. Tyler⁵⁷.

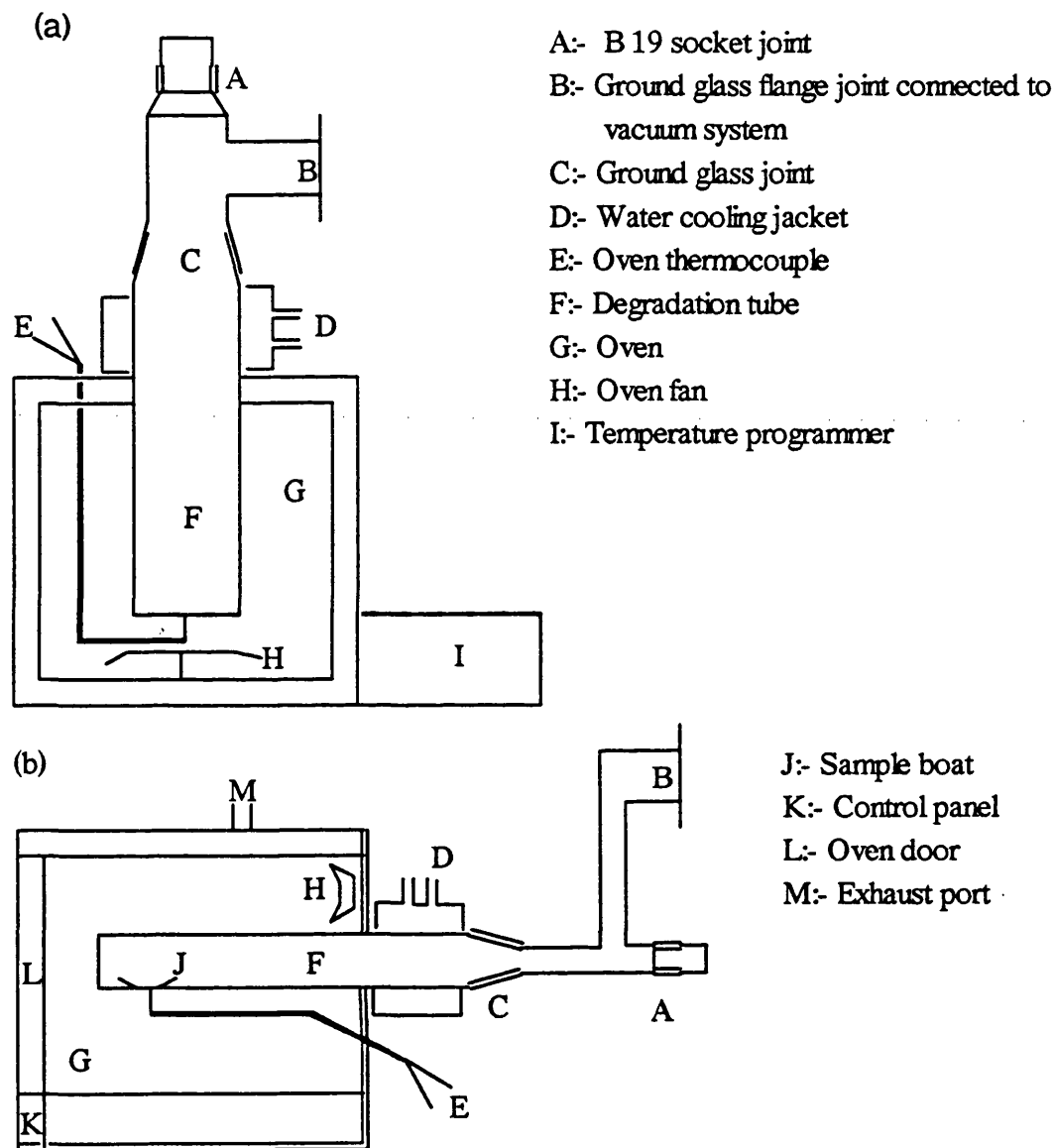


Fig. 2.4. TVA heating assembly for the degradation carried out (a) below 500°C and (b) above 500°C.

The degradation products were pumped along the TVA line and passed through the section of the TVA tube where a cold water jacket was placed around it to trap those degradation products which are volatile at the degradation temperature but

involatile at room temperature. The products collected at this point are mostly small fragments of the polymer chain and are called 'Cold Ring Fraction' (CRF). The degradation products which were not trapped at this temperature were then passed through four geometrically equivalent routes to U-shaped traps at temperatures of 0°C, -45°C, -75°C and -100°C respectively. These four routes then pass through traps at liquid nitrogen temperature (-196°C) and any products not condensed were led to the quadrupole mass spectrometer for MS analysis or to the vacuum pumps. These highly volatile products such as methane, carbon monoxide and hydrogen are termed non-condensable gaseous products. Each trap is followed by a Pirani gauge. If a compound is volatile enough to pass through any of the traps, the Pirani gauge detects the increase in pressure and the output is transmitted via interface to the computer where it is recorded continuously with oven temperature as function of time or temperature. This gives some knowledge of the volatility of the degradation products.

The degradation tubes were calibrated since due to the insulating effects of the Pyrex glass tube, the temperature inside the tube could be slightly lower than the outside. The calibration was carried out by inserting thermocouple inside the degradation tube and making sure that it was in good contact with the sample. The system was evacuated and continuously pumped to a high vacuum and then was heated as for normal TVA conditions. The same procedure was carried out without using the sample and it was made sure that the thermocouple was in good contact with the base of the tube, in the case of vertical degradation, and touching the section of the tube where the sample boat was placed, in the case of horizontal degradation. This calibration was carried out in case the sample has some effect on the thermocouple performance during degradation. These results were matched with those obtained with a thermocouple just outside the degradation tube. A typical calibration curve for the Pyrex glass degradation tube is shown in Fig. 2.5. (i) It is clear from the calibration curve that there is a 10-20°C temperature difference inside and outside of the tube. However, the calibration curve for the silica tube (Fig. 2.5. (ii)) shows lower temperature inside of the tube at the beginning which gradually narrows down and after about 200°C both curves overlap. This possibly is due to the better conducting properties of silica.

Theoretically it can be shown that same amount of volatiles passes through each of the four routes. However, one or more degradation products may condense when they pass through a cold trap so that the Pirani traces are often non-coincident for a mixture of volatile degradation products.

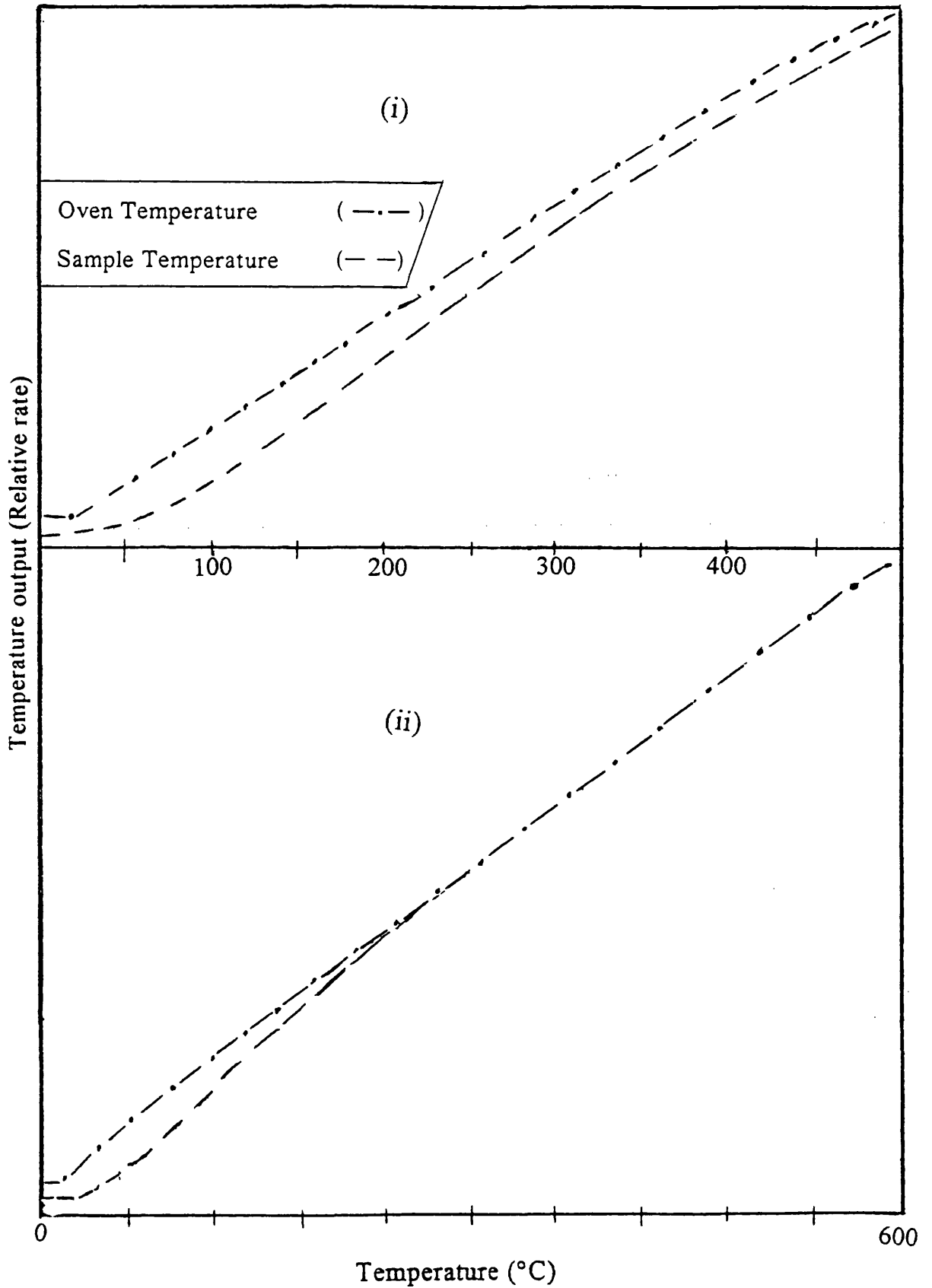


Fig. 2.5. Degradation tube temperature calibration charts for the: (i) Pyrex glass tube and (ii) silica tube.

Polymers were examined mainly as 50 mg samples and blends as 100 mg (unless indicated otherwise) in the TVA system under vacuum conditions as described above and programmed with heating rate of 10°C/min.

The individual TVA traces based on the responses of the gauges after the traps 0°C, -45°C, -75°C, -100°C and -196°C, respectively were non-coincident indicating the evolution of a mixture of degradation products of different volatilities. The values quoted for the TVA temperatures were not corrected for temperature differential across the tube base, therefore, in normal conditions, for a Pyrex glass TVA tube, the temperature of the sample would be about 15-20°C less than the oven temperature initially but the difference gradually decreases to about 8-10°C as the temperature rises to 500°C. Degradations were carried out in a silica TVA tube if samples were degraded up to 500°C or above. Since nearly all degradations started well after 200°C, the sample temperature would be similar to the oven temperature. The following convention has been used for the individual trap traces of TVA curves:

| | | |
|-----------|--------|-----------------------------------|
| — | 0°C | (and colder traps if coincident). |
| | -45°C | " |
| - - | -75°C | " |
| - · - | -100°C | " |
| - · - · - | -196°C | " |

2.2.4. The 'Sealed Tube' Degradation

Degradation products which were not condensable in liquid nitrogen under vacuum conditions, were collected by carrying out degradation in a sealed tube similar to that shown in Fig. 2.6. (a). The weighed sample was inserted through limb A and then the whole system was evacuated to a pressure of 10^{-4} to 10^{-5} torr and sealed off at point B. Limb E was then placed in an oven, modified to allow the degradation tube to enter horizontally, at the required temperature and heating rate while limb D was immersed in liquid nitrogen to trap degradation products leaving the hot zone.

After degradation the sealed tube and the cold trap were transferred to the vacuum line and the tube was connected to a gas cell (Fig. 2.6. (b)) at point H through the B14 cone (K) with break seal. The whole system was then evacuated. Section I of the gas cell was frozen with liquid nitrogen and stopcock F closed before breaking the seal using a glass covered metal weight. The system was left in this position for some time to let an

equilibrium be established between the two containers. Stopcock J was then closed, the gas cell was removed from the degradation tube and the sample was analysed by IR spectroscopy and MS. This technique is, however not suitable for quantitative purposes since only part of the sample is collected in the cell by this method.

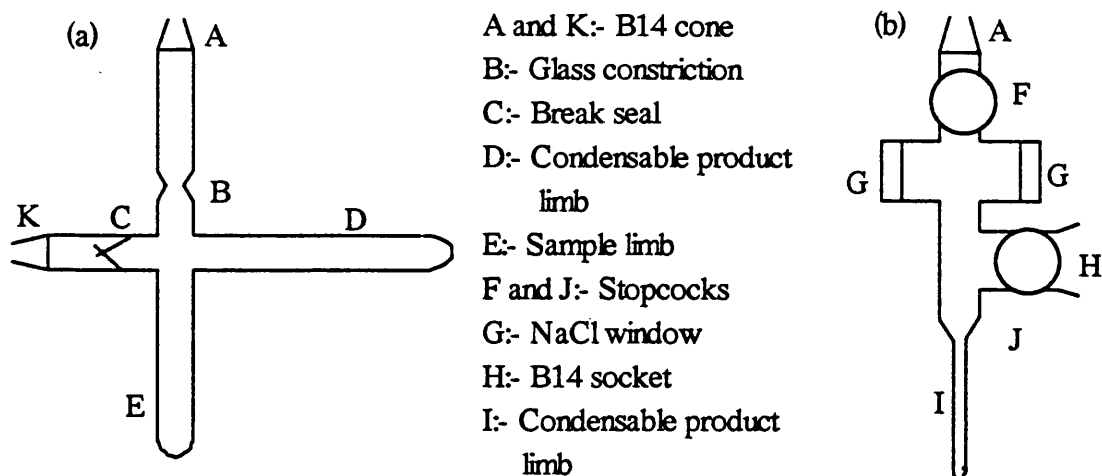


Fig. 2.6. (a) Tube for closed system degradation and (b) Gas cell for collecting non-condensable gases from the sealed tube.

2.3. SUBAMBIENT TVA (SATVA)

The volatile degradation products after degradation, other than CRF, were separated in a continuously evacuated system by the technique called Subambient TVA (SATVA)^{56, 58-60}. In the TVA line (Fig 2.3) all the volatile degradation products, trapped in the traps at 0°C to -196°C, were transferred into the subambient (SA) trap, inserted further along the TVA line, near the vacuum pumps. This U-shaped trap is surrounded by 2.5 mm glass beads contained in a Pyrex glass vessel. The glass vessel itself was cooled by submerging it into the Dewar flask containing liquid nitrogen before the degradation products were transferred into it from the other traps. The temperature of the trap was measured by inserting a thermocouple through the glass beads such that it touched the U-trap at the bottom.

After volatile degradation products had been transferred to the SA trap, stopcocks A₁ and A₄-A₈ of Fig. 2.3 were all closed and stopcock at A₂ was opened. The traps which were used for 0°C to -100°C now all contained liquid nitrogen. The dotted line shown in Fig. 2.3 represents the section of the line only opened during the subambient separation which allows the entire TVA line to be pumped continuously when stopcock A₈ was closed. Stopcock A₄ was then opened to collect the first fraction of the products. The Dewar flask containing liquid nitrogen was then removed from the SA

trap to let it warm up at a rate determined by the thickness of the surrounding jacket. As the trap warmed up, the most volatile condensed product distilled first and was collected in the first trap T_1 . The stopcock A_4 was then closed and the next one opened for the second fraction and so on. The pressure changes associated with the distillation of the products from SA trap to traps T_1 - T_4 were measured by Pirani gauge P_5 . Pirani response and SA trap temperature were recorded as a function of time to give a trace similar to that in Fig. 2.7 (a) showing at least four separable fractions. Usually liquid fractions were collected together.

The products were then distilled from each -196°C trap to evacuated sample collecting vessels attached to the limbs at points C_1 to C_4 for analysis. The collecting vessels were usually IR gas cells (Fig. 2.7 (b) for collecting gaseous products and a small liquid sample tube for collecting liquids.

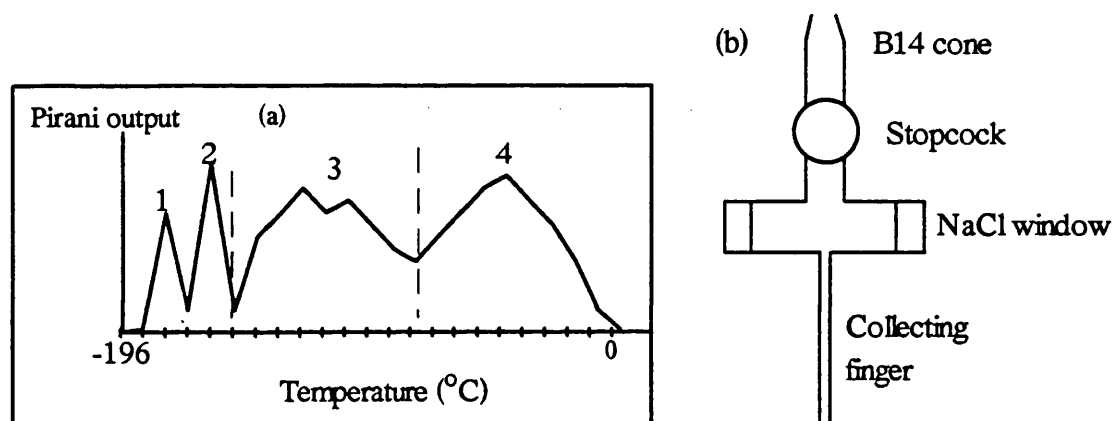


Fig 2.7. (a) Typical SATVA trace and (b) Gas cell for collecting gaseous products for IR analysis.

2.4. ANALYSIS OF DEGRADATION PRODUCTS

Degradation products can be classified as:

- (i) non-condensables
- (ii) condensables
- (iii) cold ring fraction (CRF)
- (iv) involatile residue

Non-condensables (e.g. hydrogen, methane, oxygen, carbon monoxide) are those materials which are not condensable at -196°C and can only be collected if the degradation is carried out in a closed system^{61, 62}, usually in a tube sealed under vacuum as shown in Fig 2.6 (a). Volatile degradation products are then transferred into an evacuated IR gas cell or gas sample tube for analysis. Alternatively, non-condensables could be fed into a quadrupole mass spectrometer attached to the TVA line, as soon as

they are produced. This method also gives information on the component formed at a certain temperature if there is more than one non-condensable product.

Condensables are those materials which are volatile at degradation and ambient temperature but condense at -196°C or above in a continuously pumped system. These materials were easily separated using subambient thermal volatilisation analysis (SATVA) by subsequent distillation into IR gas cells or liquid sample tubes attached at points $\text{C}_1\text{-C}_4$ as shown in Fig. 2.3, thus allowing separation of up to four fractions or products. They were then identified by using IR spectroscopy and mass spectrometry (MS) if gases and IR spectrometry and gas chromatography-mass spectrometry (GC-MS) if liquids or solids at room temperature.

The cold ring fraction (CRF) is usually analysed by IR spectroscopy, GC, NMR spectroscopy, HPLC and GLC but in the present work only IR spectroscopy, GC and NMR spectroscopy were used.

The involatile soluble residue could be analysed by IR spectroscopy either as a film cast on a NaCl plate or as a solution. Insoluble residues were analysed spectroscopically as KBr disc or Nujol mull by first grinding the material as fine powder. It was also possible to examine the residue by NMR spectroscopy if it was soluble in a suitable solvent.

2.5. ANALYTICAL TECHNIQUES USED IN THIS RESEARCH WORK

Infrared Spectroscopy

Most of the infra red spectra for the purpose of this thesis were recorded on a Philips PU 9800 FT-IR Spectrometer while a Perkin-Elmer Infrared Data Station 983 with PE 3600 data system and having a range of $4000\text{-}200\text{ cm}^{-1}$ was also used for analysing residues from blends with inorganic fillers. Polymer samples, CRFs from all degradations carried out and residues from pure degraded polymers were examined by casting a film on a NaCl plate, from dichloromethane if the component was soluble at room temperature or from 1-chlorobutane if it required heating. Insoluble CRFs and residues from blends were studied as KBr discs. Most blends formed rubbery and/or insoluble residues and were difficult to grind. Consequently, it should be kept in mind for all blends mentioned later in various chapters that if the residue is described as rubbery and/or insoluble then it was impossible to grind it. Therefore, possibly only small and thin fragments/sections allowed the transmittance of light resulting in some cases in spectra lacking in detail. The identification of degradation products from their IR spectra was based on references⁶³⁻⁷².

Elemental Analysis

Polymers, especially EEA copolymer were characterised from elemental analysis carried out on a Carlo Erba Model 1106 Elemental Analyser. This method was found particularly useful in calculating the proportion of ethyl acrylate (EA) units in EEA copolymer. The percentage weight of carbon and hydrogen were calculated by this method and percentage weight of oxygen was obtained by difference. The number of ethyl acrylate repeat units in the polymer chain were calculated on the basis of number of oxygen atoms in the empirical formula. The percentage content of each comonomer was calculated by using the following equation:

$$\% \text{ content of EA by weight} = (\text{total weight of EA units in the empirical formula} \times 100) / \text{total weight of the empirical formula}$$
$$\% \text{ content of ethylene by weight} = 100 - \% \text{ content of EA by weight}$$

Nuclear Magnetic Resonance Spectrometry (NMR)

NMR provides a powerful tool for the compositional and structural analysis of a component. This method can be used to provide useful information about the distribution of monomers in a copolymer if there is at least one functional group in a comonomer different from the other.

Spectra were obtained using either a Bruker WP 200 SY 200 MHz or a Bruker AM 200 SY 200 MHz spectrometer.

Mass Spectrometry

The mass spectra of gaseous products including non-condensables were obtained using a Kratos M512 mass spectrometer in conjunction with a DS55C data system. A Leda Mass Multiquad quadrupole mass spectrometer, coupled directly to a TVA-SATVA system (Fig. 2.3) was also used to analyse degradation products, mainly non-condensables, of some samples.

Gas Chromatography

CRFs and liquid fractions obtained from SATVA separation were analysed by gas chromatography using a Hewlett-Packard 5880A Gas Chromatograph fitted with a CP Sil 5 CB (Chrompack) fused silica capillary column (25m x 0.32mm I.D. x 0.12 μ m) and

a flame ionisation detector. Injections were operated in split mode (50:1) and helium was used as a carrier and make-up gas with flow rates of 2ml/min and 25ml/min, respectively. The temperature of the column was programmed from 50°C (2 min) to 210°C (5 min) with heating rate of 5°C/min for products from SATVA separation, while for CRF it was programmed from 80°C (2 min) to 150°C (1 min) with heating rate of 30°C/min and then to 280°C (30 min) with a heating rate of 3°C/min for CRF. The injection port and detector temperatures were set at 20°C and 15°C, respectively lower than the column temperature. Products were identified by comparing the retention times to those of standards where possible but in most cases it was difficult to get the standard compounds.

Gas Chromatography-Mass Spectrometry (GC-MS)

GC peak assignments was made mainly by obtaining mass spectra for each peak. This was made possible by using a Hewlett-Packard 5971 mass selective detector interfaced to a 5890 series II gas chromatograph and computer (Vectra TQ5/165). The Gas chromatograph was equipped with a HP1 fused silica capillary column (12.5m x 0.2mm I.D. x 0.33 μ m). Injection and temperature programming conditions were kept similar to those described for GC above. Retention times from the total ion current and flame ionisation detector chromatographs were in reasonable agreement. Mass spectra were recorded in the continuous scanning mode.

Electron Microscopy

A Philips SEM 500 scanning electron microscope was used to examine the surfaces of some of the residues while the degree of agglomeration in the fillers and sliced thin sections after degradation up to 480°C were examined by transmission electron microscopy with a JEOL 100C type electron microscope. Residue from blend 26 after 650°C was also examined by transmission electron microscopy.

2.6. BLEND PREPARATION

Most blends were prepared in a Brabender laboratory blender by melt compounding at 150°C under dynamic nitrogen except for blends 15, 16, 40, 51, 52, 53, 54 and 55. Preparation for these blends is described in chapters 6 (blends 15 and 16) and 7.

CHAPTER 3

ETHYLENE AND ETHYL ACRYLATE COPOLYMER

3.1. INTRODUCTION

It is important as a basis to understand the thermal degradation behaviour of pure low density polyethylene (LDPE) and poly(ethyl acrylate) (PEA) before considering the effect of altering the chemical structure of LDPE by introducing polar ethyl acrylate (EA) units into the polymer chain randomly. Thus initial investigations were carried out on the thermal degradation of PE and PEA.

3.2. THERMAL DEGRADATION OF LOW DENSITY POLYETHYLENE (LDPE)

3.2.1. Introduction

There are different types of polyethylenes: cross-linked, linear low-density, branched low-density and high density polyethylenes. The division is somewhat arbitrary and is based on preparation methods, physical and chemical properties, the commercial system of naming and the uses of the polymer. Polyethylenes like other polyolefins possess an attractive balance of chemical, electrical, thermal and mechanical properties, therefore they have become commonly used industrial polymers.

Most LDPE homopolymer applications are packaging films which include containers and bags for food and clothing, industrial liners, vapour barriers, agricultural film, household products and shrink and stretch wrap film. LDPE is also the choice for wire and cable insulation because of its superior dielectric properties and ability to be cross-linked. High density polyethylene (HDPE) is used in thinner films, blow moulded bottles and mouldings when stiffness is preferred over clarity. Linear LDPE (LLDPE) is used for producing stronger films at equivalent resin density, thus reducing the raw material cost by reducing the film thickness without compromising product strength.

PE has extremely poor adhesion properties, therefore, for many of its applications, it needs to be improved by introduction of polar groups into the polymer chain. These polar groups can be introduced by many means according to the chemical use of the polymer.

Thermal stability and degradation behaviour of PEA and PE have been studied previously. Wall and Straus⁷³, studied the thermal decomposition of high-pressure polyethylene i.e. LDPE. Oakes and Richards⁷⁴ on the other hand examined partial degradation of branched polyethylene by infrared (IR) spectroscopy. In each case it has been concluded that branched polyethylenes do not decompose by random chain scission as does the linear PE. Branching introduces the presence of the more reactive tertiary hydrogen atoms and the weaker carbon-to-carbon bonds attached to the ternary or quaternary carbon atoms, thus these weaker bonds are ruptured first, lowering the thermal stability. The presence of branching also increases intramolecular transfer at the expense of intermolecular transfer, thus producing more volatile unsaturated hydrocarbons. IR studies of partially degraded polyethylenes have indicated some preferred rupture near the branching points of the chain⁷⁴. It has been observed that the rate of volatilisation increases with increasing the amount of branching in the polymer backbone. However, it was revealed that the nature of the degradation products does not change greatly.

The thermal degradation and stability properties of PEA have been investigated by Grassie and Speakman⁷⁵ in great detail. It has been concluded that the mechanism of breakdown is by random chain scission and that about 50% of the volatile degradation products consist of ethanol produced by cyclisation along the chain after polymer chain scission.

Copolymers such as ethylene ethyl acrylate (EEA) copolymer have been the subject of previous studies but not in detail. Barrall, Porter and Johnson⁷⁶ and Bombaugh, Cook and Clampitt⁷⁷ investigated the products of thermal degradation of random copolymers of ethyl acrylate and methyl acrylate respectively with ethylene. In each case it has been concluded that the mode of degradation of random copolymer is discernibly different from either of the homopolymers or from a block copolymer because of the relatively isolated position of the individual comonomer units. It was also concluded that the amount of alcohol decreases with increasing ethylene content and that its production, at the expense of ethylene when a large amount of EEA copolymer is pyrolysed in bulk, is possibly due to a secondary reaction between ethylene and the residue.

In order to compare the effect of polar groups (acrylate units) and additives (inorganic fillers, salts, acids and polymer) on the thermal degradation behaviour of EEA copolymer as compared with the previous TVA/SATVA studies on PEA and LDPE, a further more detailed study has been undertaken which is reported as follows.

3.3. EXPERIMENTAL

3.3.1. Preparation and Purification of PEA

The polymer used in the present investigation was a commercial EniChem Elastomeri spa sample of PEA with molecular weight of over one million. This PEA was purified by precipitation from a 3:1 solution of distilled water and methanol at 0°C. The rubbery white material was dried in a vacuum oven at about 50°C for 3 days before subsequent analysis. The PEA-additive blends (discussed in chapters 5, 6 and 8), however, were made from the original polymer sample. PEA, with molecular weight of 1.47×10^6 , was also prepared in the laboratory for comparison. Synthesis was carried out as in the literature⁷⁵.

3.3.2. Source of LDPE and EEA Copolymer

LDPE and EEA copolymer were also commercial samples and were used without purification.

3.3.3. Microanalysis

Microanalysis data for the PEA and EEA copolymer samples are shown below in Table 3.1.

Table 3.1. Microanalysis results for PEA and EEA copolymer.

| | Elements: | C (%) | H (%) | O (%) |
|---------------------------|-------------|-------|-------|-------|
| Laboratory prepared PEA: | Found: | 60.10 | 8.60 | 31.30 |
| | Calculated: | 59.97 | 8.07 | 31.96 |
| Commercial sample of PEA: | Found: | 60.16 | 7.97 | 31.87 |
| | Calculated: | 59.97 | 8.07 | 31.96 |
| EEA copolymer: | Found: | 81.35 | 13.39 | 5.26 |

The microanalysis results show that in the EEA copolymer there are about 18 units of ethylene for every ethyl acrylate unit and that ethyl acrylate comprises about 16.54 wt.% of the structure.

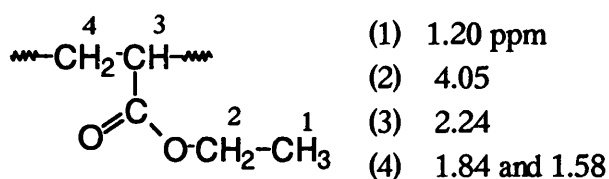
3.3.4. Infrared Spectra

Infrared spectra (films cast from CH_2Cl_2) of laboratory prepared PEA and commercial PEA are given in Fig. 3.1. There are very small differences between the two samples. For instance, the peaks in the region $1750\text{-}625\text{ cm}^{-1}$ are similar, only there is some difference for the intensities of the methyl and methylene groups in the region $2980\text{-}2860\text{ cm}^{-1}$. The IR spectra are in good agreement with those in the literature^{75, 78}.

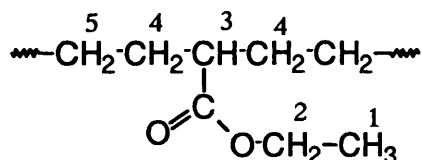
IR spectra of LDPE and EEA copolymer are shown in Fig. 3.2 (a) and (b) respectively.

3.3.5. ^1H NMR Spectra

Nuclear magnetic resonance (NMR) spectroscopy, Fig. 3.3 (a), was used to determine the stereoregularity of radically polymerised PEA. Since there is no overlap of the ester methyl protons, triplet located at 1.18, 1.27 and 1.35 ppm, the diad tacticity of the polymer was determined from the backbone methylene proton absorption from 1.50 to 2.30 ppm. The results show that both laboratory prepared and commercial (purified and unpurified) samples consist of a random configuration having about 33% of isotactic diads. Uryu, Shiroki, Okada, Hosonuma and Matsuzaki⁷⁹, using the same conditions of polymerisation, mention 51% of isotactic diads. The results are given below:



^1H NMR spectrometry (Fig. 3.3 (b)) was also used to determine the relative proportions of ethylene and ethyl acrylate units in the EEA copolymer. Results are given in Table 3.2.



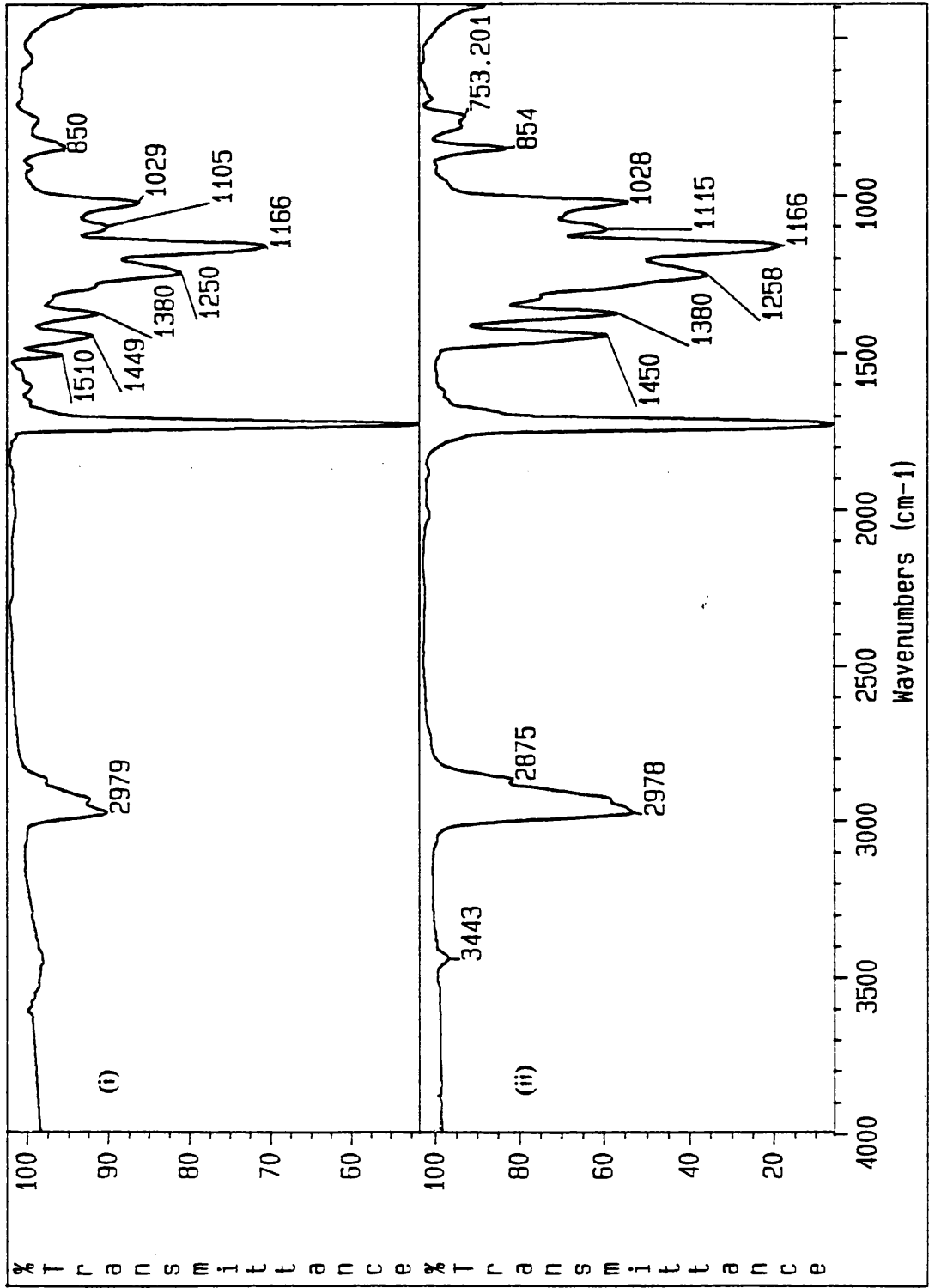


Fig. 3.1. IR spectra for (i) commercial PEA and (ii) laboratory prepared PEA.

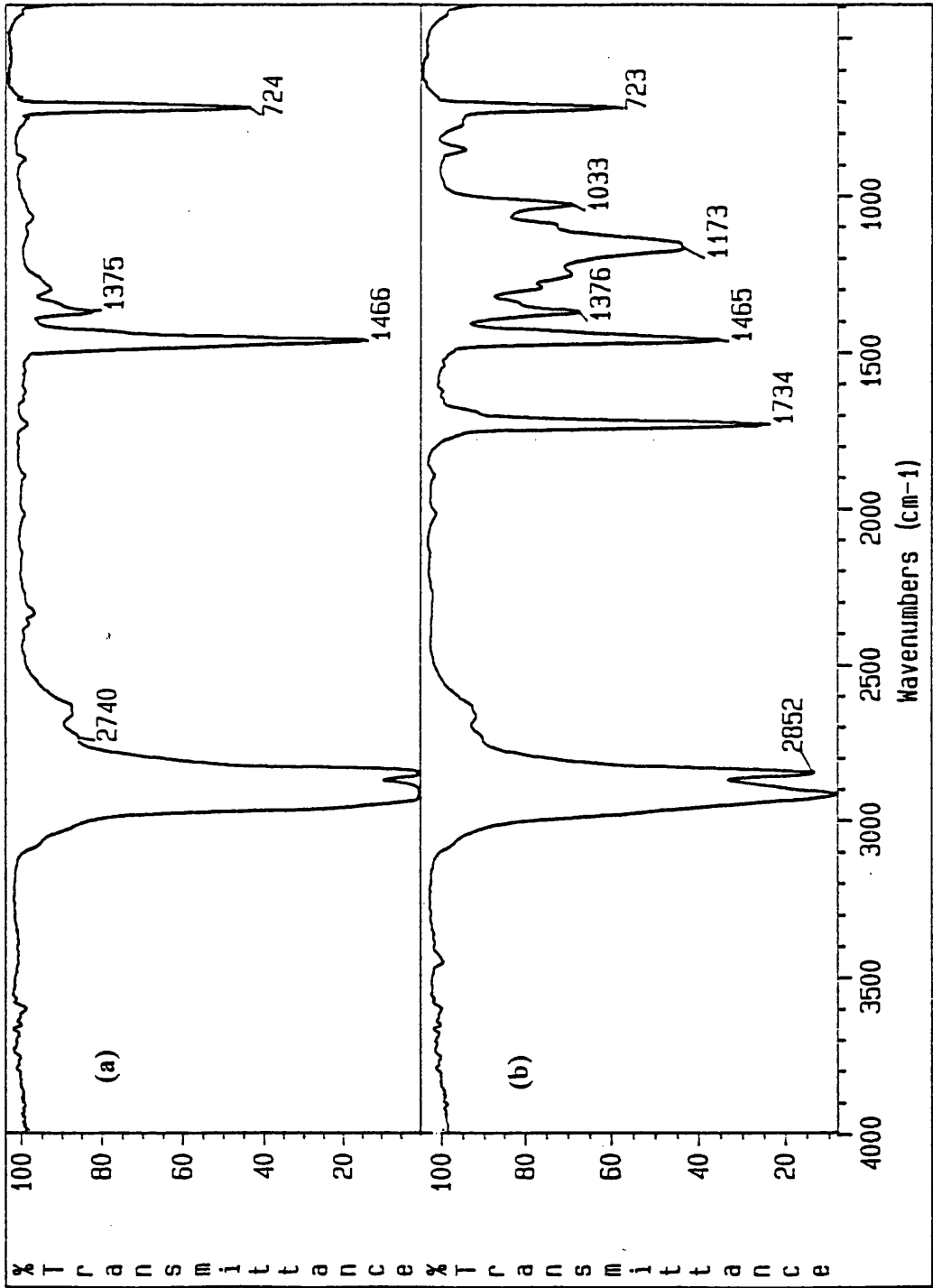


Fig. 3.2. Infrared spectra for (a) LDPE:BP77 and (b) EEA copolymer.

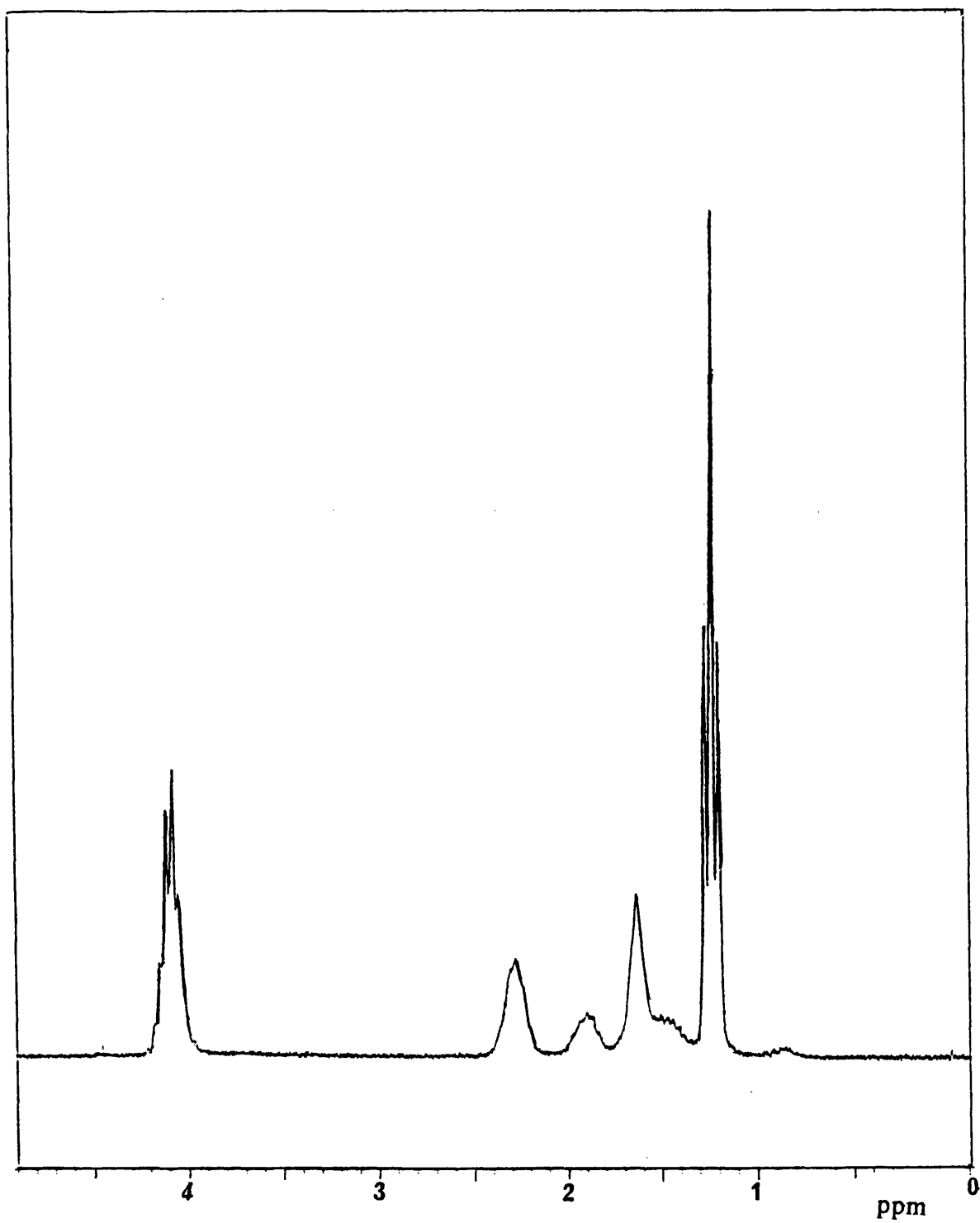


Fig. 3.3. (a) ^1H NMR spectrum for PEA

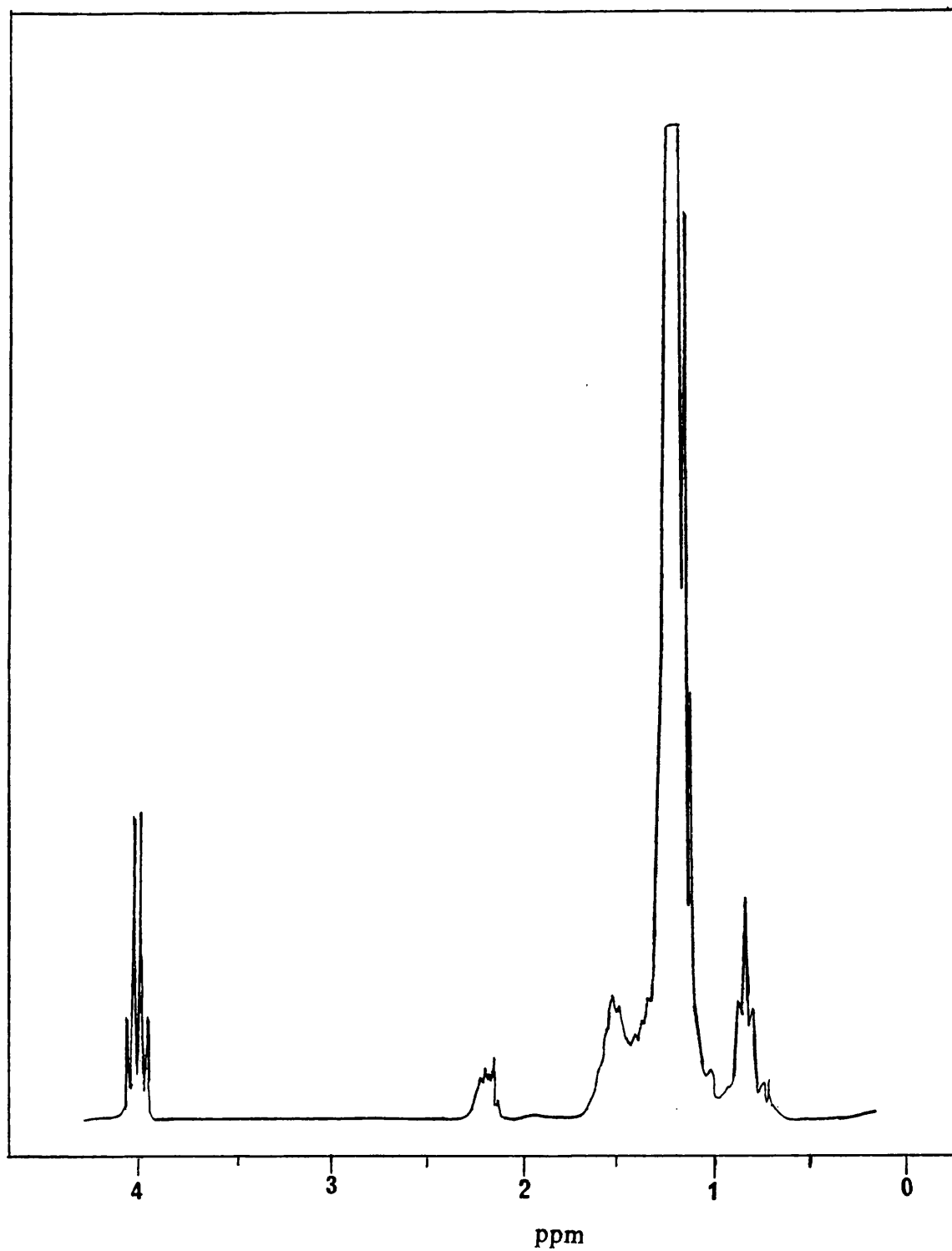


Fig. 3.3. (b) ^1H NMR spectrum for EEA copolymer.

Table 3.2. ^1H result for EEA copolymer

| C-H groups | NMR values (ppm) | Intensity | Ratio |
|------------|------------------|-----------|-------|
| 1 | 0.75 | 2.268 | 2.57 |
| 2 | 4.00 | 1.999 | 2.26 |
| 3 | 2.20 | 0.883 | 1.00 |
| 4 | 1.50 | 5.082 | 5.76 |
| 5 | 1.20 | 36.031 | 40.81 |

Since with every ethyl acrylate unit, the NMR spectrum would show similar absorption for two methylene groups near to a methine group, one of which belongs to an ethylene unit, it is concluded that for each EA unit, there are 18.56 ethylene units. The ^1H NMR result, therefore, agree with the microanalysis result.

3.3.6. Thermal Decomposition of PEA, LDPE and EEA Copolymer

3.3.6.1. Thermogravimetry (TG)

TG results in dynamic nitrogen and air are given in Table 3.3 (a) and (b) respectively.

3.3.6.1.1. TG-DTG Under Nitrogen

The TG curves obtained for the PEA samples, Fig. 3.4, indicate that the weight loss occurs almost in a single step during thermal degradation and that both laboratory and commercial samples begin to volatilise before 300°C. The temperature of maximum rate of evolution (T_{max}) for both samples, however, is different. The laboratory prepared sample reaches T_{max} at 392°C while the commercial sample reaches T_{max} at 425°C. The T_{max} value for the laboratory prepared sample agrees within 3-8°C with literatures^{75, 78}. The residue at 600°C is 2.25-6% of the total weight of the sample degraded.

Weight loss of low density polyethylenes (LDPEs), all with different degree and length of branching, starts at almost 387°C but all three samples show slightly different threshold and half weight loss temperatures (Figs. 3.5 (a) - (b)), while T_{max} of LDPE:BP77 only differs 2°C from the others. The residue at 600°C for the sample LDPE:BP77 is 1.75% while for the other LDPEs (LD5310 and LD1310) is about 0.125-0.25% of the total weight of the polymer sample degraded.

Weight loss of the EEA copolymer starts at 350°C and reaches T_{max} at 464°C. The residue at 600°C is 0.9% of the total weight of the polymer sample degraded. The TG trace is reproduced in the Fig. 3.6.

3.3.6.1.2. TG-DTG Under Air

The thermogravimetric experiments were performed for LDPE:BP77 and EEA copolymer under an atmosphere of air for purpose of comparison with the results obtained under nitrogen. These results show lower degradation temperatures, starting at 240°C and 237°C respectively. It was also observed that while LDPE:BP77 showed a single stage degradation (Fig. 3.5 (b)), EEA copolymer showed a complex degradation pattern (Fig. 3.6).

Table 3.3. (a) TG results under nitrogen

| Sample | T_{onset} (°C) | T_{max} (°C) | T_{50} (°C) | T_{stop} (°C) | % residue at 600°C |
|---------------|------------------|----------------|---------------|-----------------|--------------------|
| PEA* | 300 | 392 | 378 | 500 | 6.0 |
| PEA | 300 | 425 | 407 | 500 | 2.25 |
| PE:LD5310 | 387 | 482 | 465 | 500 | 0.13 |
| PE:LD1310 | 387 | 478 | 460 | 500 | 0.12 |
| LDPE:BP77 | 387 | 480 | 462 | 495 | 1.75 |
| EEA Copolymer | 350 | 464 | 444 | 500 | 0.9 |

Table 3.3. (b) TG results under air

| Sample | T_{onset} (°C) | T_{max} (°C) | T_{50} (°C) | T_{stop} (°C) | % residue at 600 (°C) |
|---------------|------------------|----------------|---------------|-----------------|-----------------------|
| LDPE:BP77 | 240 | 480 | 462 | 495 | 1.75 |
| EEA copolymer | 237 | 464 | 444 | 500 | 0.9 |

3.3.6.2. Differential Scanning Calorimetry (DSC)

The DSC curve for EEA copolymer exhibits two endothermic transitions as shown in Fig. 3.7. The peak temperatures occur at about 97°C and 460°C (average) and can be assigned to melting point, T_m , and the maximum rate of degradation of the copolymer, T_{max} , respectively. The temperature for the maximum rate of degradation agrees well with the TG results.

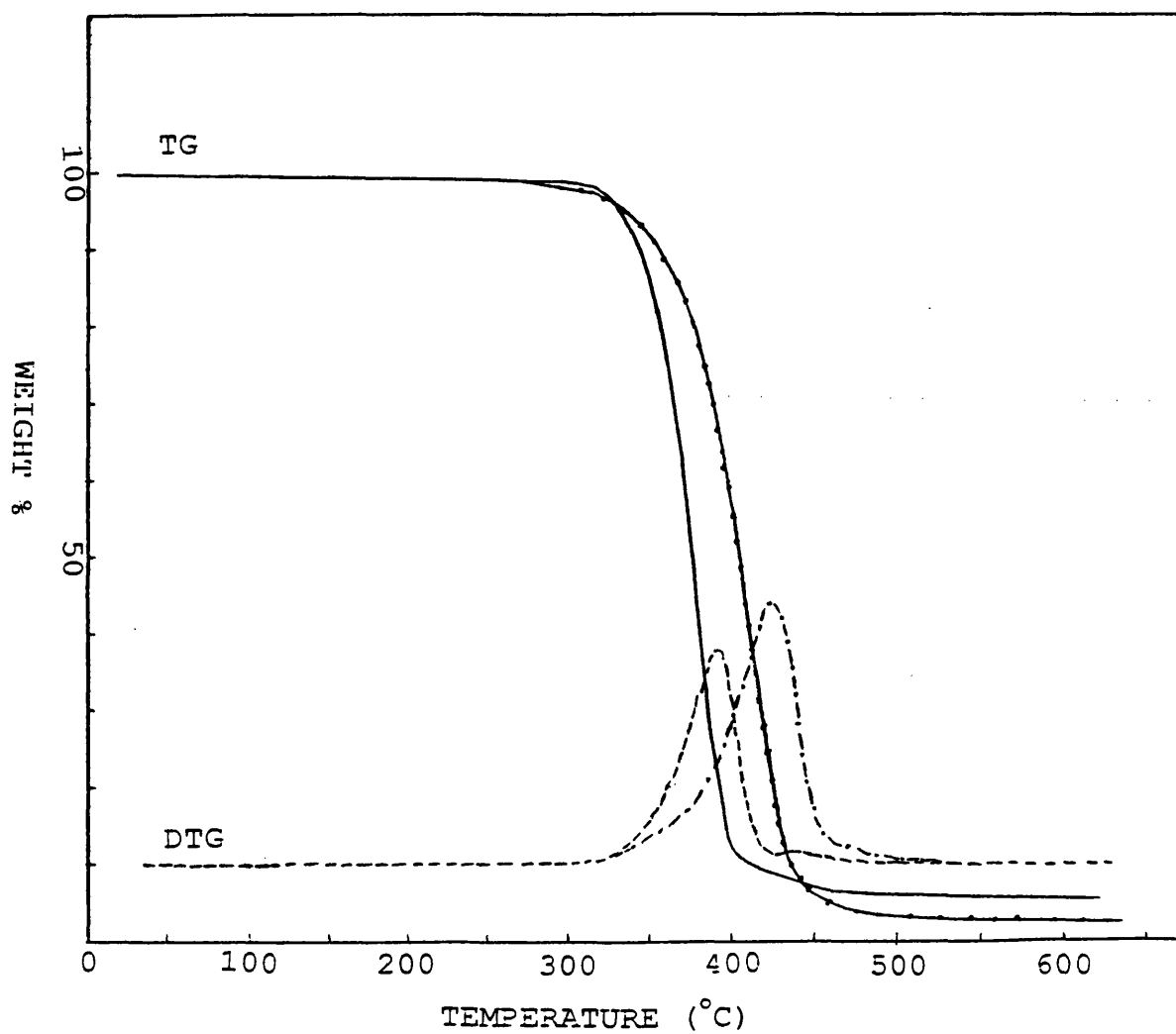


Fig. 3.4. Thermogravimetric traces for laboratory prepared PEA (—; ----) and commercial PEA (— — —; - · - · -) under nitrogen.

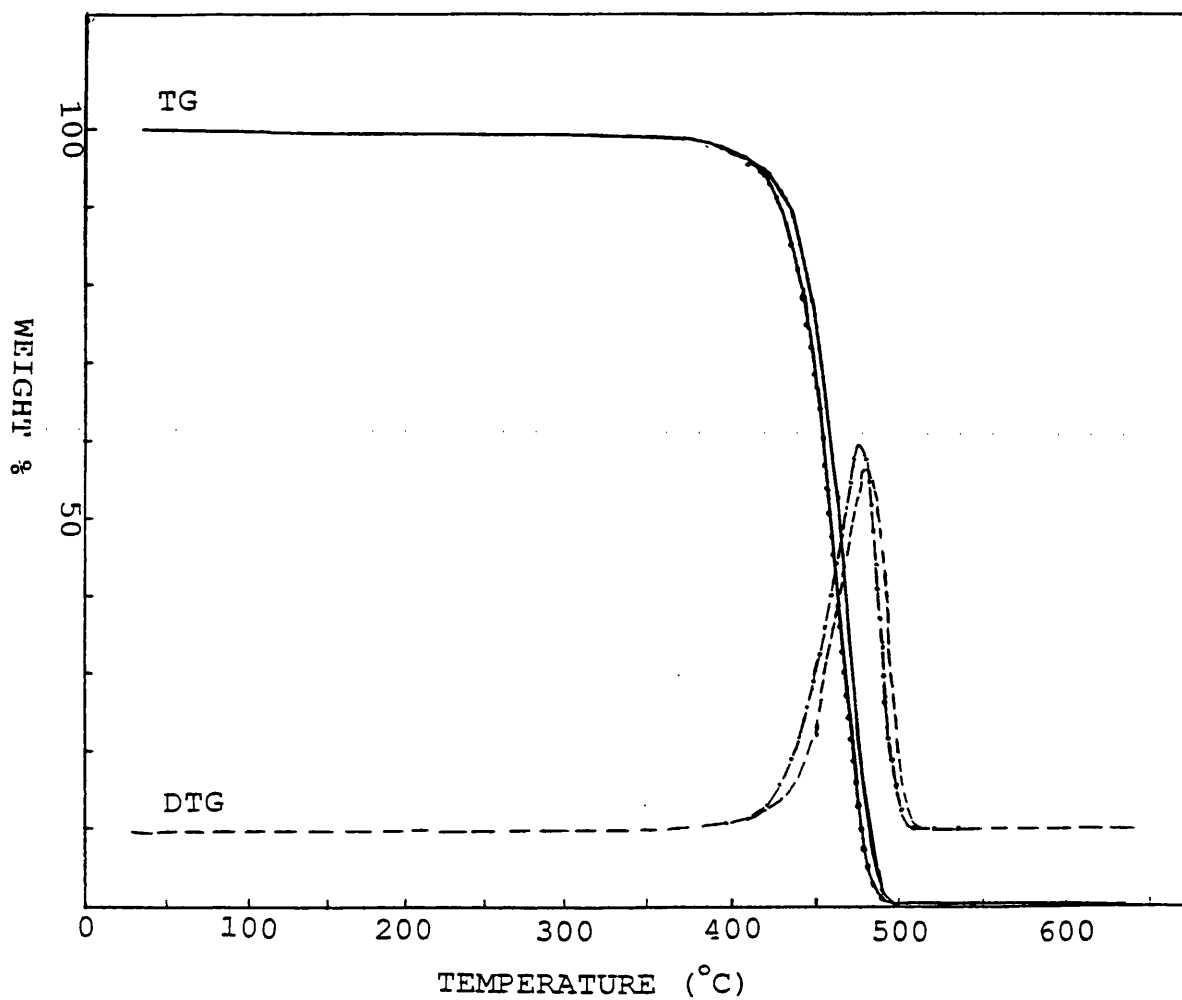


Fig. 3.5. (a) TG-DTG traces for LDPEs: LD1310 (—; ----) and LD5310 (—•—; -•-•-) under nitrogen.

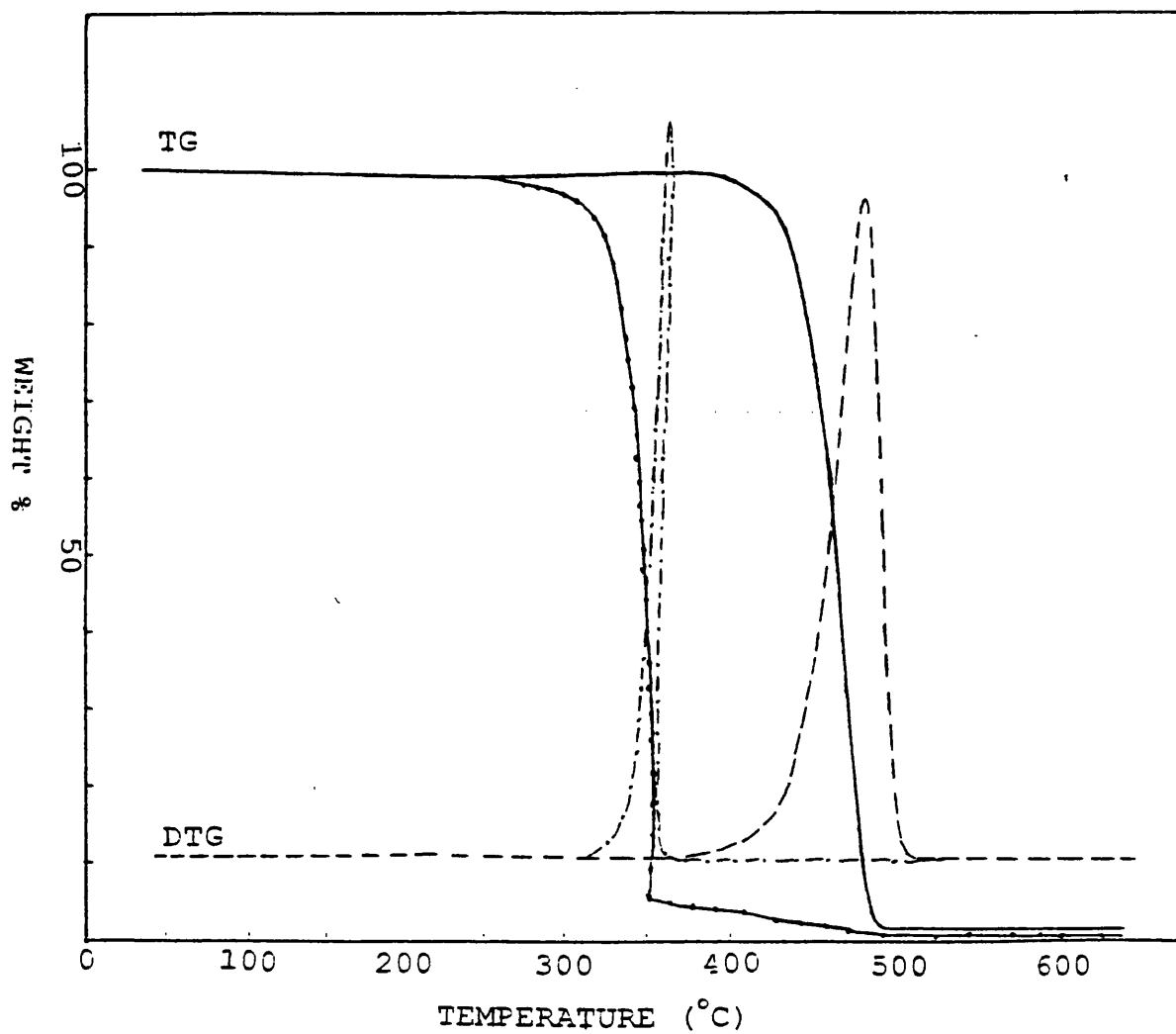


Fig. 3.5. (b) TG-DTG curve for LDPE:BP77 under nitrogen (—; ----) and air (— — —; - · - · -).

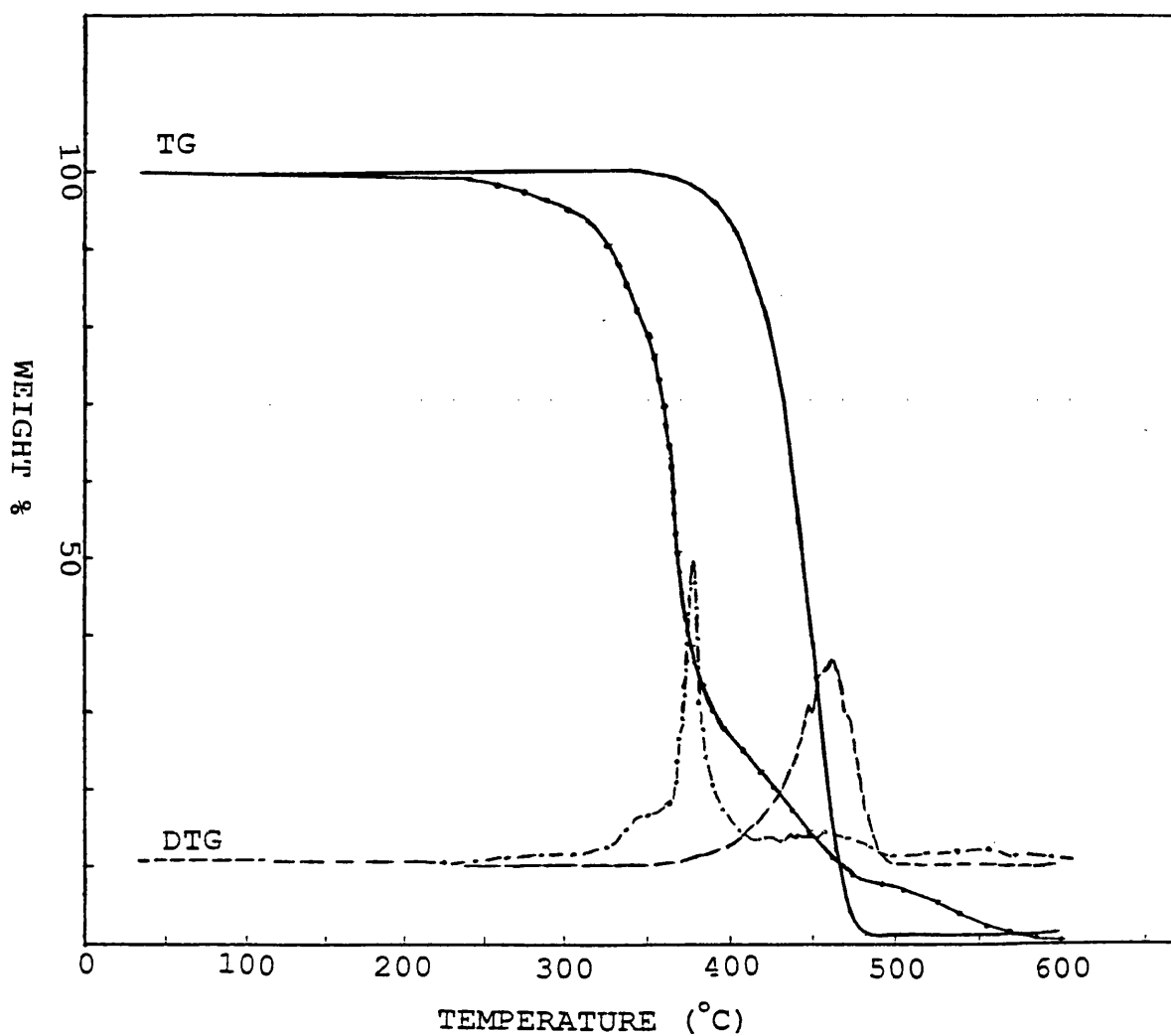


Fig. 3.6. TG-DTG traces for EEA copolymer under nitrogen (—; ----) and air (— · —; · · · · ·).

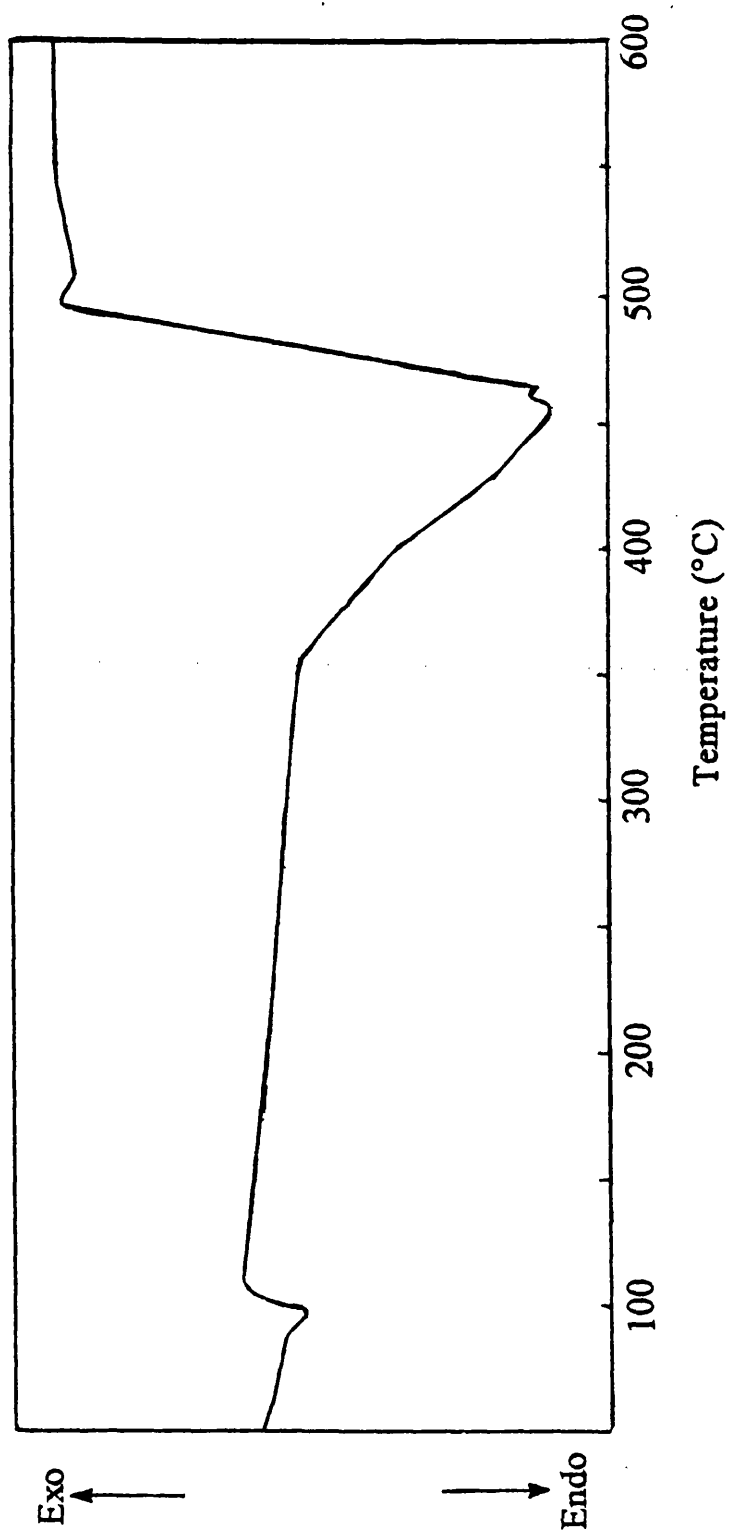


Fig. 3.7. DSC curve for EEA copolymer under nitrogen.

3.3.6.3. *Thermal Volatilisation Analysis (TVA) and SATVA Separation of Condensable Degradation Products*

PEA

The TVA curves (Fig. 3.8) of the laboratory prepared (degraded as 100 mg sample) and commercial PEA show that each polymer starts to volatilise at about 285°C (T_{onset}) and reaches maximum rate of product evolution at a temperature (T_{max}) of 420°C and 430°C, respectively. Laboratory prepared PEA (PEA*) also shows a small secondary peak at 470°C. Both samples show evidence for the evolution of non-condensable gaseous products (degradation products not trapped at -196°C under normal TVA conditions), identified as carbon monoxide, methane and hydrogen by the quadrupole mass spectrometer. The data of Grassie and Speakman^{63, 68} do not show the plateau region at the beginning.

The SATVA trace for the separation of the condensable volatile products of degradation of PEA, from either sample (Fig. 3.9), shows three peaks or three fractions. The first fraction was identified as ethylene by IR spectroscopy from the absorption bands at 950 cm^{-1} , 1443 cm^{-1} and 1890 cm^{-1} and by MS from the peaks at $m/e = 28$ (100%) $m/e = 27$ and m/z at 26. The second fraction was identified as carbon dioxide (CO_2) as seen from the absorption bands at 2320 cm^{-1} and 665 cm^{-1} in the IR spectrum and from the molecular ion peak at $m/e = 44$ (100%) in the mass spectrum of the fraction. Traces of ketene, as seen by a doublet in the IR spectrum at 2160 cm^{-1} and 2130 cm^{-1} and a peak in the mass spectrum at $m/e = 42$ are also present in the second fraction of the SATVA separation from the degradation products of commercial PEA and also when a large degradation sample is used in the case of PEA*. IR spectrum of peaks 1 and 2 is given in Fig. 3.10.

Fraction 3 of degradation products from PEA was identified mainly by GC-MS (Fig. 3.11) since IR spectroscopy only reveals the presence of the functional groups present and not a clear identity of each product. The results for identified degradation products from PEA are given in Table 3.4. It is shown that the major degradation product from PEA is ethanol which amounts to almost half of the degradation products.

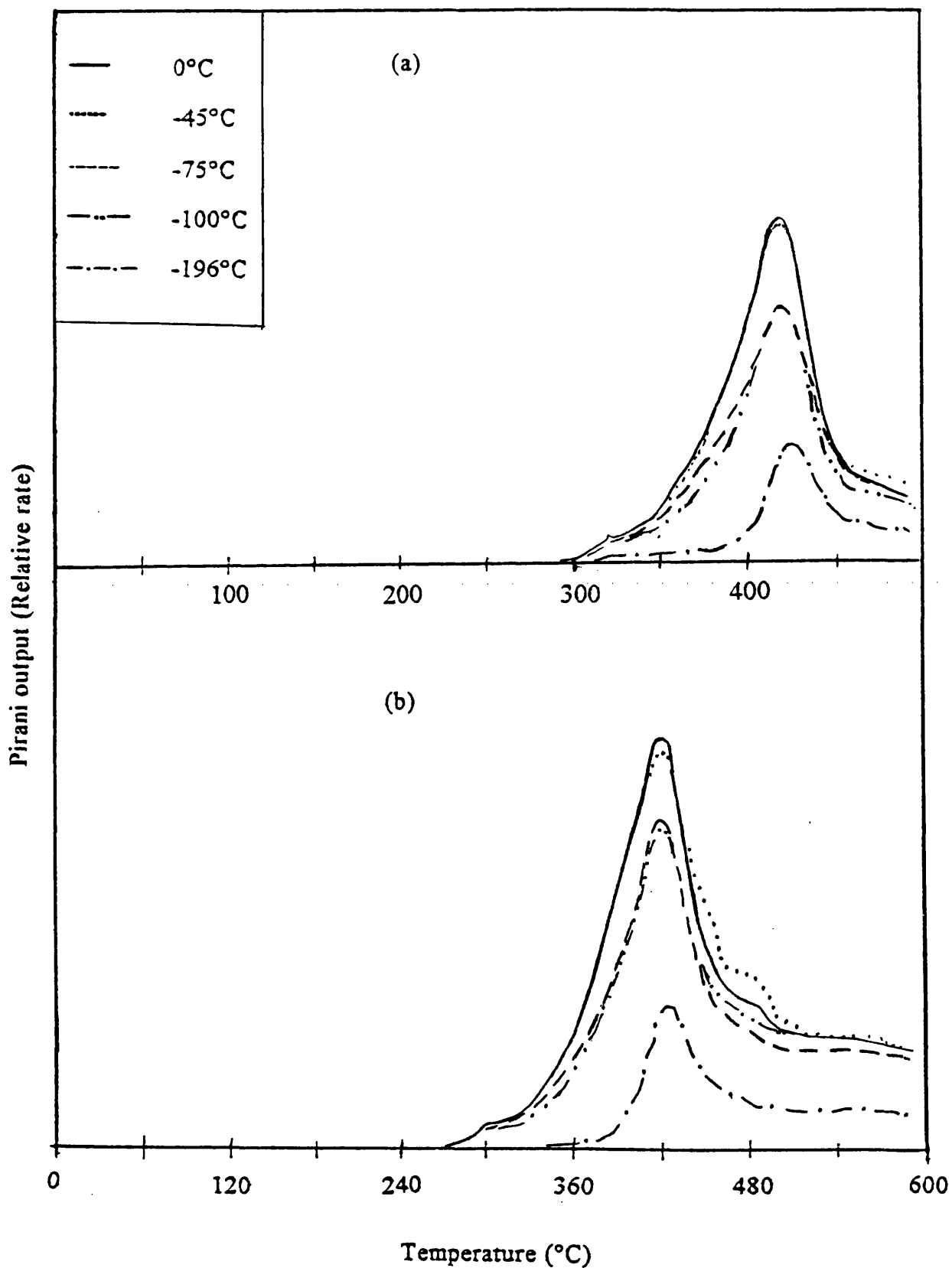


Fig. 3.8. TVA traces for (a) commercial PEA (b) laboratory prepared PEA.

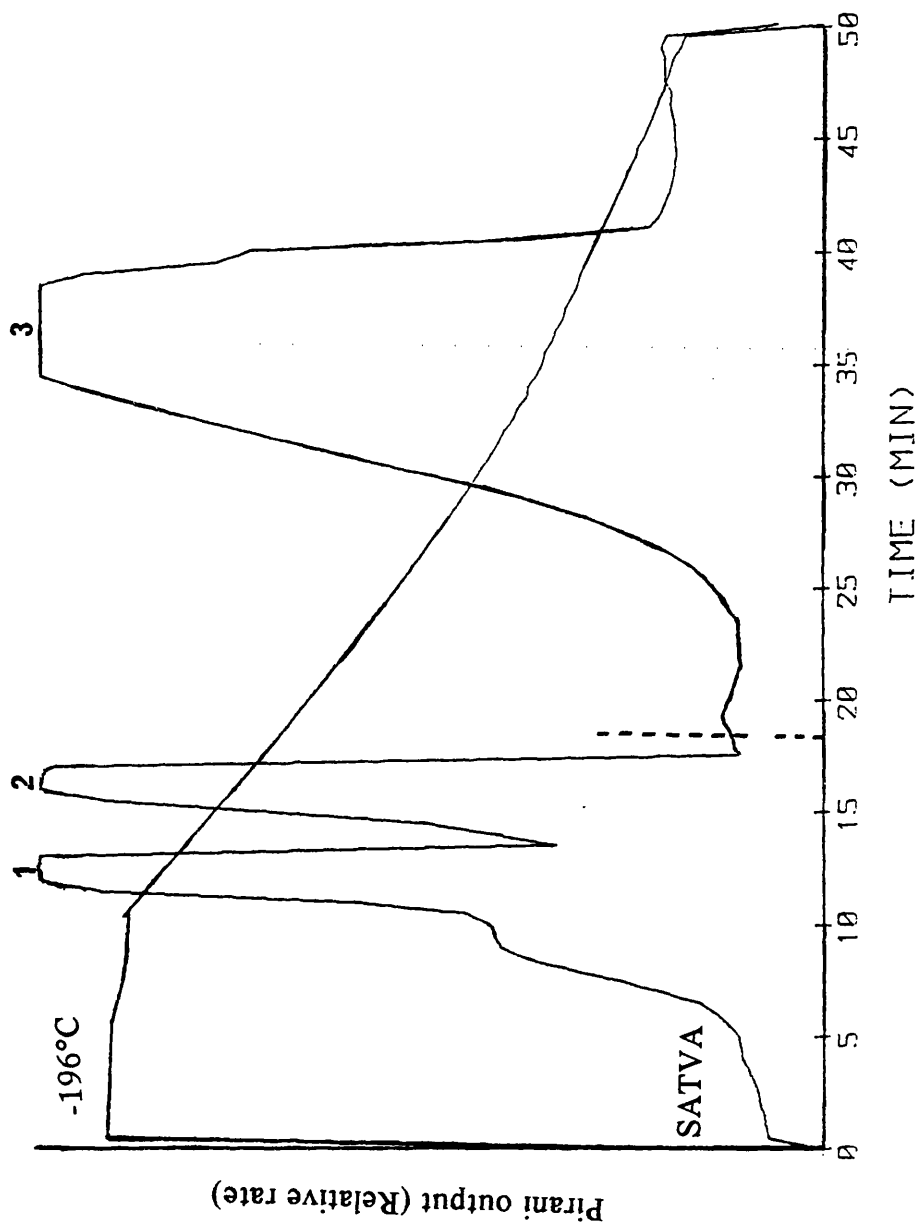


Fig. 3.9. Subambient TVA traces for warm up from -196°C to ambient temperature of condensable volatile products from degradation of PEA to 600°C .

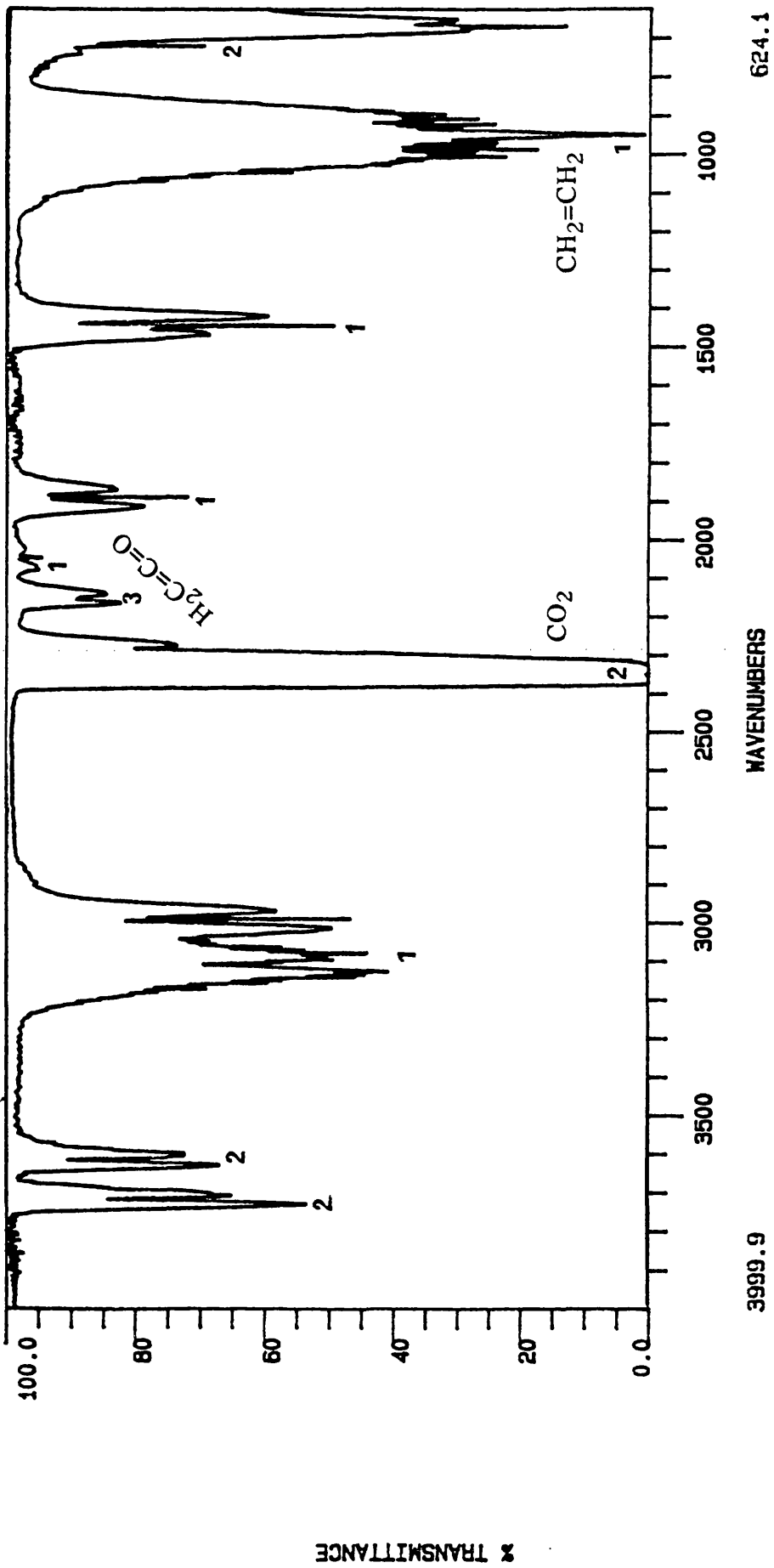


Fig. 3.10. IR spectrum for peaks 1 and 2 from SATVA analysis of products of degradation of PEA.

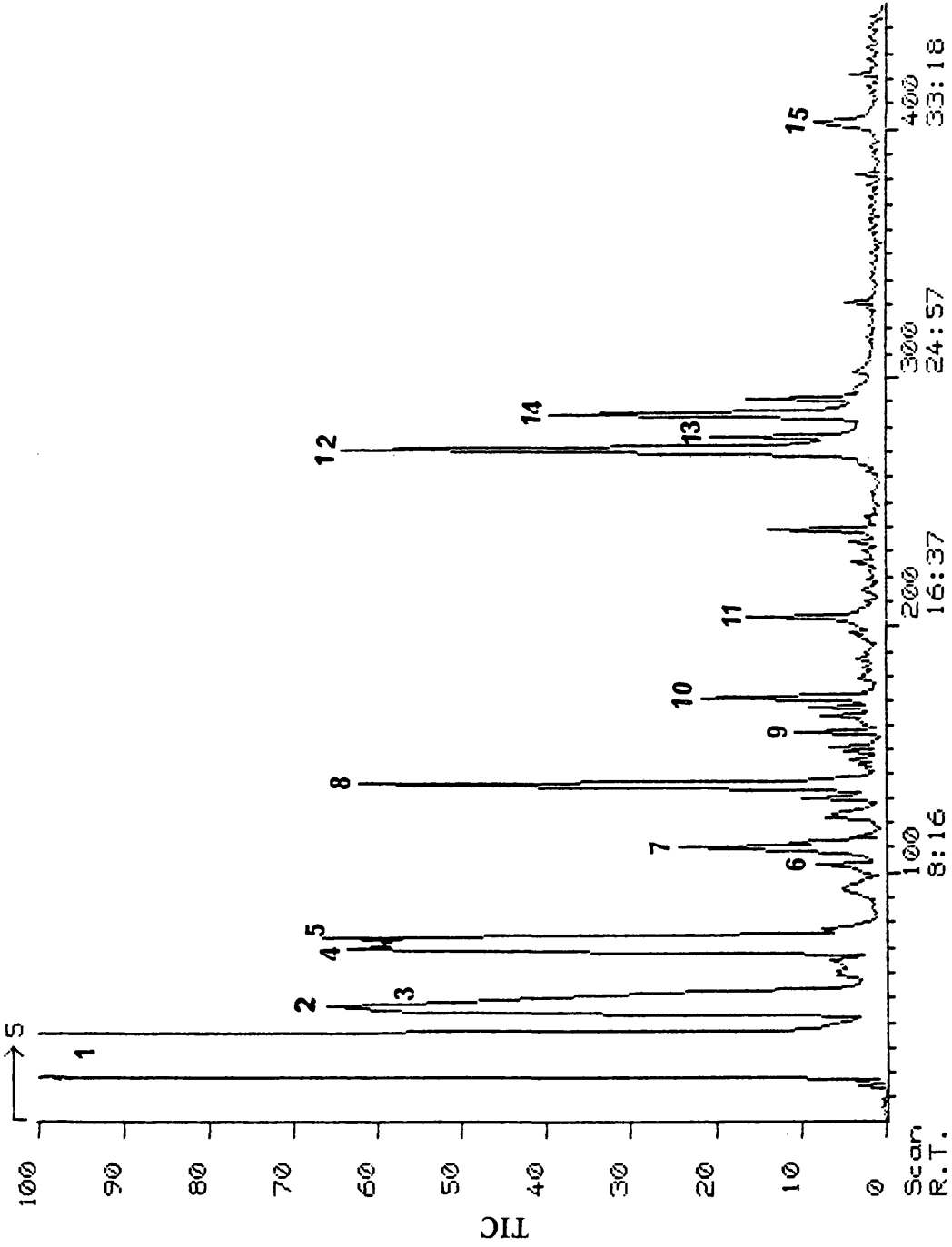
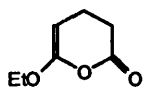
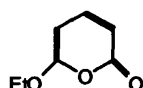
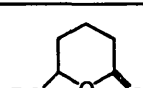
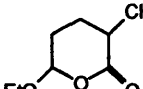
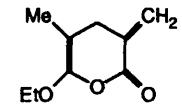
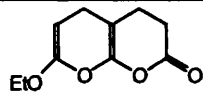


Fig. 3.11. Gas chromatograph for the liquid fraction in SATVA separation of products from the degradation of PEA.

Table 3.4. Mass Spectrum m/e data and assignments for Fraction 3 from SATVA of PEA (heated up to 480°C)

| Peak | m/e (% abundance) | Structure/Name |
|------|---|--|
| 1 | 31(100), 45(75), 46(65), 43(55), 44(40), 42(20), 47(4) | EtOH, Ethanol |
| 2 | 55(100), 45(15), 43(15), 73(15), 99(8), 82(4), 85(3), 100(2) | CH ₂ =CH-CO ₂ Et, Ethyl acrylate |
| 3 | 57(100), 75(38), 74(36), 102(10) | CH ₃ -CH ₂ -CO ₂ Et, Ethyl propanoate |
| 4 | 69(100), 41(78), 39(38), 99(30), 86(18), 114(10) | CH ₂ =C(Me)-CO ₂ Et, Ethyl methacrylate |
| 5 | 43(100), 71(95), 41(40), 88(38), 60(30), 55(25), 101(5), 116(3) | CH ₃ -CH(Me)-CO ₂ Et, Ethyl isobutyrate |
| 6 | 55(100), 83(60), 100(22), 113(20), 54(18), 128(15), 56(12), 69(5), | MeCH=C(Me)-CO ₂ Et, Ethyl 2-propanoate, |
| 7 | 55(100), 83(30), 54(28), 56(25), 128(10), 69(10), 60(5), 100(5) | CH ₂ =CH(CH ₂) ₂ -CO ₂ Et, Ethyl 4-propanoate |
| 8 | 41(100), 69(85), 67(76), 97(60), 112(60), 95(58), 55(22), 113(15), 142(10), 140(5) |  αβ-unsaturated, γ-lactone |
| 9 | 41(100), 67(85), 95(40), 112(50), 140(20), 56(26), 111(10), 97(6), |  |
| 10 | 41(100), 67(85), 95(80), 140(45), 112(40), 111(20), 97(8) | Isomer of above |
| 11 | 68(100), 41(22), 69(30), 97(25), 112(18), | Unidentified |
| 12 | 143(100), 115(80), 114(76), 87(70), 42(60), 55(48), 43(40), 142(30), 73(20), 144(6) |  |
| 13 | 157(100), 128(95), 101(85), 55(80), 99(75), 56(60), 83(55), 129(45), 156(40), 102(30), 73(20), 158(5) |  |

| | | |
|----|---|--|
| 14 | 98(100), 99(50), 154(50), 155(49), 127(40), 126(38), 53(25), 81(20), 69(8), 156(3), 168(1) |  |
| 15 | 140(100), 112(80), 113(70), 111(55), 168(52), 67(45), 169(35), 95(28), 55(20), 192(5), 196(2) |  |

The cold ring fraction (CRF) was a viscous yellowish brown liquid while the residue which spreads on the bottom of the tube on melting, was brownish black. CRF and residue were analysed by IR spectroscopy.

The IR spectrum of the CRF from PEA (Fig. 3.12), run in dichloromethane is similar to the spectrum of the parent polymer except in the following respects:

- two shoulders around 1760 cm^{-1} and 1801 cm^{-1} appear on the carbonyl peak at 1730 cm^{-1} , and the C-O stretching peak at 1165 cm^{-1} becomes broadened. There is also a weak absorption at 1630 cm^{-1} and this absorption along with absorption at 1760 cm^{-1} accounts for the presence of an $\alpha\beta$ -unsaturated 6-membered cyclic lactone. The carbonyl peak at 1801 cm^{-1} along with 1760 cm^{-1} is possibly due to the anhydride formed from the acid groups introduced during the decomposition of ester groups. GC-MS results, however, did not show the presence of anhydride.
- carbonyl peak and the peaks in the region $1500\text{-}1000\text{ cm}^{-1}$ show general broadening which increases when degradation temperature is increased.
- there is also an absorption at 950 cm^{-1} not present in the parent polymer and possibly due to C=C double bonds formed at the chain ends. However, there is not any absorption for unsaturated C-H stretch in the $3000\text{-}3100\text{ cm}^{-1}$ region.

The IR spectrum of the residue from PEA showed following principal changes:

- the C-H stretching frequency for the methyl groups at 2980 cm^{-1} almost disappears, while the C-H stretching peak for the methylene groups at 2940 cm^{-1} decreases in size but does not disappear altogether. This would be expected if the principal degradation reactions resulted in the removal of ethyl groups from the ester units and only the methylene and methine groups on the polymer chain are left.
- the carbonyl peak at 1730 cm^{-1} becomes broadened and the C-O stretch at 1166 cm^{-1} is hardly noticeable. The other peaks in the region $1500\text{ cm}^{-1}\text{-}1000\text{ cm}^{-1}$ either show a general broadening or are no longer existing.
- there is a broad peak at 1620 cm^{-1} attributed to unsaturated C=C structure.

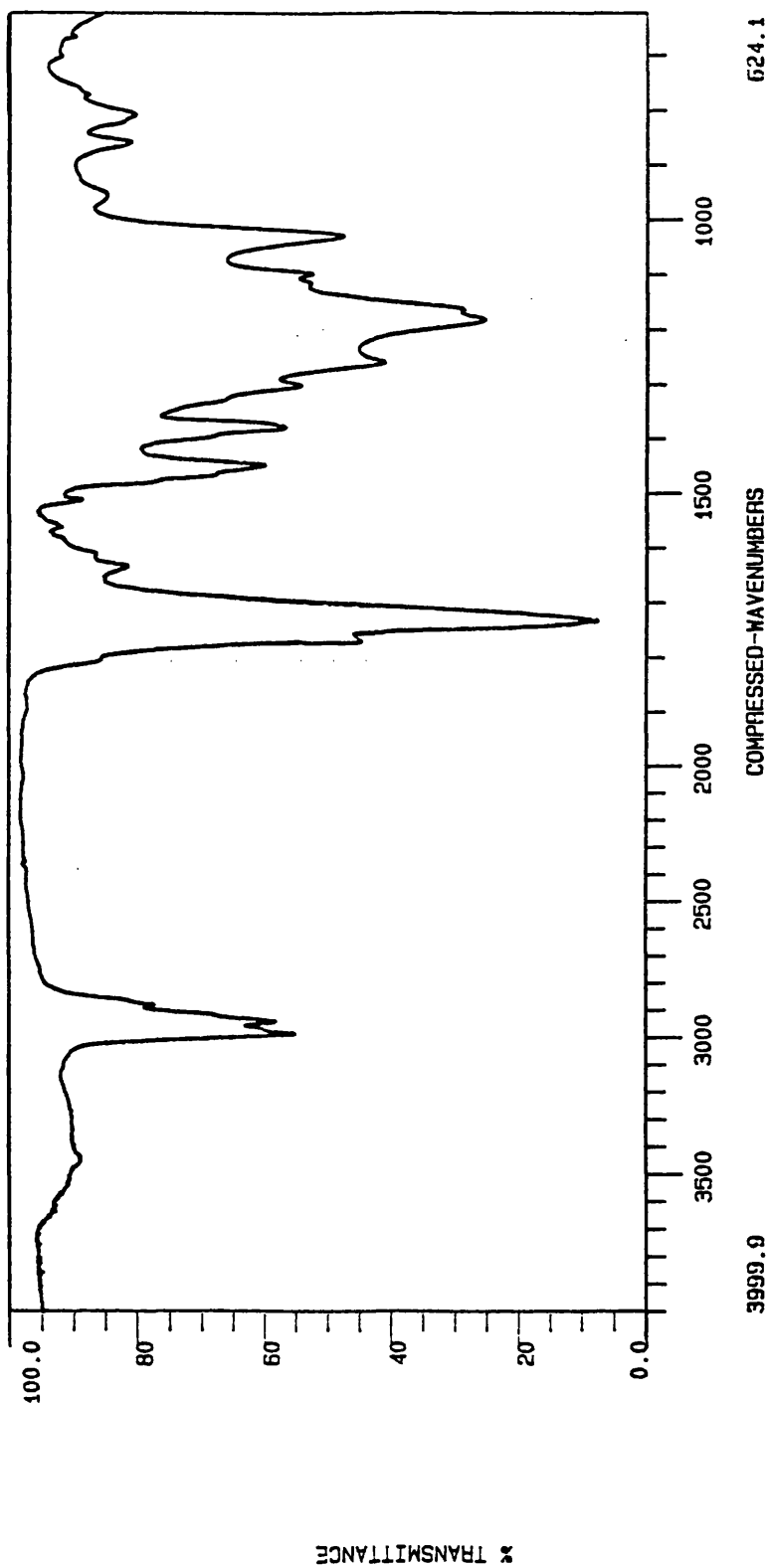


Fig. 3.12. IR spectrum for CRF from PEA.

LDPE

The TVA curve of the LDPE:BP77 (Fig. 3.13 (a)) shows that volatilisation starts at about 380°C and leads to a single peak with T_{\max} at 475°C. The TVA trace after the liquid nitrogen trap (-196°C) shows a very small rise from the baseline indicating a very small amount of non-condensable gaseous products, identified as H_2 and CH_4 by the quadrupole mass spectrometer attached to the TVA line.

The SATVA trace (Fig. 3.14 (a)) for the separation of the condensable volatile products of degradation of LDPE:BP77 shows a very small peak at the beginning due to ethylene and ethane and two sharp peaks after which the trace becomes broad with poorly resolved peaks. The later material was collected as one fraction. The second fraction was shown by IR spectroscopy and MS to consist of propene and propane while the third fraction was due to butene and butane. The final fraction was identified by GC-MS (Fig. 3.15) and results are given in Table 3.5. It is obvious that the major degradation products are saturated and unsaturated linear hydrocarbons while there are branched hydrocarbons also present.

The CRF collected, a white solid of which some was powdery while other parts were elastomeric like the original polymer, accounts for at least 80-90% of the total weight loss during the degradation. The IR spectrum of the CRF (Fig. 3.16 (a)) is similar to that of the original polymer except that it now shows absorptions for the unsaturated C=C bonds. The residue which spreads on the bottom of the tube was also white but was too small in quantity for analysis.

EEA Copolymer

The EEA copolymer starts to degrade at about 350°C and reaches T_{\max} at 450°C. The shape of the TVA trace (Fig. 3.13 (b)) is similar to that of the TVA trace for PEA except that it starts at a higher temperature and does not show the second degradation peak. The presence of non-condensable gaseous products was indicated by the rise in the trace for the -196°C trap. These gaseous products were identified as soon as they were formed by the quadrupole mass spectrometer attached to the TVA line and were found to be mainly hydrogen and carbon monoxide with traces of methane. It was found that degradation starts with evolution of H_2 and that CO is given off right through the degradation process.

The SATVA trace (Fig. 3.14 (b)) for the separation of the condensable volatile products of degradation of EEA copolymer showed three gaseous product peaks; and the remaining material gave a broad, poorly resolved peak showing a number of different

degradation products. The first peak was due to ethylene and ethane, the second peak was identified as carbon dioxide (major) and ketene while the third peak was attributed to propene, butene and their corresponding saturated hydrocarbons. The final fraction was collected as a liquid and showed pale yellow and colourless layers, being yellow at the top. The GC-MS technique was applied to identify this fourth complex mixture of compounds; the GC-MS trace and its results are given in Fig. 3.17 and in Table 3.6, respectively. The results show some compounds which are identical to the degradation products of either PE or PEA while others are new.

The IR spectrum of the volatile liquid products in the gas phase showed a broad peak at 1760 cm^{-1} . The formation of a lactone, which would absorb at this frequency, again could be possible if two or more ethyl acrylate units were together. However, it is difficult to tell the presence of a lactone from the GC-MS results.

The CRF of the EEA copolymer collected was a gummy pale yellow material while the residue was very small and almost the colour of the copolymer. Both were analysed by IR spectroscopy (Fig. 3.16 (b)). It was obvious from the examination of the TVA tube that the polymer spreads on the surface of the TVA tube on melting.

The IR spectrum of the CRF is similar to that of the undegraded copolymer except for the following differences:

- there are absorptions at 990 cm^{-1} , 965 cm^{-1} and 910 cm^{-1} which are characteristic for the unsaturated group of the type $\text{RHC}=\text{CH}_2$ and absorption at 3075 cm^{-1} confirms for this type of group.
- there are extra absorptions for the carbonyl groups at 1708 cm^{-1} and 1815 cm^{-1} . Acrylic acid units, formed due to the decomposition of the ester units in the copolymer chain, could account for the absorption at 1708 cm^{-1} . The absorption at higher frequency could be due to $\alpha\beta$ -unsaturated cyclic anhydride if the original peak at 1736 cm^{-1} was also due to the anhydride. Also two new weak peaks in the region $1025\text{-}1030\text{ cm}^{-1}$, due to C-O stretching, which is characteristic of 6-membered ring anhydride develop. However, this type of structure is only possible if two or more ethyl acrylate units were together in the copolymer chain. Since ethyl acrylate comprises about 16 wt.% of the structure, most of these units would be isolated, but there would still be some units together. There is also a weak absorption at 1642 cm^{-1} possibly due to the $\alpha\beta$ -unsaturated carbonyl compound.
- the absorptions in the region $1300\text{ cm}^{-1}\text{-}1260\text{ cm}^{-1}$ show a general decrease in intensity.

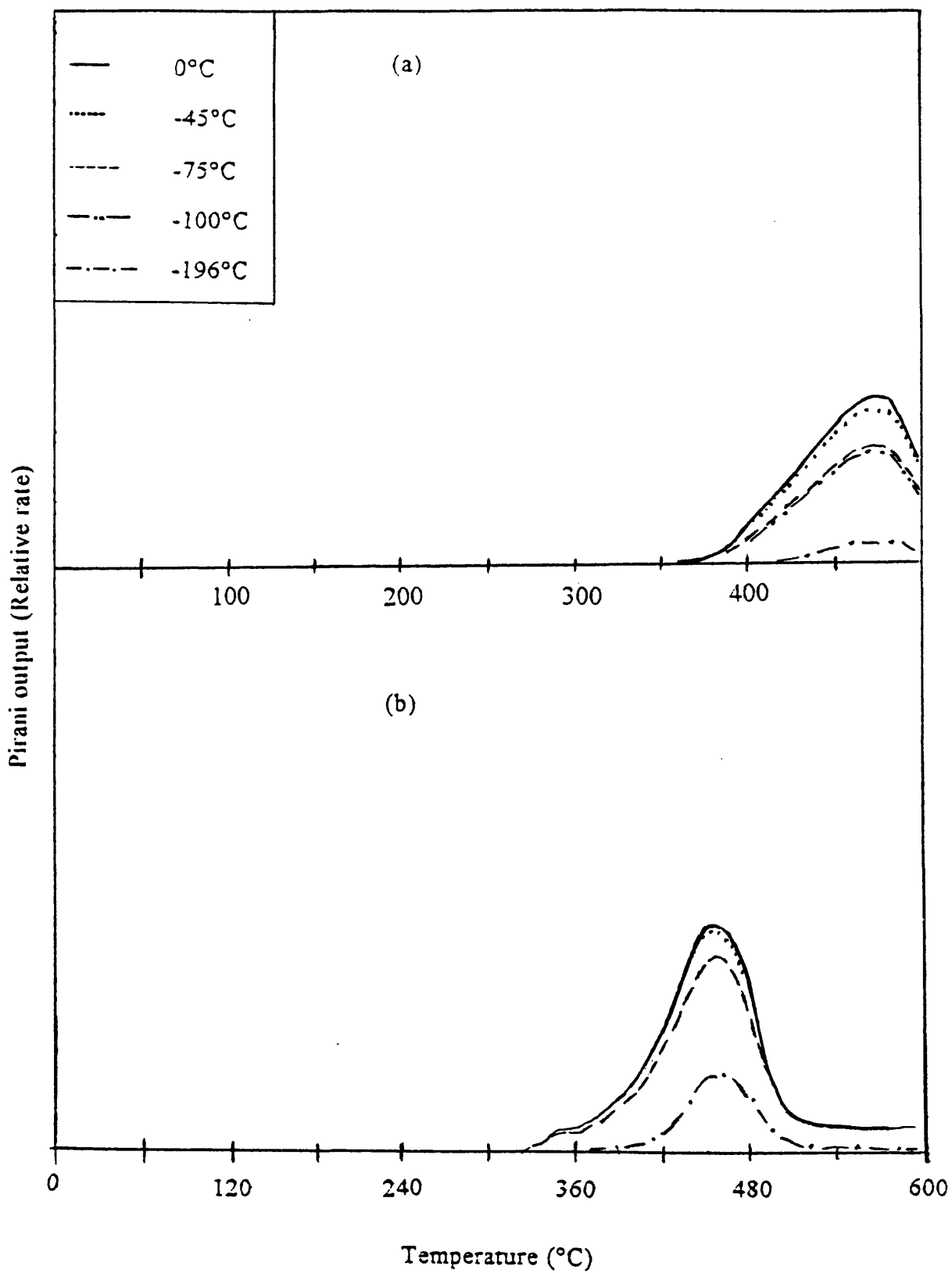


Fig. 3.13. TVA traces for (a) LDPE:BP77 and (b) EEA copolymer.

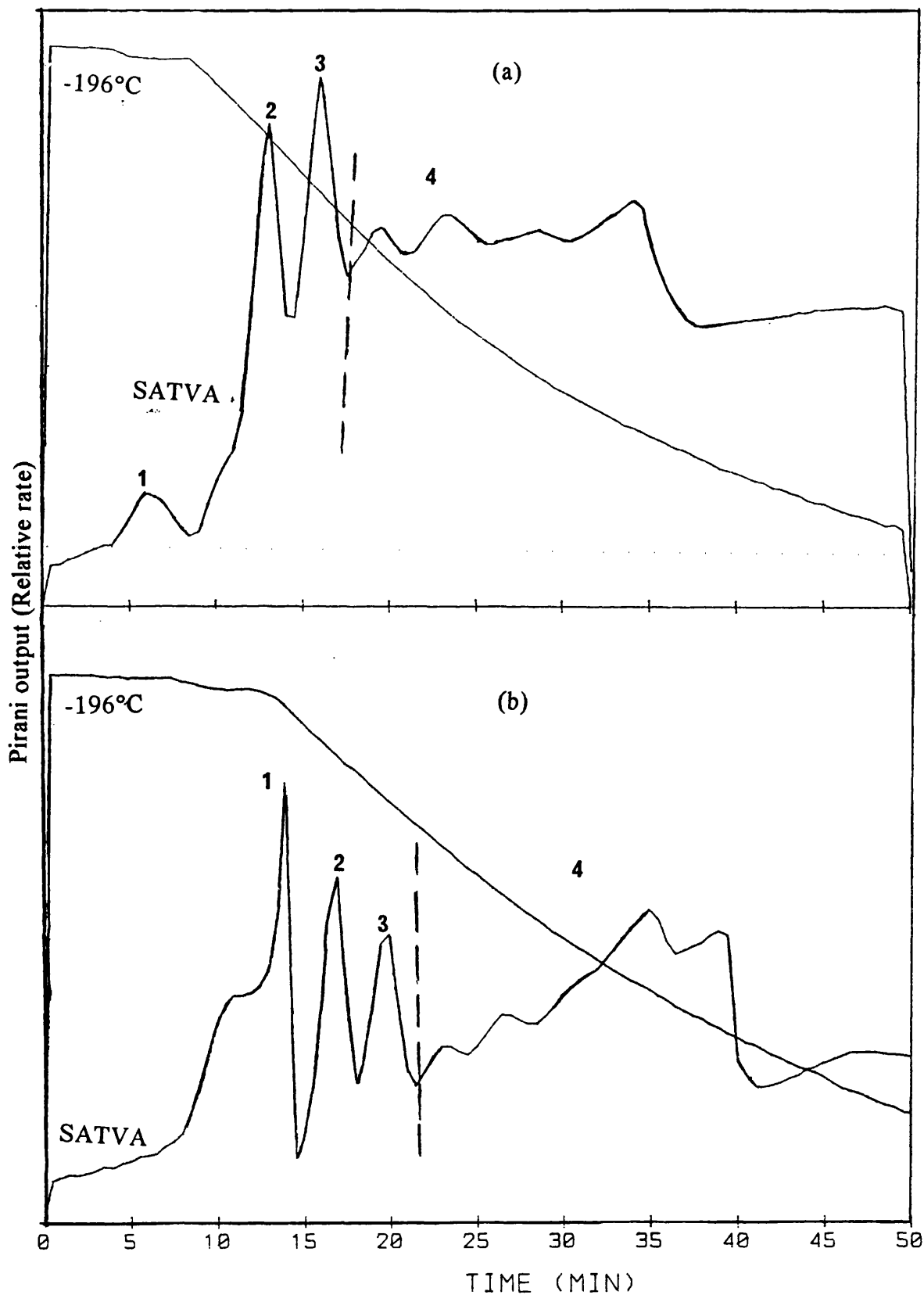
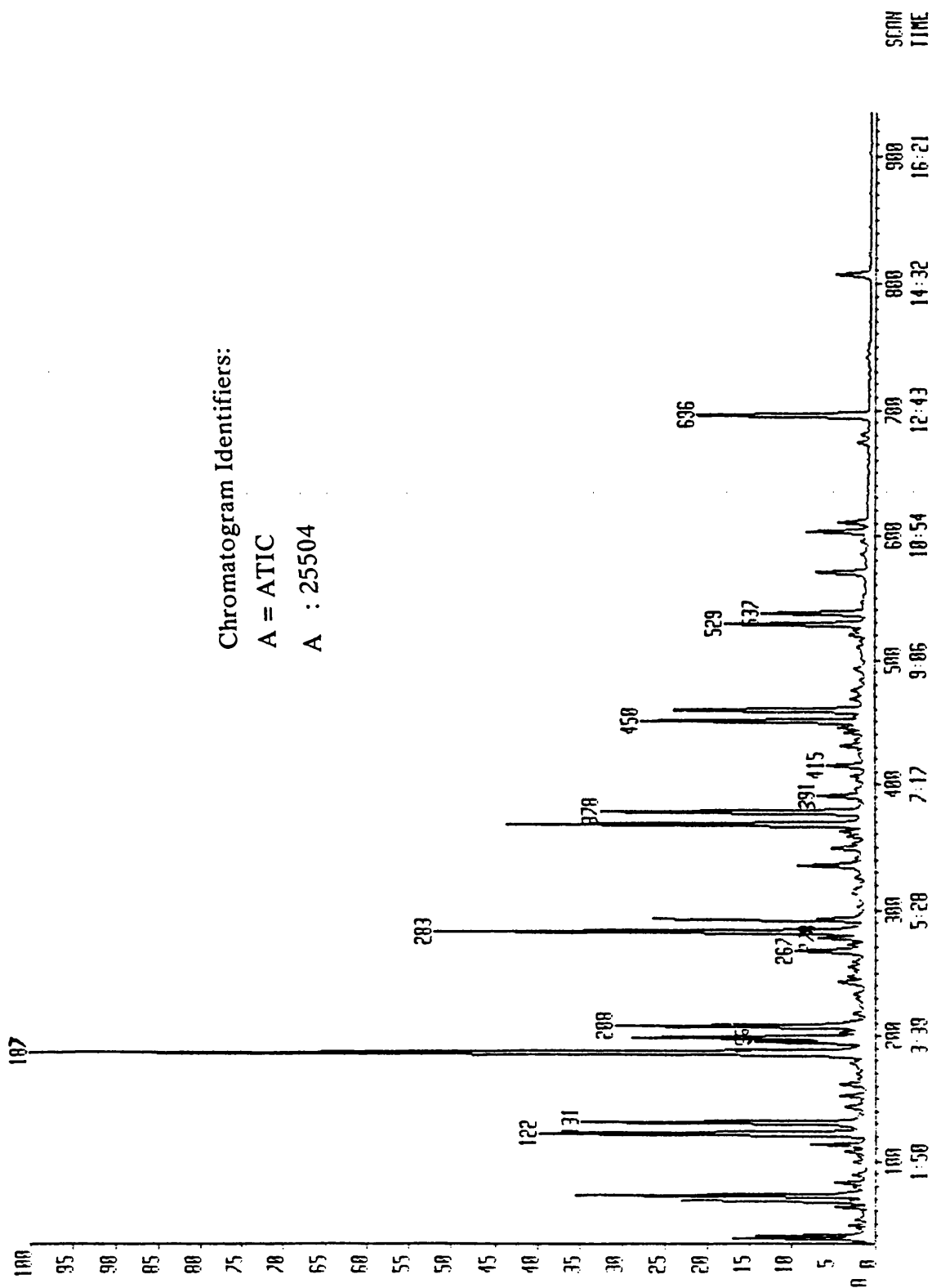


Fig. 3.14. SATVA traces for warm up from -196°C to ambient temperature of condensable volatile products from degradation of (a) LDPE:BP77 (b) EEA copolymer.



- there is also an extra weak peak at 2120 cm^{-1} and accounts for the ketene formed during the formation of ethanol.

The IR spectrum of the residue is again similar to that of the undegraded copolymer except that it shows absorptions for unsaturated C=C structures, the peak at 1736 cm^{-1} disappears and a very weak peak around 1710 cm^{-1} seems to develop. The absorption at 2980 cm^{-1} (C-H stretch of methyl groups) disappears. This shows evidence of the ester group decomposition. Also the absorptions in the region $1300\text{ cm}^{-1} - 800\text{ cm}^{-1}$ decrease.

The mass spectrum of the CRF gives a base peak at m/z 43 and the highest m/z is at 714 with six other peaks at high intensities: 69 (60.2%); 71.5 (58.5%); 83 (53.9%); 40 (41.6%); and 111 (25.0%). This type of mass spectrum is usually given by hydrocarbons and this gives some indication that the CRF contains mainly small chain fragments of the copolymer.

Table 3.5. Mass Spectrum m/e data and assignments for Fraction 3 from SATVA of LDPE:BP77 (heated up to 480°C).

| Scan | m/e (% abundance) | Structure/Name |
|------|---|---|
| 38 | 41(100), 56(95), 42(70), 55(62), 43(58), 39(40), 69(30), 84(20) | 1-Hexene |
| 40 | 41(100), 57(65), 69(55), 43(52), 56(50), 42(40), 39(30), 84(28), 86(5) | Hexane |
| 63 | 67(100), 54(68), 41(48), 82(40), 39(38), 97(2), 100(1) | $\text{CH}_2=\text{CH}-\text{C}_4\text{H}_8-\text{OH}$ 5-Hexene-1-ol |
| 68 | 41(100), 56(90), 55(75), 70(55), 42(50), 39(38), 69(37), 57(30), 43(20), 98(8), | 1-Heptene |
| 73 | 43(100), 41(58), 71(52), 57(51), 56(30), 70(25), 42(25), 55(18), 100(5) | Heptane |
| 113 | 43(100), 57(75), 85(57), 41(55), 56(40), 84(30), 39(8), 100(0) | 2, 4-Dimethylpentane |
| 122 | 70(100), 55(98), 41(58), 42(35), 43(30), 56(28), 39(22), 69(18), 83(10), 112(4) | Heptane, 3-methylene |

| | | |
|-----|---|---|
| 131 | 43(100), 41(41), 57(40), 85(39), 71(30), 56(22), 70(18), 55(12), 114(3) | Octane |
| 187 | 104(100), 78(99), 103(99), 51(60), 77(58), 50(25), 52(22), 105(20), 63(18) | 1, 3, 5, 7- Cyclooctatetraene |
| 195 | 70(100), 55(90), 41(50), 42(25), 56(20), 69(18), 71(17), 97(15), 83(10), 126(3) | 1-Octene-3-one |
| 198 | 43(100), 56(99), 55(90), 41(87), 69(60), 70(57), 42(42), 39(32), 57(26), 83(23), 97(20), 126(3) | 1-Nonene |
| 208 | 43(100), 57(83), 41(40), 85(30), 71(26), 56(22), 55(18), 39(15), 99(5), 128(3) | Nonane |
| 267 | 56(100), 55(35), 41(30), 57(28), 70(20), 69(19), 83(5), 97(3), 140(2) | Nonane, 5-methylene |
| 278 | 55(100), 70(80), 41(58), 69(39), 56(37), 43(30), 83(22), 97(20), 111(5), 140(2) | Cyclodecane |
| 283 | 56(100), 55(95), 41(90), 70(80), 43(73), 69(70), 57(70), 83(35), 97(20), 111(5), 140(2) | 1-Decene |
| 293 | 57(100), 43(98), 41(40), 71(39), 85(30), 56(20), 55(17), 99(3), 113(2), 142(1) | Decane |
| 335 | 57(100), 43(42), 71(30), 41(28), 55(19), 85(18), 98(12), 70(8), 126(4) | Branched alkane |
| 349 | 56(100), 55(45), 57(43), 41(42), 70(40), 43(38), 69(37), 82(9), 98(8), 112(4), 154(2) | C ₁₁ H ₂₂ , Branched alkene |
| 363 | 55(100), 70(85), 41(75), 56(72), 69(60), 43(40), 57(37), 83(35), 97(20), 125(4), 154(2) | 2-Decene, 8-methyl-, (Z)- |
| 368 | 55(100), 43(98), 41(95), 56(94), 70(90), 69(85), 57(65), 83(58), 97(30), 154(2) | 1-Undecene |
| 378 | 57(100), 43(95), 71(50), 41(40), 85(30), 98(5), 113(4), 156(3) | Undecane |
| 391 | 57(100), 70(63), 55(62), 41(60), 69(52), 43(50), 56(49), 98(35), 85(30), 111(4), 139(3), 168(0.5) | 3-Undecene, 6-methyl-, (E) |

| | | |
|-----|--|---|
| 415 | 57(100), 43(58), 71(45), 41(38), 85(25), 98(5), 112(4), 140(3), 168(0.4) | 2-Undecene, 5-methyl- |
| 431 | 56(100), 57(43), 55(41), 69(40), 41(39), 43(34), 83(15), 97(8), 111(5) | 1-Undecene, 2-methyl- |
| 445 | 70(100), 55(75), 41(55), 69(40), 43(34), 56(32), 83(25), 97(8), 139(3), 168(1) | 5-Undecene, 3-methyl-, (E) |
| 450 | 55(100), 43(99), 41(93), 56(92), 69(82), 70(80), 83(60), 97(40), 111(8), 168(1) | 1-Dodecene |
| 460 | 57(100), 43(85), 71(55), 41(39), 85(35), 98(5), 112(4), 170(1) | Dodecane |
| 468 | 55(100), 57(96), 43(95), 41(90), 70(90), 69(87), 71(85), 44(74), 83(60), 97(23), 112(18) | Branched alkane, C ₁₂ H ₂₆ |
| 493 | 57(100), 43(65), 41(42), 71(40), 85(30), 98(7), 111(5), 154(4) | Branched alkane, C ₁₂ H ₂₆ |
| 520 | 55(100), 41(78), 67(60), 81(58), 69(55), 44(53) 82(50), 95(35), 97(33), 109(8) | 1, 12-Tridecadiene, C ₁₃ H ₂₄ |
| 529 | 55(100), 43(99), 41(96), 69(82), 57(80), 56(78), 83(75), 97(42), 111(16), 182(2) | 1-Tridecene |
| 537 | 57(100), 43(65), 71(58), 41(38), 85(37), 99(4), 112(3), 184(1) | Tridecane |
| 603 | 43(100), 55(99), 41(95), 57(90), 69(89), 83(78), 70(75), 97(50), 111(18), 196(1) | 1-Tetradecene |
| 611 | 57(100), 43(80), 71(60), 43(38), 85(37), 99(5), 198(1) | Tetradecane |
| 674 | 55(100), 43(99), 57(90), 41(88), 69(78), 83(60), 97(50), 111(8) | 1-Pentadecene |
| 680 | | Pentadecane |
| 696 | | Contamination |

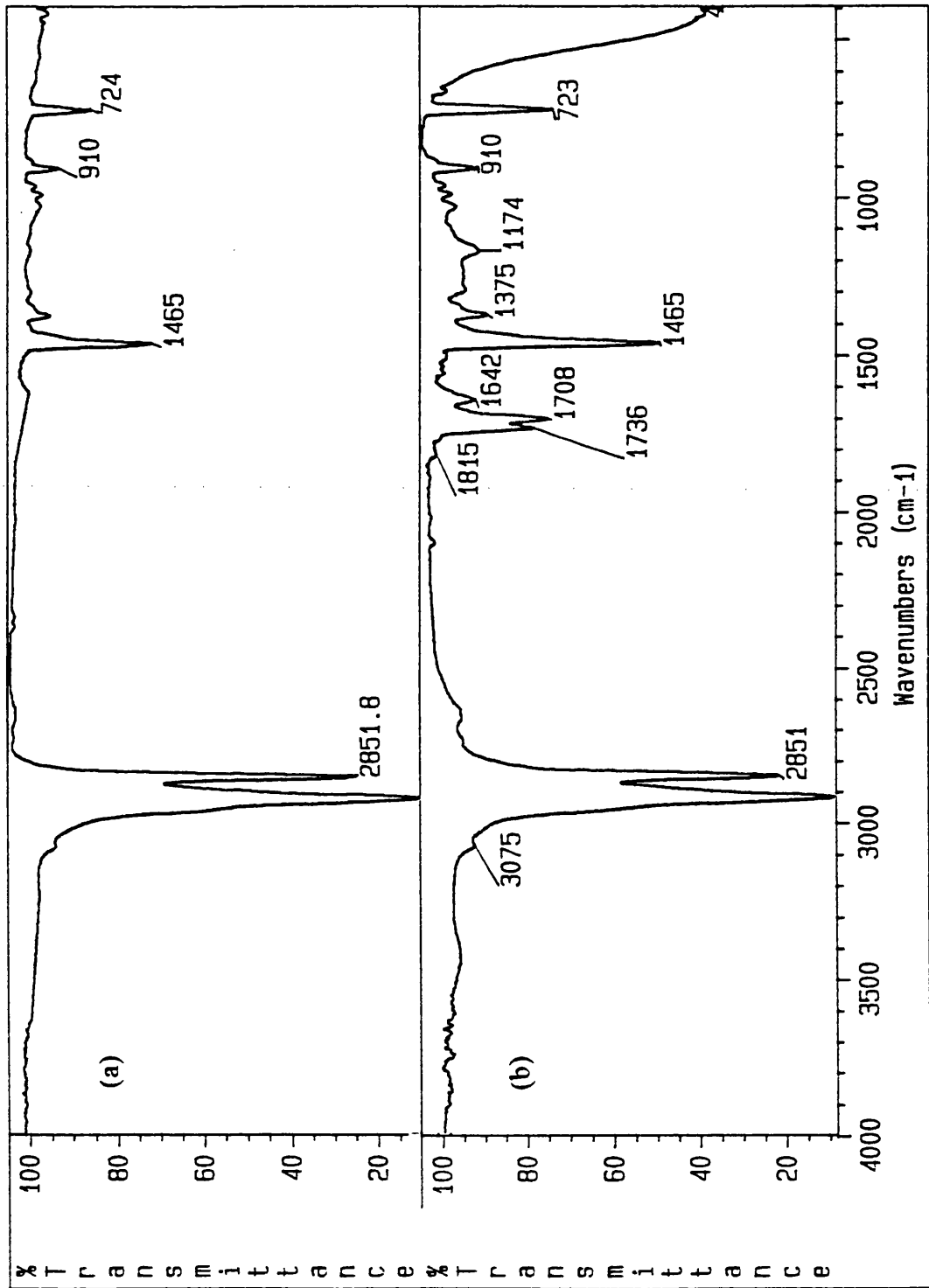


Fig. 3.16. IR spectra for CRFs from (a) LDPE:BP77 and (b) EEA copolymer.

Chromatogram Identifiers:

A = ATIC

Trace: A

Scan : 804

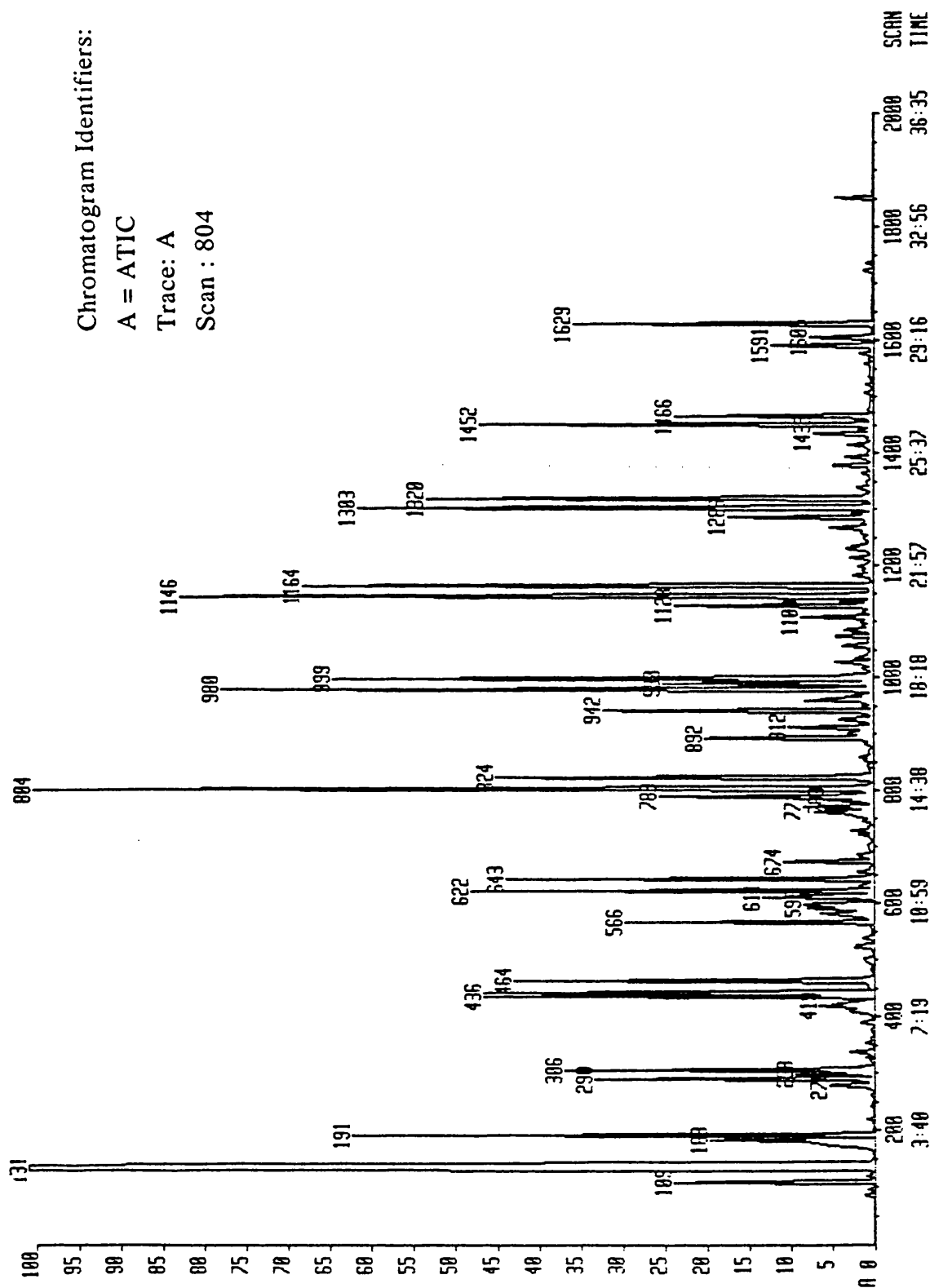


Fig. 3.17. GC trace for the liquid fraction in SATVA separation of products from the degradation of EEA copolymer.

Table 3.6. Mass Spectrum m/e data and assignments for Fraction 3 from SATVA of EEA copolymer (heated up to 480°C).

| Scan | m/e (% abundance) | Name/Structure |
|------|---|---|
| 109 | | Ethanol |
| 180 | 43(100), 45(80), 60(50) | Ethanoic acid, CH ₃ CO ₂ H |
| 183 | | 1-Hexene |
| 191 | 43(100), 45(18), 61(15), 70(10), 73(5), 88(2) | Ethyl ethanoate, CH ₃ CO ₂ Et |
| 278 | 55(100), 45(18), 56(9), 73(8), 99(2), 100(0) | Ethyl propenoate, C ₂ H ₃ CO ₂ Et |
| 290 | | 1-Heptene |
| 298 | 57(100), 45(18), 75(15), 74(12), 102(5) | Ethyl propanoate, C ₂ H ₅ CO ₂ Et |
| 306 | | Heptane |
| 339 | 83(100), 55(95), 41(30), 98(30), 42(19), 39(18), 70(10) | Methyl, cyclohexane |
| 390 | 91(100), 92(50), 65(8), 51(5), 39(5), 63(3) | 1, 3, 5-Cycloheptatriene |
| 419 | 43(100), 60(90)*, 41(75)*, 57(60), 39(39)*, 85(38), 42(35)*, 55(27), 73(20)*, 84(15), 45(12)*, 88(1.0)* | Butanoic acid*, C ₃ H ₇ CO ₂ H + some branched hydrocarbon |
| 436 | 43(100), 71(99), 88(45), 41(40), 60(30), 42(21), 45(20), 73(15), 101(5), 116(0) | Ethyl butanoate, C ₃ H ₇ CO ₂ Et |
| 440 | 70(100), 55(98), 41(58), 42(35), 39(22), 112(12) 56(10), 69(8), 83(6) | Heptane, 3-methylene |
| 445 | 43(100), 41(78), 56(70), 42(60), 55(50), 39(40), 69(38), 70(20), 83(18) | 1-octene + some other compound |
| 464 | | Octane |
| 566 | 55(100), 83(65), 100(35), 39(27), 113(25), 82(15), 54(15), 53(14), 69(4), 128(3) | 2-Ethyl propenoic acid, ethyl ester, CH ₂ =C(Et)-CO ₂ Et |
| 582 | 55(100), 39(27), 54(27), 41(23), 83(20), 56(18), 81(7), 100(5), 82(5), 69(4) | Ethyl 4-pentenoate, CH ₂ =CHC ₂ H ₄ -CO ₂ Et |

| | | |
|-----|---|---|
| 592 | 57(100), 43(55), 41(50), 55(48), 98(8), 85(4), 100(4), 114(0) | Pentane, 2, 2, 4- trimethyl |
| 598 | 60(100), 41(80), 55(60), 67(58), 39(43), 56(40), 96(36), 73(35), 83(15), 45(10), 102(0) | Pentanoic acid, $C_4H_9CO_2H$ + some other compound |
| 611 | 85(100), 57(95), 88(95), 41(60), 60(55), 73(35), 101(25), 61(25), 45(25), 70(20), 130(0) | Ethyl pentanoate, $C_4H_9CO_2Et$ |
| 615 | 70(100), 55(95), 41(60), 39(22), 83(4), 97(2), 126(1) | Branched alkene, C_9H_{18} |
| 622 | 43(100), 41(95), 56(93), 55(80), 69(50), 70(40), 42(40), 39(38), 57(24), 83(23), 97(20), 126(3) | 1-Nonene |
| 643 | | Nonane |
| 674 | 43(100), 71(60), 116(55), 41(36), 55(32), 99(22), 101(20), 39(35), 87(10) | 2,2-Dimethyl butanoic acid, $C_5H_{11}CO_2H$ |
| 687 | 43(100), 88(65), 73(58), 55(35), 41(30), 39(20), 99(3), 116(0) | 2-ethyl butanoic acid $C_5H_{11}CO_2H$ |
| 729 | 57(100), 41(50), 43(35), 55(22), 39(18), 69(10), 98(5) | Unidentified |
| 762 | 60(100), 41(60), 73(40), 55(30), 39(25), 43(25), 45(18), 88(5), 97(5), 116(0) | Hexanoic acid, $C_5H_{11}CO_2H$ |
| 771 | 56(100), 41(35), 55(30), 57(20), 70(18), 69(16), 83(5), 140(2) | Nonane, 5-methylene |
| 783 | 55(100), 41(80), 54(60), 67(40), 81(35), 39(34), 68(20), 95(5), 110(5) | Unidentified |
| 789 | 88(100), 43(95), 99(60), 60(50), 41(40), 73(30), 45(34), 61(33), 101(33), 115(5), 144(0) | Ethyl hexanoate |
| 804 | 41(100), 55(95), 56(92), 43(78), 70(75), 57(60), 69(58), 83(38), 97(22), 111(5), 140(2) | 1-Decene |
| 824 | 43(100), 57(96), 41(46), 71(39), 85(30), 56(20), 55(17), 99(3), 142(1) | Decane |
| 892 | 41(100), 55(95), 87(60), 86(58), 39(52), 69(40), 111(39), 43(38), 81(30), 115(25), 99(15), 128(8), 156(3) | Ethyl heptenoate, $C_6H_{11}CO_2Et$ |

| | | |
|------|--|--|
| 912 | 57(100), 41(58), 43(56), 55(30), 71(25), 68(23), 69(21), 39(20), 85(10), 98(10), 126(5) 110(3), 154(0) | 2-Decene, 5-methyl-, (Z)- |
| 927 | 60(100), 43(70), 41(50), 73(47), 55(35), 57(30), 39(18), 87(10), 45(8), 130(0) | Heptanoic acid, $C_6H_{13}CO_2H$ |
| 942 | 55(100), 41(97), 88(60), 56(58), 68(56), 39(48), 69(45), 110(40), 82(30), 158(0) | Ethyl heptanoate, $C_6H_{13}CO_2Et$ |
| 959 | 41(100), 55(80), 67(57), 54(55), 69(40), 82(37), 81(35), 95(12), 152(0) | 1, 8-Nonadiene, 2, 8-dimethyl, $C_{11}H_{20}$ |
| 963 | 88(100), 43(58), 41(50), 55(30), 60(30), 113(28), 101(25), 73(18), 158(0) | Ethyl heptanoate, $C_6H_{13}CO_2Et$ |
| 969 | 55(100), 41(93), 56(90), 70(88), 69(35), 43(32), 57(25), 83(5), 154(0) | 2-Decene, 8-methyl-, (Z)- |
| 980 | | 1-Undecene |
| 990 | 57(100), 116(80), 101(70), 41(50), 55(35), 73(35), 88(18), 127(12), 144(5) | Unidentified |
| 999 | 43(100), 57(99), 71(50), 41(40), 85(30), 98(5), 113(4), 156(3) | Undecane |
| 1004 | 73(100), 88(85), 41(52), 57(35), 43(30), 39(18), 69(10), 101(4), 116(2) | Unidentified |
| 1028 | 57(100), 70(63), 55(62), 41(60), 69(52), 43(50), 56(49), 98(35), 85(30), 111(4), 139(3), 168(0.5) | $C_{12}H_{24}$, 3-Undecene, 6-methyl-, (E) |
| 1057 | 55(100), 41(97), 69(65), 43(40), 57(38), 70(25), 87(16), 81(8), 95(6), 115(6), 125(2) | Unidentified |
| 1074 | 57(100), 43(65), 41(45), 71(38), 55(30), 85(12), 98(3), 112(3), 140(2), 168(0) | 1-Decene, 3,4-dimethyl-, (E), $C_{12}H_{24}$ |
| 1085 | 60(100), 41(70), 73(65), 43(59), 55(57), 39(20), 69(12), 85(10), 101(6), 115(2), 144(0) | Octanoic acid $C_7H_{15}CO_2H$ |
| 1108 | 55(100), 56(90), 41(80), 69(40), 43(35), 39(30), 88(15), 96(12), 111(5), 124(3), 128(2), 170(0) | Ethyl 3-octenoate, (Z) $C_7H_{13}CO_2Et$ + hydrocarbon |

| | | |
|------|--|--|
| 1128 | 41(100), 88(98), 55(94), 101(44), 57(42), 69(40), 43(40), 81(30), 127(22), 116(15), 95(10), 172(0) | Ethyl octanoate, $C_7H_{15}CO_2Et$ + some other compound |
| 1136 | 70(100), 55(70), 41(60), 56(38), 69(35), 57(25), 83(18), 97(4), 168(0) | 2-Undecene, 3-methyl, |
| 1146 | 41(100), 43(99), 55(93), 56(92), 69(82), 70(80), 83(50), 97(40), 111(8), 168(1) | Dodecene |
| 1164 | | Dodecane |
| 1182 | 55(100), 41(96), 43(60), 69(52), 57(50), 70(35), 83(25), 97(8), 102(5), 112(1) | |
| 1231 | 57(100), 43(80), 41(75), 55(40), 71(35), 69(25), 85(15), 97(5), 170(0) | Methyl, undecane |
| 1268 | 41(100), 55(98), 69(60), 88(50), 96(35), 101(20), 73(18), 138(4), 81(3), 184(0) | 10-Undecenoic acid + Ethyl 8-nonenoate |
| 1286 | 55(100), 41(98), 88(60), 67(40), 81(37), 101(20), 95(15), 141(4), 186(0) | Ethyl nonanoate, $C_8H_{17}CO_2Et$ + hydrocarbon |
| 1294 | 70(100), 56(60), 55(58), 41(50), 69(20), 83(5), 142(3), 182(0) | Cyclobutane, 2-hexyl-1, 1, 4-trimethyl, $C_{13}H_{26}$ |
| 1303 | | 1-Tridecene |
| 1320 | | Tridecane |
| 1393 | 101(100), 55(80), 41(75), 144(30), 73(30), 83(8), 67(7), 115(5), 167(3) | Unidentified |
| 1415 | 56(100), 41(45), 55(42), 69(18), 83(3), 98(2), 196(0) | Tridecane, 7-methylene |
| 1435 | 55(100), 41(98), 88(45), 67(40), 70(38), 81(35), 95(15), 101(8), 155(2), 200(0) | Ethyl decanoate, $C_9H_{19}CO_2Et$ + hydrocarbon |
| 1452 | | 1-Tetradecene |
| 1466 | | Tetradecane |
| 1591 | | 1-Pentadecene |

| Scan | m/e (% abundance) | Name/Structure |
|------|-------------------|----------------|
| 1605 | | Pentadecane |

3.3.7. Thermal Degradation of PEA at Lower Temperatures

Degradation of PEA was also performed from room temperature to 375°C, 425°C and 470°C respectively as a film on a stainless steel plate at 10°C/min under normal TVA conditions.

There was only a very small peak for volatile gaseous products when PEA was heated up to 375°C. The peak was shown by IR spectroscopy and MS to be due to CO₂. Other volatile degradation products were liquids (which accounted for about 50%-60% of total liquid products when degradation was carried out from room temperature to 470°C, i.e. full degradation of the polymer) and IR spectroscopy showed the presence of ethanol but it was clear from the appearance of the SATVA trace that a complex mixture of products was present, although their identification by IR spectroscopy was not possible due to their small quantities.

The spectrum of the residual polymer after degradation showed, with other minor changes, a major change which was the development of two shoulders in the carbonyl region at 1803 cm⁻¹ and 1713 cm⁻¹. Also the frequency for the carbonyl of the ester groups increased from 1736 cm⁻¹ to 1747 cm⁻¹ which shows that the ester groups were strained.

When the polymer was further heated up to 425°C, the spectrum of the residual polymer showed a considerable decrease in the intensity for the -CH₂-O- rocking band at 854 cm⁻¹, wagging at 1380 cm⁻¹ and bending at 1460 cm⁻¹. There was also a dramatic decrease in the intensities of the CH₃ and CH₂ stretching. A shoulder was developed in the carbonyl region at 1761 cm⁻¹ and the frequency for the carbonyl of the ester groups decreased from 1747 cm⁻¹ to 1732 cm⁻¹.

There was a major change in the region 1900-1000 cm⁻¹ when PEA was further heated up to 470°C. The shoulder on the carbonyl peak at 1761 cm⁻¹ disappeared and absorption for the carbonyl of ester group at 1732 cm⁻¹ shifted to 1728 cm⁻¹. There were now absorptions for unsaturated C-H stretch at 3047 cm⁻¹ and 3024 cm⁻¹. Peaks in the region 1200-1000 cm⁻¹ for C-O stretching disappeared and peaks in the region 1800-1300 cm⁻¹ diminished. The broad carbonyl peak at 1728 cm⁻¹ could be due to an αβ-unsaturated ester.

3.4. DISCUSSION

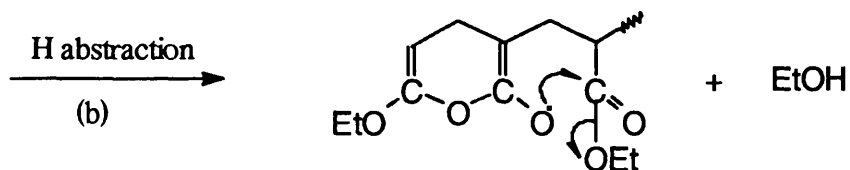
The onset temperatures (T_{onset}) for the evolution of the volatile degradation products and the temperatures at which the degradation processes occur at a maximum rate (T_{max}), obtained by each method, are in general agreement for all three samples. The T_{max} temperatures recorded under vacuum, in the case of TVA, for LDPE and PEA are lower than those measured under dynamic nitrogen by the TG and DTG techniques, as small volatile degradation products will diffuse more readily from the polymer bulk in a continuously evacuated system.

The thermal stability of LDPE and EEA copolymer is remarkably decreased in air as is observed from TG results carried out under air. This possibly is due to the chemical changes occurring in polymer chain during oxidation and result in introducing new groups such as hydroperoxide. This results in the formation of ketones and peracids at lower temperatures^{80, 81}.

The observed thermal behaviour of PEA is comparable to that found by Grassie et al.^{75, 82}.

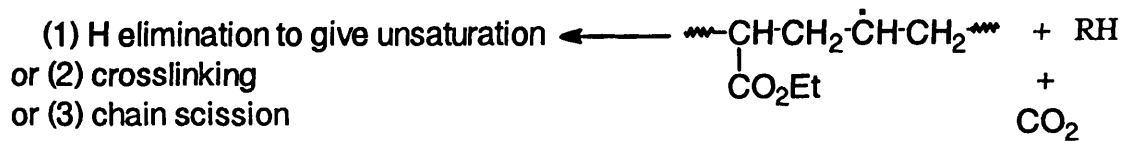
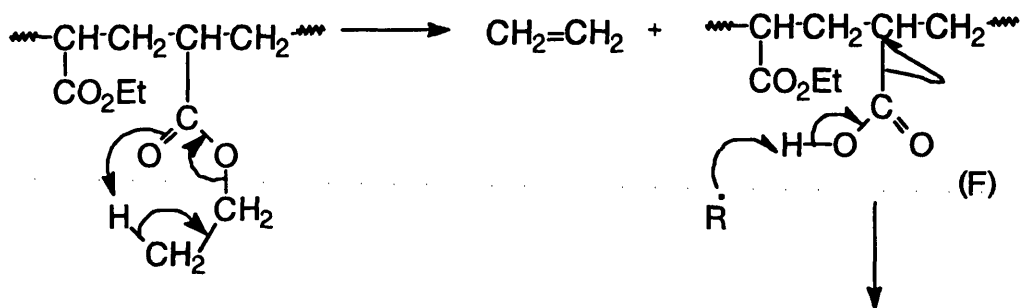
The TVA, TG and DTG curves of PEA, LDPE and EEA copolymer indicate that evolution of volatile degradation products occurs in almost a single step over a relatively narrow temperature range. It is obvious from the behaviour of the individual TVA traces that there are various degradation products (TVA traces of PEA and EEA copolymer have small plateau regions at the beginning of the main peak while PEA also has a small secondary peak at the end).

PEA produces some monomer but it is in very small amount when compared with the total degradation products indicating that degradation is by some other means than depolymerisation. The thermal degradation of PEA is initiated via random chain scission of C-C bonds and results in the formation of radicals of the type (A) and (B). (A) type radicals are relatively stable while (B) radicals are unstable and attack tertiary hydrogens and form more stable radicals of the type (C) and stable molecules of type (D). These reactions are followed by modification (main reaction) or total elimination of the ester groups attached to the polymer backbone. The modification of the ester groups results in the formation of ethanol through cyclisation along the chain of the ester groups and changes the chemical nature of the repeated units in the macromolecule. The mechanism shown below is proposed which is in good agreement to the previous work carried out by other workers^{75, 82-86} on primary poly(alkyl acrylates).

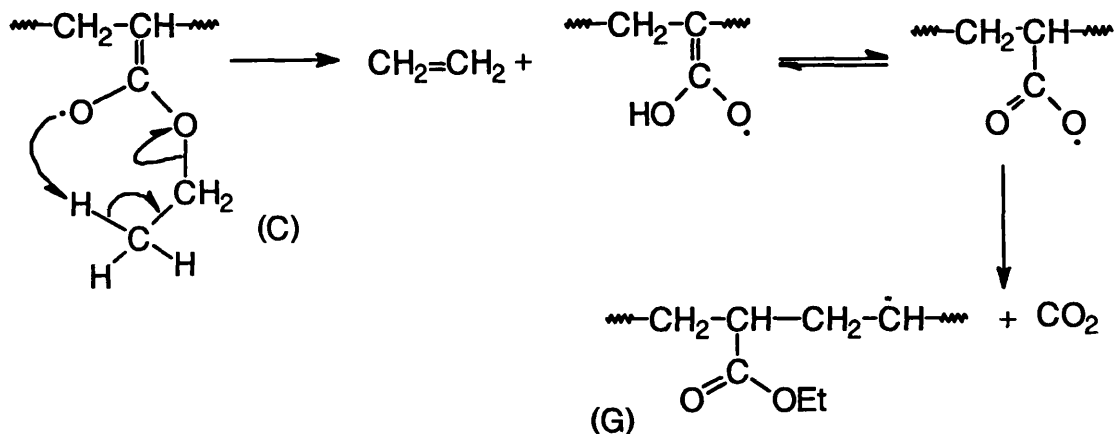


Repeat of (a) and (b) along the polymer chain would result in further production of ethanol. Chain of the type (E) also results in the formation of cyclic lactones as shown in Table 3.4.

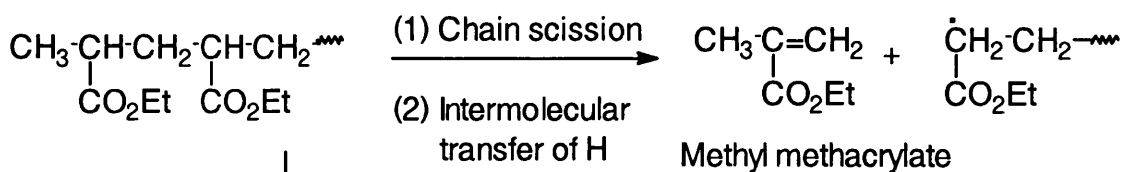
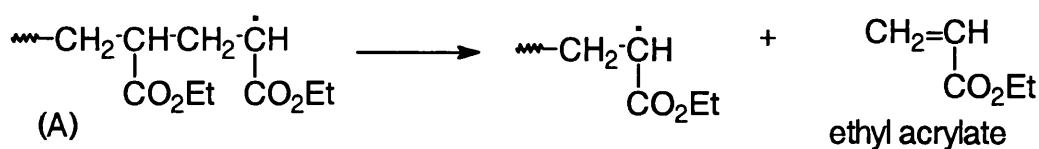
Formation of Ethylene and CO₂



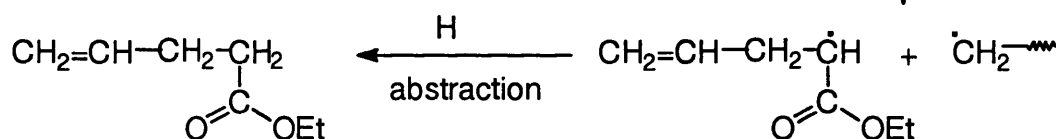
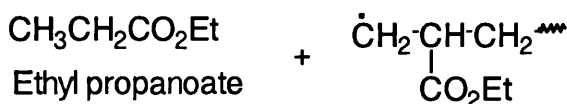
Radical (C) also results in the formation of ethylene and CO₂.



Other Degradation Products



(1) Chain scission
(2) H abstraction



3.5.2. Mechanism of Formation of Degradation Products from LDPE

It can be considered from the degradation products that the thermal degradation of LDPE is not due to a simple depolymerisation process since there is hardly any monomer produced and neither due to random chain scission. Thermal decomposition is initiated by scission at weak links followed by inter- and intra-molecular transfer reactions, which lead to crosslinking and the production of alkenes and alkanes as shown. Production of hydrogen occurs at higher temperatures than the initial temperature indicating that the degradation did not start by removal of the tertiary hydrogen. A reaction mechanism for the thermal degradation of branched polyethylene is shown in Scheme 3.1 True weak links in the structure are probably introduced by peroxide groups due to a small amount of oxidation during preparation, storage and processing of the polymer. Other weak links could be due to unsaturated structures.

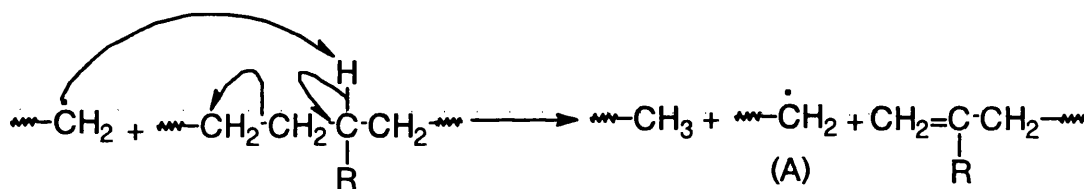
These weak links break down to form radicals which abstract hydrogen atoms in unbranched parts of the molecules or at or near chain branches.

Scheme 3.1. Thermal Decomposition of LDPE

(i) *Initiation by scission at weak links:*

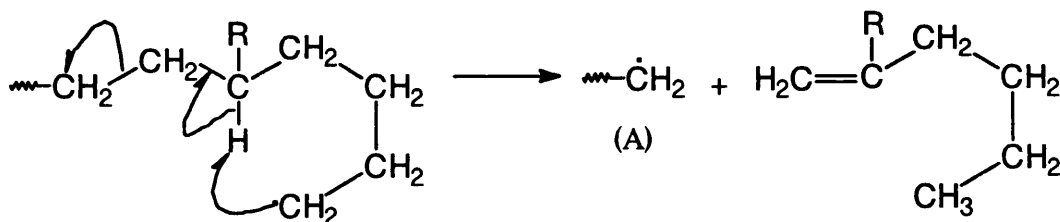


(ii) *Propagation by Intermolecular Transfer*



or

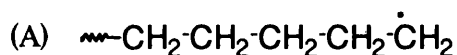
(iii) *Propagation by Intramolecular Transfer:*

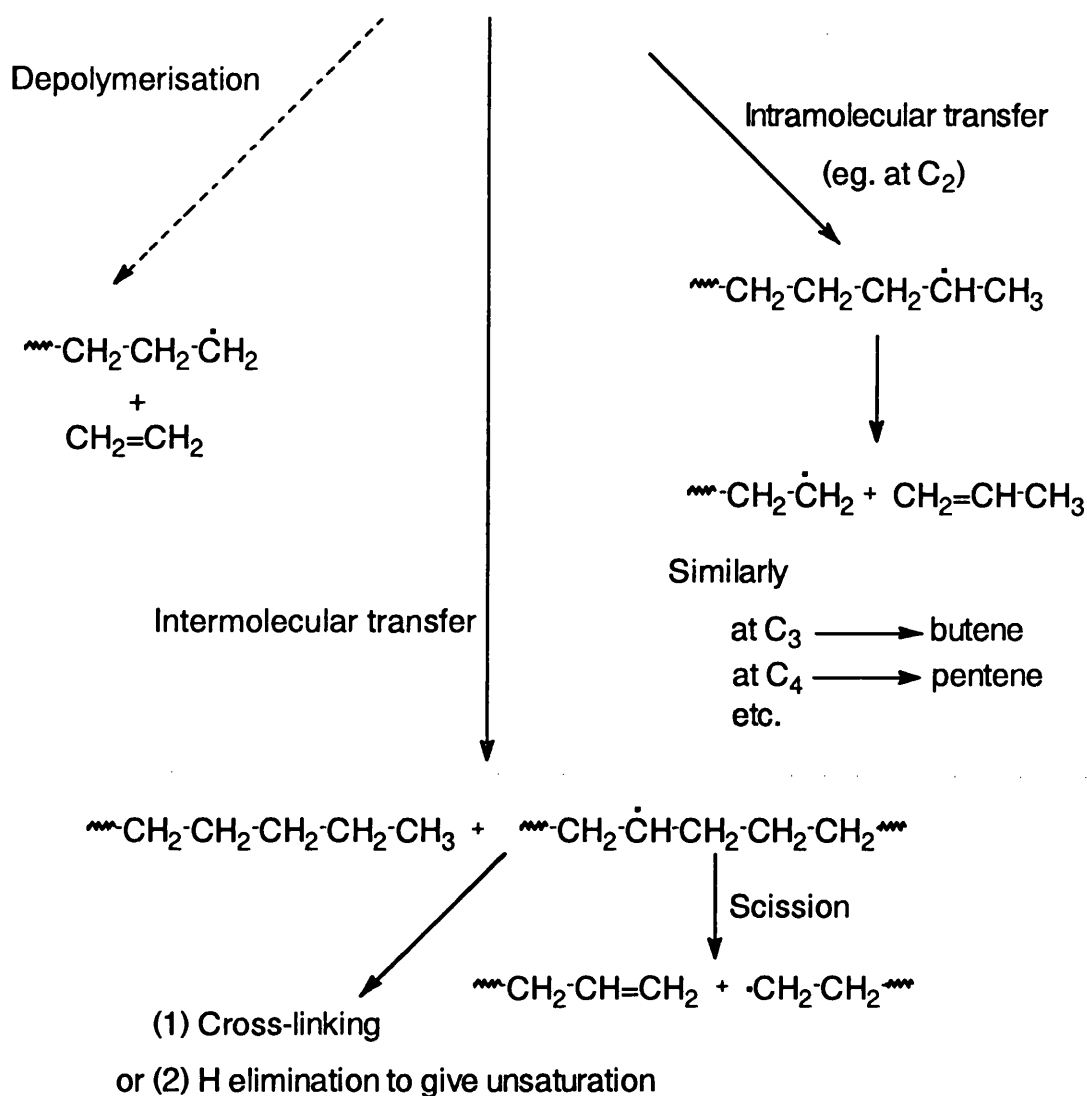


(iv) *Termination by collision of two 'live' radicals*

This leads to cross-linking in the polymer molecule.

Formation of Linear Alkenes and Alkanes





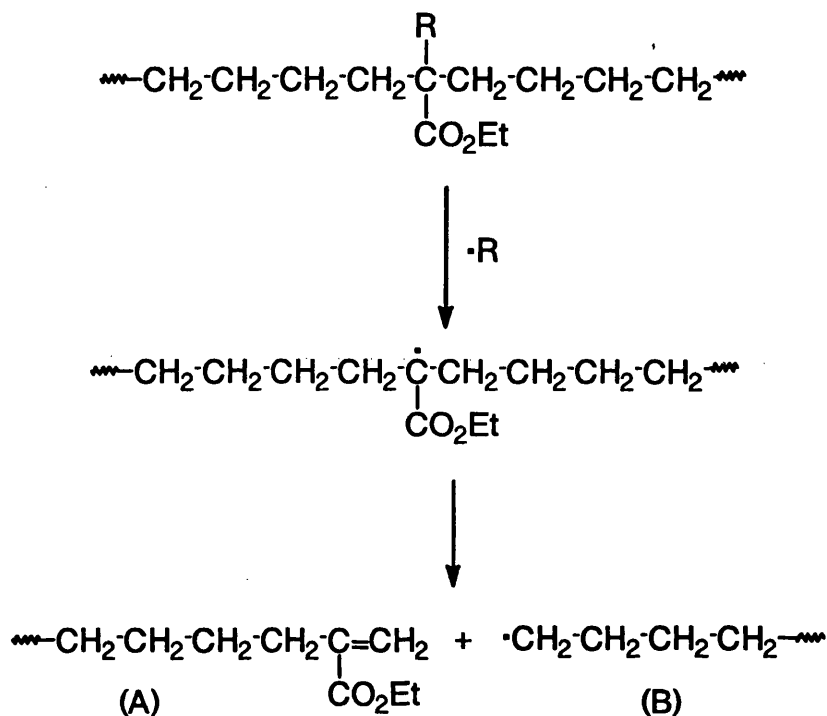
3.5.3. Mechanism of Formation of Degradation Products from EEA Copolymer

It has been shown that introduction of ethyl acrylate units into the LDPE chain thermally destabilises the polymer by 37°C. This loss in stability is reflected in the bond strengths present in the polymer and the formation of the new bonds with tertiary hydrogen introduces weak points. Degradation studies with MS attached to the TVA line confirm that the initial degradation starts with the evolution of small amounts of hydrogen. However, the amount of less volatile products (CRF) are reduced considerably.

EEA copolymer produces ethylene due to the decomposition of the ethyl acrylate (EA) units and small amounts of EA. Again simple depolymerisation is ruled out and chain scission at weak points, mainly due to branching or tertiary hydrogen atoms (minor), is suggested. The quadrupole mass spectrometer results show that only traces

of hydrogen start to evolve from the beginning of the degradation while the production of carbon monoxide starts when the main degradation starts. The production of ethanol is mainly through the route by which CO is a by-product. This reaction introduces unsaturation into the polymer chain thus more weak links. Acids are also produced after the decomposition of the ester groups to ethylene. The mechanism of degradation products from EEA copolymer is given as follows:

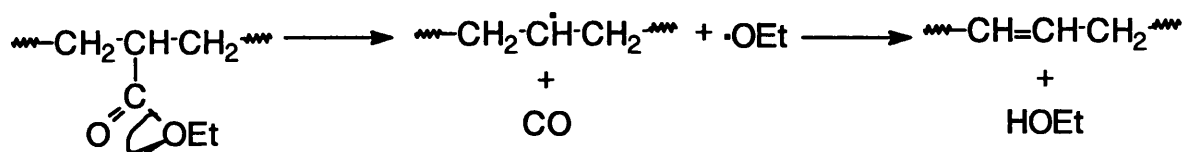
Formation of Alkenes and Alkanes

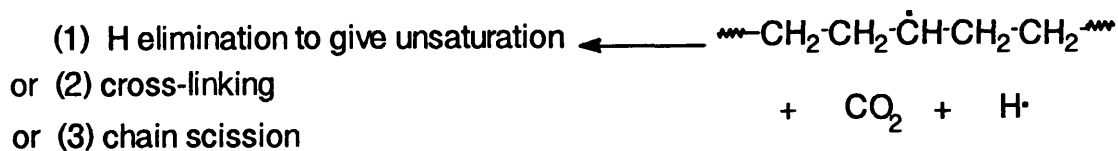


Radical (B) behaves similarly to that of PE to give saturated and unsaturated hydrocarbons by intramolecular and intermolecular transfer. Depolymerisation of the polymer chain also occurs but is a minor reaction. The unstable radical R, would abstract one of the tertiary hydrogen atoms and stabilise itself but would produce another less reactive radical.

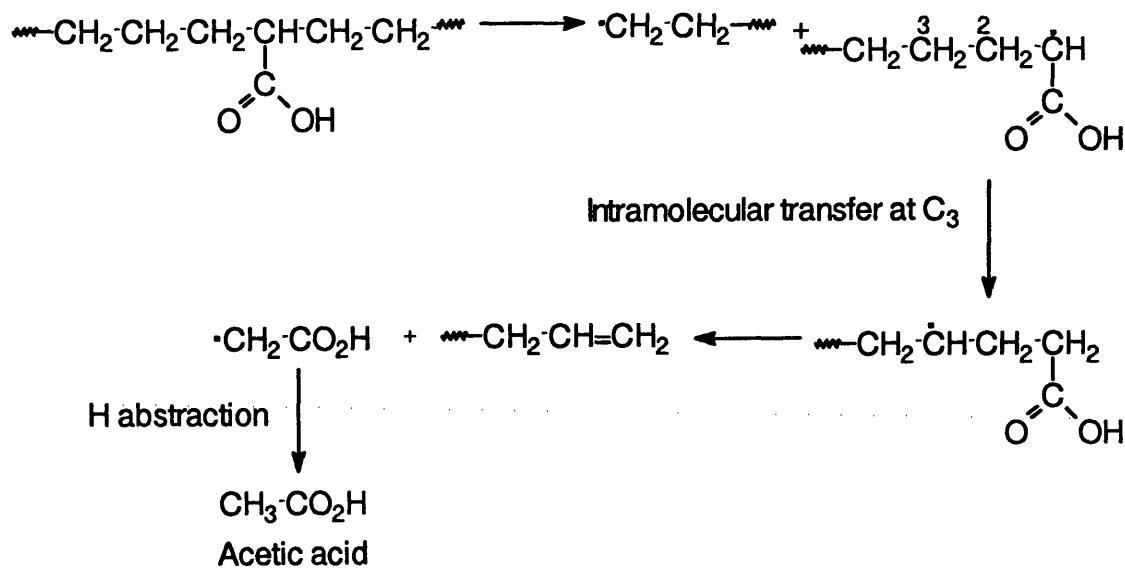
Alcohol Production

The simplest and main route for alcohol production is:



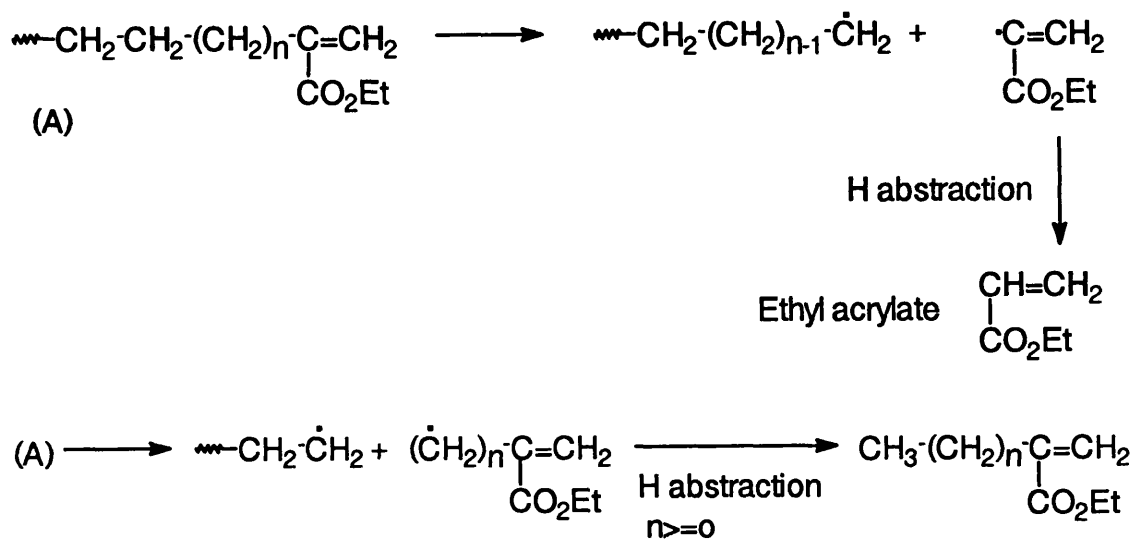


Formation of Acids



Similarly intramolecular transfer at C₄ will give propanoic acid and at C₅ butanoic acid and so on.

Formation of Unsaturated Ethyl Esters



Introduction of ethyl acrylate units to the LDPE chain thermally destabilises the polymer by 37°C.

EEA copolymer produces ethylene due to the decomposition of the ethyl acrylate (EA) units and small amounts of EA. Thermal decomposition is initiated at weak points, due to branching or tertiary hydrogen atoms. The degradation products other than gases are mainly saturated and unsaturated linear hydrocarbons and ethanol. The production of ethanol is mainly through the route by which CO is a by-product.

CHAPTER 4

DEGRADATION OF SILOXANE POLYMERS

4.1. INTRODUCTION

The field of the polyorganosilicon or "silicone" chemistry and technology is of ever increasing importance in scope, both commercially and in the volume of publications appearing. Silicones find their applications in almost all industries from food to steel since compared with other polymeric fluids, the silicones exhibit marked chemical and thermal stability in oxidative high temperature environments. Siloxanes indeed were the first useful polymers based on organometallic chemistry.

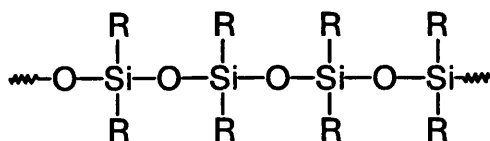
Chemically silicones are based on the heteroatomic structure of the type Si-O-Si and termed siloxane thus are called "polysiloxanes". The term silicone indeed has no place in scientific nomenclature, although it was originally introduced under the supposition that compounds of the empirical formula RR^aSiO were analogous to ketones⁸⁷; later it was used to describe related polymers⁸⁸. Siloxanes can be represented broadly by the following general formula⁸⁹:



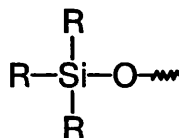
where n is large and $0 < a < 4$. In commercial silicones most R groups are methyl; other hydrocarbon groups (such as longer alkyl, fluoroalkyl, phenyl, or vinyl) or functional groups (such as methoxy, ethoxy, hydroxy or hydrogen) are substituted for specific purposes. These polymers can be combined with fillers, additives, and solvents to result in products loosely classed as silicones.

The general formula implies that the molecular structures can vary considerably to include linear, branched, and cross-linked structures.

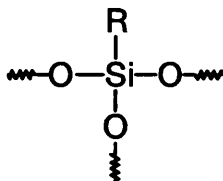
The linear polysiloxane chain with $a=2$ can be represented as:



$a = 3$ would give a monofunctional species:



This type of species usually forms the end groups where one of the R groups may be different from the others. A cross-linked structure or trifunctional species can be formulated with $a=1$:



Linear polysiloxanes possess both inorganic and organic properties⁸⁹. The polysiloxane unit, $(\text{Si-O-Si})_n$, itself is typically 'inorganic' in that it is chemically very stable. From the standpoint of physical properties inorganic characteristics are due to the high percentage of ionic character in the Si-O bond while organic characteristics are due to the substituent groups and low intermolecular forces resulting from their shielding of the siloxane skeleton. Oxidative attack and thermal decomposition occurs almost entirely at the substituent organic groups bounded to the silicon atoms.

The commercially available silicones, usually methyl- or phenyl- substituted siloxanes, have five properties which make them applicable in a large number of industries. These properties are typically associated with their heat stability and maintenance of their particular physical properties over a wide range of temperatures (-70°C to 250°C or even 300°C). Thus the rubber remains flexible over this temperature range. Siloxane exhibit water-repellency which is due in part to their ability to bond themselves to a wide range of materials so that the water shedding alkyl groups are exposed. Their excellent dielectric properties are another reason for their massive range of usage. Also of interest are their certain specific surface active effects which give rise to applications such as antifoaming; their ability to release certain materials such as rubber from metal moulds; their adhesion to other substrates and their use in polishing.

Silicones can be produced as oils, gums, rubbers or resins by altering their molecular weight, degree of cross-linking and nature of pendant groups attached to the silicon atoms. Many derived products, e.g., emulsions, greases, adhesives, sealants, coatings, and chemical specialities, have been developed. This diversity of properties and physical forms leads to silicones having an unusually large number of uses. Many of these uses are separately relatively small but combined explains why silicones products in industry and consumer production continues to increase. It is quite difficult to list all the industrial applications of silicones but a typical example is presented in Table 4.1.

Most commonly encountered silicones are methyl- and phenyl-substituted siloxanes and this is due to their heat stability that first attracted attention to the silicones.

Table 4.1. Some Typical Applications of Silicones in Industry***Fluid applications***

| | | |
|---------------------------------------|-------------|------------------|
| Plastic additives | Greases | Hydraulic fluids |
| Vibration damping | Coagulants | Lubricants |
| Cosmetic and health product additives | Antifoamers | Release agents |
| Heat-transfer media | Polishes | Dielectric media |
| Particle and fibre treatments | Surfactants | Water repellence |

Resin applications

| | | |
|------------------------------|--------------|-------------------|
| Electrical insulation | Varnishes | Junction coatings |
| Molding compounds | Paints | Adhesives |
| Protective coatings | Laminates | Release coatings |
| Pressure-sensitive adhesives | Encapsulants | |

RTV rubber applications

| | | |
|-----------------------|-----------|---------------|
| Electrical insulation | Adhesives | Sealants |
| Encapsulants | Glazing | Surgical aids |
| Medical implants | Gaskets | Molding parts |
| Conformal coatings | Foams | Mold making |

Heat-cured rubber applications

| | | |
|---|-------------------|------------------|
| Wire-cable insulation | Tubing and hoses | Laminates |
| Fuel-resistant rubber parts | Belting | Medical implants |
| Electrical conducting rubber | Extruding | Surgical aids |
| Embossing-calendering rollers | Penetration seals | Molded parts |
| Autoignition cable and spark-plug boots | Fabric coating | Foams |

(RTV -- Room temperature vulcanised)

In medical and surgical applications silicone fluids are used in gastric disorders (as antifatulents) and for antibiotic storage. Treatment of wound dressings with silicone fluids prevents sticking. Plasma bottles are treated to avoid blood coagulation and prevent the blood from wetting the bottle, facilitating draining. Rubber parts are used for surgical tubing, and RTV rubber is used as a dental mold material. Medical-grade elastomers are used for heart valves, prosthetic parts, and contact lenses. RTV materials are used to encase pacemakers and to coat catheters.

Silicone oligomers and fluids are used in cosmetic applications. Antiperspirant and deodorant formulations contain volatile oligomers to provide a moisture barrier and such products do not feel oily or sticky. Silicones in skin creams and lotions provides softness and smoothness and prevents the soaping of other ingredients. Hair products made with silicone fluids facilitate handling and provide sheen without an oily feeling.

In the electrical and electronic industries, silicone fluids are used as dielectric media in transformers, resins for molding compounds to make enclosures, heat-cured rubber for wire and cable coatings, and RTV silicone encapsulants to protect delicate circuitry.

In the current research work, the thermal degradation properties of the methyl-substituted siloxane, polydimethylsiloxane, (PDMS) are investigated. PDMS serves as the basis of a number of silicone products widespread in industrial manufacture. Besides, the derivatives of PDMS play a significant role in inorganic polymer chemistry. Accordingly, it is quite obvious that the thermal stability of PDMS and its derivatives have been attracting the interest of scientists since 1943.

It is difficult to predict the future importance of any branch of science but from the standpoint of conservation of natural resources, it is interesting to know that the synthesis of polydimethylsiloxanes does not require petroleum feed-stock unlike the great majority of commercial polymeric materials as they are prepared at the present time. The supply of petroleum is not infinite and with the increasing hunger of mankind for these useful, natural hydrocarbon products, their cost will inevitably increase. On the other hand, of the raw materials for the production of silicones, SiO_2 is infinite in relation to man's existence on the earth, and methanol can be made from the reduction of carbon monoxide (CO) with hydrogen (H_2).

The production of silicones relies heavily on electrical energy which in the future will probably come from atomic energy (fission or fusion) or directly from the sun by the use of giant solar cells.

4.2. PHYSICAL PROPERTIES OF SILICON AND ITS COMPOUNDS

4.2.1. Introduction

It is important to understand the basic physical chemistry of silicon and its compounds⁹⁰⁻⁹⁵ in order to study and understand the degradation behaviour of the silicones. Although C and Si are found close to each other and in the same group (Group IV) of the Periodic Table, their properties are not as similar to each other as in Cl and Br; Li and Na; or Mg and Ca. Thus prediction of the properties of silicones is not usually reliable on the basis of knowledge gained in organic polymer systems alone.

Some fundamental properties of Group IV elements and Bond Dissociation Energies and bond Lengths of some elements with Si and C are given in Tables 4.2 and 4.3 respectively.

Table 4.2. Properties of Group IV Elements

| Property | Carbon | Silicon | Germanium | Tin | Lead |
|---|---------|---------|-----------|---------|------|
| Atomic radius (Å) | 0.772 | 1.176 | 1.225 | 1.405 | 1.53 |
| Electronegativity | 2.5-2.6 | 1.8-1.9 | 1.8-1.9 | 1.8-1.9 | 1.8 |
| relative electron density: atomic number/atomic radius | 13.0 | 8.6 | 17.4 | 18.0 | 22.9 |

Table 4.3. Approximate Average Bond Energies and Bond Lengths

| | Average Bond Energies (KJ mol ⁻¹) | Bond lengths (Å) |
|-------|---|------------------|
| C-C | 356 | 1.54 |
| Si-Si | 210-250 | |
| C-O | 336 | 1.41 |
| Si-O | 368 | 1.63 |
| C-H | 416 | |
| Si-H | 323 | |
| Si-C | 250-335 | 1.89 |
| C-F | 485 | 1.39 |
| Si-F | 582 | 1.60 |
| C-Cl | 327 | 1.78 |
| Si-Cl | 391 | 2.05 |

Atomic radius and electronegativity of silicon are clearly unexpected and low electronegativity in particular is significant. This implies that bonds between silicon and elements such as O, N, F and Cl would be more ionic and thus stronger than the corresponding bonds with carbon and Table 4.3 confirms this hypothesis.

The characteristic bonds of silicones are those to oxygen and to carbon. Since silicon is more electropositive than carbon and oxygen, polarisation of Si-C and Si-O bonds occurs and there is a tendency for the nucleophilic attack to occur at silicon, i.e. $\text{Si}^{\delta+}-\text{C}^{\delta-}$. The Si-O bond is ca 50% ionic while the Si-C bond is slightly ionic, i.e. 12% on the basis of Pauling's scale of electronegativities⁹⁴, with silicon being positive in both cases.

The Si-C bond like the Si-O bond is quite stable towards homolytic fission, but is readily cleaved by ionic reagents, either by initial nucleophilic attack at Si or by electrophilic attack at C. Since C-H bonds break in the same direction, $\text{C}^- \text{H}^+$, as do C-Si bonds, $\text{C}^- \text{Si}^+$, then a good indication of the likely behaviour of the C-Si bond can be predicted by consideration of an analogous C-H bond. Thus in a competitive situation, a C-Si bond is more reactive towards oxygen and halogen nucleophiles/bases, whereas a C-H bond is more reactive towards carbon and nitrogen nucleophiles/bases. Similarly parallels can also be drawn for O-H and O-Si bonds but with the opposite emphasis, i.e. O-H bonds can be cleaved more readily than O-Si bonds. Thus the -Si-O-Si-O- backbone of siloxanes is very different from the -C-C-C- backbone of hydrocarbon polymers.

The Si-Cl bond is also important in silicone chemistry considering silicones are generally made from organochlorosilanes.

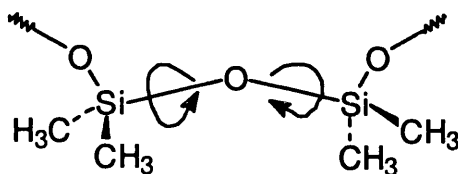
The Si-H bond is only 2% ionic therefore is much more reactive and sensitive to heterolytic cleavage than C-H. Silane, an extreme example, is spontaneously flammable in air and readily hydrolysed by water, whereas methane is comparatively inert. Under certain conditions the Si-H bond adds across a carbon-carbon multiple bond and this has become an important synthetic pathway in organosilicon chemistry.

Silicon cannot form multiple bonds, thus Si=Si, Si=C or Si=O compounds are rare and normally unstable. Although many attempts have been made in vain to isolate such compounds⁹⁶, the nearest claim is by Barton and McIntosh⁹⁷, to have trapped and identified $\text{Me}_2\text{Si}=\text{CH}_2$ using low temperature infra-red spectroscopy. The compound $\text{Me}_2\text{Si}=\text{C}(\text{SiMe}_3)_2$ is also claimed to be detected in the gas phase by mass spectrometry. Other workers also have confirmed the synthesis of structures with silicon double bond.⁹⁸⁻¹⁰⁰

Silicon has 3d-orbitals available for bonding but possibly due to steric reasons and in common with the other elements in the second short period, probably never uses more than two of them, so that the co-ordination number never exceeds six. The best known example of a compound which uses the d-orbitals of silicon is the hexafluorosilicate ion, $(\text{SiF}_6)^{2-}$, in which fluorine atoms are arranged octahedrally about the silicon atom. Thus it seems that silicon, in its ground state, greatly prefers to make four single covalent bonds.

Reactions involving free radicals are not common in silicon chemistry. The addition of Si-H bonds to unsaturated systems are of this type. The cracking and polymerisation of the simple hydrides and alkyls are probably also free radical processes, but these do not occur readily except under fairly rigorous conditions¹⁰¹⁻¹⁰². However, the small polarity of the C-H bond causes a high reactivity during contact with radicals. A marked change in the structure of the substituents takes place in a medium in which radicals are formed; when oxygen is present, partial oxidation and then complete oxidation of the substituents follows. A structural change of the hydrocarbon groups in the majority of cases results in a change in macromolecular structure of the polydimethylsiloxane. The original linear macromolecule will branch.

Bond lengths between silicon and certain other elements, especially oxygen and fluorine, are abnormally short, even after correction for the electronegativity differences of the atoms¹⁰³. The silicon-oxygen chain that constitutes the backbone of these polymers is predominantly responsible for their uniqueness. A segment of methylsiloxane chain is shown below¹⁰⁴:



Commonly accepted bond angles^{89, 105, 106} are C-Si-C = 112° , Si-O-Si = 143° (which is much larger than C-O-C bond angle in aliphatic ethers, $105-115^\circ$) and O-Si-O = 110° . The siloxane chain flexes and rotation is fairly free about the Si-O axis, especially with the small substituents e.g. methyl, on the silicon atoms¹⁰⁷. Rotation is also free in the methyl silicon compounds. As a result of the freedom of motion, the intermolecular distances between methylsiloxanes are greater than between hydrocarbons, and intermolecular forces are smaller¹⁰⁸. The small rotation barriers contribute to properties such as low modulus, low glass transition temperature and high permeability. The relationships between ring and chain forms in siloxane systems can be explained by the high flexibility of the chains.

Further structural considerations explain the weak temperature dependence of many physical properties. The preferred conformation for methylsiloxane chains is the trans form, but the large differences between successive bond angles in the chain causes this conformation to be of low spatial extension. Greater extension requires an increase in the number of higher energy states, resulting in a greater distance between the ends of methylsiloxane chains at higher temperatures. Thus increasing molecular entanglement compensates for the normal increase in molecular mobility with increasing temperatures. The viscosity of a simple methylsilicone fluid, for example, changes little with temperature, in contrast to hydrocarbon polymers, which have a stiffer structure.

4.3. THERMAL DEGRADATION OF POLYDIMETHYLSILOXANE

4.3.1. Introduction

The thermal degradation of polydimethylsiloxane, PDMS, has been studied in great detail by several groups of workers. It has been demonstrated that the thermal degradation of linear PDMS, under vacuum, results in depolymerisation liberating volatile cyclic oligomers^{109-112, 117}.

Patnode and Wilcock¹¹⁰ who were first to study the composition of thermal degradation products of PDMS, found that in a dynamic nitrogen atmosphere PDMS decomposes at 350-400°C to form low molecular weight cyclic products with the following percentage:

$[(\text{CH}_3)_2\text{SiO}]_3$ (D₃) 44%

$[(\text{CH}_3)_2\text{SiO}]_4$ (D₄) 24%

$[(\text{CH}_3)_2\text{SiO}]_5$ (D₅) 9%

$[(\text{CH}_3)_2\text{SiO}]_6$ (D₆) 10%

above cyclic hexamer 13%

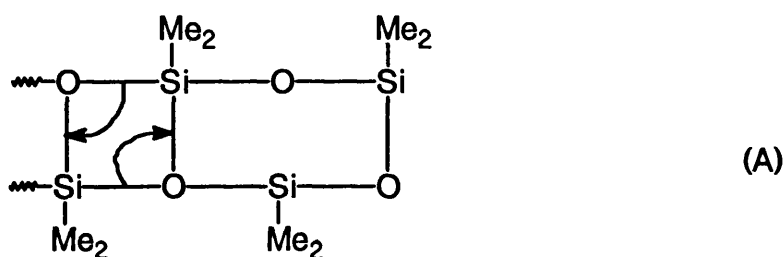
Production of cyclic products indicates that the thermal degradation of PDMS involves rupture of the silicon-oxygen bond.

Thomas and Kendrick¹¹¹ found that under nonequilibrium conditions in a catalyst-free environment, the cyclic degradation products from trimethylsiloxy end-blocked PDMS after 5 hours of heating in the vacuum at 420°C had the following composition:

| | | | |
|-----------------------|-------|-------------------|-------|
| D ₃ | 43.7% | D ₄ | 23.5% |
| D ₅ | 9.7% | D ₆ | 10.9% |
| D ₇ | 7.2% | D ₈₋₁₂ | 5.0% |
| octamethyltrisiloxane | 1.0% | | |

There was no evidence of the rupture of the Si-C bond.

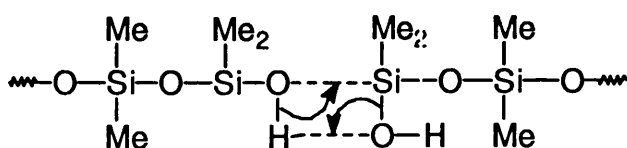
They suggested that thermal depolymerisation of trimethylsilyl end-blocked polymer occurs by a mechanism involving a randomly initiated, intramolecular cyclic, four-centred transition state with siloxane bond rearrangement (A). It was also suggested that the relatively low activation energy (i.e. 42 kcal/mol) compared to the siloxane bond energy (108 kcal/mol) is a result of silicon d-orbital participation in the transition state.



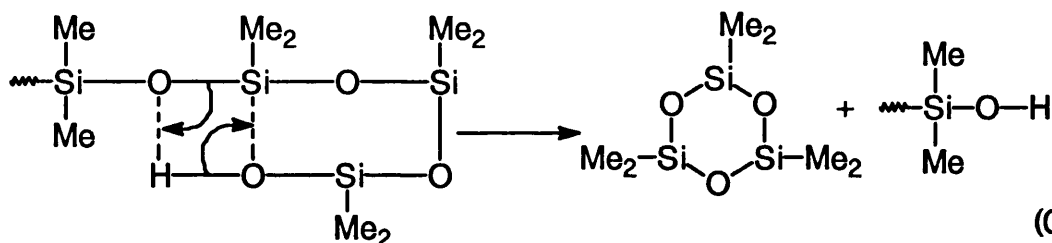
Rode, Verkhotin and Rafikov¹¹³ have found by analysis 99 weight percent dimethylcyclic trimer as the degradation product from hydroxy end-blocked PDMS, but they also found that the intrinsic viscosity of the polymer increased due to an increase in molecular weight before weight loss started. The increase in molecular weight was concluded to be the result of polycondensation involving terminal hydroxyl groups (B).

Kucera et al.¹³⁴⁻¹³⁷ have shown that the thermal stability of PDMS sharply decreases in the presence of trace impurities capable of attacking the siloxane bond or of catalysing the oxidation of methyl groups.

Grassie and MacFarlane¹⁰⁹ have shown that hydroxyl terminated PDMS is less thermally stable than the end-blocked polymer. They concluded from a combination of TG, TVA and molecular weight measurements that thermolysis of a catalyst-free polymer leads initially to condensation at the chain ends (B) accompanied by depolymerisation initiated at the chain ends (C).

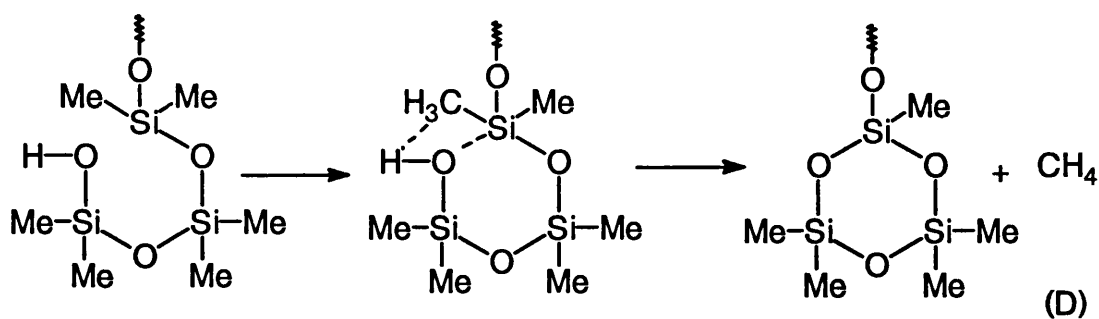


(B)

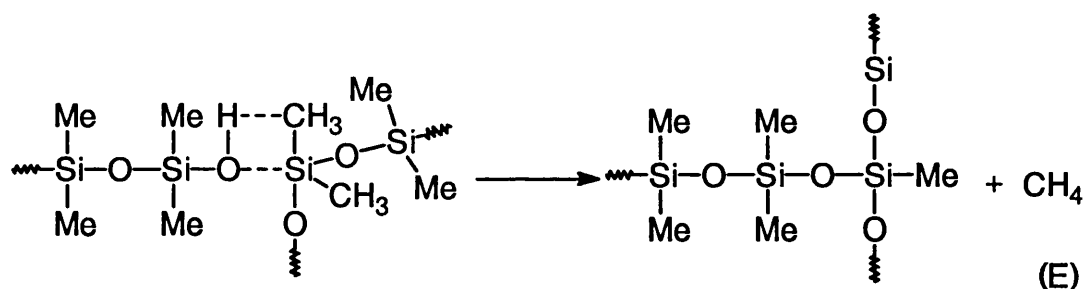


(C)

Andrianov et. al.¹¹⁴ expected and Aleksandrova et. al.¹¹² observed the presence of methane and to a lesser extent hydrogen in the degradation products of hydroxyl-end-blocked PDMS. They proposed a mechanism involving chain ends in an intramolecular reaction to account for the former (D). Andrianov et. al.¹¹⁴ working on similar samples, observed Si-C scission above 350°C with subsequent loss of sample solubility. The involvement of hydroxyl end groups in intermolecular displacement of methyl groups was suggested (E). These results conflict with the results of the other workers^{109, 111, 113, 115}.



(D)



(E)

The purpose of the present work was to investigate the thermal degradation properties of high molecular weight PDMS with vinyl end groups. This type of PDMS has been used for some applications in the industry but a very limited amount of work has been published on the degradation properties of it. Polymer samples with other end groups (e.g. hydroxy and trimethylsilyl end groups) and with a high percentage of vinyl groups have also been studied in order to make comparisons. The polymer samples used were commercial and used without any further treatment unless indicated otherwise.

4.4. EXPERIMENTAL

4.4.1. Thermal Analysis of Polydimethylsiloxane

The thermal degradation behaviour of a commercial sample of PDMS with vinyl ($-\text{CH}=\text{CH}_2$) end groups was investigated to study the thermal degradation properties in vacuo. The polymer was analysed by IR spectroscopy (Fig. 4.1 (a)). The silicone polymer with high vinyl content was also investigated to compare the thermal degradation behaviour with that of PDMS with vinyl end groups. The IR spectrum is given in Fig 4.1 (b). The thermal degradation behaviour of commercial samples of PDMS with trimethyl and hydroxyl end groups were also investigated to provide a basis for the comparison with vinyl end grouped PDMS. The IR spectra for these other samples of PDMS are given in Fig. 4.2 (a) and Fig 4.2 (b) respectively.

4.4.1.1. Thermogravimetry

PDMS With Vinyl End Groups

Thermogravimetric (TG) analysis was carried out in both dynamic nitrogen atmosphere and air with a flow rate of 50 ml/min, heating from ambient temperature to 600°C at 10°C/min in each case. The TG curves, illustrated in Fig. 4.3, show that weight loss occurs in both cases in a single step over a narrow temperature range. Weight loss of PDMS in dynamic nitrogen starts at 250°C, reaches T_{max} at 325°C and there is a negligible amount (less than 1% of original polymer weight) of residue left at the end of the degradation. Weight loss of PDMS in air starts at about 25°C later than in dynamic nitrogen, reaches T_{max} at 333°C and there is a 3.5% residue left at the end of the degradation. Knight¹¹⁸, on the other hand, found weight loss in air starting at 300°C with 50% residue at the end of the degradation (500°C), while in nitrogen starting at 340°C with no residue at the end of the degradation (575°C).

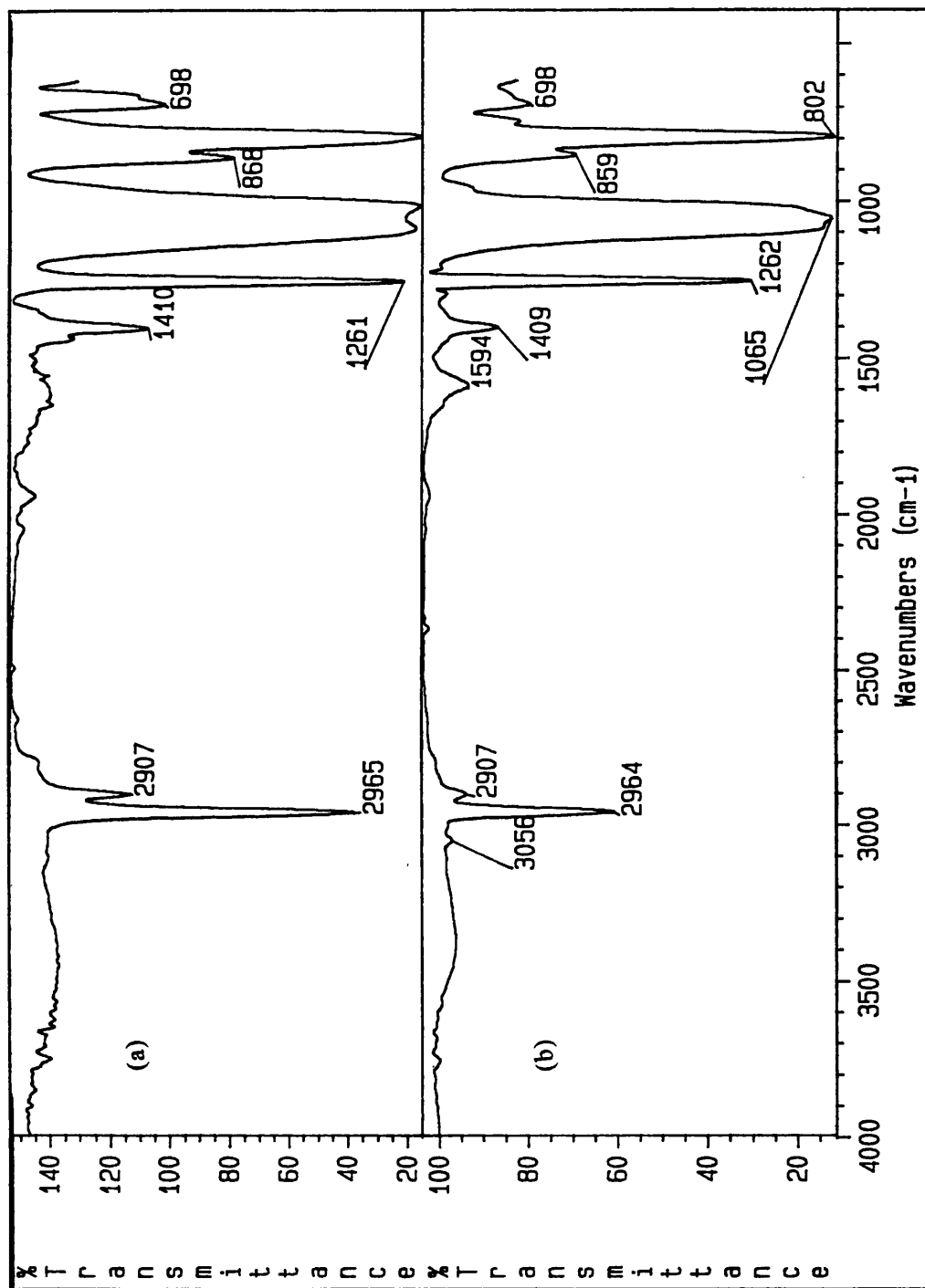


Fig. 4.1. IR spectra for PDMS with (a) vinyl end groups and (b) high vinyl content.

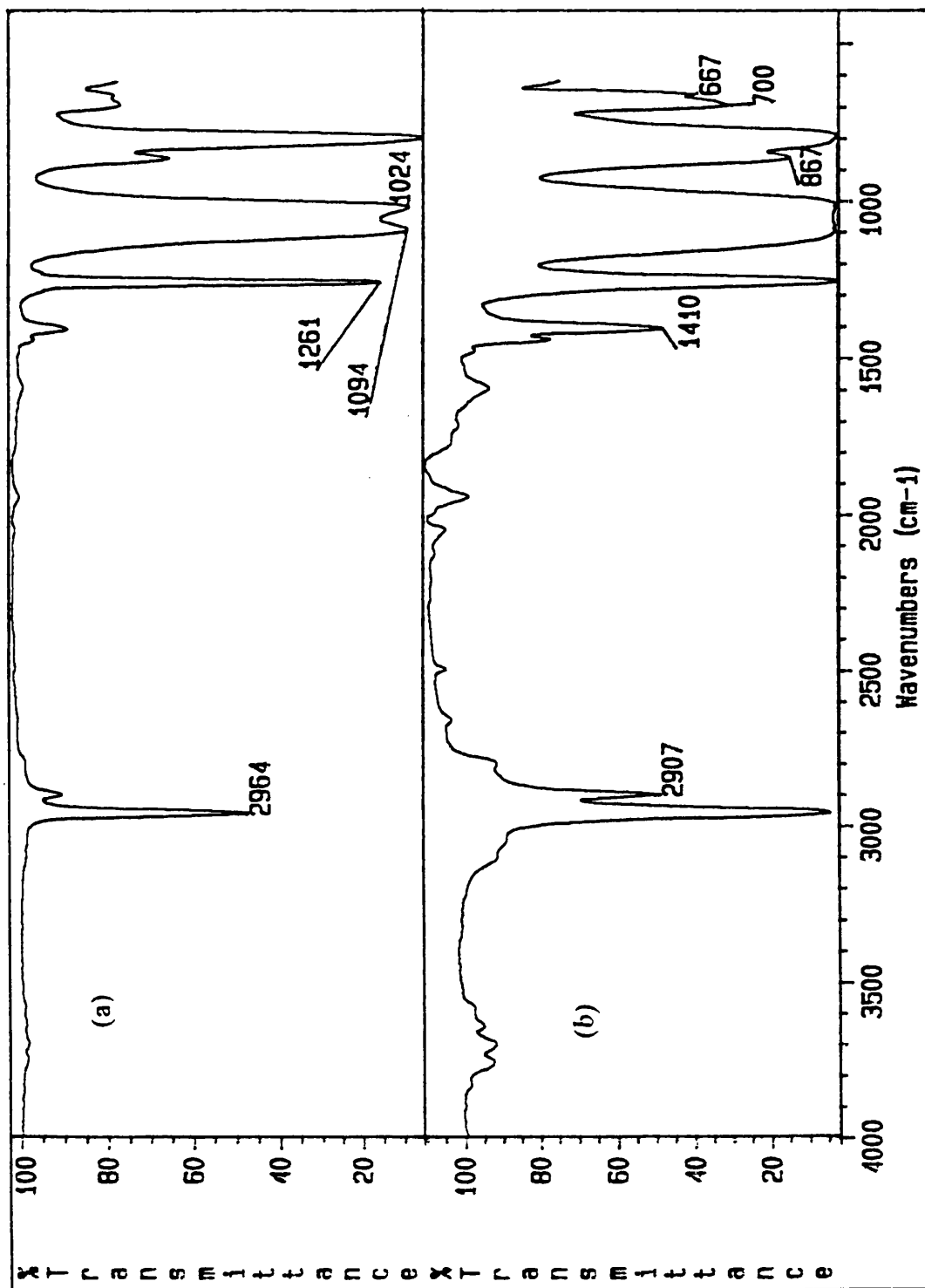


Fig. 4.2. IR spectra for PDMS with (a) trimethyl end groups and (b) hydroxyl end groups.

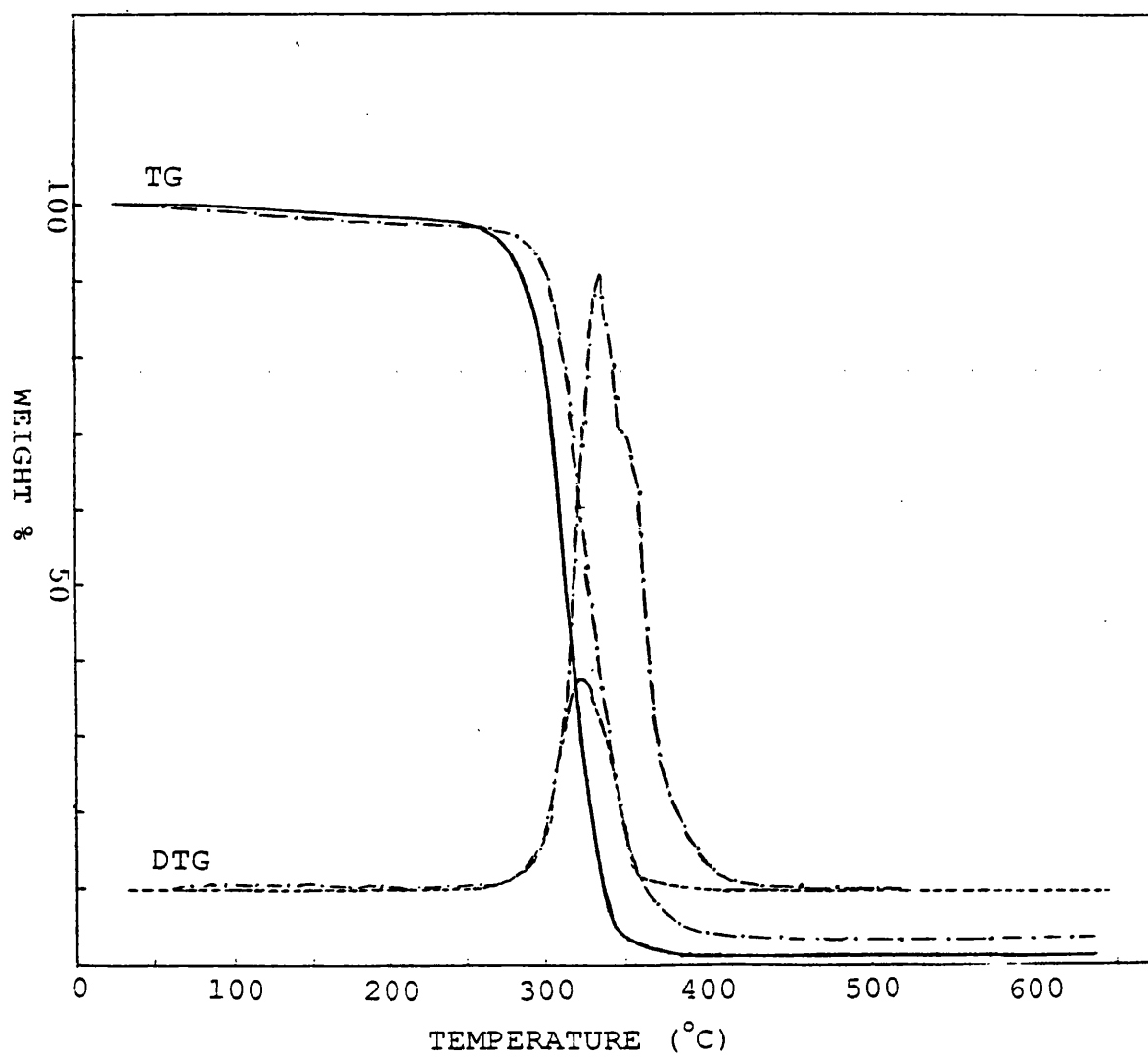


Fig. 4.3. TG-DTG curves for PDMS with vinyl end groups under nitrogen (—; ----) and air (-.-).

PDMS With Other End Groups

TG traces for other PDMS samples with different end groups were obtained in dynamic nitrogen only. TG curves are presented in Fig. 4.4 and results are given in Table 4.4.

Table 4.4. TG results in dynamic nitrogen.

| Sample | T _{thresh} (°C) | T _{max} (°C) | T ₅₀ (°C) | T _{stop} (°C) | % residue |
|----------------------|--------------------------|-----------------------|----------------------|------------------------|-----------|
| PDMS | 250 | 325 | 315 | 375 | 1.00 |
| PDMS-VMS | 250 | 325 | 314 | 375 | 1.25 |
| PDMS-OH | 350 | 460 | 450 | 500 | 0.05 |
| PDMS-Me ₃ | 275 | 331, 362 | 352 | 425 | 0.01 |

PDMS = PDMS with vinyl end groups or low vinyl content.

PDMS-VMS = PDMS with high vinyl content (Vinylmethylsiloxane (VMS) copolymer).

PDMS-OH = PDMS with hydroxyl end groups.

PDMS-Me₃ = PDMS with trimethyl end groups.

4.4.1.2. Differential Scanning Calorimetry

The Differential Scanning Calorimetry (DSC) curve (Fig. 4.5) obtained for PDMS (with vinyl end groups) under dynamic nitrogen with a flow rate of 50 ml/min and heating rate of 10°C/min reveals two endothermic transitions. The broad peak approximately in the region 50-150°C corresponds to the melting point of the polymer (T_m) while the larger peak in the region 275-325°C arises from depolymerisation. The irregular shape of the second endothermic transition is probably due to gaseous products bubbling from the viscous liquid polymer. Indirectly, this indicates that cross-linking has probably not occurred up to this point. The DSC curve rises gradually to exothermic from about 400°C onwards at the end of the degradation.

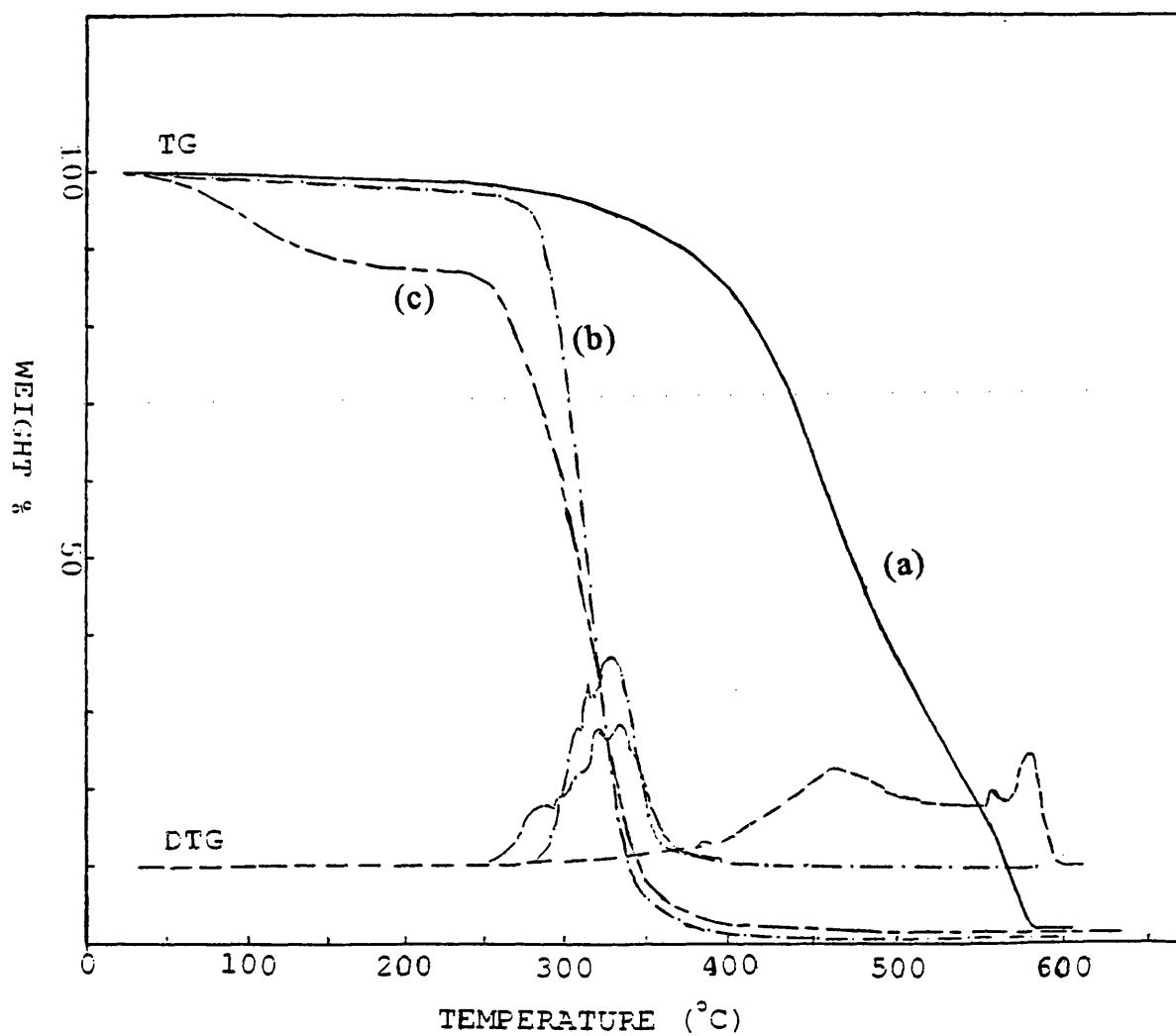


Fig. 4.4. TG-DTG traces for PDMS with (a) hydroxyl end groups (—; - - -) (b) trimethyl end groups (- · -) and (c) high vinyl content (- - -) under nitrogen.

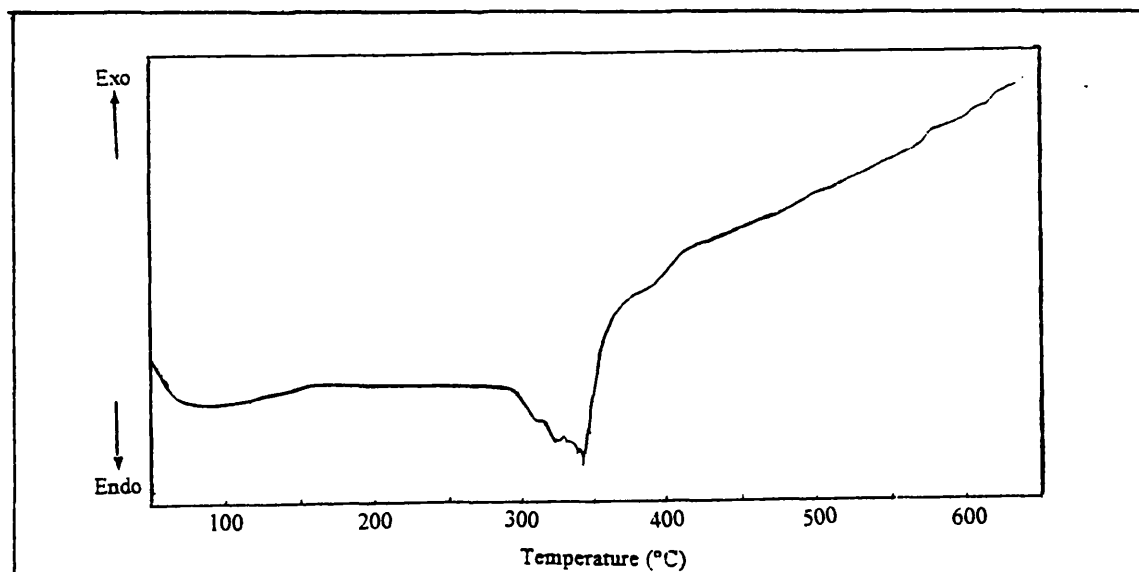


Fig. 4.5. DSC trace for PDMS with vinyl end groups.

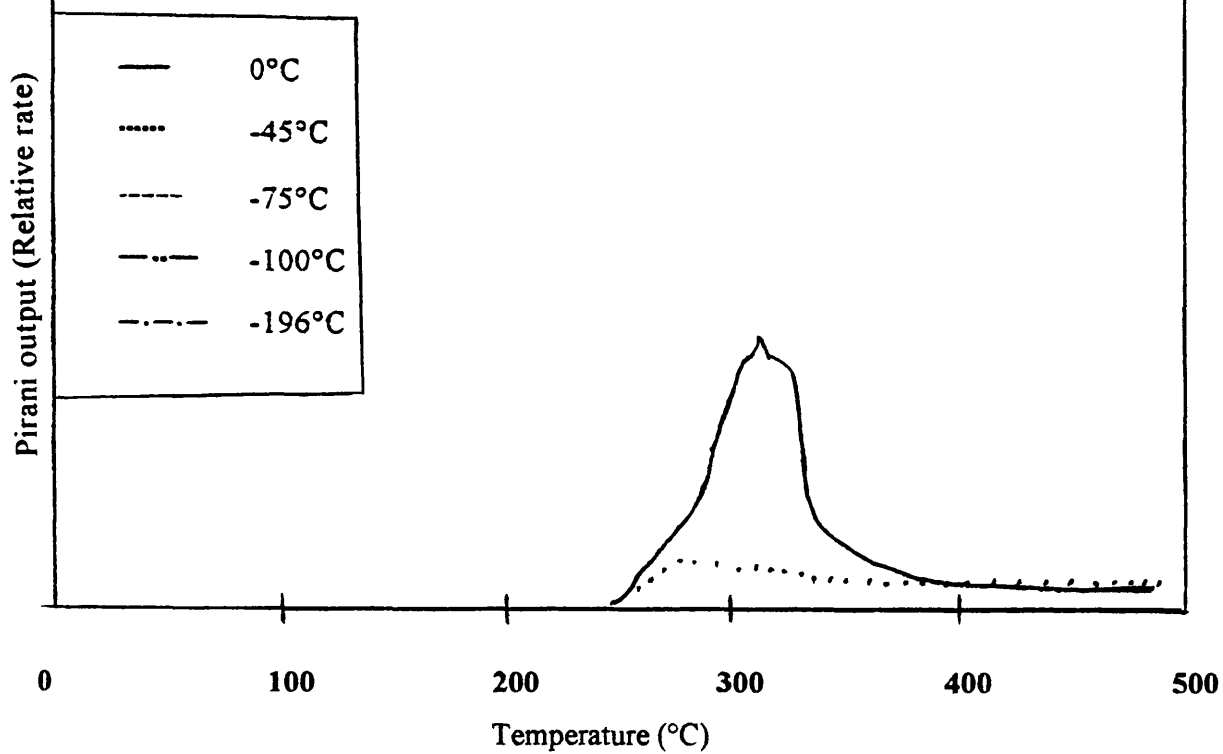


Fig. 4.6. TVA trace for PDMS with vinyl end groups.

4.4.1.3. *Thermal Volatilisation Analysis*

PDMS With Vinyl End Groups

The Thermal Volatilisation Analysis (TVA) curve (50 mg sample), Fig. 4.6, illustrates a single stage production of volatile compounds from PDMS starting at 250°C with T_{\max} at about 325°C. By examining the individual trap traces, it can be seen that most of the gaseous products are sufficiently volatile to pass through the two higher temperature traps (0°C and -45°C) but are trapped at the lower temperatures (-75°C, -100°C and -196°C). There is no evidence for non-condensable products such as methane or hydrogen since there is no rise in the -196°C trace which would indicate their presence.

The cold ring fraction (CRF) produced during the degradation was a colourless liquid. The IR spectrum was mainly similar to that of the original polymer, thus indicating that it consists of siloxane units of the type $\text{OSi}(\text{Me}_2)$. GC analysis revealed that the CRF was indeed made up of larger cyclic oligomers of which D_7 to D_{24} were positively identified. Trace amounts of linear compounds with vinyl end groups were also present. Larger cyclics may also be formed but it was not practical to heat the GC column any higher than already done.

The IR spectrum of the residue (flaky type, partially insoluble and in very small amount) was also similar to the IR spectrum of the polymer. Any changes which might have been introduced during degradation, e.g. cross-linking, would be impossible to detect from the IR spectrum since other absorptions due to siloxane groups are also at same frequencies.

PDMS With Other End Groups

PDMS with high vinyl content starts to volatilise at 250°C, reaches T_{\max} at 325°C and degradation is complete at 400°C (Fig. 4.7. (a)). Again there is no rise for the lower temperature traces as noticed for the other samples. However, the residue (0.5%) was fibre-like (more fibre-like than the residue from PDMS with vinyl end groups), insoluble and floated on the surface of the dichloromethane when dissolution was attempted.

PDMS with hydroxyl end groups starts to volatilise at about 300°C but volatilisation is extremely slow up to 350°C such that it reaches T_{\max} at 462°C (Fig. 4.7. (b)). There are no non-condensable gaseous products formed and the residue left is only 0.029% of the sample weight. This trace is identical to that obtained by

McFarlane¹⁰⁹ for PDMS with hydroxyl end groups, but in his case the volatilisation started at about 350°C.

The TVA trace (Fig. 4.7. (c)) for PDMS with trimethyl end groups shows that volatilisation starts at about 250°C but the onset of the first T_{\max} is at 331°C while the second is at 362°C. Degradation stops before 450°C and there is no production of non-condensable gaseous products. There was hardly any residue left at the end of the degradation.

PDMS with vinyl end groups was purified by dissolving it in dichloromethane and then washing the solution with distilled water, followed by shaking the solution of reprecipitated polymer with molecular sieves. Degradation of this purified PDMS, with low vinyl content, started at about 320°C but the main degradation started at 400°C and reached at T_{\max} at about 475°C. A small amount of methane was produced at 450°C. The production of methane is explained by a radical reaction.

4.4.1.4. SATVA Separation of Thermal Degradation Products

The SATVA trace for PDMS with vinyl end groups (Fig. 4.8. (a)) does not show any volatile gaseous products. There is a single large peak with a shoulder at the beginning. IR spectroscopy gave absorptions mainly for D_3 and D_4 . GC-MS results revealed the volatile degradation products to be cyclic oligomers ranging from D_3 to D_7 with D_3 being the dominant product.

The SATVA trace of PDMS with hydroxyl end groups shows an extra shoulder for the cyclic products. The degradation products are again cyclic siloxane oligomers, with cyclic trimer the major product.

The SATVA trace of PDMS with trimethyl end groups is similar to the SATVA trace of the PDMS with vinyl end groups and the degradation products are mainly cyclic siloxane oligomers with traces of linear siloxanes with trimethyl end groups.

PDMS with high vinyl content has a different shaped SATVA trace than the others (Fig. 4.8. (b)) and shows a minute peak for gaseous product(s). GC-MS analysis indicated the presence of the normal cyclic siloxane oligomers plus cyclic oligomers with at least one siloxane unit with vinylmethyl group of the type $(O-Si(CH=CH_2)Me)$. The GC trace is shown in Fig. 4.9 while MS results and interpretation are presented in Table 4.6. The structures of the compounds with vinyl groups are based on the

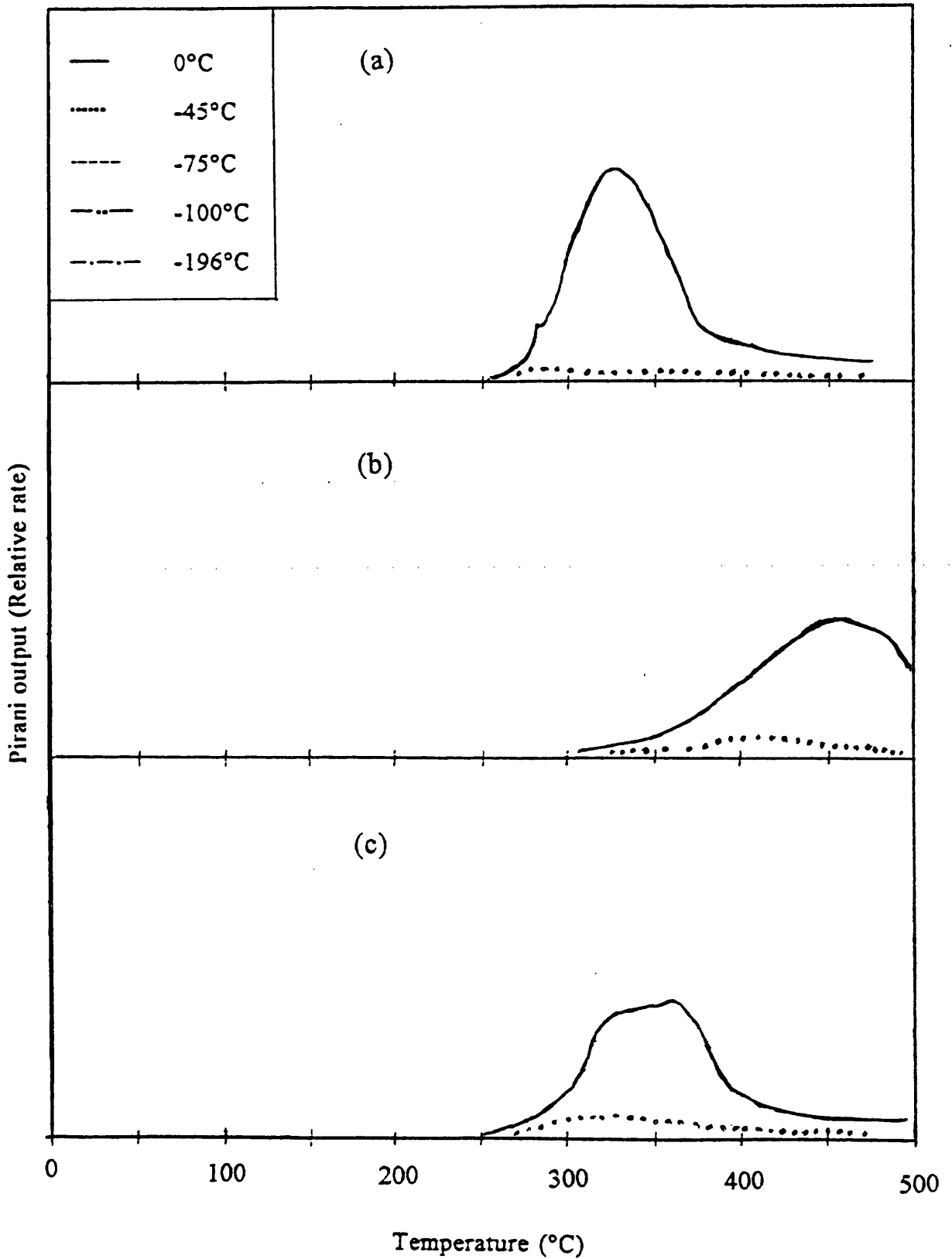


Fig. 4.7. TVA traces for PDMS with (a) high vinyl content (b) hydroxyl end groups and (c) trimethyl end groups.

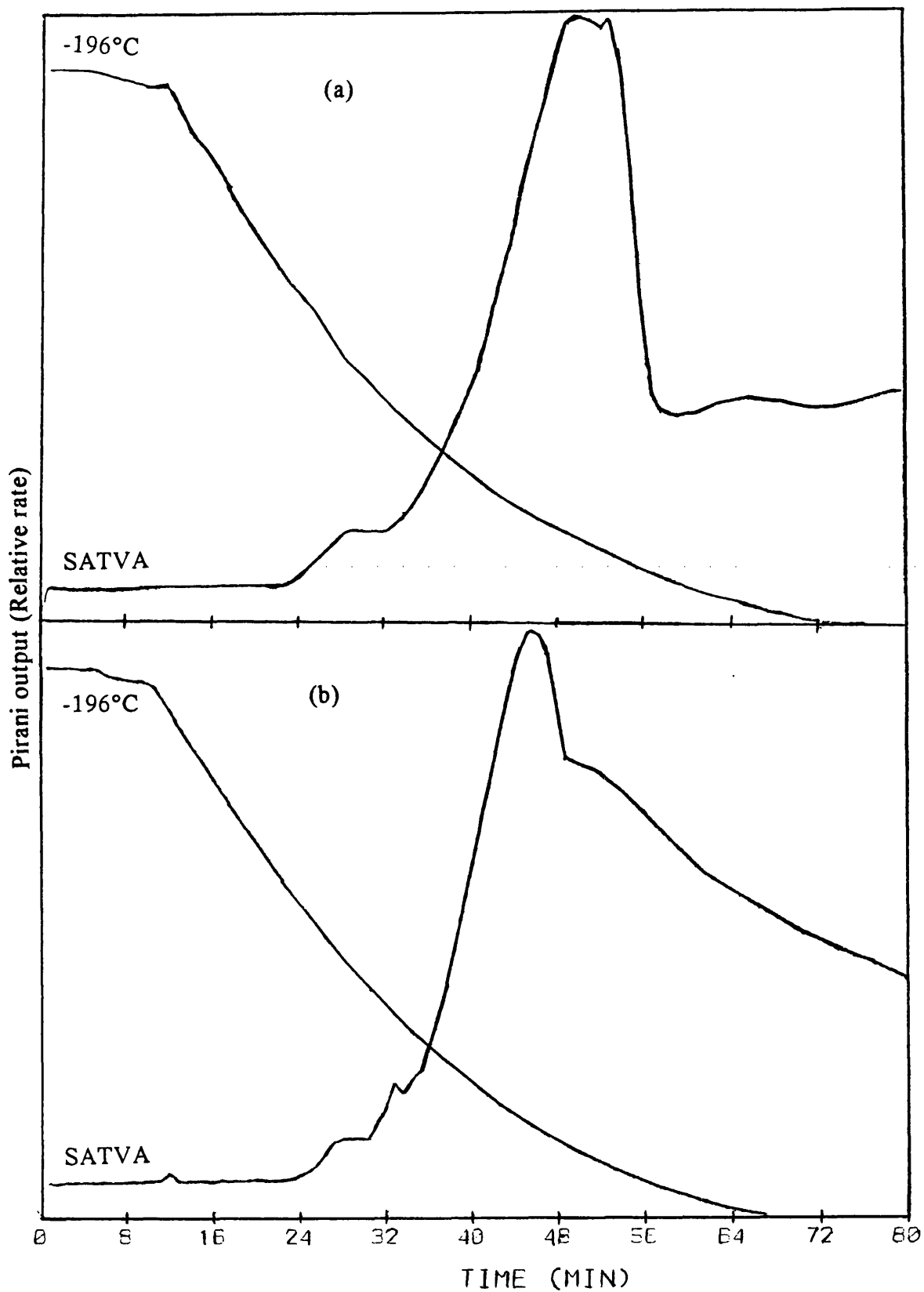


Fig. 4.8. SATVA traces for warm up from -196°C to ambient temperature of condensable volatile products from degradation for PDMS (a) vinyl end groups and (b) high vinyl content.

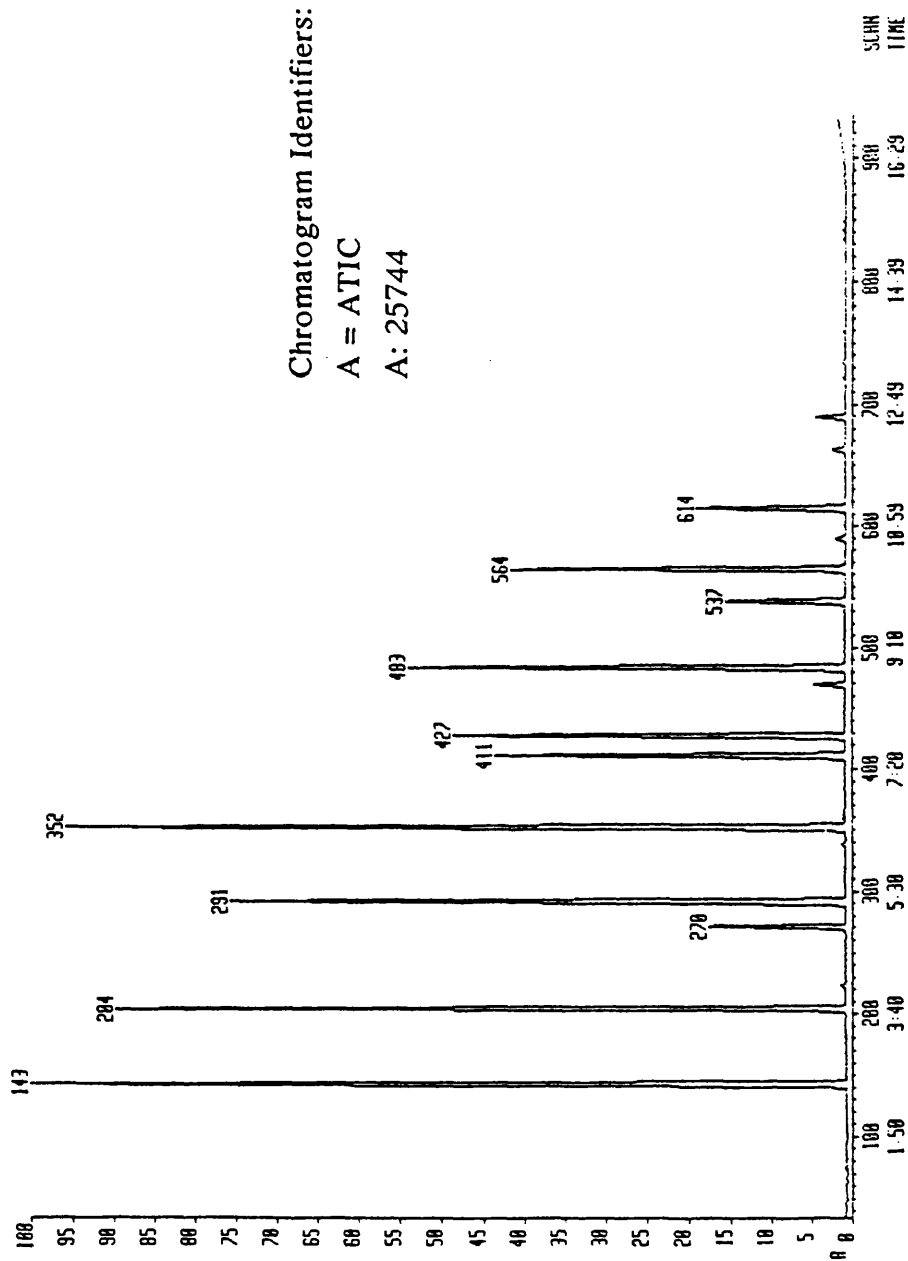
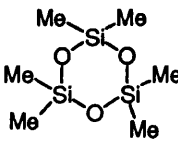
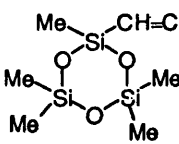
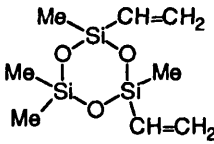
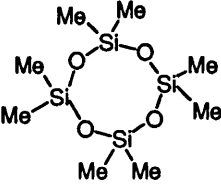
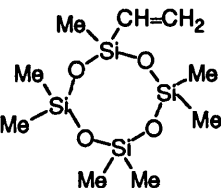
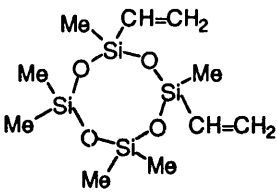
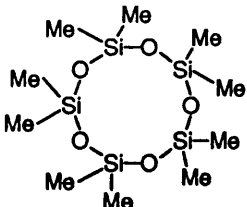
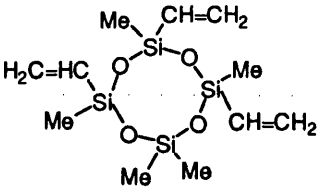
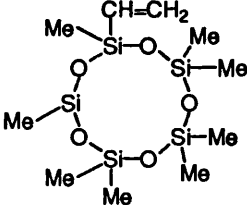
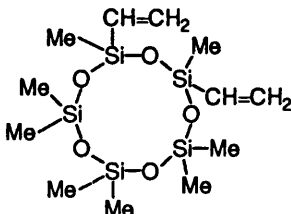


Fig. 4.9. GC trace for the liquid fraction in SATVA separation of products from the degradation of PDMS with high vinyl content.

fragmentation pattern of the ion peaks. Such an example is given in Table 4.7 for cyclotrimers and cyclic tetramers.

Table 4.6. Mass Spectrum m/e values of assignments from SATVA separation of condensable volatile products of degradation of PDMS with high vinyl content.

| Scan | m/e (%) | Name/Structure and Boiling Points ¹¹⁹ |
|------|---|--|
| 143 | 207(100), 208(22), 96(18), 209(12), 191(9), 133(7), 177(4), 119(3), 147(2), 222(0) |  <p>B.P. = 135°/760</p> <p>Hexamethylcyclotrisiloxane (D₃)</p> |
| 204 | 219(100), 193(60), 220(40), 89(38), 207(35), 203(30), 133(25), 221(20), 191(18), 102(10), 163(8), 234(0) |  <p>BP = 56°/23</p> <p>1,1 3, 3, 5-Pentamethyl-5-vinylcyclotrisiloxane</p> |
| 270 | 231(100), 203(45), 232(20), 177(10), 233(7), 89(5), 246(0) |  <p>1,1 3, 5-Tetramethyl-3, 5-divinylcyclotrisiloxane</p> |
| 291 | 281(100), 282(30), 283(20), 265(15), 193(10), 133(13), 191(12), 249(12), 73(12), 296(0) |  <p>BP = 175.8°/760, 74°/20</p> <p>Octamethylcyclotetrasiloxane (D₄)</p> |
| 352 | 293(100), 265(60), 294(45), 295(30), 193(25), 277(20), 281(19), 73(18), 125(10), 207(5), 308(0) |  <p>BP = 62-64°/11, 84°/20</p> <p>1,1 3, 3, 5, 5, 7-Heptamethyl-7-vinylcyclotetrasiloxane</p> |

| | | |
|-----|--|---|
| 411 | 305(100), 251(30), 306(25), 277(23), 307(18), 265(17), 193(15), 293(10), 118(8), 163(5), 320(1) |  <p style="text-align: center;">BP = 71-73°/11, 96°/19.5</p> <p style="text-align: center;">1,1 3, 3, 5, 7-Hexamethyl-5, 7-divinylcyclotetrasiloxane</p> |
| 427 | 73(100), 355(50), 267(45), 356(10), 357(5), 268(4), 193(4), 249(3), 323(3), 370(0) |  <p style="text-align: center;">BP = 210°/760</p> <p style="text-align: center;">Decamethylcyclopentasiloxane (D₅)</p> |
| 469 | 317(100), 289(80), 251(60), 263(50), 249(38), 274(30), 193(28), 318(25), 290(20), 73(15), 207(10), 332(0) |  <p style="text-align: center;">BP = 84-86°/11</p> <p style="text-align: center;">1,1 3, 5, 7-Pentamethyl-3, 5, 7-trivinylcyclotetrasiloxane</p> |
| 483 | 73(100), 85(60), 367(59), 267(40), 368(15), 279(10), 193(5), 249(4), 45(4), 154(3), 207(3), 281(2), 382(0) |  <p style="text-align: center;">1,1 3, 3, 5, 5, 7, 7, 9-Nonanemethyl- 9-vinylcyclopentasiloxane</p> |
| 537 | 85(100), 73(97), 379(60), 97(50), 59(40), 279(30), 267(29), 380(25), 44(15), 251(10), 193(8), 147(5), 323(4), 394(0) |  <p style="text-align: center;">1,1 3, 3, 5, 5, 7, 9-Octamethyl-7, 9-divinylcyclopentasiloxane</p> |

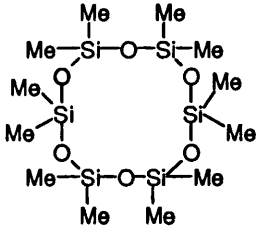
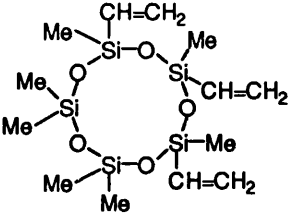
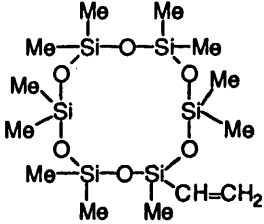
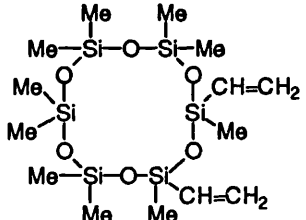
| | | |
|-----|---|--|
| 564 | 73(100), 341(55), 147(25), 429(20), 325(10), 59(5), 207(4), 251(3), 444(0) |  <p style="text-align: right;">BP = 245°/760</p> <p style="text-align: center;">Dodecamethylcyclohexasiloxane (D₆)</p> |
| 590 | 85(100), 97(80), 73(77), 391(48), 59(35), 279(15), 207(8), 363(5), 147(4), 406(0) |  <p style="text-align: right;">1,1 3, 3, 5, 7, 9-Octamethyl-5, 7, 9-trivinylcyclopentasiloxane</p> |
| 614 | 73(100), 85(40), 341(40), 441(35), 353(30), 59(18), 147(12), 442(8), 207(5), 456(0) |  <p style="text-align: right;">1,1 3, 3, 5, 5, 7, 7, 9, 9, 11- Decamethyl-11-vinylcyclohexasiloxane</p> |
| 663 | 73(100), 85(70), 353(30), 59(27), 97(17), 341(16), 453(15), 207(10), 147(8), 468(0) |  <p style="text-align: right;">1,1 3, 3, 5, 5, 7, 7, 9, 11- Nonamethyl-9, 11-divinylcyclohexasiloxane</p> |
| 689 | 73(100), 147(45), 281(40), 327(7), 415(4), 207(3), 503(2), 518(0) | <p style="text-align: center;">C₁₄H₄₂O₇Si₇ Octadecamethylcycloheptasiloxane (D₇)</p> |

Table 4.7. Fragment Ions in the Mass Spectra of D_3 and $D_3(CH=CH_2)_n$ (where $n = 0$ to 3)

Note: D_3V_1 = Cyclic trimer with one vinyl group of the type $-CH=CH_2$
 D_3V_2 = Cyclic trimer with two vinyl group of the type $-CH=CH_2$
 D_3V_3 = Cyclic trimer with three vinyl group of the type $-CH=CH_2$

| m/e | D_3 | D_3V_1 | D_3V_2 | D_3V_3 | Ion type |
|-----|-------|----------|----------|----------|--|
| 59 | | | | | $[(C_2H_7Si)^+]$ |
| 73 | 5 | 2 | 2 | | $[(CH_3)_3Si]^+$ |
| 75 | 5 | 4 | 3 | | |
| 87 | 1 | | | | $[(CH_3)_3SiCH_2]^+$ |
| 89 | 3 | 38 | 8 | | $[(CH_3)_3SiO]^+$ |
| 96 | 18 | 4 | 3 | | $[D_3 - 2CH_3]^{2+}$ $[D_3V_1 - CH_2CH - CH_3]^{2+}$, $[D_3V_2 - 2(CH_2=CH)]^{2+}$, |
| 102 | | 15 | | | $[D_3V_1 - 2CH_3]^{2+}$ |
| 108 | | | 5 | | $[D_3V_2 - 2CH_3]^{2+}$ |
| 133 | 30 | 25 | 10 | | $[(CH_3)_3Si_2O_2]^+$ |
| 147 | 5 | 3 | 1 | | |
| 161 | 2 | | | | |
| 163 | 6 | 10 | 5 | | $[(CH_3)_5Si_2O_2]^+$ |
| 177 | 20 | 15 | 16 | | $[D_3 - CH_3 - C_2H_6]^+$ $[D_3V_1 - CH_3 - (CH_2=CH)]^+$ $[D_3V_2 - CH_3 - C_4H_6]^+$ |

| m/e | D ₃ | D ₃ V ₁ | D ₃ V ₂ | D ₃ V ₃ | Ion type |
|-----|----------------|-------------------------------|-------------------------------|-------------------------------|---|
| 191 | 30 | 10 | 3 | | [D ₃ -CH ₃ -CH ₄] ⁺ D ₃ V ₁ -CH ₄ -(CH ₂ =CH) ⁺ [D ₃ V ₂ -CH ₂ =CH ₂ -(CH ₂ =CH)] ⁺ |
| 193 | 5 | 58 | 8 | | [D ₃ -C ₂ H ₃] ⁺ [D ₃ V ₁ -C ₃ H ₅] ⁺ [D ₃ V ₂ -C ₄ H ₅] ⁺ |
| 203 | | 18 | 40 | | [D ₃ V ₁ -CH ₃ -CH ₄] ⁺ [D ₃ V ₁ -CH ₃ -CH ₂ =CH ₂] ⁺ |
| 207 | 100 | 20 | | | [D ₃ -CH ₃] ⁺ [D ₃ V ₁ -(CH ₂ =CH)] ⁺ |
| 222 | < 1 | 2 | 1 | | [D ₃] ⁺ |
| 219 | | 100 | 10 | | [D ₃ V ₁ -CH ₃] ⁺ [D ₃ V ₂ -(CH ₂ =CH)] ⁺ |
| 234 | | <1 | | | [D ₃ V ₁] ⁺ |
| 231 | | | 100 | | [D ₃ V ₂ -CH ₃] ⁺ |
| 246 | | | 0 | | [D ₃ V ₂] ⁺ |

4.2.2. DEGRADATION IN AIR

PDMS (with low vinyl groups) was also degraded in air in a silica pot with a chimney at the top. The degradation product was mainly white solid material which was identified by IR spectroscopy as silicon dioxide. This is an indication of Si-C bond rupture and oxidation of CH₃ groups along with crosslinking of the polymer chains, thus reducing the amount of cyclic oligomers that can be formed. The volatile gaseous products were not collected. There was a very small amount of flaky residue left. The IR spectra for white solid material and residue are given in Fig. 4.10.

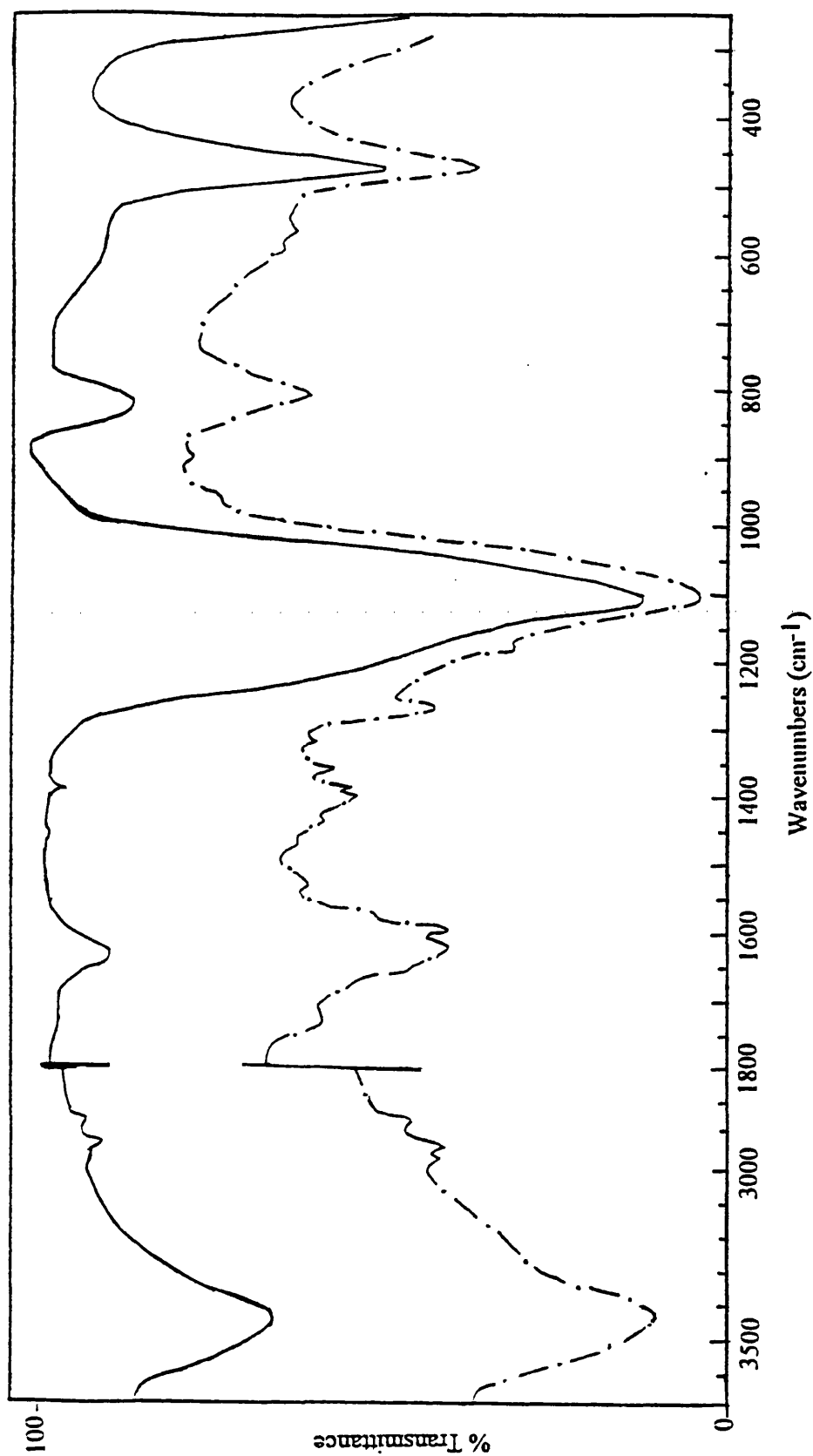


Fig. 4.10. IR spectra for degradation products from PDMS (with vinyl end groups) heated in air, white solid material (—) and flaky residue (—·—).

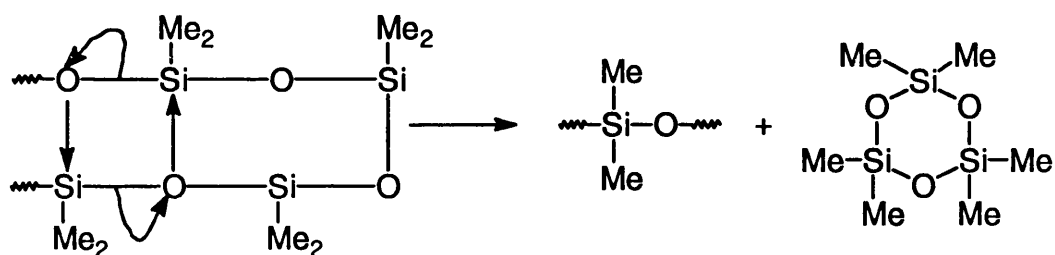
4.5. DISCUSSION

TG, DTG, DSC and TVA data clearly indicated that weight loss occurs in a single step during the thermal degradation of PDMS with vinyl end groups. The onset and rate maximum temperatures are in good agreement for all techniques applied.

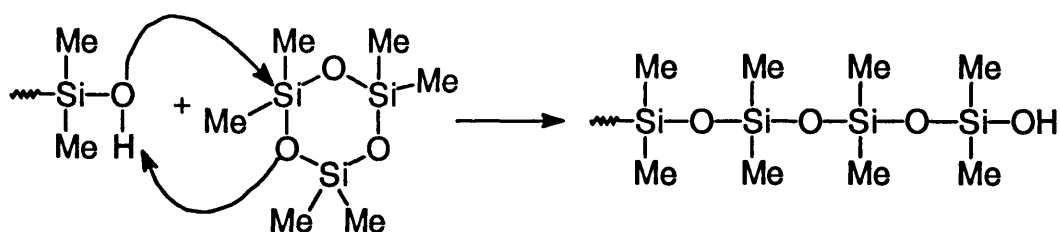
The TVA trace indicates that there is no production of methane which results from Si-C bond rupture thus indicating Si-O bond breaking only. The insolubility of the residue indicates some degree of cross-linking. Other PDMS samples with different end groups also showed only Si-O bond rupture, but the mechanism of degradation depends on the end groups of the polymer chain. The degradation products were mainly cyclic siloxane oligomers with dimethyl groups in all cases except in the case of PDMS with high vinyl content which has cyclic siloxane oligomers with dimethyl groups but also units with methylvinyl group of the type $(\text{O-Si}(\text{CH}=\text{CH}_2)\text{Me})$. The main features of the degradation mechanism of polydimethylsiloxanes with different end groups are discussed as follows:

(a) *Depolymerisation by Random Elimination*

Random elimination of cyclic trimer and larger cyclic oligomers may occur without chain scission from the polymer with non-active chain ends such as trimethyl end groups^{109, 112} and vinyl end groups of the type $\text{O-Si}(\text{Me})_2\text{-CH}=\text{CH}_2$.

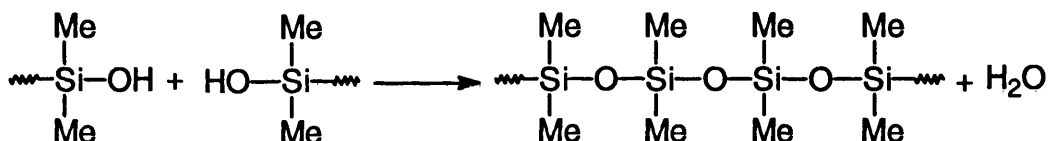


This would result in the formation of cyclic siloxane oligomers and small amounts of linear siloxanes with end groups similar to those of the parent polymer. GC-MS analysis has confirmed the presence of such linear compounds but due to higher molecular weight, they were relatively in small amount.



(d) Intermolecular Condensation of Terminal Hydroxyl Groups

This reaction, which is also called chain extension and would lead to an increase in molecular weight has been studied by other workers¹⁰⁹, , again in the present work these reactions were not distinguished.



4.6. CONCLUSIONS

TG, DTG (both in nitrogen and in air) DSC and TVA data clearly indicate that weight loss occurs in a single step during the thermal degradation of PDMS with vinyl end groups. PDMS with hydroxyl and trimethyl end groups is more stable than that with vinyl end groups. The polymer with vinyl end groups, however, becomes more stable if purified as described before. This indicates that even small amounts of impurities affect the degradation behaviour and stability of the polymer.

Oxygen has a profound effect on the degradation behaviour of the PDMS and the degradation product is mainly silicon dioxide which results after methyl groups are oxidised and removed.

PDMS (with vinyl end groups) mainly gave cyclic siloxane oligomers and D₃-D₂₄ have been identified with D₃ the major product at temperatures up to 470°C. Trace amounts of linear compounds with vinyl end groups in the case of PDMS with vinyl end groups and trimethyl end groups in the case of PDMS with trimethyl end groups were also present

PDMS (with high vinyl content) gave cyclic siloxane oligomers with difunctional units dimethyl (OSiMe_2) and vinylmethyl ($\text{OSi}(\text{CH}=\text{CH}_2)\text{Me}$). Cyclic oligomers with only one vinylmethyl group are formed in greater quantities than the cyclic oligomers with more than one vinylmethyl group.

There is no Si-C bond rupture and degradation products are formed by Si-O bond breaking only. If, however, the polymer is stabilised by removing impurities it initiates the production of methane and thus Si-C bond rupture at the higher temperature, at which normally the polymer almost degrades to completion. The insolubility of the residue indicates some degree of cross-linking. Other PDMS with different end groups also indicate Si-O bond rupture only but the mechanism of degradation depends on the end groups.

CHAPTER 5

BLENDS OF POLYOLEFINS AND INORGANIC FILLERS

5.1. INTRODUCTION

Polyethylene and its copolymers possess an excellent balance of chemical, electrical and mechanical properties but their flammability is a major limitation in their usage. Their behaviour, however, can be modified to reduce the risks from fire by addition of additives which would either absorb heat from the hot zone and thus reduce flame propagation or prevent flame reaching the plastic by introducing charred or intumescent matter.

In the past fire retardants such as antimony oxide and halogenated compounds have been used to achieve the required standards for safety reasons. However, concern about the toxicity and corrosive effects of acid and halogen containing flame retardants has attracted research interest towards non-halogenated additives¹²⁰, especially inorganic fillers such as $\text{Mg}(\text{OH})_2$, $\text{Al}(\text{OH})_3$, MgO , CaCO_3 and others. These fillers are used as heat sinks to remove heat from the polymeric materials and thus reduce their decomposition to some degree.

Inorganic fillers with polyolefins have been used before by other workers. Delfosse et. al^{121, 122} showed that metallic hydroxides added to polymeric material as fire retardants, eventually catalysed the oxidation of the char formed during combustion. The catalytic effects were found to be due to the metal oxides formed during the decomposition of the metallic hydroxide. These metal oxides introduced the surface oxidation of carbonyl groups to CO_2 . Rychlý et. al^{123, 124} found that the activation energies of the decomposition of polyethylene (PE) and polypropylene (PP) in the presence of $\text{Mg}(\text{OH})_2$ in air were notably higher than those for the polymers while the $\text{Al}(\text{OH})_3$ showed opposite effect on these polymers. It was also shown that these hydroxides were effective fire retardants for ethylene-vinyl acetate (EVA) copolymers if present in more than 60% by weight and that the acetic acid formed from the first stage of decomposition of the EVA copolymer reacted with the metal oxides to form the corresponding ionic salts. These workers made their investigations mainly in air. The work carried out for the purpose of this thesis, however, was mostly carried out in an inert atmosphere and all the volatile degradation products were collected and analysed to find out the mechanism of decomposition of the polymeric material and the formation of these degradation products in the presence of inorganic fillers.

This chapter deals with the blends of LDPE, PEA and EEA copolymer with calcium carbonate. EEA copolymer is also considered with other inorganic fillers such as $Mg(OH)_2$, $Al(OH)_3$, MgO , TiO_2 and different sized (coated and uncoated) $CaCO_3$.

5.2. EXPERIMENTAL

5.2.1. Preparation and Compositions of Blends

All blends were prepared as described in Chapter 2. The compositions of the inorganic fillers and polymer/copolymer were based on weight and are given in Table 5.1.

Table 5.1. Characterisation of samples examined

Note:- * = Uncoated

| Sample | Polymer | Additive | Mean particle size (μ) | Type |
|----------|---------------|----------------|------------------------------|--------------|
| Blend 1 | LDPE:BP77 | 50% $CaCO_3$ | 1.5 | Whiting |
| Blend 2 | PEA | 31.6% $CaCO_3$ | 1.5 | Whiting |
| Blend 3 | EEA copolymer | 31.6% $CaCO_3$ | 1.5 | Whiting |
| Blend 4 | EEA copolymer | 50% $CaCO_3$ | 1.5 | Whiting |
| Blend 5 | EEA copolymer | 50% $CaCO_3$ | 1.5 | Calcite* |
| Blend 6 | EEA copolymer | 50% $CaCO_3$ | 0.9 | Calcite |
| Blend 7 | EEA copolymer | 50% $CaCO_3$ | 5.0 | Calcite |
| Blend 8 | EEA copolymer | 50% $CaCO_3$ | 0.06 | Precipitated |
| Blend 9 | EEA copolymer | 50% $Al(OH)_3$ | | |
| Blend 10 | EEA copolymer | 50% $Mg(OH)_2$ | | |
| Blend 11 | EEA copolymer | 50% MgO | | |
| Blend 12 | EEA copolymer | 50% TiO_2 | | |

5.2.2. Thermal Analysis of Blends of Polyolefins and Inorganic Fillers

The thermal behaviour of these blends was investigated using TG-DTG, TVA and SATVA mostly while in some cases DSC is also used. The experimental procedure had been described in Chapter 2. The blends used for these investigations were cut into small fragments before degradation.

The thermal degradation of polyolefins alone has been discussed in Chapter 3 and TG-DTG, TVA and SATVA curves are illustrated therein.

5.2.2.1. Thermogravimetry

TG results in dynamic nitrogen and air are given in Table 5.2 (a) and (b), respectively. The behaviour of each blend predicted, assuming no interaction between the components, was calculated from the TG curves of the components and their relative amounts.

5.2.2.1.1. TG-DTG Under Nitrogen

Blend of LDPE and CaCO₃

Weight loss of blend 1 (LDPE, 50% CaCO₃) started at 387°C and reached T_{max} at 481°C. There was not any effect on the stability as seen from the TG-DTG curve (Figs. 5.1) which shows that the calculated TG curve coincides with the experimental TG curve.

Blend of PEA and CaCO₃

The TG curves obtained for the blend 2 (PEA, 31.6% CaCO₃) showed mainly a single stage degradation process starting at 325°C with T_{max} at 409°C and completed by 450°C (Fig. 5.2). The residue at this temperature was 39.0%, 3.0% more than the expected value, assuming that there was no interaction between the filler and the polymer. There was also a very small second degradation step beginning at 475°C and with T_{max} at 490°C. This second degradation stage was not present when PEA was degraded alone. The TG curve showed about 5-15°C of stabilisation at the beginning up to about 11% weight loss and after this there was destabilisation which gradually increased to about 15°C, however, the dynamic weight loss curve moved again towards higher temperature after 60% weight loss at 435°C. The residue at 600°C amounted to 33.25% by weight of the total original weight of the blend degraded.

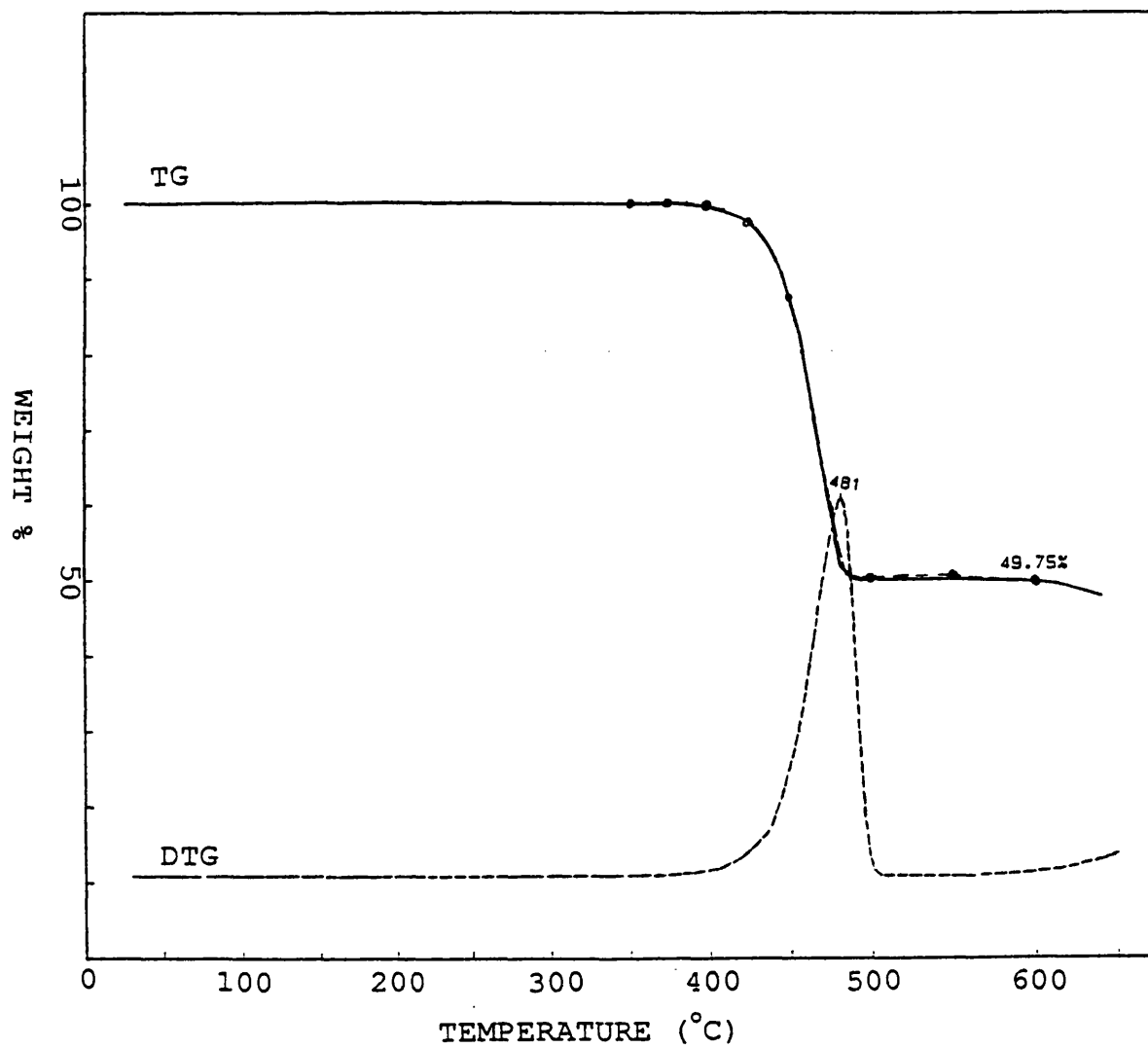


Fig. 5.1. TG-DTG traces for blend 1: experimental (—; ···) and calculated (---) under nitrogen.

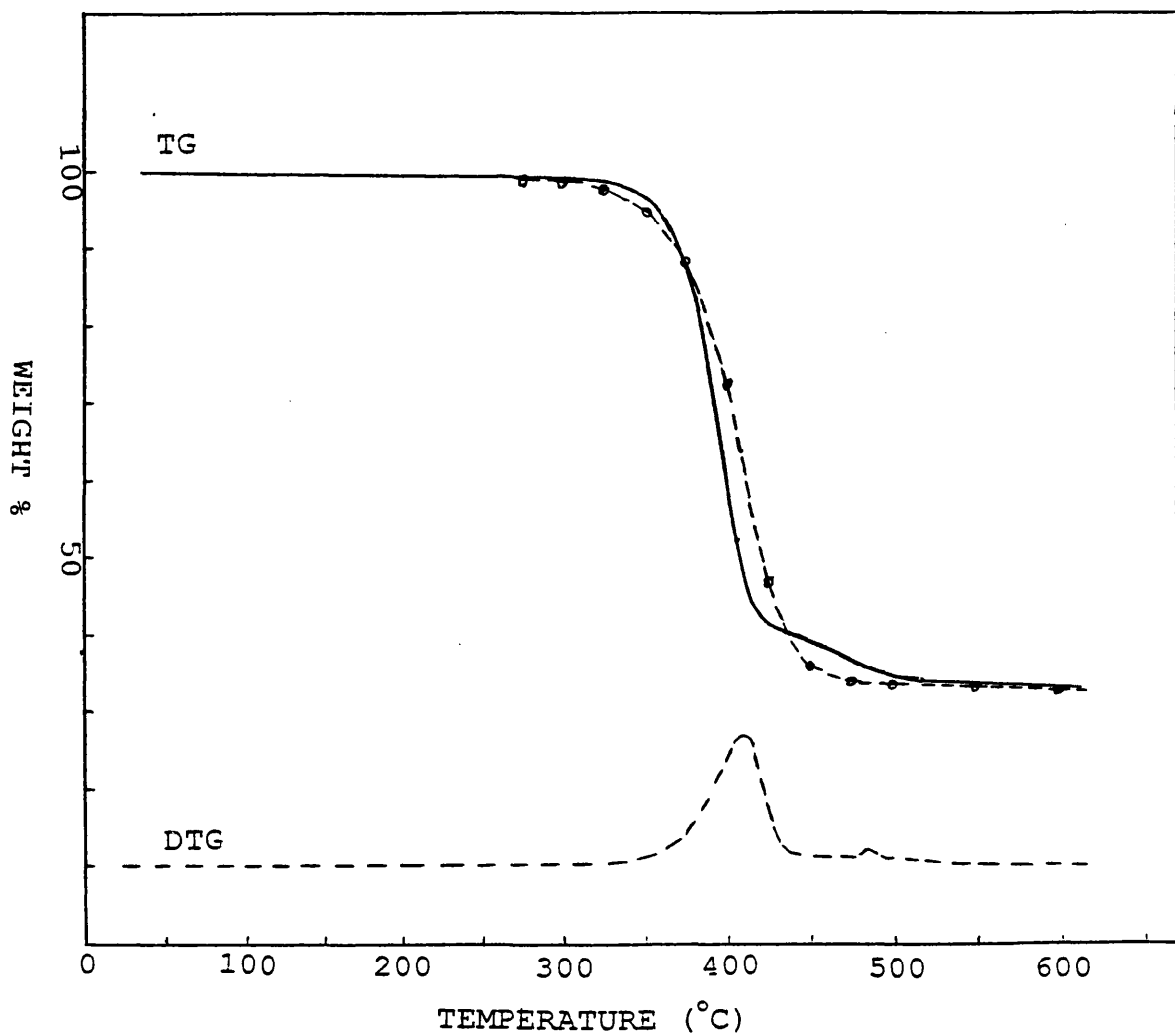


Fig. 5.2. TG-DTG curves for blend 2: experimental (—; ----) and calculated (↔↔↔) under nitrogen.

Blends of EEA Copolymer and CaCO₃

Weight loss of all EEA copolymer and CaCO₃ blends showed two stage degradation as seen from the TG-DTG curves (Fig. 5.3 to Fig. 5.8) while the EEA copolymer alone showed only one main degradation stage. This indicates that the mechanism of the formation of the degradation products has been changed and this change would only be possible if there was a chemical interaction between the filler and the polymeric material.

The first stage of degradation of blend 3 (EEA copolymer, 31.6% CaCO₃) and blend 4 (EEA copolymer, 50% CaCO₃), in both cases using coated CaCO₃ with particle size of 1.5 microns, started at about 350°C and reached T_{max} at 440°C and 435°C respectively while the second (main) stage of degradation reached T_{max} at 471°C and 475°C respectively. Although these blends were slightly less stable initially than predicted, after about 20% weight loss the degradation process slowed down and there was a drift towards higher temperature in the dynamic weight loss curve of about 10-20°C at the end. The residue at 600°C was 31.00% and 49.55% respectively of the total weight of the blend degraded.

Blend 5 (EEA copolymer, 50% CaCO₃ (uncoated, 1.5 microns)) did not show stabilisation initially but after 2.5% weight loss stabilisation was apparent and there was a drift towards higher temperature of about 15°C at the end. The first and second stages of degradation reached T_{max} at 450°C and 484°C respectively.

Blend 6 (EEA copolymer, 50% CaCO₃ (coated, 0.9 microns)), initially showed destabilisation but after 6% weight loss, the degradation process slowed down such that the TG curve was displaced 20-30°C towards higher temperature near the end of the degradation. This blend showed three degradation stages ((Fig. 5.6) instead of the two shown by the others. The first stage of degradation started at about 275°C but the degradation was quite slow such that it reached T_{max} at 437°C. The second and third stages of degradation reached T_{max} at 481°C and 492°C, respectively.

Blend 7 (EEA copolymer, 50% CaCO₃ (coated, 5.0 microns)) started to volatilise at 367°C and the first stage of degradation reached T_{max} at 448°C while the second stage of degradation reached T_{max} at 480°C (Fig. 5.7). This was the only blend of EEA copolymer and CaCO₃ which showed stabilisation at the beginning and throughout the degradation but the stabilisation is only 2-12°C.

Blend 8 (EEA copolymer, 50% CaCO₃ (coated, precipitated, 0.06 microns)) initially did not show stabilisation, but after 4% weight loss there was about 10-15°C

stabilisation. Like blend 6 this blend also showed three degradation stages instead of the two shown by the others. The first stage of degradation commenced at 350°C and reached T_{\max} at 437°C while the second and third stages of degradation reached T_{\max} at 478°C and 483°C, respectively. However, the second and third stages of degradations are so close to each other that they could be considered as one with average T_{\max} at 480°C (Fig. 5.8).

Blends of EEA Copolymer and Other Inorganic Fillers

The first stage of degradation of blend 9 (EEA copolymer, 50% $\text{Al}(\text{OH})_3$) which is due to the decomposition of $\text{Al}(\text{OH})_3$ to Al_2O_3 and water, started at about 225°C and finished at about 350°C (Fig. 5.4(a)). $\text{Al}(\text{OH})_3$, when decomposed alone, started to volatilise at about 174°C and reached T_{\max} at 223°C. It seems that the polymer melt retards the volatilisation of the water for some time. The second stage of degradation commenced at about 350°C, reached T_{\max} at 477°C and stopped at 525°C. The stabilisation, which was evident throughout the degradation, was up to 40°C and the residue at 600°C was 35.25%, about 2.55% more than the expected value.

The first stage of weight loss of blend 10 (EEA copolymer, 50% $\text{Mg}(\text{OH})_2$), which was due to the decomposition of the filler, started at 305°C and reached T_{\max} at 417°C. There was also small shoulder at the start of the first stage which was not present when the filler was degraded alone. The second stage of degradation started at 423°C and reached T_{\max} at 485°C (Fig. 5.10). There was slight destabilisation initially but after 2% weight loss stabilisation reached up to 20°C and was maintained throughout the degradation.

Blend 11 (EEA copolymer, 50% MgO) almost showed one stage degradation starting at 325°C with T_{\max} at 484°C. However, there was a small hump with T_{\max} at 387°C (Fig. 5.11). The stabilisation which started after 5% weight loss reached up to about 17°C.

Weight loss of blend 12 (EEA copolymer, 50% TiO_2) only showed one stage degradation starting at about 350°C and with T_{\max} at 473°C (Fig. 5.12). Nevertheless, there was a stabilisation, starting from the beginning and gradually increasing up to about 8°C. After about 48.5% weight loss at 480°C, however, the blend showed destabilisation compared to the calculated behaviour.

Table 5.2. (a) TG Results Under Nitrogen

Temperatures shown in brackets are calculated values assuming that there was no interaction between the components.

| Sample | T _{thresh} (°C) | T ₅₀ (°C) | T _{max} (°C) | T _{stop} (°C) | % residue at 600°C |
|---------------------|--------------------------|----------------------|-----------------------|------------------------|--------------------|
| Blend 1 | 387 (375) | | 481 | 490 (490) | 49.75 (49.75) |
| Blend 2 | 325 (300) | 408 (422) | 409, 490 | 550 (550) | 33.25 (32.90) |
| Blend 3 | 350 (350) | 461 (457) | 440, 471 | 525 (525) | 31.00 (31.98) |
| Blend 4 | 350 (350) | 500 (550) | 435, 475 | 500 (500) | 49.55 (49.23) |
| Blend 5 | 350 (350) | 505 | 450, 485 | 505 (500) | 49.75 (49.75) |
| Blend 6 | 275 (350) | 512 (500) | 437, 485 | 512 (500) | 49.75 (49.50) |
| Blend 7 | 367 (350) | 500 | 448, 480 | 500 (500) | 49.75 (50.00) |
| Blend 8 | 275 (300) | 490 (482) | 437, 480 | 510 (500) | 47.50 (48.50) |
| Blend 9 | 225, 375 (212), (375) | 471 (455) | 320, 477 | 515 5000 | 35.25 (32.70) |
| Blend 10 | 305, 423 (305), (410) | 476 (457) | 419, 485 | 515 (500) | 36.00 (35.30) |
| Blend 11 | 325 (325) | 486 (472) | 484 | 505 (495) | 46.50 (48.00) |
| Blend 12 | 350 (350) | 482 | 473 | 500 (500) | 48.25 (50.45) |
| CaCO ₃ | 375 | | | | 97.75 |
| Al(OH) ₃ | 212 | | 292 | 325 | 64.50 |
| Mg(OH) ₂ | 325 | | 405 | 450 | 70.25 |
| MgO | 25 | | | 400 | 95.25 |
| TiO ₂ | | | | | 100 |

5.2.2.1.2. TG-DTG Under Air

Thermogravimetric experiment was performed for blend 4 under an atmosphere of air for the purpose of comparison with the results obtained under nitrogen.

Blend 4 started to decompose at 250°C but the degradation process was extremely slow such that it reached the main T_{\max} at 448°C. There was not any stabilisation initially (Fig. 5.4) but after 4% weight loss at 325°C, the degradation process slowed down and TG curve moved up to 50°C towards higher temperature. The degradation process speeded up again after 43% weight loss and another degradation stage started to develop at 575°C. The degradation process is much more complicated than when degradation was carried out in inert atmosphere. TG results (Table 5.2 (a-b)) and traces (Fig. 5.4) show that blend 4 is 50-75°C more stable in inert atmosphere than in the air. However, there was a significant shift towards higher temperature in the dynamic weight loss curve in air but not in nitrogen.

Table 5.2. (b) TG Results Under Air

Temperatures shown in brackets are calculated values assuming that there was no interaction between the components.

| Sample | T_{thresh} (°C) | T_{max} (°C) | T_{50} (°C) | T_{stop} (°C) | % residue at 600°C |
|-------------------|--------------------------|-----------------------|---------------|------------------------|--------------------|
| Blend 4 | 325 (300) | 355 and 445 | 463 | 468 (550) | 49.50 (50.00) |
| CaCO ₃ | 375 | | | | 97.75 |

5.2.2.2. Differential Scanning Calorimetry (DSC)

DSC was carried out from room temperature to 650°C at a programmed rate of 10°C/min under an atmosphere of dynamic nitrogen, with a flow rate of 50 ml/min. The sample size was approximately 6.67 mg.

The DSC curve for blend 4 exhibits three endothermic transitions as shown in Fig. 5.13. The peak temperatures occur at about 110°C and 448°C (average) 485°C (average). The first can be assigned to the melting point, T_m , while the other two are due to degradation of the copolymer. The temperature for the maximum rate of degradation agrees within 10-13°C with the TG results.

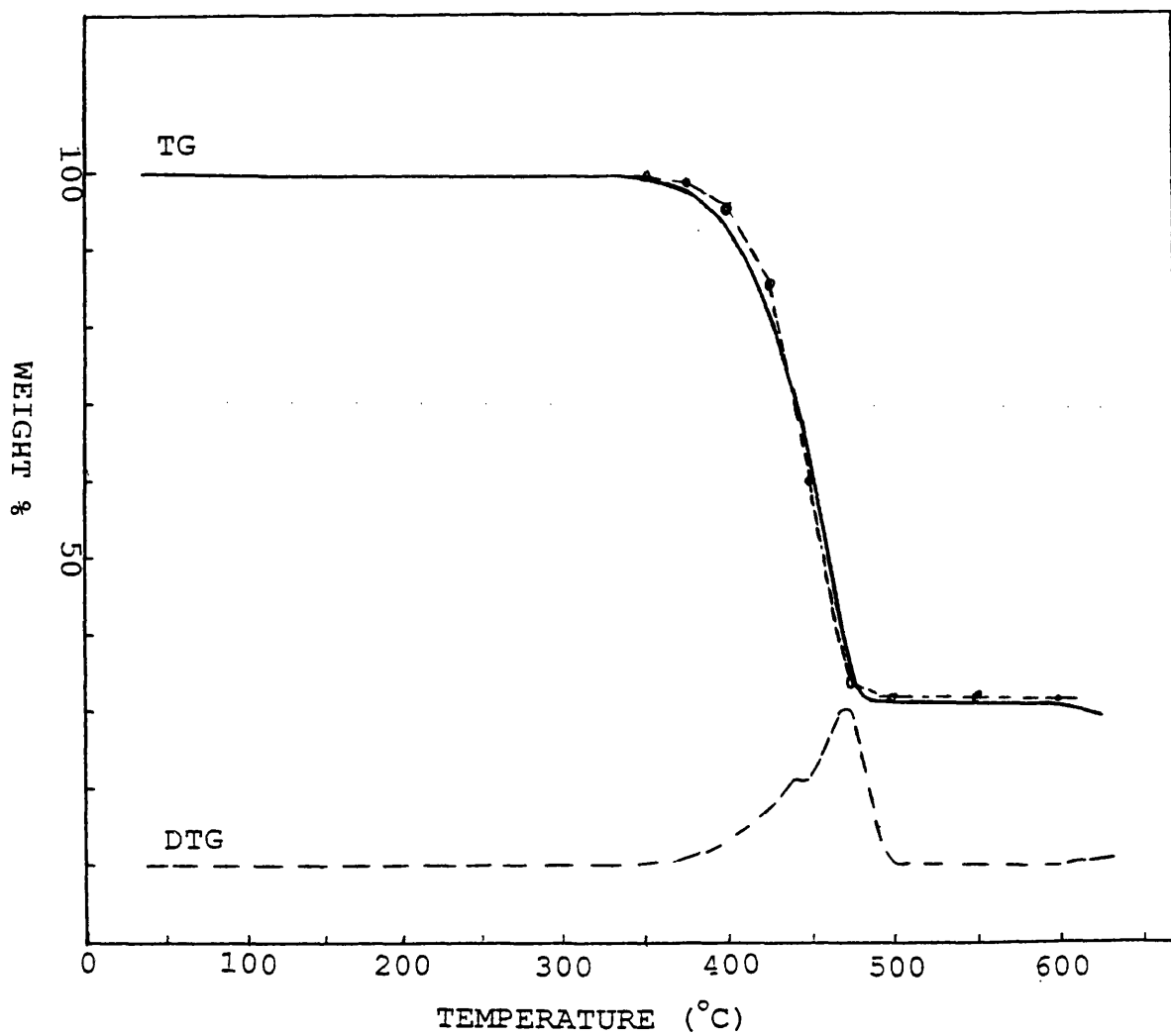


Fig. 5.3. TG-DTG curves for blend 3: experimental (—; ----) and calculated (◆◆◆) under nitrogen.

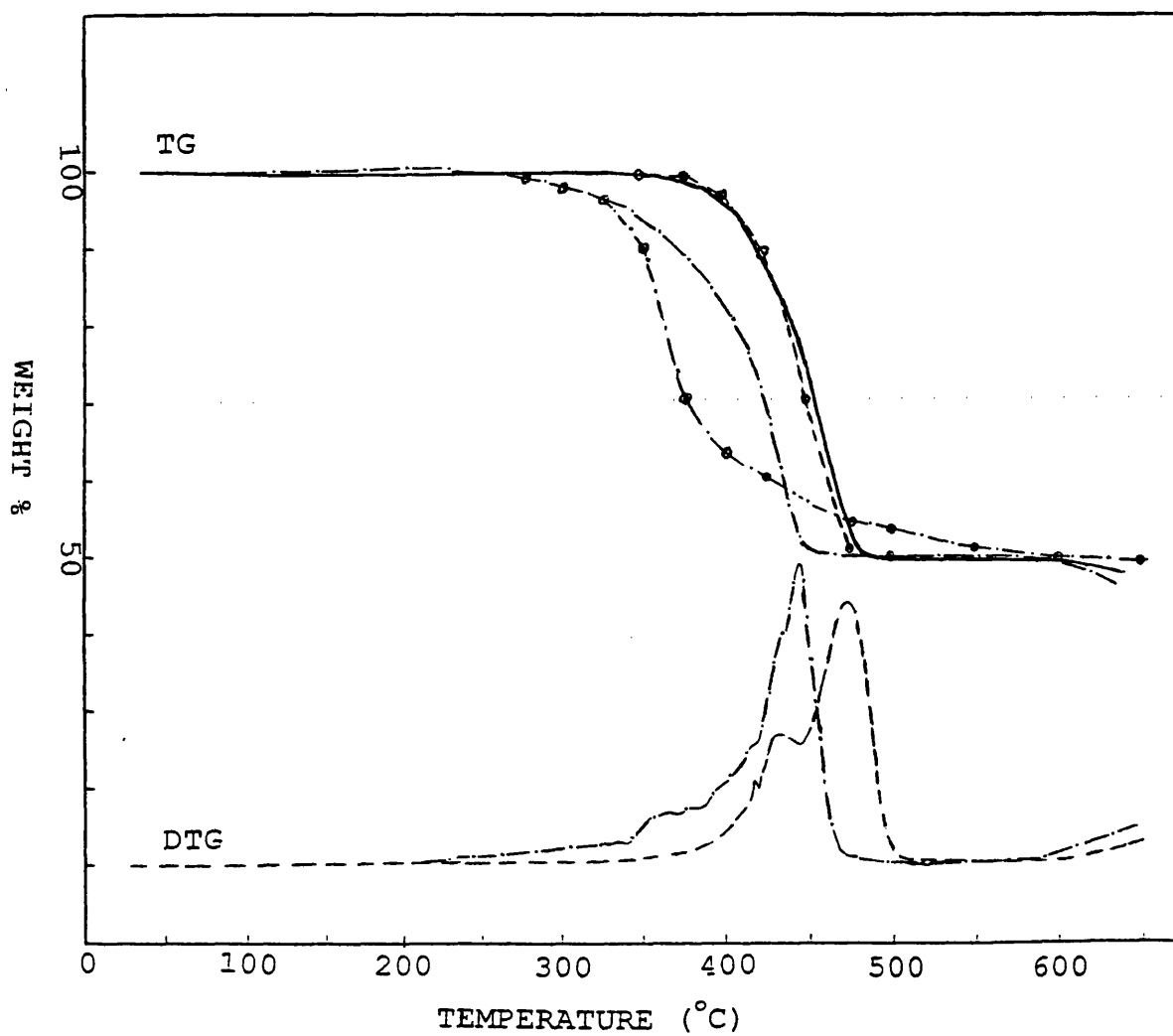


Fig. 5.4. TG-DTG traces for blend 4 under nitrogen: experimental (—; ----) and calculated (—•—), and air: experimental (---) and calculated (—•—).

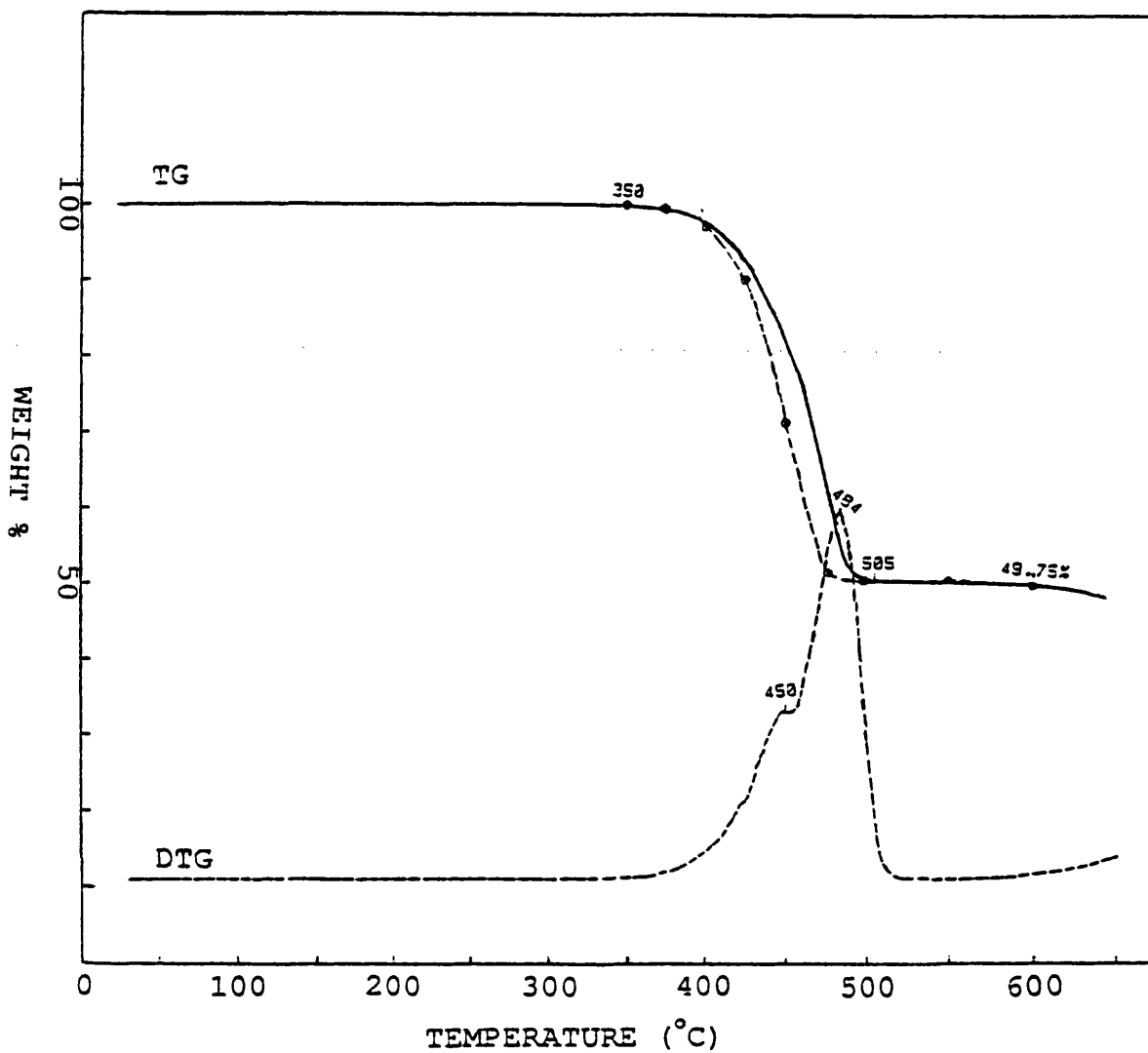


Fig. 5.5. TG-DTG traces for blend 5 under nitrogen: experimental (—; ----) and calculated (— · —).

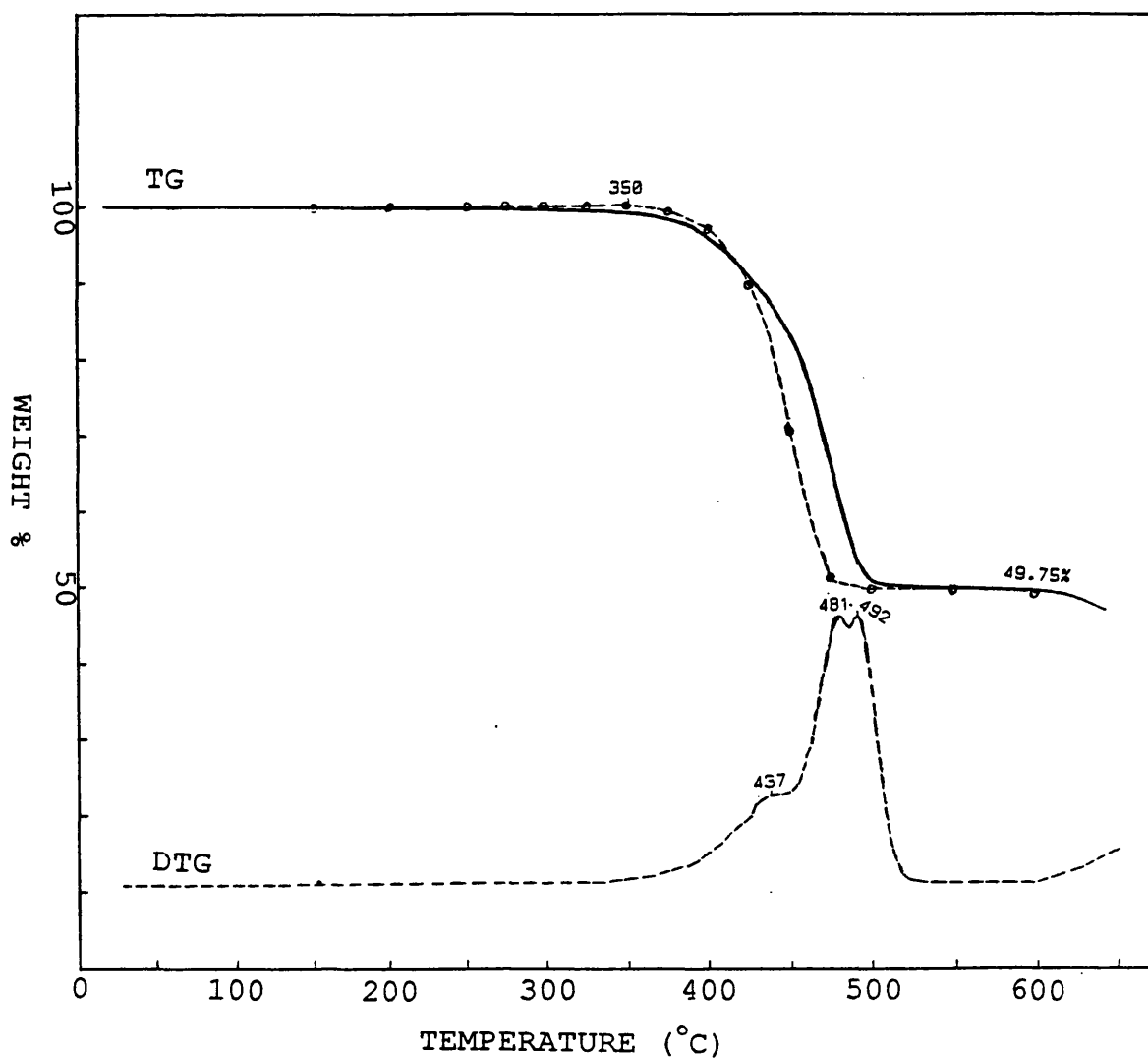


Fig. 5.6. TG-DTG traces for blend 6 under nitrogen: experimental (—; ----) and calculated (— + —).

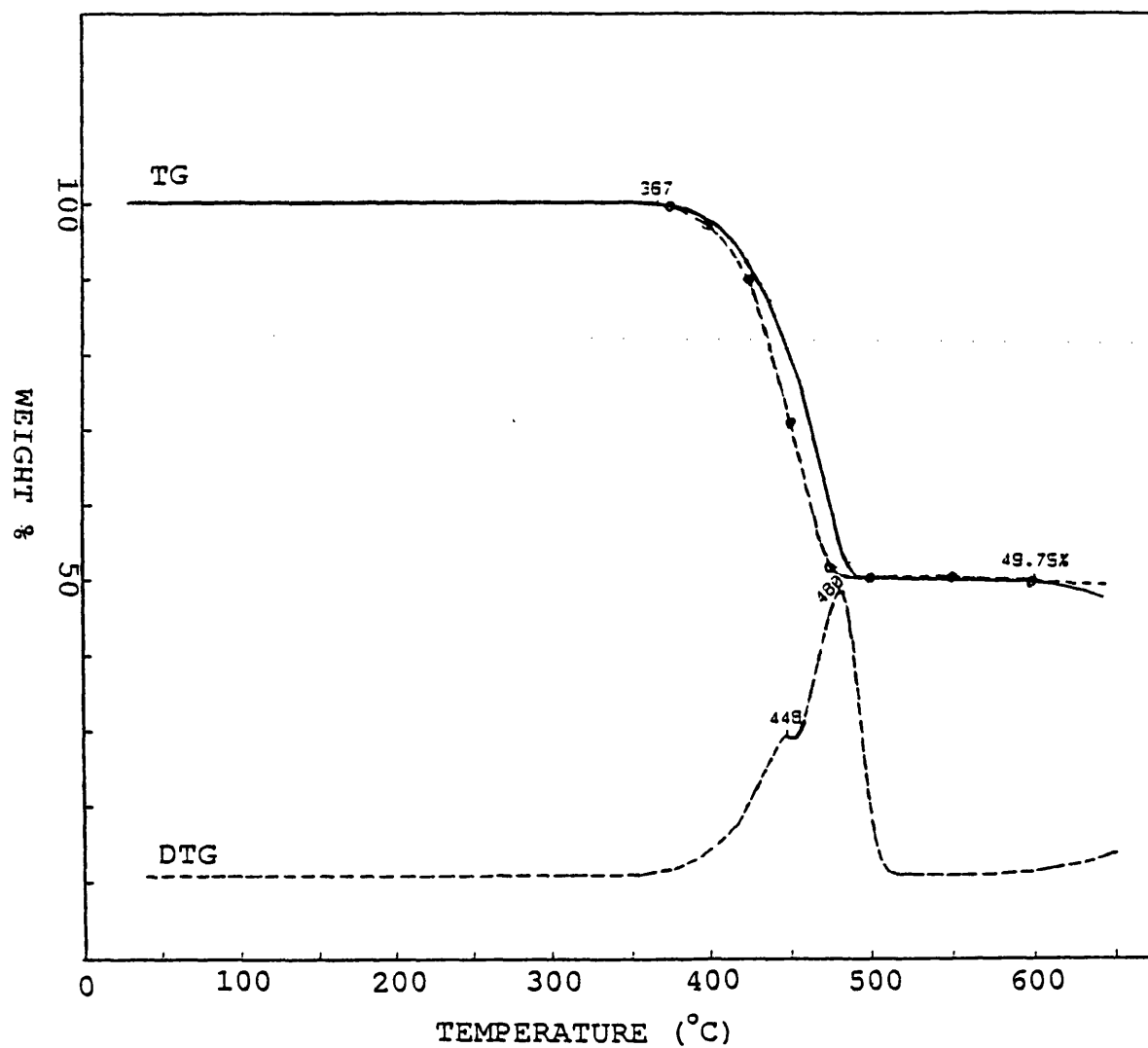


Fig. 5.7. TG-DTG traces for blend 7 under nitrogen: experimental (—; ----) and calculated (— · —).

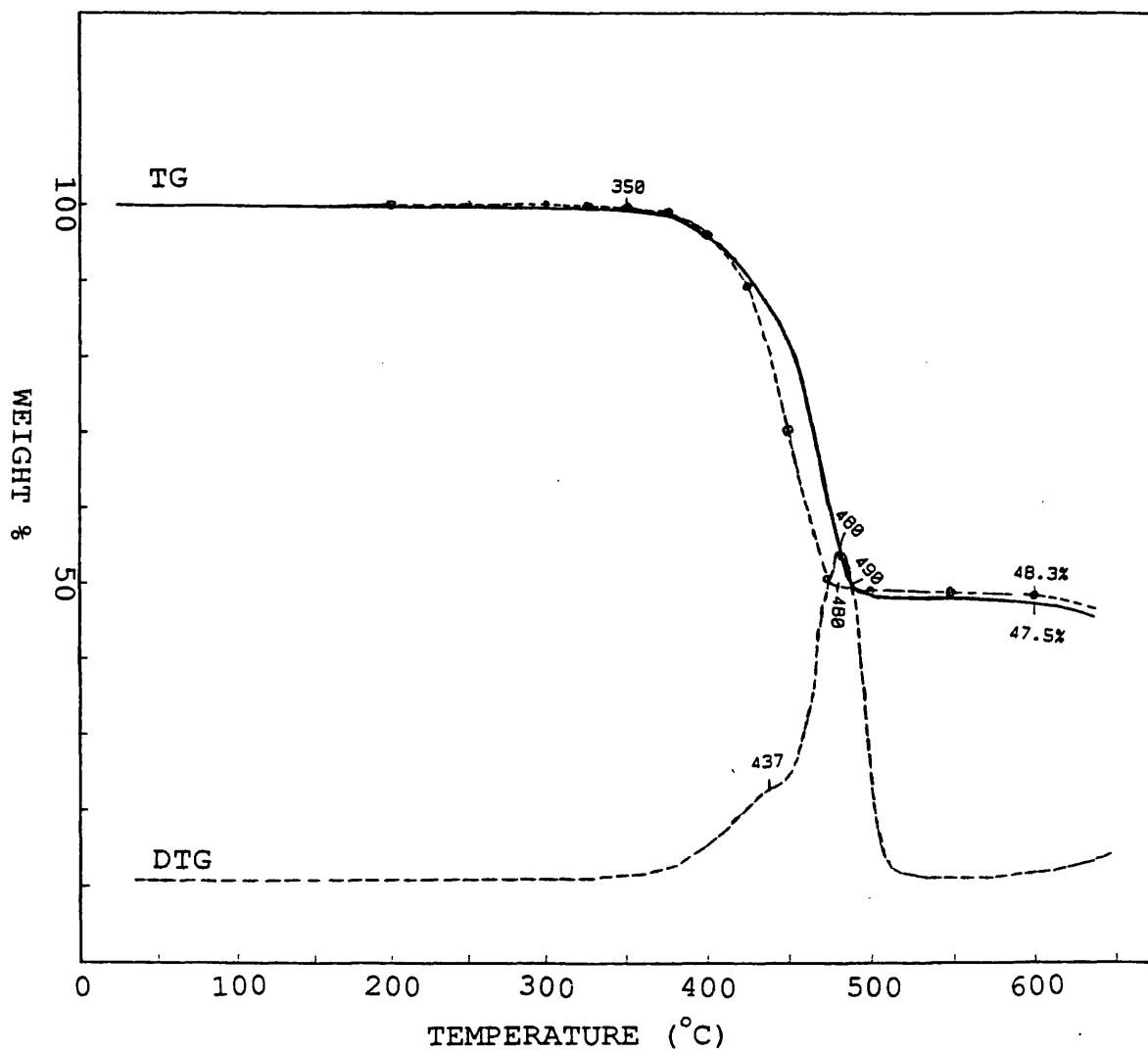


Fig. 5.8. TG-DTG traces for blend 8 under nitrogen: experimental (—; ···) and calculated (— · —).

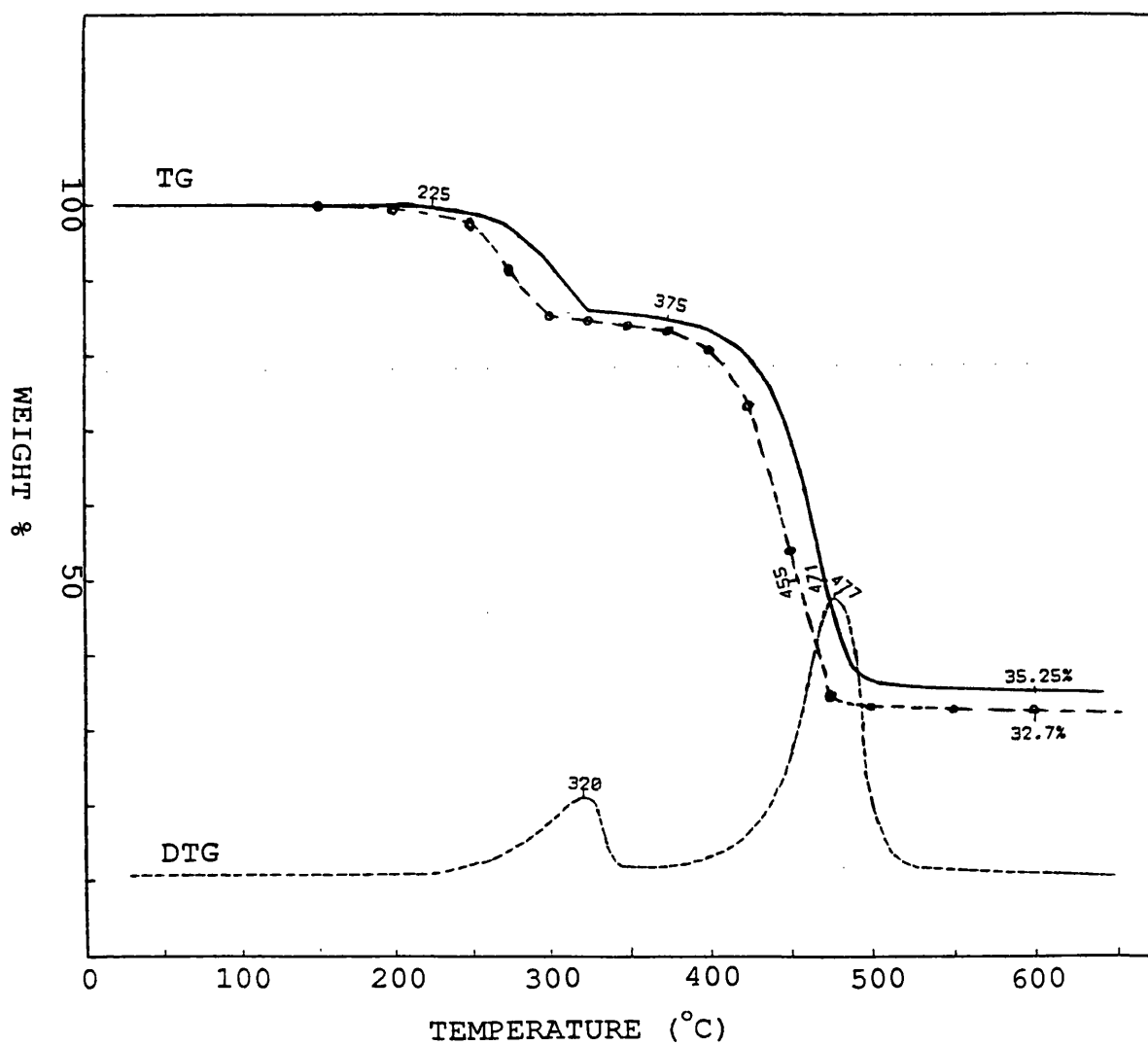


Fig. 5.9. TG-DTG traces for blend 9 under nitrogen: experimental (—; ----) and calculated (—→—).

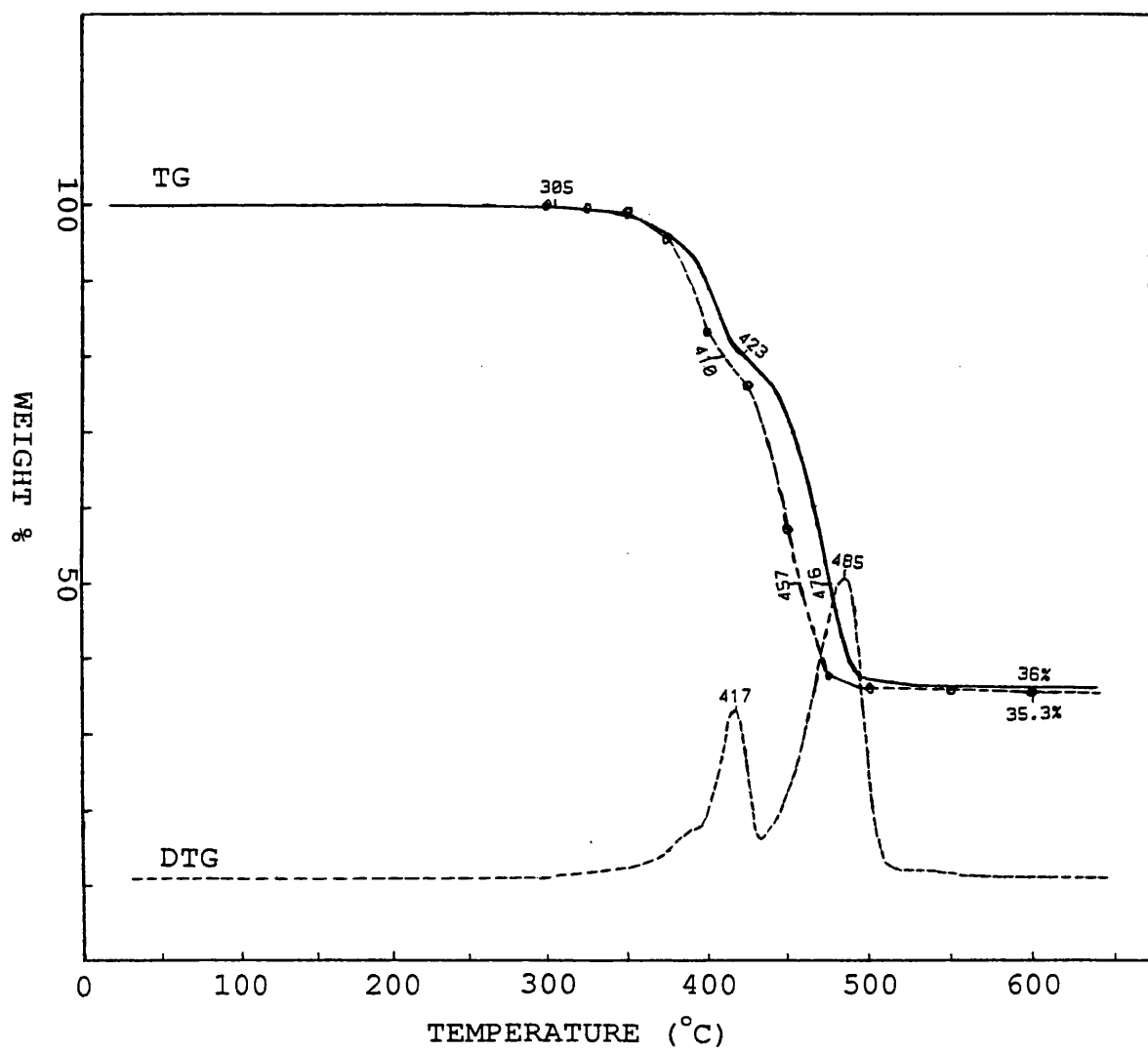


Fig. 5.10. TG-DTG traces for blend 10 under nitrogen: experimental (—; ----) and calculated (— + —).

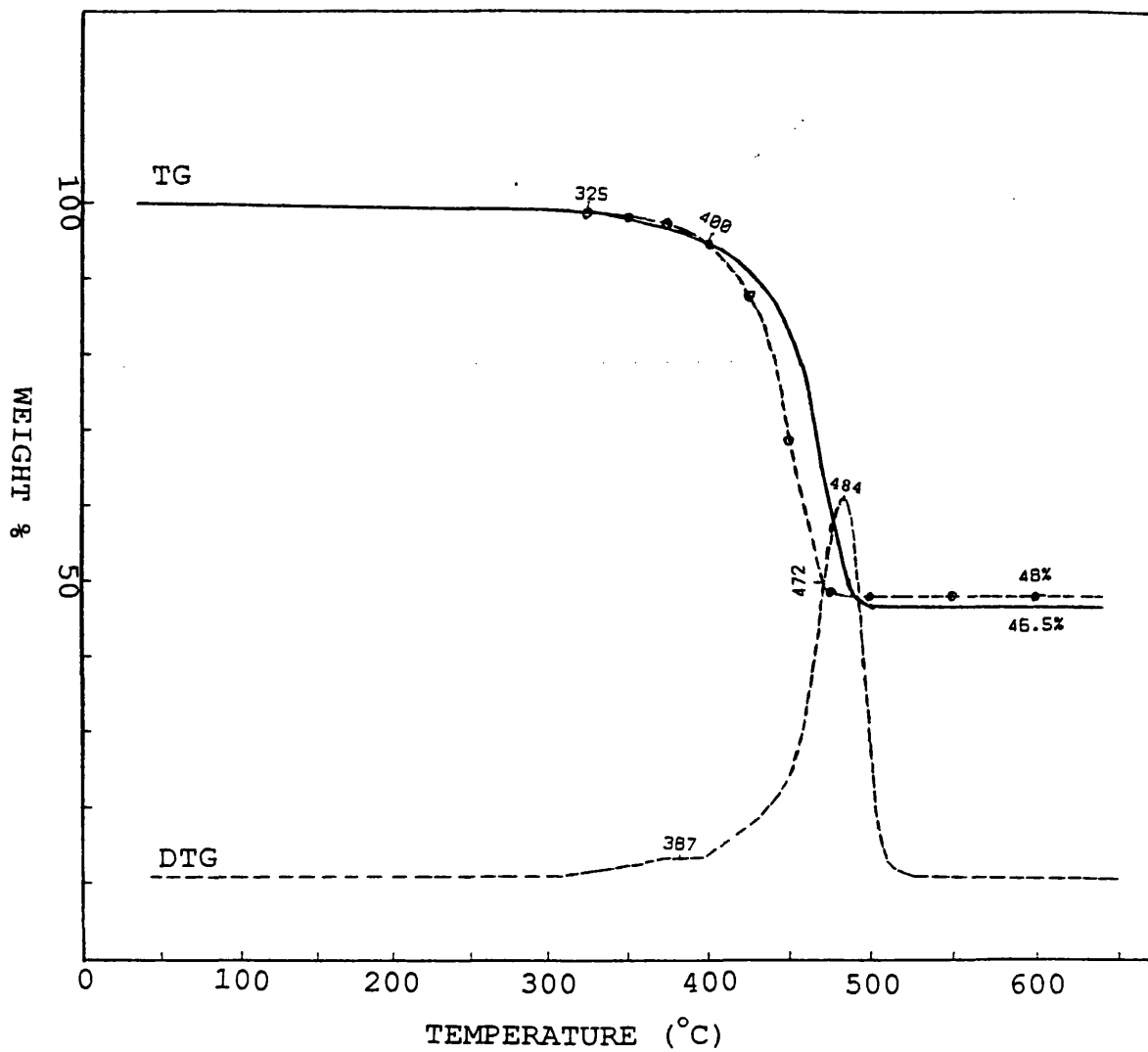


Fig. 5.11. TG-DTG traces for blend 11 under nitrogen: experimental (—; ----) and calculated (—•—).

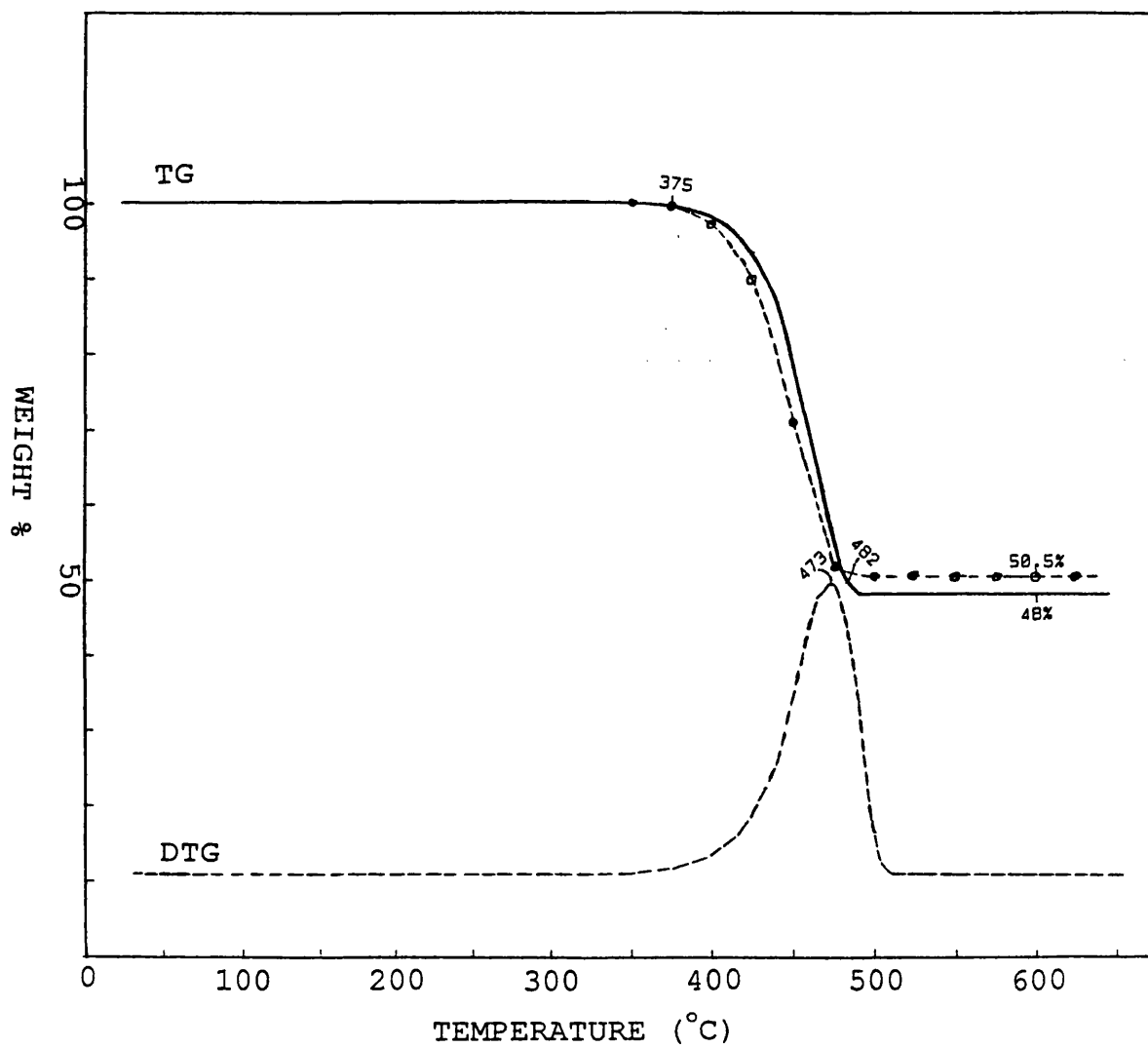


Fig. 5.12. TG-DTG traces for blend 12 under nitrogen: experimental (—; —) and calculated (—○—).

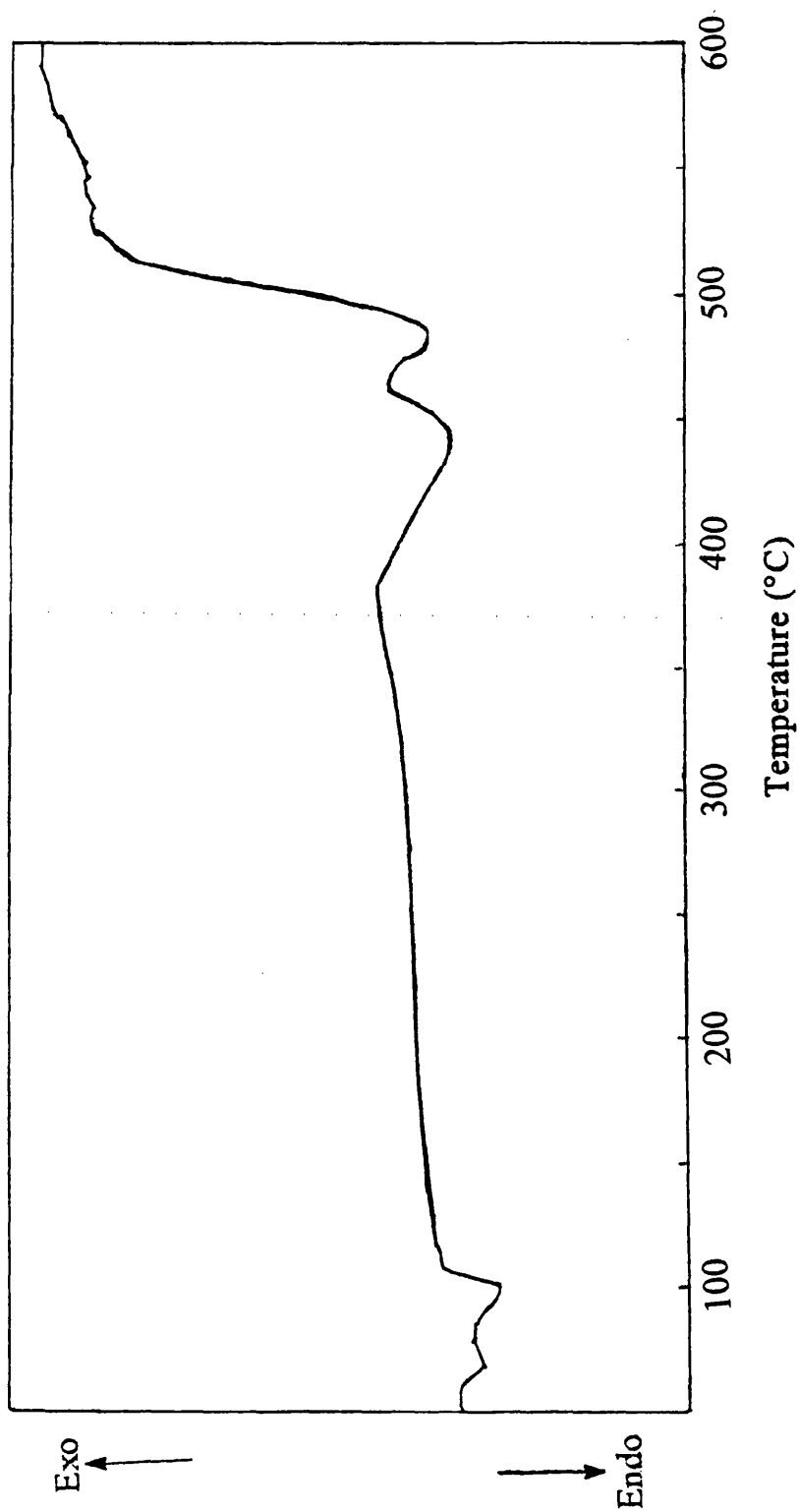


Fig. 5.13. DSC trace for blend 4 (EEA copolymer + 50% coated CaCO_3 with mean particle size of 1.5μ) under nitrogen.

5.2.2.3. Thermal Volatilisation Analysis (TVA) and SATVA Separation of Condensable Degradation Products

Blend of LDPE and CaCO₃

The TVA curve of blend 1 (Fig. 5.14) showed that volatilisation started at about 387°C and led to a single peak with T_{\max} at 476°C. The TVA trace from the gauge after the liquid nitrogen trap (-196°C) showed a very small rise, almost negligible, from the baseline indicating a very small amount of non-condensable gaseous products, identified as H₂ and CH₄ by the quadrupole mass spectrometer attached to the TVA line.

The SATVA trace (Fig. 5.14 (a)) for the separation of the condensable volatile products of degradation of blend 1 did not show a peak at the beginning due to ethylene and ethane, however, two sharp peaks were present, after which the trace became broad with poorly resolved peaks. The later material was therefore collected as one fraction. The first fraction was shown by IR spectroscopy and MS to consist of propene and propane while the second fraction was due to butene and butane. The final fraction was characterised by GC-MS and the results show that the degradation products are similar to those when LDPE was degraded alone (results are given in Table 3.5, Chapter 3) but smaller in quantity.

The CRF collected was a white solid material of which some was powdery while other parts were elastomeric like the original polymer. The IR spectrum of the CRF was similar to that of the original polymer except that in the present case it showed absorptions for the unsaturated C=C bonds. A similar observation was made in the case of the CRF from LDPE when it was degraded alone (Fig. 3.16 (a), Chapter 3).

The residue spread on the surface of the tube on melting covering a large area of the degradation tube like the original polymer when degraded alone, and was easily to be removed from the surface of the tube. The IR spectrum of the residue (similar in appearance to that of CaCO₃) did not show absorptions due to the undegraded or partially degraded polymer thus indicating complete decomposition of the polymer.

Blend of PEA and CaCO₃

TVA trace of blend 2 (Fig. 5.14 (b)) was similar in shape to that of the original polymer when degraded alone but showed 10-15°C stabilisation. Volatilisation started just before 300°C and reached maximum rate (T_{\max}) at a temperature of about 440°C. There was evidence for the evolution of non-condensable gaseous products (degradation

products not trapped at -196°C under normal TVA conditions), identified as carbon monoxide and with traces of H_2 by the quadrupole mass spectrometer attached to the TVA line.

The SATVA trace for the separation of the condensable volatile products of degradation of blend 2, showed three peaks or three fractions similar to the SATVA trace from PEA when it was degraded alone (Fig. 3.9, Chapter 3). The degradation products were also found to be identical to the degradation products when PEA was degraded alone (GC-MS results are given in Table 3.4, Chapter 3). However, the quantity of the degradation products varies as was seen from the area under the SATVA traces, IR spectra and GC traces. It was found that the production of ethylene and CO_2 was almost equal when PEA was degraded alone while in the present case the production of CO_2 was less than ethylene while the total production of CO_2 and ethylene increased than in the case of pure polymer. There was also increase in the production of ketene, $\text{CH}_2=\text{C}=\text{O}$.

The cold ring fraction (CRF) of degradation products was a viscous yellowish brown liquid while the residue was dark brown and was difficult to break. It was obvious from the state of the residue that the polymer did not spread on the surface of the TVA tube on melting whereas it spread on the surface of the TVA tube when it was degraded alone. CRF and residue were analysed by IR spectroscopy.

The IR spectrum (Fig. 5.15. (a)) of the CRF was found to be similar to the IR spectrum of the CRF from PEA when degraded alone (discussed in Chapter 3) except that in the present case the carbonyl peak at 1734 cm^{-1} became slightly broadened instead of splitting into peaks with absorptions at 1760 cm^{-1} and 1801 cm^{-1} .

The IR spectrum of the residue (Fig. 5.15. (a)) was similar to the IR spectrum of coated CaCO_3 showing weak absorptions due to C-H stretching of the methylene groups at 2928 cm^{-1} and 2872 cm^{-1} . These bands show that there is small amount of polymeric material present in the residue but without ester groups. Any other changes which might have occurred were masked by the strong carbonate ion absorption and to see these changes, the residue was extracted with dichloromethane to separate polymeric material, but without any success. This shows that there was some interaction between the components.

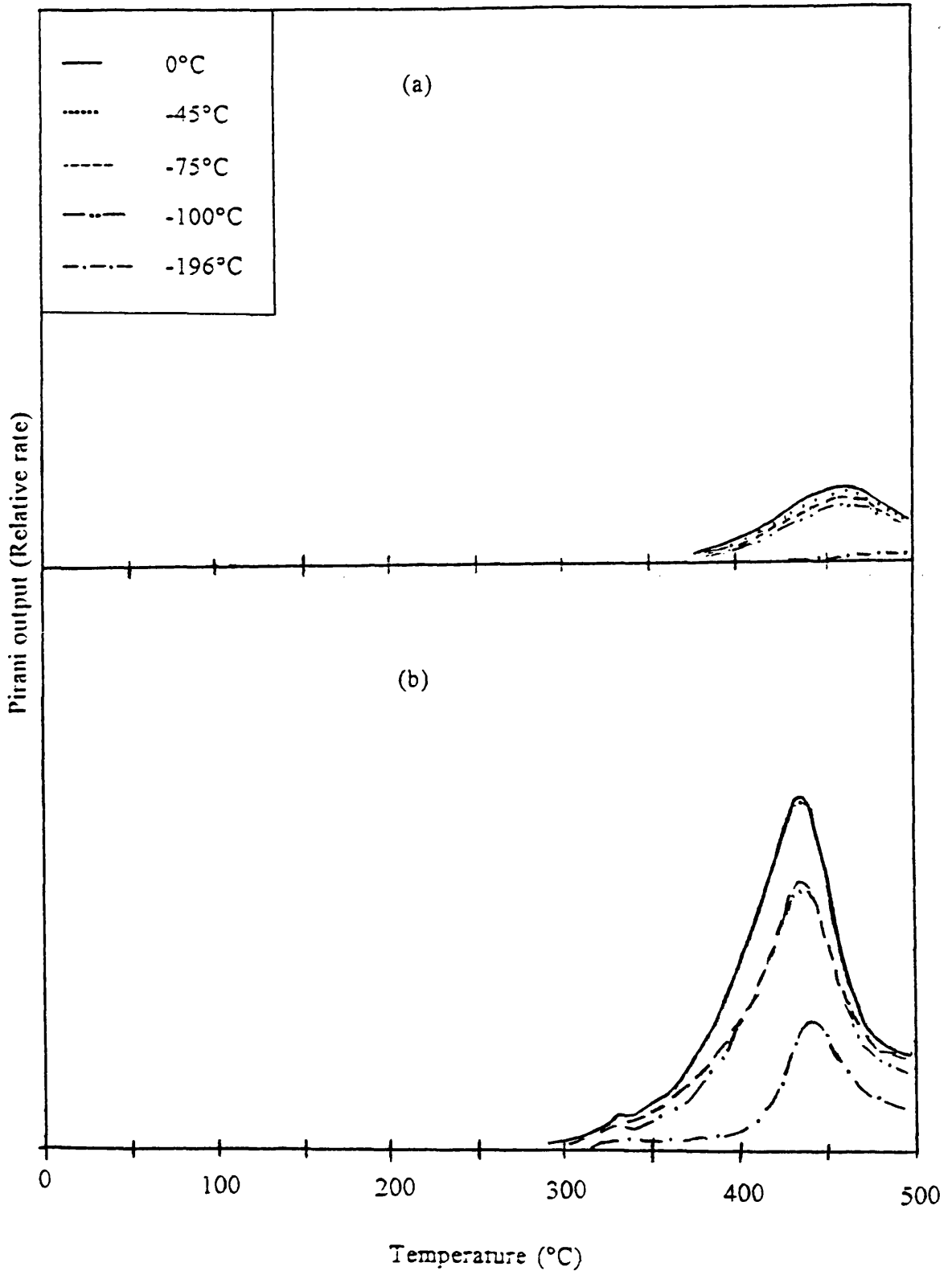


Fig. 5.14. TVA traces for blends: (a) blend 1 (LDPE:BP77 + 50% CaCO₃) and (b) blend 2 (PEA + 31.6% CaCO₃), in both cases using coated CaCO₃ with mean particle size of 1.5 μ .

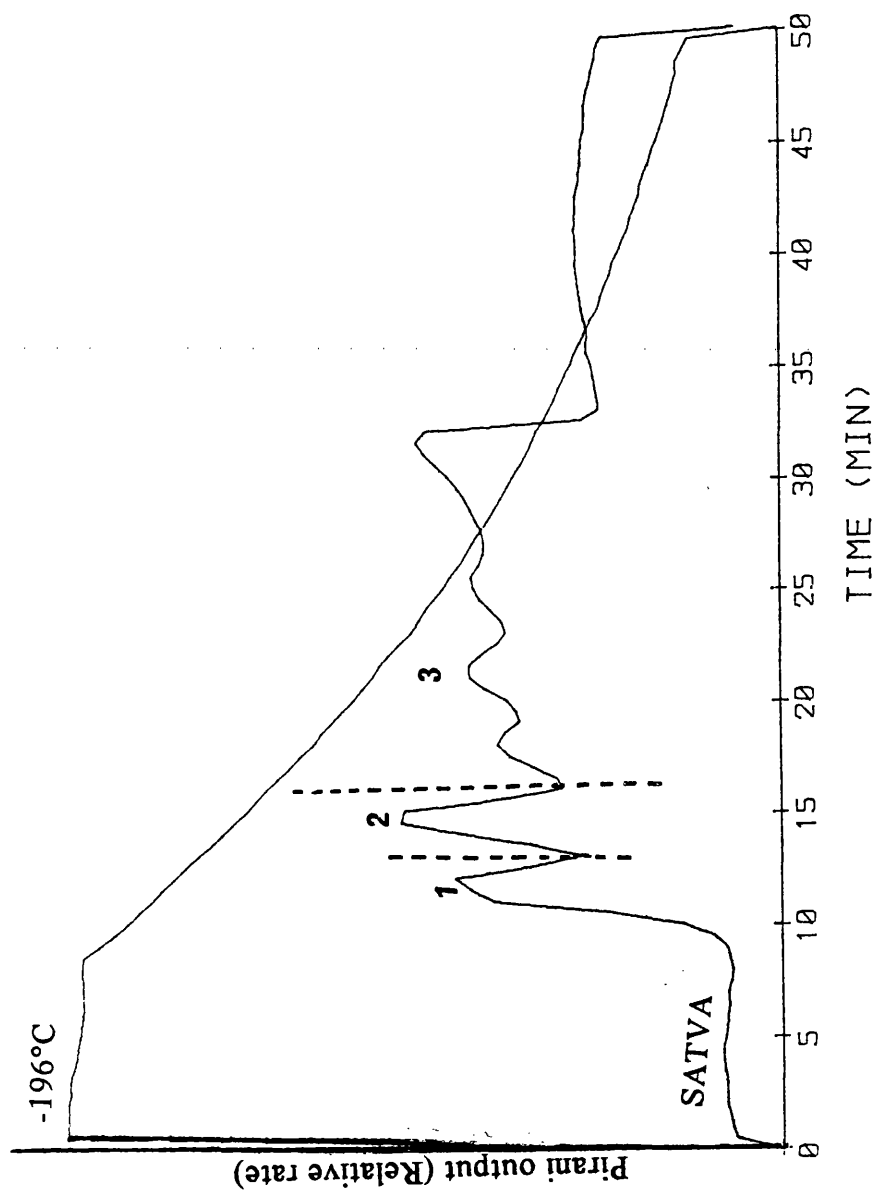


Fig. 5.14. (a) SATVA trace for warm up from -196°C to ambient temperature of condensable volatile products from degradation for blend 1 (LDPE:BP77 + 50% CaCO₃).

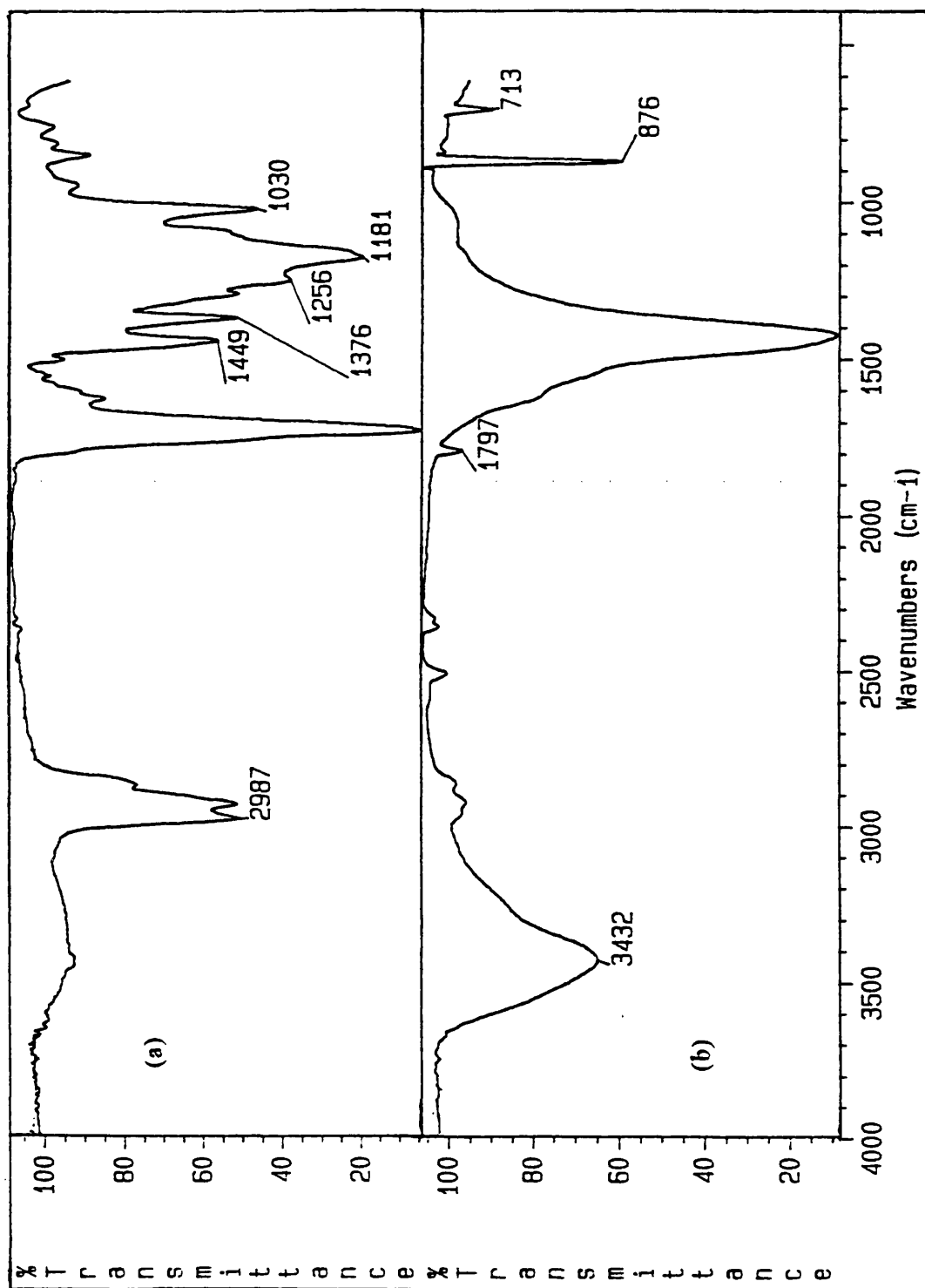


Fig. 5.15. IR spectra of (a) CRF and (b) residue from blend 2.

Blends of EEA Copolymer and CaCO₃

The TVA curves of the blends 3 and 4 started to decompose at the normal decomposition temperature of EEA copolymer at about 350°C (T_{onset}) but the degradation in this case was in two stages instead of just one stage as was the case when EEA copolymer was degraded alone.

The TVA traces of the blends 5-8 (blends of EEA copolymer with different particle sized, coated and uncoated CaCO₃) showed that all nearly started to volatilise at about 343°C, showed two stage degradation followed by a low plateau region, had less level of rate of volatilisation for the non-condensable gaseous products and gave similar volatile compounds but the amount of the degradation products varied from one blend to the other as was seen from the area under the peaks in the SATVA traces and under the IR absorption peaks. TVA traces of blends 4 and 7 are given in Figure 5.16.

The non-condensable products, identified as soon as they were formed using the quadrupole mass spectrometer attached to the TVA line, were found to be mainly carbon monoxide and hydrogen with traces of methane, in smaller amount than when EEA copolymer was degraded alone (discussed in Chapter 3) or with PDMS or with PDMS and CaCO₃ (discussed later in Chapters 6 and 8, respectively). The TVA trace also showed two degradation stages instead of just one as in the case of EEA copolymer.

The CRFs from all blends were darker in colour than the CRF from the EEA copolymer when degraded alone. Microanalysis results for the CRF from the blend 4 showed decrease in oxygen and hydrogen content which may be due to the decomposition of about half of the ester groups and introduction of unsaturation possibly at those points. GC trace (Fig. 5.17) shows the presence of alkenes and their corresponding alkanes up to C₃₈H₇₆. These long chained hydrocarbons are also result of the decomposition of the ester groups. The IR spectroscopy of the CRFs also showed decrease of ester groups and the presence of C=C double bounds. The IR spectra of the CRFs were similar to the IR spectrum of the CRF from the EEA copolymer (discussed in Chapter 3) except there was no absorption at 1815 cm⁻¹ and 1708 cm⁻¹ while there was an extra absorption at 1725 cm⁻¹.

Residues from all blends were yellow in colour, except from blend 8, tended to spread slightly on the TVA tube, were difficult to remove from the tube and did not crumble to powder. Their IR spectra gave absorptions for the C-H stretch of CH₂

groups at 2923 cm^{-1} and 2849 cm^{-1} . The residue from blend 8 (with precipitated filler) was slightly lighter colour than the others, puffed up like pop corn and crumbled to powder when disturbed. The IR spectra of residues from blends 4 and 8 are given in Fig. 5.18 (a) and (b) respectively.

The SATVA trace for the separation of the condensable volatile products of degradation of blends 3-8 showed three gaseous product peaks, and the remaining material gave a broad, poorly resolved peak showing a number of different degradation products. The first peak was due to ethylene and ethane, the second peak was due to carbon dioxide (major) and ketene (trace amount in most blends) while the third peak was attributed to propene, butene and their corresponding saturated hydrocarbons.

SATVA traces of blends 6 and 8 (both with coated CaCO_3 0.9 and 0.06 microns, respectively) showed that peak 2 which was due to CO_2 and ketene was larger than that due to ethylene while other blends in this series showed the reverse affect. However, the IR spectra of products from peak 2 showed that blends 6 and 8 gave negligible amount of ketene while other blends in this series gave at least trace amount of ketene. This indicates that ketene production also decreased when the particle size of the filler was decreased and the filler was also coated. IR spectra of condensable gaseous products (peaks 1 and 2 from SATVA separation) of degradation from blends 6 and 7 are given in Fig. 5.19 (a) and 5.19 (b) respectively.

The final fraction was collected as a liquid and showed pale yellow and colourless layers, being yellow at the top. The GC-MS technique was applied to characterise this fourth complex mixture of compounds. The results of the GC-MS trace (Fig. 5.20) from blend 4 are given in Table 5.3. The results show that the major degradation products are identical to the degradation products of EEA copolymer when degraded alone except that in the present case production of acids such as acetic and propanoic acid, produced when EEA copolymer was degraded alone, is either in a trace amount or absent.

Although the degradation products of all blends were similar, their quantities varied from one blend to another as discussed above. It was difficult to analyse every compound quantitatively because of the complex mixture of the compounds. Ethanol was analysed semi-quantitatively, however, by measuring area under the GC peak for ethanol. It was found that blend 7 gave more ethanol than other blends while blend 8 gave least.

The IR spectra of the volatile liquid products from the blends, in the gas phase, showed a broad peak at 1760 cm^{-1} . The formation of a lactone, which would absorb at this frequency, could be possible if two or more ethyl acrylate units were together and GC-MS results give evidence from fragmentation pattern, the presence of lactone.

Blend of EEA Copolymer and CaCO_3 Heated up to 600°C

Blend 4 was also degraded up to 600°C and the TVA trace (Fig 5.16 (b)) showed two degradation stages with T_{max} temperatures at 427°C and 480°C respectively. The degradation was completed at about 500°C . The rise for the -196°C trace which was due to the presence of non-condensable degradation products was much less than in the case when EEA copolymer was degraded alone up to 600°C .

The SATVA trace was similar to that when blend 4 was degraded up to 480°C and to that of EEA copolymer when degraded to any temperature above 450°C except that an extra shoulder developed in the broad, poorly resolved peak region. The area under the IR spectrum showed that the production of ethylene was almost same as in the case of pure copolymer while the production of CO_2 was more than double. The production of ketene was almost half of that in the case of copolymer.

The residue was 49.32% which would indicate complete decomposition of copolymer leaving only filler yet the IR spectrum of the residue gave absorptions for the C-H stretch of CH_2 groups at 2923 cm^{-1} and 2849 cm^{-1} . This indicates the presence of residual organic material and hence that some of the filler must have decomposed. Decomposition of filler normally starts after 600°C . There was no indication by TVA of any decomposition occurring between 500°C and the maximum temperature of the experiment, 600°C , so that any filler decomposition must have occurred below 500°C .

Blend of EEA Copolymer and CaCO_3 heated up to 400°C

Blend 4 was also heated up to 400°C and the SATVA trace showed the presence of CO_2 while there was no formation of ethylene which normally accompanies CO_2 production. EEA copolymer when heated up to 400°C did not show presence of CO_2 while there was very small amount of ethylene present. Other degradation products were found to be more than in the case of pure copolymer and the IR spectrum showed that

ethanol was the major product in the case of blend 4 while it was present in a trace amount in the case of pure copolymer.

The residue was smooth and pale yellow in colour at the outside surface when blend 4 was heated up to 400°C and 480°C and turned black when heated up to 600°C while the underlying layer stayed dark grey and was difficult to break or scrape with a spatula due to its smooth outside surface. If, however, the blend was degraded in slightly large lumps, then the middle of the residue was easily broken since it did not become smooth and was more like the original blend before degradation. The residue also only occupied the area where the sample was originally placed before degradation, while it was obvious from the examination of the TVA tube that EEA copolymer when degraded alone spread and spattered on the surface of the TVA tube after melting. IR spectroscopy of the residue (KBr disc), after heating up to 480°C, showed that there still might be some undegraded polymeric material left as the C-H stretch was much more intense than when EEA copolymer was degraded alone. C-H deformations were overlapped by the broad and intense absorption of the CO_3^{2-} ions. EEA copolymer when degraded alone showed very weak and broad absorption at 1710 cm^{-1} , such an absorption would also be masked by the intense and broad absorption of CO_3^{2-} ions.

The residue (after heating up to 400°C) was heated to 110°C in 1-chlorobutane in an attempt to extract the copolymer from the filler. It was noticed that the solvent stayed clear although it was possible to break the residue with a spatula or crush between the fingers. The copolymer did not dissolve. Undegraded blend under the same heating conditions formed a cloudy suspension in the solvent within 5 minutes and the filler and the copolymer could be separated on cooling since the copolymer deposited on the walls of the container while the filler settled at the bottom. However, when thick sections of the blend were degraded then extracted, some cloudiness appeared in the solvent after heating for about an hour but the outside surface still did not dissolve even after long period of heating. This observation was also made when blend 4 was heated up to 480°C. This could only be possible if there was some interaction between the polymer and the filler at least on the surface.

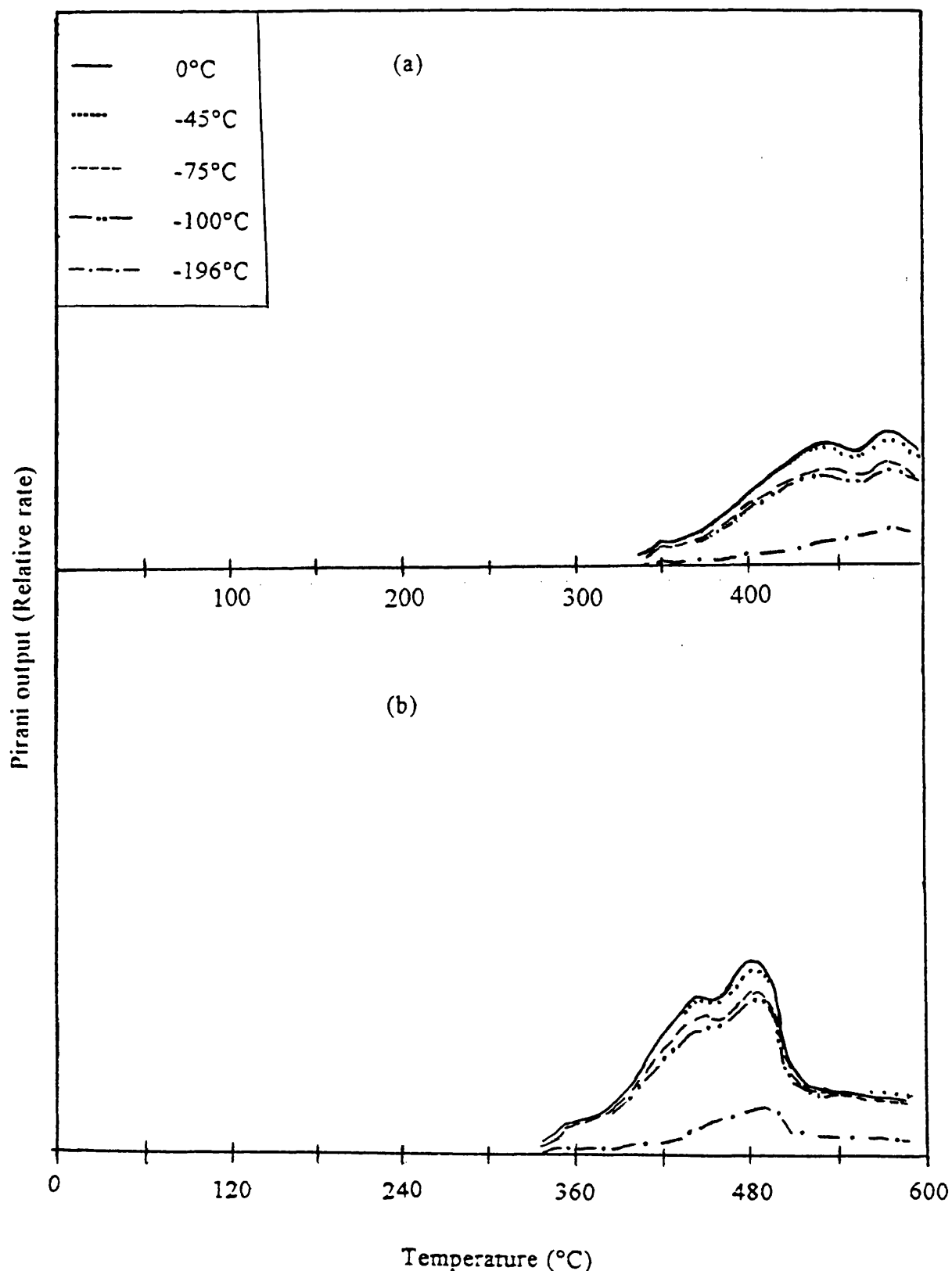
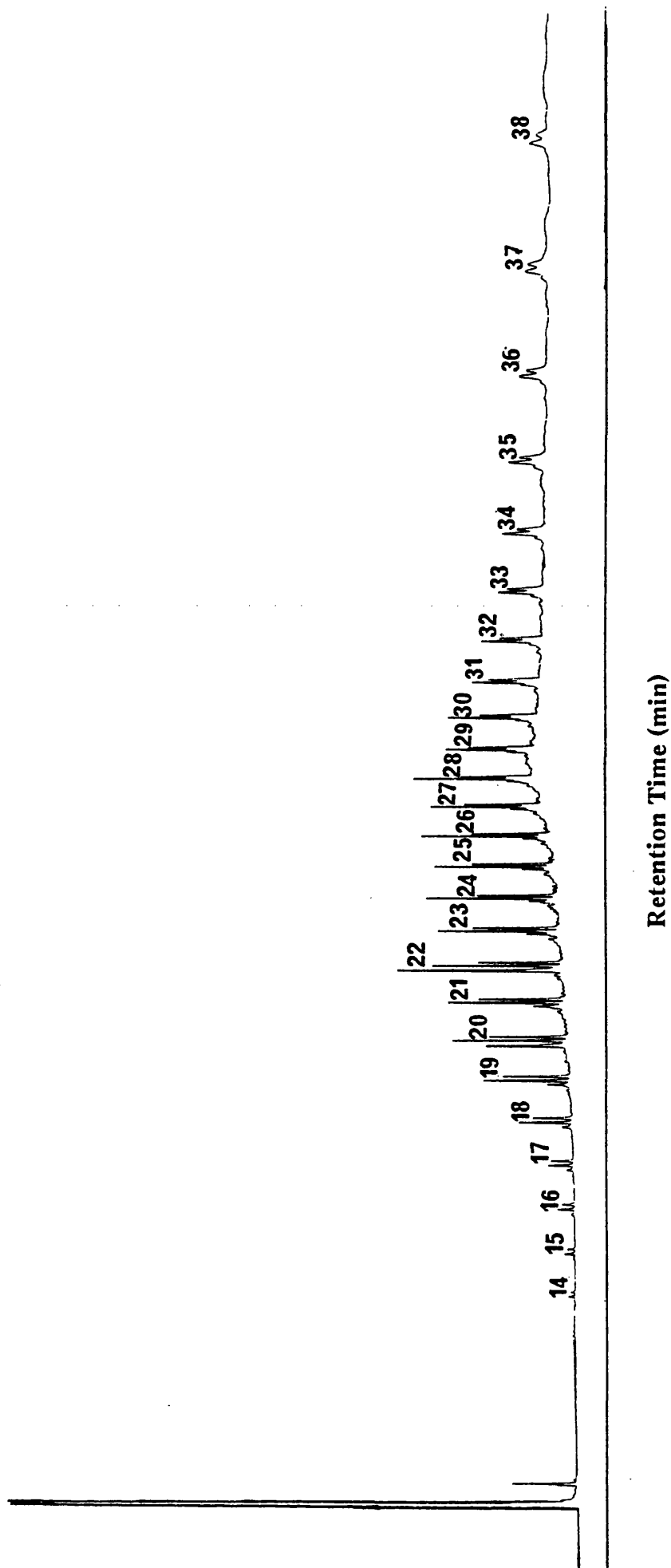


Fig. 5.16. TVA traces for blends of EEA copolymer and 50% coated CaCO_3 : (a) blend 7 (with mean particle size of 5μ) and (b) blend 4 (with mean particle size of 1.5μ).

Fig. 5.17. GC trace for the CRF from blend 4 (EEA copolymer and 50% coated CaCO_3 with mean particle size of 1.5μ).



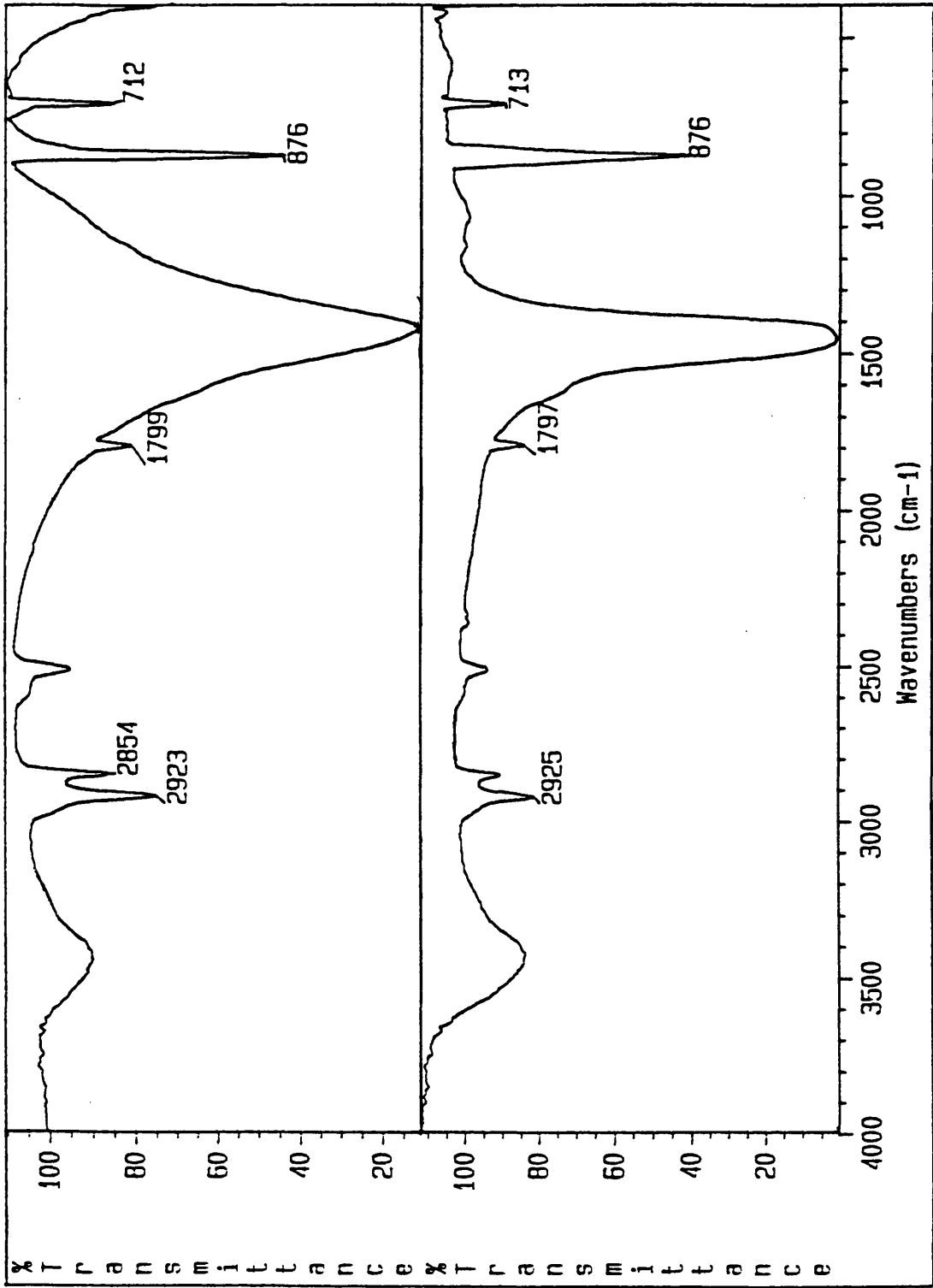


Fig. 5.18. IR spectra for residues from blends of EEA copolymer and 50% coated CaCO₃: (a) blend 4 (with mean particle size of 1.5 μ) and (b) blend 8 (precipitated and with mean particle size of 0.06 μ).

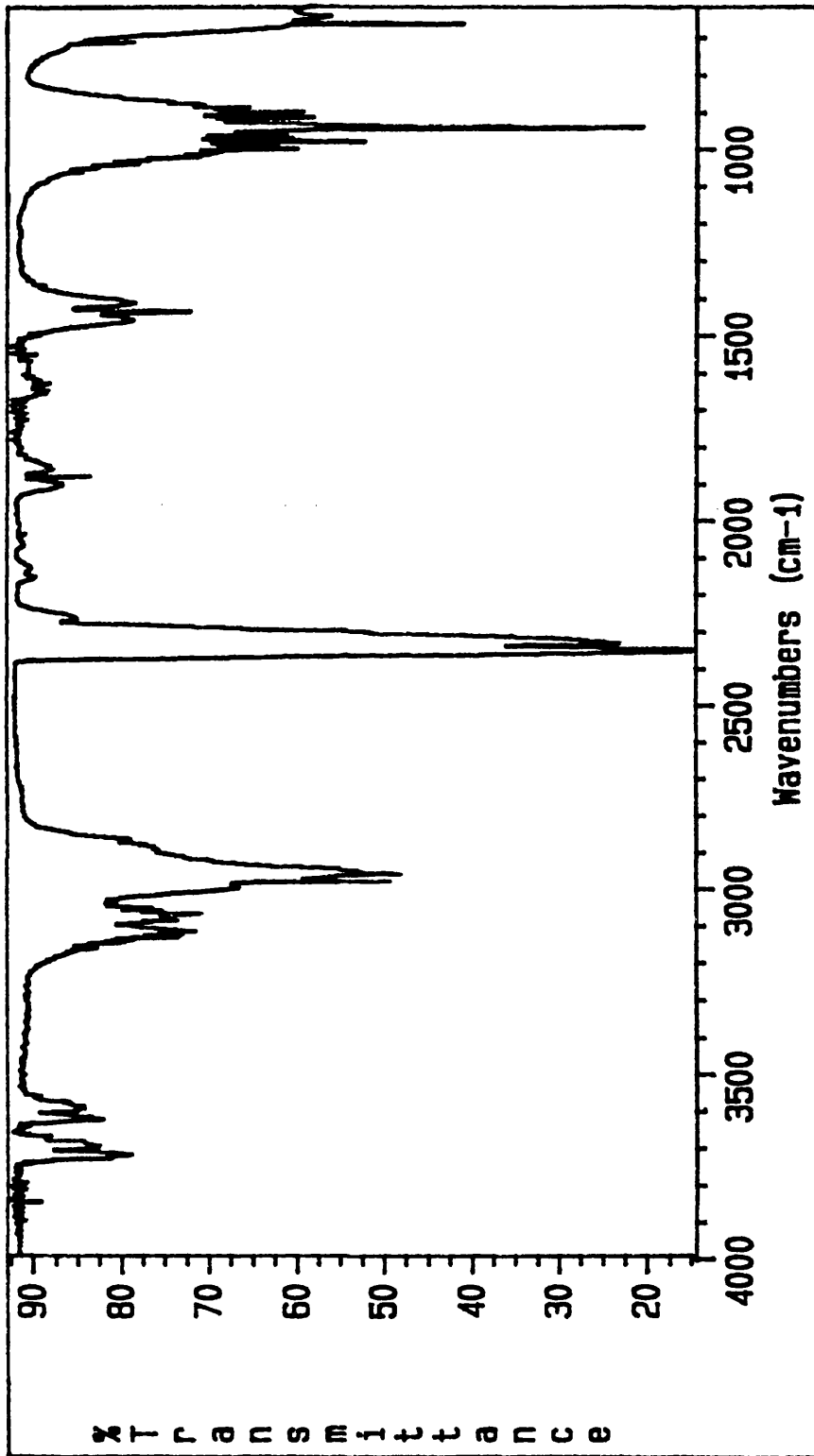


Fig. 5.19. (a) IR spectra of the volatile products from the first two peaks of SATVA from the degradation of blend 6 (EEA copolymer and 50% coated CaCO₃ with mean particle size of 0.9 μ).

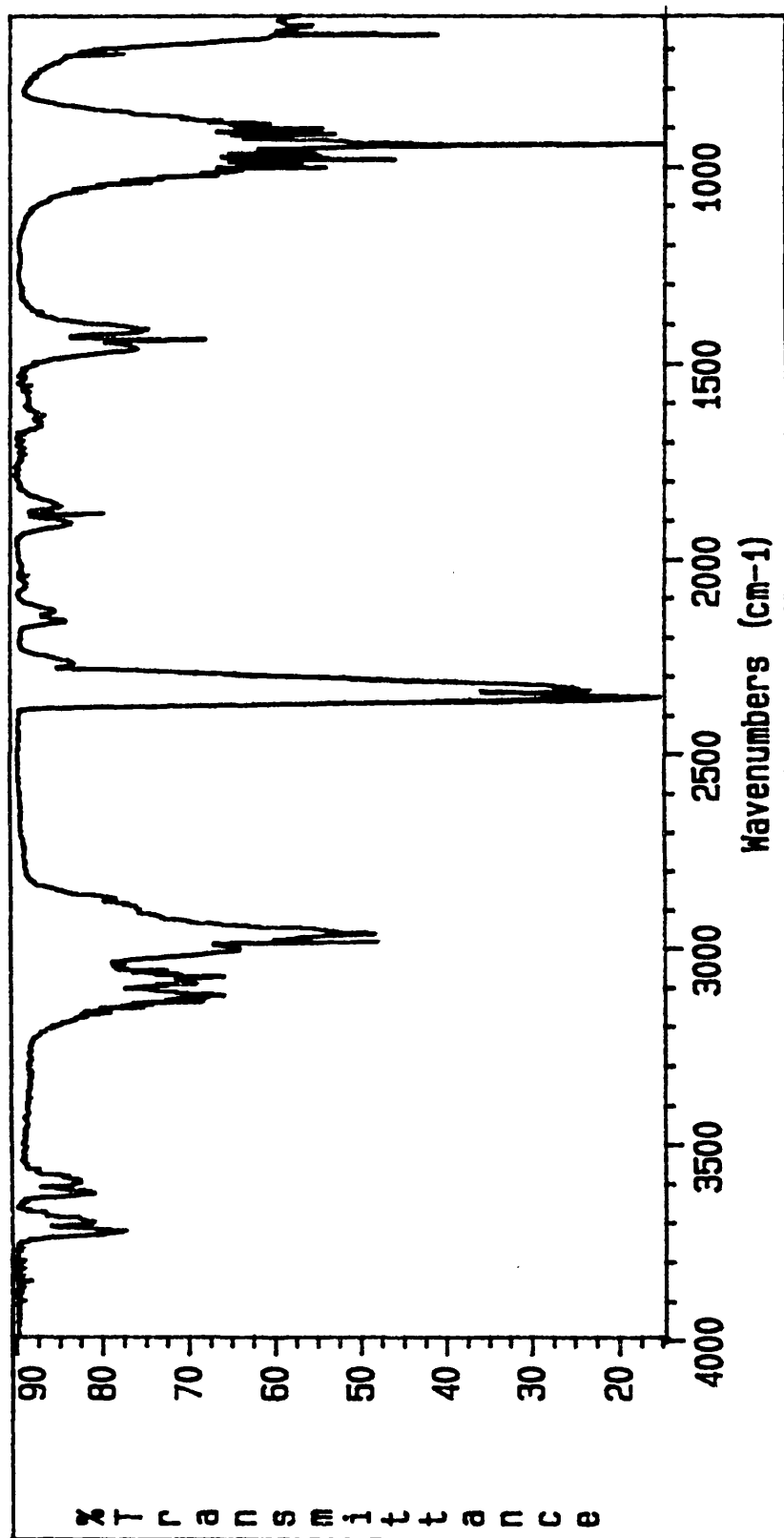


Fig. 5.19. (b) IR spectra of the volatile products from the first two peaks of SATVA from the degradation of blend 7 (EEA copolymer and 50% coated CaCO_3 with particle size of 5μ).

Table 5.3. Mass Spectrum assignments for the final from SATVA of blend 4.

| Scan | Name/Structure | Scan | Name/Structure |
|------|---|------|--|
| 130 | Ethanol | 842 | Decane |
| 212 | 1-Hexene | 956 | Ethyl heptanoate, C ₆ H ₁₃ CO ₂ Et |
| 221 | Hexane | 992 | 1-Undecene |
| 294 | Acetic acid, vinyl ester | 1003 | Lactone ? |
| 323 | 1-Heptene | 1011 | Undecane |
| 339 | Heptane | 1137 | Ethyl octanoate, C ₇ H ₁₅ CO ₂ Et + hydrocarbon |
| 467 | Ethyl butanoate, C ₃ H ₇ CO ₂ Et | 1154 | Dodecene |
| 475 | 1-Octene | 1172 | Dodecane |
| 495 | Octane | 1291 | Ethyl nonanoate, C ₈ H ₁₇ CO ₂ Et + hydrocarbon |
| 594 | CH ₂ =C(Et)-CO ₂ Et | 1308 | 1-Tridecene |
| 613 | 2-Heptanoate, C ₇ H ₁₄ O | 1324 | Tridecane |
| 648 | 1-Nonene | 1438 | Ethyl decanoate |
| 668 | Nonane | 1453 | 1-Tetradecene |
| 698 | 2,2-Dimethyl butanoic acid ? | 1468 | Tetradecane |
| 791 | Nonane, 5-methylene | 1591 | 1-Pentadecene |
| 822 | 1-Decene | 1605 | Pentadecane |

Blends of EEA Copolymer and Other Inorganic Fillers

The first stage of degradation of blend 9 (with 50% Al(OH)₃), which was due to the decomposition of Al(OH)₃ to Al₂O₃ and water, started at about 227°C and finished at about 353°C (Fig. 5.21 (a)). Al(OH)₃, when decomposed alone, started volatilisation at about 174°C and showed T_{max} at 223°C. It seems that the polymer melt retarded the volatilisation of the water for some time yet the residue spattered on the surface of the

TVA tube indicating the rapid evolution of volatile material from the polymer melt. The second stage of degradation began at about 369°C and reached T_{\max} at 448°C.

The SATVA trace (Fig. 5.22) of blend 9 gave similar compounds as were found from blend 4, except that there was a large amount of water also formed due to the decomposition of the filler. However, the IR spectra of the volatile gaseous products indicated the presence of ethylene (more than from blend 11 (MgO)), CO_2 (less than from blend 10 ($\text{Mg}(\text{OH})_2$)) and blend 11, ketene (less than from blends 10 and 12 (TiO_2)) and other hydrocarbons (less than from blends 10 and 11).

The IR spectrum of the CRF was similar to that of the CRF from EEA copolymer when degraded alone, giving the absorptions for both acid and ester groups as well as absorptions at 1813 cm^{-1} indicating the presence of cyclic six membered $\alpha\beta$ -unsaturated anhydride. This also indicates that there are some ester groups which are not isolated.

The IR spectrum of the residue (Fig 5.24 (a)) was similar to that of the Al_2O_3 but there were absorptions for $-\text{CH}_3$ and $-\text{CH}_2$ groups. There were also absorptions in the region $1640\text{-}1540\text{ cm}^{-1}$ and $1473\text{-}1418\text{ cm}^{-1}$ and such absorptions are known to be shown by the acid salts. The residue crumbled to powder possibly because any polymeric material left was no longer elastomeric.

The first stage of the degradation of blend 10 (with $\text{Mg}(\text{OH})_2$), which was due to the decomposition of the filler to MgO and water, started at about 318°C and reached T_{\max} at 390°C. The TVA trace (Fig. 5.21 (b)) shows that some volatile product(s) which were non-condensable at 0°C but condensable at -45°C started to evolve at 390°C and reached T_{\max} at 418°C. The second degradation stage started at about 431°C and reached T_{\max} at 479°C. The TVA trace of the first degradation stage also reveals the evolution of small amounts of other highly volatile products including non-condensable gaseous products identified as carbon monoxide with trace amounts of hydrogen and methane. The non-condensable degradation products from the second degradation stage and up to second T_{\max} were mainly hydrogen and CO with small amounts of methane while hydrogen with trace amount of methane were the only non-condensable products after the second T_{\max} . The decomposition of $\text{Mg}(\text{OH})_2$ when degraded alone, started at about 264°C with T_{\max} at 321°C. The TVA trace showed the absence of non-condensable products. This shows that the polymer melt retarded the volatilisation of the water by up to 54°C.

The SATVA trace (Fig. 5.23) for blend 10 indicates the absence of ethylene which is a by-product of the decomposition of the ester groups to acid groups. IR of the first fraction showed the presence of CO_2 and a trace amount of ketene. The SATVA trace of the filler showed very small amounts of CO_2 . Therefore, the presence of large amounts of CO_2 indicates that some of the ester groups have been converted to acid groups but by some other mechanism than in the normal case when EEA copolymer was degraded alone. The GC trace of the liquid products resembled the GC trace from blend 4 except that it did not show the presence of acids or esters. The GC results showed that the area under the ethanol peak was as large as expected from the assumption that most ester groups would end up as ethanol, since there were very weak absorptions in the IR spectrum of the CRF for the carbonyl groups at 1813 cm^{-1} , 1736 cm^{-1} (being the weakest absorption compared to other two) and 1718 cm^{-1} (strongest). The absorptions in the region $1300\text{--}1100\text{ cm}^{-1}$ almost disappeared while the absorption at 1641 cm^{-1} , possibly due to an $\alpha\beta$ -unsaturated carbonyl compound, was as intense as the absorption at 1718 cm^{-1} . The IR spectrum of the CRF was otherwise similar to that of the CRF from the EEA copolymer when degraded alone.

The only explanation of such behaviour is the nucleophilic attack of the hydroxyl groups on the surface of the filler at the ester groups as indicated in Scheme 5.4. This would leave only the backbone of the polymer giving an IR spectrum much similar to the IR spectrum of the LDPE. The presence of an $\alpha\beta$ -unsaturated carbonyl compound which could only result if at least two ester groups were adjacent, also indicates that this reaction mainly takes place at isolated ester groups. Other volatile products were similar to those in the case of blends 4, 9, 11 and 12.

The residue puffed up like popcorn and neither spattered nor spread on the surface of the TVA tube. This indicates that dehydration of the remaining unreacted filler did not take place as a sudden release of water from the polymer melt. The IR spectrum of the residue (Fig 5.24 (b)) showed absorptions for MgO and at 2924 cm^{-1} and 2853 cm^{-1} for $-\text{CH}_2$ groups while absorptions due to ester and acid groups were negligible. There were also absorptions in the region $1638\text{--}1560\text{ cm}^{-1}$ and $1473\text{--}1458\text{ cm}^{-1}$ and such absorptions are shown by acid salts. It seems, therefore, that quite a lot of ester groups ended up as acid salts.

Blend 11 (with 50% MgO) started to volatilise at about 276°C which was possibly due to the decomposition of the impurity, $\text{Mg}(\text{OH})_2$, to MgO and water. The degradation was extremely slow such that the first stage of degradation reached T_{max} at

373°C. The second and third stages of degradation started at about 394°C and 450°C respectively (Fig. 5.25 (a)).

The SATVA trace (Fig 5.26) for condensable volatile degradation products from blend 11 (with 50% MgO) was similar to that for blend 4 but the area under the SATVA curve showed that ethylene production was less than in the case of blends 9 and 12 while production of other products was increased. This could be possibly due to the impurity, $\text{Mg}(\text{OH})_2$, (shown in the IR spectrum of the filler by a slightly weak but sharp band at 3695 cm^{-1}) which was making the filler show some properties like blend 10.

The CRF was yellow and its IR spectrum was similar to that of blend 4. The residue did not spread on the TVA tube, was hollow inside and crumbled to powder when disturbed. The IR spectrum was similar to IR spectrum of the residue from blend 10.

The TVA trace (Fig. 5.25 (b) of blend 12 (with 50% TiO_2) was similar in every aspect in appearance to that of EEA copolymer when degraded alone. The SATVA trace of blend 12 was also similar to that of blend 4 but the IR spectrum revealed that absorption due to ketene was nearly 2/5 of the absorption due to CO_2 and this is the only example of the blends so far examined where ketene was produced in such a large quantity. The GC trace revealed that the production of acids was also much more than when EEA copolymer was degraded alone or with other fillers. However the production of hydrocarbons of higher molecular weight was less than for any of the other blends.

The CRF was much darker than the CRFs from other blends in this series but the IR spectrum was similar to that of the CRF from EEA copolymer.

It was obvious from the state of the residue that the blend did not spread on the surface of the TVA tube. The residue puffed up like a bubble and crumbled to powder when disturbed. The IR spectrum was similar to the IR spectrum of TiO_2 but there were also weak absorptions at 2921 cm^{-1} and 2851 cm^{-1} due to $-\text{CH}_3$ and $-\text{CH}_2$ groups.

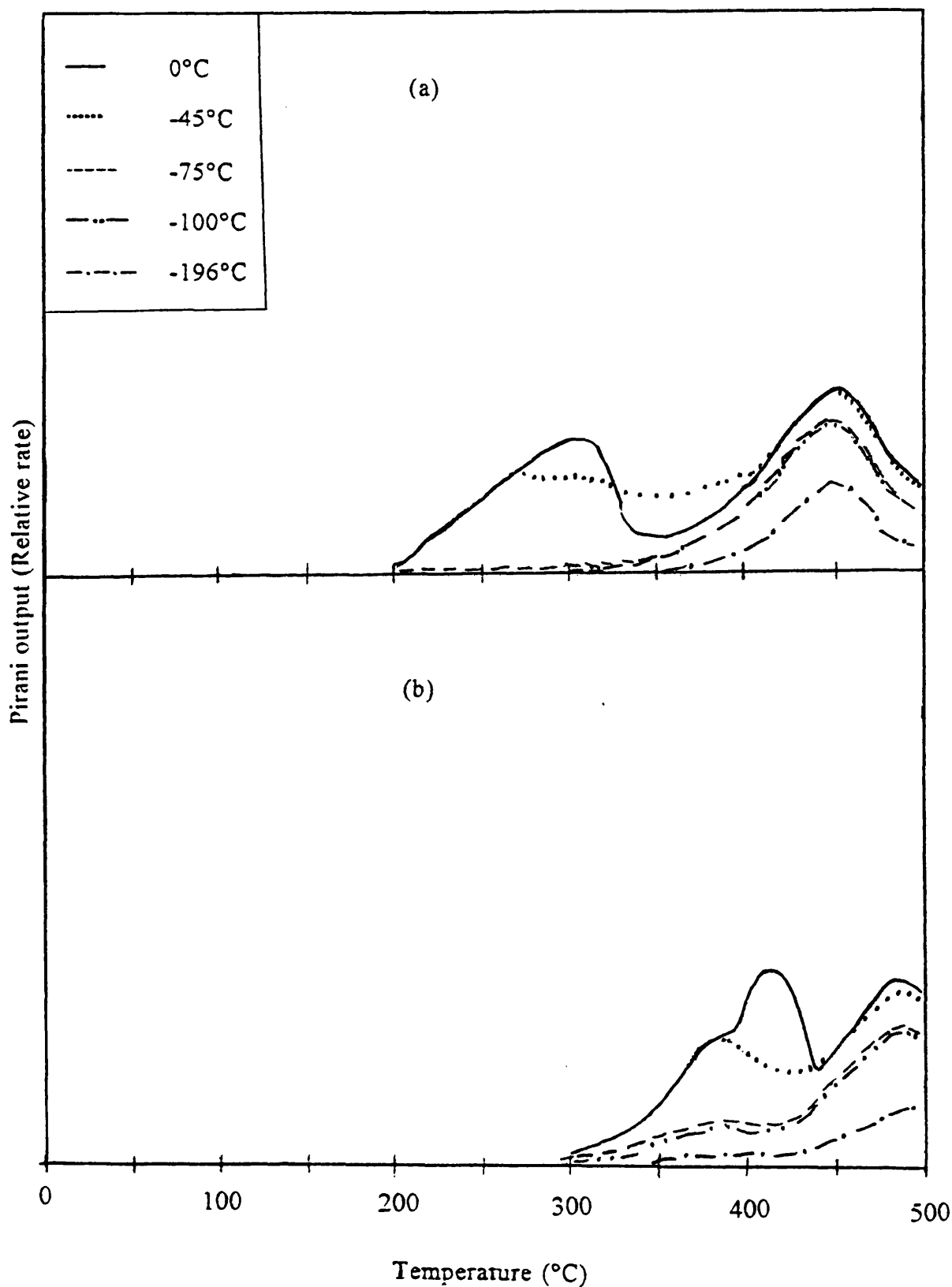


Fig. 5.21. TVA traces for blends of EEA copolymer and 50% inorganic fillers (a) blend 9 with $\text{Al}(\text{OH})_3$ and (b) blend 10 with $\text{Mg}(\text{OH})_2$.

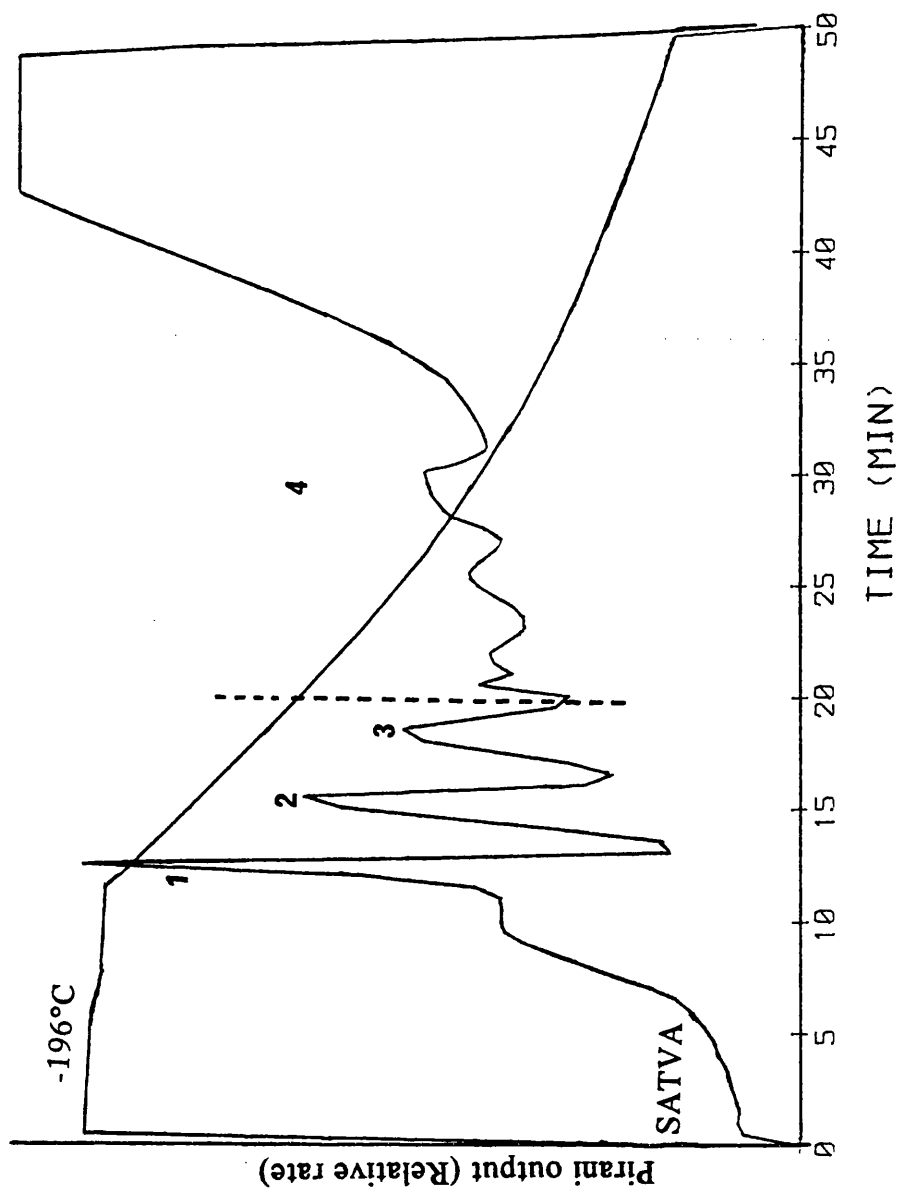


Fig. 5.22. SATVA trace for warm up from -196°C to ambient temperature of condensable volatile products from degradation for blend 9 with 50% $\text{Al}(\text{OH})_3$.

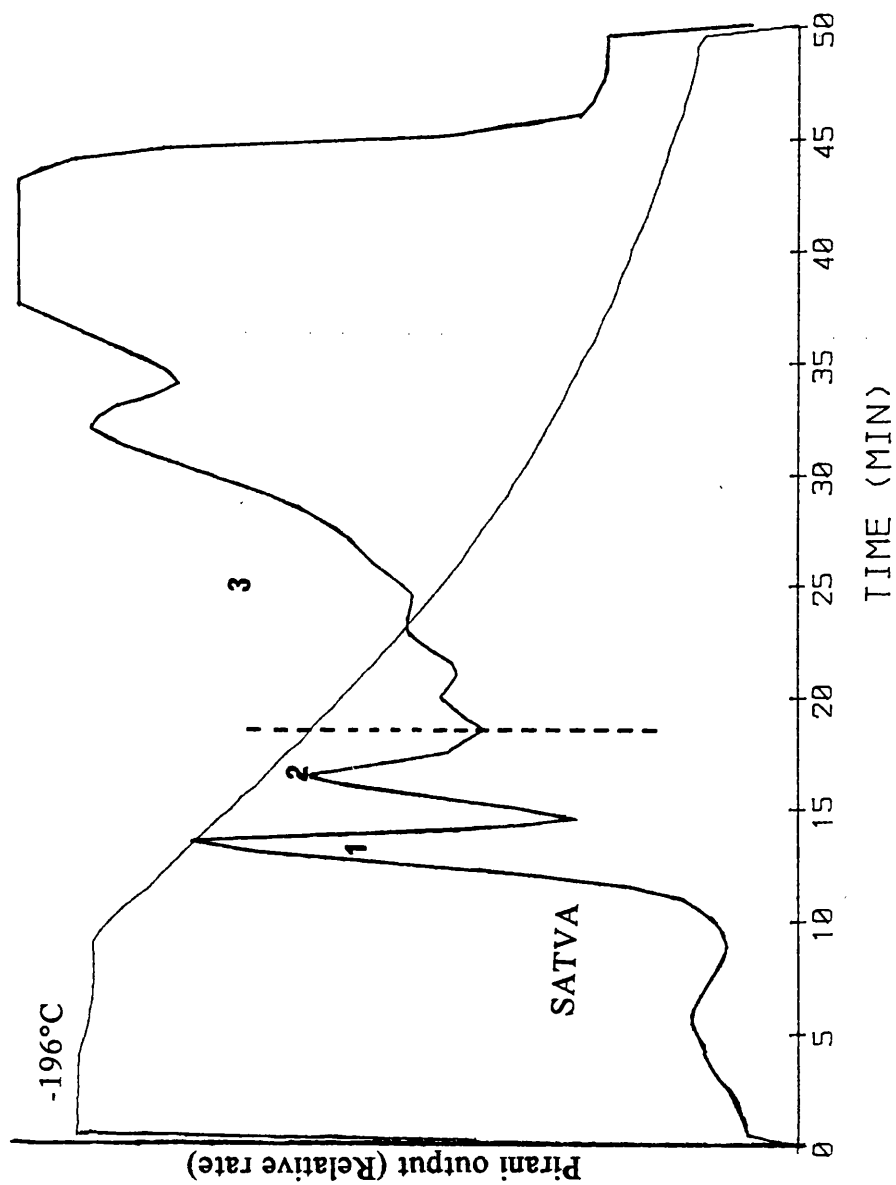


Fig. 5.23. SATVA trace for warm up from -196°C to ambient temperature of condensable volatile products from degradation for blend 10 with 50% Mg(OH)₂.

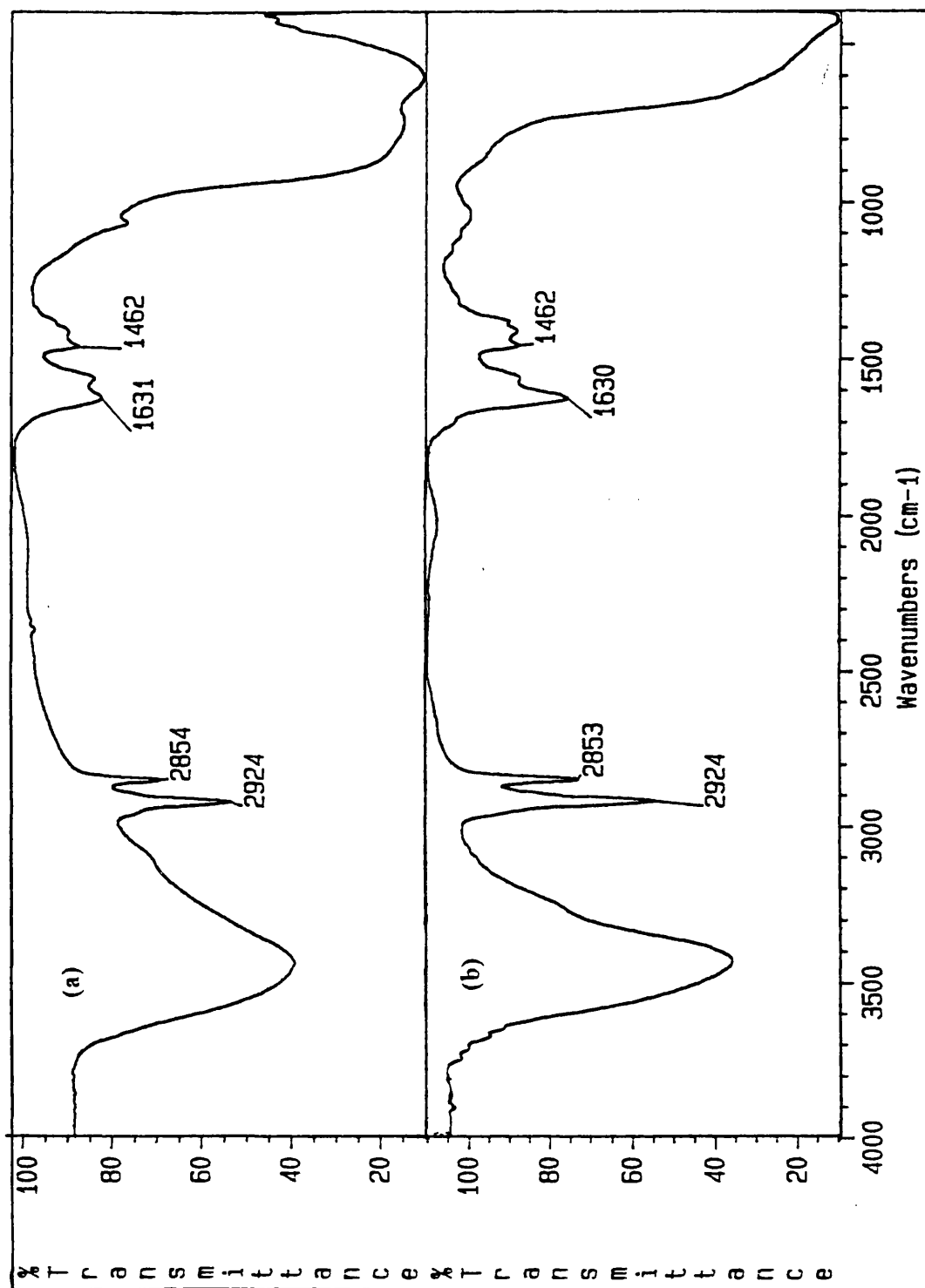


Fig. 5.24. IR spectra for residues from blends of EEA copolymer with 50% inorganic fillers: (a) blend 9 (Al(OH)₃) and (b) blend 10 (Mg(OH)₂).

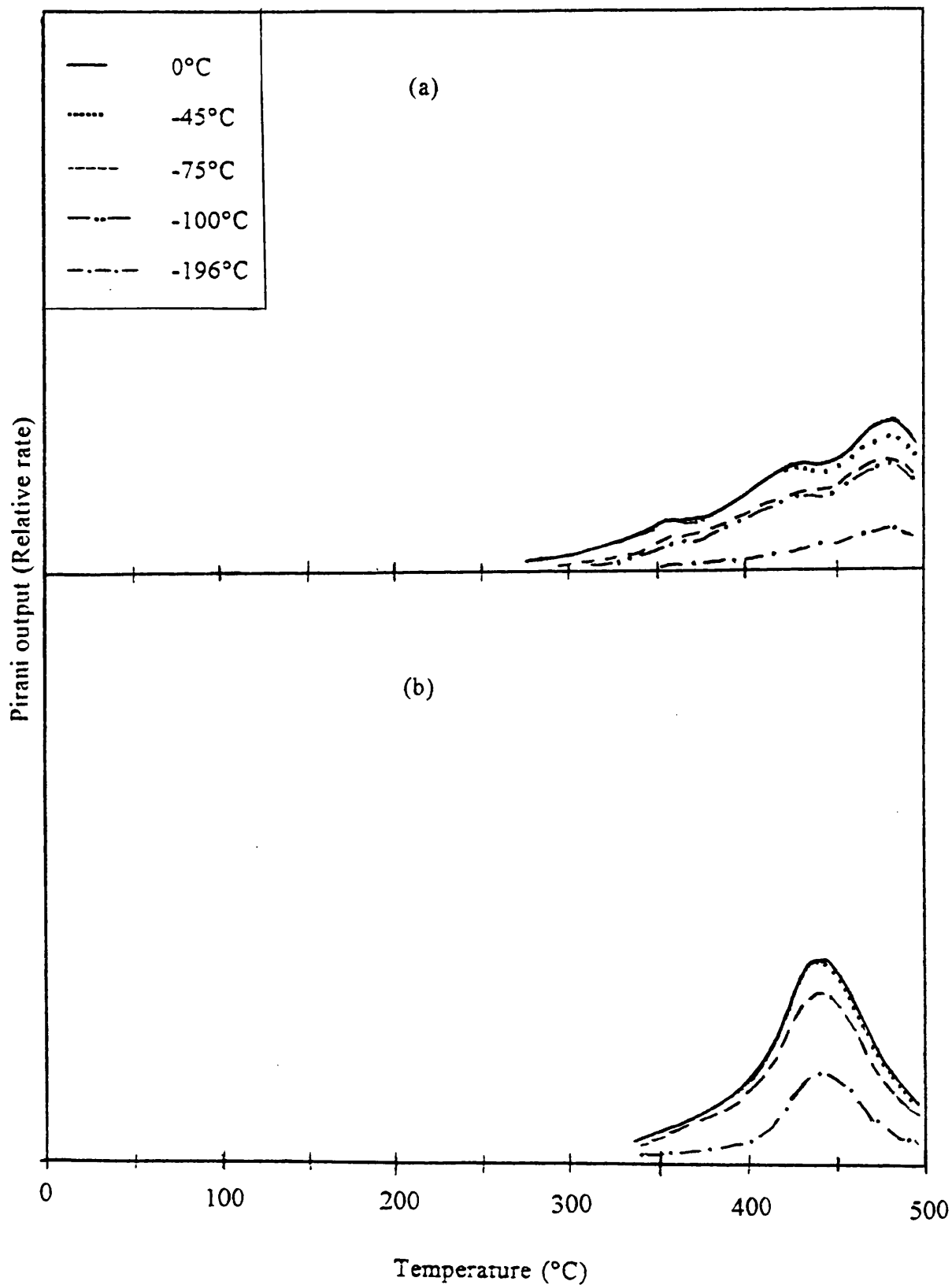


Fig. 5.25. TVA traces for blends of EEA copolymer and 50% inorganic fillers: (a) blend 11(MgO) and (b) blend 12 (TiO₂).

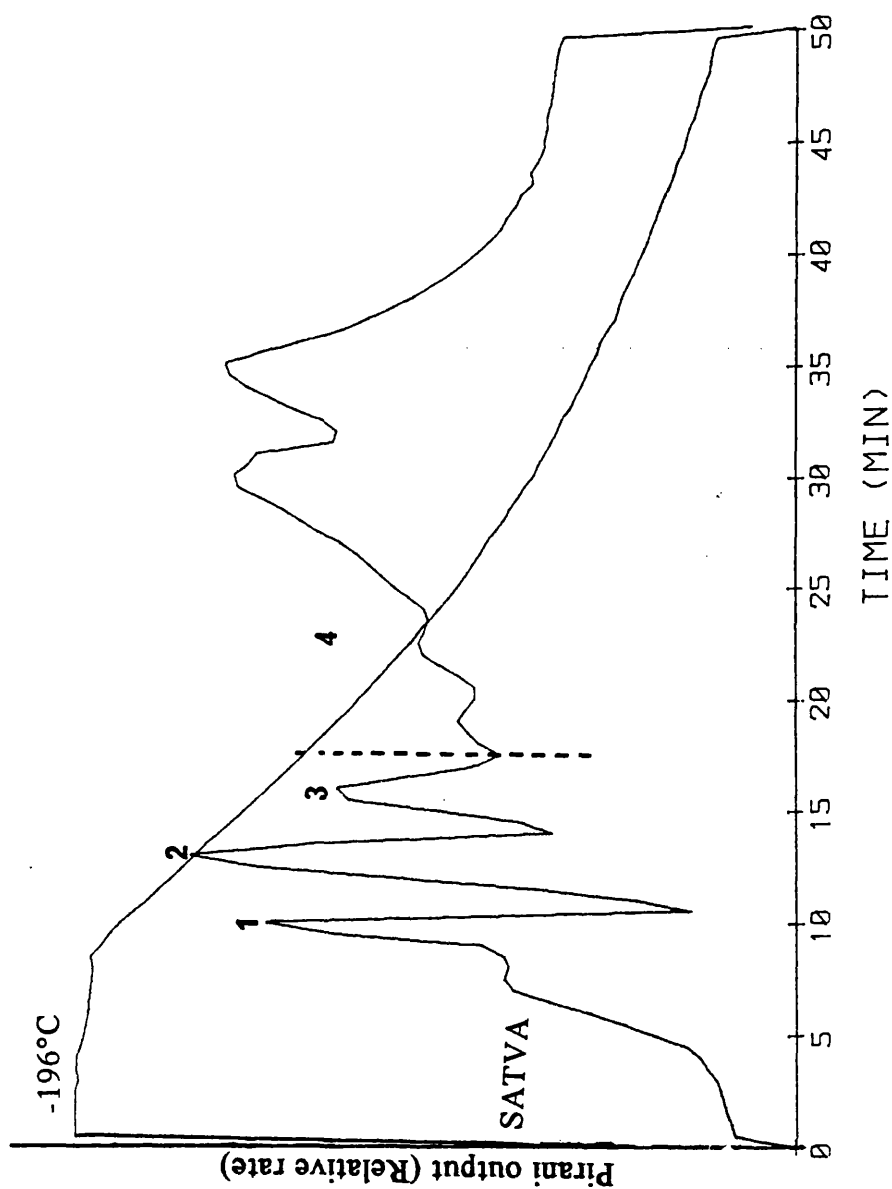


Fig. 5.26. SATVA trace for warm up from -196°C to ambient temperature of condensable volatile products from degradation for blend 11 (EEA copolymer + 50% MgO).

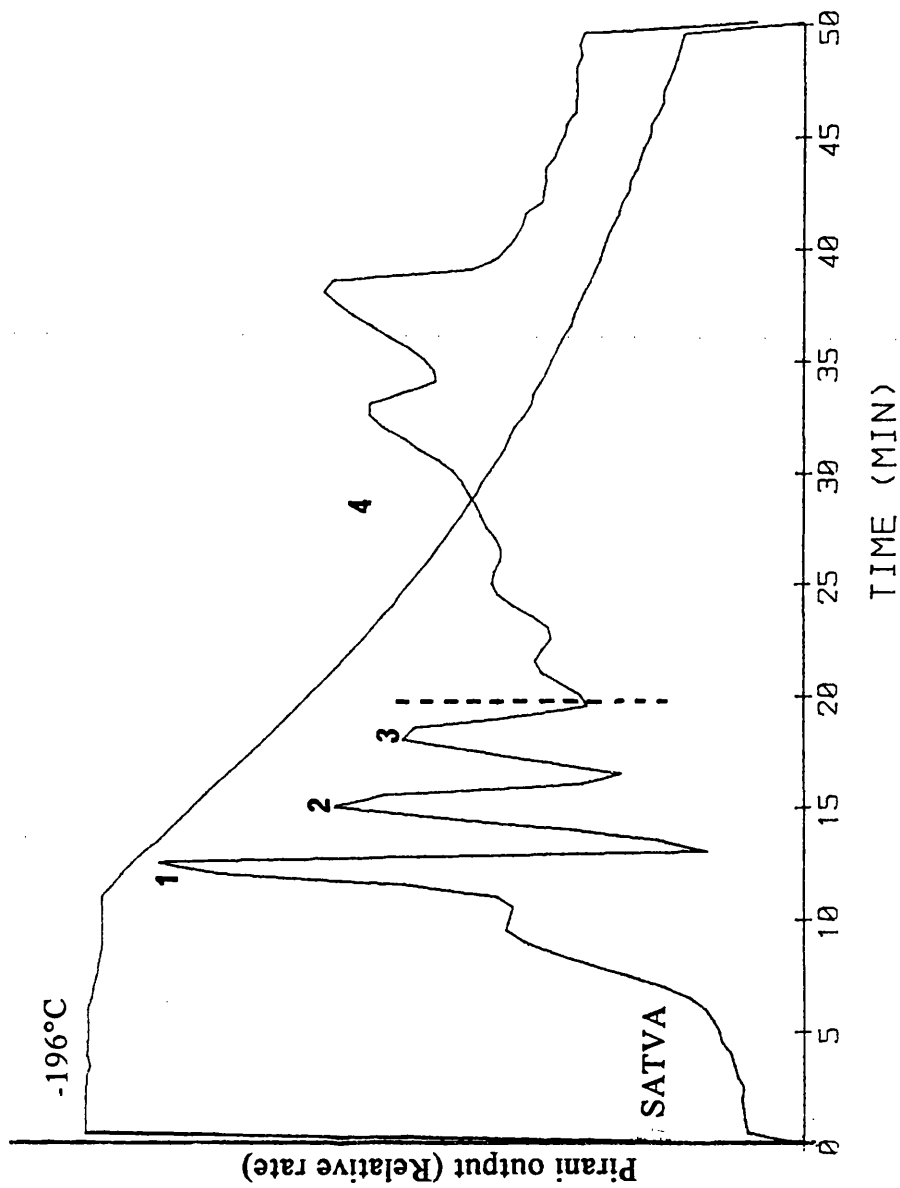


Fig. 5.27. SATVA trace for warm up from -196°C to ambient temperature of condensable volatile products from degradation for blend 12 (EEA copolymer + 50% TiO_2).

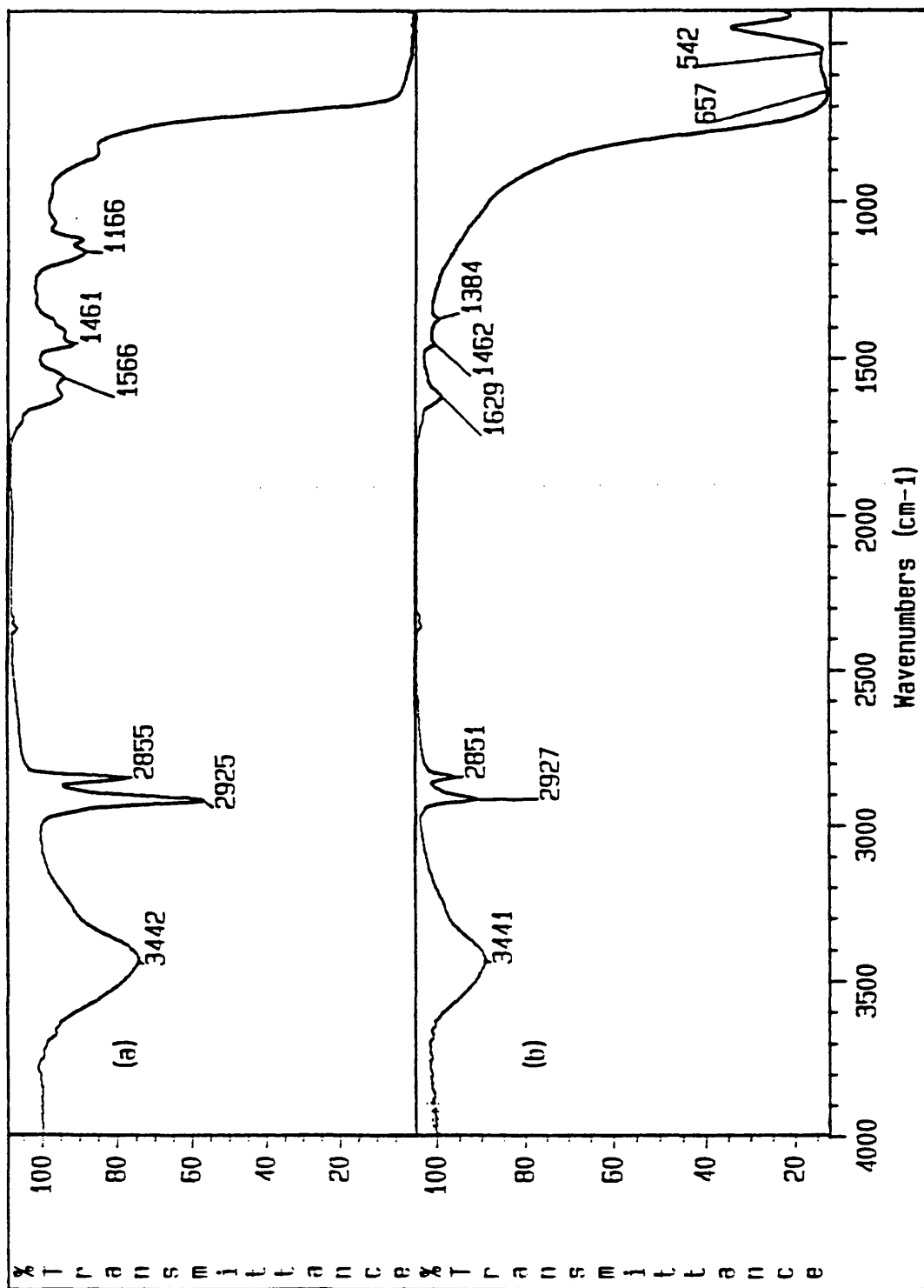


Fig. 5.28. IR spectra for residues from blends of EEA copolymer with 50% inorganic fillers: (a) blend 11 (MgO) and (b) blend 12 (TiO₂).

5.3. DISCUSSION

The onset temperatures (T_{onset}) for the evolution of the volatile degradation products and the temperatures at which the degradation processes occur at a maximum rate (T_{max}), obtained by each method, are in general agreement for all blends.

Blends of LDPE and CaCO₃

The TVA and TG-DTG curves of blend 1 indicate that evolution of volatile degradation products occurred in a single step and that there was no effect of the filler on the stability of the polymer although the volatile degradation products, especially smaller molecular weight compounds, were less in quantity. This suggests that the filler was acting as heat sink by simple dilution of the polymer and thus reducing the production of low molecular weight degradation products. The mechanism of formation of the degradation products, therefore did not change.

Blends of PEA and CaCO₃

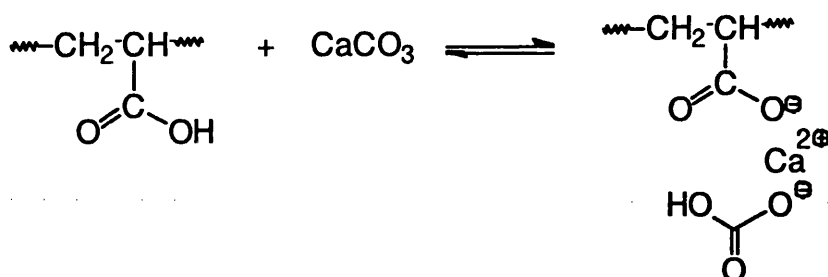
The stabilisation of blend 2 at the beginning was possibly due to the filler acting as a heat sink by simple dilution of the polymer and thus delaying the degradation of the polymer. It was obvious from the presence of the small second degradation step in the TG-DTG curve not observed when PEA was degraded alone, from the nature and properties of the residue and from the different quantity of the degradation products than normal that the filler was chemically interacting with the polymer.

The decrease in the formation of CO₂ indicates that some of the acid groups introduced during the ethylene production do not decompose to CO₂ instead possibly interact with the filler and form stable salts. Weak absorptions at 2928 cm⁻¹ and 2872 cm⁻¹ due to the stretching frequencies of methylene groups indicate the presence of polymeric material in the residue. The absence of the methyl groups in the residue indicates that all of the ester groups were decomposed. The ability of this polymeric material to stay intact with the filler after degradation suggests the chemical interaction of the components. The mechanism in Scheme 5.1. was proposed for the interaction after the introduction of the acid groups into the polymer chain. This interaction results in the formation of ionic salts.

Stability of blend 2 at the end could possibly be due to the formation of these ionic salts in the polymer chain since it was found (discussed in Chapter 3) that ethylene production, which accompanies formation of acid groups in the chain, started after 375°C and ceased before 425°C while CO₂ which is formed from the decomposition of

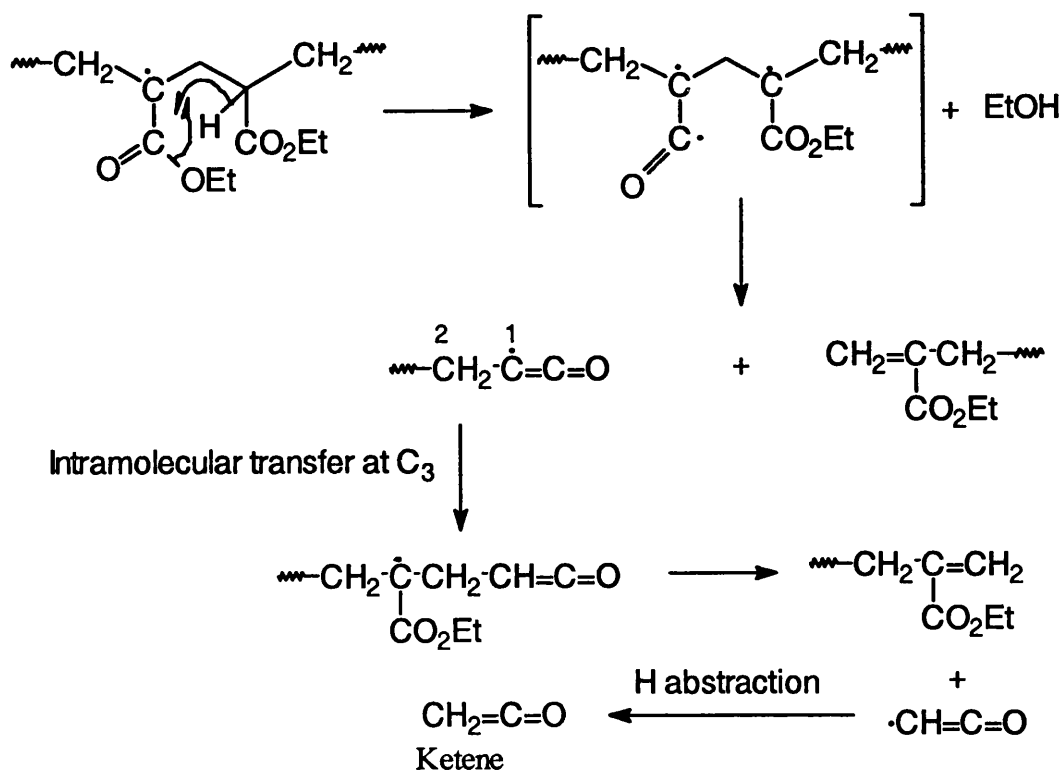
acid groups in the chain, continued after 425°C. However it was found in the case of blend 2 that CO₂ formation ceased before 425°C and this was possibly due to the formation of ionic salts. These ionic salts formed would be more stable than the acid groups. However, it would be difficult for this reaction to occur in the environment where there is crowding of the neighbouring groups but in the temperature region 375-435°C most of the ester groups would decompose leaving the backbone less crowded. Destabilisation of blend 2 in the region 375°C-435°C is difficult to understand but it might be due to the reaction in Scheme 5.3 which has been described later in the chapter.

Scheme 5.1.



The mechanism in Scheme 5.2. has been proposed for the formation of ketene and this mechanism also leads to the formation of ethyl acrylate and ethanol. This type of reaction was negligible in the case of pure polymer.

Scheme 5.2.



The presence of the broad and strong carbonyl peak at 1734 cm^{-1} in the IR spectrum of the CRF indicates that most of the CRF was made up of the chains mainly with undegraded ester groups. This would imply less formation of volatile degradation products such as ethanol and it was found that the liquid degradation products were less than in the case of pure polymer.

Blends of EEA Copolymer and CaCO_3

The fact that at least one extra degradation stage was shown by all blends of the EEA copolymer with CaCO_3 implies that the mechanism of formation of the degradation products has been changed in the presence of the filler and this was also confirmed by the trace amounts or total absence of acid groups and the negligible amount of ketene, $\text{H}_2\text{C}=\text{C}=\text{O}$. The acid groups introduced during the production of ethylene in the chain must react with the filler to produce ionic salts which being more stable would decompose at higher temperature than the normal TVA temperature. The proposed mechanism for the interaction of the filler with acid groups, introduced during the decomposition of the esters in the copolymer, is similar to that contracted for blend 2. However, this reaction would be facilitated in the blends of EEA copolymer because most of the ester groups are isolated so there is no crowding in the neighbourhood.

The formation of CO_2 at temperatures up to 400°C without ethylene suggests that CO_2 was produced by some method other than ester decomposition and the fact that after heating blend 4 (EEA copolymer and 50% CaCO_3) up to 400°C it is not possible to extract the copolymer from the residue shows that the interaction between the components (at points other than with acid groups) also took place during this period. This was also the temperature region when destabilisation of the blends occurred and the degradation products, especially ethanol, were more than in the case of pure copolymer. The formation of ethanol in the absence of ketene and carbon monoxide indicates that ethanol also was produced by some method, other than indicated in Chapter 3, which resulted in the production of either ketene (minor process) or carbon monoxide. The following mechanism (Scheme 5.3) was proposed for the interaction of the components without acid groups being involved and which resulted in the formation of CO_2 and ethanol. The reduction in the total amount of carbon monoxide, which was a by-product of ethanol formation in the case of pure copolymer, also confirms the mechanism introduced in Scheme 5.3.

The absence of methyl groups in the residue at 480°C in the form of salt (A) indicates that it decomposes before 480°C . The presence of CO_2 and larger quantities of ethanol than expected at temperatures below 400°C show that salt (A) was unstable and decomposed before 400°C , hence destabilising the system in this region. It is

difficult to tell whether salt (B) decomposed completely to salt (C) before 400°C or decomposition was still taking place at this temperature, since the first degradation stage which seems to be mainly due to the decomposition of these salts, formed in Scheme 5.3, ends at about 440°C. This difficulty arises because pure EEA copolymer gave large quantities of ethylene and CO₂ in the region 400°C-450°C.

The presence of the salt (C) in the residue is difficult to detect from the IR spectrum because of the strong carbonyl absorption due to the carbonate ions. IR spectroscopy of the residue (KBr disc), after heating up to 600°C, showed the presence of some undegraded polymeric material as the C-H stretch was much more intense than when EEA copolymer was degraded alone. C-H deformations were overlapped by the broad and intense absorption of the CO₃²⁻ ions. EEA copolymer when degraded alone showed very weak and broad absorption at 1710 cm⁻¹, such an absorption would also be masked by the intense and broad absorption of CO₃²⁻ ions.

Reaction through route (iii) possibly only takes place at temperatures above 500°C since the IR spectrum of the residue did not show the presence of calcium oxide at degradation temperatures below 500°C.

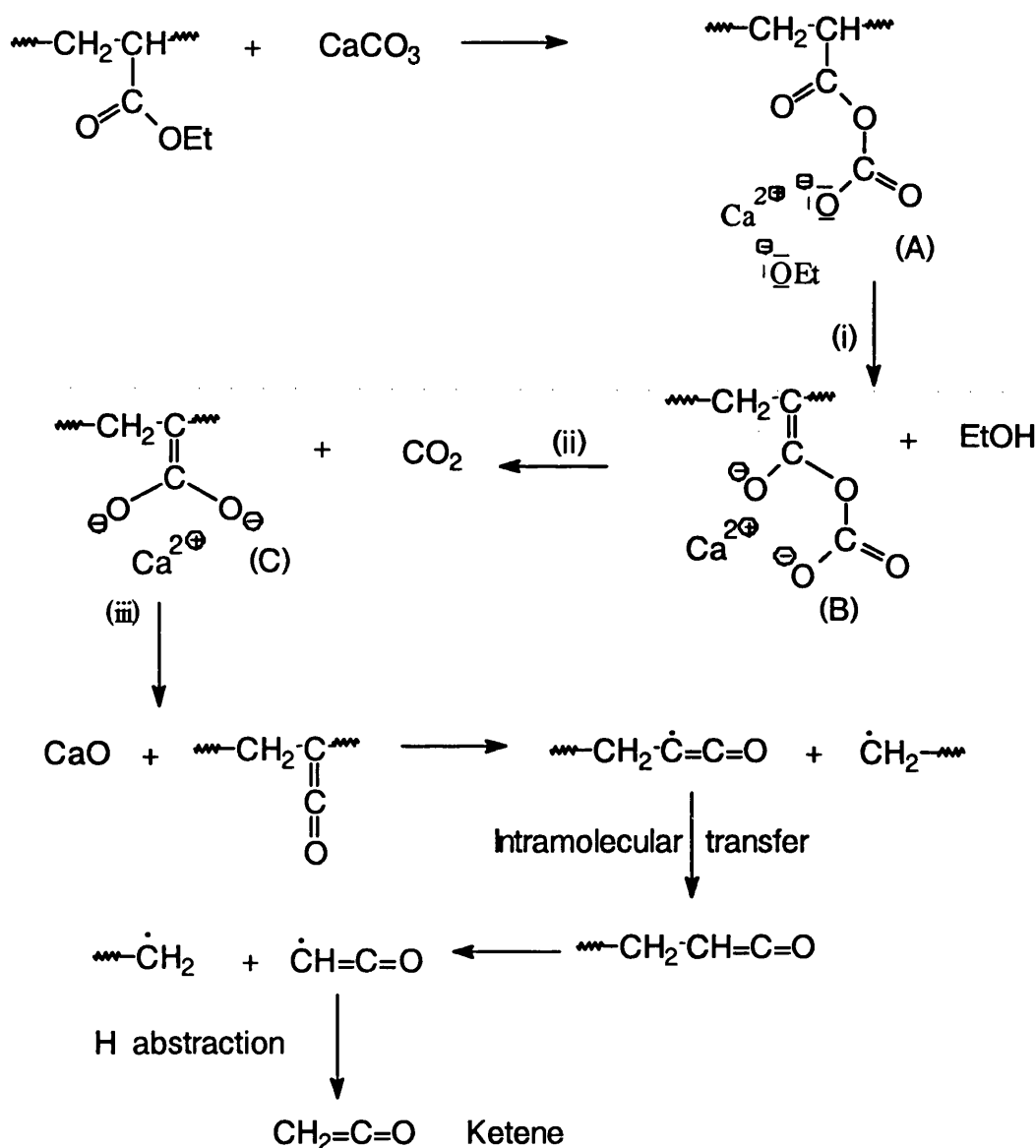
The type of reaction described in Scheme 5.3 would be impossible at the start of the degradation in the case of blend 2 at places other than at the chain ends because of the crowding of the neighbouring groups, but in the temperature region 375-435°C most of the ester groups would decompose leaving the backbone less crowded. The destabilisation shown by blend 2 might be possibly due to this interaction for the same reasons as described for blend 4 since degradation products in the case of blend 2 increased in this region.

Calcium carbonate samples with different particle size and type have slightly different effects on the copolymer. Calcite type calcium carbonate with larger particle size, whether coated or uncoated, does not destabilise the copolymer initially like the other types and gives stabilisation throughout the degradation. Coated calcium carbonate with smaller particle size of either type destabilises the copolymer initially but the overall stabilisation is more than with larger particle sized calcium carbonate. It should be kept in mind for blends with coated CaCO₃ that there would be interaction of the type shown in Scheme 5.1 between the filler and the acid groups of the stearic acid. This observation was made when coated filler was heated alone and was found that decomposition due to coating started at 375°C and formed hydrocarbons up to C₁₁.

The greater stabilisation in blend 8, containing the precipitated form of the filler, could be explained in terms of the surface treatment of the filler to give it a high degree

of dispersion thus providing a specific surface area several times larger than other types of grades. The larger surface area would provide more sites for interaction and more surface area to remove the heat from the polymer since the dispersion through the polymeric material would be much better so most of the filler would be in contact with the polymer.

Scheme 5.3. Interaction of the Components and Formation of Ionic Salts



The largest stabilisation in blend 6, which contains calcite type calcium carbonate, is difficult to understand since if the stability were due to the smaller particle size then it would have shown less stabilisation than blend 8. The only differences which may be contributing to the greater stabilisation, are impurities in it (such as ferric oxide, Fe_2O_3 , sulphate and magnesium oxide) and its different type while blend 8 contains a precipitated, and therefore highly purified, form of calcium carbonate. Metal oxides are

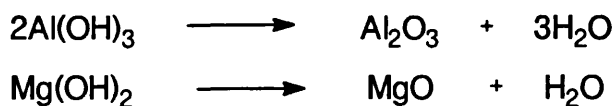
known to react with acid groups formed in the polymer chain (discussed later under the heading "Blends of EEA Copolymer and Other Inorganic Fillers").

The decrease in the level of ketene production with coated and smaller particle size filler at temperature below 500°C is possibly due to the larger surface area available for the interaction with ester groups in the copolymer. The resulting ionic salt (A) decomposes and eventually forms salt of the type (C) which being more stable, decompose at temperatures higher than in most of the TVA experimental work carried out, to give metal oxide and ketene. This was confirmed by degrading blend 4 up to 600°C and it was found that the level of ketene increased slightly and the IR spectrum of the residue showed the presence of trace amounts of the metal oxide. The greater quantity of CO₂ than ethylene (a by-product in the formation of CO₂ by the ester decomposition) for the blends with smaller particle sized filler also supports a high level of interaction of these fillers with the copolymer, thus increasing the production of decomposition products of these salts.

The greater stabilisation shown by blend 4 in an inert atmosphere than in air can be explained as described in chapter 3 for the pure polyolefins. The higher degree of stabilisation than expected shown by blend 4 in air was possibly due to the large loading of filler preventing oxygen reaching the copolymer and also possibly due to interaction of the filler with acid groups (e.g. peracids) introduced into the copolymer chain during oxidation.

Blends of EEA Copolymer and Other Inorganic Fillers

The stabilisation in blends 9 and 10 apparently is due to the high filler content resulting in the filler acting as solid phase diluent. Both metal hydroxides also decompose endothermically on heating and produce water and inert metal oxides:



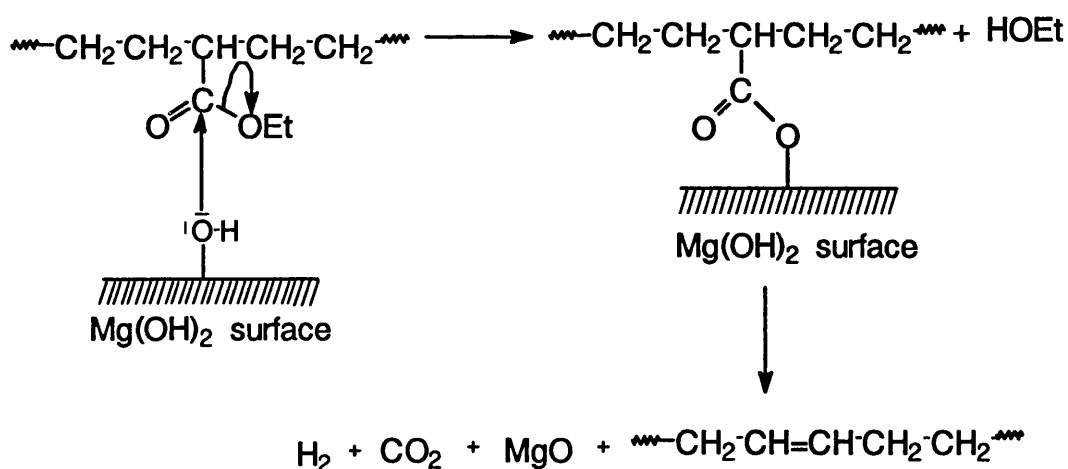
Endothermic decomposition of these metal hydroxides withdraws heat from the substrate thus retarding the rate of the thermal degradation. The accompanying release of inert gas (water vapour) cools decomposing material and dilutes the combustible polymer degradation products. Thus the heat capacity of both the fire-retardant additives and inert decomposition products further reduce the thermal energy available to degrade the substrate.

Magnesium oxide being basic, reacts with the acid groups and forms corresponding ionic salts which are more stable than the acid groups in the polymer chain.

Dehydration of aluminium hydroxide at a relatively low temperature forms γ - Al_2O_3 which is quite reactive and reacts with both acids and bases. γ - Al_2O_3 has a considerable capacity for adsorption, so some of the degradation products may adsorb on the surface of the filler for some period of time thus reducing the evolution of degradation products at lower temperatures. This is possibly another factor which is contributing towards the stability shown by blend 9. Alumina itself has been for long used as a filler to modify the physical properties and in certain applications to reduce the effective cost of the synthetic polymer.

However, there is some other factor involved in stabilising blend 10. The formation of large amounts of CO_2 in the absence of ethylene for blend 10 indicates that some of the ester groups have been converted to carboxylate structures but by some other mechanism than in the normal case when EEA copolymer was degraded alone. The only explanation of such behaviour is the nucleophilic attack of the $-\text{OH}$ groups on the surface of the filler at the ester groups as indicated in Scheme 5.4 below:

Scheme 5.4. *Nucleophilic attack of the $-\text{OH}$ groups on the surface of the filler at the ester groups*



The extremely weak absorptions due to the carbonyl groups in the IR spectrum of the CRF supports this hypothesis. This effect is not caused by the Al(OH)_3 possibly because the interaction between the components would occur at higher temperature than the dehydration temperature of Al(OH)_3 . This is confirmed by the TG curve of aluminium hydroxide which shows that the extensive water loss (31.5%) takes place between 200°C and 325°C and the remaining 3.12% weight loss takes place in period

325-600°C. It is not clear whether the remaining 3.12% weight loss is due to water within the matrix diffusing slowly from the oxide body as the temperature rises further or residual undecomposed hydroxide. The TG curve of blend 9 shows that expected weight loss (31.5%) due to decomposition of the filler finishes well before the second degradation starts, due to the decomposition of the EEA copolymer. Any $\text{Al}(\text{OH})_3$ remaining may interact with the copolymer.

The above interaction between the components also results in the formation of ethanol and hydrogen gas. However, this was not the only route for the production of ethanol since carbon monoxide and trace amount of ketene show that ethanol was also produced from the normal mechanisms by which CO (major) and ketene were by-products during ethanol formation (described in Chapter 3). These reactions were only favoured by the isolated ester groups. This indicates that not all isolated ester groups reacted with hydroxide groups possibly because there are not enough free hydroxide groups to react with all isolated ester groups.

The difference in the residues for the blends of both hydroxides is also due to the fact that the polymer is held intact within the magnesium hydroxide due to interaction and therefore, on the decomposition of the remaining filler, the residue puffs up like popcorn instead of spattering or spreading on the surface of the TVA tube.

The stability of blend 11 is partially due to the same reasons as for blend 10 since MgO contains $\text{Mg}(\text{OH})_2$ as impurity. The high filler content acts as a solid phase diluent. The acid groups are not present in the degradation products of blends 9 and 11 because they react with the filler to produce ionic salts with the metal oxides.

The evolution of volatile degradation products in a single step for blend 12 indicates that the mechanism of formation of the degradation products has not changed and that the filler stabilises the copolymer initially by decreasing rates of heat transmission from the heat source to the matrix. As a result the evolution of the decomposition products occurs at a higher temperature. The destabilisation of the blend near the end and almost total decomposition of the copolymer indicates that at higher temperatures the filler activates the decomposition of the residual polymer and increases the quantity of degradation products, especially larger molecular weight compounds.

The increase in the formation of ketene and acids for blend 12 indicates that the production of ethanol is also favoured by the route in which ketene is a by product (discussed in Chapter 3) and that most of the acid groups introduced in the copolymer chain are converted to acids instead of CO_2 . The preference of some of the degradation

products over the others indicates that the mechanism of degradation has changed and as a result some routes of degradation were preferred to the others.

5.4. CONCLUSIONS

Calcium carbonate did not stabilise LDPE, however it reduced the formation of the low molecular weight hydrocarbons by simple dilution of the polymer.

Calcium carbonate stabilises PEA initially by simple dilution of the polymer. The mechanism for the formation of some of the degradation products changes because of some interaction between the components.

Calcium carbonate interacts with polyolefins if polar groups are introduced by copolymerisation and stabilises the copolymer, the stabilisation depending on the percentage content, the particle size, type and coating of the filler.

Calcite type calcium carbonate leads to more stabilisation than whitening or precipitated form. Smaller particle size and coated surface of the filler also plays part in stabilising the copolymer.

The filler prevents the formation of acids, such as acetic acid and propanoic acid, which are produced in the case of pure copolymer, by interacting with the acid groups on their formation in the chain. This interaction contributes towards the stabilisation of the EEA copolymer. The mechanism for the formation of some of the degradation products changes. The production of ethanol is mainly through the route by which carbon monoxide is a by-product while the alternative route by which ketene was a by-product is almost prohibited in most cases.

The blend of EEA copolymer and calcium carbonate, like the pure copolymer, is more stable in an inert atmosphere than in the air. Nevertheless, calcium carbonate stabilises copolymer more in air than in nitrogen.

More higher molecular weight compounds are formed from degradation of the blend of EEA copolymer and calcium carbonate than from the pure copolymer.

Metal hydroxides stabilise the polymer system by decomposing endothermically and producing inert decomposition products which further reduce the thermal degradation of the substrate by reducing the thermal energy available to the substrate. However, if a metal hydroxide does not decompose until high temperature, then at lower temperatures it interacts with the polymer system with reactive groups and changes the mechanism for the formation of the degradation products.

CHAPTER 6

BLEND OF POLYOLEFINS AND POLYDIMETHYLSILOXANE

6.1. INTRODUCTION

Although non-halogenated additives, especially inorganic fillers such as $Mg(OH)_2$, $Al(OH)_3$, MgO , $CaCO_3$ and others are now becoming popular in the plastic industry as fire retardants, heavy loadings of these fillers are required to meet increasingly restrictive safety standards. As a result, most of the resins in which these fillers are incorporated suffer in physical performance. Silicones have also been tested in polyolefins as non-halogenated fire retardants, especially to be used in electrical applications, but it was found that uncrosslinked polyolefins do not achieve good fire retardancy¹²⁵⁻¹²⁷.

In this chapter, the degradation of high molecular weight polydimethylsiloxane (PDMS) with vinyl end groups was examined in presence of LDPE, PEA and EEA copolymer to investigate if introduction of polar groups into the uncrosslinked LDPE chain could give useful stabilisation in the PDMS blends.

6.2. EXPERIMENTAL

6.2.1. Preparation and Composition of Blends

All blends were prepared as described in Chapter 2 except for samples 15, 16, 17 and 19. Samples 17 and 19 were unmixed components and films were cast, at room temperature and normal atmosphere, in a twin-limbed TVA tube specially designed for the degradation of such systems. Blends 15 and 16 were prepared by dissolving both components in a common solvent and then casting a film, inside the twin-limbed TVA tube in the case of blend 15 and on a stainless steel plate in the case of blend 16. The compositions were based on weights of components and are given in Table 6.1.

Table 6.1. Compositions of samples examined

| Sample | Polymer | Additive |
|--------------|---------------|------------|
| Blend 13 | LDPE:BP77 | 50% PDMS |
| Blend 14 | PEA | 7.1% PDMS |
| Blend 15** | PEA* | 50% PDMS |
| Sample 16** | PEA* | 50% PDMS |
| Blend 17*** | PEA* | 50% PDMS |
| Blend 18 | EEA copolymer | 7.14% PDMS |
| Sample 19*** | EEA copolymer | 7.14% PDMS |
| Blend 20 | EEA copolymer | 50% PDMS |

Note: PEA* = Laboratory prepared PEA, *** = Unmixed components where ** = blends not prepared on a Brabender laboratory batch melt mixer by melt compounding.

6.3. RESULTS

6.3.1. Thermogravimetry

TG results under dynamic nitrogen and air are given in Table 6.2 (a) and (b) respectively.

6.3.1.1. TG-DTG Under Nitrogen

Blend of LDPE and PDMS

The TG-DTG curve (Figs. 6.1) of the blend 13 (LDPE, 50% PDMS) showed two stage degradation as expected but the degradation started at 325°C, which was about 75°C higher than predicted and reached T_{max} at 405°C, while the second stage of the degradation began at 435°C and reached T_{max} at 485°C. The stabilisation was shown almost throughout the degradation but the second stage, which was mainly due to the decomposition of the LDPE, only showed stabilisation of 5-10°C. The residue at 600°C amounted to 1.5% by weight of the total original weight of the blend degraded compared with 1.4% expected.

Blends of PEA and PDMS

The TG-DTG curve (Fig. 6.2) obtained for blend 14 (PEA, 7.1% PDMS) was similar to the TG-DTG curve of pure PEA showing mainly a single stage degradation process starting at 325°C with T_{\max} at 412°C. The TG-DTG curve showed up to 75°C of stabilisation initially, up to about 31% weight loss. However, destabilisation of up to 10°C started after 36% weight loss. The system became stable again when there was only 15% blend left. The residue at 600°C amounted to 7.25% by weight of the total original weight of the blend degraded compared with 2.11% expected.

Blends of EEA copolymer and PDMS

Weight loss of blend 18 (EEA copolymer + 7.1% PDMS) showed only one main degradation stage (Fig. 6.3) starting at 350°C with T_{\max} at 460°C. The TG-DTG curve showed up to 75°C of stabilisation initially, up to about 12% weight loss, but after about 16% weight loss, the degradation process speeded up and there was a drift towards destabilisation in the dynamic weight loss curve of up to 10°C. The residue at 600°C was 1.0% of the total weight of the blend degraded.

The TG-DTG curve of blend 20 (EEA copolymer, 50% PDMS) showed higher stability than predicted (Fig. 6.3), 125°C more at the start which gradually became less and was only 25°C more than the calculated value at 85% weight loss. The shape of the TG-DTG curve was not similar to TG-DTG curves of pure EEA copolymer or blend 18 with 7.14% PDMS. Blend 20 showed two main degradation stages, the first one starting at 375°C with T_{\max} at 459°C. The second stage according to the DTG curve (difficult to distinguish from the TG curve) started at 475°C and reached T_{\max} at 484°C. There was another broad and small degradation stage starting at about 500°C when there was 89% weight loss. The residue at 600°C amounted to 3.5% by weight of the total original weight of the blend degraded compared with 0.95% expected.

6.3.1.2. TG-DTG Under Air

TG data for blend 20 were also obtained under an atmosphere of air for the purpose of comparison with the results obtained under nitrogen.

Blend 20 like the EEA copolymer showed a complex TG-DTG curve but with two distinguishable degradation stages (Fig. 6.4). The first stage of degradation started at 275°C with T_{\max} at 373°C while the second started at about 425°C with T_{\max} at 457°C. Blend 20 showed a stabilisation of about 50°C at the beginning which gradually increased up to 150°C at end of the degradation. The residue at 600°C amounted to

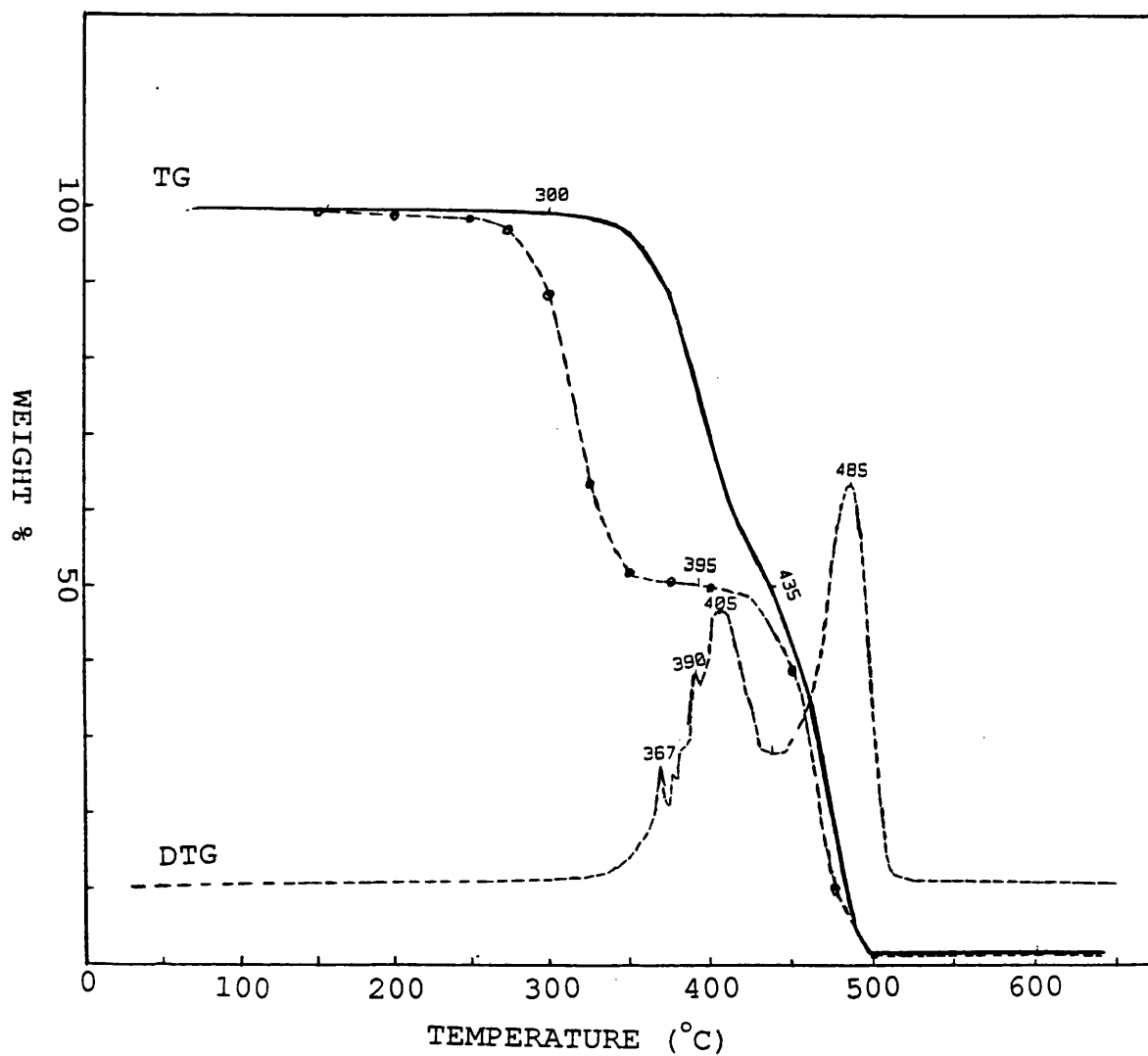


Fig. 6.1. TG-DTG traces for blend 13 (LDPE:BP77 + 50% PDMS) under nitrogen: experimental (—; ····) and calculated (—·—·).

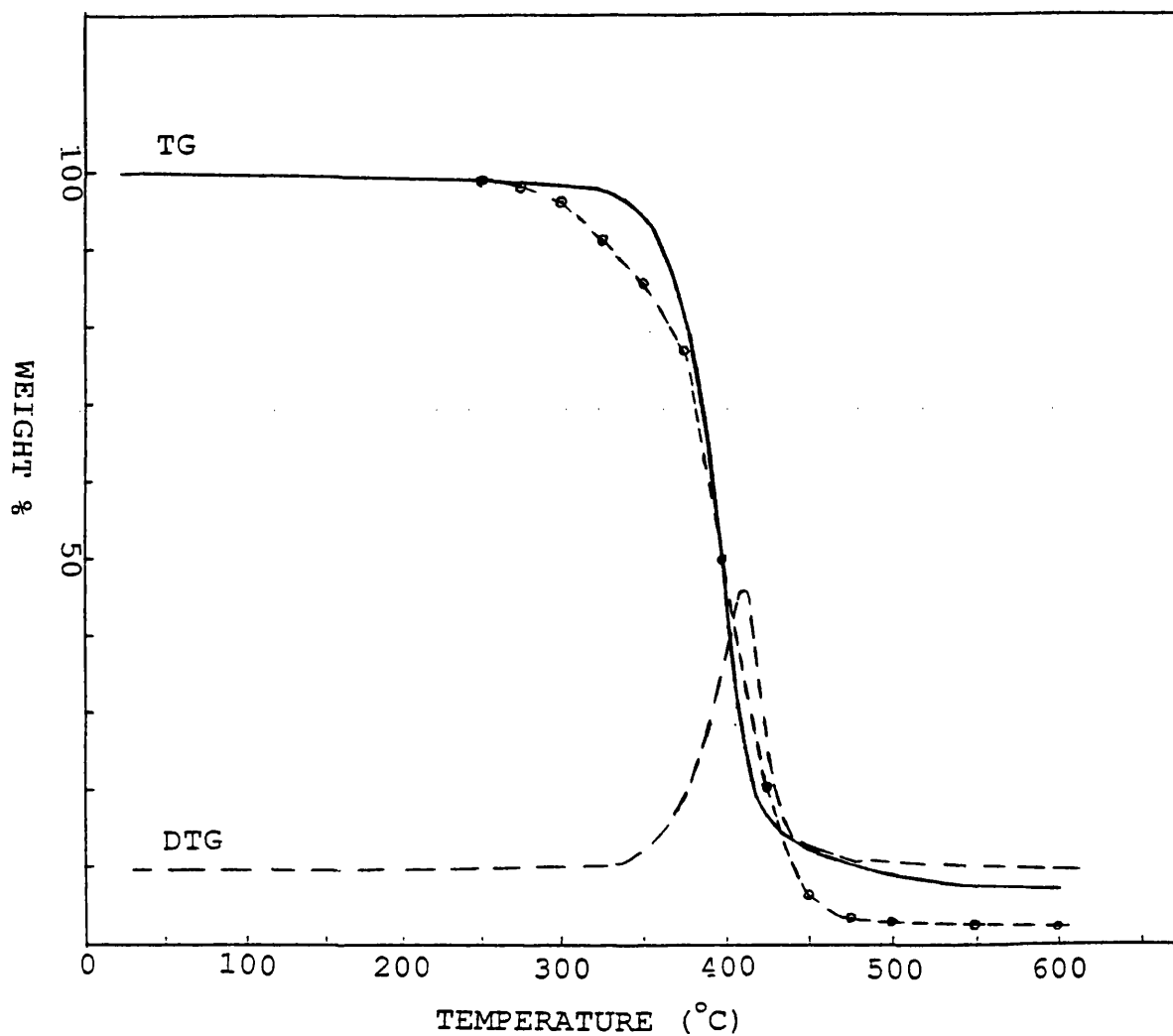


Fig. 6.2. TG-DTG traces for blend 14 (PEA + 7.14% PDMS) under nitrogen: experimental (—; ----) and calculated (-.-.).

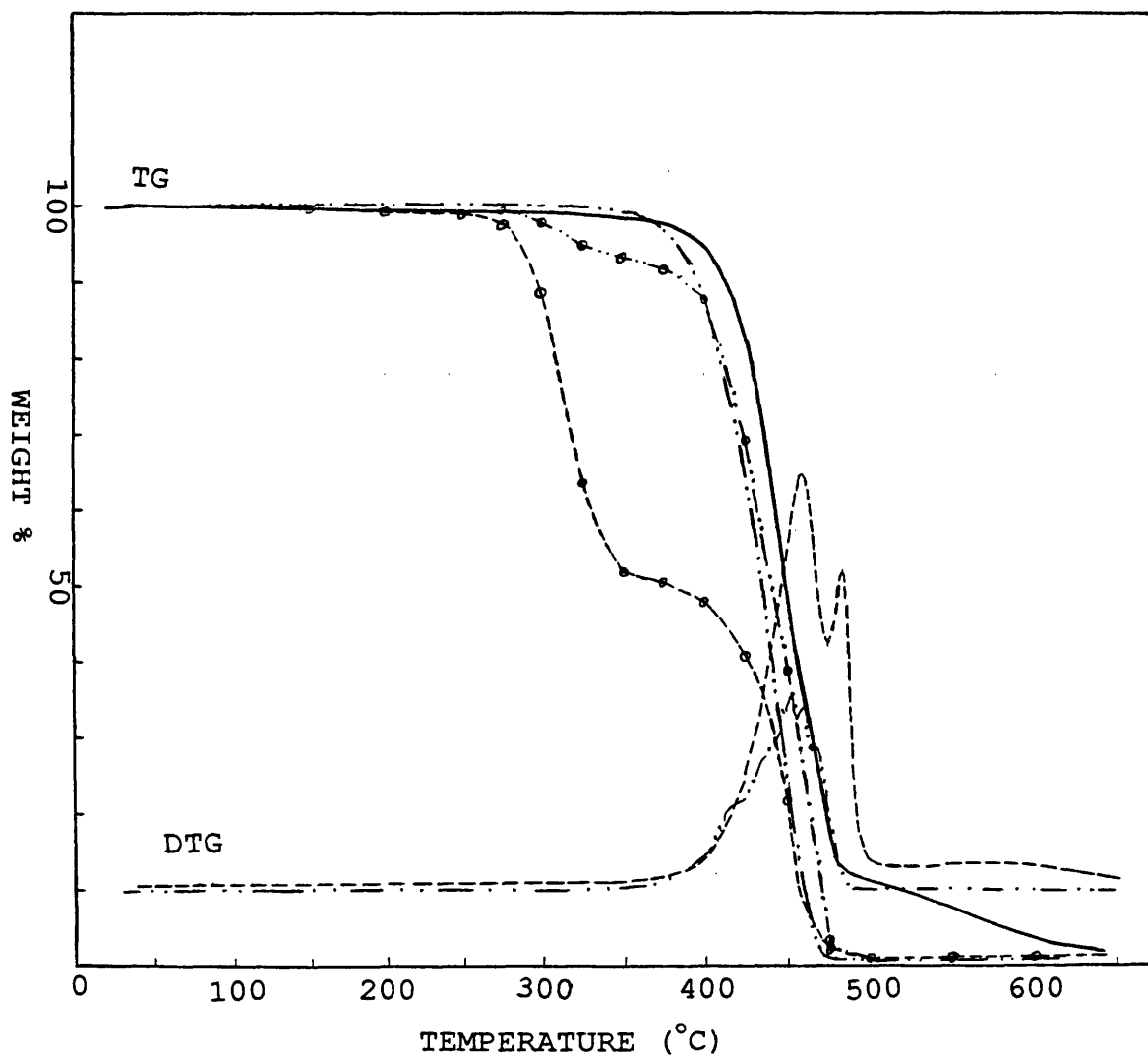


Fig. 6.3. TG-DTG traces for blends of EEA copolymer and PDMS under nitrogen: blend 18 with 7.14% PDMS (experimental (---) and calculated (---)) and blend 20 with 50% PDMS (experimental (—; ----) and calculated (---)).

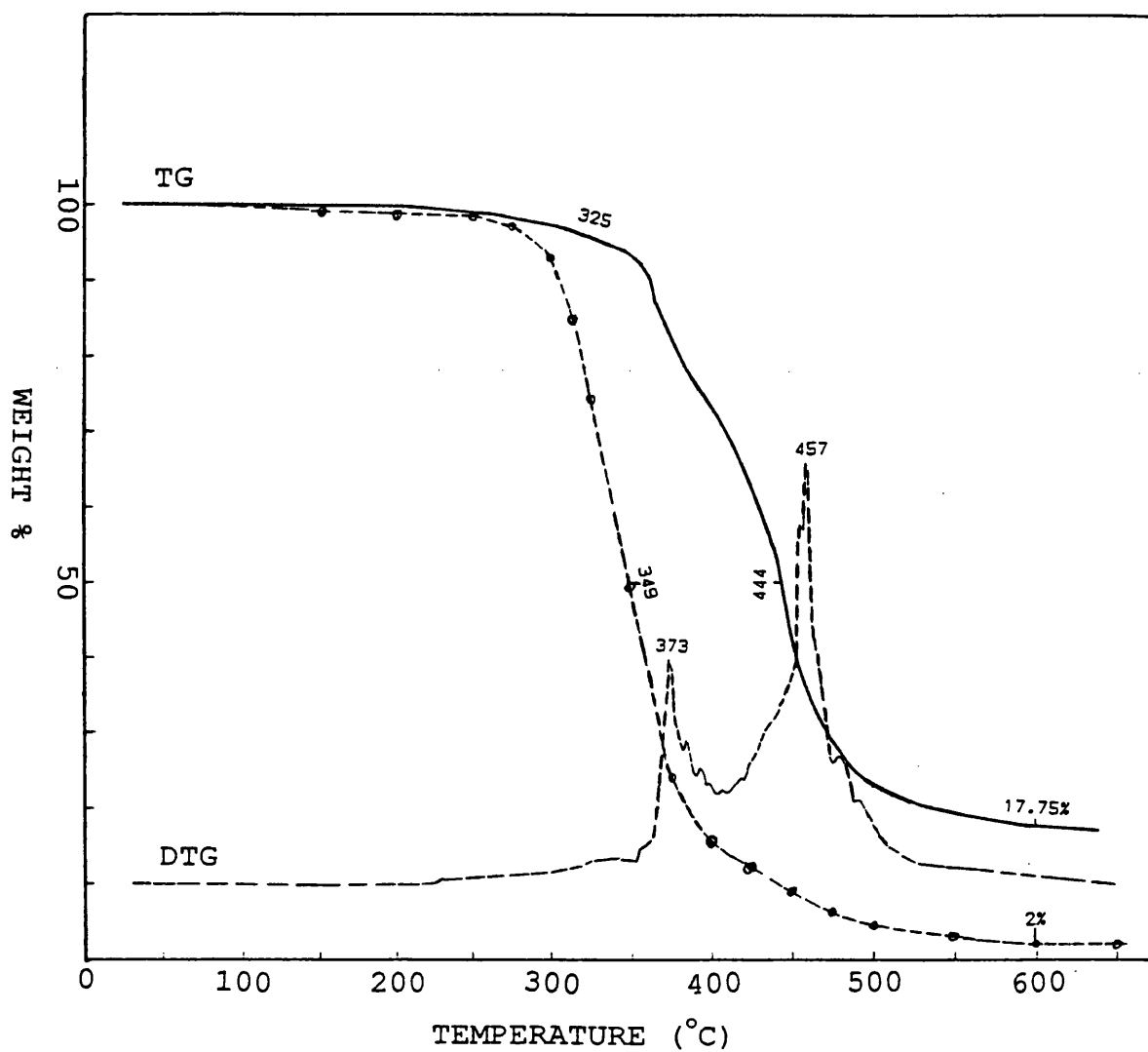


Fig. 6.4. TG-DTG traces for blend 20 (EEA copolymer + 50% PDMS) under air: experimental (—; ----) and calculated (—•—).

17.75% by weight of the total original weight of the blend degraded compared with 2.0% expected.

The TG-DTG results (Table 6.2 (a) and (b)) show that blend 20 is up to 75°C more stable at the beginning in the inert atmosphere than in the air. The stabilisation decreases gradually such that after 65% weight loss the TG-DTG curve in air showed more stabilisation.

Table 6.2.

(a) TG results under nitrogen

Temperatures shown in brackets are calculated values assuming that there was no interaction between the components while T_{50} = Temperature for 50% weight loss

| Sample | T_{thresh} (°C) | T_{50} (°C) | T_{max} (°C) | T_{stop} (°C) | % residue at 600°C |
|----------|--------------------------|---------------|-----------------------|------------------------|--------------------|
| Blend 13 | 325 (250) | 435 (395) | 405, 485 | 510 (500) | 1.5 (1.4) |
| Blend 14 | 325 (250) | 399 (405) | 412 | 500 (500) | 7.25 (2.11) |
| Blend 18 | 350 (250) | 436 (442) | 452 | 490 (500) | 1.0 (0.84) |
| Blend 20 | 375, 488 (250), (350) | 450 (355) | 459, 484 | 650 (500) | 3.5 (0.95) |

(b) TG results under air

| Sample | T_{thresh} °C | T_{50} °C | T_{max} °C | T_{stop} °C | % residue at 600°C |
|----------|------------------------|-------------|---------------------|----------------------|--------------------|
| Blend 20 | 275 (237) | 444 (349) | 373, 457 | 550 (550) | 17.75 (2.00) |

6.3.2. Differential Scanning Calorimetry (DSC)

The DSC curve for blend 13 (carried out under dynamic nitrogen) exhibited two well defined endothermic transitions as shown in Fig. 6.5. The peak temperatures occurred at about 122°C (average) and 495°C. However, there seemed at least two more endotherms in the regions 325-350°C and 377-450°C. The first was assigned to the melting point, T_m , while the others to degradation of the components. There was also a small exotherm shown just before the decomposition started with T_{max} at 318°C.

This may be due to the small amount of cross-linking. The temperature for the maximum rate of degradation agreed within 7-13°C with the TG-DTG results.

6.3.3. Thermal Volatilisation Analysis (TVA) and SATVA Separation of Condensable Degradation Products

Blend of LDPE and PDMS

The first stage of the degradation of blend 13 (Fig. 6.6), due to the decomposition of the PDMS, started at about 246°C (volatilisation started at 250°C when PDMS was degraded alone), reached T_{\max} at 326°C and did not show any rise for the -196°C TVA trace. The second stage of degradation, which started at about 373°C, showed a small rise for the -196°C trace indicating a very small amount of non-condensable gaseous products. The two stage TVA curve obtained was as expected, assuming no interaction between the two components.

The SATVA trace for the separation of the condensable volatile products of degradation of blend 13 showed two gaseous product peaks. The third fraction gave a poorly resolved peak showing a number of different degradation products while the fourth fraction gave two peaks (Fig. 6.7). The first fraction was due to propene and propane and the second to butene and butane. The SATVA trace did not show the presence of ethylene and ethane which were present in small amounts when LDPE was degraded alone.

Fractions 3 and 4 of degradation products from blend 13 were identified mainly by GC-MS since IR spectroscopy only reveals the presence of the functional groups present and not a clear identity of each product. The results for identified degradation products from blend 13 were mainly similar to the degradation products from pure LDPE plus degradation products from PDMS. It was clear from the SATVA curve that most of the degradation products were oligomers of cyclic siloxanes and larger hydrocarbons while there were very small amounts of new products present as well. Table 6.5 shows mass spectrum m/e data and assignments for the new products.

The CRF collected was a white material showing patches on the TVA tube due to oligomers from both type of components. The CRF was not dripping or running down the TVA tube on cooling as in the case of pure PDMS. The IR spectrum of the insoluble CRF showed absorptions similar to both PDMS and LDPE except that there were two extra absorptions, one at 3075 cm^{-1} due to the unsaturation in the hydrocarbons and the other at 1053 cm^{-1} due to the asymmetric Si-O-Si stretching vibration in siloxanes. There was also a weak but sharp peak at 665 cm^{-1} possibly due to either CH_2 rocking in

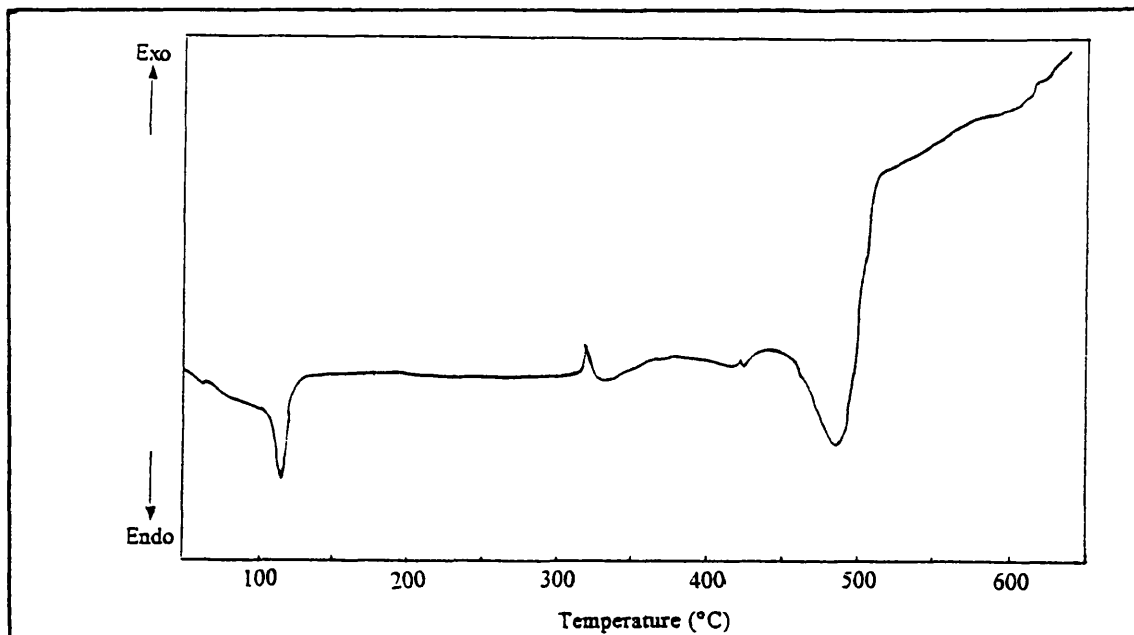


Fig. 6.5. DSC trace for blend 13 (LDPE:BP77 + 50% PDMS) under nitrogen.

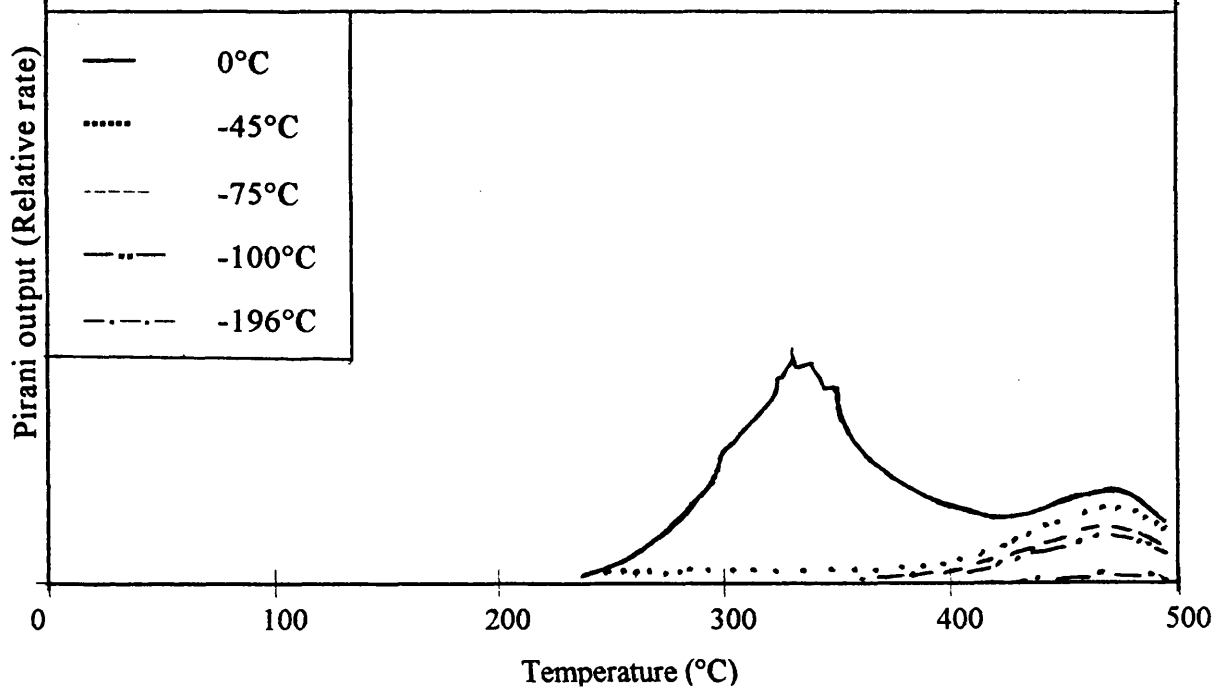


Fig. 6.6. TVA trace for blend 13 (LDPE:BP77 + 50% PDMS).

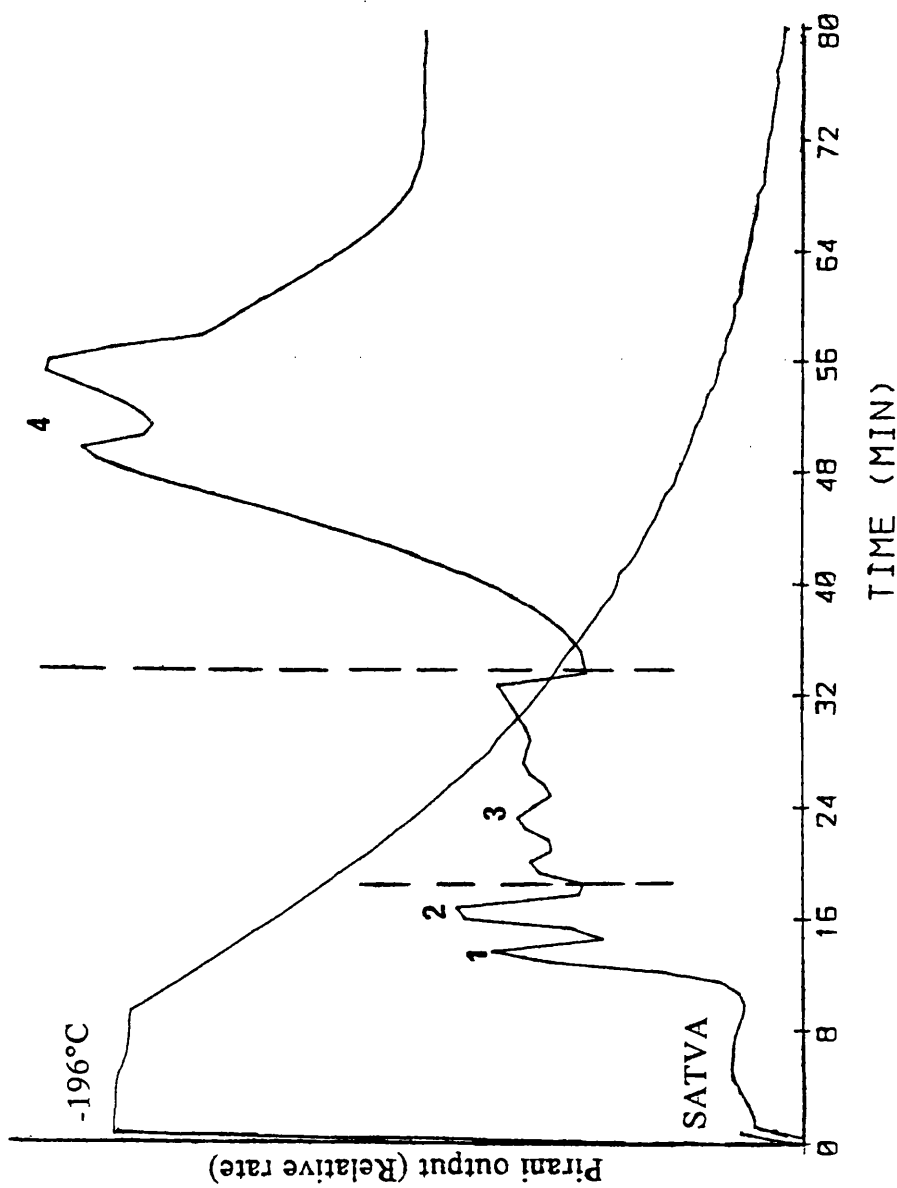


Fig. 6.7. SATVA trace for warm up from -196°C to ambient temperature of condensable volatile products from degradation for blend 13 (LDPE:BP77 + 50% PDMS).

the methylene chains substituted on silicon atoms or Si-C stretching in the Si-Et grouping. The absorptions for the asymmetric Si-O-Si stretching vibration for the siloxanes broadened indicating different alkyl groups substituted on silicon atoms. Absorption at 665 cm^{-1} can only be possible as a result of structures formed by radical reactions.

The residue was more than expected and there were very small patches due to components boundaries. The IR spectrum of the soluble residue, at room temperature, was similar to the IR spectrum of the CRF from PDMS except that the absorptions for the asymmetric Si-O-Si stretching vibration for the siloxanes broadened. There were also very weak absorptions similar to those in the LDPE spectrum. The IR spectrum of the insoluble residue, at room temperature, showed strong absorptions associated with LDPE and weak absorptions associated with PDMS, except that there were extra peaks at 910 cm^{-1} and 930 cm^{-1} due to the unsaturation of the hydrocarbons. There was also a strong absorption at 1160 cm^{-1} which was not assigned but could be due to the Si-CH₂-CH₂-Si type of structure. This type of junction between the two silicon atoms is only possible if some radical reactions occur.

Blends of PEA and PDMS

Volatilisation of blend 14 (commercial PEA + 7.14% PDMS) started at about 300°C and had a main peak with T_{max} at 434°C , compared with 430°C for pure PEA. The shape of the TVA curve (Fig. 6.8 (a)) was similar to that for pure PEA.

Volatilisation of blend 15 (PEA* + 50% PDMS) started at 325°C and reached T_{max} at 417°C (Fig. 6.8 (b)). It was clear from the areas under peaks corresponding to the different cold traps that there were some degradation products which were not as volatile as in the case of pure PEA. A second degradation started at about 450°C but the degradation products seemed to be only volatile enough to pass through the cold traps at temperatures 0°C and -45°C . Siloxane compounds show such kind of behaviour so it was concluded that the second stage of degradation was due to the decomposition of PDMS. There was evidence for non-condensable gaseous products at the first stage but not at the second stage. It was obvious from the nature of the TVA trace that some of the PDMS degraded during the first stage as well.

The TVA trace for blend 16 (50% PDMS), degraded on a stainless steel plate as a thin film, was similar to that of blend 15 except that the second degradation stage started at about 475°C , just before the degradation was stopped. Again like blend 15, the first stage of degradation showed the presence of products volatile enough to pass through

-100°C cold trap and also non-condensable gaseous products, but the second stage products were condensed at temperatures of -75°C and below.

The TVA trace (Fig. 6.8 (c)) of the unmixed sample 17 (50% PDMS) was similar to that of blend 15 except it did not show the presence of the second degradation stage.

The SATVA trace for the separation of the condensable volatile products of degradation of blend 14 showed three peaks or three fractions and a fourth broad, unresolved region. The first fraction was identified as ethylene while the second fraction was identified as carbon dioxide. Traces of ketene were also present in the second fraction of the SATVA separation of the degradation products of blend 14. The absorptions present and their assignments for the IR spectrum of the fraction 3 in both the gas phase and on the salt plate are given in table 6.3.

Table 6.3. Assignments for the IR spectrum of fraction 3 in both gas phase and on salt plate as liquid

| Wavenumber (cm ⁻¹) | Interpretation |
|--------------------------------|---|
| 3660 | O-H stretching in ethanol |
| 2982 and 2918 | C-H stretch in methyl and methyl groups |
| 1760 | carbonyl stretch in an $\alpha\beta$ -unsaturated 6-membered lactone |
| 1730 | carbonyl stretch in ester group |
| 1716-1713 | carbonyl stretch in $\alpha\beta$ -unsaturated ester group |
| 1638 | C=C stretch in $\alpha\beta$ -unsaturated carbonyl compound |
| 1450 | C-H deformation in the methyl and ethyl groups |
| 1410 | O-H bending |
| 1395 | symmetrical deformation of the methyl groups in ethanol |
| 1260 | Si-CH ₃ symmetrical deformation of methyl groups on silicon atom |
| 1305 and 1196 | C-O stretching in all classes |
| 1242 | C-H deformation in the methyl and ethyl groups of ethanol |
| 1067 | C-O stretching in ethanol |
| 1090 and 1049 | asymmetric Si-O-Si stretching vibration |
| 806 | Si-C stretching of methyl groups in O-SiMe ₂ type of structure |

Note: All assignments are based on references 63-72.

The IR spectrum of fraction 3 both on a salt plate (Fig. 6.9) and in gas phase showed the presence of both saturated (minor) and unsaturated (major) ester groups.

The IR spectrum of the fraction 4 in the gas phase showed the presence of cyclic siloxane compounds only. The assignments for the present absorptions are given in Table 6.4.

Table 6.4 Assignments for the IR spectrum for fraction 4 in both gas phase and on salt plate as liquid

| Wavenumber (cm ⁻¹) | Interpretation |
|--------------------------------|---|
| 2965, 2920 and 2860 | C-H stretch of methyl groups on silicon atom |
| 1410 | Si-CH ₃ antisymmetric deformation of the methyl groups |
| 1260 | Si-CH ₃ symmetric deformation of methyl groups on silicon atom |
| 1085 and 1030 | asymmetric Si-O-Si stretching vibration |
| 815 | Si-C stretching of methyl groups in O-SiMe ₂ groups |

All siloxane compounds, whether cyclic or linear, show at least one strong band between 1124-1020 cm⁻¹ arising from an asymmetric Si-O-Si stretching vibration. The position of such absorptions depends on the mass and inductive effect of the substituents on the silicon.

Fractions 3 and 4 of degradation products from blend 14 were also identified by GC-MS since IR spectroscopy only gave a clear indication of the presence of the ethanol and for the other products only revealed the presence of the functional groups present and did not permit identification of each product. The results for identified degradation products from blend 14 showed that these were mainly similar to the degradation products from pure PEA plus degradation products from PDMS, as reported in Chapters 3 and 4 respectively, but there were also small amounts of new products present, mainly similar to those found in blend 13. Table 6.5 shows the mass spectrum m/e data and assignments for the new products.

It was obvious from the area under the SATVA trace for the peak 2 that the formation of CO₂ was reduced considerably in comparison with the cases of pure polymer or blend 2 (PEA + CaCO₃)

The cold ring fraction (CRF) of degradation products was a viscous yellowish brown liquid, without any noticeable presence of the less viscous liquid CRF from PDMS, while the residue was black. The IR spectrum of the CRF from blend 14, run in dichloromethane, was similar to the IR spectrum of the CRF from pure PEA except in the following respects:

The shoulder around 1760 cm^{-1} was not well defined while the original carbonyl peak at 1730 cm^{-1} was as strong as in the undegraded PEA. There were also extra absorptions at 1260 cm^{-1} , 1098 cm^{-1} , 1028 cm^{-1} , 804 cm^{-1} and 857 cm^{-1} due to the presence of siloxane groups. The IR spectrum of the CRF from blend 14 was in fact like the IR spectrum of the CRF from blend 2 (Chapter 5) except that absorptions due to the siloxane groups were also present.

The absence of the absorption due to acid groups in both cases indicates that the formation of these acid groups is either prohibited or they interact with the other component on their formation and stay in the residue due to their change in chemical nature after interaction instead of forming small molecular weight acid products.

The IR spectrum of the residue from blend 14 showed mainly the presence of siloxane groups based on the PDMS repeat structure. However if these siloxane absorptions were subtracted from the spectrum then it resembled the spectrum of the residue from pure PEA.

The SATVA trace for the separation of the condensable volatile products of degradation of blend 15, (Fig. 6.8 (i)) showed 4 fractions. The first fraction was identified as ethylene, the second fraction was identified as carbon dioxide (CO_2) with traces of ketene. The IR spectrum of fraction 3 was similar to the IR spectrum of fraction 3 from pure PEA except that there were extra absorptions at 1260 cm^{-1} , 1035 cm^{-1} and 818 cm^{-1} , all due to the siloxane groups.

The IR spectrum of fraction 4 was similar to the IR spectrum of the volatile degradation products from the pure PDMS showing mainly the presence of the cyclic trisiloxane and cyclic tetrasiloxane.

The IR spectrum of the CRF was essentially the sum of those of the cold ring fractions from the components.

The residue from blend 15 was insoluble and it was clear from the patchy appearance that this blend was not uniformly mixed, since the boundaries of each

component were more noticeable after degradation since PEA leaves dark brown patches on the container while PDMS leaves clear patches. The IR spectrum of the residue showed absorptions only for siloxanes as in the IR spectrum of the residue from the pure PDMS. No changes were detectable because the spectrum was only taken of the surface of the residue due to its insolubility and difficulty to grind. Also absorptions due to any changes e.g. cross-linking, would be masked by the strong absorptions for the Si-O-Si structure.

The SATVA trace for separation of the condensable products of degradation of blend 16 was also similar to that of blend 15 products except fractions 4 and 5 were much less than in the case of blend 15. The IR spectra of the CRF and residue (insoluble) were also similar to those obtained for blend 15. However, the residue was more in the case of blend 16.

The SATVA trace (Fig. 6.8 (ii)) for separation of the condensable volatile products of degradation of sample 17 showed 4 fractions. The first fraction was identified as ethylene, the second fraction as carbon dioxide (CO₂) but with no traces of ketene. The IR spectrum of fraction 3 was similar to the IR spectrum of fraction 3 from blend 15 except that there was extra absorption at 915 cm⁻¹. Fraction 4, due to siloxane compounds, was much more than in the case of any of the mixed blends and showed absorptions which were the sum of the absorptions from the fractions 3, 4 and 5 from blends 14 and 15 except there were weak absorption for ethanol and there was no absorption at 1760 cm⁻¹.

The CRF was smaller in amount than expected and its IR spectrum was the sum of those of the CRFs from both components.

The residue from the PDMS was soluble and its IR spectrum was similar to the IR spectrum of the residue from pure PDMS.

Blends of EEA Copolymer and PDMS

The TVA traces for blends 18 (Fig. 6.10 (a)) and 19 were similar in shape to that for pure EEA copolymer and showed onset of decomposition (T_{onset}) at the normal decomposition temperature of EEA copolymer at about 350°C but reached maximum rate of product evolution (T_{max}) at 460°C compared with 450°C for EEA copolymer. The TVA trace of blend 20, in which case degradation was carried out up to 600°C, showed two degradation stages, the main degradation stage starting at the normal

degradation temperature of the pure EEA copolymer but reaching T_{\max} at 459°C. A shoulder developed at about 485°C that only was revealed from the 0°C cold trap. A second small degradation stage started at about 540°C and gave no evidence for the non-condensable gaseous products. There was also only a response from the gauge after the 0°C trap, indicating the low volatility of the degradation products. This type of behaviour was observed in the case of blends 14, 15 and 16 except that the TVA traces of these blends also showed a response in the -45°C trace.

The SATVA curve for the separation of the condensable volatile products of degradation of blends 18-20 showed three gaseous product peaks. The remaining material gave broad, poorly resolved peaks showing a number of different degradation products. The first peak was due to ethylene and ethane, the second peak to carbon dioxide (major) and ketene, while the third peak was attributed to propene, butene and their corresponding saturated hydrocarbons. The IR spectra of the volatile products of degradation in the fourth fraction from blends 18 and 20, in the gas phase, were similar to those from pure EEA copolymer except for the following changes:

- the broad peak at 1760 cm^{-1} for the carbonyl group split into three poorly resolved peaks with absorptions at 1785 cm^{-1} , 1740 cm^{-1} and 1710 cm^{-1} .
- the intensity of the bands at 1642 cm^{-1} and 1590 cm^{-1} was reduced.
- there were extra absorptions due to siloxane compounds at 1415 cm^{-1} (weak and slightly broad) and at 1262 cm^{-1} (strong and sharp) due to the antisymmetric and symmetric stretching vibrations of methyl groups on silicon atoms (Si-CH₃) respectively; the absorption at 1067 cm^{-1} became more strong due to presence of siloxane Si-O-Si group; there was a weak absorption at 1030 cm^{-1} also due to the Si-O-Si group; there were bands at 865 cm^{-1} (weak but sharp) and 808 cm^{-1} (strong and sharp) both due to the Si-C stretching of methyl groups in O-Si-(Me)₂ groups.
- the strong absorption at 910 cm^{-1} became weak and there was an extra absorption at 710 cm^{-1} (medium and sharp).

The IR spectra of the volatile products of degradation of the small portion at the beginning of the fourth fraction from blends 18 and 20, in the gas phase, were mainly similar to that of the degradation products from pure PDMS, showing the presence of cyclic hexamethyltrisiloxane and cyclic octamethyltetrasiloxane.

The GC-MS technique was also applied to identify the complex mixture of compounds in the fourth fraction. The results for degradation products of both mixed and unmixed samples showed the presence of new peaks with ion peaks for both siloxanes and hydrocarbons but their identification was difficult because there were no parent ion peaks present. It is clear, however, that the new compounds contain at least 3 siloxane units (OSiMe_2) shown by the intense ion peak for one of these compounds at m/e 207. These new compounds possibly contain large alkyl groups substituted on at least one of the silicon atoms thus result showing ion peaks for both type of fragments. This result shows that some of the radical reactions between the products from two components were taking place in the gas phase. Ion peaks and assignments for some new siloxane compounds are given in Table 6.5.

GC-MS results from products from mixed systems showed only negligible amounts of acids such as acetic and propanoic while these acids were present in products from the unmixed system.

It was clear from the area under the peak in the SATVA trace and the IR spectrum of the gaseous products that blends of EEA copolymer and PDMS gave less gaseous products than in the case of pure EEA copolymer. Thus, the formation of CO_2 was at least 4 times less than in the case of pure copolymer. However, formation of ketene almost doubled compared with pure copolymer. The amount of CO_2 was almost twice that of ketene in the case of blends 18 and 20 while it was about 4 times more in the case of the copolymer. The formation of ethylene decreased in the mixed systems as seen from the SATVA trace. Formation of siloxane cyclic oligomers was also reduced in the mixed systems.

The CRFs from blends 18-20 were lighter in colour (lemon yellow) than that CRF from the EEA copolymer when degraded alone and were not smooth i.e. were in patches. The IR spectra of the CRFs were similar to the IR spectrum of the CRF from the copolymer except that there were absorptions at 800 cm^{-1} , 860 cm^{-1} , 1020 cm^{-1} , 1095 cm^{-1} and 1260 cm^{-1} which were characteristic of siloxanes of the type $(\text{Me}_2)\text{SiOSi}(\text{Me}_2)$.

The IR spectra of the residues were again similar to that of the residue from the EEA copolymer except that the absorptions at 1736 cm^{-1} and 2980 cm^{-1} (C-H stretch of methyl groups) did not totally disappear. This shows that some of the ester groups survived through decomposition. Also there were extra absorptions due to the siloxane groups at 800 cm^{-1} , 1020 cm^{-1} , 1090 cm^{-1} and 1262 cm^{-1} .

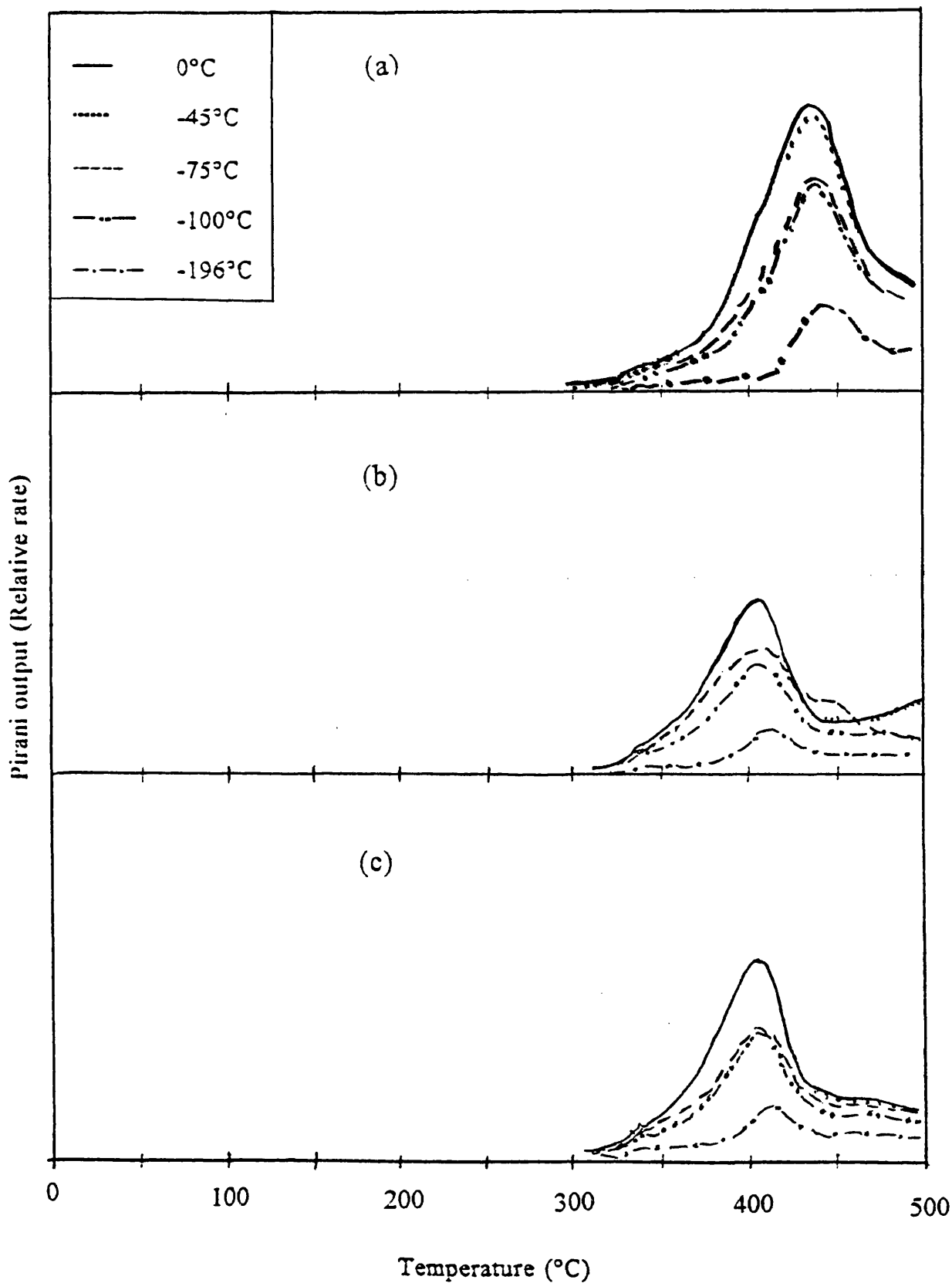


Fig. 6.8. TVA traces for blends of PEA and PDMS: (a) blend 14 (7.1% PDMS), (b) blend 15 (50% PDMS) and (c) unmixed sample 17 (PEA and PDMS (1:1)).

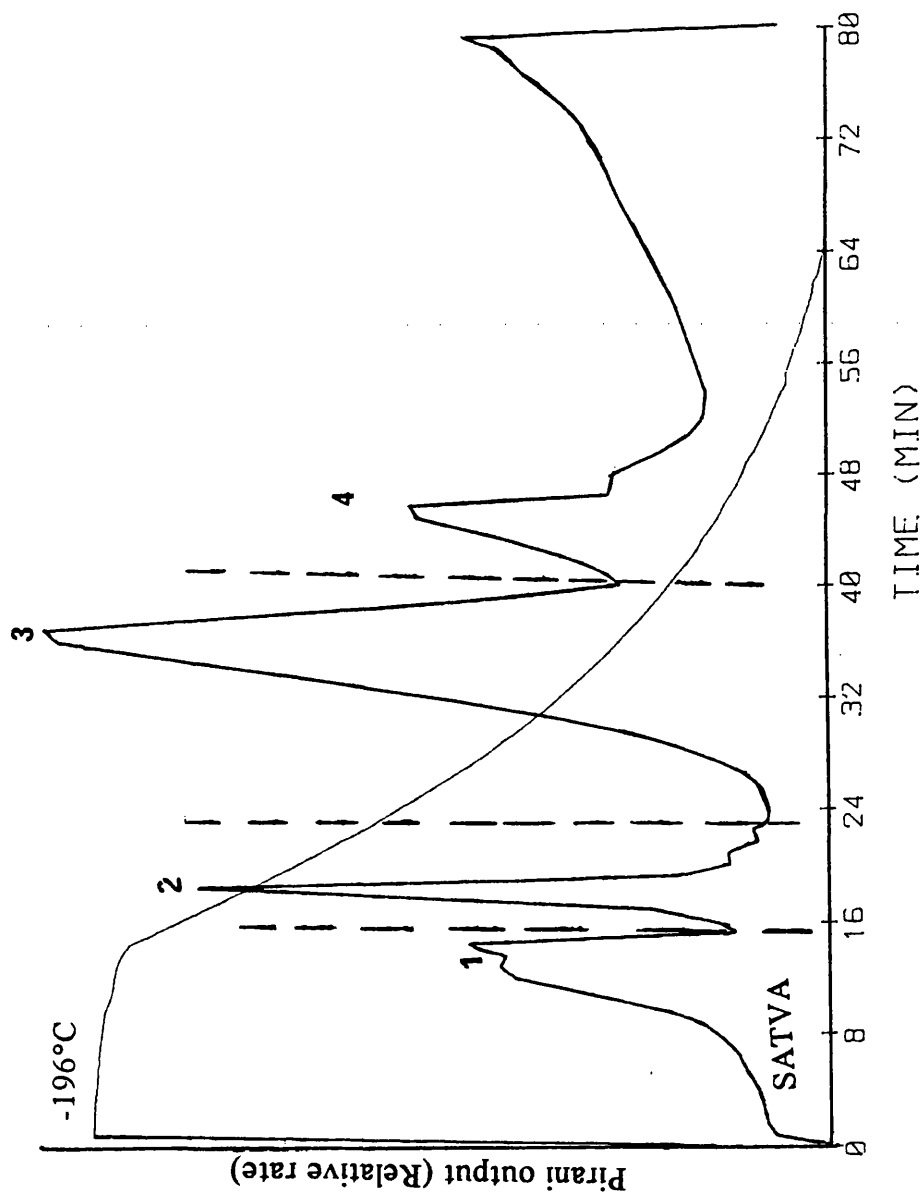


Fig. 6.8. (i) SATVA trace for warm up from -196°C to ambient temperature of condensable volatile products from degradation for blend 15 (PEA + 50% PDMS).

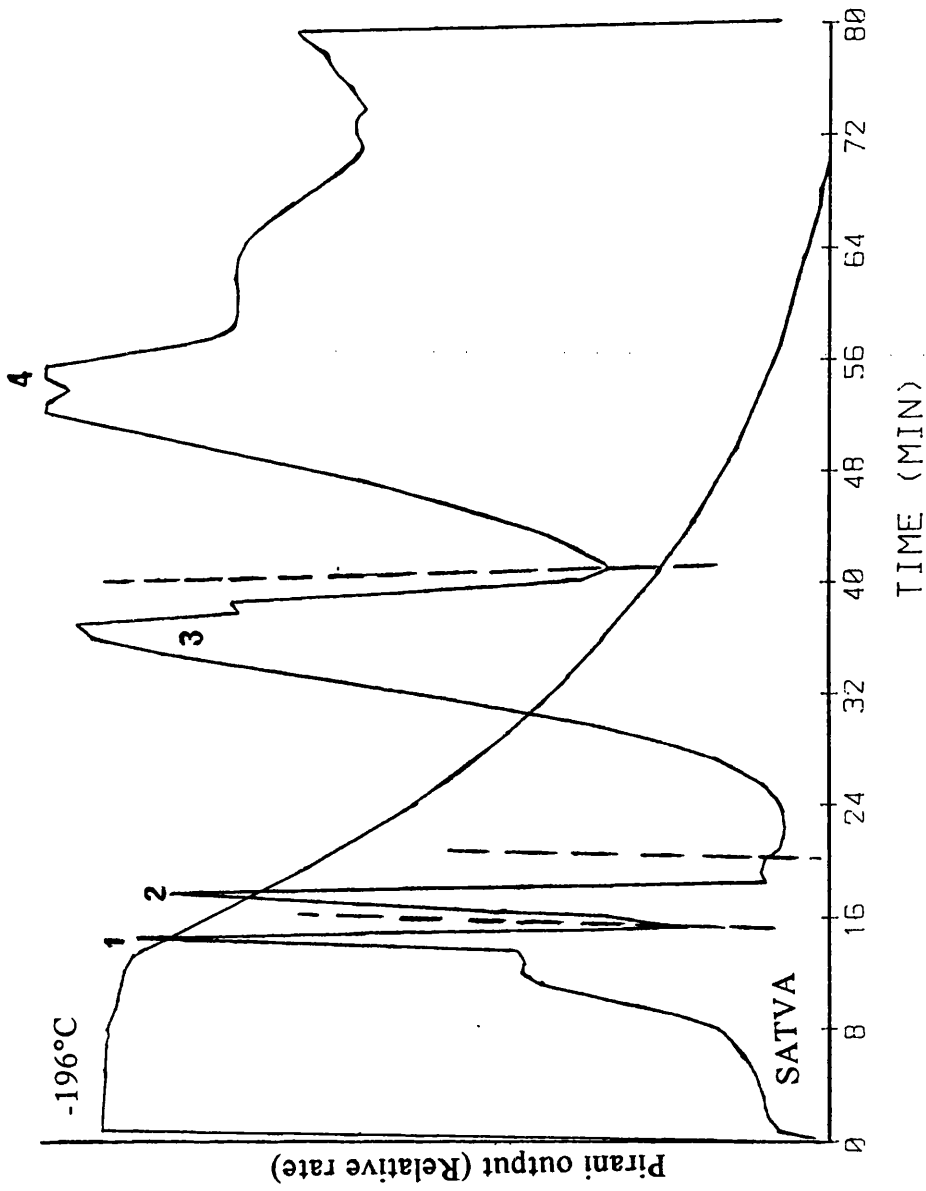


Fig. 6.8. (ii) SATVA trace for warm up from -196°C to ambient temperature of condensable volatile products from degradation for unmixed sample 17 (PEA and PDMS 1:1).

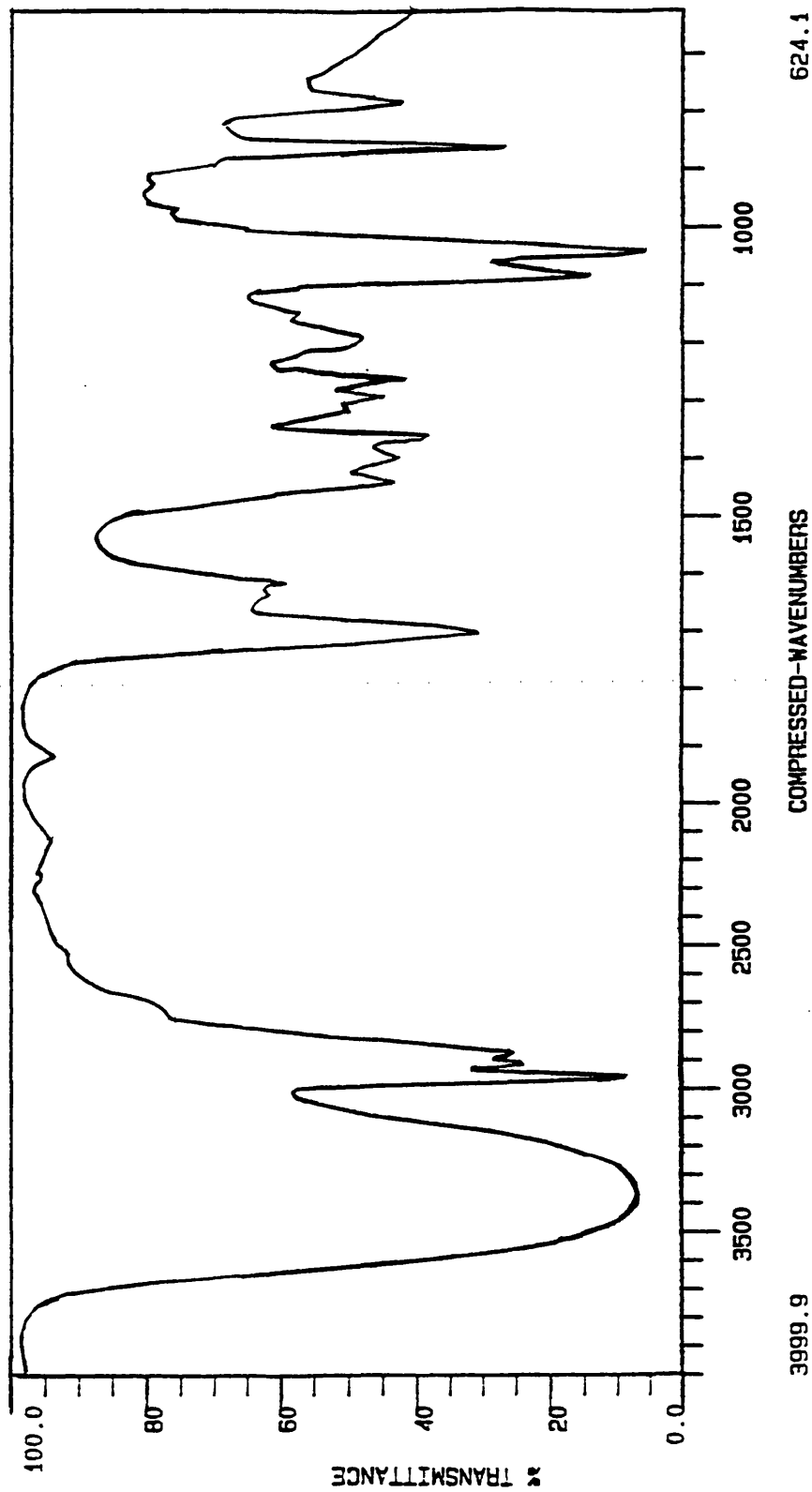


Fig. 6.9. IR spectrum of fraction 3 in SATVA separation of products from the degradation of blend 14 (PEA + 7.14% PDMS).

3999.9

COMPRESSED-WAVENUMBERS

624.1

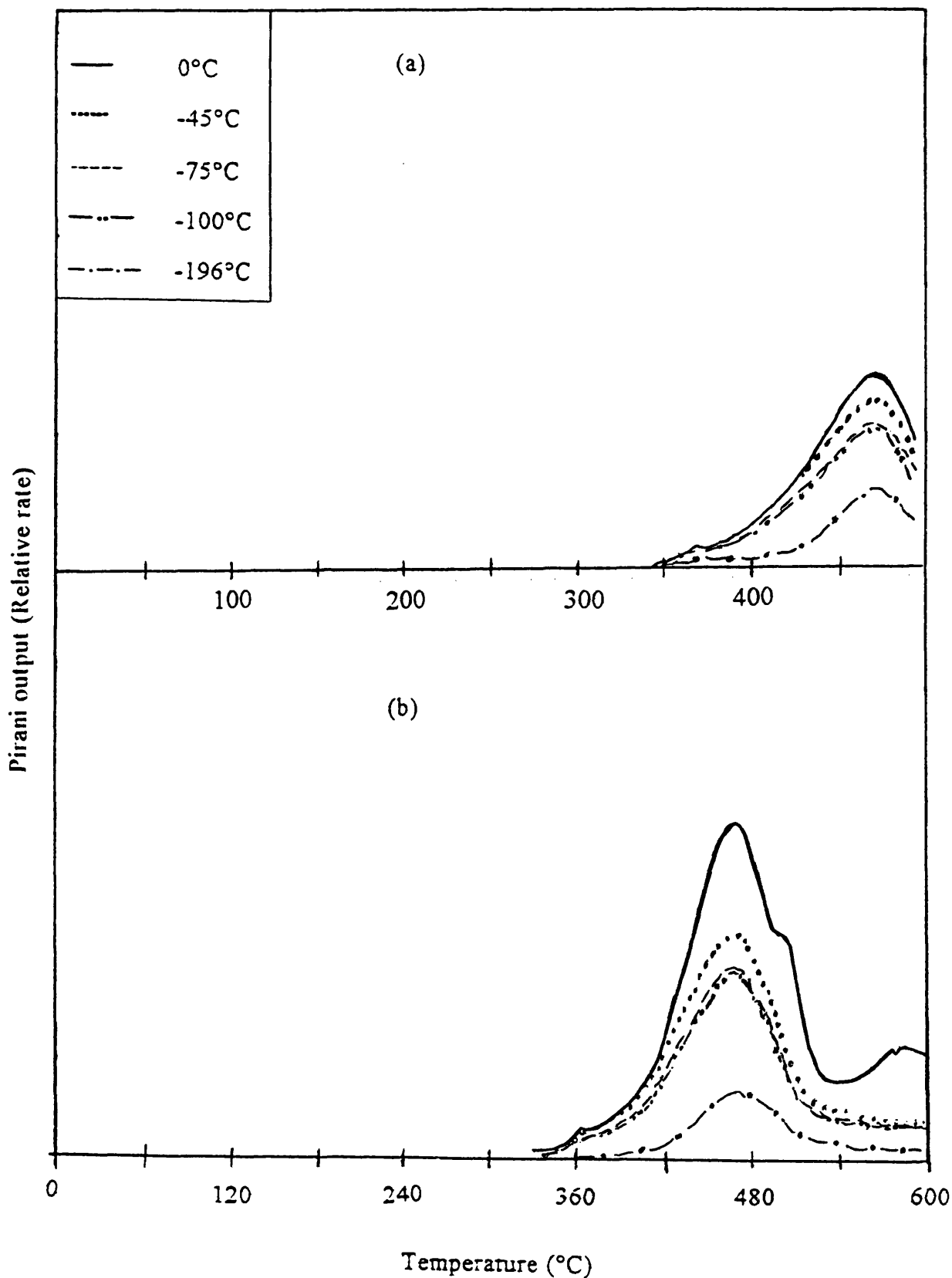


Fig. 6.10. TVA traces for blends of EEA copolymer and PDMS: (a) blend 18 (7.1% PDMS) and (b) blend 20 (50% PDMS).

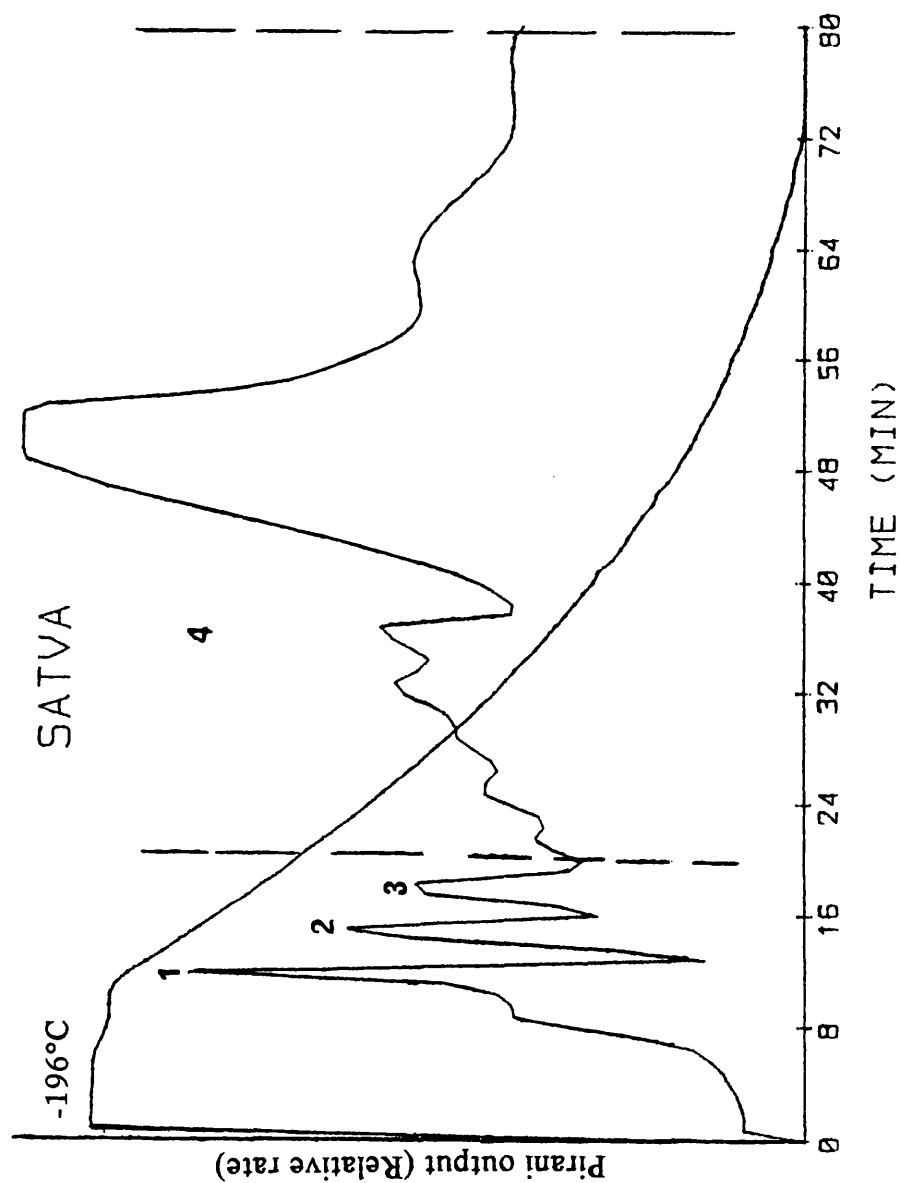
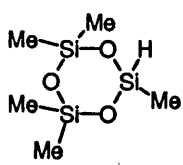
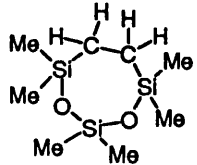
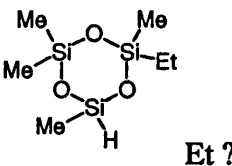
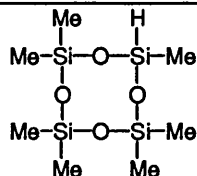


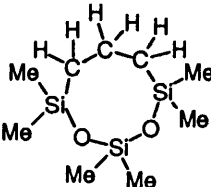
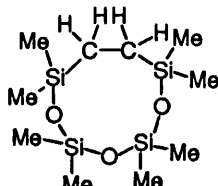
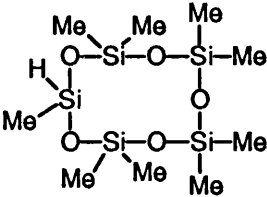
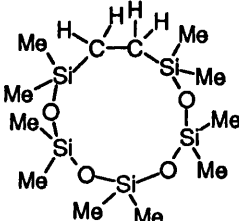
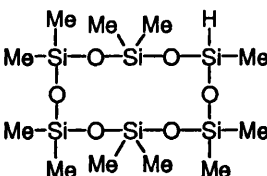
Fig. 6.11. SATVA trace for warm up from -196°C to ambient temperature of condensable volatile products from degradation for blend 20 (EEA copolymer + 50% PDMS).

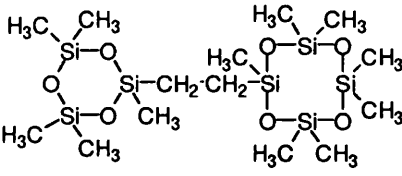
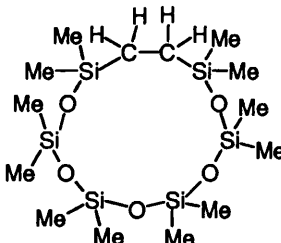
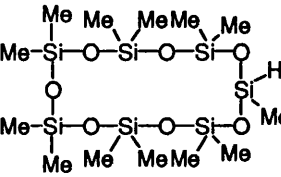
PDMS

Nearly all of the above experiments showed stabilisation of the PDMS and it was difficult to explain the stabilisation of PDMS in an unmixed sample. Therefore, other degradations were carried out on PDMS alone. The degradation conditions (e.g. film was cast on the degradation tube and 7-25 mg polymer sample was taken) were kept similar to those as the above samples. It was found that under these conditions, the degradation of PDMS samples started at 300-321°C but the main degradation started at 350-375°C; depending on the sample size, the smaller samples starting at higher temperatures. Thus film thickness is important in PDMS degradation with thicker films showing lower stability.

Table 6.5. Mass spectrum m/e data and assignments for the new siloxane compounds.

| Scan | m/e (% abundance) | Structure/Name | Comments |
|------|---|--|-----------------------------------|
| 57 | 193(100), 194(19), 89(18), 133(15), 195(14), 207(9), 177(8), 163(6), 75(5), 103(3), 191(2), 208(0) |  | Trace*** |
| 105 | 219(100), 89(25), 220(20), 193(18), 133(15), 207(13), 102(8), 163(5), 75(3), 234(0) |  | Minor* |
| 115 | 207(100), 193(31), 206(20), 208(18), 221(15), 133(12), 191(12), 89(10), 96(6), 177(4), 222(5) |  | Minor only seen in blend 20 |
| 134 | 267(100), 268(28), 193(20), 269(15), 281(12), 191(10), 73(10), 133(7), 282(3) |  | Minor** |
| 147 | 57(100), 43(80), 41(40), 71(38), 83(28), 207(20), 98(8), 208(8), 142(7), 193(6), 209(5) | Possibly tricyclicsiloxane compound with alkyl group substituted on at least one silicone atom. | Trace** |

| | | | |
|-----|--|--|------------------------------------|
| 148 | 55(100), 87(85), 86(70), 111(60), 41(60), 113(58), 69(55), 112(45), 128(35), 283(20), 282(18), 156(10) | ? | Trace only seen in blend 20 |
| 149 | 231(100), 203(40), 233(20), 219(15), 177(10), 133(8), 89(5), 73(3), 246(0) |  <p>(D₃C₃); 1, 1, 3, 3, 5, 5-Hexamethyl-1, 3, 5-trisila-2, 4-dioxacyclooctane</p> | Trace* |
| 170 | 207(100), 208(22), 209(16), 193(13), 96(10), 97(9), 191(8), 133(6), 75(4), Parent ion(0) | Possibly Dimer of cyclic trimer (D ₃) joined by Si-Si linkage Or may be D ₃ with larger alkyl group on at least one Si atom | Minor, only seen in blend 20 |
| 192 | 293(100), 294(25), 193(25), 265(20), 73(18), 281(10), 207(6), 59(5), 308(0) |  | Minor*** |
| 200 | 281(100), 101(80), 294(77), 116(75), 57(70), 73(40), 282(38), 296(30), 127(20), 193(18), 195(18), 266(16) | Possibly D ₃ with larger alkyl groups substituted on siloxane atoms. | Trace** |
| 220 | 73(100), 267(90), 341(85), 253(15), 59(7), 193(5), 59(18), 355(3), 356(0) |  | Trace*** |
| 279 | 73(100), 85(50), 367(25), 267(16), 59(15), 279(5), 207(4), 368(3), 281(2) |  | Minor* |
| 314 | 73(100), 341(35), 59(18), 327(15), 325(12), 415(10), 147(8), 133(6), 207(3), 311(2), 430(0) |  | Trace*** |

| | | | |
|-----|---|--|----------|
| 340 | 207(100), 96(25), 208(20), 209(18), 281(14), 55(13), 133(10), 191(9), 282(5) |  | Trace** |
| 368 | 73(100), 85(36), 341(15), 59(12), 441(10), (147(7), 442(4), 207(3), 456 |  | Minor* |
| 400 | 73(100), 147(20), 281(15), 327(12), 59(10), 133(5), 207(4), 415(3), 401(1), 504(0) |  | Trace*** |

Notes: All structures of the compounds mentioned above are based on the fragmentation pattern of the ion peaks.

* = found in all mixed samples, ** = found in all samples and *** = found in blends 15 and 20.

6.4. DISCUSSION

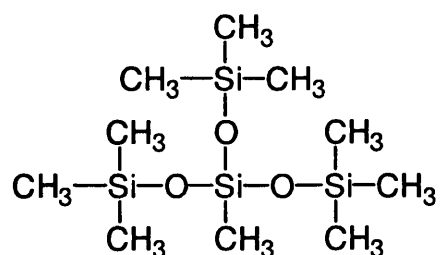
The threshold temperatures for the evolution of the volatile degradation products and the temperatures at which the degradation processes occurred at a maximum rate (T_{\max}), obtained by each method, were generally in agreement for samples 18-20. Blend 13, however, showed up to 75°C stabilisation under dynamic nitrogen by the TG technique, while degradation carried by TVA under continuous evacuation did not show this stabilisation. The T_{\max} temperature recorded under vacuum, in the case of TVA, for blend 14 (PEA + 7.14% PDMS) was 22°C lower than that measured under dynamic nitrogen by the TG-DTG technique.

A difference of 10-15°C between the two techniques is understandable as small volatile degradation products will diffuse more readily from the polymer bulk in a continuously evacuated system but the larger differences shown by the above blends are difficult to understand.

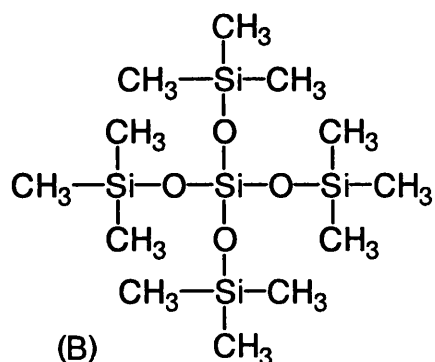
The decomposition of PDMS in blend 13 at its normal degradation temperature under continuously pumped and high vacuum conditions indicated that there was no interaction between the components at the beginning of the degradation. The stabilisation shown by PDMS in a system which was not under continuous evacuation was obviously due to the fact that the degraded products from PDMS were not removed from the LDPE melt as soon as they were formed. As the degradation products at the lower temperatures are mostly larger cyclic oligomers, the evolution of these large compounds in a non-evacuated system in a melt with another polymer depends on the permeability of these oligomers through the other component. If the permeability is poor then the evolution of these oligomers would occur at a higher temperature. Under such conditions the possibility of repolymerisation of these compounds exists and this also reduces the weight loss of the polymer.

The presence of an extra band at 1053 cm^{-1} in the IR spectrum of the CRF from blend 13 indicates the presence of some new siloxane material with different chemical structure than cyclic dimethylsiloxane oligomers. The IR spectra of the linear siloxane compounds give absorptions in the $1060\text{-}1040\text{ cm}^{-1}$ region⁶⁷ but the absorption in question is much less in these model compounds $(\text{CH}_3\text{-(Me)}_2\text{Si-O-})_n\text{-SiMe}_3$ compared with the degraded material. Another possibility is the Si-O stretching vibration of the group Si-O-CH_3 ⁷⁰. Both above explanations would imply a large concentration of new end groups in the degraded polymer in turn implying considerable chain scission almost inevitably involving a rather complex mechanism that is not easy to formulate.

Wright and Hunter⁶⁷ have reported the presence of strong bands occurring at 1055 cm^{-1} and 1068 cm^{-1} respectively in the IR spectra of the branched compounds 3-trimethylsiloxyheptamethyltrisiloxane (A) and 3, 3-di(trimethylsiloxy)hexamethyltrisiloxane (B)



(A)



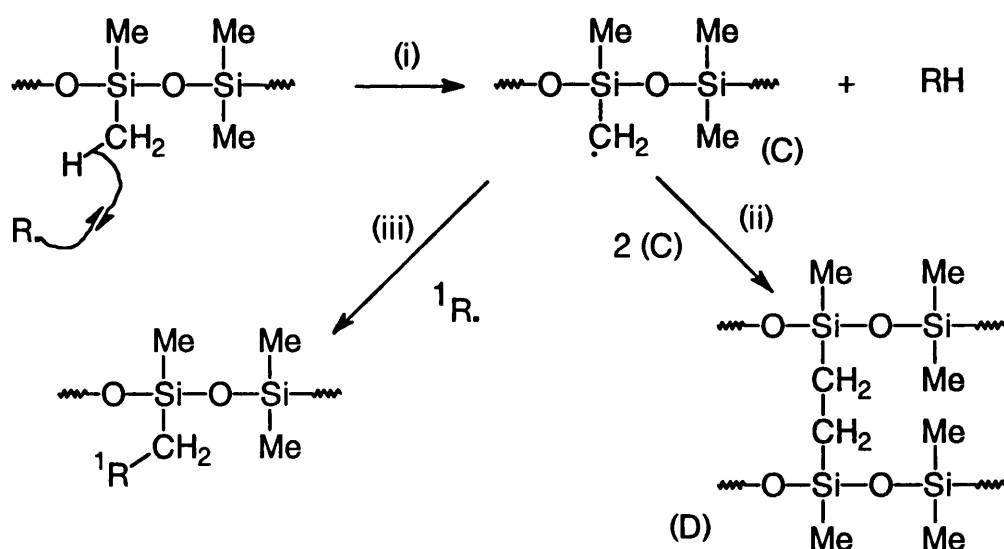
(B)

Macfarlane and Grassie¹⁰⁹ reported an absorption at 1062 cm^{-1} in the IR spectrum of PDMS degraded in a limited amount of oxygen and concluded that it was due to crosslinking, on the basis that the residue showed swelling in carbon

tetrachloride. They did not show the chemical structure or the mechanism of crosslinking.

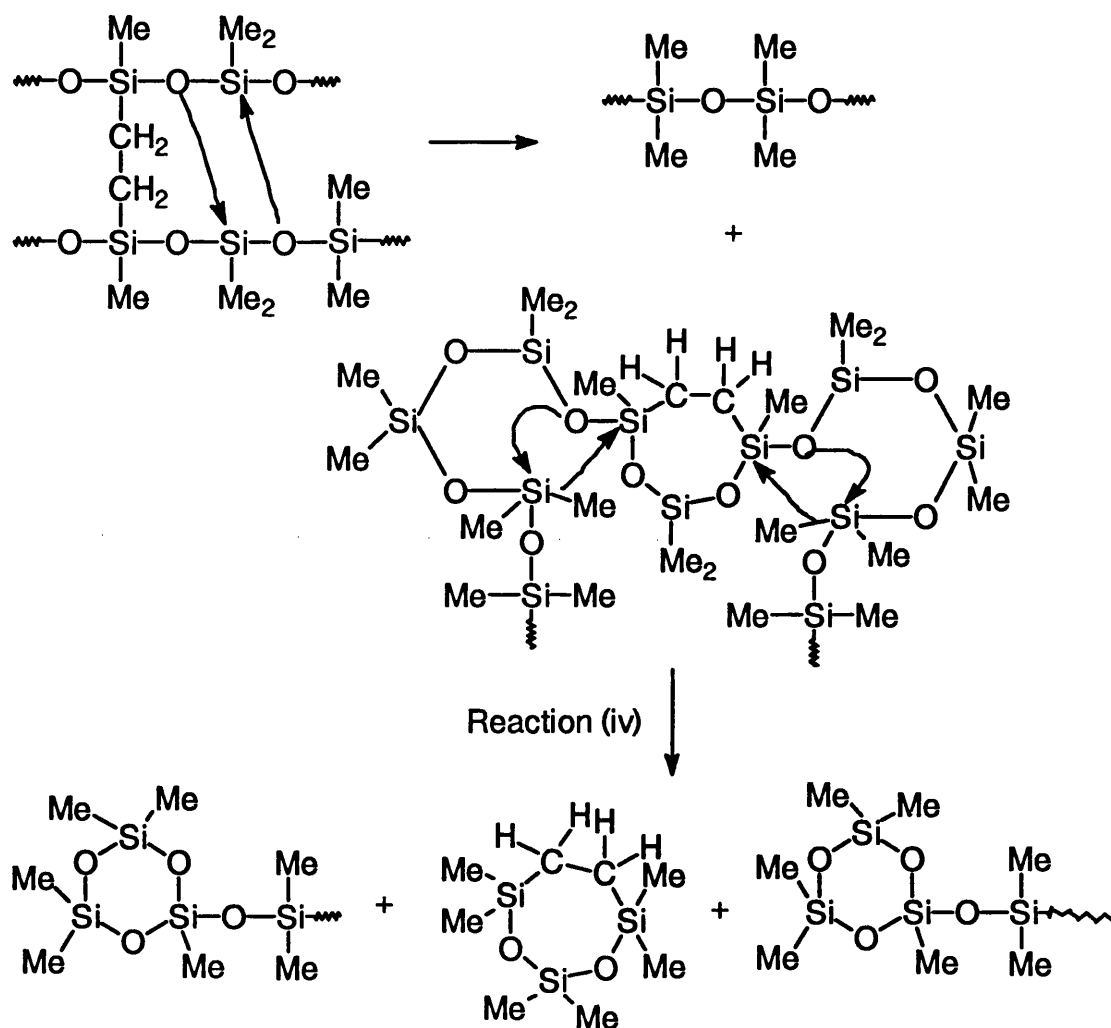
The formation of structures of the type (A) and (B) in the absence of oxygen is not possible also the PDMS in the present research did not have trimethyl end groups. The other explanation is that the actual shape of the spectrum in the region $1100\text{-}1000\text{ cm}^{-1}$ depends on the nature of the substituent alkyl groups attached to the silicon atoms. Linear polymethyldecylsiloxane fluid gives a strong band centred at about 1053 cm^{-1} . Thus there is possibility that crosslinking between the components results in formation of different alkyl groups on the silicon atoms through radical reactions.

Although radical reactions are not common in silicon chemistry, the small polarity of the C-H bond of the methyl group substituted on silicon cases a high reactivity during contact with radicals. So crosslinking in PDMS chains could be very easily introduced in an environment rich in radicals. Since degradation of LDPE, source of the radicals in the melt of the components, begins well before the degradation of PDMS ceases, there would be crosslinking and formation of new alkyl groups on the silicon atoms in reasonable amounts. Thus the new band at 1053 cm^{-1} could be explained¹²⁸. The insolubility of the residue and formation of new siloxane compounds can also only be explained in the terms of radical reactions taking place after the degradation of LDPE starts. The following mechanism has been proposed for the crosslinking in the polymer chains that results in insolubility of the residue and for the formation of certain alkyl bridged cyclic compounds from radical reactions.



Radicals R and 1R are any radicals from LDPE but reactions between the bulky radicals would only take place on the boundaries of the two components. Silicones with alkyl substituents other than dimethyl or phenylmethyl are considerably less stable and

their stability decreases as the length of the alkyl group increases¹²⁹. Crosslinked chain (D) then results in the formation of one of the new homologous series of compounds with ethylene linkage from the following mechanism:



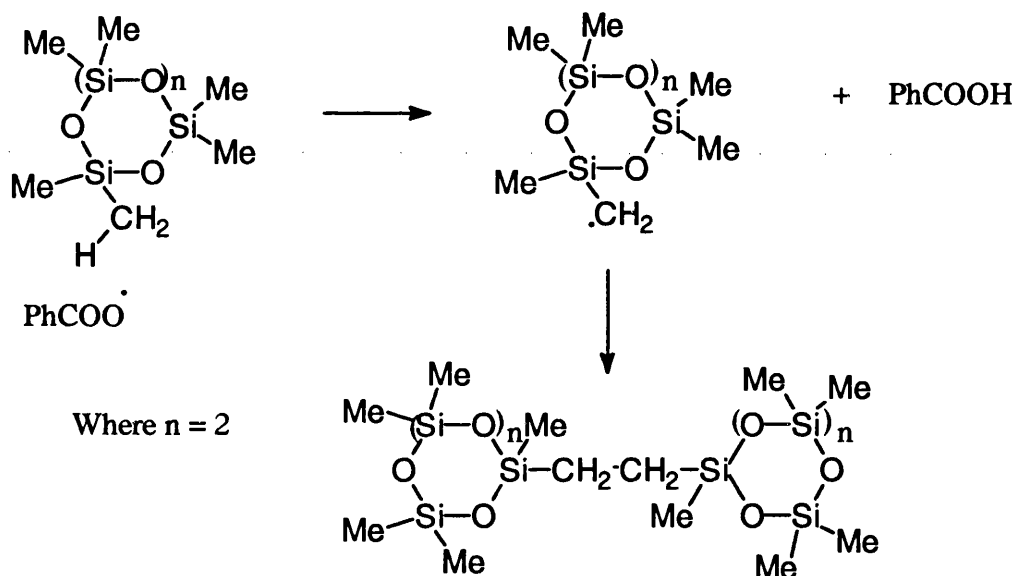
Products through reaction (iv) were only present when degradation was carried out above 480°C.

The insolubility of the residues from all mixed blends also confirms the high degree of crosslinking introduced from the radicals. It seems more possible, for crosslinking across the boundaries, that small alkyl radicals formed from polyolefins during decomposition reactions diffuse across the boundaries and induce radical reactions in the PDMS that result in crosslinking but other radicals, especially of the EtO. type, are also involved in polymer systems with ester groups.

Organic peroxides, such as tert-butyl peroxide (Me₃C-O-O-CMe₃), have been used for curing high molecular weight polysiloxanes¹³⁰. The action depends on the

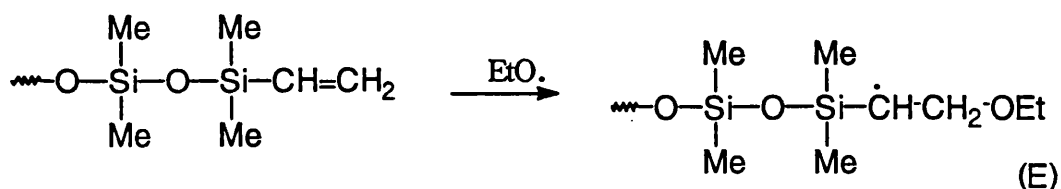
ability of free radicals of the type $RO\cdot$, arising from their decomposition at elevated temperatures, to abstract hydrogen atoms from methyl groups. Links of the type $-CH_2-CH_2-$ are thus formed between the chains¹³¹. Ethoxy ($EtO\cdot$) radicals may therefore, abstract hydrogen from the methyl group substituted on the silicon atom in the same manner as those radicals arising from the peroxides. Two ethoxy radicals would be required for one crosslink as indicated by the structure (D) and in turn two molecules of ethanol are formed.

The above type of reactions through routes (i) and (ii) to form structures of the type (C) and (D) have been demonstrated by Bobear¹³². It was found that bis(heptamethylcyclotetrasiloxanyl)ethane was formed when octamethylcyclotetrasiloxane was heated with *t*-butyl perbenzoate ($C_6H_5CO_2-O-C(Me)_2CH_3$).

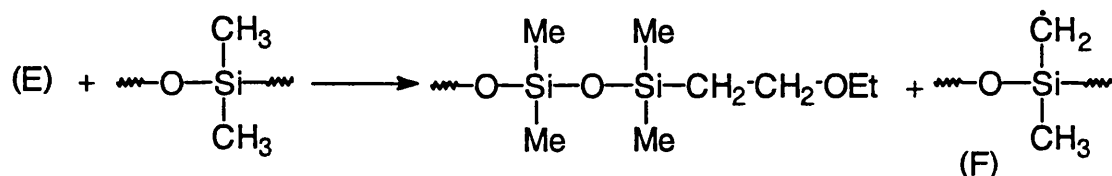


The possibility of such dimers from two identical cyclics or two different cyclics exists both in condensed and gas phase and a compound of this type containing cyclic hexamethyltrisiloxane and cyclic octamethyltetrasiloxane is thought to be the one of the new degradation products.

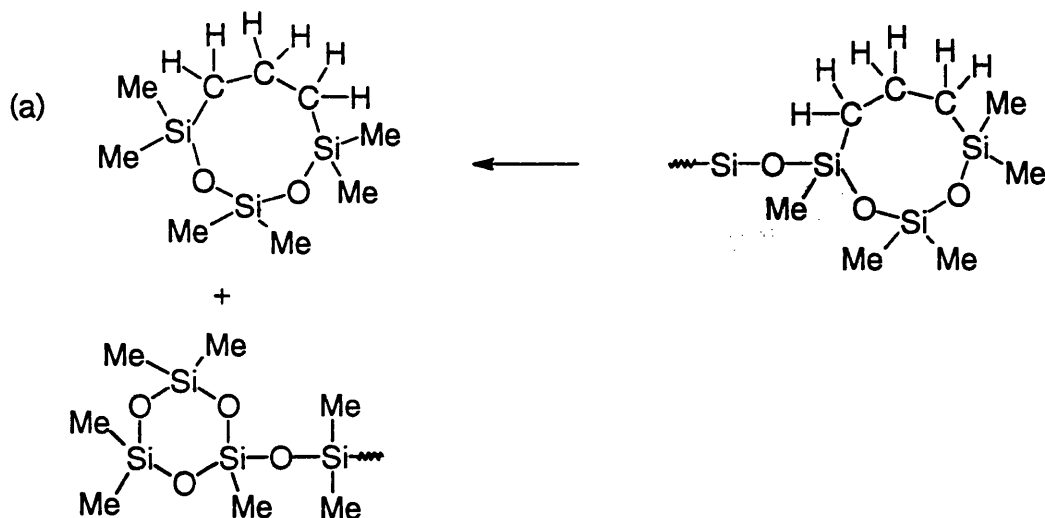
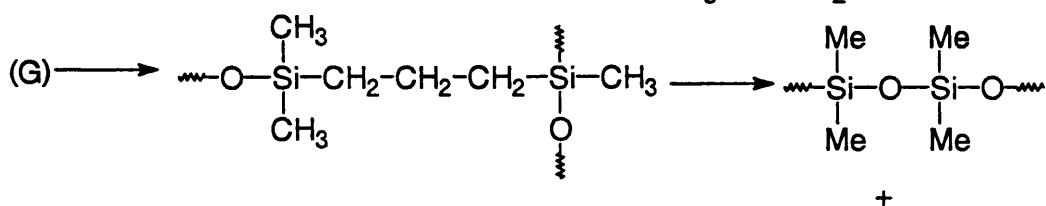
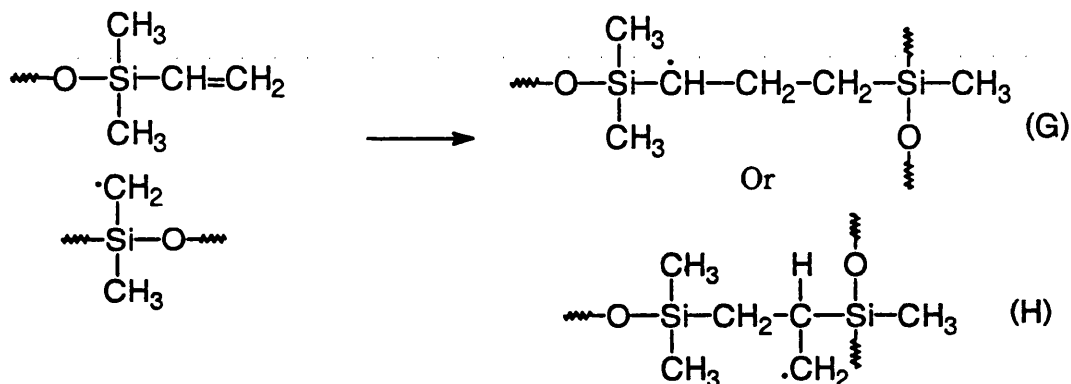
Vinyl groups in PDMS are known to react vigorously with free radicals from decomposition of peroxides. The PDMS used in this research has vinyl end groups and again radicals such as ethoxy radicals may react with these end groups as indicated below:



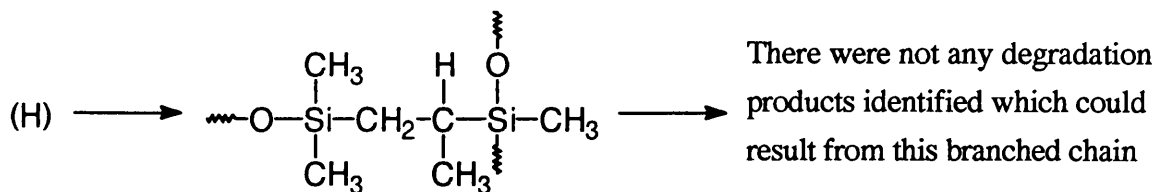
Abstraction of hydrogen from a methyl group leads to cross linking via formation of radical (F).



Two radicals of type (F) either crosslink and result in formation of structures of the type (D) or may react resulting in branching through alkyl bridges as follows:



Homologous series of compounds of the type (a) have been identified from the GC-MS results of degradation products from blends 16 and 20.

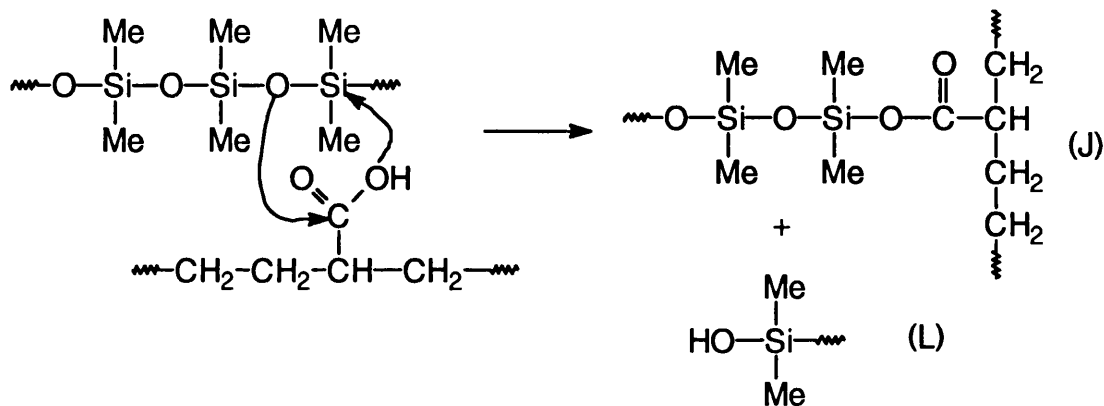


Since radicals (G) and (H) behave similarly to radical (E) and thus carry on forming radicals in the polymer chain. The above mechanism accounts for the experimental observation made by Bobear¹³² that the number of crosslinks depends on the concentration of peroxide instead of on the number of vinyl groups present in the PDMS.

The failure of PDMS to volatilise in mixed systems at 250°C, at its normal decomposition temperature, suggests interaction between the components but it is difficult to explain the failure of PDMS to volatilise at this temperature in an unmixed system. Reaction taking place in the gas phase appears unlikely since there is difference between the decomposition temperatures of the two components, about 36°C in the case of blends 14-17 and about 100°C in the case of blends 18-20. However, it was found (discussed in Chapter 4) that thin films of PDMS cast on any surface started decomposition at higher temperature than expected and that is the only reason for the decomposition of PDMS starting at higher temperature in an unmixed system. As in the present research blends which were prepared from solutions, were degraded as thin films cast on the surface of the TVA tube or stainless steel plate, these would decompose at higher temperature than samples made in a blender.

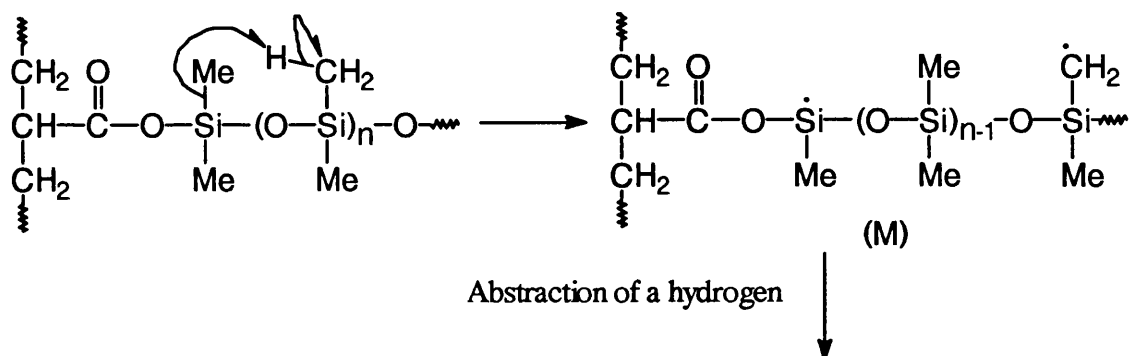
The decomposition of most PDMS, in all mixed samples except for blend 13, in the second degradation stage indicates that PDMS was stabilised up to 200°C. This considerable stabilisation can only be due to the interaction of the components before decomposition of either of the component begins. The following mechanism has been proposed:

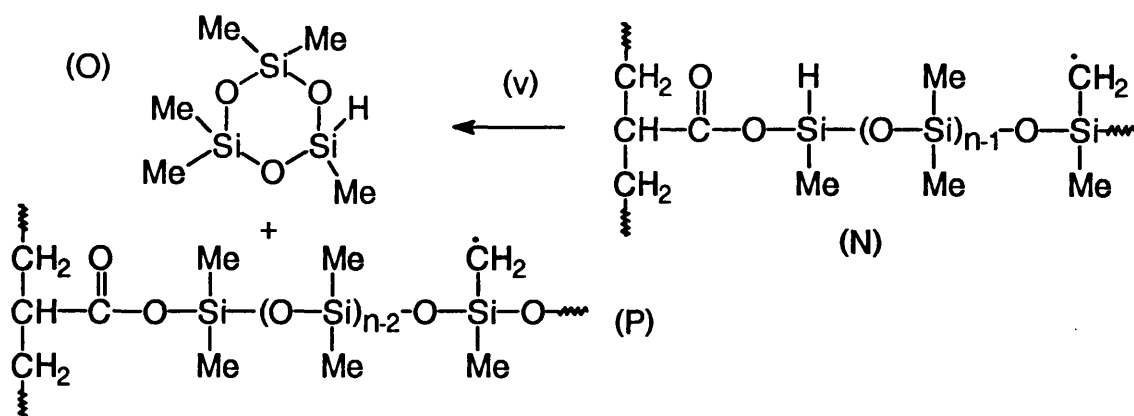
The negligible amount of acids such as acetic and propanoic in mixed samples is possibly due to the reduction of ethylene formation by side group scission so there would be fewer acid groups formed on the backbone. It is also possible that elimination of carbon dioxide follows immediately on the formation of acid groups. A further possibility is that of interaction between the PDMS and the acid units may occur as shown below but there is no real proof of such reaction:



Chain (L) forms a new end group and degradation of such chain occurs through the mechanism which involves depolymerisation from chain ends destabilising the PDMS.

Other degradation products identified in the case of blends 15 and 20 can only be possible from ester bridged chain of the type (J) which has a weakening effect on the neighbouring Si-CH₃ bonds due to its ability to withdraw electrons both by inductive effect and resonance. The following mechanism is proposed for the formation of these compounds:





Reaction through (v) then produces the homologous series of compounds of the type (O). These compounds are however more in quantity in blend 20 than in blend 15 possibly because crowding of ester groups in PEA only allows interaction at the chain ends.

There might be trace amounts of other new degradation products formed but their presence was not detected since GC traces of polyolefins are extremely crowded with complex mixture of compounds.

6.5. CONCLUSIONS

PDMS was stabilised in polymer systems which contained polar groups under all conditions while in a non-polar system it was only stabilised in nitrogen atmosphere.

Decomposition of PDMS in a blend where the other component had polar groups, occurred after the decomposition of that component.

Stabilisation of the polyolefins with polar groups increased with increasing percentage content of PDMS. Stabilisation of PDMS in turn increased with decreasing percentage content of the polyolefins.

The formation of low molecular weight volatile degradation products from polyolefins was reduced in the presence of PDMS.

The formation of low molecular weight volatile degradation products from PDMS was also reduced in the presence of polyolefins due to interaction of the components which increased the decomposition temperature of PDMS.

Crosslinking occurred in PDMS through radical reactions introduced by the diffusion of radicals from polyolefins across phase boundary to PDMS. The degree of crosslinking was more in systems in which the degradation of the components, other than PDMS, occurred at lower temperatures.

Insolubility and quantity of the residue in blends of PEA and EEA copolymer increased with increasing the percentage content of PDMS.

Blend 20 shows initially more stabilisation in an inert atmosphere than in air but gradually stabilisation in air overcomes the stabilisation shown in inert atmosphere.

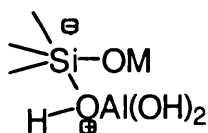
CHAPTER 7

BLENDS OF POLYDIMETHYLSILOXANE AND ADDITIVES

7.1. INTRODUCTION

The investigation of the thermal degradation of blends of PDMS with PE, PEA and EEA copolymer has demonstrated that PDMS was stabilised in each case, formed cross links by radical reactions and seemed to interact with the polymers which possessed reactive groups, thus changing the degradation mechanism. It was of interest therefore, to investigate the thermal behaviour of PDMS with additive systems other than organic polymers.

The thermal degradation of PDMS has been studied by several groups of workers, as described in Chapter 4. Anionic polymerisation of polydimethylsiloxane from octamethylcyclotetrasiloxane (cyclic tetramer) which proceeds from the active centres, formed when a strong base reacts with the siloxane bonds, remain as "living" during the course of the entire reaction and are very reactive. These reactive sites can be represented as $-\text{SiOM}$ (where M may be Cs, Rb, K, Na, R_4N^- , or R_4P^- (where R is an alkyl group)). Active chain ends such as R_4P^- can be decomposed by heating at 150°C while others cannot. Lewis¹³³ and Kučera et al¹³⁴⁻¹³⁷ were mainly concerned with the destructive effects of the residual basic catalyst on the thermal stability of PDMS. They concluded that these active chain ends, at which polymerisation of the polysiloxane rings originates, were also centres of depolymerisation and induced an ionic breakdown mechanism at temperatures below the true depolymerisation temperature. Kučera et al¹³⁴ reduced the weight loss by incorporating substances such as $\text{Al}(\text{OH})_3$ into the polymer which react with the "active sites" present in the polymer and transform them into stable complexes of the type:



It was found that there was no change in the molecular weight of polymer on contact of the active centres with $\text{Al}(\text{OH})_3$ so it was concluded that splitting of the above complex into MOH and $-\text{SiOAl}(\text{OH})_2$ was unlikely or it was proceeding very slowly at 270°C . It was reasoned that if such was not the case then released MOH would immediately

attack neighbouring siloxane bonds so that the final result would be a substantial decrease in the molecular weight of the polymer.

The stability effects of Al_2O_3 , Fe_2O_3 , BeO , SiO_2 , CdO , HgO , TiO_2 and ZnO have been studied previously.^{138, 139, 140} It was shown that oxides with a small cation (e.g. Al_2O_3 , Fe_2O_3 , BeO , SiO_2) form complexes on the active centres and stabilise basic active centres in PDMS at least to some extent, although some of them possibly do so with considerable difficulty. CdO and HgO , which are used for improving some of the mechanical properties of siloxane elastomers, were practically found to be without any effect¹³⁵. It was also found that the stability of the polymer was not improved by TiO_2 and ZnO ; therefore, it was concluded that they did not react with the reactive centre. It was also found that none of the above oxides could prevent the oxidative degradation of methyl groups on prolonged exposure at elevated temperatures.

Osipchik et al.¹⁴¹ examined the products of degradation of polydimethylsiloxane in the presence of ceramic oxides such as Al_2O_3 , TiO_2 and MgO by pyrolysis gas chromatography (with a pyrolysis attachment) at temperatures ranging from 200°C to 900°C . They observed that the qualitative composition of products of pyrolysis of PDMS was identical, while their quantitative yields depended on the type of filler and the degradation temperature. They concluded from the degradation products that during thermal degradation chain scission apparently occurred both at Si-O and Si-C bonds, but in the presence of Al_2O_3 and MgO it occurred mainly at Si-C bonds and that the content of volatile degradation components also decreased significantly in presence of these two fillers. They found that thermal degradation temperatures increased with TiO_2 , Al_2O_3 and MgO by $90\text{-}100^\circ\text{C}$, $60\text{-}65^\circ\text{C}$ and $10\text{-}20^\circ\text{C}$, respectively.

Zdorikova et al.¹⁴² studied the effects of aluminium oxide trihydrate particle size on the combustion of PDMS. They concluded that the size of the flame-retardant particles affected the physico-mechanical characteristics and combustion of polymeric compositions based on polydimethylsiloxane and that the processes of interaction of the polymer and the filler during thermal degradation definitely played an important role in the general mechanism of combustion termination. They attributed the evolution of methane and easy destruction of PDMS to the formation of strong hydrogen bonds between hydroxyl groups of the filler surface and methyl groups of PDMS. Kharitonov and Ostrovsky¹⁴³ pointed out that the quantity of evolved methane depended certainly on the content of the hydroxyl groups on the surface of the filler. Thus filler with smaller

particle size would have a higher concentration of OH groups on its surface due to the relatively larger surface area.

Despite the great number of investigations of the thermal stability of PDMS containing trace catalyst impurities, which have been carried out in the presence of additives, such as metal oxides, only a limited amount of work has been published in detail on the thermal stability and degradation properties of catalyst-free PDMS in the presence of additives. The study of flame retarding silicone rubber appears to be a question of understanding the solid state reactions. It has been claimed by various groups of workers that different combinations of platinum, fused silica, titanium dioxide, quartz, group II metal oxides, carbon black, manganese carbonate and triphenylphosphite are effective¹⁴⁴⁻¹⁵⁵.

The objective of the current chapter was to study the thermal degradation properties of PDMS in the presence of fire-retardant systems, mainly inorganic fillers, in detail and to gain an insight into the fundamental processes, final products of degradation in the presence of additives and thus mechanisms that operate when polymer-additive systems are subjected to high temperatures.

7.2. EXPERIMENTAL

7.2.1. Preparation and Compositions of Blends

All blends were prepared as described in Chapter 2 except for the samples 40, 51, 52, 53, 54 and 55. These blends were prepared by mixing PDMS with additive thoroughly in a very small amount of dichloromethane at room temperature. The compositions of the PDMS and additives were based on percentage by weight and are given in Table 7.1.

Table 7.1. Characteristics of samples examined

| Sample | Polymer | Additive | Mean particle size (μ) | Type |
|-----------|----------------------|--------------------------------------|------------------------------|--------------|
| Blend 21 | PDMS | 1.0% CaCO ₃ | 1.5 | Whiting |
| Blend 22 | PDMS | 2.0% CaCO ₃ | 1.5 | Whiting |
| Blend 23 | PDMS | 5.0% CaCO ₃ | 1.5 | Whiting |
| Blend 24 | PDMS | 10.0% CaCO ₃ | 1.5 | Whiting |
| Blend 25 | PDMS | 30.0% CaCO ₃ | 1.5 | Whiting |
| Blend 26 | PDMS | 50.0% CaCO ₃ | 1.5 | Whiting |
| Blend 27 | PDMS | 70.0% CaCO ₃ | 1.5 | Whiting |
| Blend 28 | PDMS | 86.0% CaCO ₃ | 1.5 | Whiting |
| Blend 29 | PDMS | 50.0% CaCO ₃ | 5.0 | Calcite |
| Blend 30 | PDMS | 50.0% CaCO ₃ | 0.9 | Calcite |
| Blend 31 | PDMS | 50.0% CaCO ₃ | 0.06 | Precipitated |
| Blend 32 | PDMS | 50.0% CaCO ₃ | 0.7 | Calcite** |
| Blend 33 | PDMS | 50.0% CaCO ₃ | 1.5 | Calcite** |
| Blend 34 | PDMS | 50.0% CaCO ₃ | 5.0 | Calcite** |
| Blend 35 | PDMS-Me ₃ | 50.0% CaCO ₃ | 1.5 | Whiting |
| Blend 36 | PDMS | 50.0% MgCO ₃ | 2.0 | |
| Blend 37 | PDMS | 50.0% Mg(OH) ₂ | | |
| Blend 38 | PDMS | 50.0% Al(OH) ₃ | 1.0 | |
| Blend 39 | PDMS | 1.0% Ca(OH) ₂ | | |
| Blend 40* | PDMS | 50.0% (CaO + Ca(OH) ₂) | | |
| Blend 41 | PDMS | 50.0% MgO | | |
| Blend 42 | PDMS | 50.0% Al ₂ O ₃ | | |
| Blend 43 | PDMS | 50.0% TiO ₂ | | |
| Blend 44 | PDMS | ~66% Silica | | |

| Sample | Polymer | Additive | Mean particle size (μ) | Type |
|-----------|-----------------------------------|-------------------------|------------------------------|---------|
| Blend 45 | PDMS | 1.0% Calcium stearate | | |
| Blend 46 | PDMS | 5.0% Calcium stearate | | |
| Blend 47 | PDMS | 1.0% Stearic acid | | |
| Blend 48 | PDMS | 5.0% Stearic acid | | |
| Blend 49* | PDMS | 20.0% Stearic acid | | |
| Blend 50 | PDMS | 1.0% DHT-4A | | |
| Blend 51 | PDMS-CH ₃ | 1.0% DHT-4A | | |
| Blend 52* | PDMS | 50.0% MgSO ₄ | | |
| Blend 53* | PDMS | 50.0% CaCl ₂ | | |
| Blend 54* | PDMS-VMS | 50.0% CaCO ₃ | 1.5 | Whiting |
| Blend 55* | D ₃ and D ₄ | 33.0% Baked MgO | | |
| Blend 56* | D ₃ and D ₄ | CaCO ₃ | 1.5 | Whiting |

Note: Calcium carbonate was stearate coated in all blends except where indicated otherwise as ** = Uncoated calcium carbonate; while * = blends not prepared by melt compounding.

Mean particle size is not known in some cases.

Vinyl end grouped PDMS was used in all blends unless indicated otherwise as: PDMS-VMS = PDMS with high vinyl content; PDMS-Me₃ = PDMS with saturated or trimethyl end groups; PDMS-OH = PDMS with hydroxyl end groups.

DHT-4A ($Mg_{4.5}Al_2(OH)_{13}CO_3 \cdot 3.5H_2O$) is a hydrocalcite like material.

7.2.2. Thermal Analysis of PDMS with Additives

The thermal behaviour of these blends was investigated mainly using TG-DTG, TVA and SATVA, while in some cases DSC was also used. Experimental procedures are described in detail in Chapter Two.

7.3. RESULTS AND DISCUSSION

7.3.1. Electron Microscopy

Some of the fillers were examined by transmission electron microscopy (TEM) to see the degree of agglomeration in the fillers since it is not correct to judge the properties of the composites from the average particle size. It is necessary to regard the crystallite size and agglomeration as separate factors. It was difficult to see the dispersion of the filler in the polymer because as soon as the sample was left under the electron beam, the polymer melted and formed a thick rubbery sheet on the top surface as seen in Figure 7.1.

It was clear from the TEM photographs of different types and grades of CaCO_3 that the degree of agglomeration decreased with increasing particle size. The degree of agglomeration was also reduced by a coating on the surface of the filler.

7.3.2. Thermogravimetry

TG curves of additives are also given if appropriate along the blend in question. TG results under dynamic nitrogen and air are given in Tables 7.2 (a) and (b), respectively.

7.3.2.1. *TG-DTG Under Nitrogen*

Blends of PDMS and CaCO_3

All blends of PDMS and CaCO_3 were of 1.5 microns, coated and whiting type unless indicated otherwise. PDMS used for blends was with vinyl end groups. The behaviour of each blend (21-50) predicted, assuming no interaction between the components, was calculated from the TG curves of the components and their relative amounts. Results for TG experiments are shown in Table 7.2 (a).

The TG curves obtained for blends 21-28 (with 1%, 2%, 5%, 10%, 30%, 50%, 70% and 86%, respectively) are shown in Fig. 7.2 - Fig. 7.5. There is a trend towards higher stabilisation with increasing percentage content of the filler. Stabilisation is shown throughout the degradation of up to 40°C - 250°C depending on the filler content.

The TG traces of blends 29-34 (all with 50% CaCO_3 and particle size of 5.0, 0.9, 0.06, 0.7, 1.5 and 5.0 microns respectively), whether coated or uncoated, show an



Fig 7.1. Electron micrograph of blend 26 (PDMS and coated CaCO_3 with mean particle size of 1.5μ).

increase in stability up to 75-125°C depending on the grade of the filler, as seen from the Fig. 7.6 and Fig. 7.7. Although blends 32 and 33 with uncoated grades start before the expected value, they develop stabilisation after 3-5% weight loss and this stabilisation remains throughout the degradation.

The onset of degradation of blend 35 (with saturated end grouped PDMS) also shows a dramatic increase in stabilisation up to 250°C and shows similar behaviour to that of blend 26 except it also shows a plateau region with T_{max} at 420°C and a further small amount of degradation starting at about 630°C possibly due to the decomposition of the filler, giving an additional 1.5% weight loss (Fig. 7.8).

It is clear from the TG result of blend 26, 29-34 and 35 that calcium carbonate samples with different particle size and type have slightly different effects on the polymer initially but overall there is an increase in the stabilisation with all grades and types of the filler. It is also clear that different end groups of the polymer do not affect the polymer stability.

Calcite type uncoated calcium carbonate with smaller particle size, does not stabilise the polymer initially like the other types. Coated calcium carbonate with all particle sizes and of either type stabilises the polymer from the start and throughout the degradation.

Stabilisation increases with increasing particle size because the larger the crystallite size the less agglomeration of the crystallites thus leads to a better dispersion of the particles in the polymer. This increases the effective volume of the polymer in contact with the filler for both interaction and to absorb heat from the polymer. Further, blends with coated grades show more stabilisation compared with the blends with uncoated but with the same particle sized fillers except in the case of blends 26, 31 and 35. Blend 31 shows 10-20°C more stability than blend 26 which in turn is more stable than other blends in this series.

The greater stabilisation in blend 31, containing the precipitated form of the filler, could be explained in terms of the surface treatment of the filler to give it a high degree of dispersion thus providing a specific surface area several times larger than other types of grades. The larger surface area would provide more sites for interaction and more surface area to remove heat from the polymer since the dispersion through the polymeric material would be much better so most of the filler would be in contact with the polymer.

The largest stabilisation in blends 26 and 35, which contain coated whiting type calcium carbonate, is difficult to understand since if the stability was due to the coating and particle size only then they would have shown less stability than blend 29 (coated, particle size 5.0 microns). The only differences which may be contributing to the enhanced stability are the high level of impurities (such as ferric oxide, Fe_2O_3 , sulphate and magnesium oxide and about 7 times more than in the other types) in it and its different type. Magnesium oxide is found to stabilise the polymer greatly as in the case of blend 41. Other impurities are also reported to stabilise the polymer. There was also a colour change from creamish white to greyish depending upon the temperature of degradation. None of the other blends showed this colour change. The TG results also show that decomposition of CaCO_3 did not start at 600°C as expected indicating that the filler itself had been stabilised. This could only be explained if there had been some chemical changes during the degradation.

Blend of PDMS and MgCO_3

Blend 36 shows more stabilisation than blends with CaCO_3 and starts at the decomposition temperature of the filler to MgO and CO_2 (Fig. 7.9). The DTG curve shows a complex multi-stage degradation with two main T_{max} temperatures (615°C and 626°C , respectively) and a broad shoulder with T_{max} at 550°C . The very small amount of degradation in the region 250°C - 359°C is possibly due to decomposition of the impurity, $\text{Mg}(\text{OH})_2$, but the weight loss in this region is only 2.0%. The residue at 600°C was 57.0% and at 650°C 31.25% of the total weight of the blend degraded, compared with 27.0% expected for the blend at 600°C .

Blends of PDMS and Metal Hydroxides

Blends 37 (50% $\text{Mg}(\text{OH})_2$) and 38 (50% $\text{Al}(\text{OH})_3$) show two degradation stages as expected (Fig 7.10 and Fig. 7.11, respectively) and stabilisation is maintained throughout the degradation of up to 40°C and 260°C , respectively.

The first weight loss of blend 37 starts at about 275°C which is 50°C before the dehydration of the filler so the weight loss of polymer seems to begin before the decomposition of the filler and most of the weight loss of the polymer occurs during the first stage as it accounts for almost 40% weight. The second stage of weight loss is mainly due to the decomposition of metal hydroxide to the corresponding metal oxide and water.

The first stage of degradation of blend 38 which was due to the decomposition of $\text{Al}(\text{OH})_3$ to Al_2O_3 and water started 50°C higher than the dehydration of the filler. It seems that the polymer melt retarded the volatilisation of the water for some time or there was interaction between the components which delayed the decomposition of the filler.

There is only about $6\text{-}10^\circ\text{C}$ of stabilisation shown by the blend 39 (1.0% $\text{Ca}(\text{OH})_2$) at the start which slowly decreases such that at 316°C when weight loss is 41%, destabilisation commences and reaches about 23°C near the end (Fig 7.12).

It is obvious from the TG trace of blend 38 that $\text{Al}(\text{OH})_3$ stabilises PDMS about $10\text{-}20^\circ\text{C}$ more than CaCO_3 (whiting) and up to 125°C more than $\text{Mg}(\text{OH})_2$. A considerable amount of stabilisation shown by $\text{Al}(\text{OH})_3$ is also due to the blanketing effect of the polymer surface by the released water during the decomposition of filler to metal oxide and water. The metal oxide formed further stabilises the polymer as seen from the results of the metal oxides below, by acting as a heat sink. While $\text{Mg}(\text{OH})_2$ has 75°C higher dehydration temperature than the degradation temperature of the polymer, $\text{Ca}(\text{OH})_2$ does not dehydrate in the experimental temperature region, $25\text{-}650^\circ\text{C}$. This clearly shows that the maximum stabilisation of the polymer can be maintained by using the hydroxide with lower dehydration temperature than the polymer.

Blends of PDMS and Metal Oxides

TG traces obtained for blends 41 (Fig. 7.13), 42 (Fig. 7.14), 43 (Fig. 7.14), and 44 (Fig. 7.15) show stabilisation of up to $82\text{-}250^\circ\text{C}$ higher (depending on the filler, see Table 1) than predicted. Blend 43 (50% TiO_2) shows most stabilisation among metal oxides. Blend 41 (50% MgO) although shows a stabilisation of up to 200°C but the onset of degradation is much faster than other blends.

Blend of PDMS and Other Additives

TG traces of blends 45-48 are illustrated in Figures 7.17 - 7.20, respectively while of the corresponding additives are given in Fig. 7.16. Blend 45 (with 1.0% calcium stearate) shows higher stability than estimated, 25°C more at the beginning than calculated values which gradually increases to 40°C while blend 46 (with 5.0% calcium stearate) shows 115°C stabilisation throughout the degradation. The shape of the DTG

curve of blend 45 is slightly different from the DTG curve of the pure polymer while blend 46 shows two stage degradation with a plateau region at the start.

Blends 47 and 48 (1% and 5% stearic acid, respectively) show about 50°C-75°C stabilisation, depending on the filler content, almost throughout the degradation. There is no residue left at the end of the degradation for blend 47 whereas 1% residue was expected. Blend 48 shows two stage degradation, the first with about 5% weight loss, due to the degradation of the additive.

It is clear from the results of blends 45-46 that like CaCO_3 , these additives also increase stabilisation with increasing % content of the additive.

Blends 50 (PDMS with vinyl end groups), and 51 (PDMS with trimethyl end groups) both with 1.0% DHT-4A ($\text{Mg}_{4.5}\text{Al}_2(\text{OH})_{13}\text{CO}_3 \cdot 3.5\text{H}_2\text{O}$), give the same type of behaviour, presenting a dramatic increase in stability of 150-230°C (Figs. 7.21 and 7.22, respectively). The DTG curves of both blends show two stage degradation. The first stage with onset temperature at about 400°C. This increased stabilisation shown with only 1.0% of additive is difficult to explain since in other cases such stability was only obtained after increasing the percentage content of the filler in question up to 50%. Thus DHT-4A is possibly not acting as a heat sink as in the case of the most other fillers which although they seem to interact with the silicone polymer act mainly as heat sinks.

7.3.1.2. TG-DTG Under Air

Thermogravimetric experiments were performed for some of the above blends under an atmosphere of air for the purpose of comparison with the results obtained under nitrogen.

TG thermograms of most of the blends 26 (Fig. 7.5), 35 (Fig. 7.8), 36 (Fig. 7.9), 37 (Fig. 7.10), 39 (Fig. 7.12), 41 (Fig. 7.13), 42 (Fig. 7.14), 44 (Fig. 7.15), 45 (Fig. 7.17), 46 (Fig. 7.18), 47 (Fig. 7.19), 48 (Fig. 7.20) and 50 (Fig. 7.21) show a remarkable increase in stability, the rate maximum depending on the type of filler and its content. This stability is maintained throughout the degradation for most of the blends mentioned above as seen from their TG curves. The TG-DTG thermograms show that the degradation processes for most blends are much more complicated than when degradation for these blends was carried out in an inert atmosphere since most of these blends show two main degradation stages accompanied by other small complex degradation stages.

Blend 39 (1.0% $\text{Ca}(\text{OH})_2$) shows a stabilisation of up to 25°C throughout the degradation which is more than in an inert atmosphere. Furthermore, stabilisation was only shown up to 58% weight loss under an atmosphere of dynamic nitrogen.

The TG-DTG curve of blend 41 (with 50.0% MgO) did not show stabilisation initially but after 7% weight loss at 300°C, the degradation process slowed down and the TG curve moved towards higher temperature; also the onset of degradation process was extremely slow such that the degradation ended at 535°C.

The residues at 600°C are more than the expected values from the residues of the individual components or when these blends were degraded in dynamic nitrogen except in the case of blends 42 (with 50.0% Al_2O_3), 44 (with ~66% silica).

The greater amounts of residue found for most blends than expected are possibly due to oxidative attack on the methyl groups leading to crosslinking of the polymer chains. This would reduce the weight loss giving cyclic siloxane oligomers. The resulting degradation product is mainly silica which contributes in the weight increase of the residue. This also seems the possible reason for more residue in air for most blends than in dynamic nitrogen.

The smaller residue than expected in the case of blends 42 and 44 is difficult to explain but it seems possibly that these fillers might prevent oxidative degradation of methyl groups by forming some kind of barrier on the outside surface of the sample. This may then lead to the weight loss by depolymerisation of the polymer at elevated temperatures. The residue in this case would be much less than expected in air. This, explanation however, is a contradiction of the previous work¹³⁸⁻¹⁴⁰.

The TG-DTG results (Table 7.2 (a) and (b)) show that most of the blends mentioned above show 25-50°C more stabilisation in inert atmosphere than in air while it was found that pure PDMS was 25-30°C more stable in air than in an inert atmosphere. This again can be explained due to fewer crosslinks formed in the presence of a filler because the filler would prevent the oxygen reaching the polymer thus favouring the weight loss by depolymerisation. It is also apparent that the stabilisation of blends, with different percentage content, increases in either atmosphere with increasing percentage content of the corresponding additive.

Table 7.2. (a) TG results under nitrogen

Temperatures shown in brackets are calculated values assuming that there was no interaction between the components.

| Sample | T _{thresh} (°C) | T ₅₀ (°C) | T _{max} (°C) | T _{stop} (°C) | % residue at 600°C |
|----------|--------------------------|----------------------|-----------------------|------------------------|--------------------|
| Blend 21 | 280 (250) | 348 (315) | 355 | 425 (380) | 0.65 (1.98) |
| Blend 22 | 300 (250) | 368 (315) | 382 | 450 (380) | 1.50 (2.25) |
| Blend 23 | 325 (250) | 404 (315) | 407 | 575 (380) | 3.50 (5.50) |
| Blend 24 | 375 (250) | 522 (318) | 525 | 635 (380) | 17.00 (10.65) |
| Blend 25 | 400 (250) | 569 (325) | 568 | 635 (380) | 36.00 (30.50) |
| Blend 26 | 400 (250) | 585 (315) | 540 | 600 (380) | 50.00 (50.0) |
| Blend 27 | 400 (250) | | | 625 (380) | 74.50 (69.78) |
| Blend 28 | 400 (250) | | | 620 (380) | 86.50 (84.50) |
| Blend 29 | 375 (250) | 625 | 437, 475 | 625 (380) | 51.75 (50.50) |
| Blend 30 | 325 (250) | 462 (425) | 425 | 462 (380) | 50.0 (49.5) |
| Blend 31 | 387 (250) | | 500, 570 | 625 (380) | 53.0 (48.36) |
| Blend 32 | 230 (250) | 405 | 402 | 405 (380) | 49.50 (49.75) |
| Blend 33 | 217, 350 (250) | | 287, 427 | 475 (380) | 51.50 (50.0) |
| Blend 34 | 325 (250) | | 420 | 500 (380) | 51.50 (50.0) |
| Blend 35 | 400, 635 (250) | 605 | 586 | 640 (380) | 51.0 (50.10) |
| Blend 36 | 425 (250, 365) | 605 (365) | 615, 626 | 650 (550) | 57.0 (27.0) |
| Blend 37 | 275 (250, 350) | 393 (355) | 369, 410 | 425 (425) | 40.55 (35.75) |
| Blend 38 | 225, 425 (212) | 549 (324) | 317, 525 | 612 (380) | 40.0 (32.75) |
| Blend 39 | 255 (250) | 306 (300) | 316 | 375 (380) | 1.5 (1.0) |

| Sample | T _{thresh} (°C) | T ₅₀ (°C) | T _{max} (°C) | T _{stop} (°C) | % residue at 600°C |
|---------------------|--------------------------|----------------------|-----------------------|------------------------|---------------------------|
| Blend 41 | 225 (250) | (350) | 392, 525 | 550 (380) | 50.25 (48.00) |
| Blend 42 | 350 (250) | | 402 | 475 (380) | 52.50 (50.50) |
| Blend 43 | 410 (250) | 600 | 510 | 600 (380) | 50.0 (50.50) |
| Blend 44 | 425 (250) | 571 (324) | 558 | 613 (380) | 36.75 (31.69) |
| Blend 45 | 275 (250) | 355 (313) | 372 | 425 (380) | 1.0 (1.0) |
| Blend 46 | 320 (250) | 417 (315) | 413, 432 | 550 (450) | 0.75 (2.0) |
| Blend 47 | 300 (250) | 367 (314) | 385 | 425 (380) | 0.0 (1.0) |
| Blend 48 | 150, 325 (150, 250) | 411 (312) | 200, 426 | 525 (400) | 1.0 (1.15) |
| Blend 50 | 375 (250) | 513 (314) | 520, 580 | 612 (380) | 4.0 (1.5) |
| Blend 51 | 400 (250) | 520 (315) | 513, 582 | 615 (380) | 4.5 (1.5) |
| CaCO ₃ | 375 600 (main) | | 775 | 810 | 97.75, (57.5 at 810°C) |
| MgCO ₃ | 425 | | 575 | 600 | 53.0 |
| Mg(OH) ₂ | 325 | | 405 | 450 | 70.25 (69.13) |
| Al(OH) ₃ | 212 | | 292 | 325 | 64.50 |
| MgO | 25 | | | 400 | 95.25 |
| Silica | 25 | | 60 | 100 | 96.25 |
| Stearic acid | 125 | 220 | 248 | 260 | 4.25 |
| Calcium stearate | 50, 350 | 425 | 82, 425 | 490 | 22.5 |
| DHT-4A | 30, 150, 225 | | 87, 185, 378 | 525 | 59.5 |

Note: All other type and grades of calcium carbonates start to decompose at 575°C except grades with particle size of 5.0 μ which start at 600°C. While Al₂O₃ and TiO₂ did not show any weight loss up to 650°C.

Table 7.2. (b) TG results under air

Temperatures shown in brackets are calculated values assuming that there was no interaction between the components.

| Sample | T _{thresh} (°C) | T ₅₀ (°C) | T _{max} (°C) | T _{stop} (°C) | % residue at 600°C |
|---------------------|--------------------------|----------------------|-----------------------|------------------------|--------------------|
| Blend 26 | 367 (275) | | 400 and 506 | 525 (400) | 57.5 (51.5) |
| Blend 35 | 350 (275) | 568 (322) | 395, 565 | 590 (400) | 53.25 (51.5) |
| Blend 36 | 360, 525 (275, 450) | 612 (458) | 400, 510, 631 | (600) | 54.0 (28.0) |
| Blend 37 | 325 (275) | 425 (362) | 403 and 430 | 500 (412) | |
| Blend 38 | (275) | | | | |
| Blend 39 | 286 (275) | 350 (328) | 360 | 400 (400) | 14.0 (4.47) |
| Blend 41 | 275, 350 (275) | (374) | 370 and 522 | 520 (400) | 56.25 (47.88) |
| Blend 42 | 325 (275) | 418 | 395 | 437(400) | 48.0 (51.75) |
| Blend 43 | 212 | | 292 | 325 | 64.50 |
| Blend 44 | 325, 410 (275) | | 375, 425, 507 | 525 (400) | 52.0 (61.58) |
| Blend 45 | 325, 375 (275) | 431 (320) | 362, 392, 470 | 490 (415) | 17.5 (3.63) |
| Blend 46 | 325, 393 (275) | 460 (323) | 362, 415, 473 | 550 (415) | 19.0 (4.32) |
| Blend 47 | 312 (275) | 357 (324) | 368 | 425 (400) | 2.5 (3.47) |
| Blend 48 | 150, 325 (125, 275) | 375 (323) | 212, 385 | 450 (400) | 16.0 (3.43) |
| Blend 50 | 325 (275) | 490 (320) | 362, 411, 420, 512 | 575 (400) | 26.0 (4.05) |
| MgCO ₃ | 425 | | 562 | 612 | 53 |
| Mg(OH) ₂ | 325 | | 384 | 425 | 71.25 |

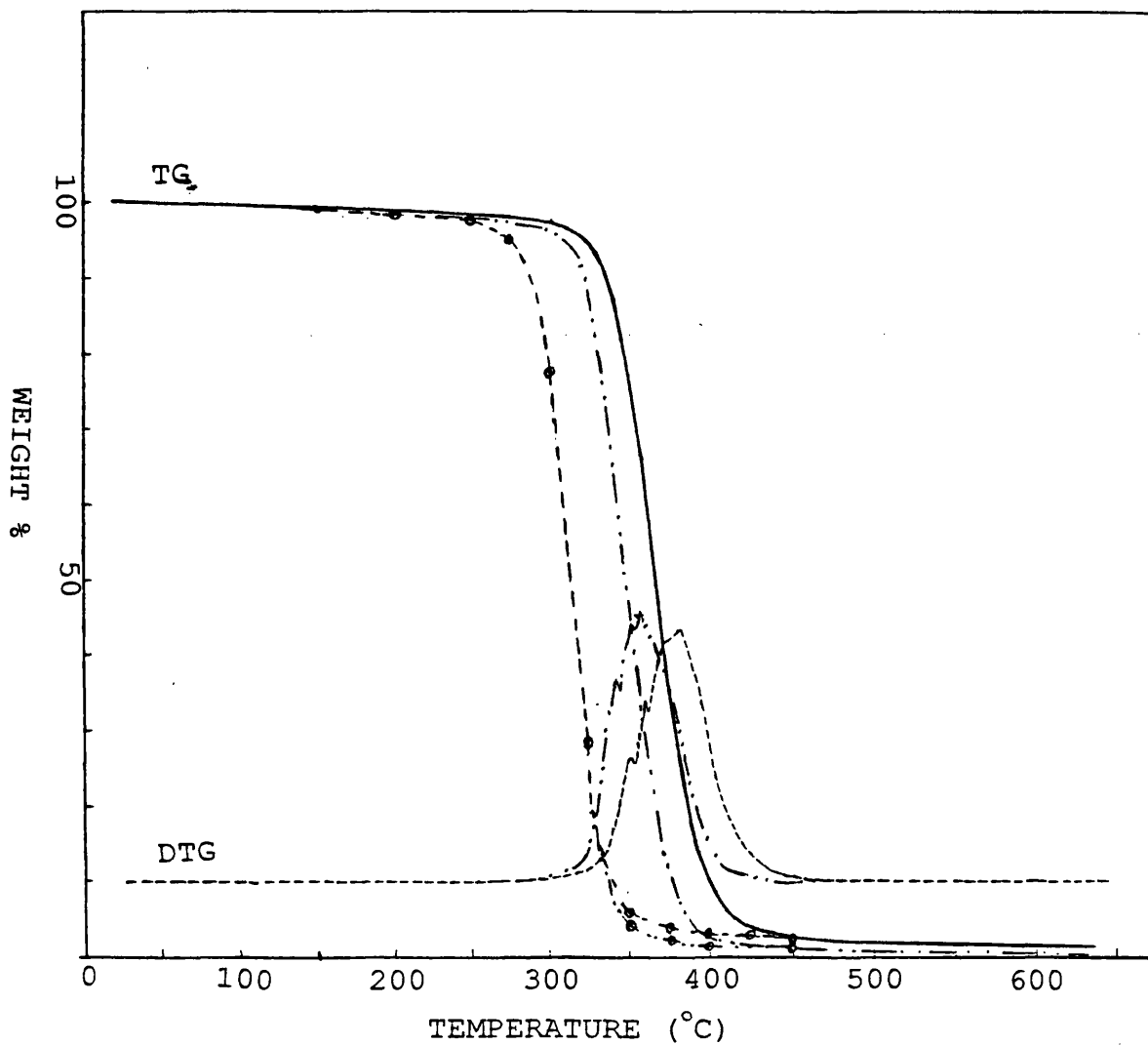


Fig. 7.2. TG-DTG traces for blends of PDMS and coated CaCO_3 with mean particle size of 1.5μ under nitrogen: blend 21 (1% CaCO_3) experimental (---) and calculated (-·-·-·-), and blend 22 (2% CaCO_3) experimental (—; ----) and calculated (-·-·-·-).

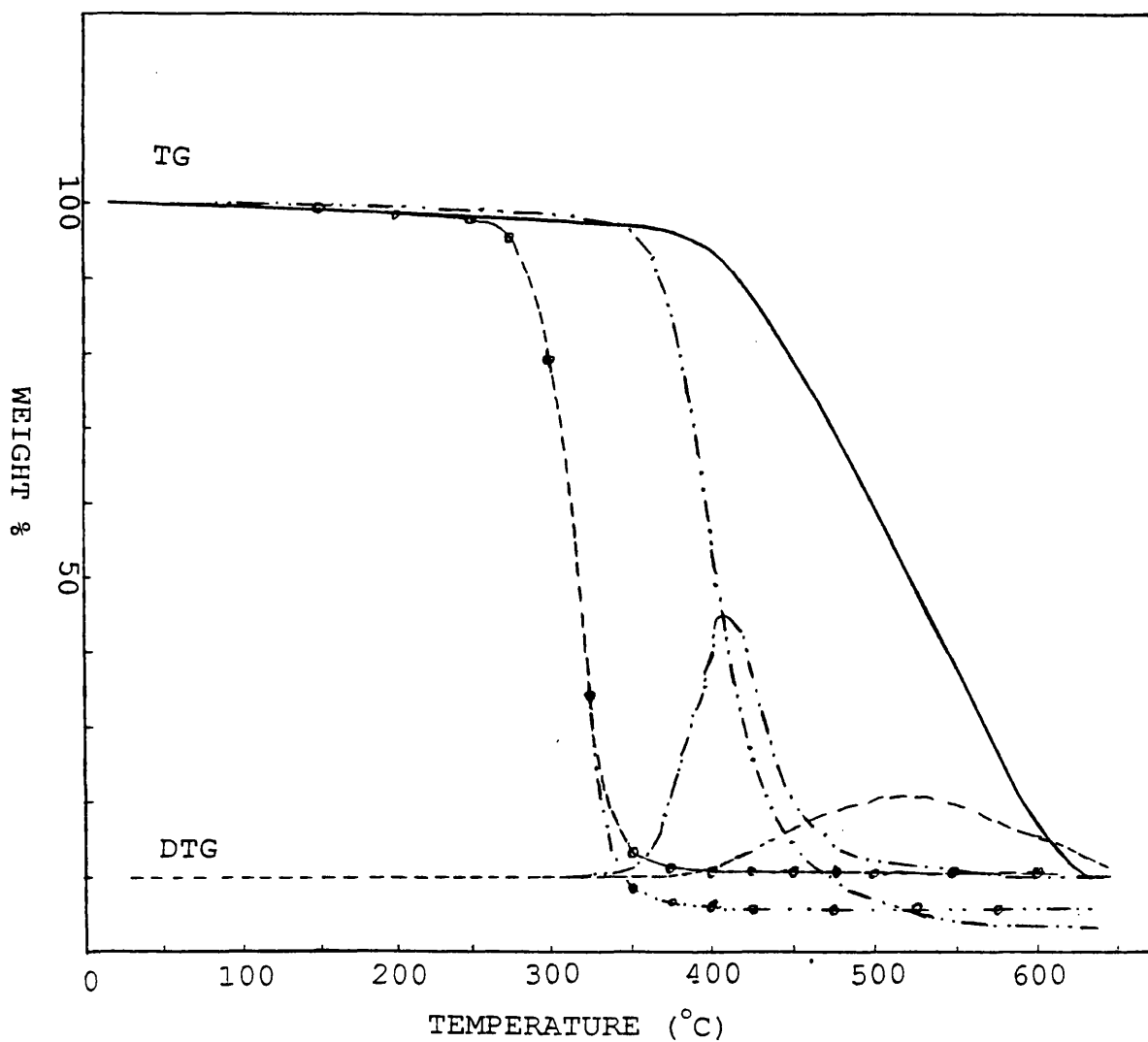


Fig. 7.3. TG-DTG traces for blends of PDMS and coated CaCO₃ with mean particle size of 1.5 μ under nitrogen: blend 23 (5% CaCO₃) experimental (---) and calculated (-·-·-), and blend 24 (10% CaCO₃) experimental (—; ----) and calculated (-·-·-).

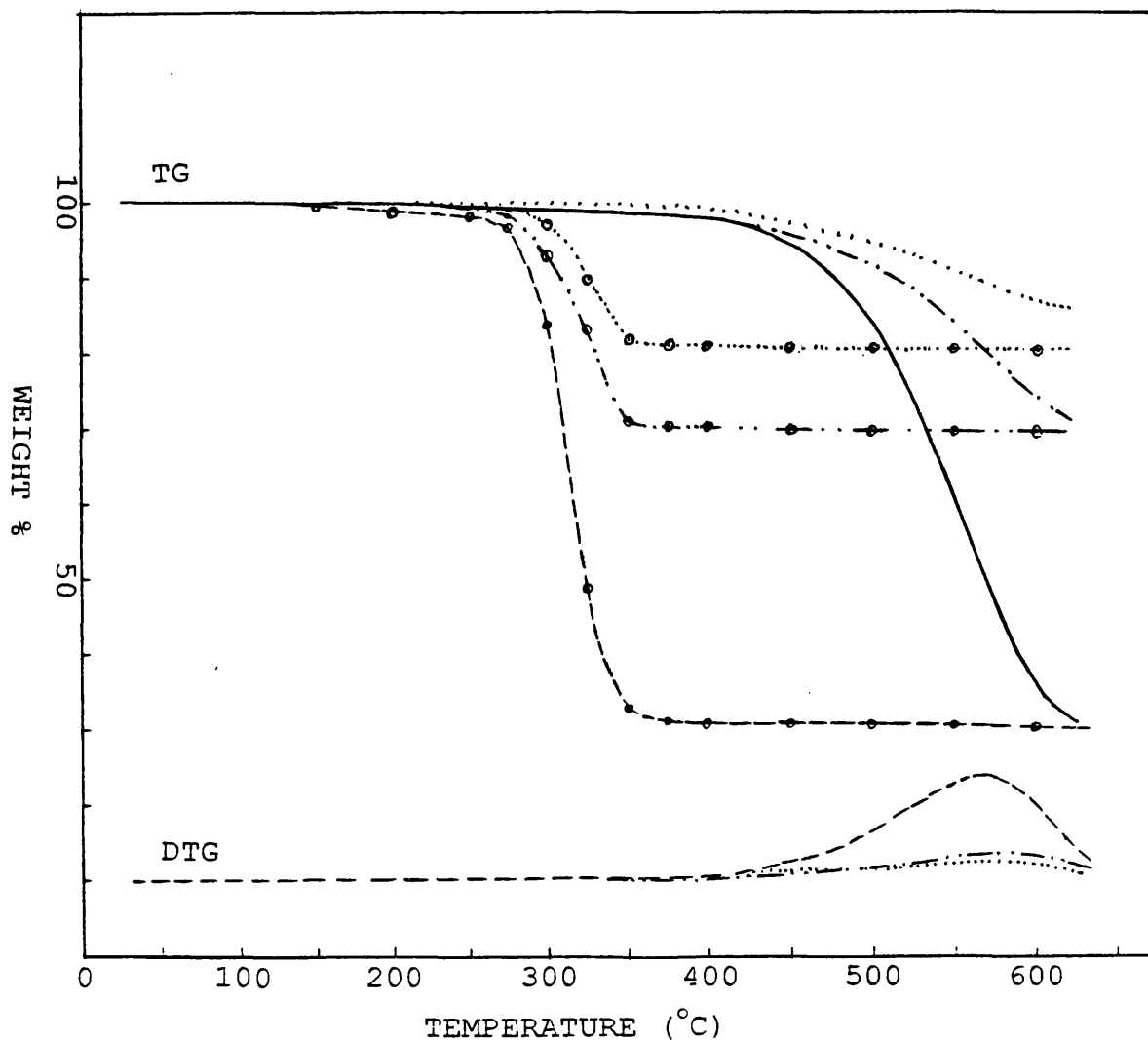


Fig. 7.4. TG-DTG traces for blends of PDMS and coated CaCO_3 with mean particle size of 1.5μ) under nitrogen: blend 25 (30% CaCO_3) experimental (—; ----) and calculated (- - -), blend 27 (70% CaCO_3) experimental (- · - ·) and calculated (- · · · - ·) and blend 28 (86% CaCO_3) experimental (---) and calculated (---).

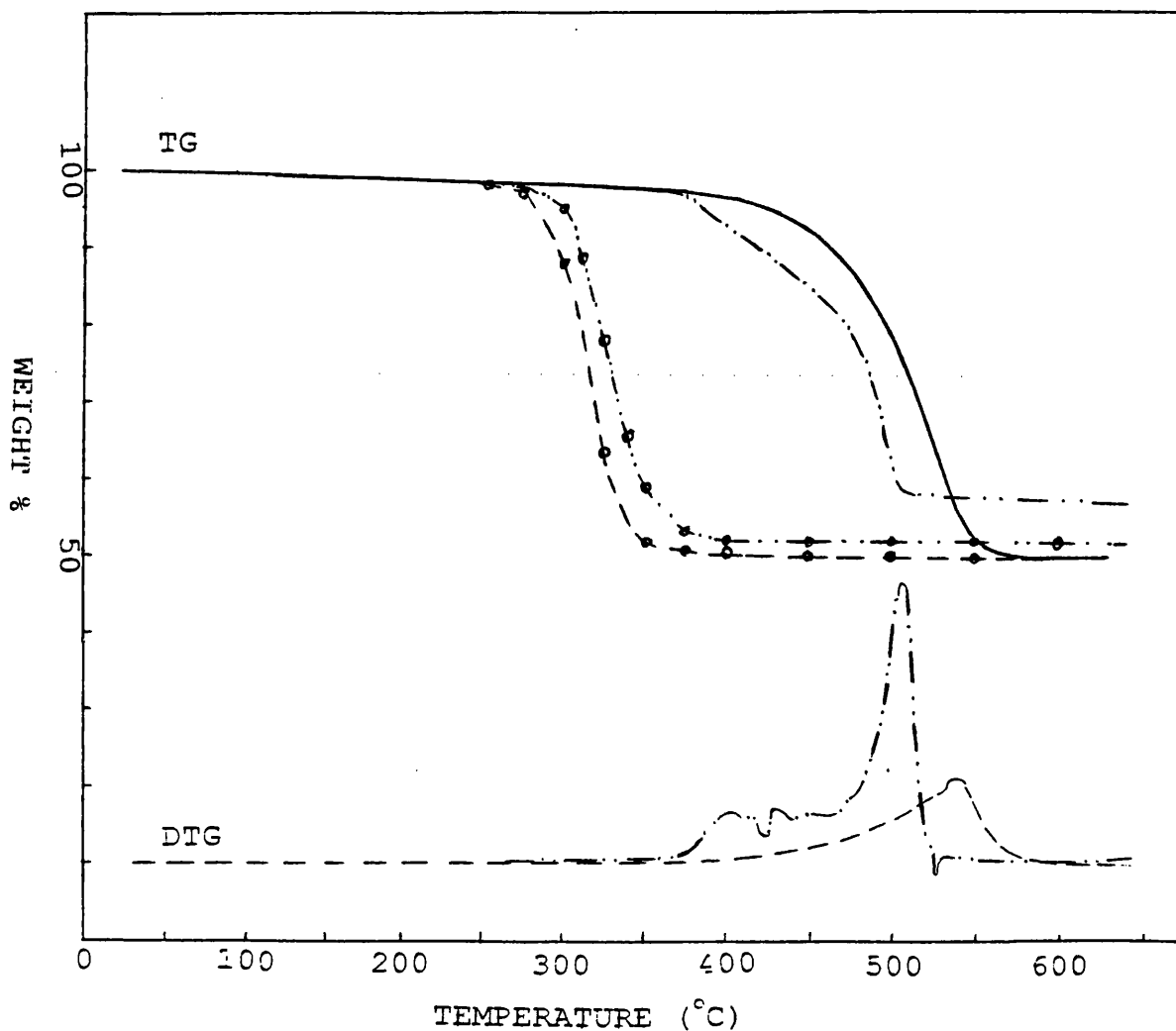


Fig. 7.5. TG-DTG traces for blend 26 (PDMS and coated CaCO₃ with mean particle size of 1.5 μ) under nitrogen: experimental (—; ----) and calculated (-+-), and air: experimental (-.-.-) and calculated (-.-.-+).

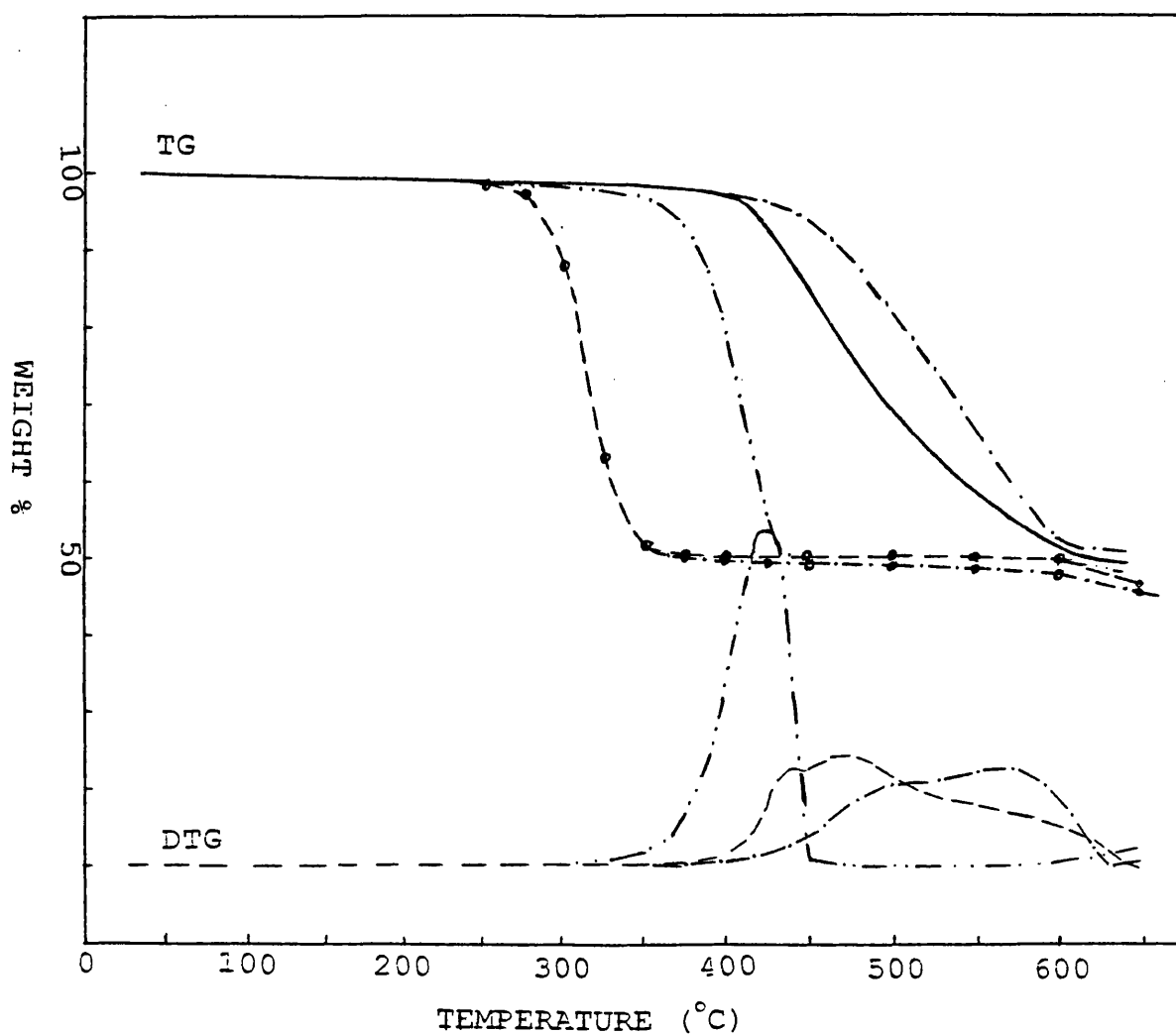


Fig. 7.6. TG-DTG traces for blends of PDMS and 50% coated CaCO_3 under nitrogen: blend 29 (with mean particle size of 5μ) experimental (—; ----) and calculated (- - - -), blend 30 (with mean particle size of 0.9μ) experimental (- · - ·) and calculated (- · - · - ·) and blend 31 (with precipitated CaCO_3 and mean particle size of 0.06μ) experimental (— · —) and calculated (- · - ·).

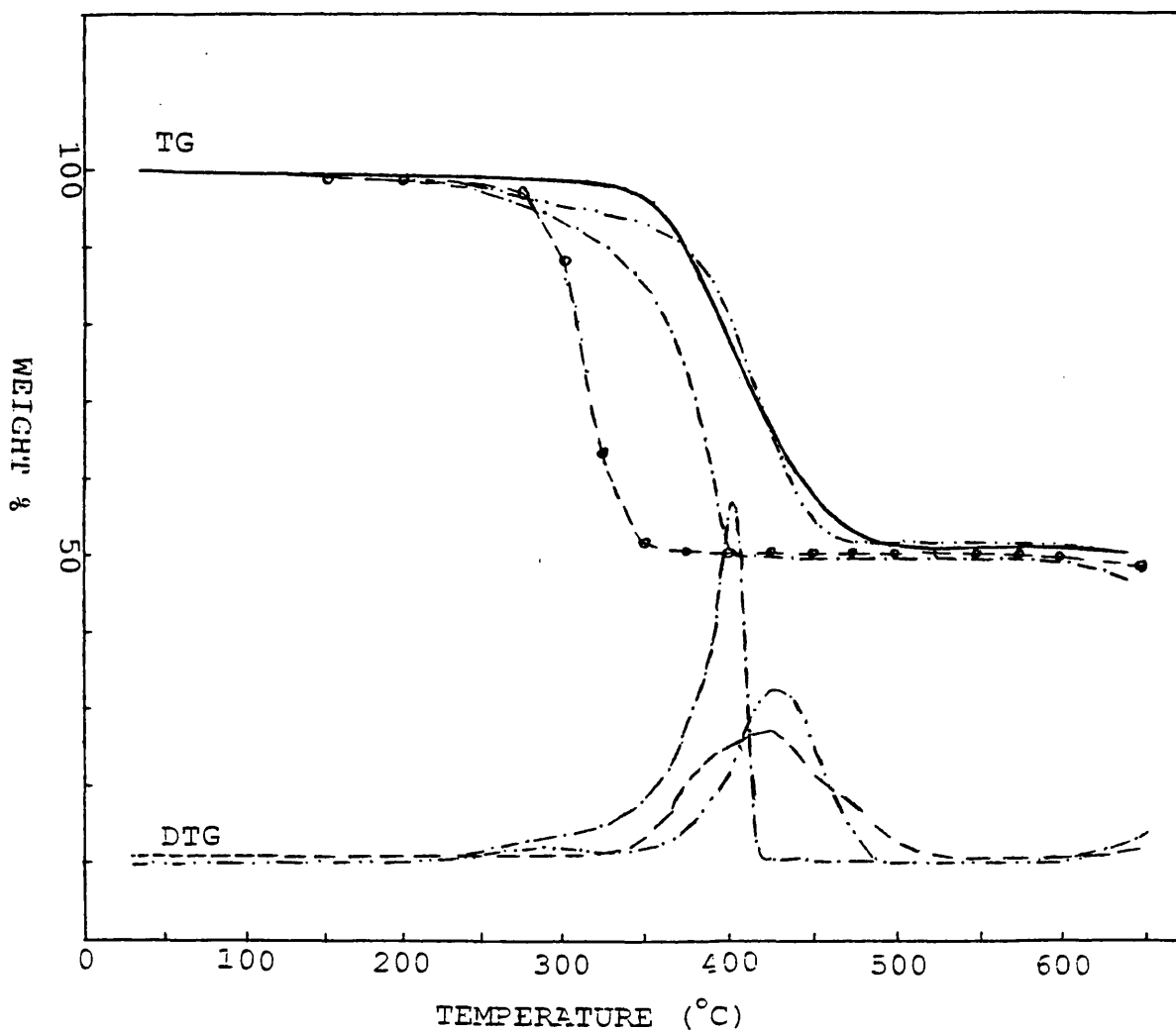


Fig. 7.7. TG-DTG traces for blends of PDMS and 50% uncoated CaCO_3 under nitrogen: blend 32 (with mean particle size of 0.7μ) experimental (---) and calculated (-.-.-), blend 33 (with mean particle size of 1.5μ) experimental (....) and calculated (-.-.-.-) and blend 34 (with precipitated and mean particle size of 5μ) experimental (—; -----) and calculated (-.-.-).

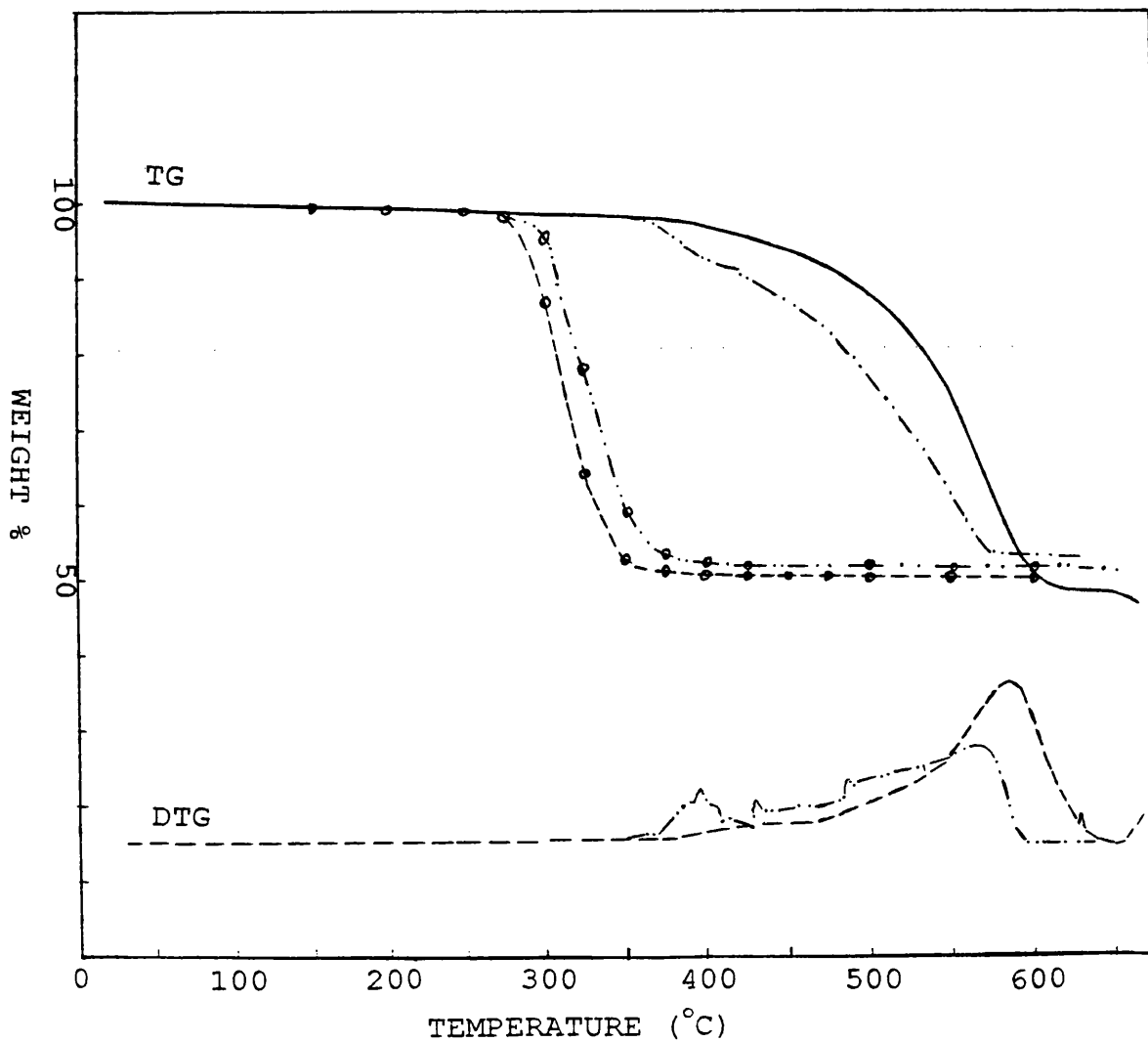


Fig. 7.8. TG-DTG traces for blend 35 (PDMS with trimethyl end groups and 50% coated CaCO_3 with mean particle size of 1.5μ) under nitrogen: experimental (—; ----) and calculated (-+ -), and air: experimental (-·-·) and calculated (-·+·-·).

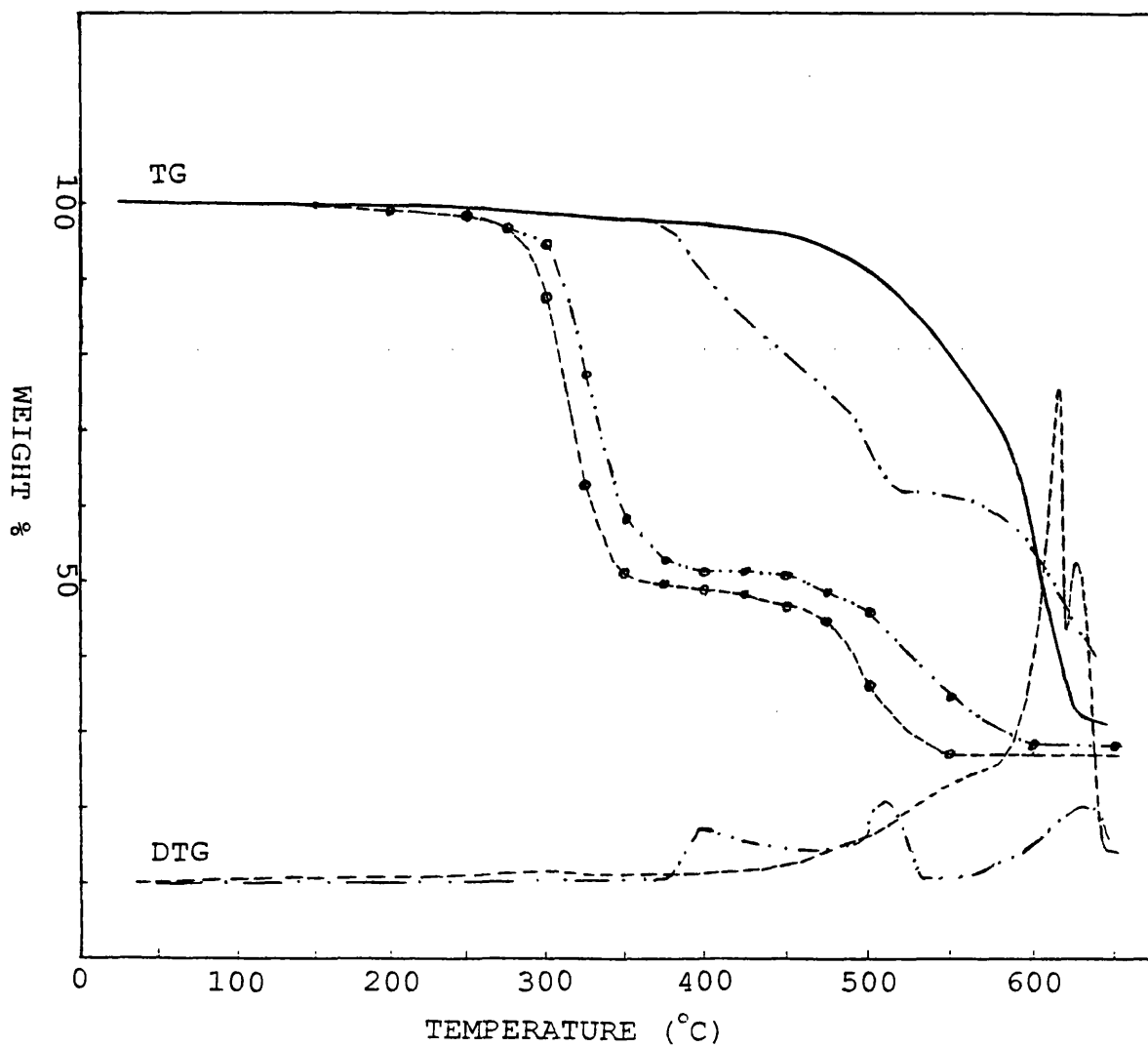


Fig. 7.9. TG-DTG traces for blend 36 (PDMS and 50% MgCO_3) under nitrogen: experimental (—; ----) and calculated (- - -), and air: experimental (- · - ·) and calculated (- · · · - ·).

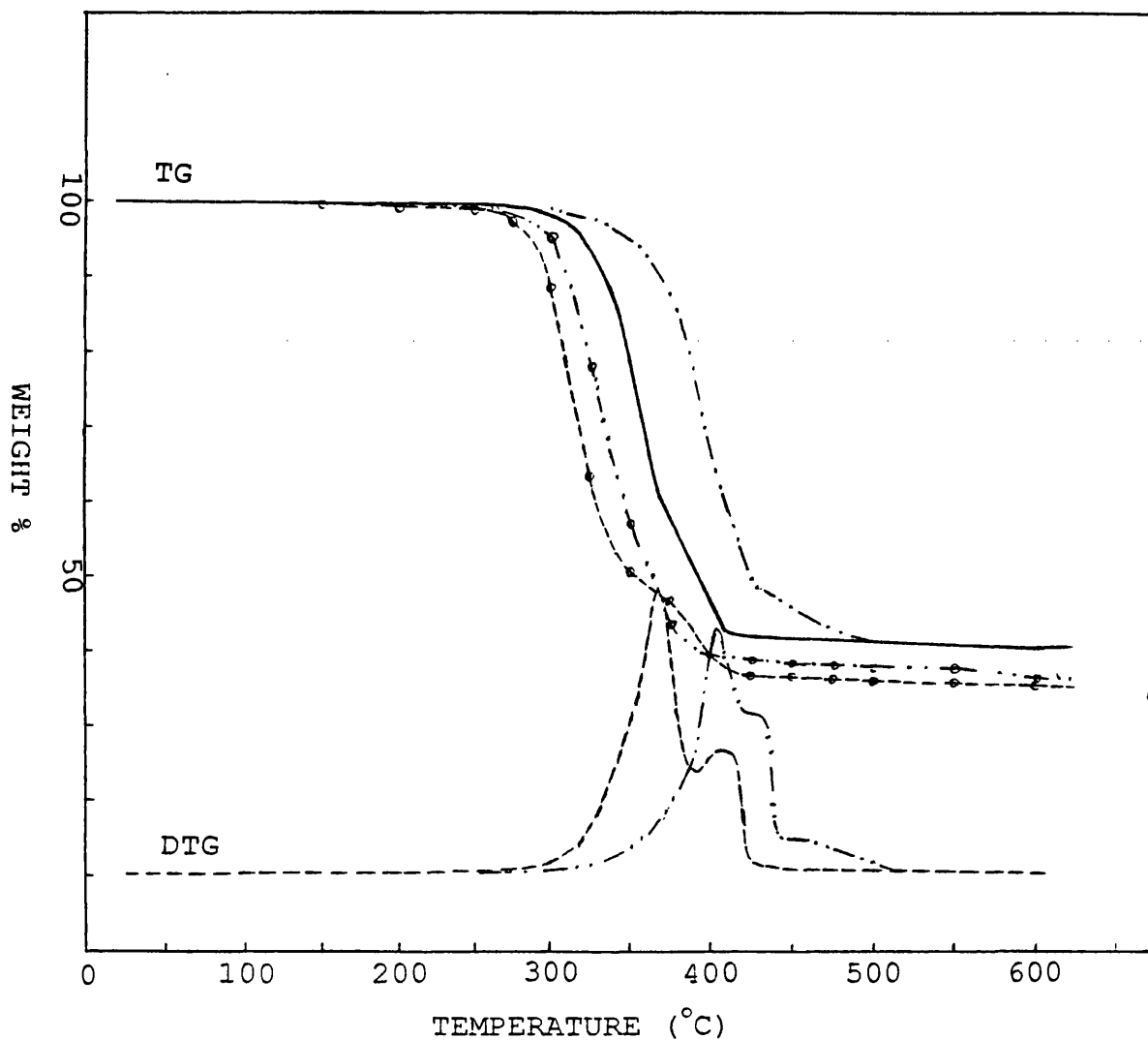


Fig. 7.10. TG-DTG traces for blend 37 (PDMS and 50% Mg(OH)₂) under nitrogen: experimental (—; ----) and calculated (-·-·-), and air: experimental (-·-·-) and calculated (-·-·-·-).

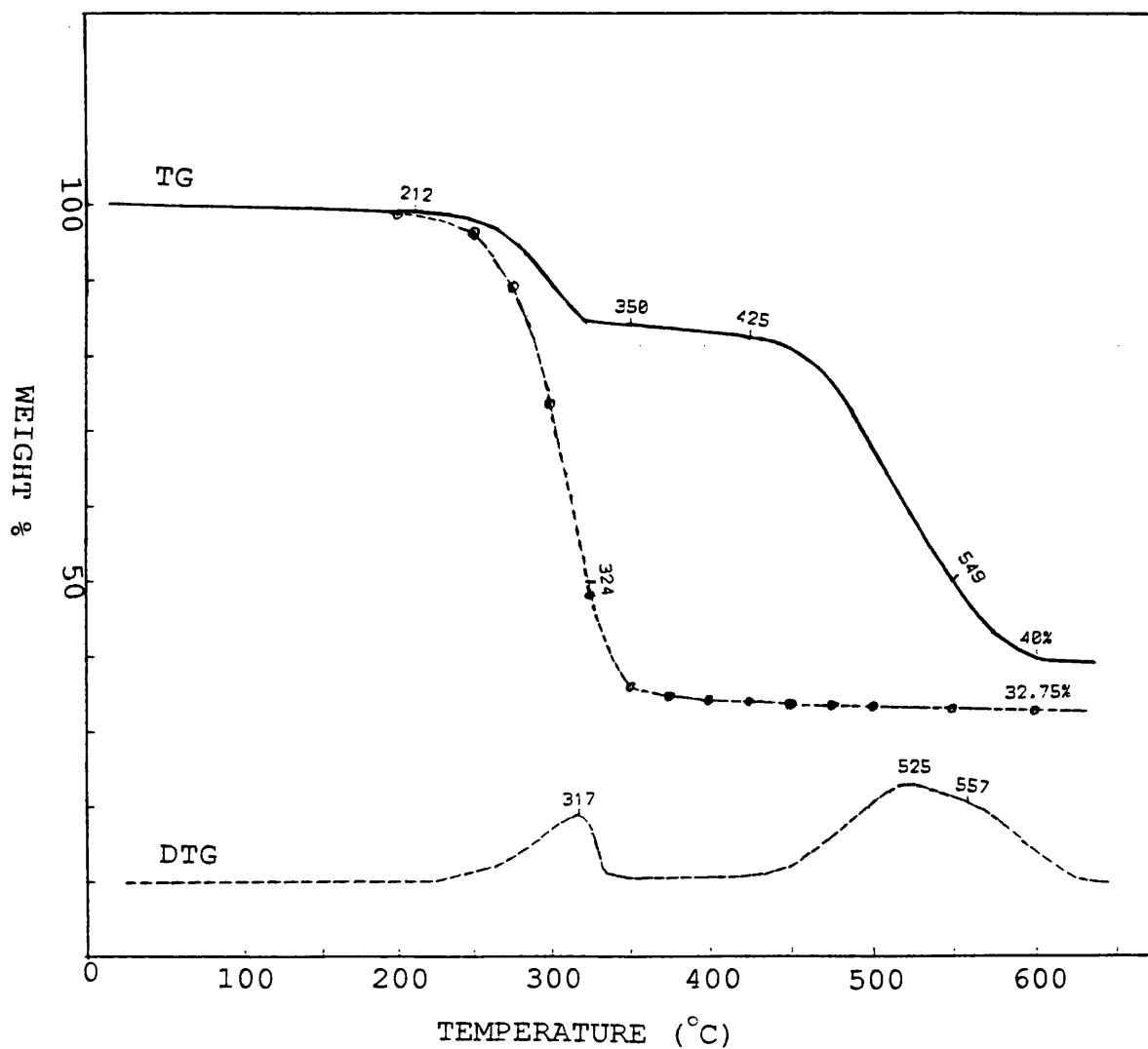


Fig. 7.11. TG-DTG traces for blend 38 (PDMS + 50% Al(OH)₃) under nitrogen: experimental (—; ----) and calculated (-•-).

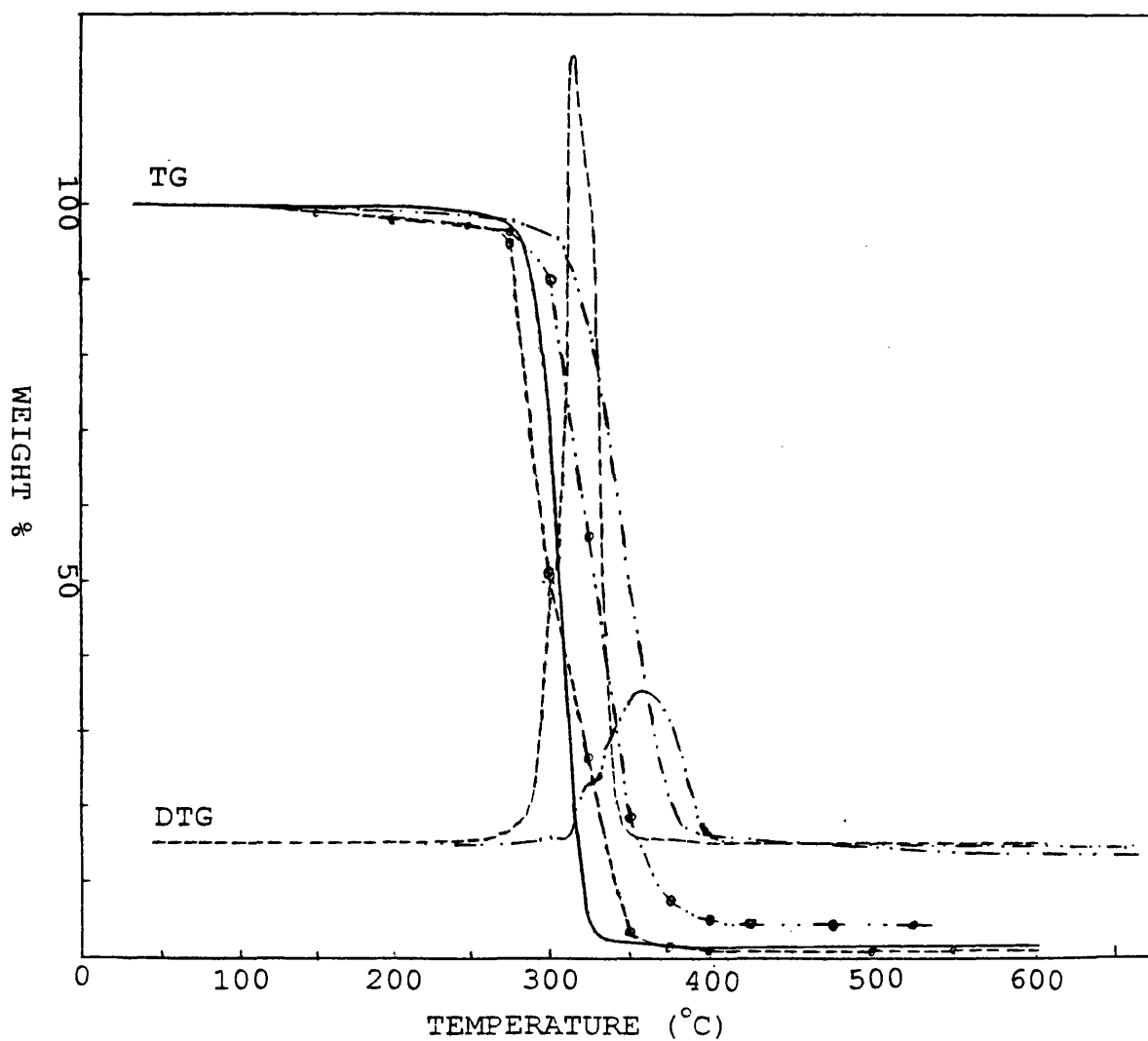


Fig. 7.12. TG-DTG traces for blend 39 (PDMS + 1% $\text{Ca}(\text{OH})_2$) under nitrogen: experimental (—; ----) and calculated (---), and air: experimental (-·-·-) and calculated (-·-·-·-).

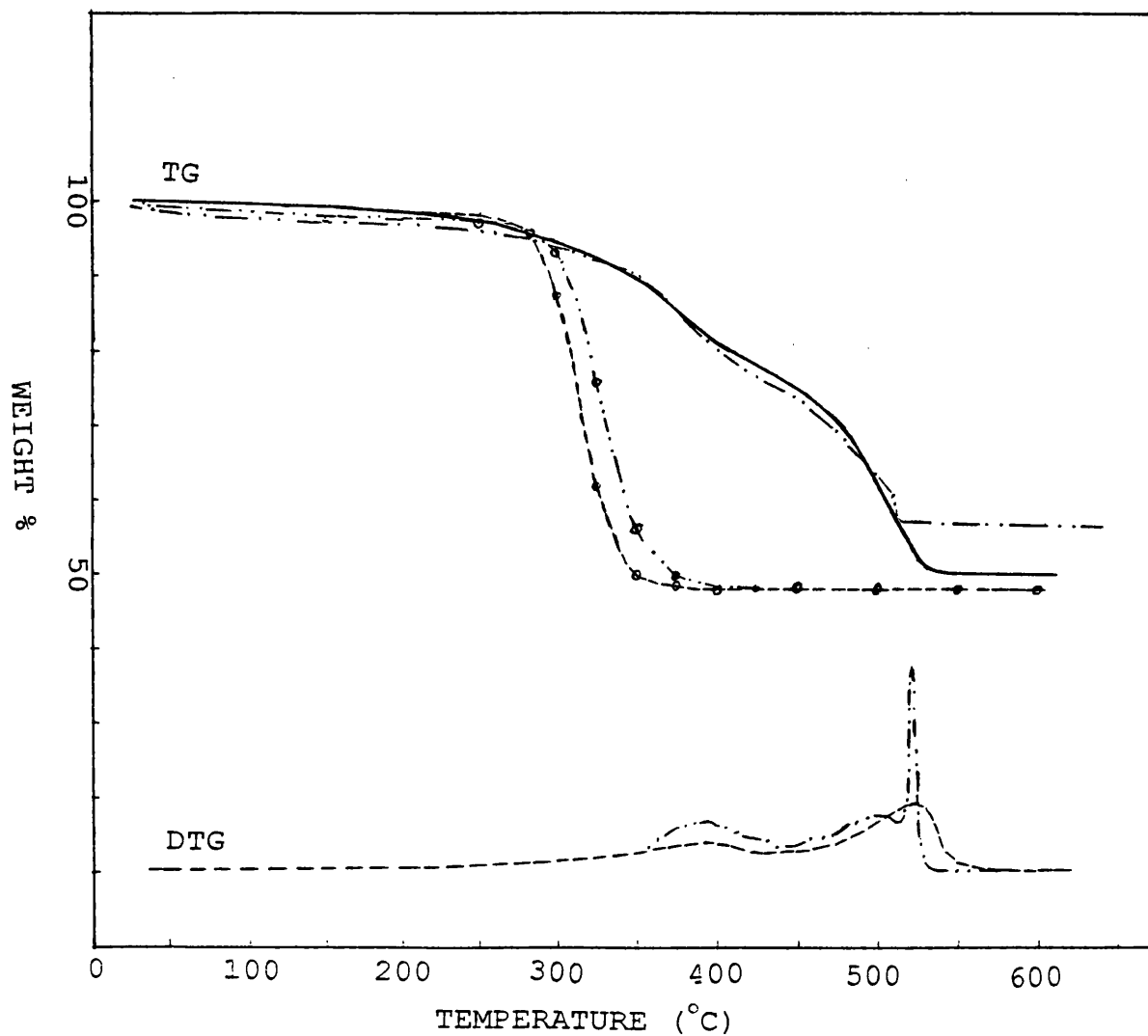


Fig. 7.13. TG-DTG traces for blend 41 (PDMS + 50% MgO) under nitrogen: experimental (—; ----) and calculated (- - - -), and air: experimental (- · - ·) and calculated (- · - · - ·).

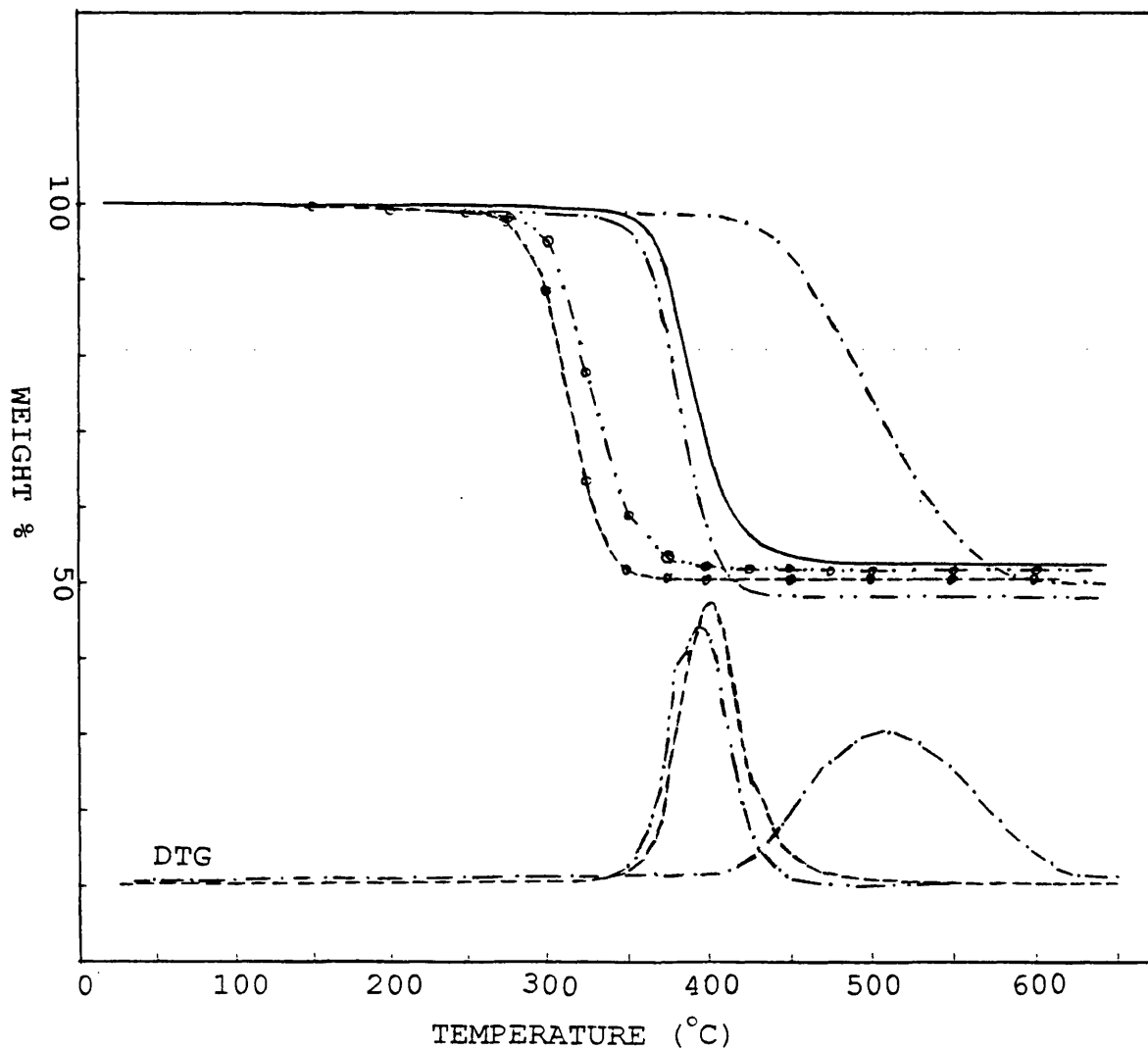


Fig. 7.14. TG-DTG traces for blends of PDMS and 50% inorganic fillers under nitrogen: blend 42 (Al_2O_3) experimental (—; - - -) and calculated (- · -), and blend 43 (TiO_2) experimental (- · -) and calculated (· - ·), and air: blend 42 experimental (- · · -) and calculated (- · · · -).

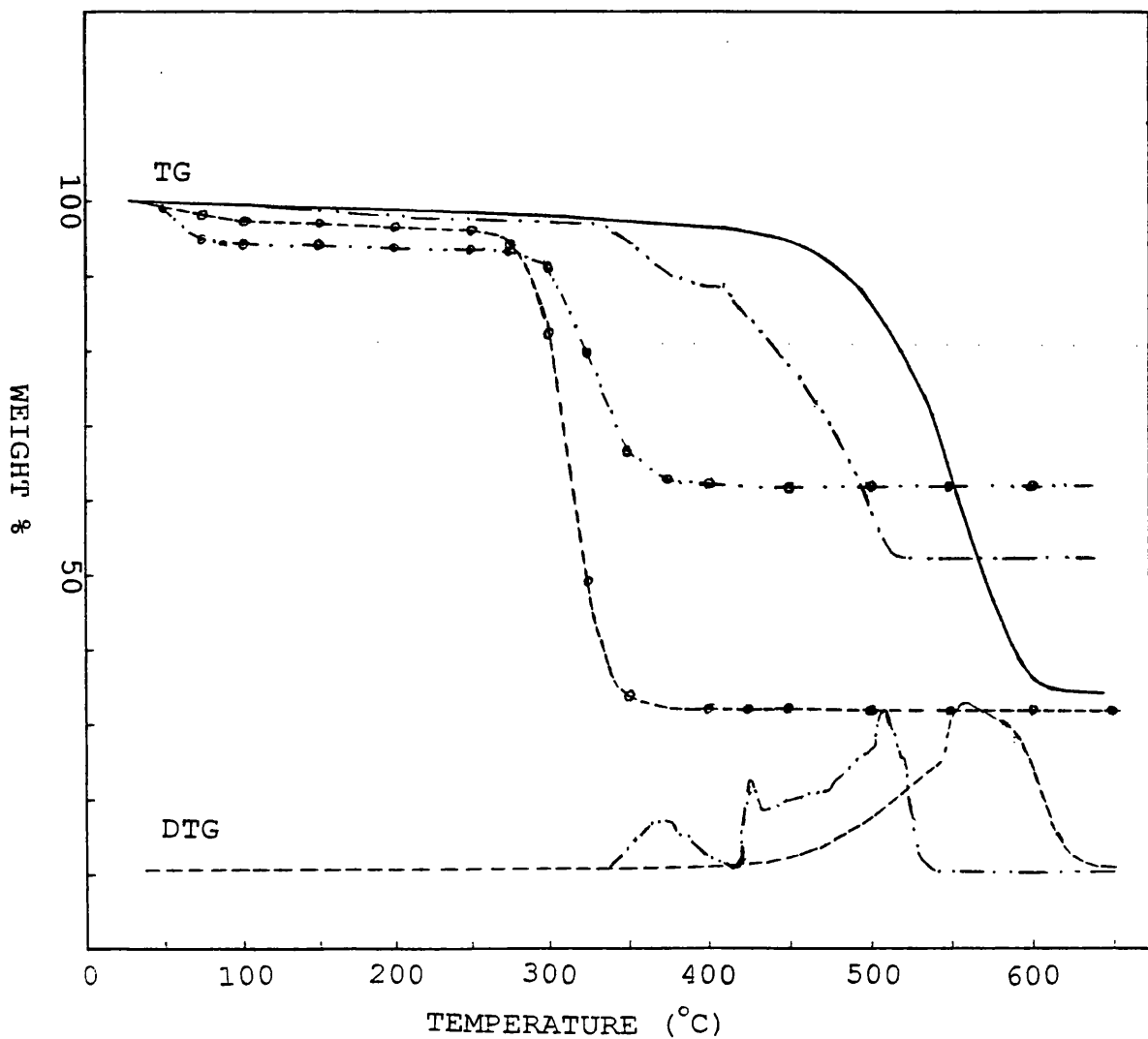


Fig. 7.15. TG-DTG traces for blend 44 (PDMS + ~ 66% silica) under nitrogen: experimental (—; ----) and calculated (---), and air: experimental (-·-·-) and calculated(-·-·-·-).

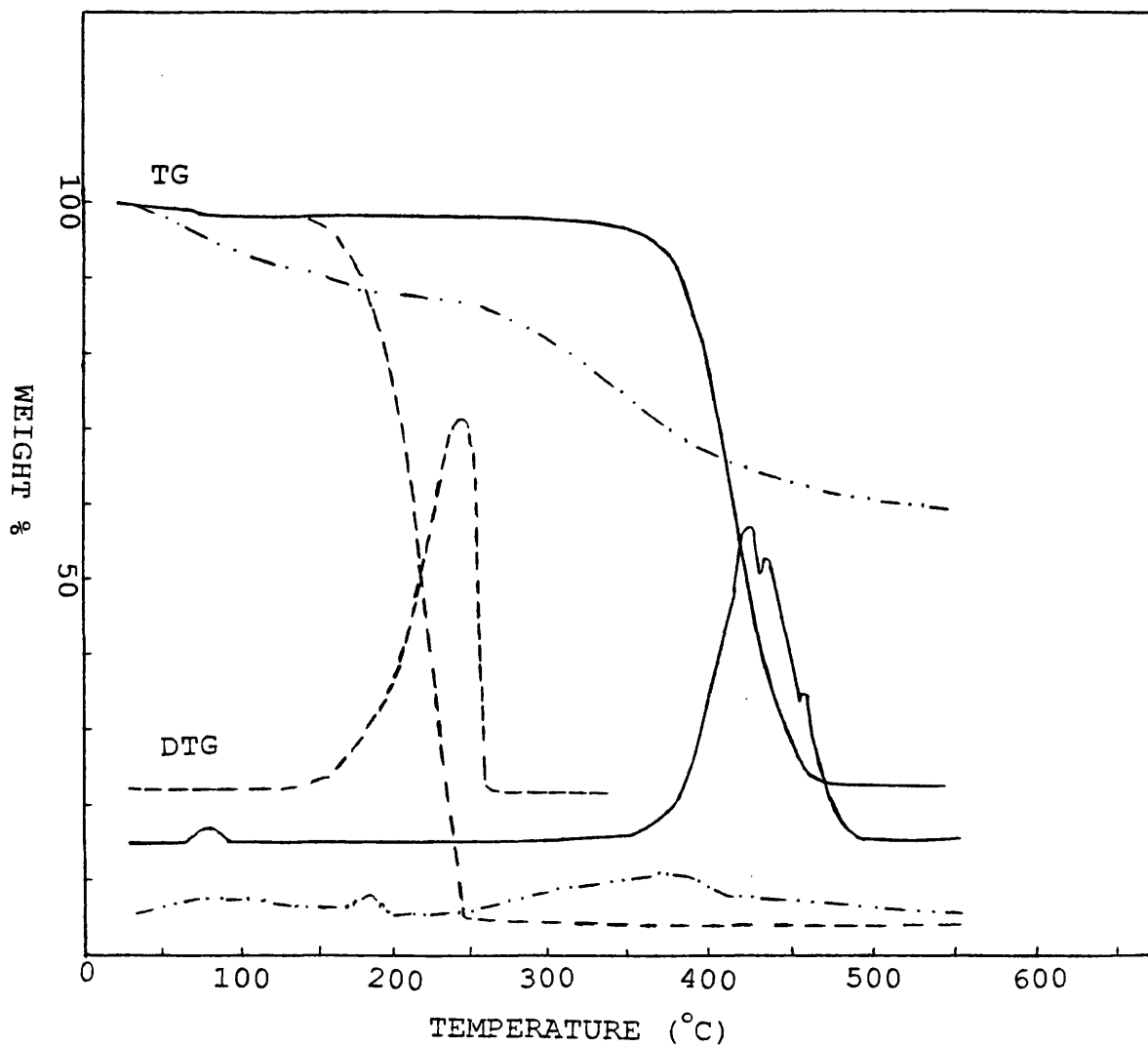


Fig. 7.16. TG-DTG traces for additives under nitrogen: calcium stearate (—), stearic acid (---) and DHT-4A (-·-·-).

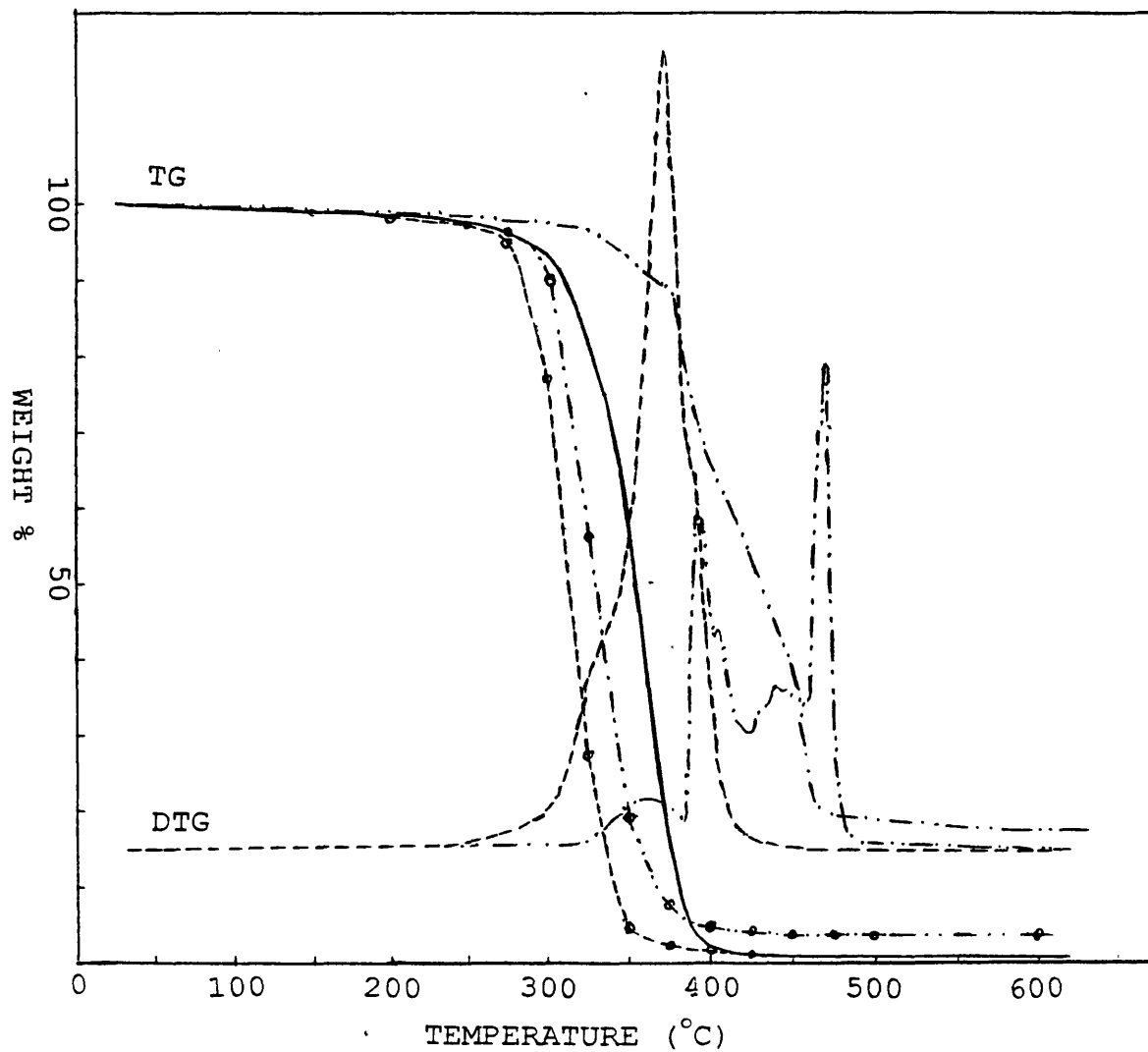


Fig. 7.17. TG-DTG traces for blend 45 (PDMS + 1% calcium stearate) under nitrogen: experimental (—; ----) and calculated (- - - -), and air: experimental (- · - ·) and calculated (- · - · - ·).

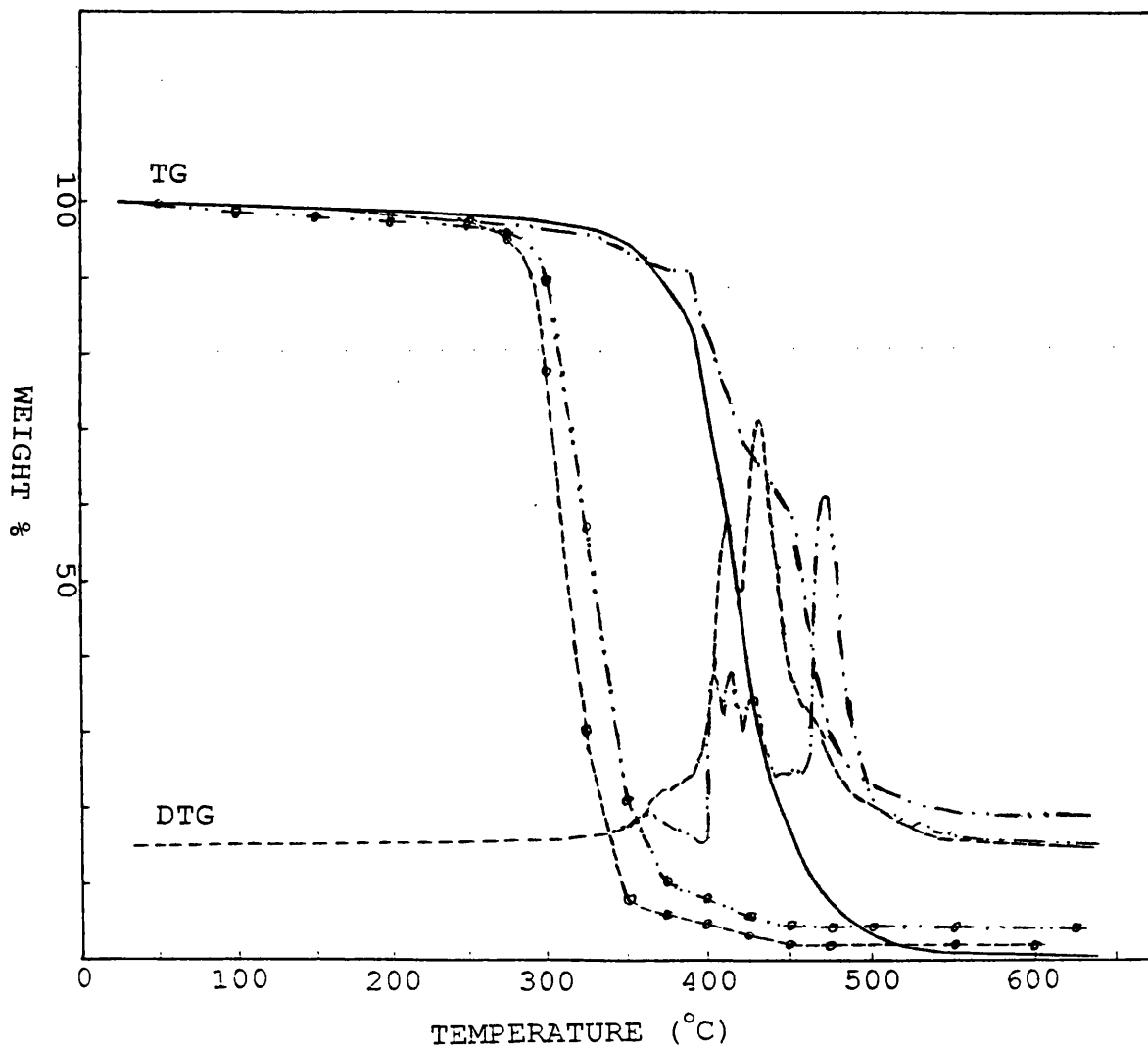


Fig. 7.18. TG-DTG traces for blend 46 (PDMS + 5% calcium stearate) under nitrogen: experimental (—; ----) and calculated (- - - -), and air: experimental (- · - ·) and calculated (- · - · - ·).

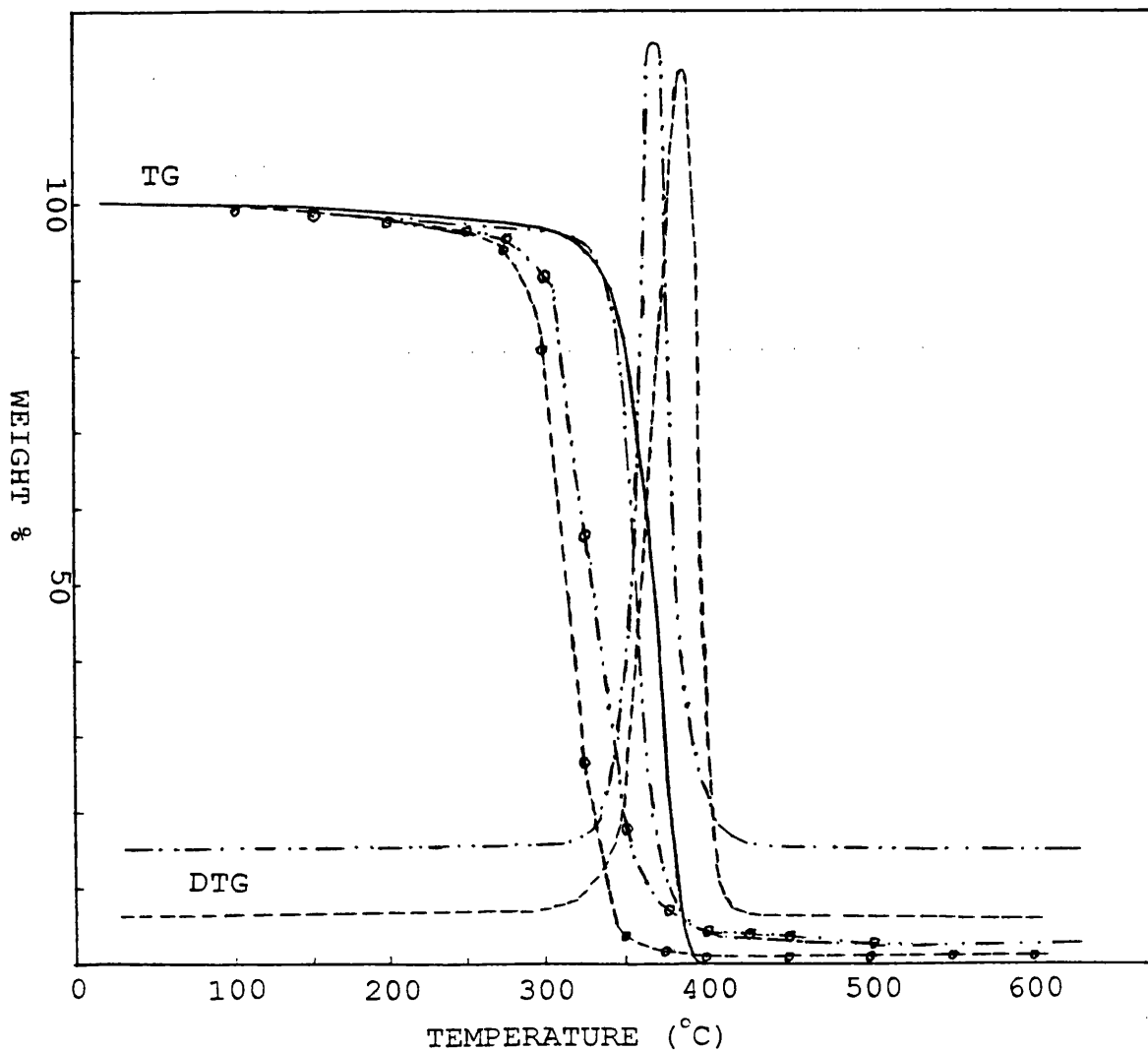


Fig. 7.19. TG-DTG traces for blend 47 (PDMS + 1% stearic acid) under nitrogen: experimental (—; ----) and calculated (-·-·-), and air: experimental (-·-·-) and calculated (-·-·-·-·-).

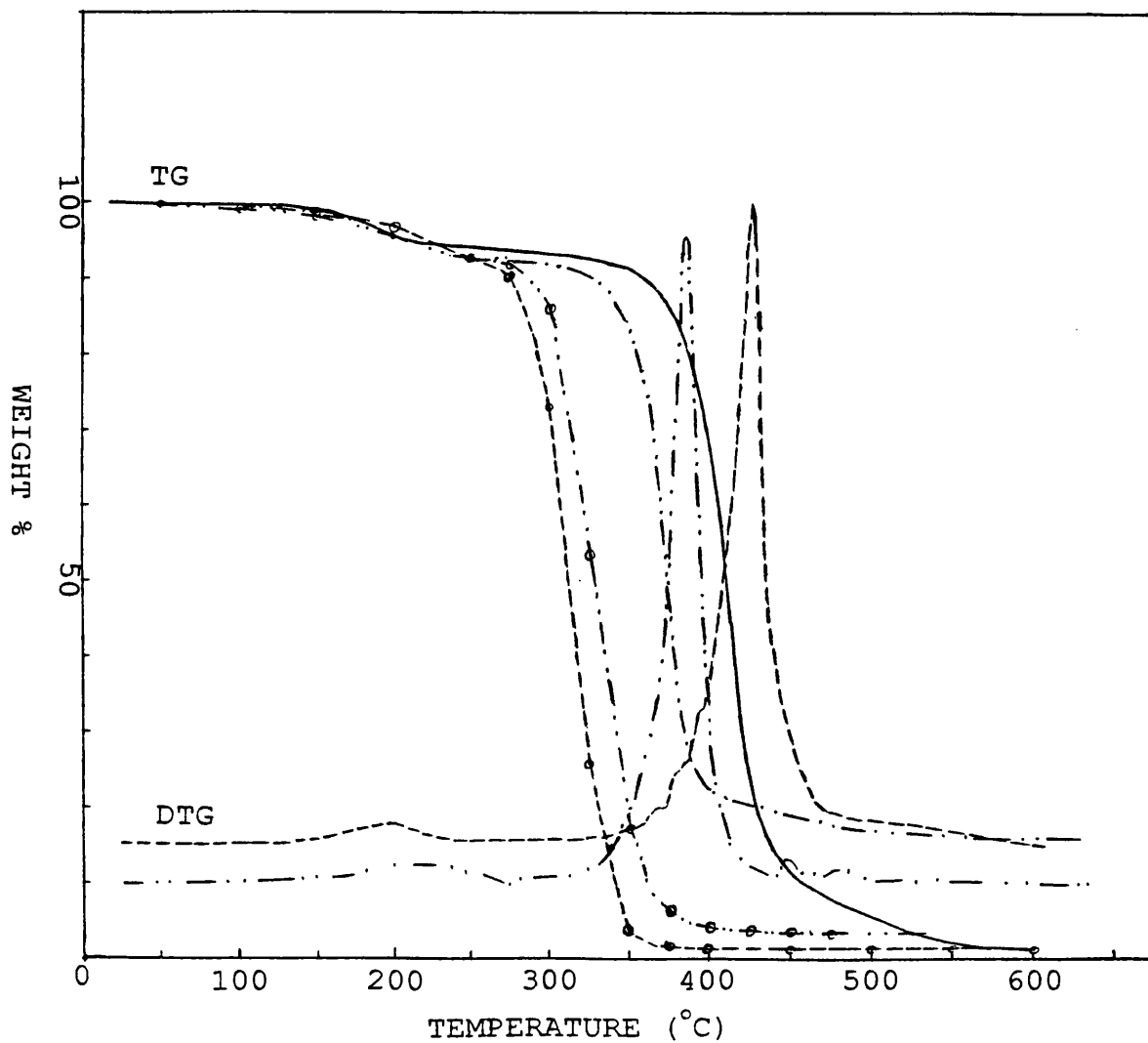


Fig. 7.20. TG-DTG traces for blend 48 (PDMS + 1% stearic acid) under nitrogen: experimental (—; ----) and calculated (- - -), and air: experimental (- · - ·) and calculated (- · - · - ·).

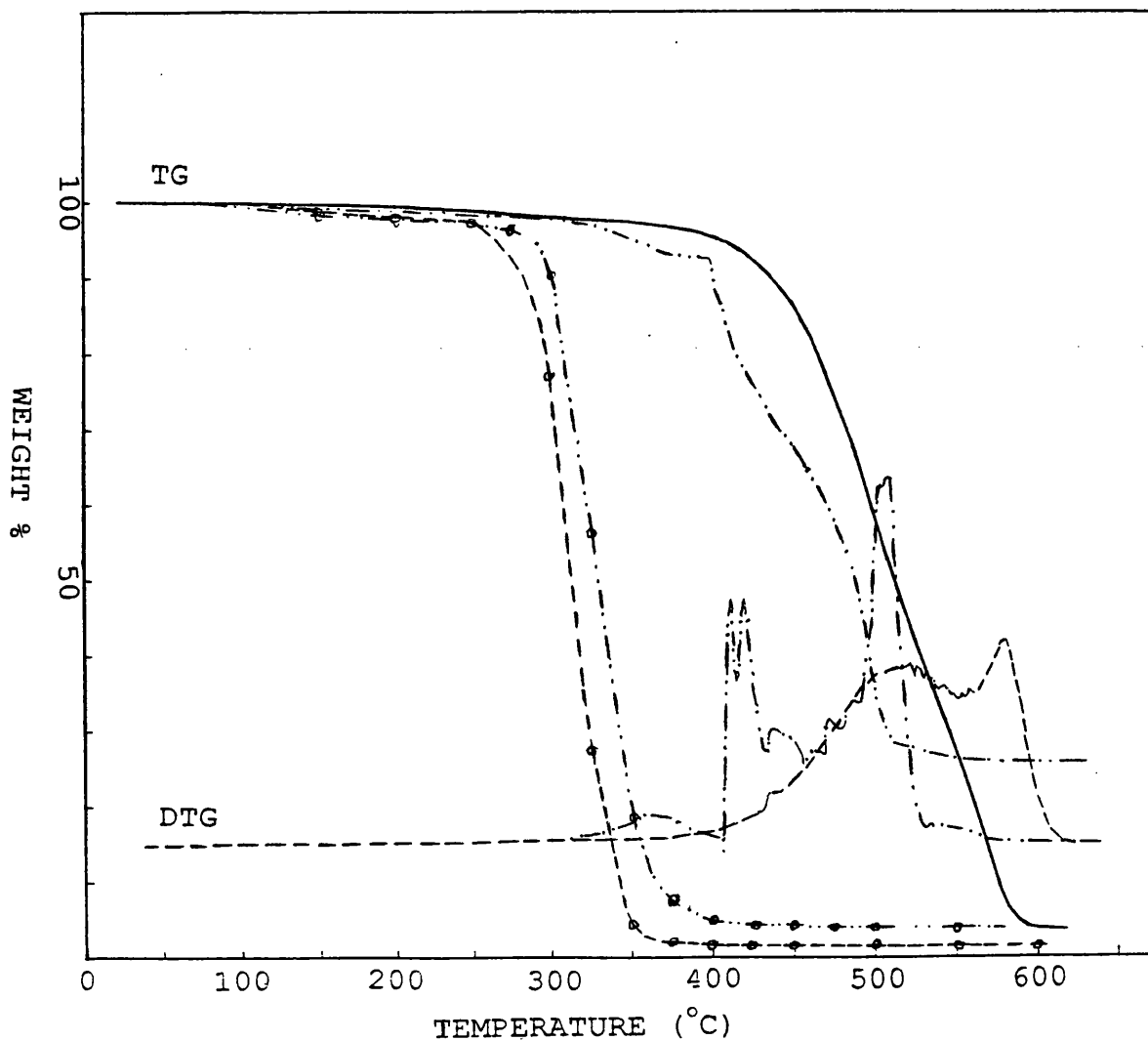


Fig. 7.21. TG-DTG traces for blend 50 (PDMS + 1% DHT-4A) under nitrogen: experimental (—; ----) and calculated (- - -), and air: experimental (- · - ·) and calculated (- · - · - ·).

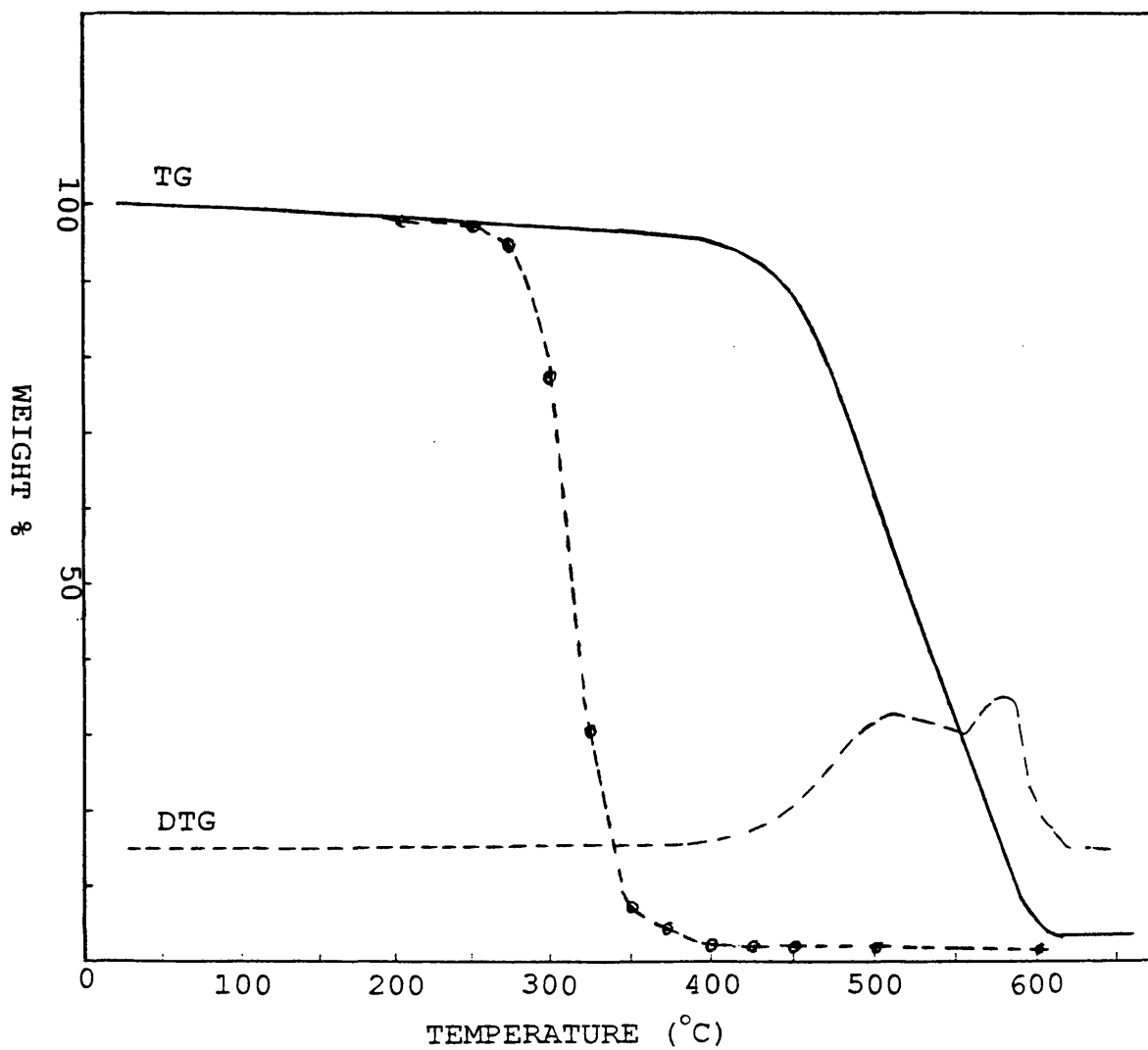


Fig. 7.22. TG-DTG traces for blend 51 (PDMS with trimethyl end groups + 1% DHT-4A) under nitrogen: experimental (—; ----) and calculated (- - -).

7.3.2. Differential Scanning Calorimetry (DSC)

Blend of PDMS with Coated CaCO₃

The DSC curves for blends 26 (with particle size of 1.5 microns), 29 (with particle size of 5.0 microns), 30 (with particle size of 0.9 microns) and 31 (with precipitated and particle size of 0.06 μ), exhibit two endothermic transitions as shown in (Fig. 7.23). The peak temperature for the first transition due to melting of the polymer occurred at about 50°C (average) while the second is poorly defined for most blends and almost a straight curve rising towards exotherm. This rise towards the exotherm is almost throughout the degradation after melting of the polymer. This shows the great degree of crosslinking occurring or/and indicates interaction between the components. The temperature for the maximum rate of degradation agreed within 7-13°C with the TG-DTG results.

Blend of PDMS with Uncoated CaCO₃

The DSC curves of blends 32, 33 and 34 (with particle size of 0.7 μ , 1.5 μ , 5.0 μ , respectively) are similar to the DSC curve of blend 30, with second endothermic transitions in the regions 350-450°C, 375-475°C and 325-425°C, respectively (Fig. 7.24).

Blend of PDMS and MgCO₃

The DSC curve of blend 36 (with MgCO₃) is similar to the DSC curve of blend 26 but the curve does not rise steeply towards the exotherm after melting of the polymer and has second endothermic transitions in the regions 225-300°C. The curve rises towards the exotherm steeply after the second transition but becomes endothermic after 583°C (Fig. 7.24). This sudden fall is due to extensive of volatilisation of the degradation products, possibly due to decomposition of the filler.

Blends of PDMS and Metal Hydroxides

Blend 38 (with 50% Al(OH)₃) shows an exotherm with T_{max} at 289°C and an endotherm with T_{max} at 324°C (Fig. 7.25) possibly due to interaction of the components and the dehydration of the filler, respectively. The interaction of the components can be seen to be associated with a weight loss at lower stages than for the normal degradation of the polymer.

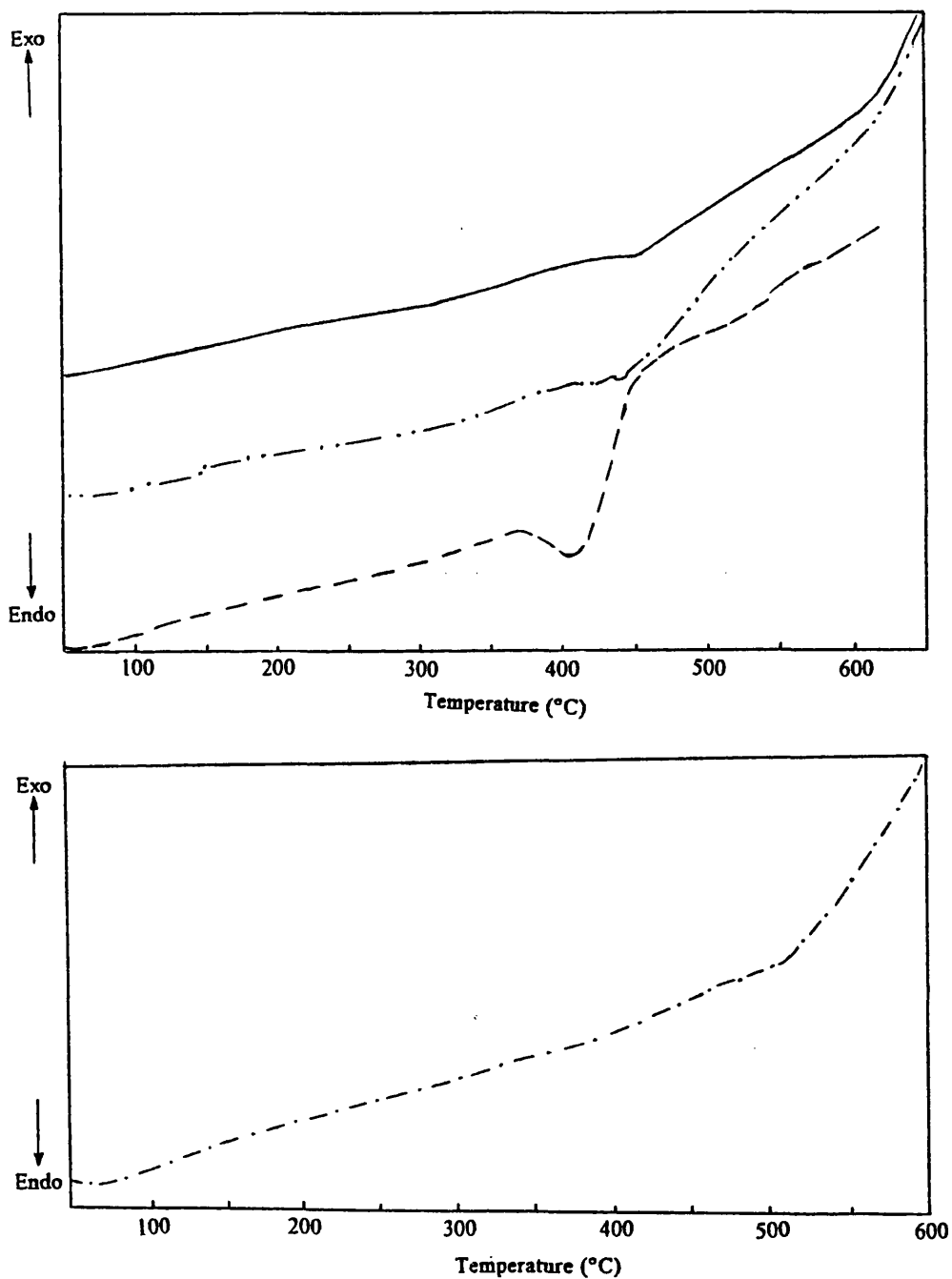


Fig. 7.23. DSC traces for blends of PDMS and 50% coated CaCO₃ under nitrogen: blend 26 with particle size of 1.5 μ (—), blend 29 with particle size of .5 μ (-·-·-), blend 30 with particle size of 0.9 μ (- - -) and blend 31 with precipitated and particle size of 0.06 μ (- - - -)

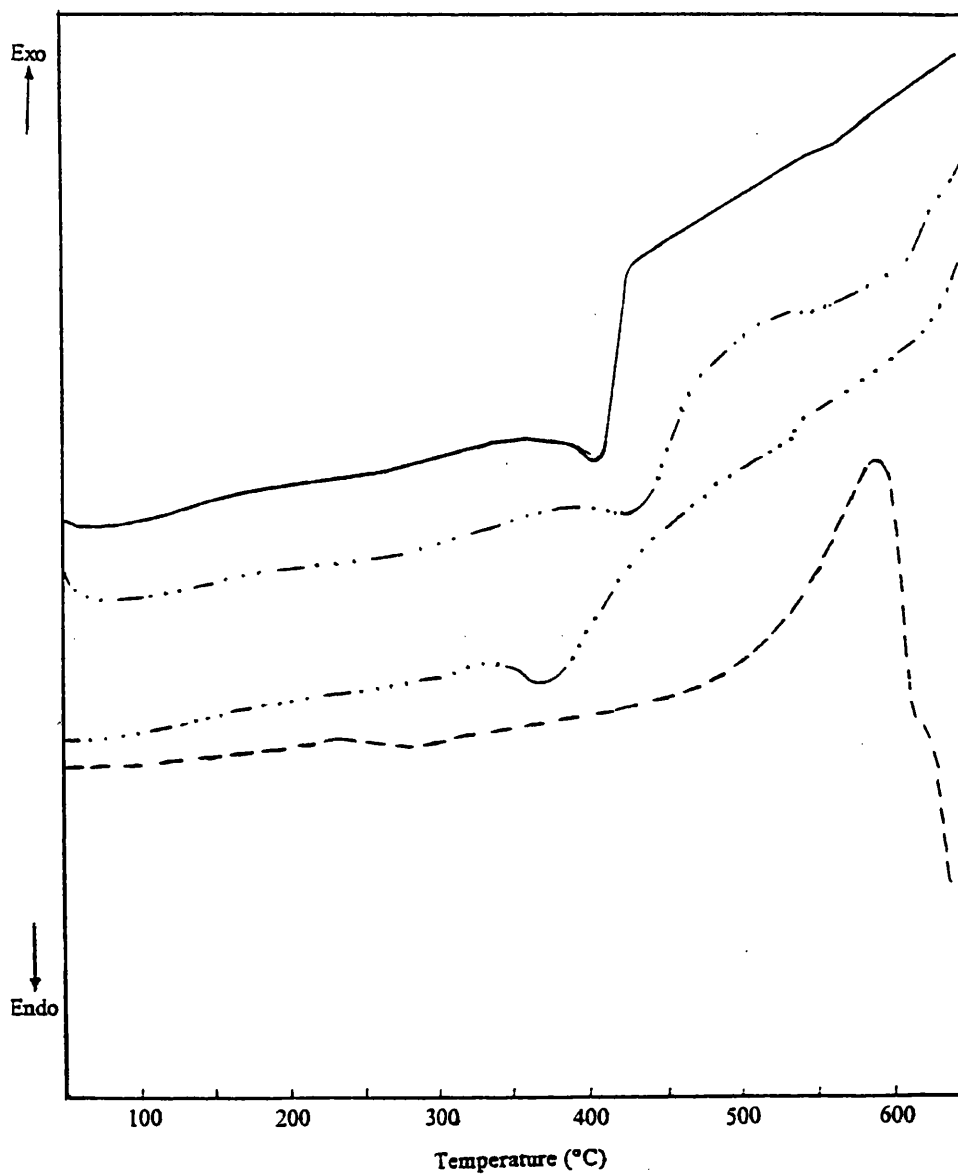


Fig. 7.24. DSC traces for blends of PDMS and 50% inorganic fillers under nitrogen: blends with uncoated CaCO₃: blend 32 with particle size of 0.7 μ (—), blend 33 with particle size of 1.5 μ (- · - · -) and blend 34 with particle size of 5 μ (- · · - · -), and blend 36 with MgCO₃ (-----).

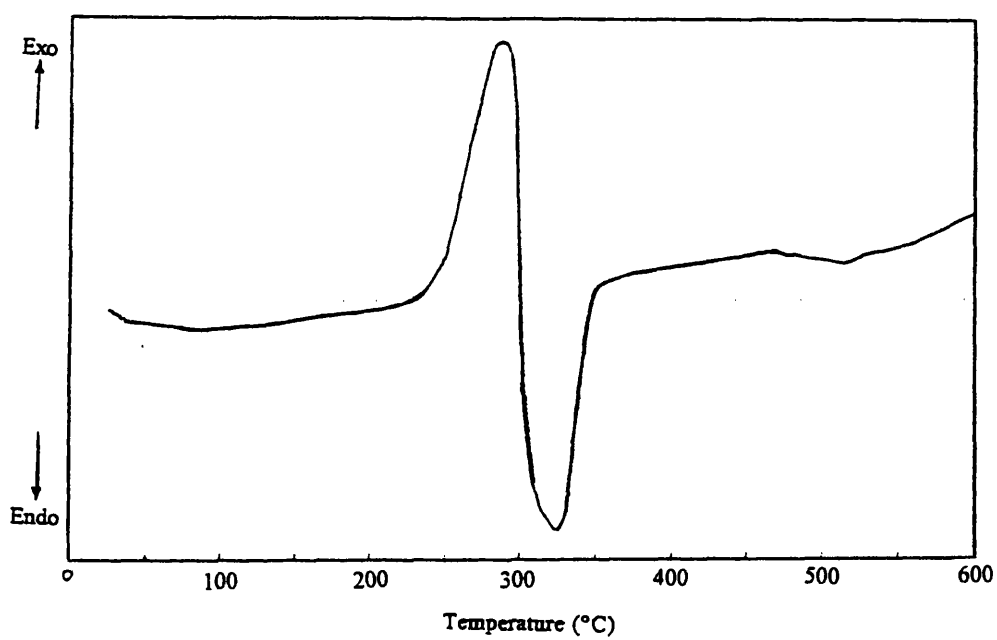


Fig. 7.25. DSC trace for blend 38 (PDMS + 50% Al(OH)₃) under nitrogen.

7.3.3. Thermal Volatilisation Analysis (TVA) and SATVA Separation of Condensable Degradation Products

Blends of PDMS and CaCO₃

The TVA trace of blend 21 (with 1.0% CaCO₃) is similar in shape to that of PDMS when degraded alone only in the present case degradation starts at 25°C later and shows 25-30°C stabilisation throughout the degradation (Fig. 7.26 (a)). The TVA trace does not show the presence of any non-condensable gaseous product. The SATVA trace is also similar to that of PDMS. The IR spectrum of the residue (1.48%) shows absorptions for both filler and siloxane groups.

The TVA curve of blend 26 (with 50.0% CaCO₃) shows volatilisation starting at about 388°C (Fig. 7.26 (b)). The TVA trace from the gauge after the liquid nitrogen trap (-196°C) shows a rise from the baseline indicating the presence of non-condensable gaseous products, identified as CH₄ by the quadrupole mass spectrometer attached to the TVA line.

The SATVA trace (Fig. 7.27) for the separation of the condensable volatile products of degradation of blend 26 shows the presence of two main fractions, after which the trace became broad with poorly resolved peaks. The IR spectrum of the first fraction (Fig. 7.28) showed bands at 2346 cm⁻¹ (strong) due to CO₂, 2164 cm⁻¹, 2138 cm⁻¹ due to ketene, 1261 cm⁻¹ with shoulders at 1256 cm⁻¹ and 1268 cm⁻¹, 1098 cm⁻¹, 1025 cm⁻¹, 862 cm⁻¹ all due to siloxane groups and at 911 cm⁻¹ due to C=C bonds which is confirmed by an absorption at 3085 cm⁻¹. The presence of a ketene can only be possible if polymer has chain ends of the type Si-O-CH=CH₂. Formation of ketene would also introduce Si-H groups in the polymer chain but the characteristic strong band for Si-H stretch which falls in the 2275-2040 cm⁻¹ was not detected. The Si-Me group in a compound H-Si(Me₂)- would absorb around 1256 cm⁻¹, while the bending modes of a single hydrogen on silicon fall between 952-768 cm⁻¹. In fact the bands at 911 cm⁻¹ and 868 cm⁻¹ could be due to the Si-H group. Tetramethylsilane also gives absorptions at 1256 cm⁻¹ and 868 cm⁻¹ but its formation would be difficult to explain. It is clear, however, that these siloxane compounds are not of the type O-Si(Me₂)-O since there was no band at 800 cm⁻¹. Whatever these siloxane compounds are, their quantity is extremely small, and therefore they are difficult to identify.

Formation of CO₂ and ketene was in a 4:3 ratio when blend 26 was heated up to 700°C. The production of CO₂ was only slightly more than when blend 26 was degraded up to 650°C indicating delay in decomposition of the filler.

The later fraction collected was characterised by GC-MS (Fig. 7.29) and the results (Table 7.7) show that the main degradation products are similar to those when PDMS was degraded alone giving cyclic siloxane oligomers while there are some new products present as well. The mechanism of formation of these compounds is given later in section 7.5.

IR spectroscopy of total degradation products including CRF shows, beside the expected siloxane absorptions, weak absorptions at 2130 cm^{-1} and 1358 cm^{-1} which could be assigned to Si-H and Si-CH₂-Si groups respectively if there were also bands at about 910 cm^{-1} and 769 cm^{-1} , respectively (Fig. 7.30). These peaks if present were masked under the strong absorptions due to the siloxane groups although there seems development of shoulders in the region $950\text{-}880\text{ cm}^{-1}$ and $800\text{-}750\text{ cm}^{-1}$. Since the Si-H group gives a strong and sharp absorption around 2130 cm^{-1} , the Si-H group if present is in very small amount. Identification of the degradation products (Table 7.7) confirms the presence of compounds with Si-H groups and also their small amount. There is also an extremely small but sharp absorption at 1709 cm^{-1} which could arise from a carbonyl stretching absorption but there is no satisfactory explanation for the formation of carbonyl groups unless they are formed from carbonate ions when the filler interacts with the silicone polymer. The GC-MS results did not show the presence of compounds containing carbonyl groups but the tiny peaks of the GC separation were not assigned.

The cold ring fraction (CRF) produced during the degradation was a colourless liquid of which a very small amount was insoluble. The IR spectrum (Fig. 7.31) of the soluble CRF was similar in most respects to that of the original polymer (see Fig 4.1 (a) in Chapter 4) and its CRF thus indicating that it consists of siloxane units of the type O-SiMe₂ except there seemed to be an extra poorly resolved absorption in the region $1092\text{-}1024\text{ cm}^{-1}$. GC analysis (Fig. 7.32) revealed that the CRF was indeed made up of larger cyclic oligomers of which D₇ to D₂₄ were positively identified on the basis of retention time from the reference compounds and from smooth plots of retention times against number of repeating units. However, it is clear from the GC trace that small amounts of other compounds are also present but were not identified due to difficulty in finding the reference compounds. High cyclics may also be formed but it was not practical to heat the GC column any higher than already done.

The IR spectrum of the insoluble CRF was mainly similar to that of the original polymer and its CRF except that the C-H stretch for the methyl groups at 2963 cm^{-1} and the absorption for the Si-Me group at 1261 cm^{-1} decreased in intensity indicating the reduction of the number of methyl groups on the silicon atoms. Any other changes which caused this small amount of CRF to become insoluble could not be detected because

of the small quantity of the sample and also the absorptions due to changes such as crosslinking, which result in reduction of methyl groups, would be masked by other siloxane absorptions.

The residue (89.98% at 480°C) was rubbery and formed an unbreakable bubble with outside surface shiny and smooth while the inside surface was slightly rough. The IR spectrum of the soluble residue (10.0% of sample and 18.12% of the total residue) was also similar to the IR spectrum of the original polymer. The IR spectrum of the insoluble residue showed absorptions for the filler and the polymer. Any changes which might have been introduced during degradation, e.g. crosslinking, would be impossible to detect from the IR spectrum since other absorptions due to siloxane groups are also in the same regions as for the polymer and others would be masked by the strong absorption due to the carbonate ions.

Note: It should be kept in mind for this blend and others mentioned later that if the residue is described as rubbery and/or insoluble then it was impossible to grind it. Therefore, possibly only small and thin fragments/sections allowed the transmittance of light and thus may have given some absorptions, giving only some detail.

The residue of blend 26 was still rubbery at 600°C (IR spectrum of the residue is given in Fig. 7.33 (b)) while it crumbled to powder when disturbed after degradation was carried out up to 650°C. The IR spectrum of the residue after heating up to 650°C was similar to the IR spectrum of the filler but there were still weak absorptions for siloxane groups at 1261 cm^{-1} , three absorptions in the region 1098-1020 cm^{-1} instead of just two and at 802 cm^{-1} . However, the intensity of band at 1261 cm^{-1} due to Si-Me group was much less than the intensity for Si-O-Si groups indicating a high degree of crosslinking. The band due to Si-Me almost disappeared when blend was heated up to 700°C while bands due to Si-O-Si group were still present (Fig. 7.33 (c)). This shows that the crosslinking increased as the degradation temperature was raised.

Note: Assignments of peaks in the IR spectra from all fractions are given in Table 7.5 while Table 7.6 shows the effects on the absorbance frequencies of the Si-O-Si group of hydrogen substitution on silicon atoms and the molecular size of the compounds, to clarify the differences seen in the IR spectra of different fractions. These two tables are based on assignments in IR spectra from all of the blends.

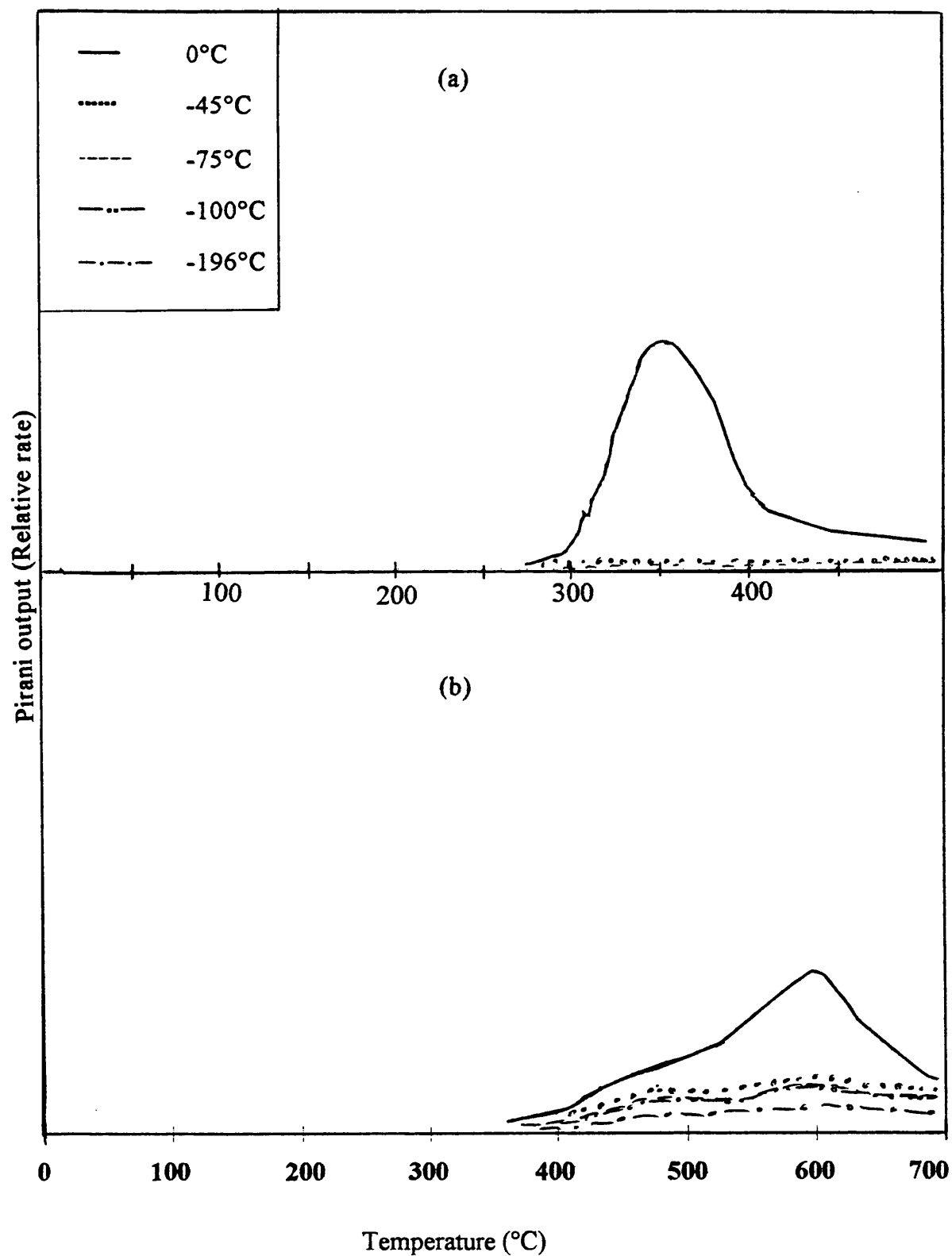


Fig. 7.26. TVA traces for blends of PDMS and coated CaCO₃ with particle size of 1.5 μ : (a) blend 21 (with 1% CaCO₃) and (b) blend 26 (50%).

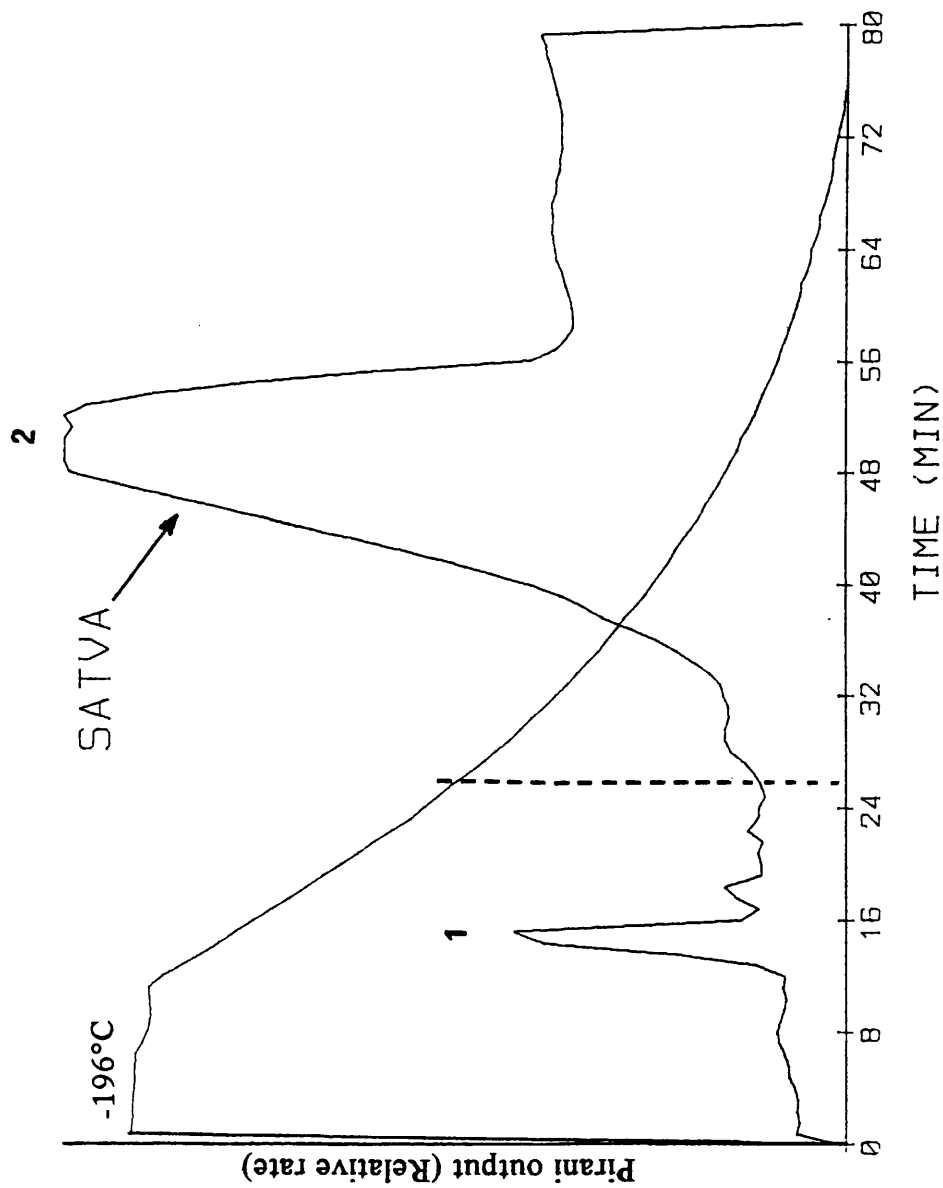


Fig. 7.27. SATVA trace for warm up from -196°C to ambient temperature of condensable volatile products from degradation for blend 26 (PDMS + 50% coated CaCO_3 with particle size of $1.5\ \mu$) after heating up to 700°C .

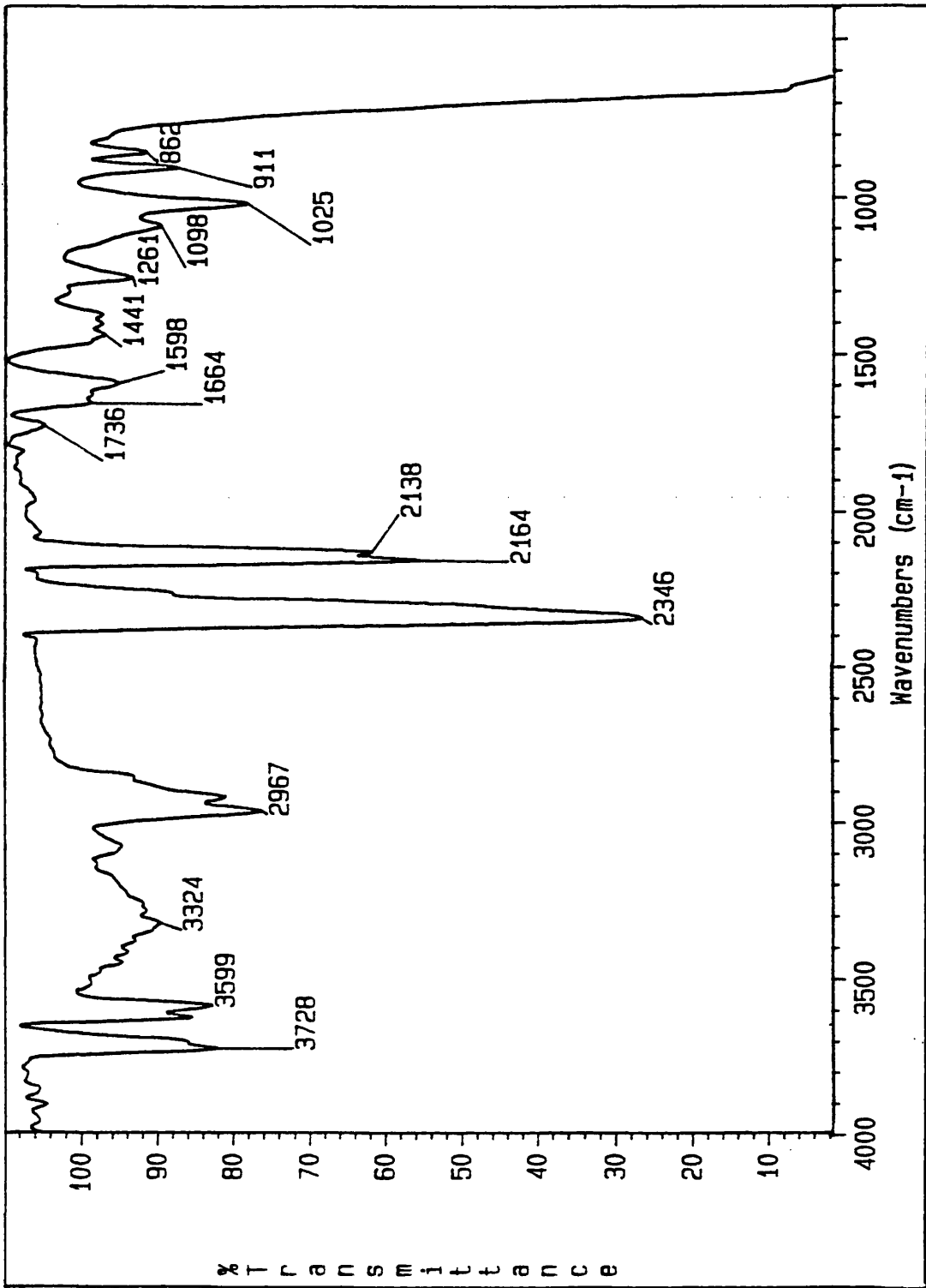


Fig. 7.28. IR spectrum (transmittance $\times 10$) of fraction I in SATVA separation of products from the degradation of blend 26 (PDMS + 50% coated CaCO_3 with particle size of 1.5μ).

Chromatogram Identifiers:
 A = ATIC
 Trace: A
 Scan : 314

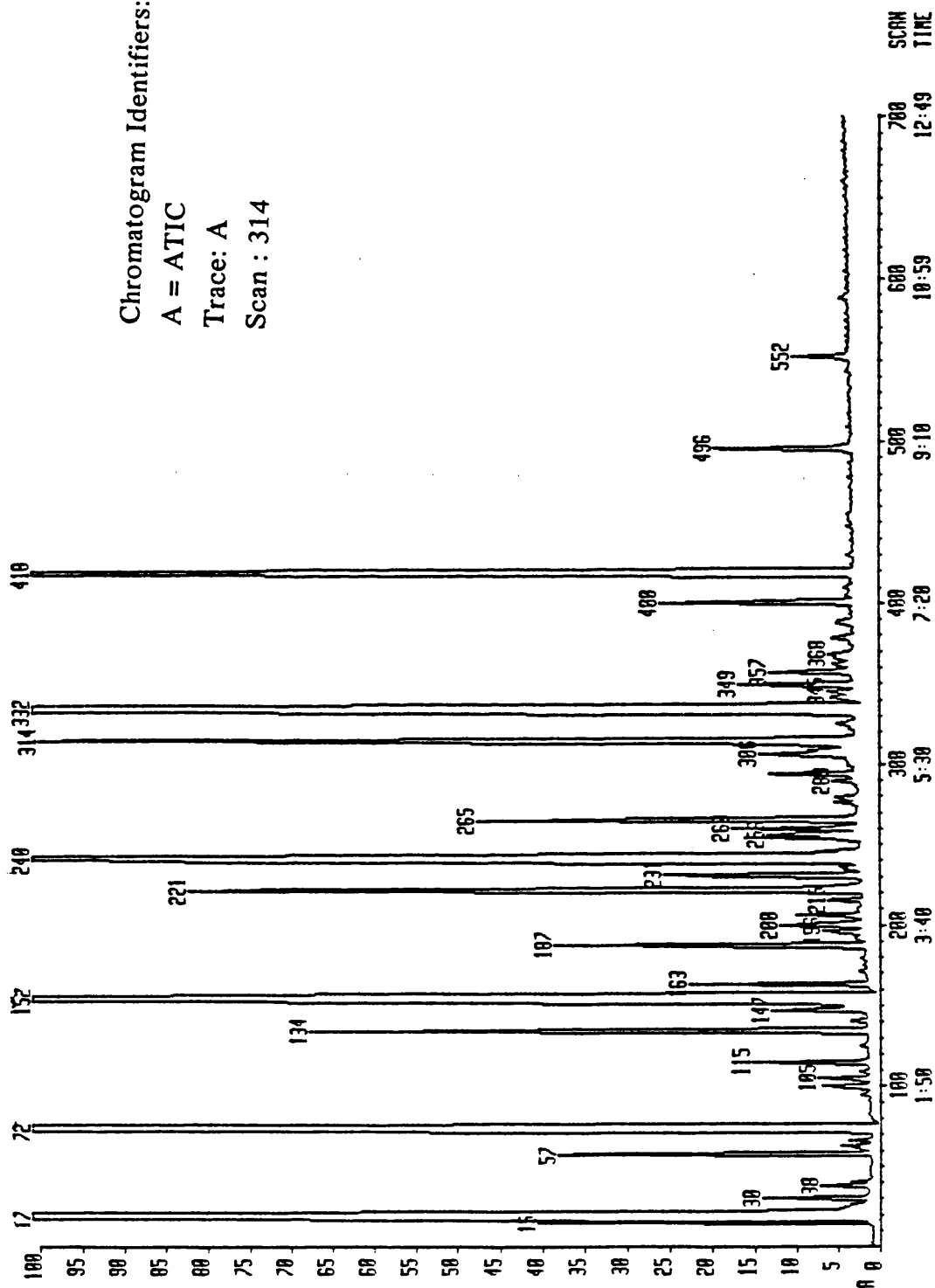


Fig. 7.29. GC trace for the liquid fraction in SATVA separation of products from the degradation of blend 26 (PDMS + 50% coated CaCO_3 with particle size of 1.5μ)

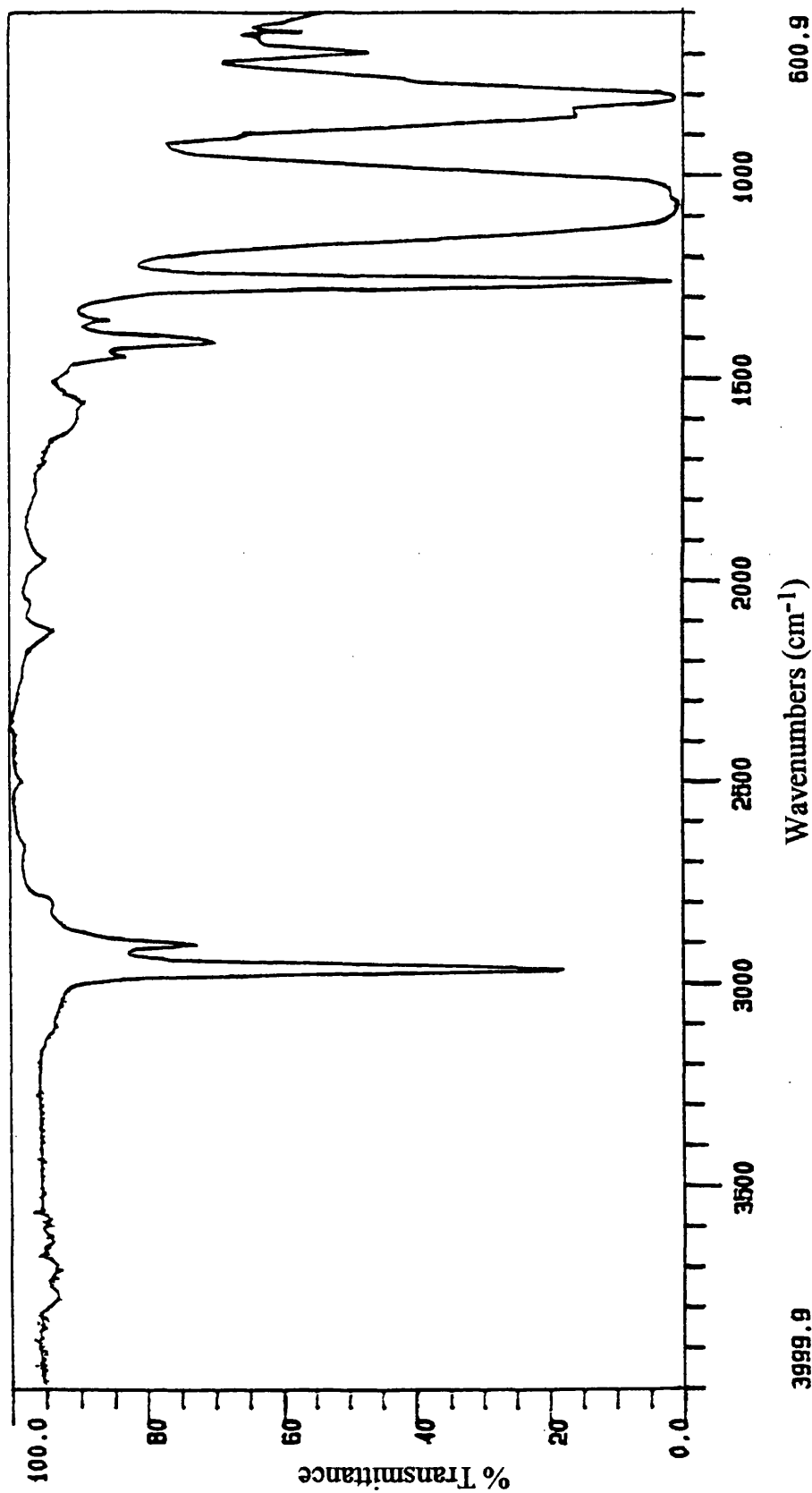


Fig. 7.30. IR spectrum of total products including CRF from the degradation of blend 26 (PDMS + 50% coated CaCO₃ with particle size of 1.5 μ).

3999.9

Wavenumbers (cm⁻¹)

600.9

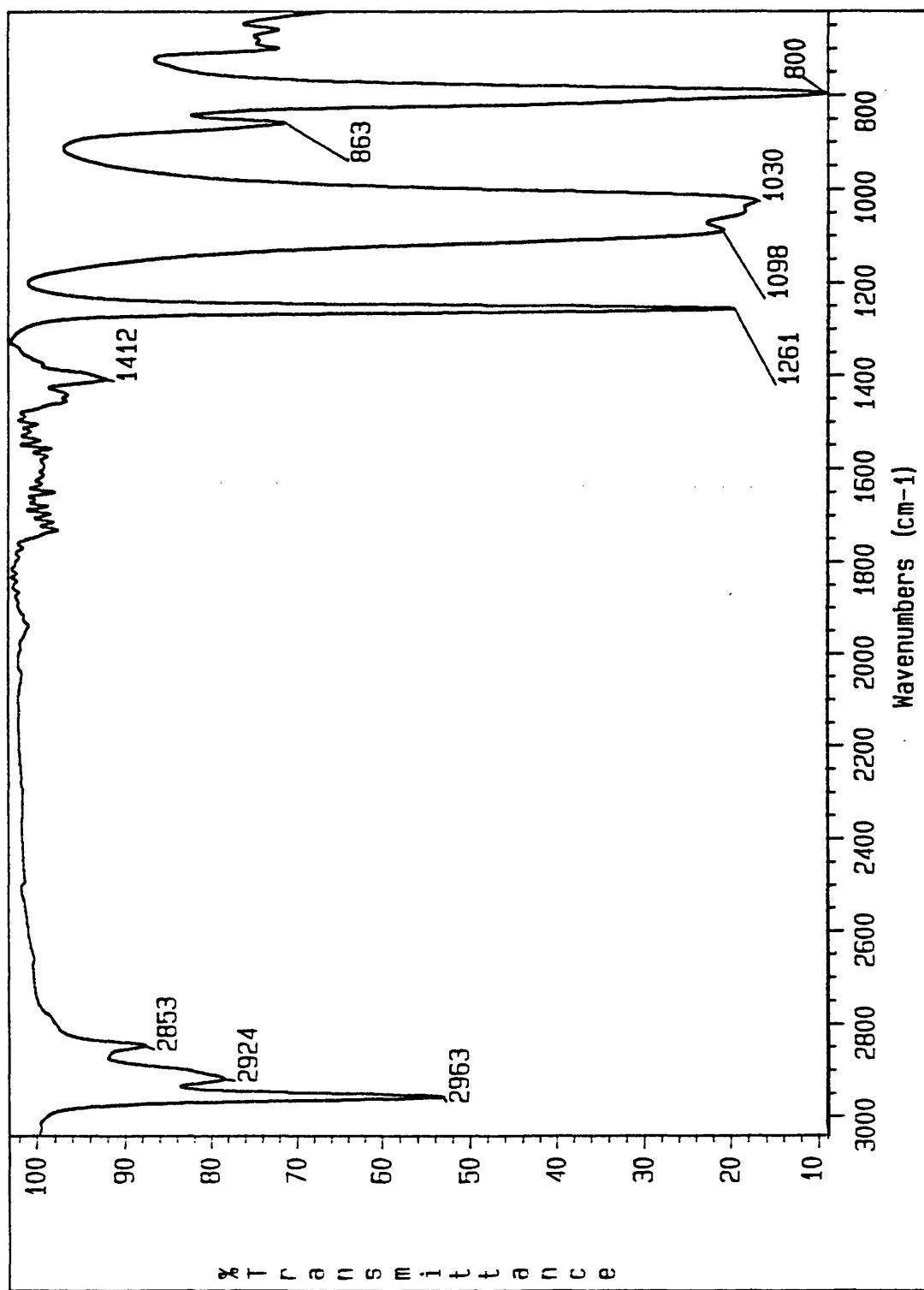


Fig. 7.31. IR spectrum of CRF from the degradation of blend 26 (PDMS + 50% coated CaCO₃ with particle size of 1.5 μ) after heating up to 700°C.

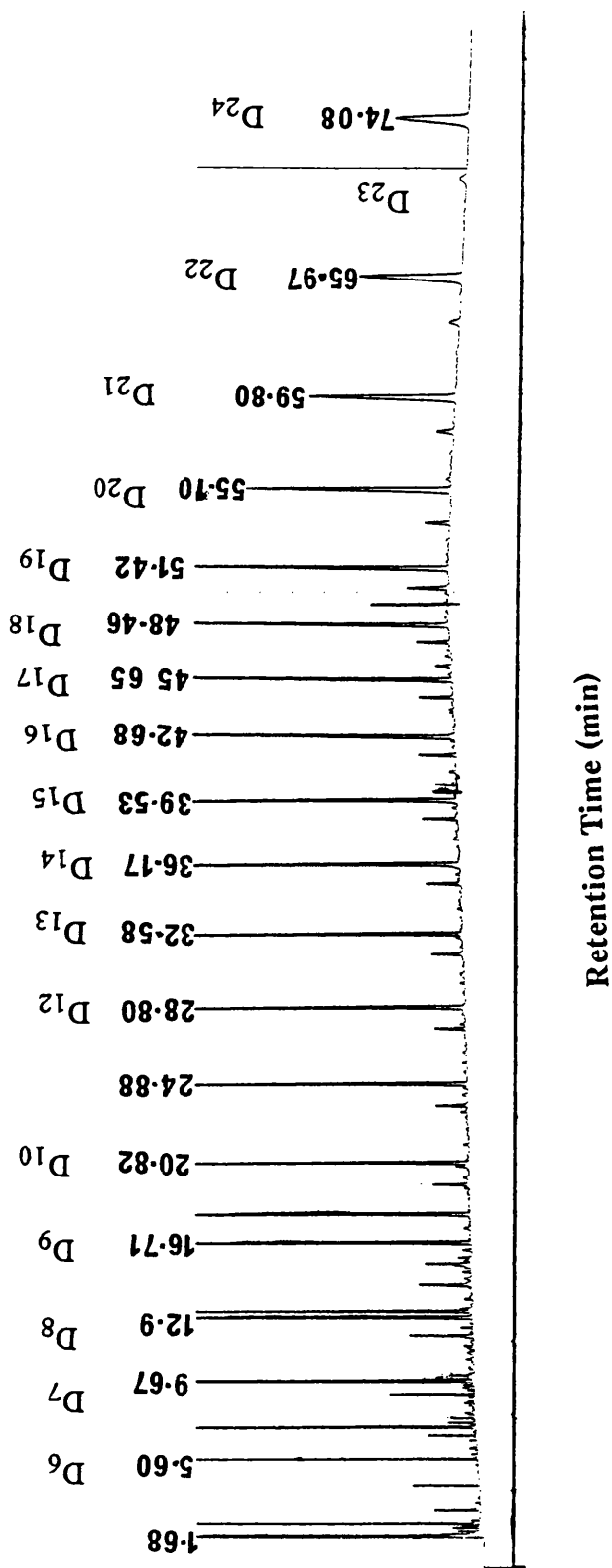


Fig. 7.32. GC trace for the CRF from the degradation of blend 26 (PDMS + 50% coated CaCO₃ with particle size of 1.5 μ).

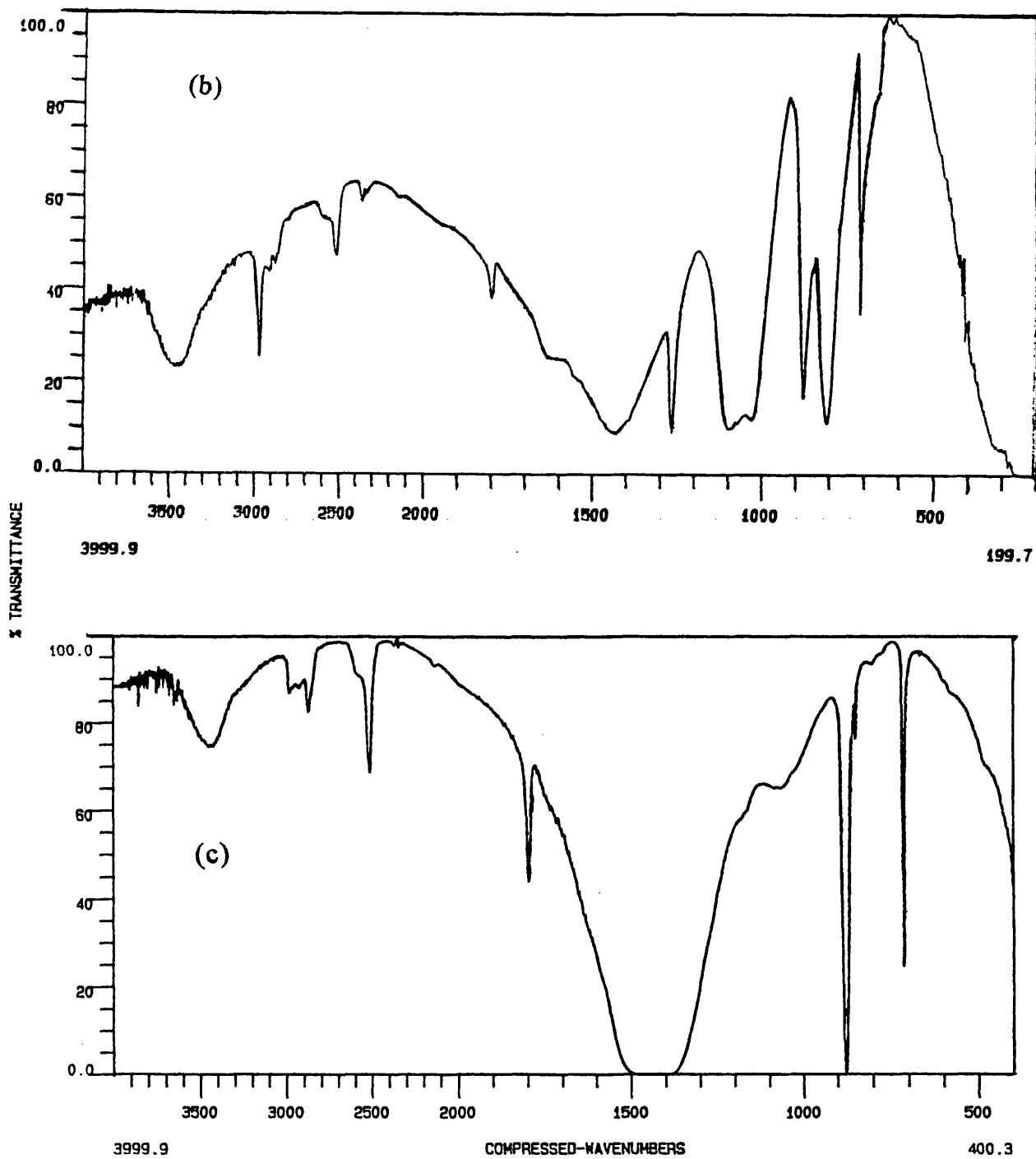


Fig. 7.33. IR spectra of residues from the degradation of blend 26 (PDMS + 50% coated CaCO_3 with particle size of 1.5μ) after heating up to (b) 600°C and (c) 700°C .

Degradation of Extract from Blend 26 after Degrading it up to 480°C

The TVA trace of the extract from the residue of the blend 26 looked quite similar to the TVA curve of the blend itself except it did not show evolution of methane. The extract also started to volatilise at the volatilisation temperature of the blend, 388°C but the rate was very slow and the main volatilisation of the degradation products started at about 427°C. A rubbery and mostly insoluble residue (58.2%) was left after heating the extract up to 480°C. The SATVA trace did not show evidence for any gaseous products. This shows that the extract was either already crosslinked or there was a radical source introduced which later resulted in crosslinking hence made the residue insoluble.

ELECTRON MICROSCOPY

The residues from blend 26 after heating to 480°C and 650°C, respectively, were examined by scanning electron microscopy (SEM) while sliced thin sections after 480°C were also examined by transmission electron microscopy (TEM).

The scanning electron micrograph of the residue at 480°C was fairly similar to that obtained from the undegraded blend. It was a closed cell rubbery material, the walls of which were studded with what appear to have been bubbles, or were punctured by holes apparently formed by breaking of such bubbles. It was difficult to see filler in the thick walled rubbery material. The scanning electron micrograph of the residue (Fig. 7.34) at 650°C showed the presence of the polymer mainly on the area of the filler particles which were rough. Continuous membrane or interconnected webbing seen at 480°C was no longer seen around the larger filler particles but only in the case of extremely small particles. This indicates that the highly crosslinked polymer after degradation remains on the surface of the filler and possibly makes it stable to decomposition at its normal temperature.

Transmission electron micrographs (Fig. 7.35) of the residue showed clearly the web like structure in which filler particles were held firmly from the point of their rough areas. There seemed to be small holes in the continuous web-like structure possibly made by the escaping volatile products. This indicates that the filler interacts with the polymer and results in the formation of a rubbery texture. It is also clear that the surface of the filler plays an important role in the formation of such interactions.

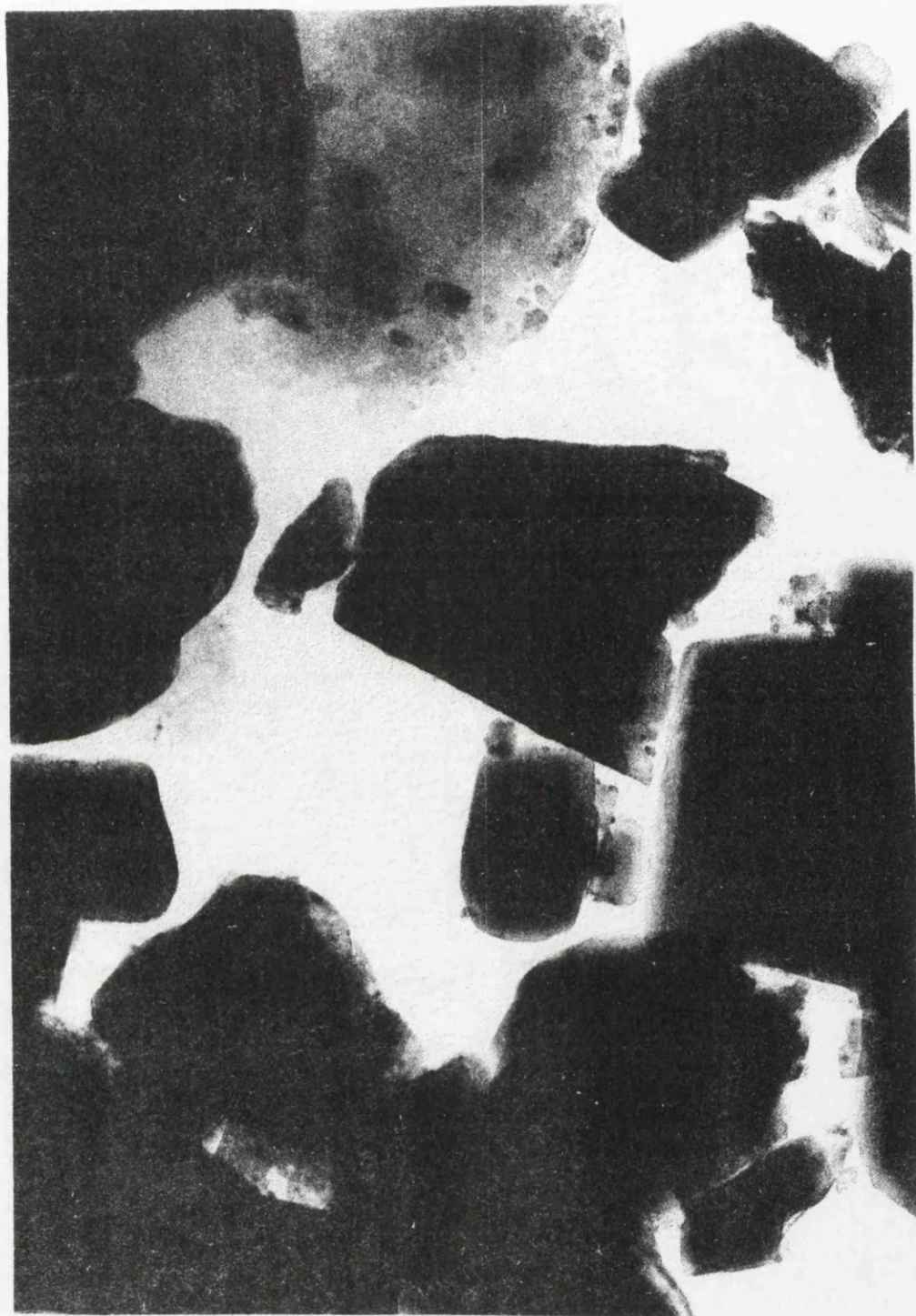


Fig. 7.34. Scanning electron micrographs for residue from blend 26 (PDMS and coated CaCO_3 with particle size of 1.5μ) after heating up to 650°C .



Fig. 7.35. Transmission electron micrograph of sliced thin sections of residue from blend 26 (PDMS and coated CaCO_3 with particle size of 1.5μ) after heating up to 480°C .

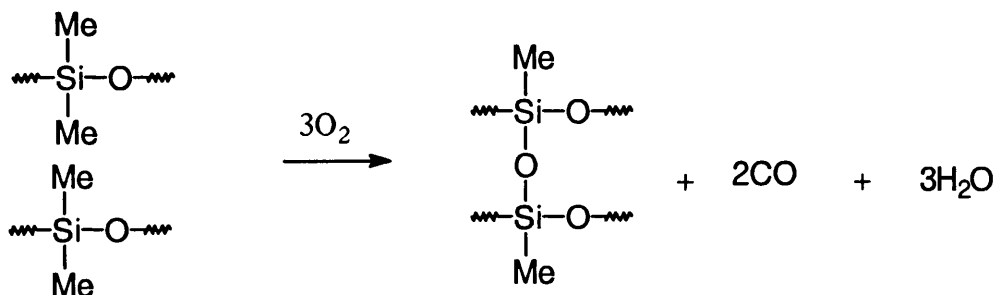
Degradation of Other Blends with Different Filler Content

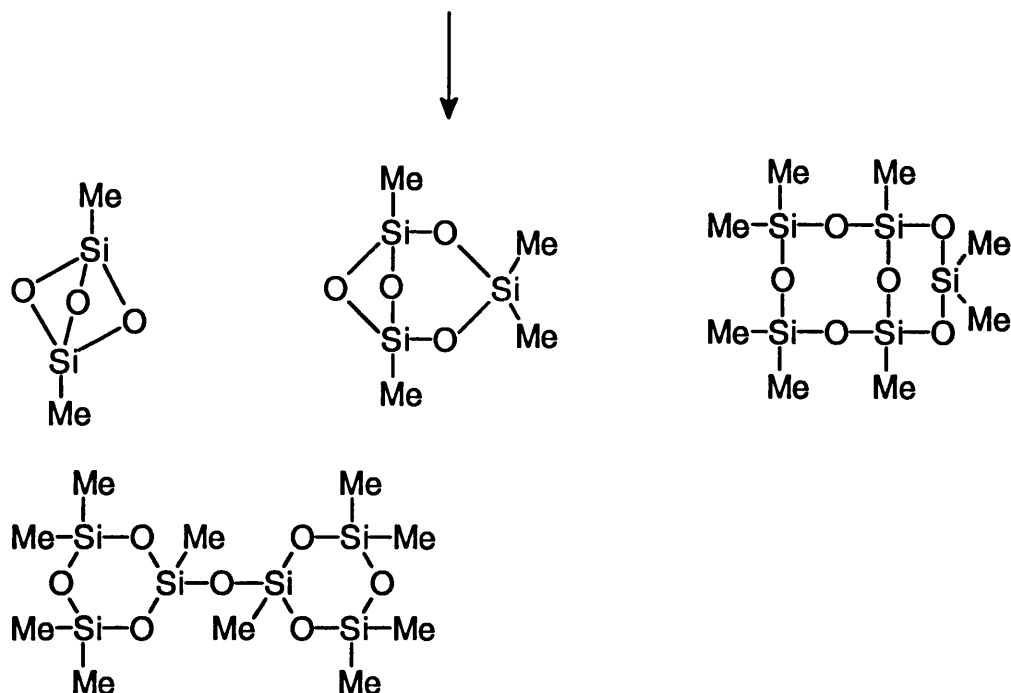
Other blends with different filler content were also degraded from room temperature to 480°C and the degradation products were found to be identical to those from blend 26. However, the quantity of the minor degradation products which were the result of radical reactions, differed from one blend to the other. These minor compounds were almost negligible in the case of blend 21 while they started increasing in quantity as the filler content was increased but around 50% filler content the quantity seemed to become steady.

Degradation up to 600°C in a Limited Amount of Oxygen

Blends 25-28 were also degraded from room temperature to 600°C in silica tubes sealed under vacuum. The IR spectrum of the total condensable degradation products (under 1.0×10^{-4} mbar of pressure) showed a strong absorption at 2853 cm^{-1} arising from the C-H stretching frequencies of methylene groups bound directly to the siloxane units. This could only be possible by reduction of the number of methyl groups, absorbing at 2959 cm^{-1} , and if there was crosslinking. The intensity of the absorption due to the methyl groups was reduced and production of methane could only be explained from the crosslinking reaction. Absorption at 2920 cm^{-1} was also more intense than the absorption at 2959 cm^{-1} . There was also a small but sharp absorption at 1709 cm^{-1} which could be due to carbonyl stretching but there is no satisfactory explanation for the formation of the carbonyl groups unless they are formed from the carbonate ions when the filler interacts with the silicone polymer.

Gaseous products collected under 1.9×10^{-2} mbar of pressure were identified by IR spectroscopy (Fig. 7.36) and MS as cyclic trimer (D_3), a trace amount of cyclic tetramer (D_4), methane and a trace amount of carbon monoxide. Production of CO shows that oxidation of methyl groups has occurred. Oxidative degradation reactions probably take place initially in the organic part of the chain. Cleavage of the organic groups occurs with crosslinking of the chains through siloxane bonds as shown and the net result of these structural changes is to retard further oxidation if the oxygen supply is not limited.





These degradation products were also formed in trace amounts under normal TVA conditions possibly due to small amounts of trapped air in the blends.

Degradation products of these blends were mainly similar to the degradation products from degradation carried out under normal TVA conditions to 600°C and 650°C in the silica TVA tube. The differences are shown in the GC-MS results (Table 7.7). The residues in this case were not rubbery at 600°C. Degradation in the sealed tube, however, was not programmed at 10°C/min, instead, the temperature was raised from room temperature to 600°C in an hour. The IR spectra, however, still gave absorptions similar to those of siloxane groups instead of just CaCO₃ but the intensity of the absorptions due to siloxane groups was reduced.

Degradation at Different Temperatures

The principal degradation products were a mixture of cyclic oligomers when blend 26 was degraded from room temperature to 400°C. However, the GC-MS results showed that the large oligomer, (O-SiMe₂)₇ (D₇) was the dominant product. The amounts of degradation products were in the order D₇ > D₆ > D₃ > D₅ > D₄, with D₇ about 41% and D₆ about 33%, (where D₃ refers to cyclic hexamethyltrisiloxane, D₄ to cyclic octamethyltetrasiloxane etc.). When the same sample was further heated from room temperature to 480°C, the degradation products were in the order D₃ > D₄ > D₆ > D₅ > D₇, with D₃ now about 50-60% and D₄ about 19%.

The IR spectrum of the CRF was similar to that of the total degradation products except that the absorption at 1709 cm^{-1} was stronger, there was an extra weak but sharp band at 1377 cm^{-1} and the absorption at 2959 cm^{-1} due to methyl groups decreased while the absorption due to methylene groups at 2925 cm^{-1} and 2853 cm^{-1} increased in intensity.

The residue after heating up to 400°C was rubbery and the IR spectrum (Fig. 7.37) of the soluble residue showed an increase in the intensity for the absorption of the methylene groups and a decrease in the intensity for the methyl groups. There was also a small absorption for carbonyl groups at around 1740 cm^{-1} , a peak around 1377 cm^{-1} and there seemed development of shoulders on the siloxane peak in the region $1140\text{-}1190\text{ cm}^{-1}$. All these peaks indicate the $\text{Si-CH}_2\text{-Si}$ and $\text{Si-(CH}_2)_2\text{-Si}$ types of linkage. The absorptions in the region $1140\text{-}1190\text{ cm}^{-1}$ would be masked if the content of the Si-O-Si is high.

Blend 26 was also heated from the room temperature to 170°C , 200°C , 300°C , 325°C , 390°C and 460°C to observe the degradation temperature at which blend formed a rubbery texture and became insoluble, and to calculate the percentage weight loss at these temperatures.

It was found that there was 5.87% weight loss, possibly due to unpolymerised oligomers, when blend 26 was heated up to 170°C . There was no CRF or rubbery texture formed but the top layer of the sample was not as sticky as before heating.

The above sample was further heated to 200°C but the additional weight loss was only 0.25%. Again there was no rubbery texture formed although the top layer looked rubbery. It was possible to extract the polymer from the filler but the remaining insoluble filler showed weak absorptions due to siloxane groups.

There was about 1.03% weight loss when the above sample was further heated up to 300°C . There was negligible CRF formed and the top layer of the sample became slightly rubbery / hard and shiny but there was no formation of a bubble. It was possible to break the top layer with a spatula but complete extraction of the polymer from the filler was not possible as the most of the top layer swells in the solvent or forms a cloudy suspension (only a small amount of the sample was taken). The IR spectrum of the swollen material showed strong absorptions due to siloxane groups and slightly weaker absorptions at 1420 cm^{-1} due to the carbonate ions.

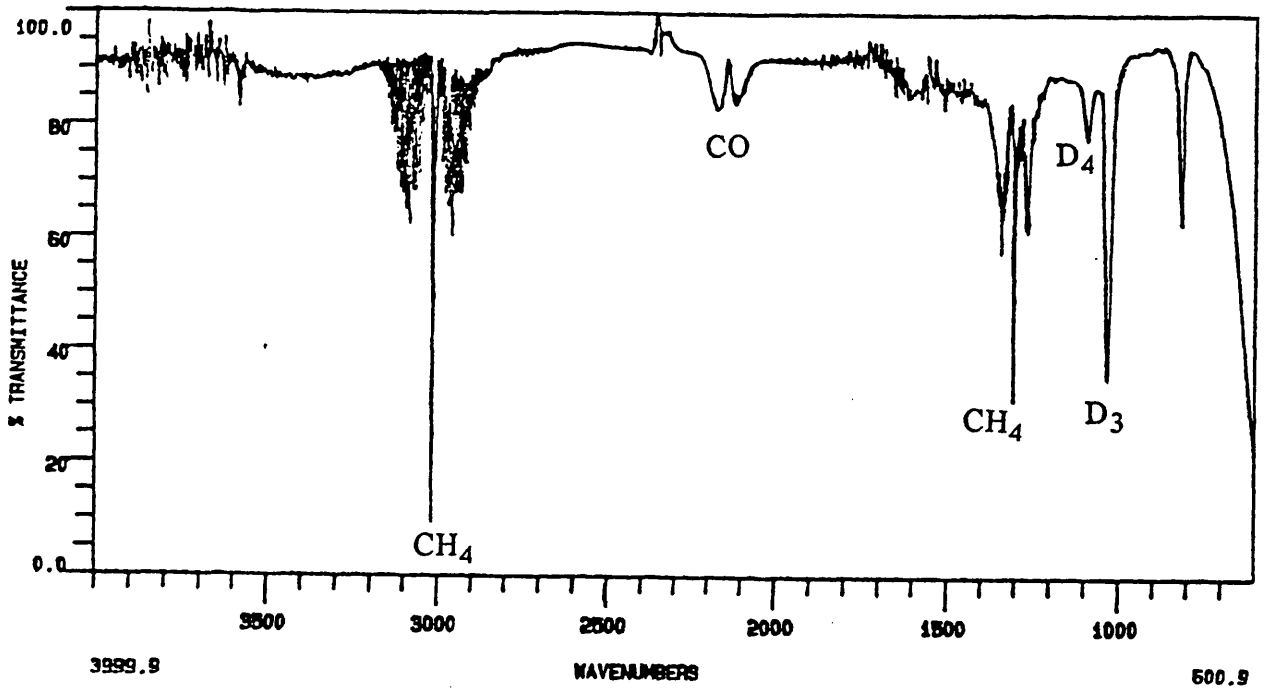


Fig. 7.36. IR spectrum of gaseous products from the degradation of blend 26 (PDMS + 50% coated CaCO_3 with particle size of 1.5μ) in a silica tube sealed under vacuum.

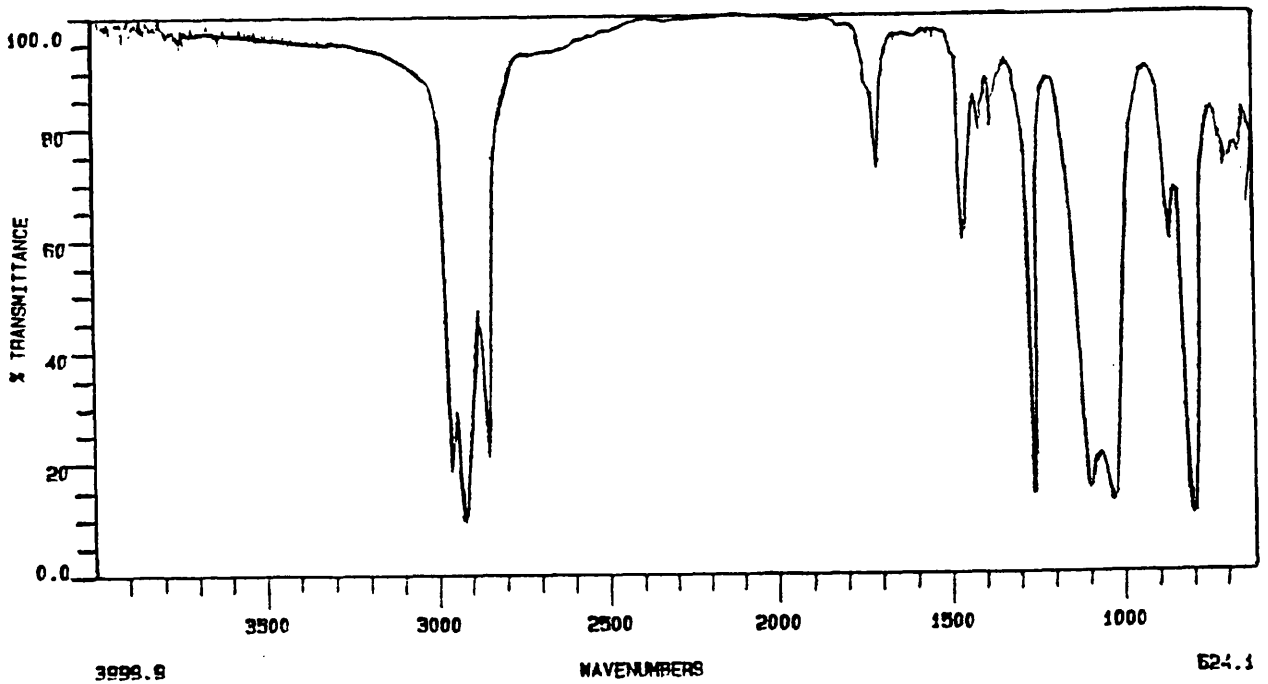


Fig. 7.37. IR spectrum of the soluble residue from the degradation of blend 26 (PDMS + 50% coated CaCO_3 with particle size of 1.5μ) after heating up to 400°C .

The sample became rubbery and a thick walled bubble was formed when it was further heated up to 325°C but the weight loss due to degradation was only 0.66%. The whole residue was then immersed in the solvent to extract the polymer from the top layer. It was possible to extract 0.43% of the polymer from the total sample degraded at 325°C. However, it was difficult to tell how much extraction was from the top since the solvent entered inside the bubble and swelled the residue.

The sample was further heated up to 390°C after drying it. The weight loss due to degradation was 0.32% while weight loss due to the extraction of the residue was 0.86%.

The weight loss was 3.68% when the above dried residue was further heated up to 460°C. The residue was further extracted and the weight loss due to the extraction was 0.73%.

Blends of Siloxane Polymer with Different Type and Particle Sized CaCO₃

Blends of siloxane polymer with different type and particle sized CaCO₃ were also degraded from room temperature to 480°C. TVA showed that all blends (29-34) gave mainly cyclic oligomers but their quantities differed. The formation of non-condensable gaseous products was restricted to blends 30, 31, 32 and 33. Small amounts of other degradation products resulting from the radical reactions were restricted to the blends which produced methane and / or had coated filler.

Blend 29 (with 50% coated and particle size of 5.0 μ) had TVA trace similar to that of blend 26 (when degraded up to 480°C) except that volatilisation started 38°C earlier than blend 26, showed negligible rise for non-condensables and reached at its first T_{max} at 437°C while blend 26 did not show any well defined T_{max} below 480°C. The amount of CO₂ (and ketene if present) was also extremely small. Other unidentified siloxane compounds, found in the first fraction of the SATVA trace from the other blends were not present. The residue formed a bubble like the residue of blend 26 but some of its inside parts were sticky i.e. contained undegraded polymer material which dissolved in dichloromethane.

The TVA curve of blend 30 (with 50% of coated CaCO₃ and particle size of 0.9 μ), resembles in most respects the TVA curve of PDMS when degraded alone but

volatilisation starts at a higher temperature and has a rise in the -196°C trace starting at 400°C , indicating the presence of non-condensable gaseous products (Fig. 7.38 (a)). The residue crumbled to powder when disturbed but there was evidence for bubble formation. The IR spectrum of the residue showed extremely weak absorptions for the siloxane groups.

The volatilisation of blend 31 (with 50% of coated, precipitated CaCO_3 and particle size of $0.06\ \mu$) started at 250°C but the degradation process was slow such that the main volatilisation started at 400°C . The shape of the TVA trace (Fig. 7.38 (b)) from the main volatilisation point onwards was like that of blend 26 but there were more gaseous products in the present case while other volatile degradation products were less and consisted mainly of smaller cyclic oligomers. The residue formed a bubble but its texture was different from the residue of blend 26 i.e. some parts of the bubble were thick while others were thin, also residue was more rubbery and sticky.

Blend 32 (with 50% of uncoated CaCO_3 and particle size of $0.7\ \mu$) degraded 50°C earlier than expected and showed two stage degradation (Fig. 7.39 (a)). However, stabilisation developed gradually and there is evidence for the formation of non-condensable gaseous products after 400°C . The degradation products were mainly larger oligomers and the condensable gaseous products such as CO_2 and ketene were evolved in greater amounts than in the other cases with complete degradation, e.g. in the case of blend 30.

The TVA trace of blend 33 (with 50% of uncoated CaCO_3 and particle size of $1.5\ \mu$) shows two well separated degradation stages (Fig. 7.39 (b)). The first degradation started 50°C earlier than in the case of pure polymer but stabilisation developed after the first degradation, of up to $50\text{-}60^{\circ}\text{C}$. There is almost negligible rise for the non-condensable trace and the SATVA trace showed that the condensable gaseous products were less than in the case of blend 30.

The residues from blends 32 and 33 crumbled to powder but there was evidence for the formation of a sponge like-texture. The IR spectra of the residues showed weak absorptions due to siloxane groups.

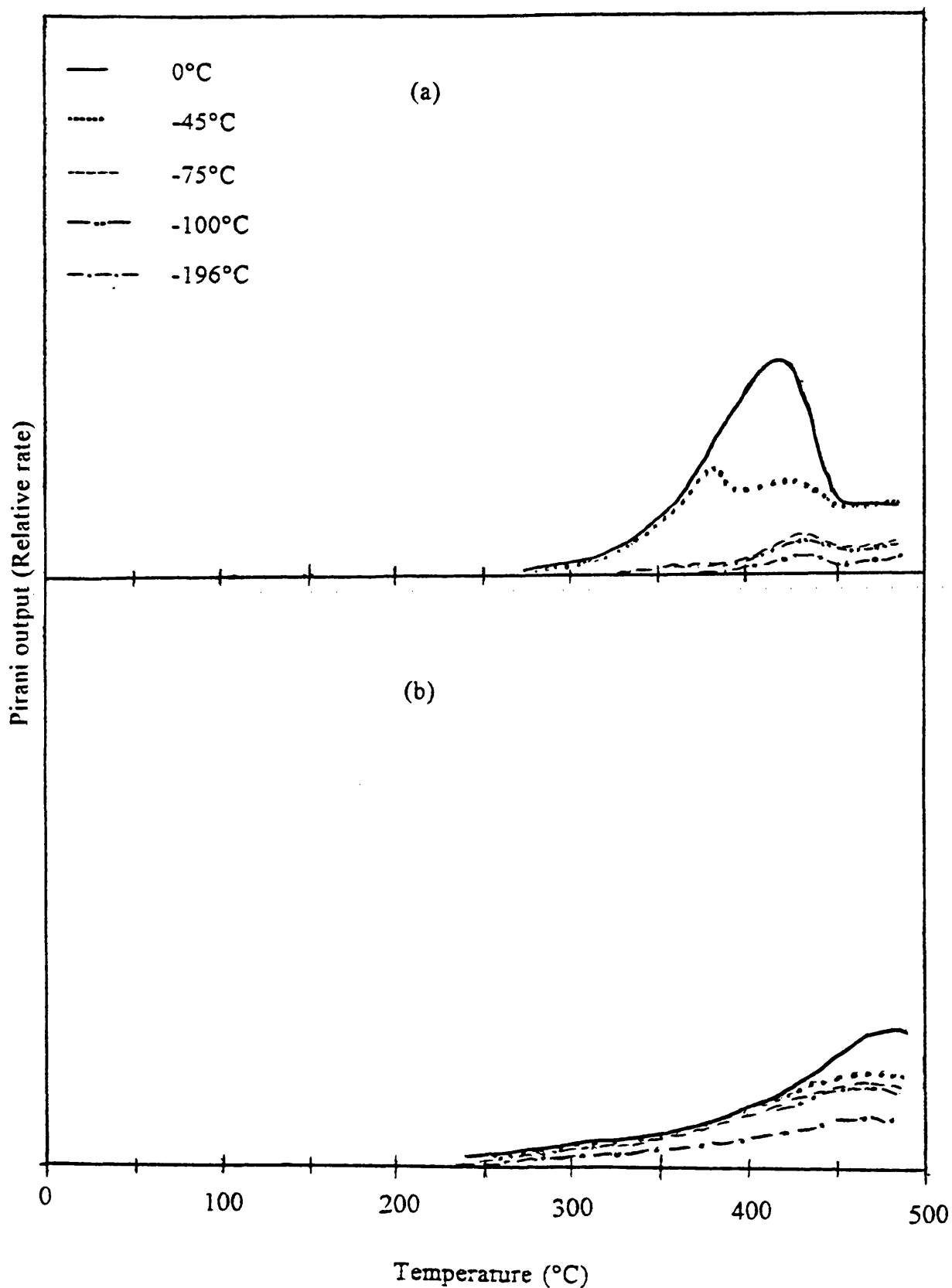


Fig. 7.38. TVA traces for blends of PDMS and 50% coated CaCO_3 : (a) blend 30 (with particle size of 0.9μ) and (b) blend 31 (with precipitated and particle size of 0.06μ).

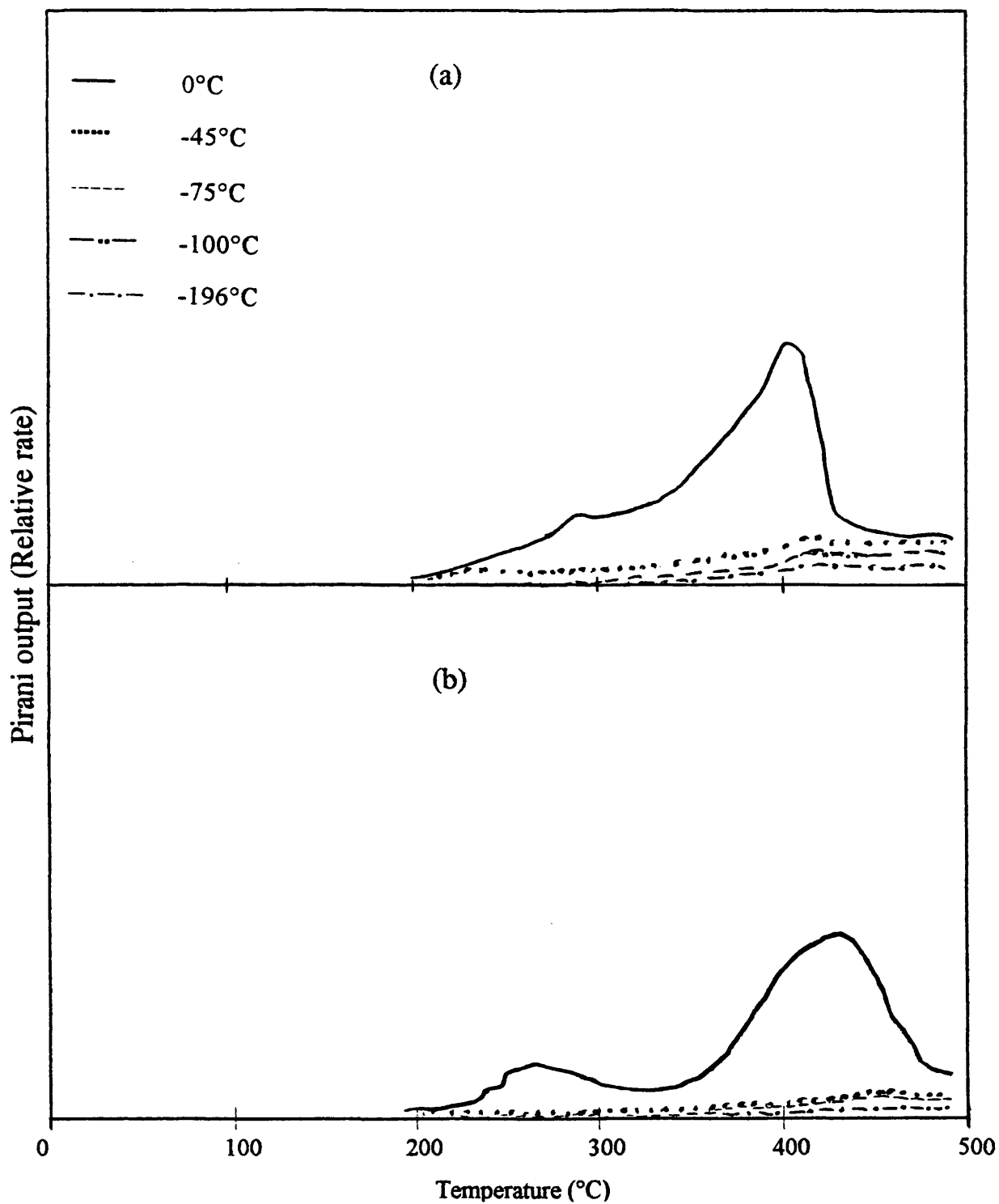


Fig. 7.39. TVA traces for blends of PDMS and 50% uncoated CaCO_3 :
(a) blend 32 (with particle size of 0.7μ) and (b) blend 33 (with particle size of 1.5μ).

The TVA trace of blend 34 (with 50% of uncoated CaCO_3 and particle size of 5.0μ) was similar to the trace of PDMS when degraded alone except it showed stabilisation of 50°C throughout the degradation. There was no formation of gaseous products and the unidentified product(s) with Si-O-Si group formed in most other blends were missing. The IR spectrum of the CRF was similar to that of the original polymer except it gave an extra absorption in the siloxane region, $1020\text{-}1100 \text{ cm}^{-1}$. The residue, which crumbled to powder when disturbed, formed thin walled bubbles which probably burst when gaseous products trapped inside escaped. The IR spectrum of the residue showed weak absorptions due to siloxane groups.

These results show that blends with coated and smaller particle sized filler form more methane than the blends with uncoated and/or larger particle sized filler. These are also the blends which show more stabilisation. The hypothesis that fillers interact with the polymer and cause the production of methane near the sites of interaction and that fillers with highly coated surface and with smaller particle size form more interactions, fits well with the observation made about the quantity of methane evolution. This also indicates that the minor degradation products would depend on the type and grade of the filler.

Coating seems to have effect on the texture of the final residue since blends with coated filler form a single bubble, the expansion and thickness of which depends on the particle size of the filler. Smaller particle sized filler forms a more expanded and thin-walled bubble, with tiny holes invisible with naked eye, while as the particle size of the filler is increased the thickness of the bubble increases and the size of the holes, possibly made by escaping degradation products, increases.

Blend of PDMS with Trimethyl End Groups and CaCO_3

Blend 35 (50% CaCO_3 and PDMS with saturated end groups) showed volatilisation at about 400°C and the TVA trace (Fig. 7.40 (a)) was identical in appearance to that of blend 26 (50% CaCO_3 and PDMS with vinyl end groups). The evolution of volatile gaseous products was extremely small while other products were also in small amount when degradation was carried out up to 480°C . Formation of carbon dioxide was about twelve times more than in the case of blend 26 when degradation was carried out up to 700°C , while other degradation products such as cyclic siloxane oligomers were almost the same in quantity. There was also the formation of a trace amount of ketene at 700°C , but its formation is difficult to explain.

The residue (93.74%) at 480°C formed a bubble, was rubbery and virtually insoluble (1.46% residue was soluble). The IR spectrum of the CRF and soluble residue were similar to those of the original polymer (discussed in Chapter 4). Other degradation products were similar to those from blend 26 with very small differences in the quantity of the degradation products other than normal cyclic siloxane oligomers.

Blend 35 was also heated from room temperature to 170°C, 200°C, 300°C, 325°C, 390°C and 460°C to determine the degradation temperature at which the blend produced a rubbery texture and became insoluble, and to estimate the percentage weight loss at these temperatures. The procedure carried out was as described for blend 26. The results for the weight loss at different temperatures are given in Table 7.4.

Table 7.4: Percentage weight loss of blend 35 at different temperatures

| Temperature (°C) | Weight loss (%) | Soluble residue (%) | CRF | Rubbery texture formation |
|------------------|-----------------|---------------------|-------------|-----------------------------|
| 170 | 1.23 | ~100 | | |
| 200 | 0.725 | | | only looks rubbery |
| 300 | 1.01 | | | rubbery, with small bubbles |
| 325 | 1.03 | 0.12 | | Unbreakable bubble formed |
| 390 | 1.28 | 0.24 | | |
| 460 | 3.42 | 0.18 | gummy solid | |

Note: Soluble residue is the % extractable from the sample remaining at the particular temperature after degradation

The difference between the two blends was that the residue after 200°C, when dissolved in solvent and left for some time to see if extraction of the polymer from the filler was possible, did not settle down; instead it stayed suspended in the solvent and made it cloudy, indicating insolubility. This could only be possible if there was some interaction between the polymer and the filler. The IR spectrum of the swollen residue showed siloxane peaks and absorptions due to carbonate ions in the region 1458-1420 cm^{-1} .

Blend of PDMS and MgCO₃

The main decomposition of MgCO₃ started at about 400°C and degradation was complete well before 600°C when heated alone. There was also a very small volatilisation in the region 150-230°C possibly due to the dehydration of the impurity, Mg(OH)₂, as seen from the IR spectrum of the second fraction of the SATVA trace, identified as water, while the first fraction was identified as CO₂. The IR spectrum of the filler (Fig. 7.41) also showed extremely weak bands at 3620 cm⁻¹, 3522 cm⁻¹ and 3460 cm⁻¹, confirming the trace amount of impurity while filler heated up to 480°C did not show these bands.

Blends 36 (with 50% MgCO₃) started to volatilise at 210°C, possibly due to dehydration of the impurity, Mg(OH)₂, but volatilisation was very slow up to 420°C. The degradation process was multi-stepped and complex (Fig. 7.40 (b)) but with one distinguishable T_{max} at 617°C. The non-condensable gaseous products started to evolve at about 280°C but their production was considerable in the region 560-700°C, which is after the decomposition of the filler to CO₂ and MgO. This clearly shows that MgO has a greater affect on Si-C bond scission than MgCO₃ or CaCO₃. Some of the methane formation before the decomposition of the filler, therefore, is due to MgO which results from the dehydration of the impurity, Mg(OH)₂ interacting with the polymer, instead of just due to interaction between the major filler and the polymer. The mechanism of interaction of the components is given later in section 7.5.

The SATVA trace (Fig. 7.42) showed two main fractions, the first one identified by IR spectroscopy (Fig. 7.43) and MS mainly as CO₂ with a small amount of ketene. The IR spectrum also showed very weak bands at, 1265 cm⁻¹, 1096 cm⁻¹, 1035 cm⁻¹, 868 cm⁻¹, 818 cm⁻¹ all due to siloxane groups and at 909 cm⁻¹ due to C=C bond. There was also some indication of a trace of ethylene while formation of ethylene was not shown by any of the other blends. The bands at 868 cm⁻¹ and 909 cm⁻¹ could be due to the Si-H group assuming that Si-H stretching band was hidden under the ketene bands, while other remaining were due to siloxane groups. The results of GC-MS of the second fraction showed that the degradation products were mainly similar to those from blend 26. The IR spectrum of the CRF after heating up to 700°C (Fig. 7.44 (a)) was also similar to that from blend 26 except it did not show an extra absorption in the region 1096 cm⁻¹ - 1035 cm⁻¹.

The residue was rubbery at 480°C and formed a bubble like the residue from blend 26, but when the blend was heated up to 700°C, the bubble formed crumbled to grey

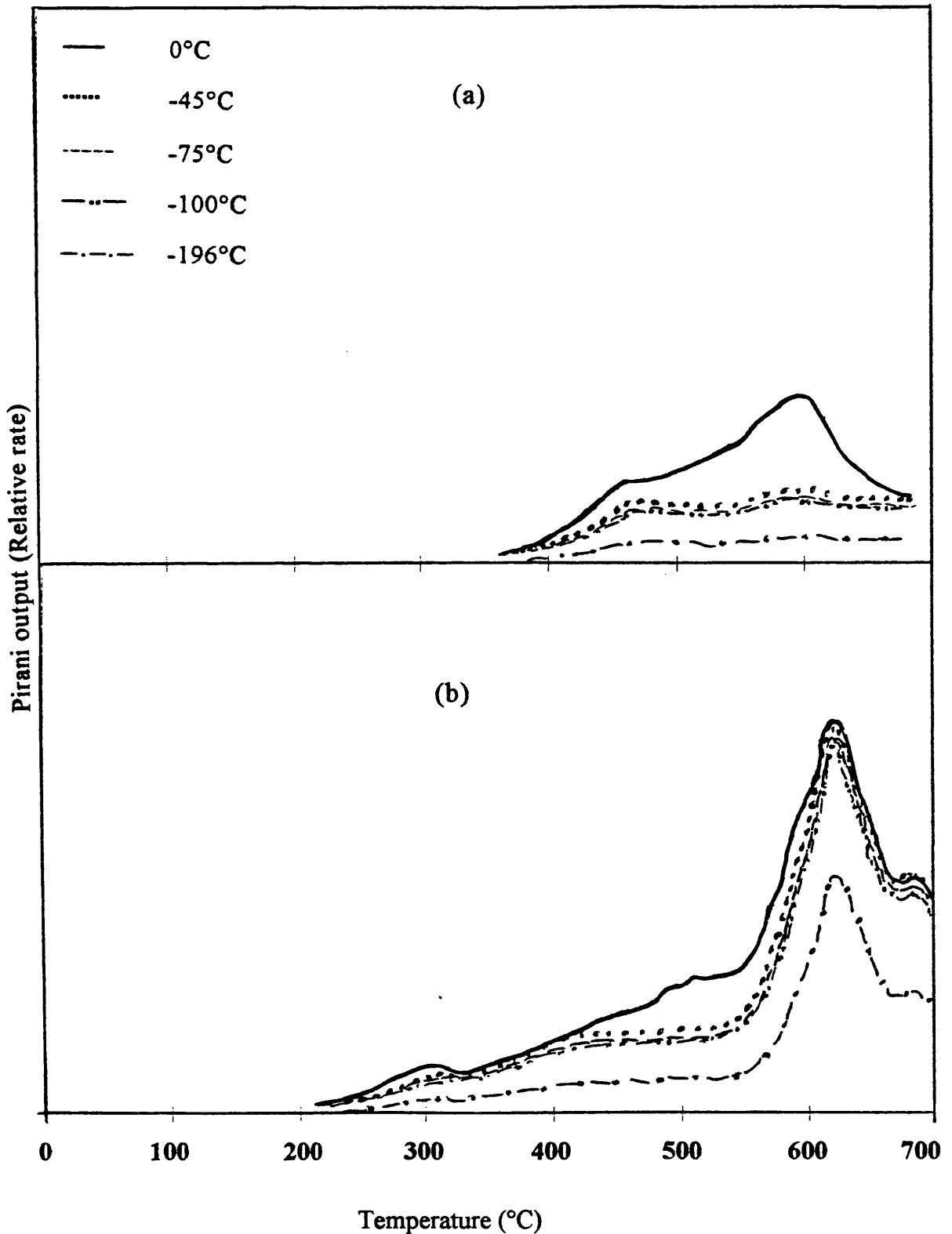


Fig. 7.40 TVA traces for blends: (a) blend 35 (PDMS with trimethyl end groups and 50% coated CaCO_3 with particle size of 1.5μ) and (b) blend 36 (PDMS + 50% MgCO_3).

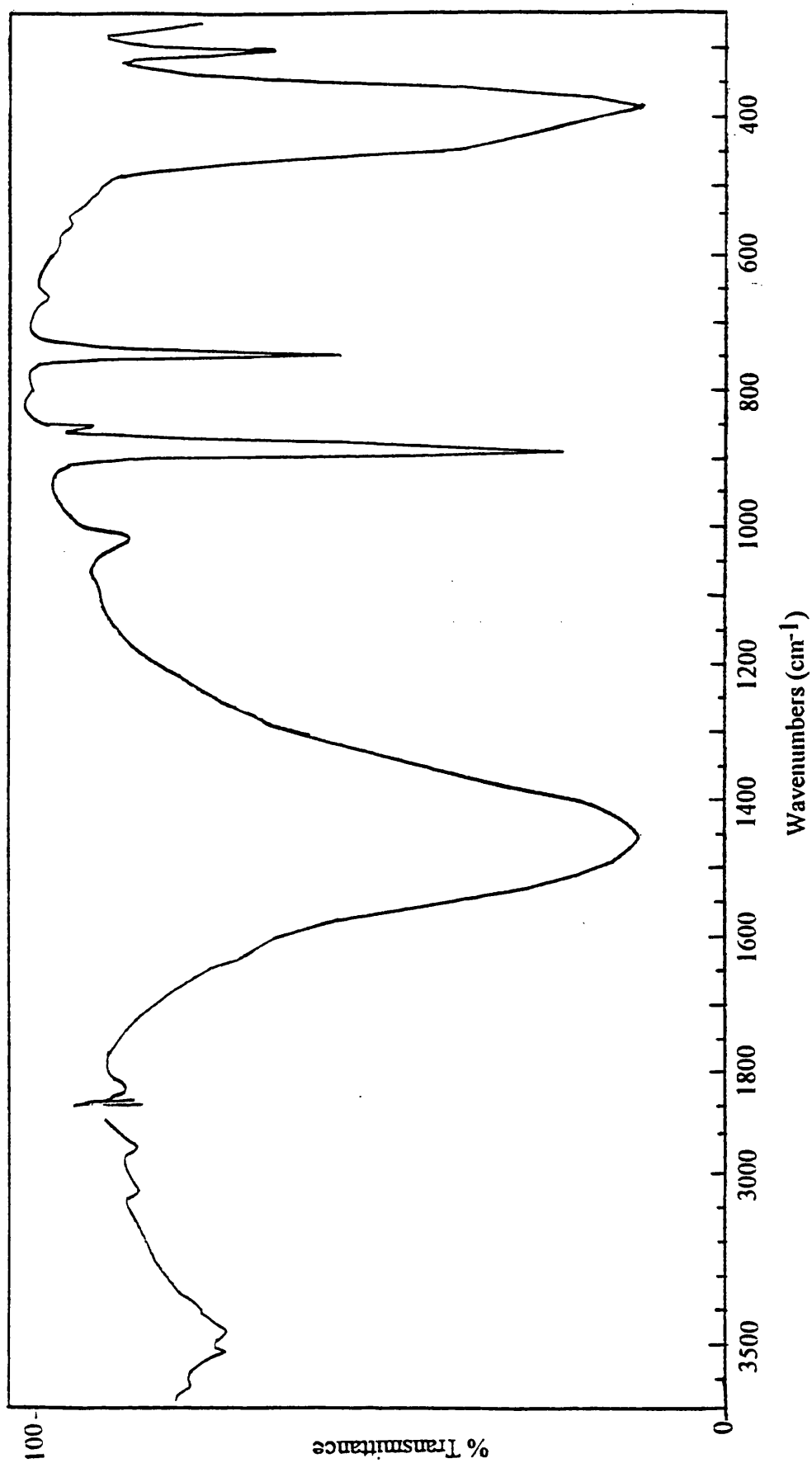


Fig. 7.41 IR spectrum of MgCO₃.

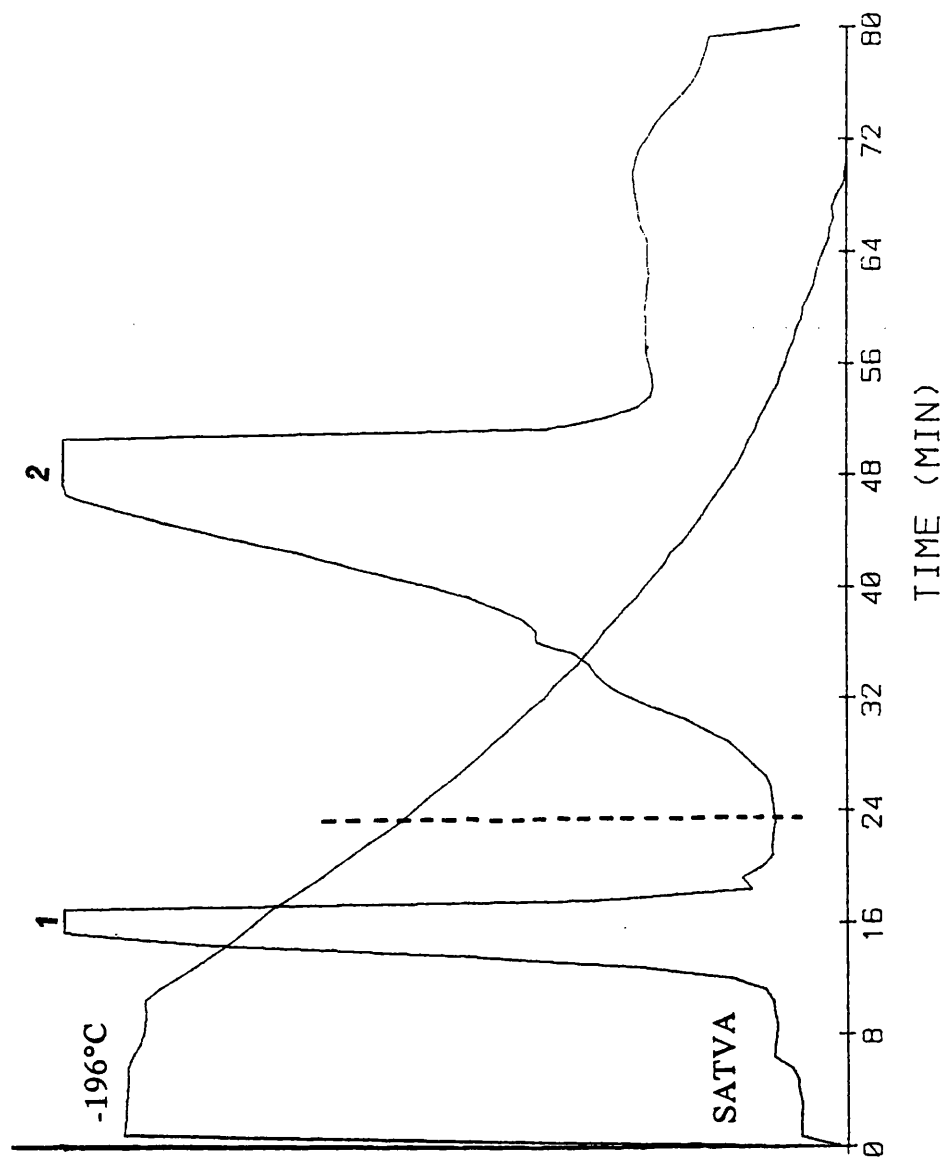


Fig. 7.42. SATVA trace for warm up from -196°C to ambient temperature of condensable volatile products from degradation of blend 36 (PDMS + 50% MgCO_3) after heating up to 700°C .

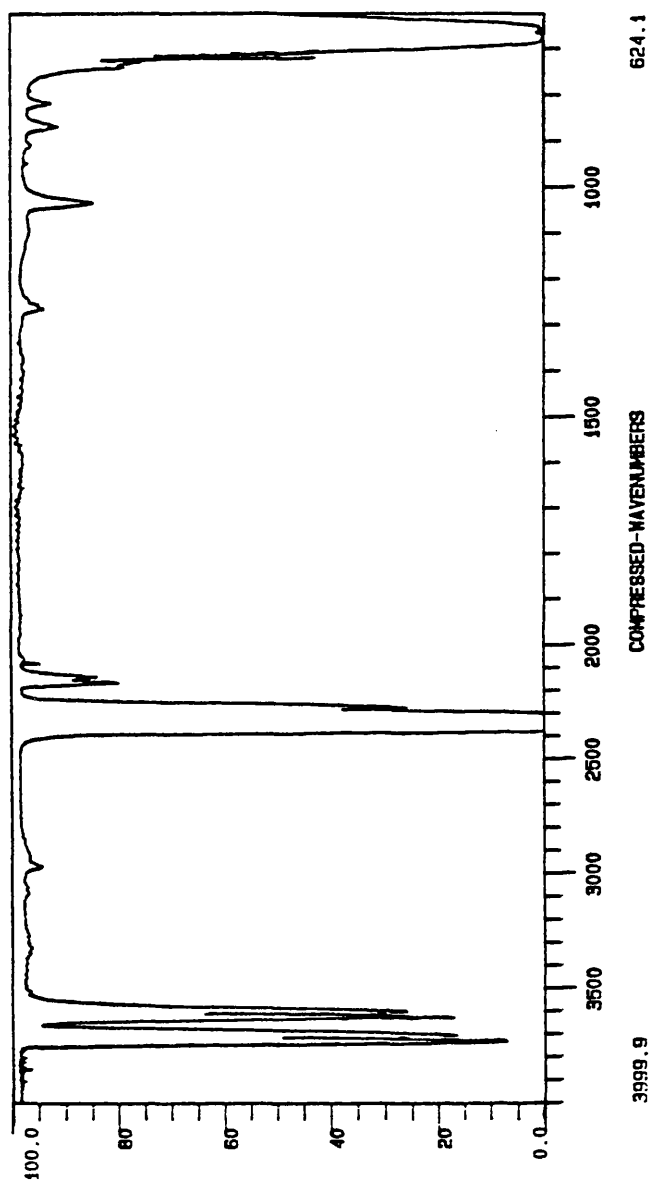


Fig. 7 43. IR spectrum of the volatile products from the first fraction of SATVA from the degradation of blend 36 (PDMS + 50% MgCO₃) after heating up to 700°C.

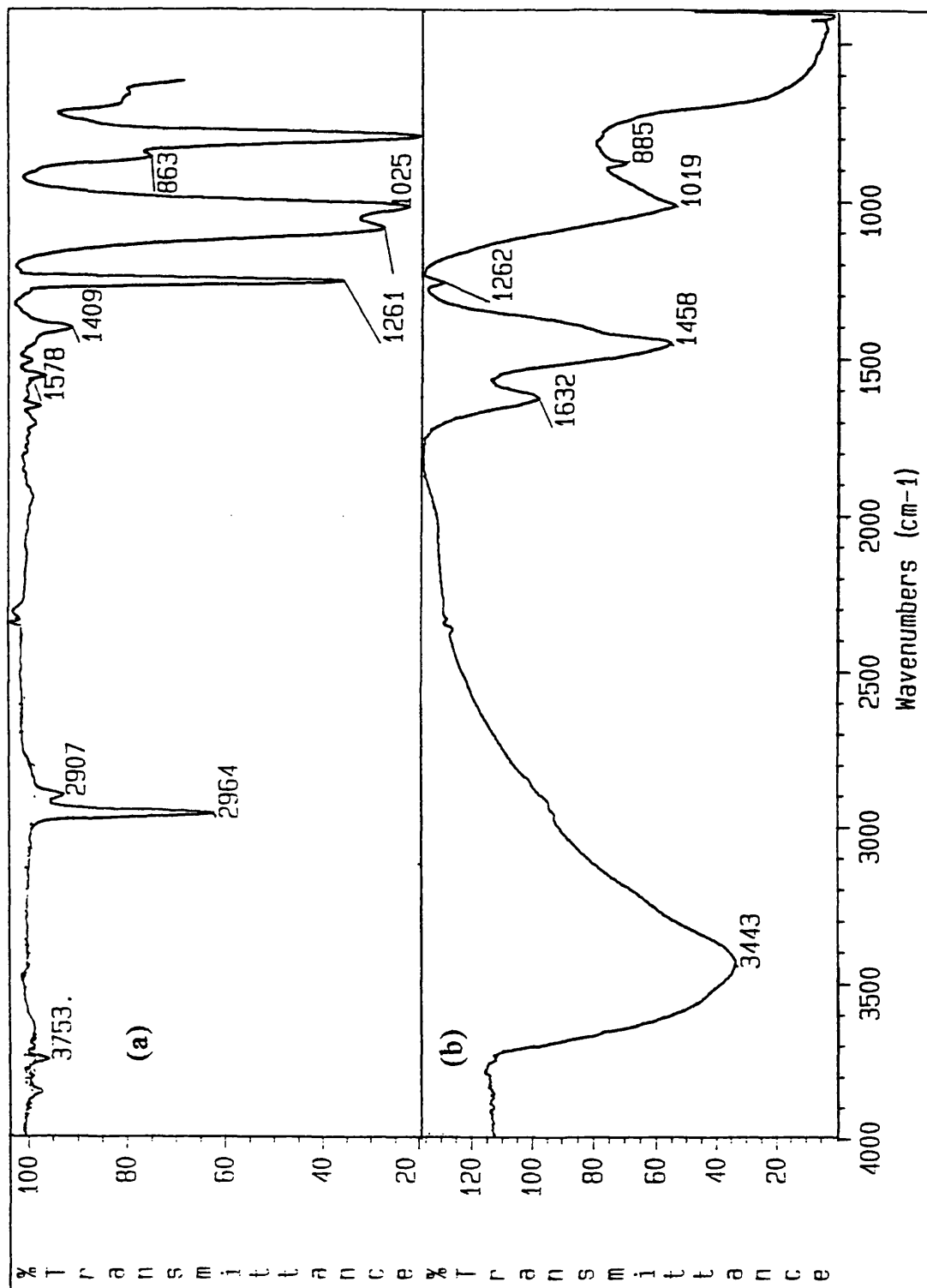


Fig. 7 44 IR spectra from the degradation of blend 36 (PDMS + 50% MgCO₃) after heating up to 700°C: (a) CRF and (b) residue.

powder when disturbed. The IR spectrum (Fig. 7.44 (b)) showed absorptions mainly due to MgO but there were still absorptions at 1458 cm^{-1} and 885 cm^{-1} due to undecomposed filler. There was also a strong band at 1019 cm^{-1} as intense as the band at 1458 cm^{-1} and a weak band at 1262 cm^{-1} . These last bands are attributed to the siloxane group, but usually both these bands are nearly of similar intensity in the siloxane compounds and PDMS. As for other blends showing a lot of methane production, this indicates a high degree of crosslinking of the polymer during degradation. The equal intensity of the carbonate ions and Si-O-Si is an indication of the interaction of the components and results in stabilisation of both components but also indicates almost complete scission of the methyl groups. The residue at 700°C was 30.88% which was 7.52% more than expected for no interaction.

Blends of PDMS and Metal Hydroxides

TVA trace of blend 37 (with 50% $\text{Mg}(\text{OH})_2$) starts at the dehydration temperature of the filler, 266°C , and shows a main T_{max} at 413°C with a shoulder with T_{max} at 356°C . It is clear from the TVA trace (Fig. 7.45 (a)) that there was evolution of highly volatile degradation products and a lot of methane was produced, starting at 300°C but with the main evolution at 375°C when the filler would be expected to dehydrate completely. Other gaseous products from the first and second fractions of the SATVA separation (Fig. 7.46 (a)) were similar to those from blend 26.

The residue left from blend 37 was slightly less rubbery, thus it was possible to grind it into fairly small fragments. IR spectrum after removing soluble residue, showed weak absorptions due to MgO (Fig. 7.47). There were also, however, very strong absorptions similar to those from MgCO_3 , which is difficult to understand since the IR spectrum of filler alone did not indicate MgCO_3 as an impurity. Other absorptions (all strong) were at 1262 cm^{-1} , 1100 cm^{-1} , 1022 cm^{-1} and 803 cm^{-1} , all due to siloxane groups. The spectrum taken without removing the soluble residue only showed absorptions due to MgO and siloxane groups. The spectrum of the soluble residue was similar to the spectrum of the original polymer except the intensity due to methyl groups at 2955 cm^{-1} had decreased considerably and there was also an absorption in the carbonyl region at about 1730 cm^{-1} . Similar results were observed when blend 26 was heated to 400°C . The IR spectrum of $\text{Mg}(\text{OH})_2$ before and after heating up to 480°C is given in Fig. 7.48.

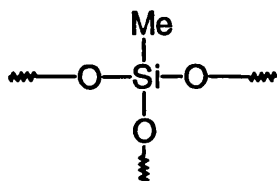
The first stage of the degradation of blend 38 (with 50% $\text{Al}(\text{OH})_3$), which was due to the decomposition of the filler to Al_2O_3 and water, starts at 195°C and shows a considerable rise due to the evolution of methane, starting at 240°C with T_{max} at 294°C . The second stage of degradation, which is mainly due to siloxane oligomers formation starts at 400°C . The evolution of methane was shown throughout the degradation, as seen in Fig. 7.45 (b) indicated by the rise of the -196°C trace.

The IR spectrum of the products from the first stage of the degradation gave absorptions due to water as expected, also absorptions due to cyclic siloxane compounds and a broad absorption at 2087 cm^{-1} possibly due to the Si-H group, but usually this group shows a sharp absorption rather than broad (Fig. 7.49 (a)). However, the band would be broad in the presence of compounds with different molecular weight as seen from Table 7.6.

The IR spectrum (Fig. 7.49 (b)) of the volatile condensable products from the first fractions of the SATVA separation (Fig. 7.46 (b)) showed the presence of CO_2 (possibly adsorbed on the surface of the filler), a trace amount of ketene and some other compounds containing Si-OH / Me-SiO₃, Si-H, O-SiMe₂ and Si-O-Si groups. Absorptions at 1256 cm^{-1} and 868 cm^{-1} could be assigned to tetramethylsilane, but its formation is difficult to formulate.

The IR spectrum of the CRF (Fig. 7.50 (a)) is much more complicated than for those from other blends, showing absorptions for a number of different types of siloxane compounds. The most abundant compounds seem to contain groups of the type Si-OH, Me-SiO₃, Si-O-Si, Si-O-Al, O-SiMe₂ (but its intensity has been reduced considerably), $\text{CH}_2=\text{CH}-$ and $\text{C}=\text{O}$.

Me-SiO₃ refers to a structure of the type shown below, possibly resulting from crosslinking



The residue from blend 38 crumbled to powder on disturbing but there was evidence for the formation of bubbles and sponge-like texture. The IR spectrum of the residue (Fig. 7.50 (b)) shows absorptions similar to that of Al_2O_3 but there were also weak absorptions due to siloxane groups. IR spectrum of $\text{Al}(\text{OH})_3$ is given in figure 7.51.

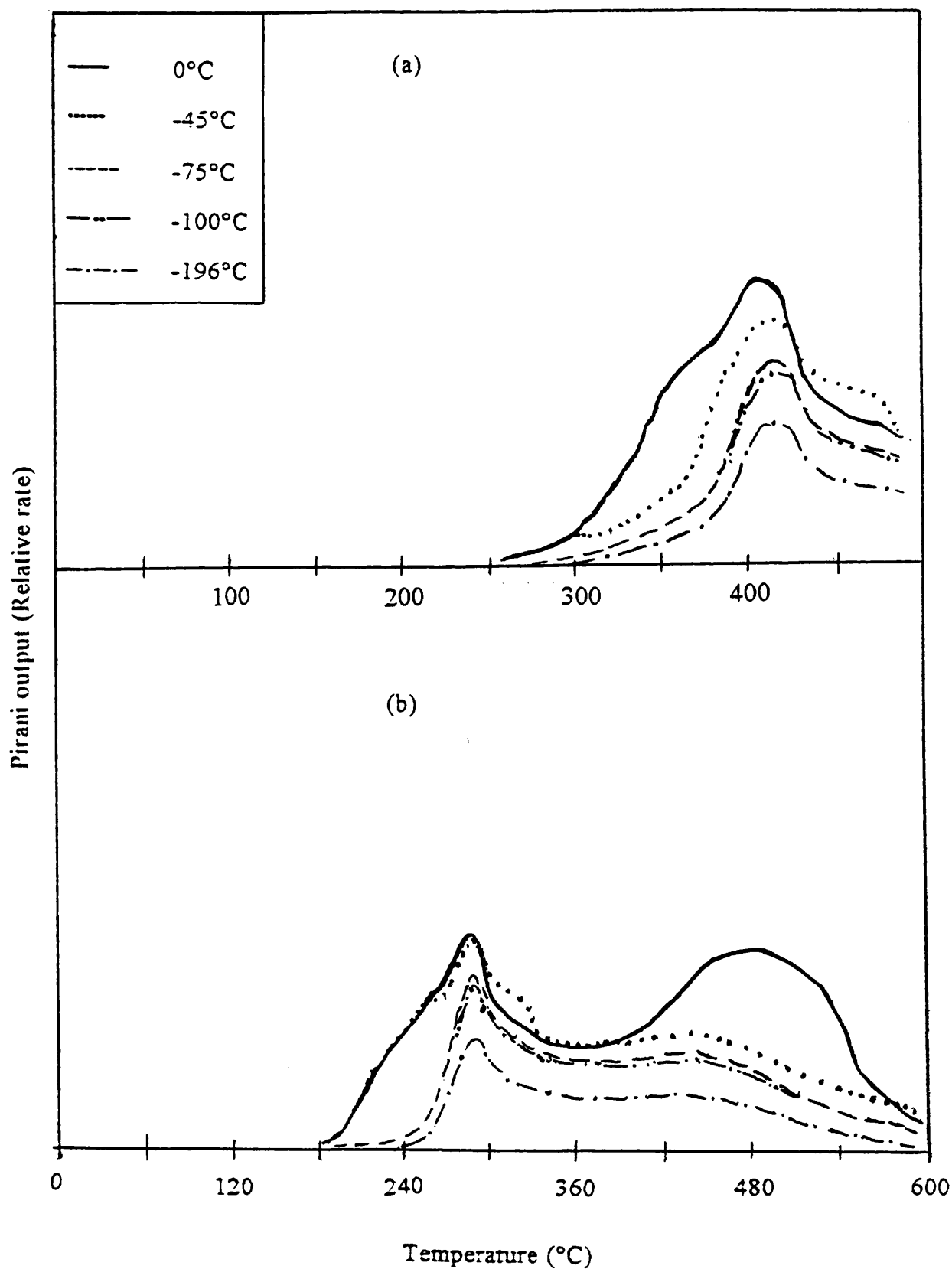


Fig. 7 45. TVA traces for blends of PDMS and 50% metal hydroxide:
 (a) blend 37 ($\text{Mg}(\text{OH})_2$) and (b) blend 38 ($\text{Al}(\text{OH})_3$).

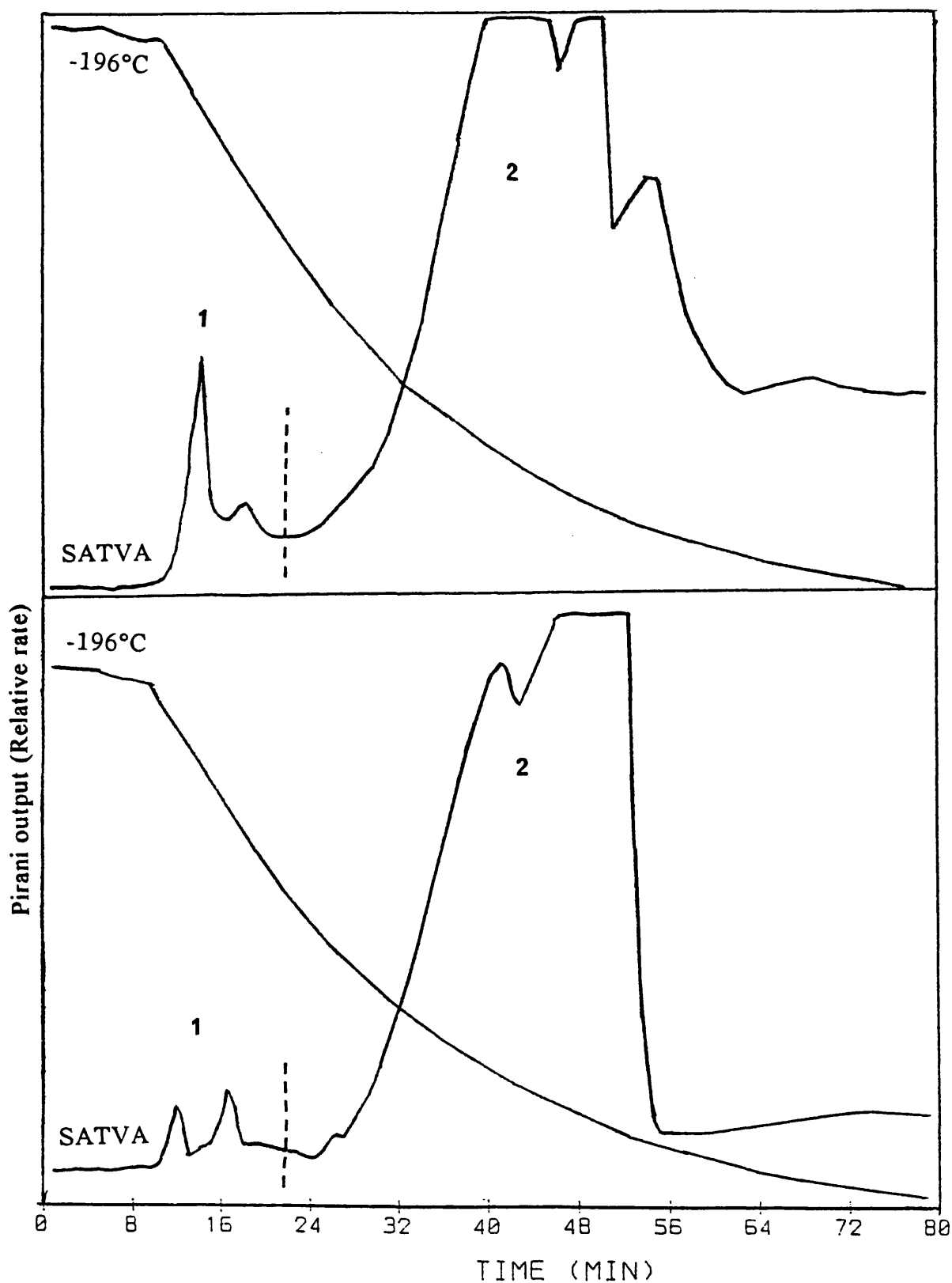


Fig. 7.46. SATVA traces for warm up from -196°C to ambient temperature of condensable volatile products from degradation for blends of PDMS and 50% metal hydroxides: (a) blend 37 ($\text{Mg}(\text{OH})_2$) and (b) blend 38 ($\text{Al}(\text{OH})_3$) after heating up to 500°C and 600°C respectively.

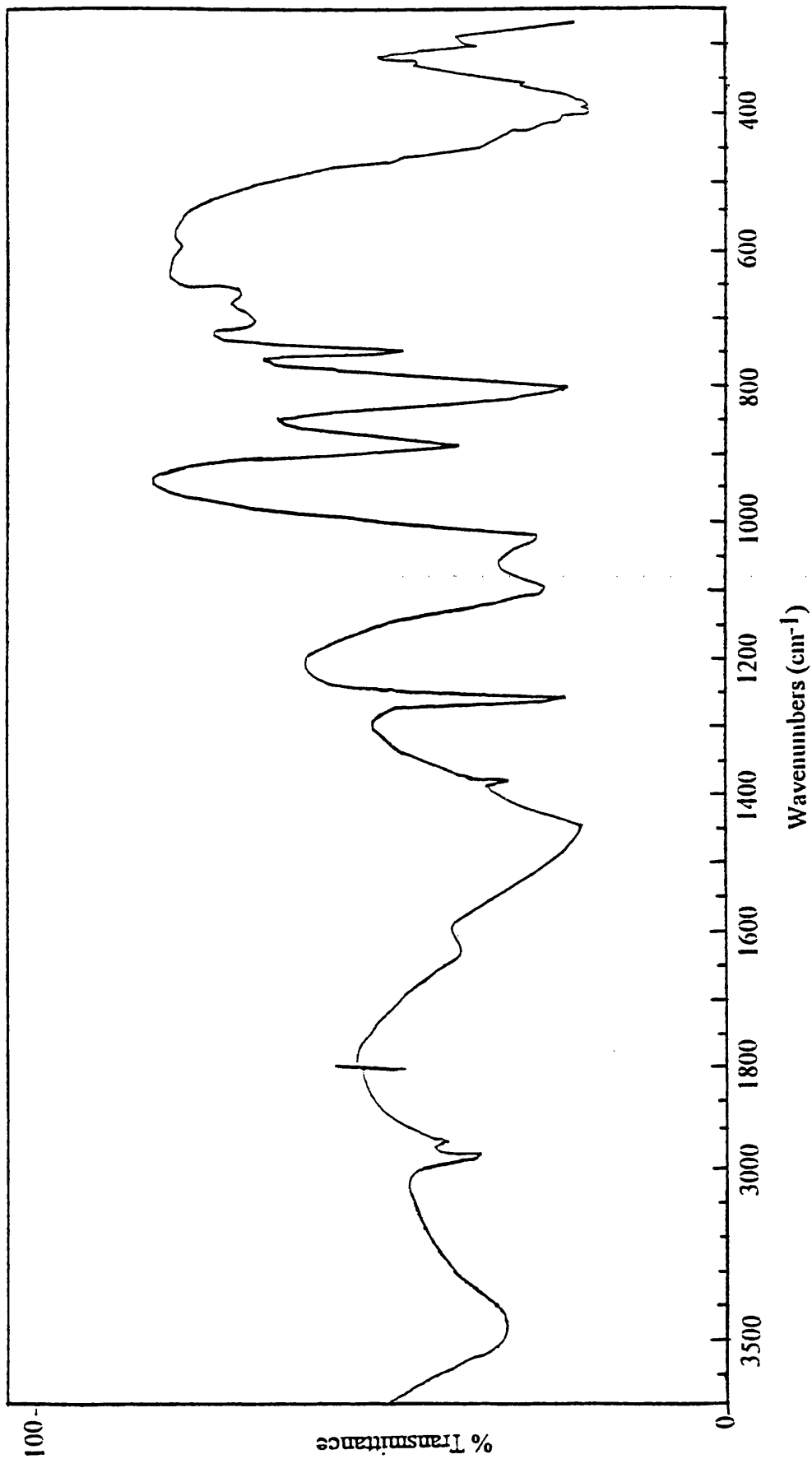


Fig. 7.47. IR spectrum of residue from the degradation of blend 37 (PDMS + 50% Mg(OH)₂) after heating up to 480°C.

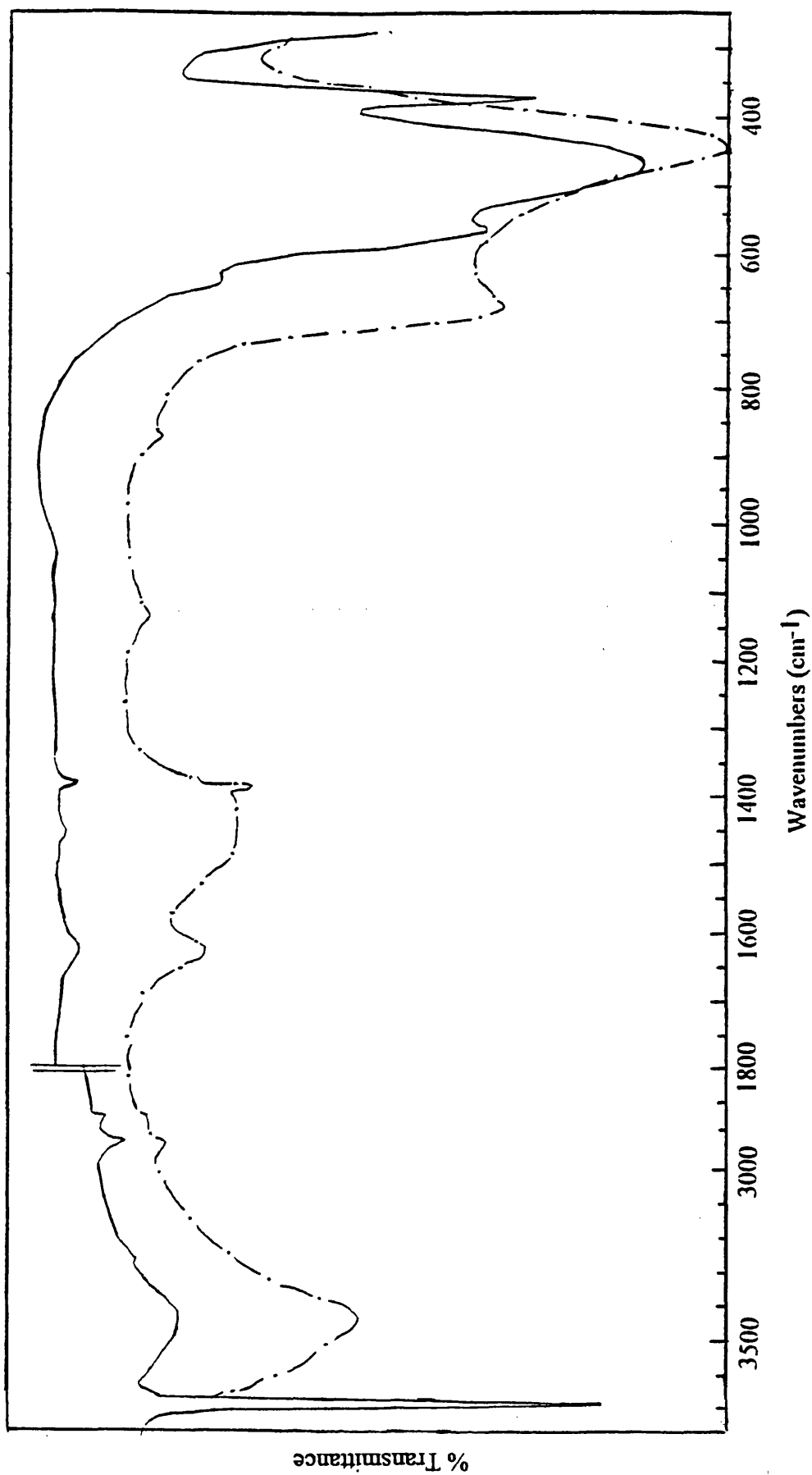


Fig. 7 48. IR spectra of Mg(OH)_2 before (—) and after (— · —) heating up to 480°C.

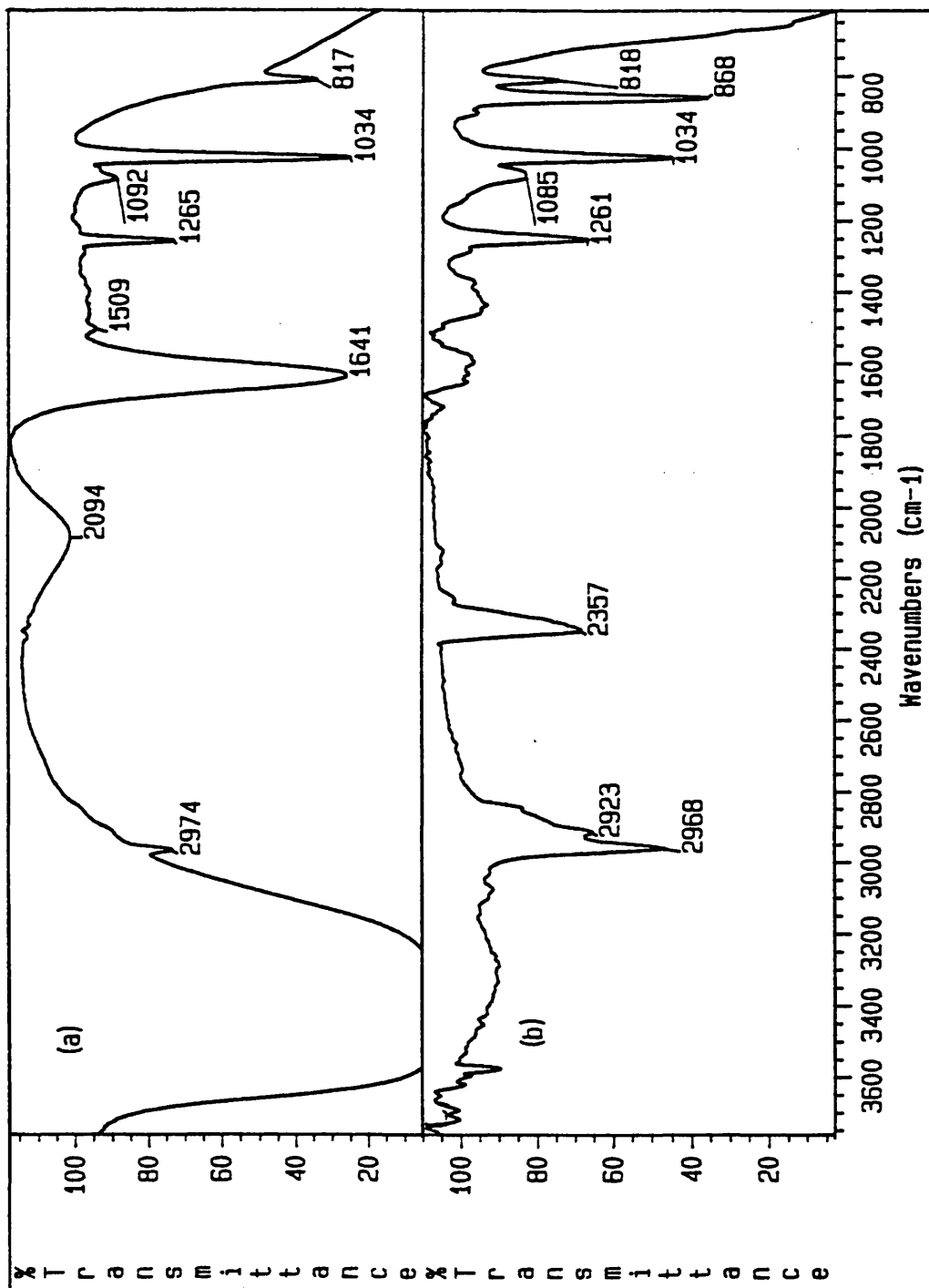


Fig. 7 49. IR spectra (transmittance x 8) of products of degradation of blend 38 (PDMS + 50% Al(OH)₃) after heating up to 600°C: (a) volatile condensable products from the first stage of degradation (b) total volatile products from the first fraction of SATVA separation.

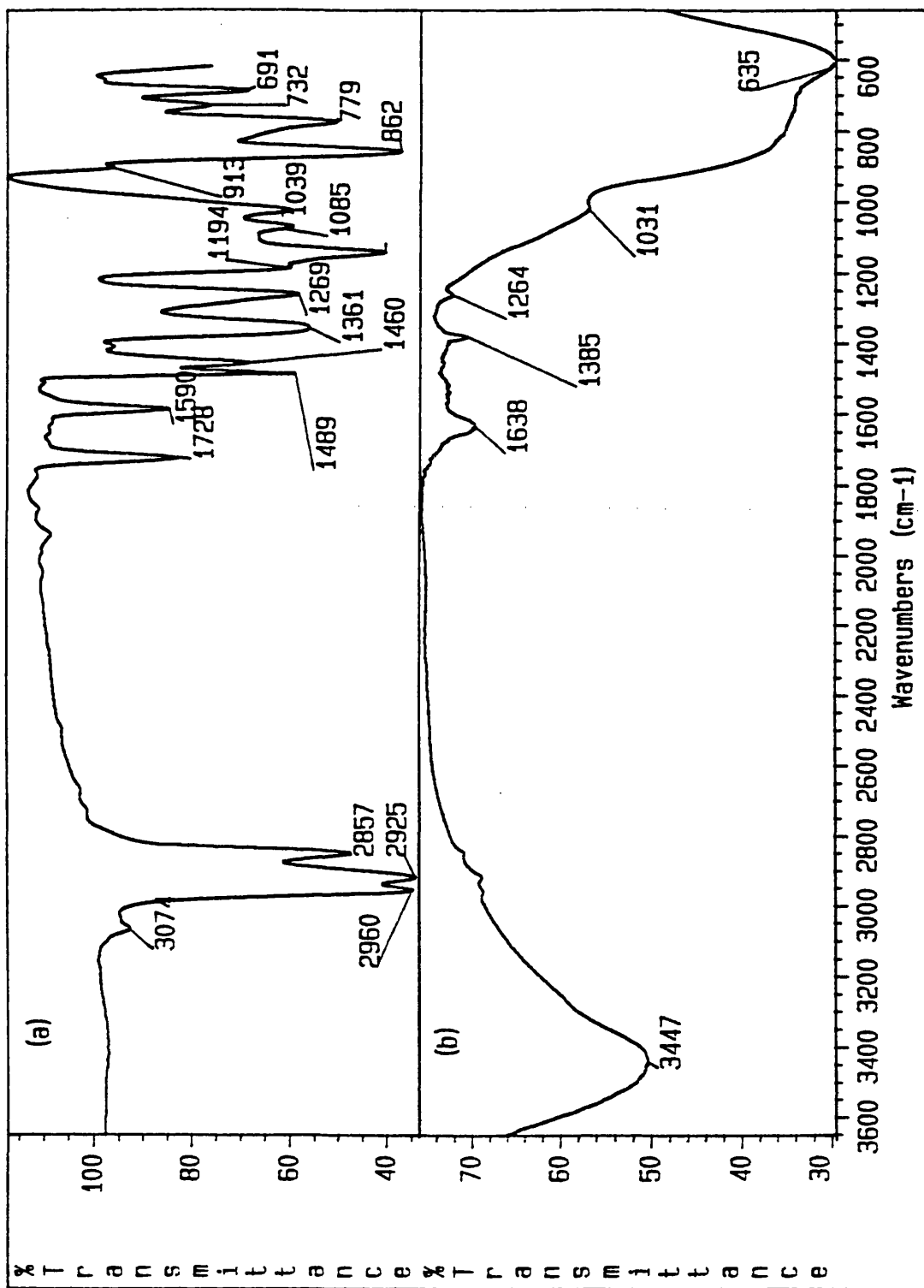


Fig. 7 50. IR spectra of products of degradation of blend 38 (PDMS + 50% Al(OH)₃) after heating up to 600°C: (a) CRF (b) residue.

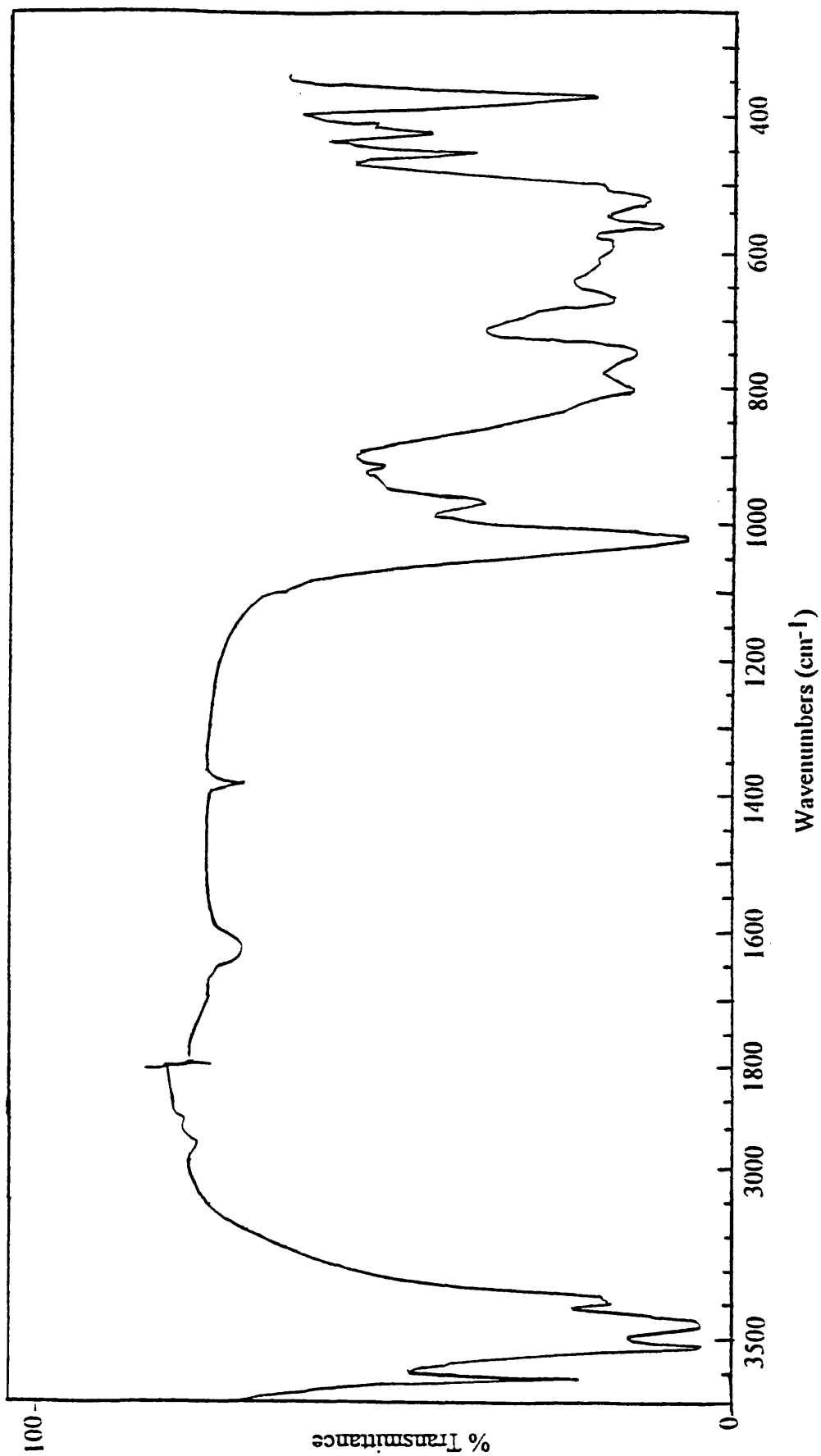
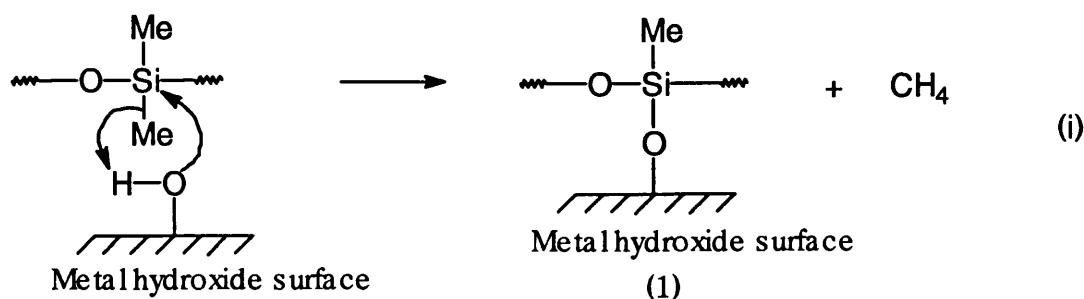


Fig. 7 51. IR spectrum of Al(OH)_3 .

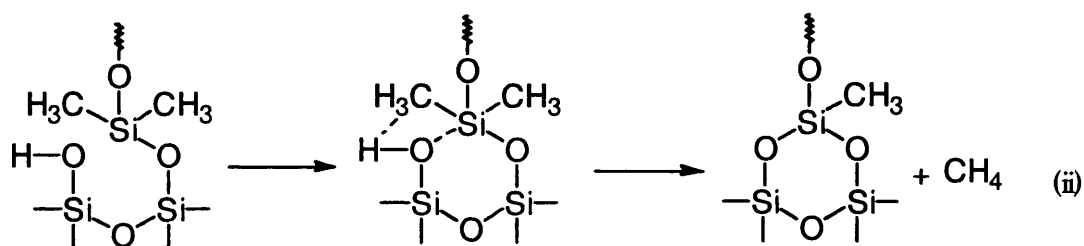
Volatilisation of blend 39 (1% $\text{Ca}(\text{OH})_2$) commenced at about 282°C , reached T_{max} at about 353°C and the degradation was complete at 415°C (Fig. 7.52 (a)). The TVA trace indicated the presence of an almost negligible amount of methane while other gaseous products such as CO_2 and ketene were not produced. Smaller cyclic oligomers, i.e. cyclic trimer and cyclic tetramer, were produced in a large quantity. The amount of the CRF was quite small and had some solid material as well as liquid. The IR spectrum of the CRF (Fig 7.53 (a)) was similar to that of the original polymer, except it showed an extra peak at 1059 cm^{-1} . The residue did not form a bubble but instead spread on the surface of the tube and crumbled to powder; it was slightly difficult to remove from the container. The IR spectrum of the residue (Fig 7.53 (b)) gave evidence for the presence of siloxane groups, besides the absorptions due to the filler. There were also absorptions at 1423 cm^{-1} , 875 cm^{-1} and 714 cm^{-1} attributable to calcium carbonate. Similar behaviour was shown by the residue of blend 37.

The evolution of methane, identified by the quadrupole mass spectrometer attached to the TVA line, especially around the decomposition temperatures of the corresponding filler could only be possible if there were some chemical bonds formed between the components. Thus the stabilisation shown by PDMS is not only due to the blanketing effect of the polymer surface by the released water and the filler but also due to the chemical interaction. The large amount of methane evolution in the case of blend 38 at the filler's dehydration temperature indicates that hydroxides with lower dehydration temperatures result in more Si-C bond cleavage than hydroxides with higher dehydration temperatures. The following mechanism is proposed for such an interaction between hydroxides and PDMS:

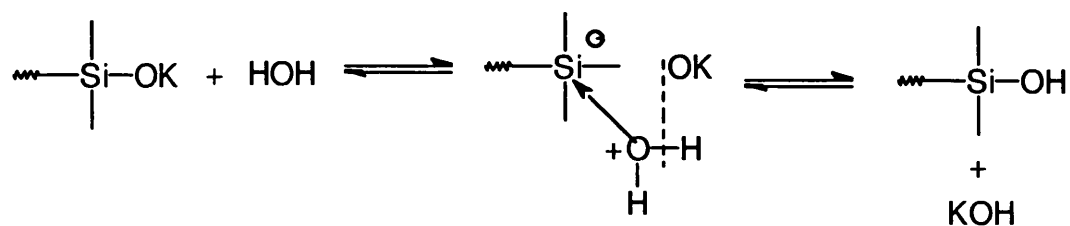


This type of reaction was also suggested by Kharitonov et al¹⁴³ in the case of PDMS degraded in the presence of $\text{Al}(\text{OH})_3$ but the main evolution of methane in the case of blend 37 after the complete dehydration of the $\text{Mg}(\text{OH})_2$ confirms that this reaction is not favoured by all hydroxides. The IR spectrum of blend 38 also confirms that this is not the only reaction taking place since it does not result in the introduction of the hydroxyl groups shown in the IR spectrum of the degradation products.

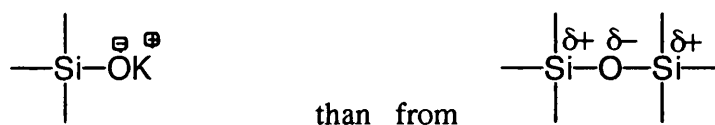
Zdorikova et al¹⁴² suggested the occurrence of hydrolysis of the main chain of polymer thus forming end fragments carrying -OH groups. These new end groups would lead to depolymerisation from the chain ends to form cyclic siloxane oligomers as described in Chapter 4. But this type of reaction would result in considerable fragmentation of the polymer chain and thus weight loss at lower temperature. The TVA traces of blends 37 and 38 conflict with this since most of the oligomers formation occurs, especially in the case of blend 38, at higher temperatures than expected. These workers¹⁴² also suggested the formation of methane from these hydroxyl end groups as follows:



Kucera et al¹³⁴ proved by heating cyclic siloxane tetramer in a sealed tube in the presence of water for 72 hours at 300-320°C that siloxane bonds are stable towards the hydrolysing effect of water. However, they found that in the presence of active sites (formed during polymerisation from the basic hydroxides i.e. KOH, used as catalysts and still active during the life of the polymer, resulting in depolymerisation of PDMS when heated: in other words they are sites for both polymerisation and depolymerisation), at 150°C, water results in hydrolysis of PDMS. They suggested that the reaction of active sites follows temporary conversion of the adjacent silicon atom to a pentavalent atom during interaction with water as follows:

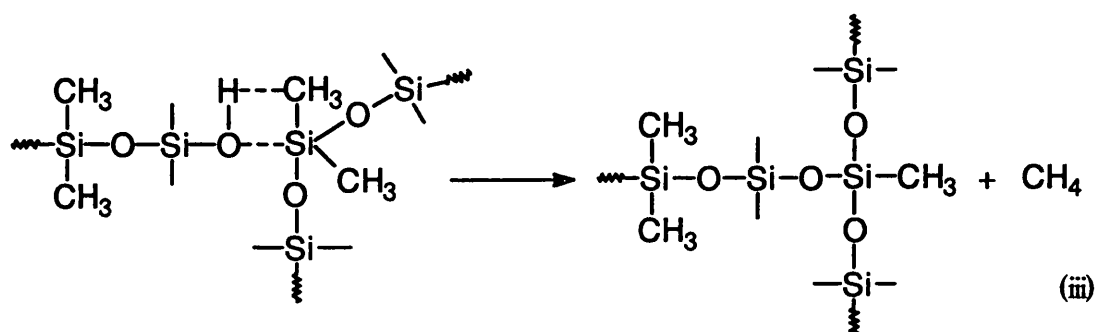


Hurd et al¹⁵⁶ also pointed out that during heating water has no effect on the normal siloxane bonds and that the co-ordination bond would be formed more easily from the group



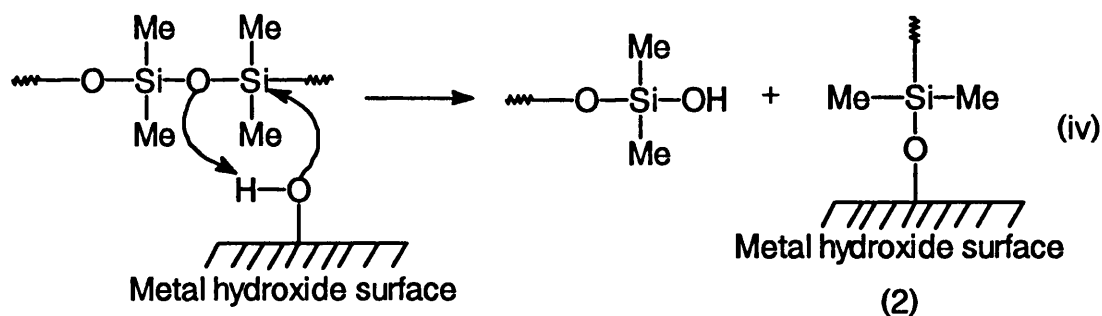
So if the hydrolysis of the chains occurs then it would happen after the formation of the active sites but by that time most of the water would volatilise from the reaction mixture.

Other workers^{112, 114} also have suggested the mechanism (ii) and the following for the formation of methane from hydroxyl end grouped PDMS when degraded alone (discussed in Chapter 4).



However, it was found in Chapter 4 that PDMS with hydroxyl end groups did not produce methane so these reactions are ruled out for the production of methane.

The formation of hydroxyl groups in the polymer seems more likely from the following mechanism at/or near the dehydration temperature of the filler:



This reaction stabilises one chain fragment while the other with hydroxyl ends results in depolymerisation at lower temperature, or if it is a low molecular weight fragment, it would volatilise from the reaction mixture and contribute as a degradation product. This mechanism seems more favoured by basic hydroxides since it does not result in the formation of methane at the dehydration temperature of the filler. However, the Si-C bond is weakened near the point of interaction due to electron withdrawing effects resulting in the formation of methane after the interactions through mechanism (i) and (iv). The continuous methane production throughout the degradation in the case of blend 38 could only be explained from the structures of the type (1) and (2) formed from these mechanisms, since the corresponding metal oxide (Al_2O_3) does not cause Si-C

bond scission as seen in the case of blend 42. The complexes formed seem to be stable at lower temperature, and at higher temperatures the underlying unreacted hydroxide groups on the surface of the metal hydroxide would continue formation of methane.

Blends of PDMS and Metal Oxides

Stabilisation of blend 40 (50% CaO with Ca(OH)_2 as impurity) was initially 50°C which gradually increased to about 120°C. The TVA trace (Fig. 7.52 (b)) shows the formation of a large amount of methane starting at about 325°C. The other degradation products were mainly smaller cyclic siloxane oligomers as was seen from the GC-MS results, thus the amount of CRF was small. There was no formation of gaseous products such as carbon dioxide or ketene. The spectrum of the residue gave strong absorptions for the siloxane groups, CaO and Ca(OH)_2 , but the intensity of the band for hydroxide groups at 3643 cm^{-1} decreased considerably.

Blend 41 (with 50% MgO containing a small amount of Mg(OH)_2 as impurity) started volatilisation at about 200°C, 50°C earlier than expected, but the onset of degradation was extremely slow such that gradually a stabilisation of up to 80-85°C was established. A lot of methane was produced, starting at about 340°C (Fig. 7.54 (a)). The residue was rubbery, but it was possible to grind it to some extent. It was not hollow (like a bubble) like the rubbery residues from other blends, but was rather hard. The spectrum of the insoluble residue gave strong absorptions for the siloxane groups in addition to the absorptions due to filler.

The TVA trace of blend 42 (with 50% Al_2O_3) was similar to the TVA trace of PDMS when degraded alone except that volatilisation started at a much higher temperature (344°C) in the case of blend 42 and reached T_{max} at 403°C (Fig. 7.54 (b)). There was no evidence for the formation of methane. The residue crumbled to a fine grey powder when disturbed. The IR spectrum of the residue did not show any absorption for siloxane groups. Blend 42 was also degraded up to 400°C to see if the stability shown by the blend was due to the filler acting as a heat sink only or if there was an interaction between the components. It was found that the residue left after heating up to 400°C was rubbery and was like a sponge rather than a bubble. The residue was left in solvent to extract filler from the polymer but it was possible to extract only some polymer, indicating that interaction between the components had occurred. The IR spectrum of the insoluble residue (Fig. 7.55) gave strong absorptions for the

siloxane groups and for the filler. The IR spectrum of the filler is given in Fig. 7.56 for comparison.

Blend 43 (with 50% TiO₂) started to volatilise at about 279°C with evolution of methane but had a threshold degradation temperature at 400°C (Fig. 7.54 (c)). Degradation products were like the degradation products of blend 31 which were mainly larger cyclic siloxane oligomers. The SATVA trace showed a negligible amount of the first fraction. However, there was evidence for some small amounts of siloxane products other than cyclic siloxane oligomers (D₃, D₄, D₅ etc.). The IR spectrum of these products showed, besides the expected siloxane absorptions, bands at 3583 cm⁻¹ due to -OH group, 3098 cm⁻¹, 1666 cm⁻¹, and 938 cm⁻¹ all three due to Si-CH=CH₂ 1716 cm⁻¹ due to C=O, 1098 cm⁻¹, and 1027 cm⁻¹ which could be assigned Si-O-Si. The formation of -OH and C=O groups is difficult to explain.

The degradation products were mainly smaller cyclic siloxane oligomers, thus the amount of CRF was very small and the IR spectrum of the CRF (Fig. 7.57 (b)) was similar to the IR spectra of the CRFs from the other blends of silicone and inorganic fillers which produced methane, except there were extra peaks at 1196 cm⁻¹, 1157 cm⁻¹, and 920 cm⁻¹. The absorption of the Si-O-Ti vibration is known⁶⁵⁻⁶⁷ to be in the region 917-926 cm⁻¹. There is possibility of the compounds containing Si-O-Ti groups resulting from the interaction of the components. The other degradation products seem to contain siloxane compounds with methylene and ethylene linkages in higher proportion than in most other blends. The mechanism of interaction is described and discussed later in section 7.5.

The residue was rubbery, sticky and formed a bubble. The rubbery texture of the residue remained after extraction with dichloromethane. The IR spectrum of the soluble residue was similar to that of the original polymer except that it showed an extra peak at 1735 cm⁻¹, assigned to C=O, but its formation cannot be explained.

Volatilisation of blend 44 (with ~66% silica) started at 350°C but the main degradation started at about 400°C. The TVA trace (Fig. 7.58 (a)) was similar to that of blend 26 but the non-condensable gaseous product, identified as methane, was only in a trace amount; while there were no condensable gaseous products such as CO₂. The GC-MS results showed that the degradation products were mainly similar to those from the other blends which produced trace amounts of methane or had some radical source. The CRF at 480°C was liquid and in small amount while the residue was hard and changed its appearance from clear to white. The SATVA trace for blend 44 is given in Fig. 7.58 (b).

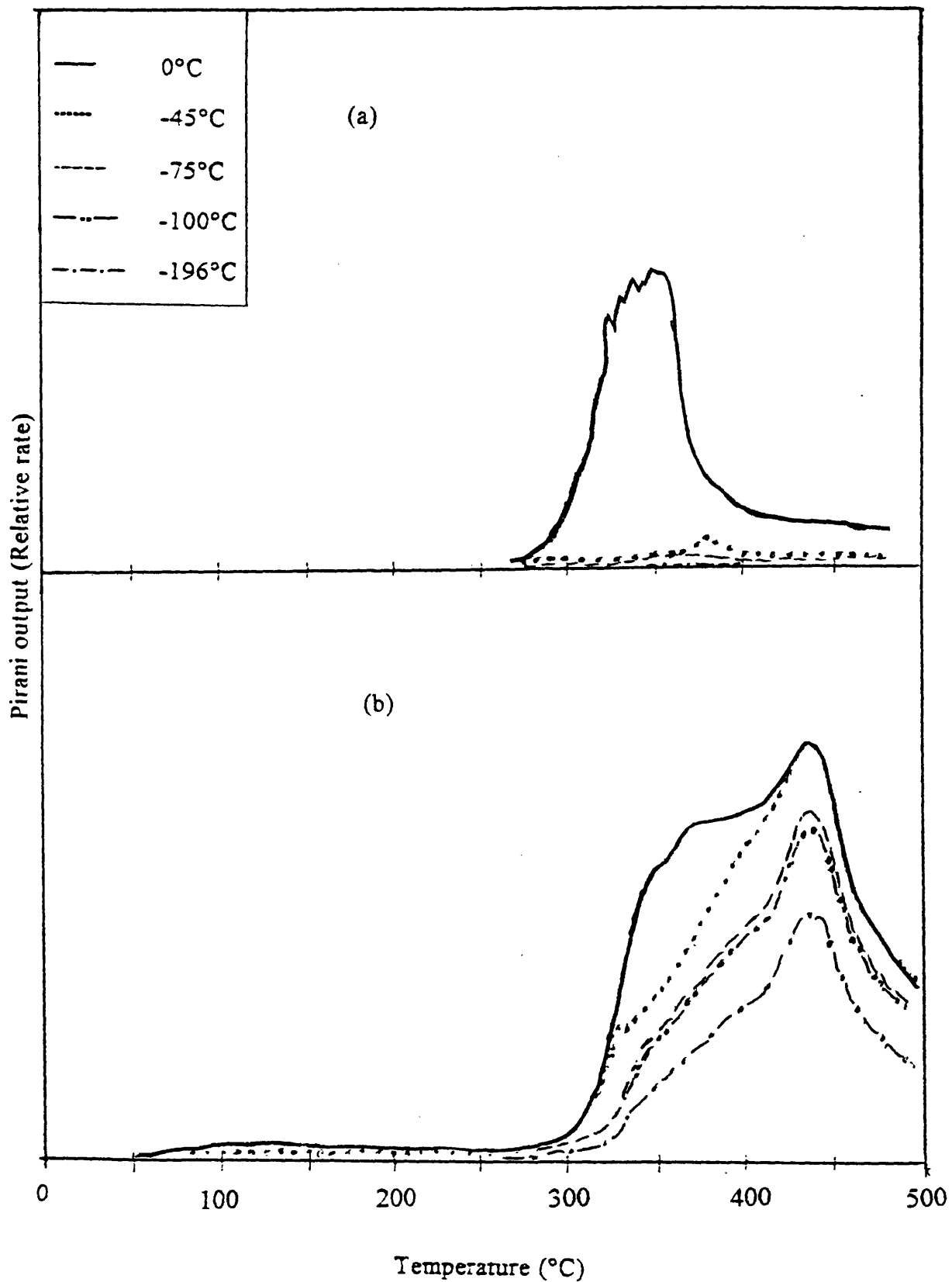


Fig. 7.52. TVA traces for blends of PDMS and inorganic fillers: (a) blend 39 (1% Ca(OH)₂) and (b) blend 40 (50% CaO).

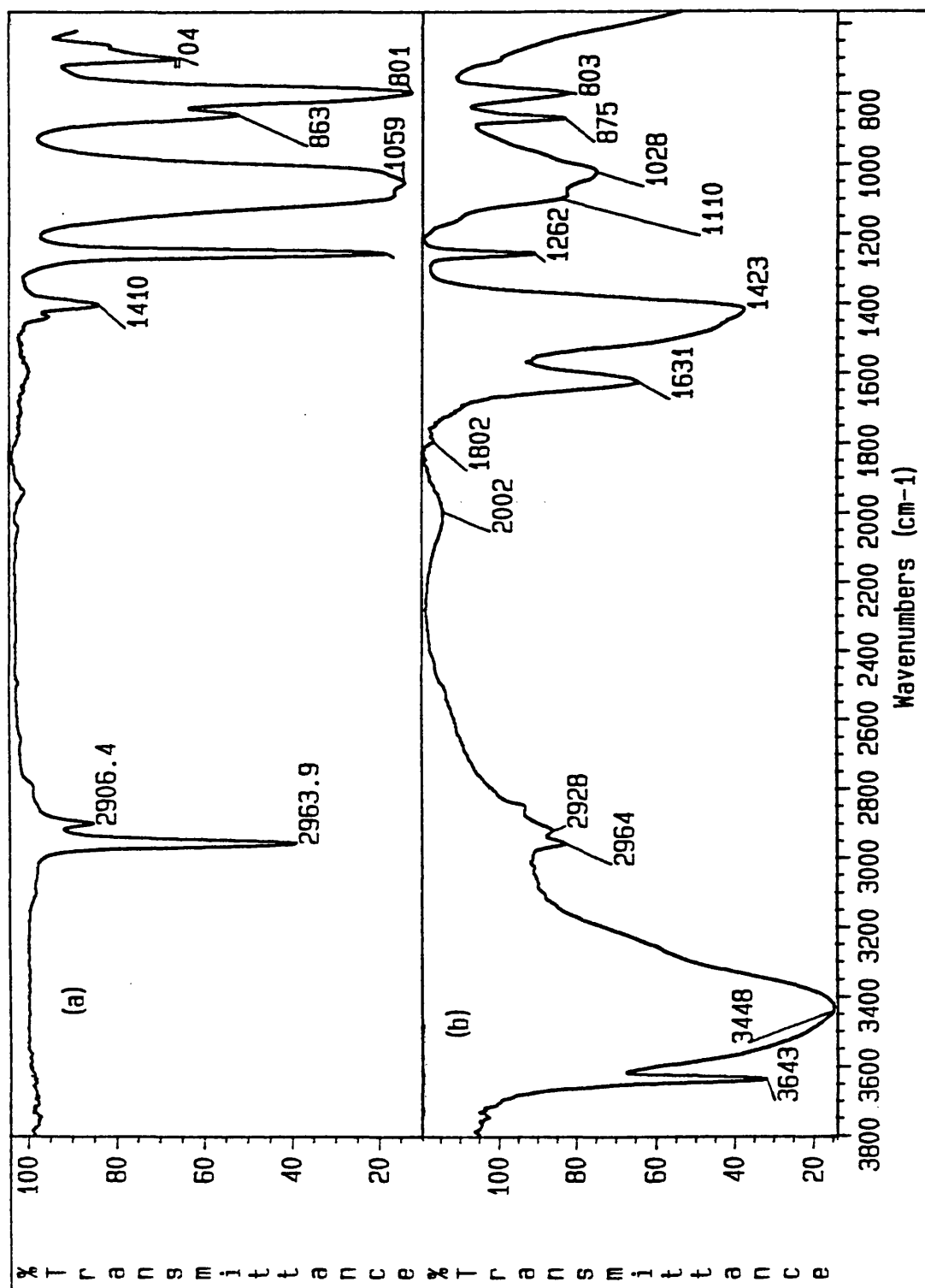


Fig. 7.53. IR spectra from the degradation of blend 39 (PDMS +1-0% Ca(OH)₂):

(a) CRF (b) residue.

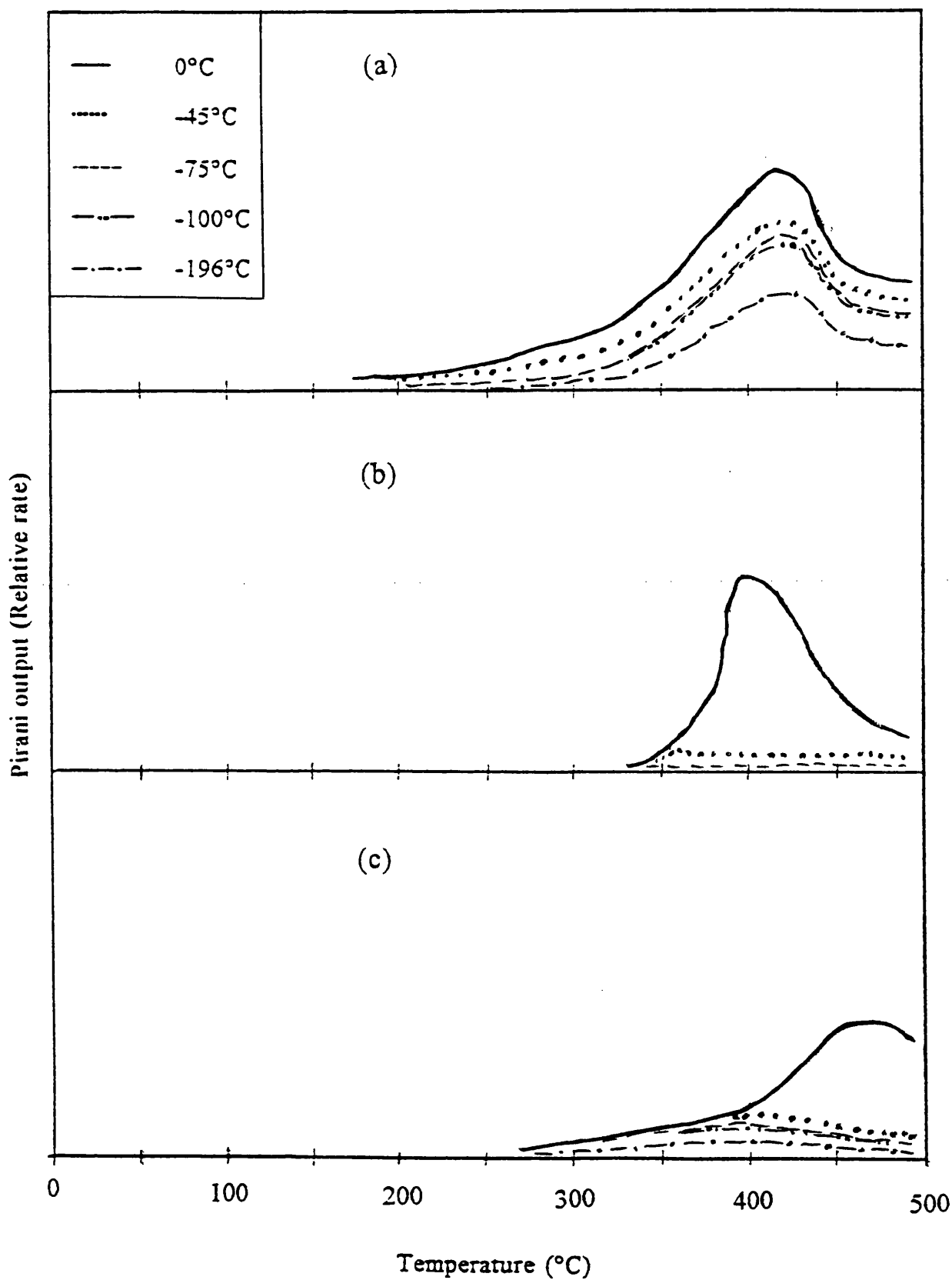


Fig. 7.54 TVA traces for blends of PDMS and 50% metal oxides: (a) blend 41 (MgO), (b) blend 42 (Al₂O₃) and (c) blend 43 (TiO₂).

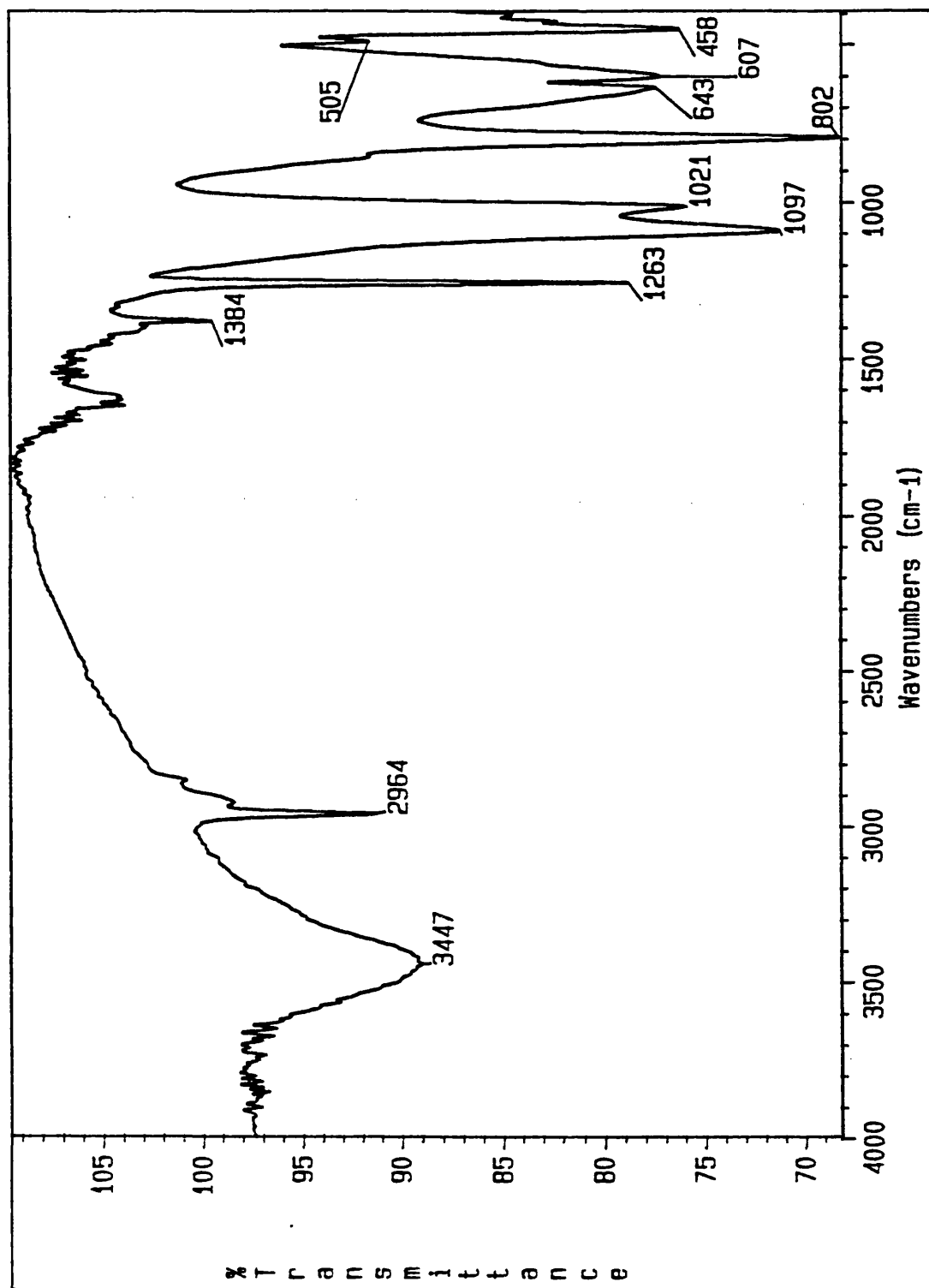


Fig. 7.55. IR spectrum of the residue from blend 42 (PDMS + 50% Al₂O₃) after heating up to 400°C.

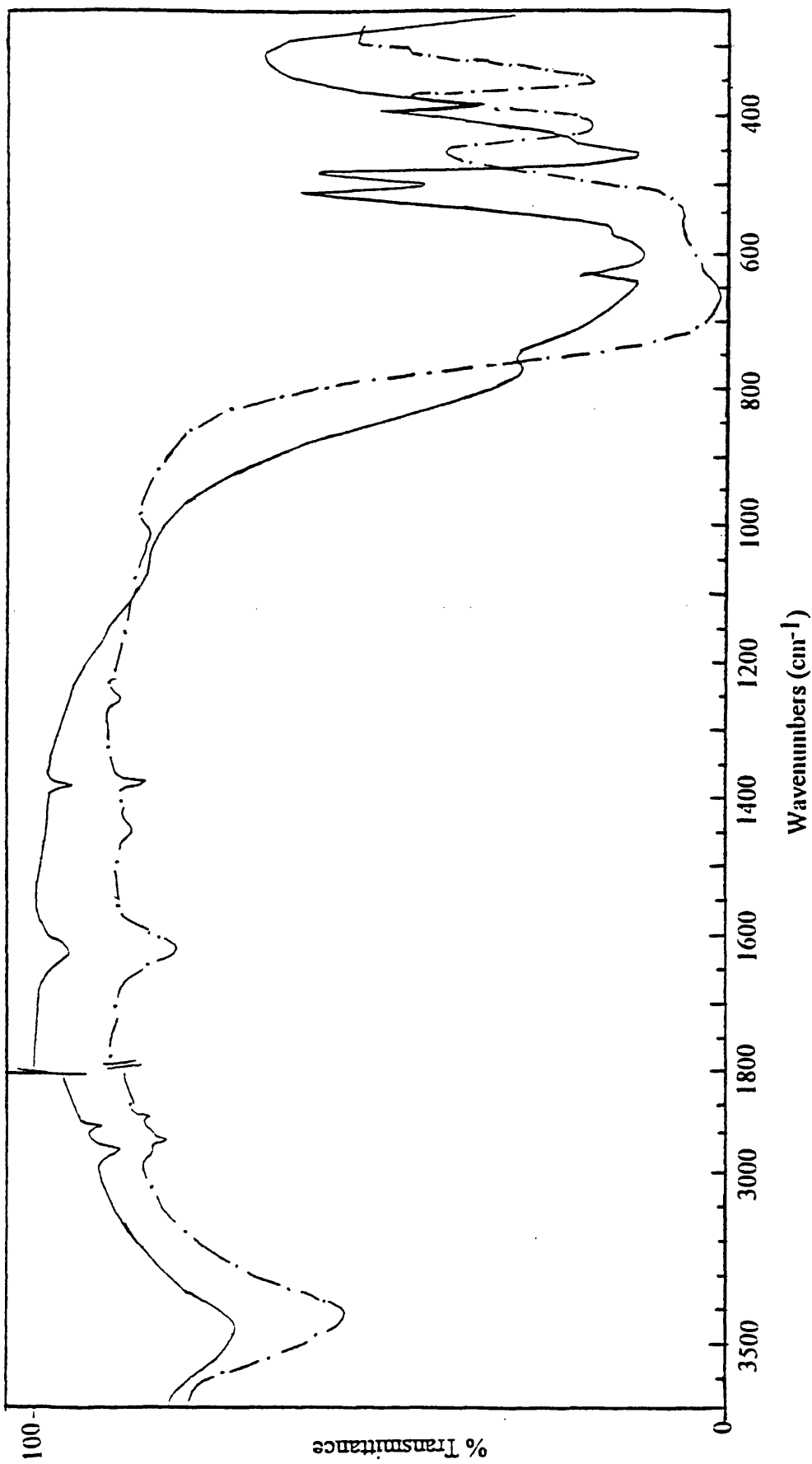


Fig. 7.56 IR spectra of the fillers: Al₂O₃ (—) and TiO₂ (— · —).

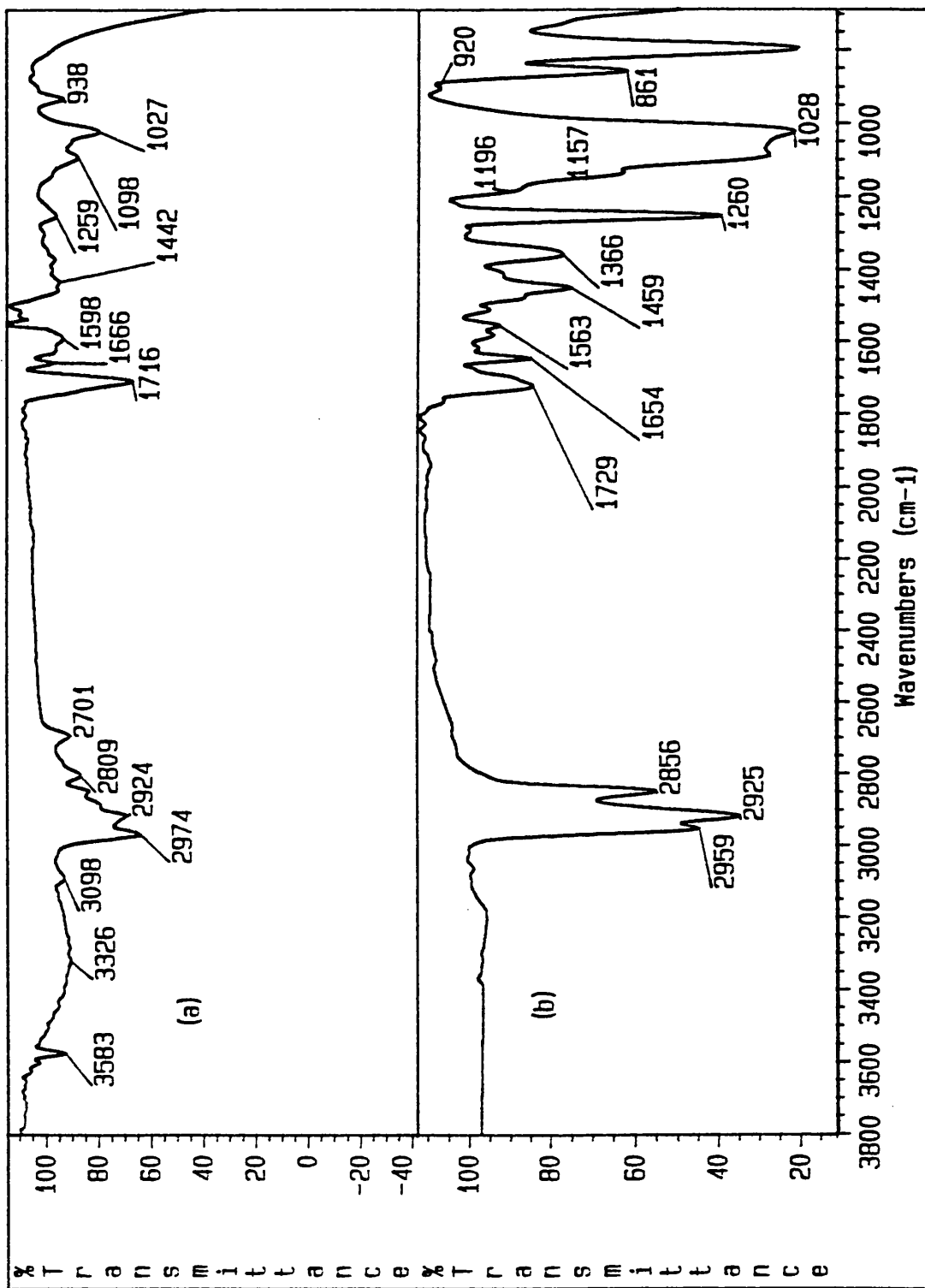


Fig. 7.57 IR spectra of the degradation products from blend 43 (PDMS + 50% TiO₂): (a) volatile degradation products (b) CRF.

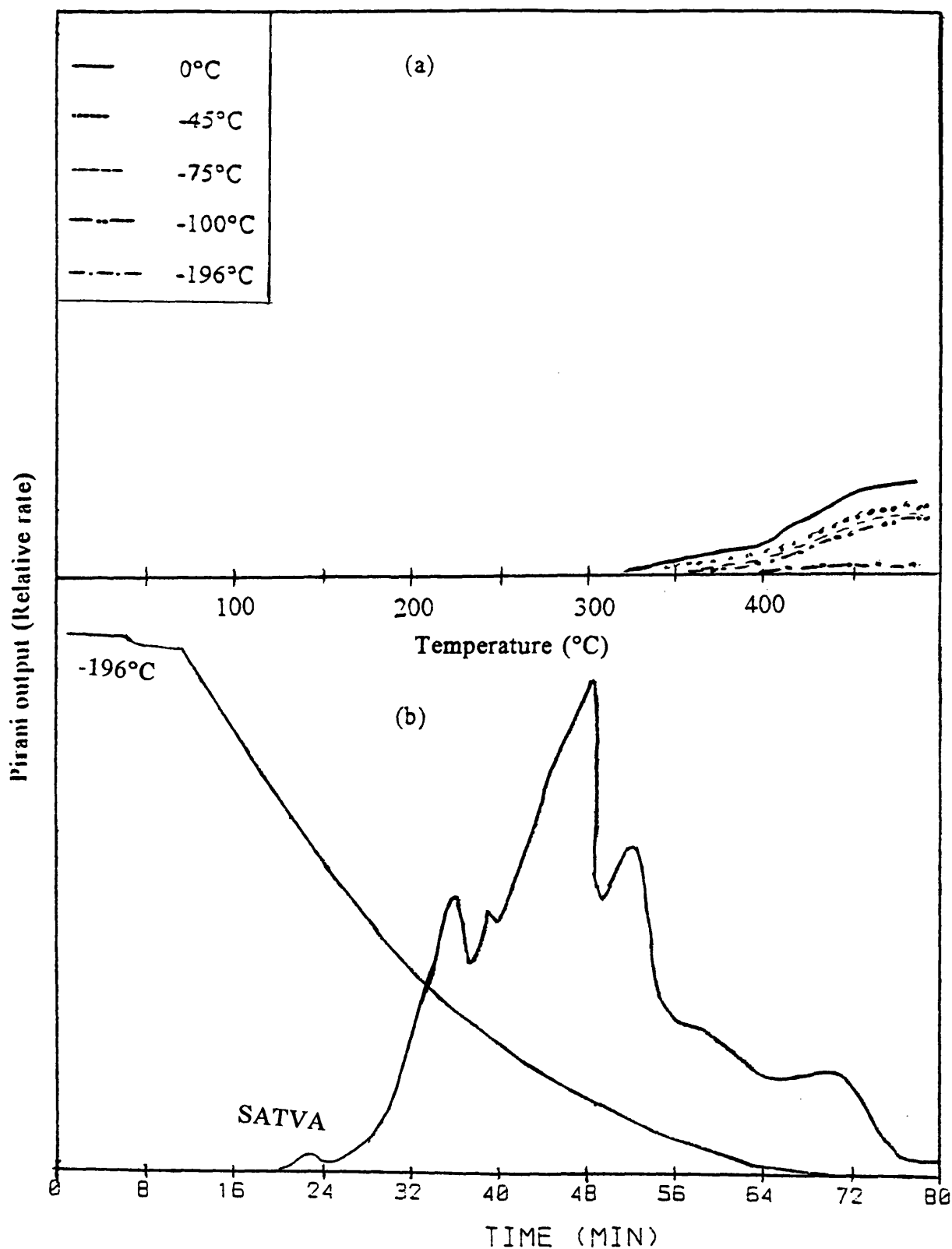


Fig. 7.58 (a) TVA trace and (b) SATVA trace for warm up from -196°C to ambient temperature of condensable volatile products from degradation of blend 44 (PDMS + $\sim 66\%$ silica).

Blends of Siloxane Polymer and Other Additives

Blend 45 (1% calcium stearate, CaSt) started to volatilise at about 290°C and the rate reached T_{\max} at 415°C (Fig. 7.59 (a)). The TVA trace was almost similar in shape to that of PDMS when degraded alone except that in this case it started at a higher temperature. The process of volatilisation was quite slow at the beginning and a very small amount of non-condensable gaseous product was evolved at about 350°C.

Blend 46 (5% CaSt) showed a two stage degradation (Fig. 7.59 (b)), the first starting at 310°C. The TVA trace showed the presence of a non-condensable gaseous product (identified as methane), starting at 440°C, in this case much more than from blend 45.

The SATVA traces for both blends mentioned above indicated that blend 45 produced less volatile gaseous products (i.e. CO₂ and ketene) and more higher molecular weight compounds (i.e. cyclic siloxane oligomers) than blend 46. The IR spectra of the gaseous products from both blends revealed absorptions for CO₂, ketene, alkenes and siloxane group. The IR spectra of the CRFs (Fig. 7.60 (a-b)), whitish gummy liquids and completely different in appearance from the others, showed extra absorptions around 1060 cm⁻¹ (strong) due to siloxane group and around 1707 cm⁻¹ (weak) due to carbonate group. These absorption were much more pronounced in the case of blend 46. It is clear from these absorptions that the filler interacted with the polymer and thus carbonate groups were introduced into the polymer chain.

The light brown residue (about 14.49% in the case of blend 46) was rubbery, sticky and insoluble. The IR spectra (KBr disc) from both blends were similar to that of the original polymer. The strong absorptions due to antisymmetrical stretching frequencies of carboxylate ions in the region 1578-1541 cm⁻¹ and in the region 1468-1426 cm⁻¹ due to alkyl group of the filler were not present. It is difficult to tell what happened to calcium but the possibility is that it was fixed into the polymer chain and thus stayed in as Si-O⁻Ca²⁺-O-Si. The IR spectra of calcium stearate and blend 46 are given in Fig. 7.61 (a) and (b) respectively.

Blend 47 (1% stearic acid, StA) started to volatilise at around 313°C and the rate reached T_{\max} at 413°C (Fig. 7.62 (a)). The TVA trace looked similar in shape to that of PDMS when degraded alone except that in the case of blend 47, it started at a higher temperature and the volatilisation of the degradation products was slow at the beginning.

The SATVA traces show the presence of a negligible amount of volatile gaseous products. The IR spectrum of the CRF (Fig. 7.63 (b)) was similar to those in the case of blends 45 and 46 but this time the extra peak around 1060 cm^{-1} was much more intense than in the other cases. This type of band was also present in the case when PDMS and LDPE were degraded together (blend 13) as discussed in Chapter 6. The foam like residue (14.51% after degradation up to 480°C) was rubbery, did not change colour from the original blend and was mainly insoluble. The IR spectrum (KBr disc) was similar to that of the original polymer. The IR spectrum of stearic acid is given in Fig. 7.63 (a).

The TVA trace of blend 48 (5% StA) shows almost two stage degradation, the first starting at 348°C (Fig. 7.62 (b)). The TVA traces of blends 47 and 48 did not show the presence of non-condensable gaseous products.

The SATVA trace demonstrated a negligible rise for the volatile gaseous products. Other volatile products, characterised by GC-MS (Fig. 7.68), were much less than in the case of blend 47. The MS results and interpretations for the volatile degradation products are presented in Table 7.7. The IR spectrum of the CRF (liquid plus white solid) showed extra absorptions at 1698 cm^{-1} (strong and sharp with small shoulders in the region $1690\text{-}1640\text{ cm}^{-1}$), 1060 cm^{-1} and shoulders at 1279 cm^{-1} , 1190 cm^{-1} and 942 cm^{-1} (Fig. 7.63 (c)). These absorptions, except for the absorption at 1060 cm^{-1} , may indicate the presence of Si-O-CO-R group, where R is an alkyl group but on the other hand if all the absorptions for the siloxane groups, including absorption at 1060 cm^{-1} were subtracted from the IR spectrum then the remaining spectrum would be nearly similar to that of the stearic acid. Stearic acid, when heated alone, under vacuum conditions, volatilised before 100°C and condensed as CRF. If such was the case then stabilisation of the PDMS is difficult to explain since all of the additive would volatilise well before the degradation of the polymer started.

Formation of the insoluble, foam-like rubbery residue (about 44.14% after degradation up to 480°C), which did not change colour, was not possible if there was no interaction between the polymer and the additive. It seems logical to think that there was some interaction between the polymer and at least some of the additive before it could volatilise from the system. This interaction was possibly introduced when the blend was prepared or during degradation when PDMS melts.

Blend 49 (with 20% StA) was prepared in the laboratory at room temperature to see if the interaction was introduced during blending. The TVA trace (Fig. 7.62 (c)) indicated some drift at the start in the base lines of the pressure readings revealing some volatilisation but products were formed as CRF which was possibly due to some of the additive volatilising from the polymer. The IR spectrum of the solid part of the CRF implied that it was composed of the additive but it was not enough to account for 20% added. The residue (20.36% at 480°C) was not as rubbery and sticky as the residue from blend 48. The TVA trace also showed the presence of a small amount of non-condensable gaseous product, in the region 350-430°C. The evolution of the degradation products also started at this temperature and reached T_{\max} at 432°C.

It seems that any interaction between the polymer and the additive occurred when both were in their melt state, but the method of preparation also seems to have some effect on the stabilisation properties of the additive. It was clear from blends 47 and 48 that the increase in additive content increased the stabilisation, but blend 49, although it had four times more additive than blend 48, showed almost the same stabilisation as blend 48. The interaction is possibly similar to that described in Chapter 6 which results in the formation of a system like a grafted copolymer. The SATVA trace was similar to that of blend 48.

The degradation products from blends 45-49 showed presence of low molecular weight hydrocarbons, identified by GC-MS which were also found from the blends which contained coated filler. There were also trace amounts of unidentified compounds containing both alkyl and siloxane groups. These additives or coatings with large alkyl groups seem to decompose by radical reactions in the presence of another component and result in formation of hydrocarbons instead of volatilising as does stearic acid. The radicals formed may abstract hydrogen from the methyl groups on the silicon atoms of the polymer as described in Chapter 6 and introduce radical reactions within the polymer chains resulting in crosslinking and branching of the polymer and eventually the formation of a rubbery and insoluble residue. The explanation also accounts for the absence of methane, since these alkyl radicals only cause the breaking of C-H bonds rather than Si-C bonds. It seems that as little as 1% and up to 5% stearic acid is enough to bring about these changes.

The formation of methane in the case of calcium stearate additive is due to the Ca embedding into the polymer chain and resulting a structure of the type $\text{Si-O}^- \text{Ca}^{2\oplus} \text{-O-Si}$. It is known that Si-C bond scission of PDMS is favoured by the formation of the above type of structures as described in section 7.5.

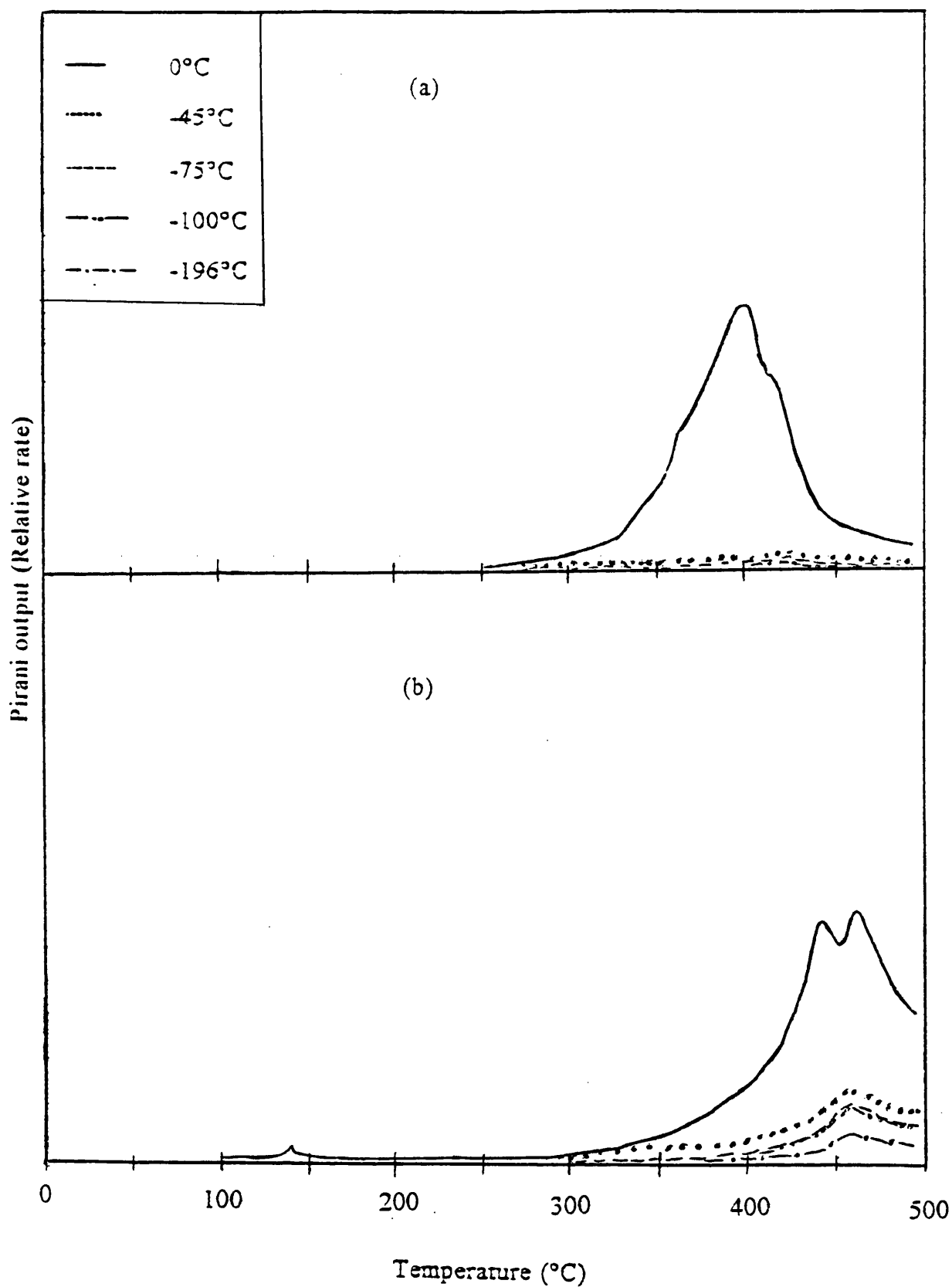


Fig. 7.59. TVA traces for blends of PDMS and calcium stearate: (a) blend 45 (1%), (b) blend 46 (5%).

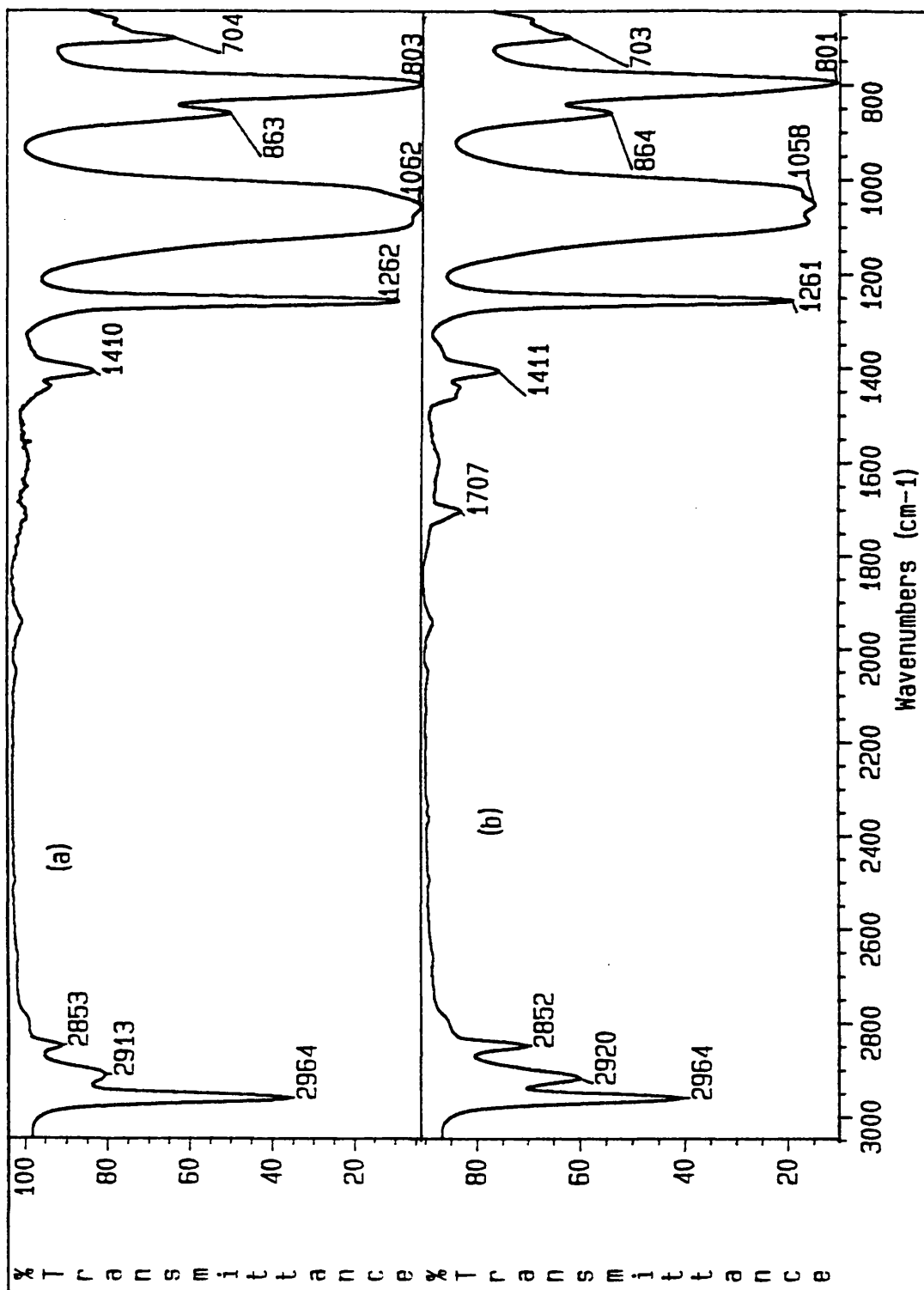


Fig. 7.60. IR spectra of the CRFs from blends of PDMS and calcium stearate:
 (a) blend 45 (1%) and (b) blend 46 (5%).

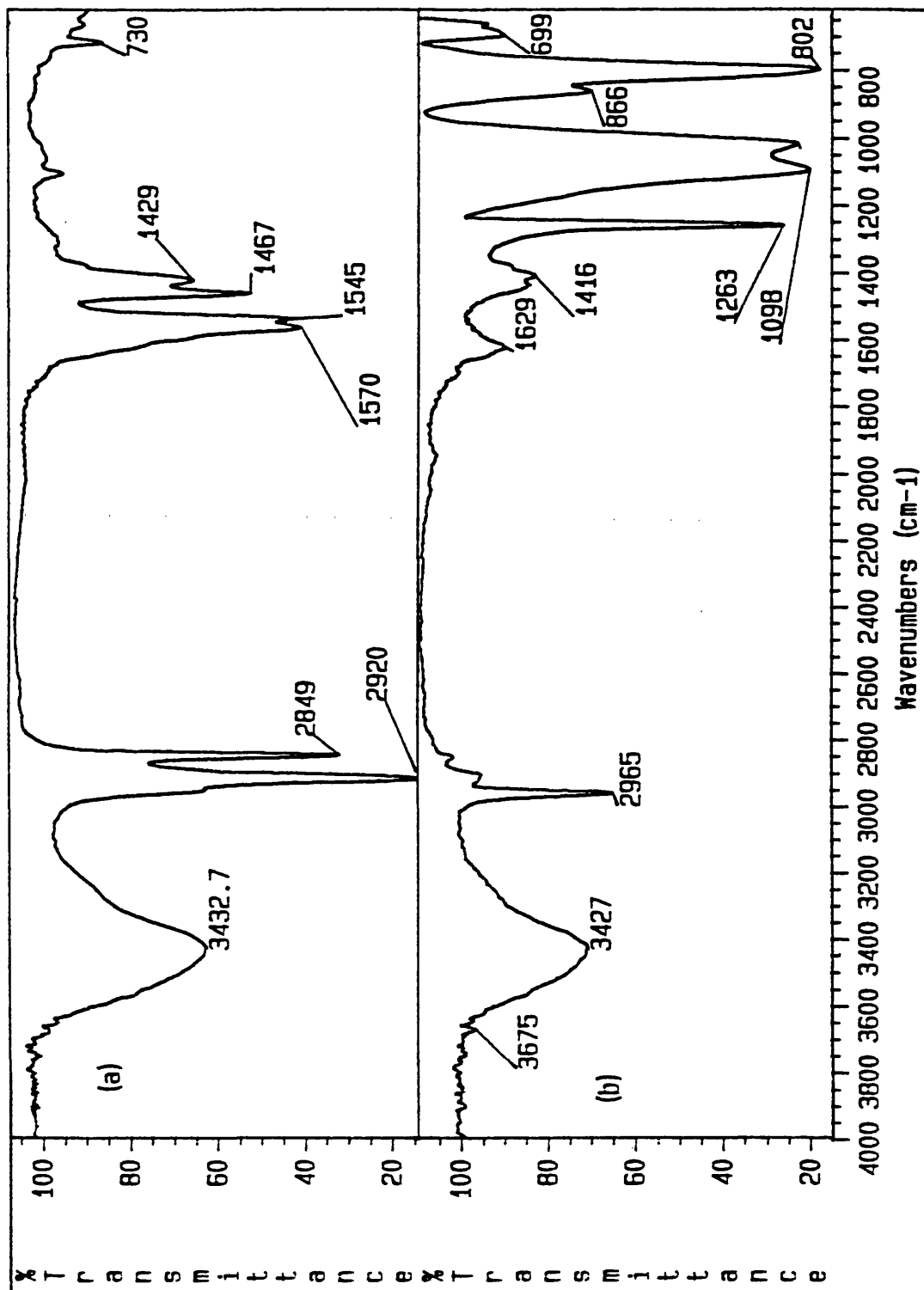


Fig. 7.61 IR spectra of (a) calcium stearate and (b) residue from blend 46 (PDMS + 5% calcium stearate).

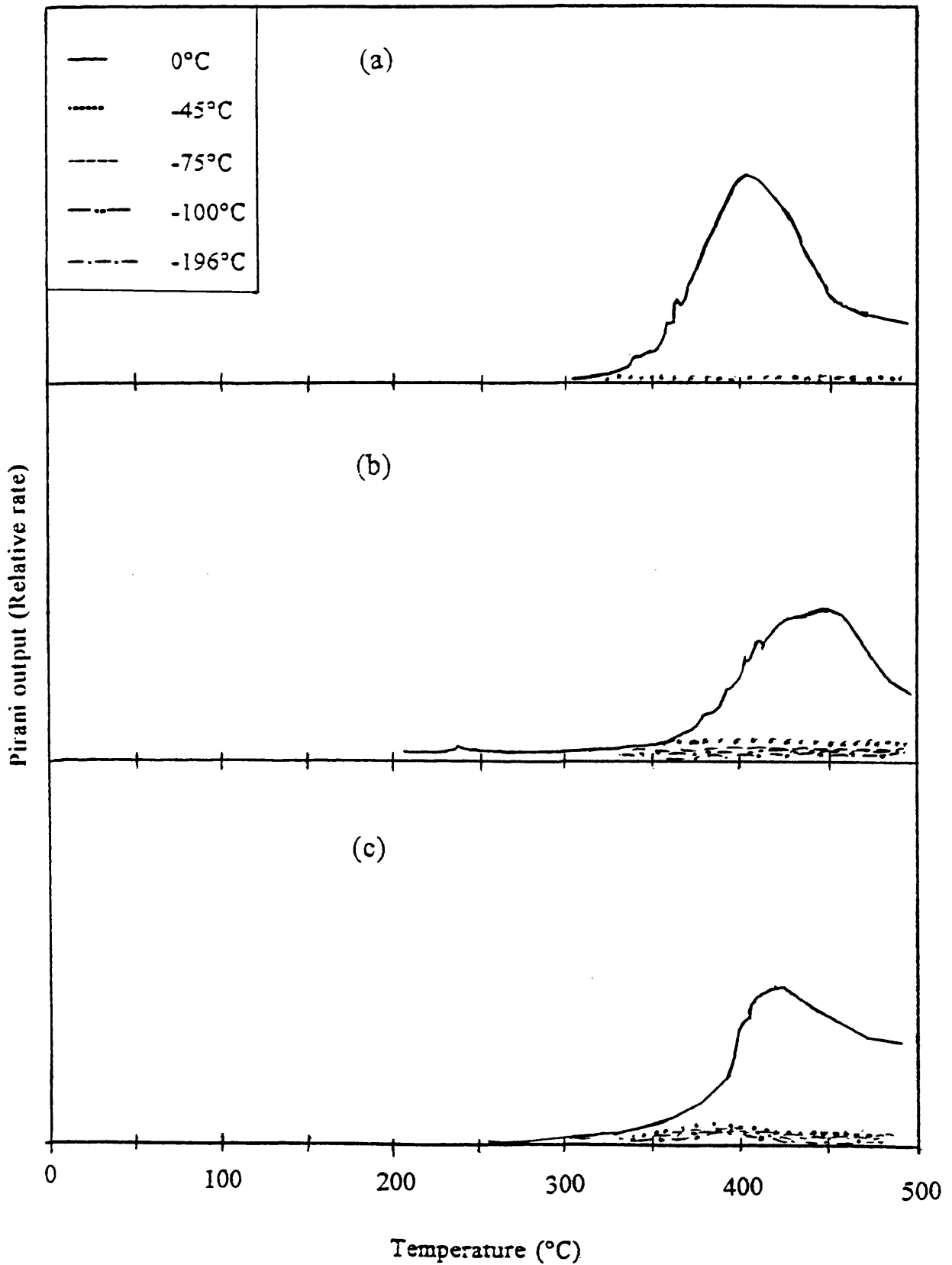


Fig. 7.62 TVA traces for blends of PDMS and stearic acid: (a) blend 47 (1%), (b) blend 48 (5%) and (c) blend 49 (20%).

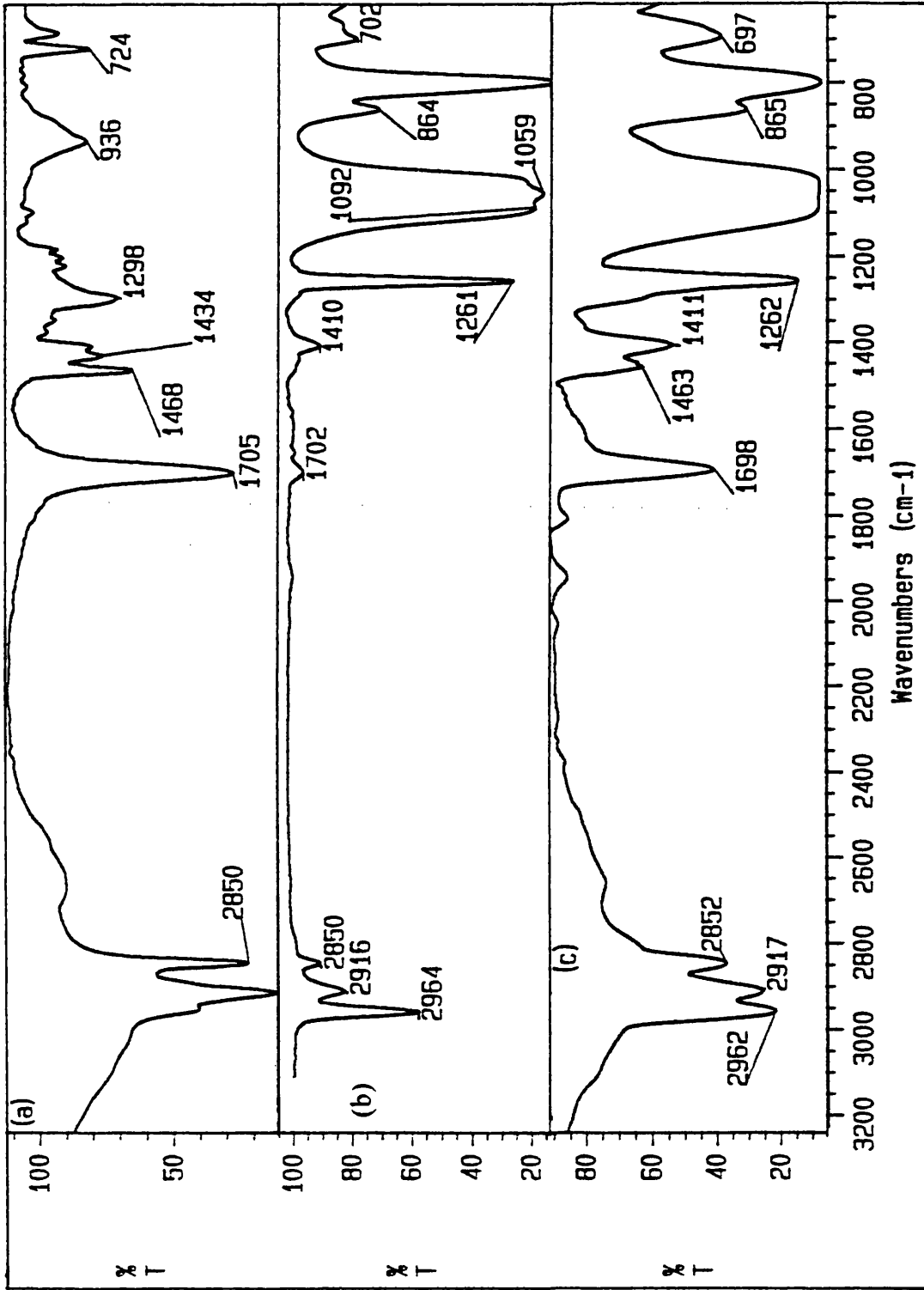


Fig. 7.63. IR spectra of (a) stearic acid, (b) CRF from blend 47 (PDMS + 1% stearic acid) and (c) CRF from blend 48 (PDMS + 5% stearic acid).

Blends 50 and 51 (silicone with saturated end groups), both with 1% DHT-4A, showed two stage degradation starting mainly at 420°C. The TVA traces of both blends (Fig. 7.64 (a-b)) were similar in shape and showed a rise mainly for the 0°C trap response and only a small rise for the -45°C trap response. There was a small amount of methane produced, starting in the region 500-650°C.

The SATVA traces for products of degradation of blends 50 and 51 at 700°C had a small peak due to CO₂ while blend 50 also showed the presence of a trace amount of ketene. The other volatile products were mainly cyclic oligomers while some trace amount of other products resulting from radical reactions were also present. The MS results and interpretations for the volatile degradation products from blend 50 are presented in Table 7.7 while GC-MS trace is given in Fig. 7.69. The IR spectra of the CRFs were similar to that of the original polymer. The residues from both blends (85.87% and 88.32%, respectively) at 480°C were rubbery, colourless, transparent, formed a smooth bubble, and were mainly insoluble. The IR spectrum of the residue from blend 50 heated at 500°C on a NaCl plate as a compressed thin film showed absorptions for both polymer and additive (Fig. 7.65 (a)) but when the blend was further heated up to 600°C (Fig. 7.65 (b)), some of the absorptions due to the additive, especially for the carbonate ions at 1368 cm⁻¹, decreased in intensity. The residues (1.18% and 0.39%, respectively) at 700°C were as colourless flakes and were not rubbery any more, but crumbled to powder. The IR spectrum of the residue at 700°C showed absorption in the region 1000-1100 cm⁻¹ due to the Si-O-Si group while the absorption due to the Si-Me group at 1261 cm⁻¹ was reduced considerably. IR spectra of DHT-4A and of the residue from blend 50 are given in Fig. 7.66 (a) and (b) respectively.

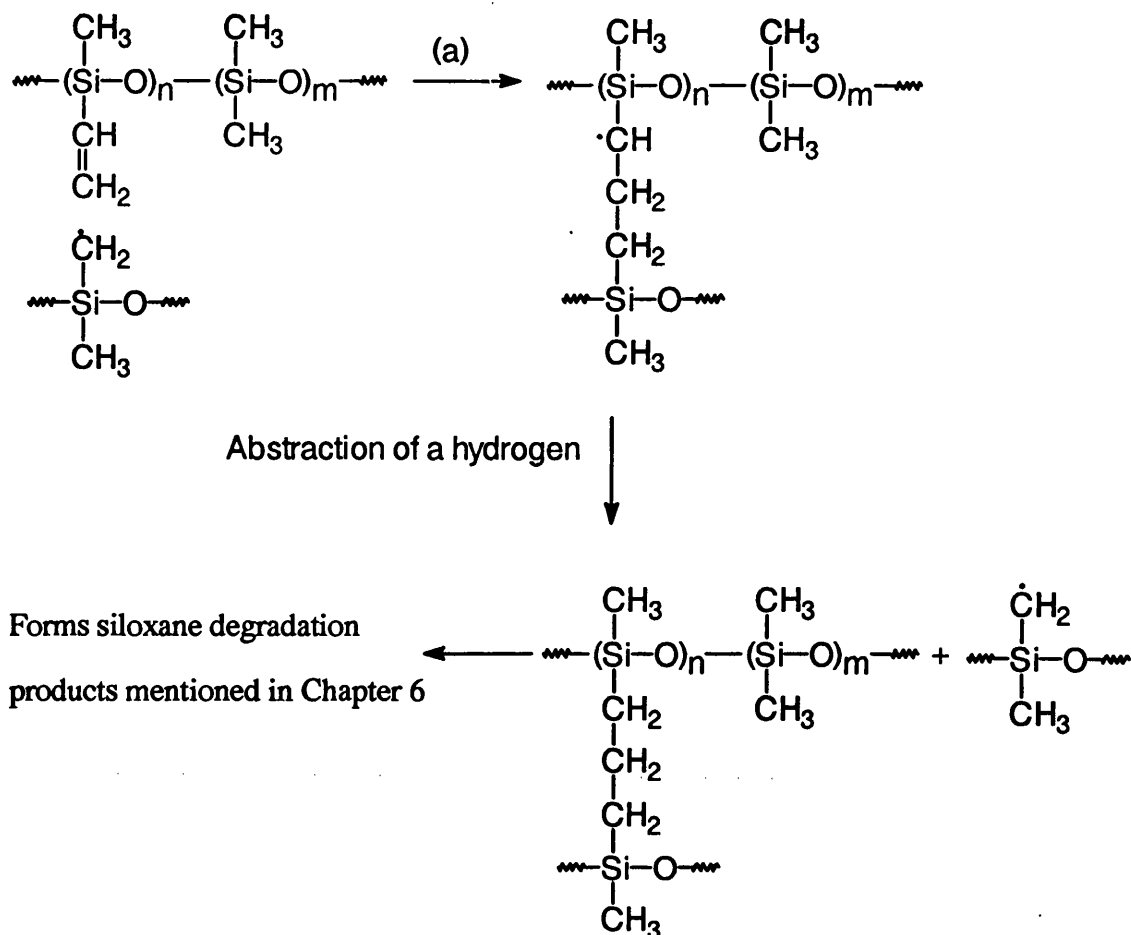
Stabilisation of blends 50 and 51 as described before is due to the catalytic effects of the additive, and the small amount of methane formed resulting from Si-C bond scission at temperatures as high as 500°C can be explained from the radical reactions taking place. The CO₂ formation is due to the additive decarboxylating as was found when it was heated alone.

The TVA trace for MgSO₄ when heated alone showed volatilisation from 50°C, with T_{max} at 120°C and the main reaction finished by 300°C. There was also a small amount of degradation starting at 325°C with T_{max} at 366°C. The main volatile product was found to be water while there was also a small amount of a gaseous product. Blend 52 (50% MgSO₄) showed a complex multistage degradation (Fig. 7.67) starting at

100°C, thus indicating the retarding of the evolution of water. The volatilisation of the non-condensable gaseous products started at 250°C and continued to 400°C. The SATVA trace showed a negligible amount of gaseous products but a lot of other volatile degradation products. The CRF was small compared to that for other blends in which degradation was complete around 500°C. The residue (36.0% at 480°C) was fluffy and did not spread on the surface of the container, but was easily broken down.

Volatilisation of blend 53 (50% CaCl₂) started at 75°C due to release of absorbed water since CaCl₂ is hygroscopic, while the degradation of the blend commenced at 375°C (Fig. 7.67 (b)) and the shape of the TVA trace was similar to that of blend 26 except the main rise was only for the 0°C trace and almost negligible rise for the -196°C trace. Degradation products were mainly low molecular weight cyclic siloxane oligomers with trace amounts of some other unidentified siloxane compounds. The residue (75.6% at 480°C) was insoluble and rubbery with a sponge-like texture and had the colour of the additive. This enhanced stabilisation and the state of the residue shows that there was an interaction between the components which results in the additive becoming unextractable from the polymer.

Sample 54 (50% CaCO₃, high vinyl silicone polymer) started to volatilise at about 308°C but the volatilisation was rather slow such that it reached T_{max} at 450°C showing a stabilisation of 50°C initially which increased to 115°C as the degradation proceeded (Fig. 7.67 (c)). The SATVA trace showed a small peak for gaseous products such as CO₂, ketene, alkenes (absorption at 912 cm⁻¹) and some volatile silicone compounds. It is logical to think that formation of ethylene from Si-CH=CH₂ bond scission would occur as in the case of Si-Me bond scission giving methane, but there was not even a trace amount of ethylene formed at temperatures up to 480°C. The GC trace of the volatile compounds showed the presence of degradation products similar to those from the pure polymer as described in Chapter 4 but there were also small amounts of other compounds resulting from radical reactions. Also, the amount of vinylmethyl-substituted cyclic siloxane oligomers decreased. This type of behaviour could be explained in terms that the vinyl groups were involved in radical reactions introduced by the coating on the filler and from the Si-Me bond scission as described in Chapter 6 and result in crosslinking.



This results in the formation of another radical in the polymer chain thus continuing the above mechanism by step (a). The role of the filler and the formation of degradation products is similar to the case of blend 26 and discussed in section 7.5.

The IR spectrum of the CRF was similar to that of the polymer. The residue (91.45%) showed small bubbles and was easily broken down to small fragments. The IR spectrum of the residue showed strong absorptions for the siloxane groups similar to those of the original polymer plus shoulders at 1165 cm^{-1} and 1385 cm^{-1} . These absorptions account for the above type of crosslinked structures (structures of the type $\text{Si}-(\text{CH}_2)_n\text{-Si}$).

7.4. Blend of Backed MgO and Cyclic Siloxane Oligomers

Backed MgO (treated to remove $\text{Mg}(\text{OH})_2$ impurity) was blended with cyclic trimer (D_3) and tetramer (D_4) of siloxane at room temperature and the blend was then heated up to 100°C under 1.9×10^{-1} mbar of pressure. The blend was further heated again from room temperature up to 480°C under normal TVA conditions. The TVA

trace indicated volatilisation throughout the heating and showed evidence for the presence of non-condensable gaseous products. The GC and MS results for the volatile products showed evidence for the presence of higher (D_3 - D_8) cyclic oligomers, with D_4 at least 4 times more than D_3 while the ratio of D_3 and D_4 was one to one in the mixture. The GC trace also showed trace amounts of other compounds found in those blends which form methane on degradation. The IR spectrum of gaseous products also gave very weak absorptions for CO_2 and at 2164 cm^{-1} , 2137 cm^{-1} due to ketene, 1265 cm^{-1} , 1091 cm^{-1} , 1026 cm^{-1} and 816 cm^{-1} due to siloxane groups. It is difficult to formulate a mechanism for the formation of ketene and there is a possibility that these absorptions in the region 2164 - 2137 cm^{-1} may be due to Si-H groups since formation of such groups could be possible from the radical reactions as discussed in section 7.5. The IR spectrum of the CRF was similar to that of pure polymer except that the absorptions at 2917 cm^{-1} and 2849 cm^{-1} were much stronger in the present case indicating the increase in methylene ($(-CH_2)_n$) groups substituted on silicon atoms.

The above kind of polymerisation was also shown when D_3 was heated with $CaCO_3$ in an evacuated sealed tube. Polymerisation in both cases was possibly carried out in the same way as the anionic polymerisation by alkaline (e.g. KOH, NaOH etc.) cleavage of D_4 e.g. in the case of MgO:

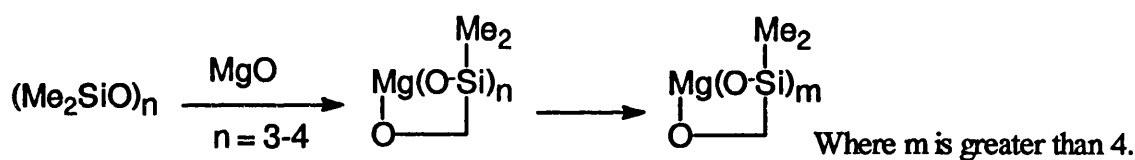


Table 7.5. IR spectra from all blends and assignments for the absorptions.

| Wavenumber (cm^{-1}) | Interpretation ⁶⁵⁻⁶⁷ |
|---------------------------------|--|
| 3584 | OH stretching of Si-OH group |
| 3085-3044 | vinyl C-H stretch, Si-CH=CH ₂ group or unsaturated hydrocarbon. |
| 2965, 2920, 2860 | C-H stretch of methyl groups on silicon atom |
| 2275-2040 | stretching absorption of Si-H |
| 1945 | overtone seen in long chained siloxane compounds |

| | |
|---------------|---|
| 1740-1709 | C=O (but there was no proof for any compound with carbonyl group from GC-MS results of volatile products) |
| 1590 | ? |
| 1489-1410 | Si-CH ₃ , antisymmetric deformation of the methyl groups |
| 1385-1352 | Si-CH ₂ -Si group |
| 1268-1256 | Si-CH ₃ , symmetric deformation of methyl groups |
| 1192-1140 | CH ₂ twisting/wagging frequency of Si-(CH ₂) ₂ -Si group (two bands) |
| 1123-1020 | asymmetric Si-O-Si stretching vibration |
| 1100-1000 | CH ₂ twisting/wagging frequency of Si-CH ₂ -Si group |
| 917 | Si-O-Ti vibration |
| 912, 826 | Si-O stretching absorption of Si-OH group |
| 952-768 | bending mode of a single hydrogen on silicon |
| 868, 874, 815 | methyl rocking and Si-C stretching of methyl group(s) |
| 858 and 800 | methyl rocking and Si-C stretching of methyl groups in O-SiMe ₂ groups |
| 714 and 669 | ? |
| 779, 750 | asymmetric Si-C-Si stretch of Si-CH ₂ -Si groups |
| 762 | methyl rocking and Si-C stretching of a single methyl on silicon atom, O-SiMe group |

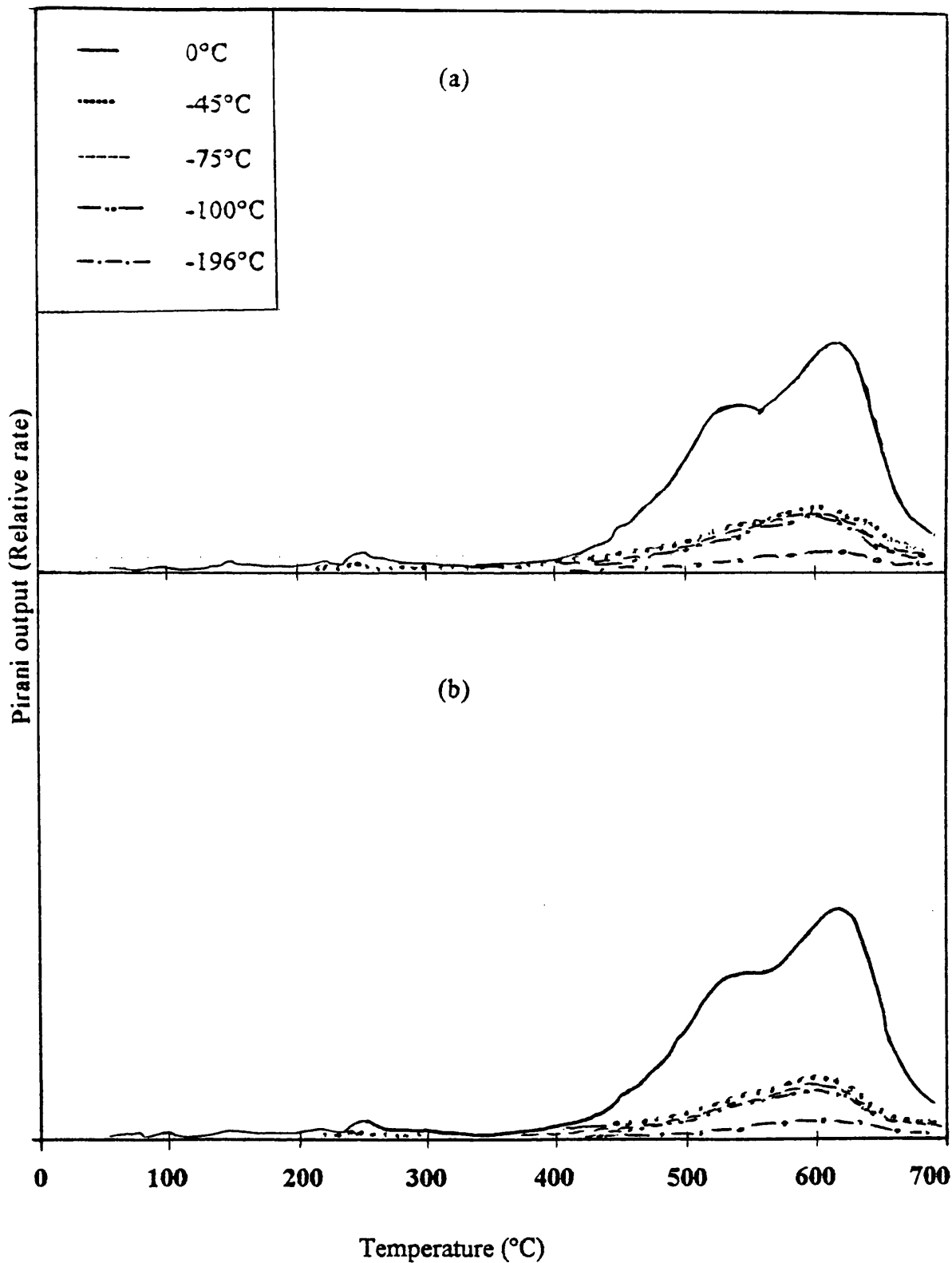


Fig. 7.64 TVA traces for blends of PDMS and 1% DHT-4A: (a) blend 50 (PDMS with vinyl end groups) and (b) blend 51 ((PDMS with trimethyl end groups).

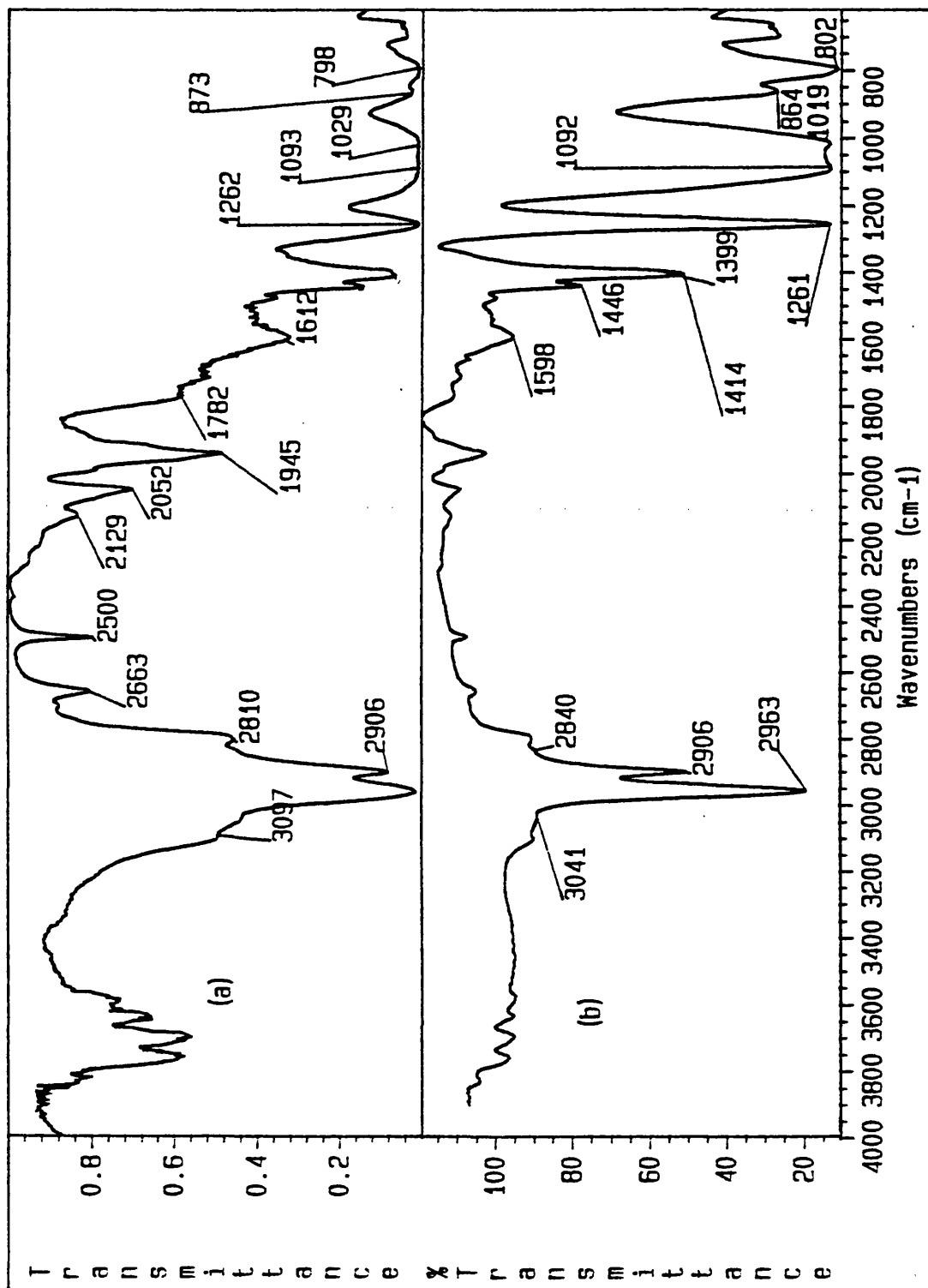


Fig. 7.65. IR spectra of residues from blend 50 (PDMS + 1% DHT-4A) heated on a NaCl plate up to (a) 500°C and (b) 600°C.

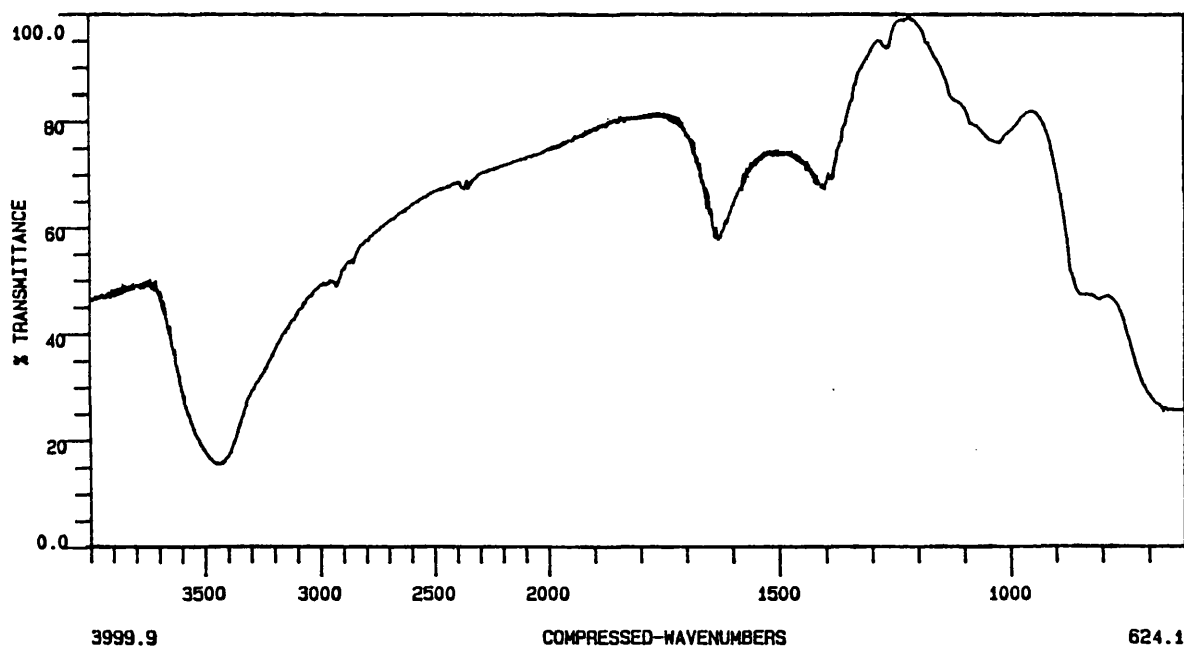
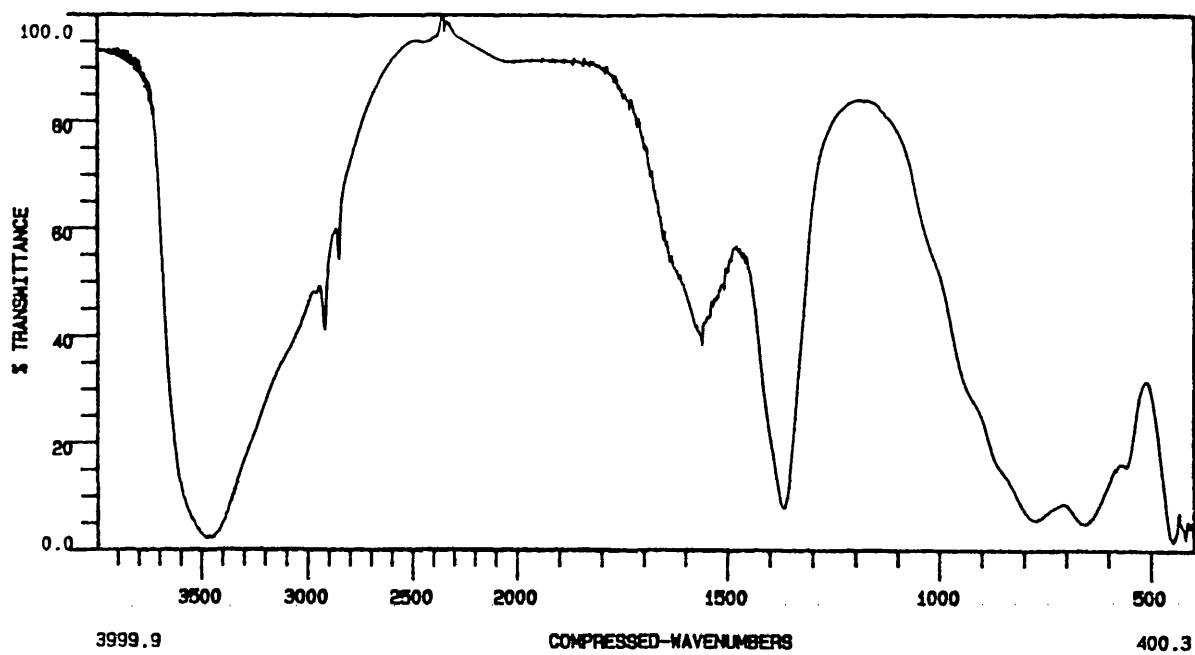


Fig. 7.66. IR spectra of (a) DHT-4A, (b) residue from blend 50 (PDMS + 1% DHT-4A) at 700°C.

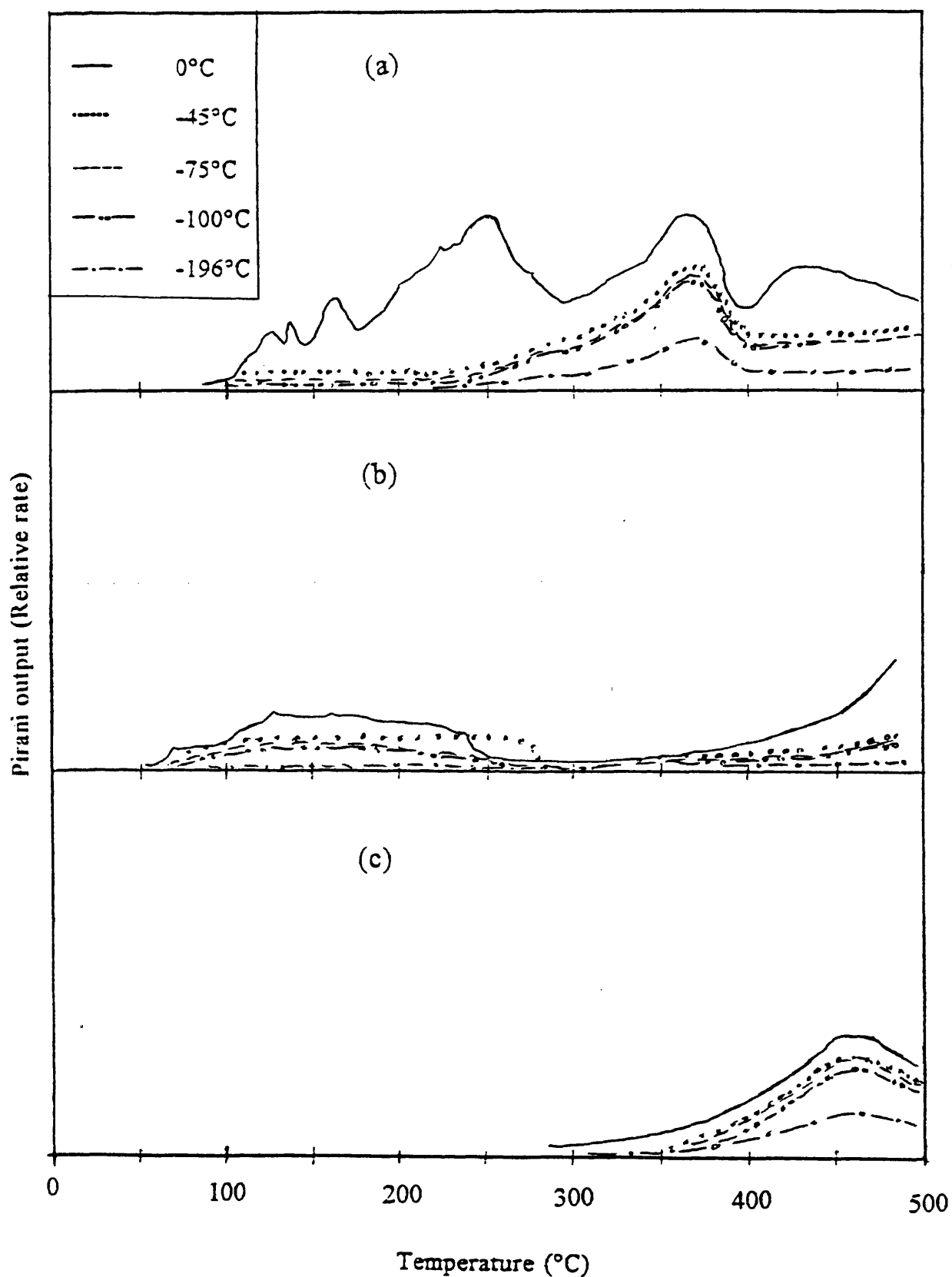


Fig. 7.67 TVA traces for blends of PDMS and 50% filler: (a) blend 52 (MgSO₄), (b) blend 53 (CaCl₂) and (c) blend 54 (PDMS with high vinyl content + CaCO₃).

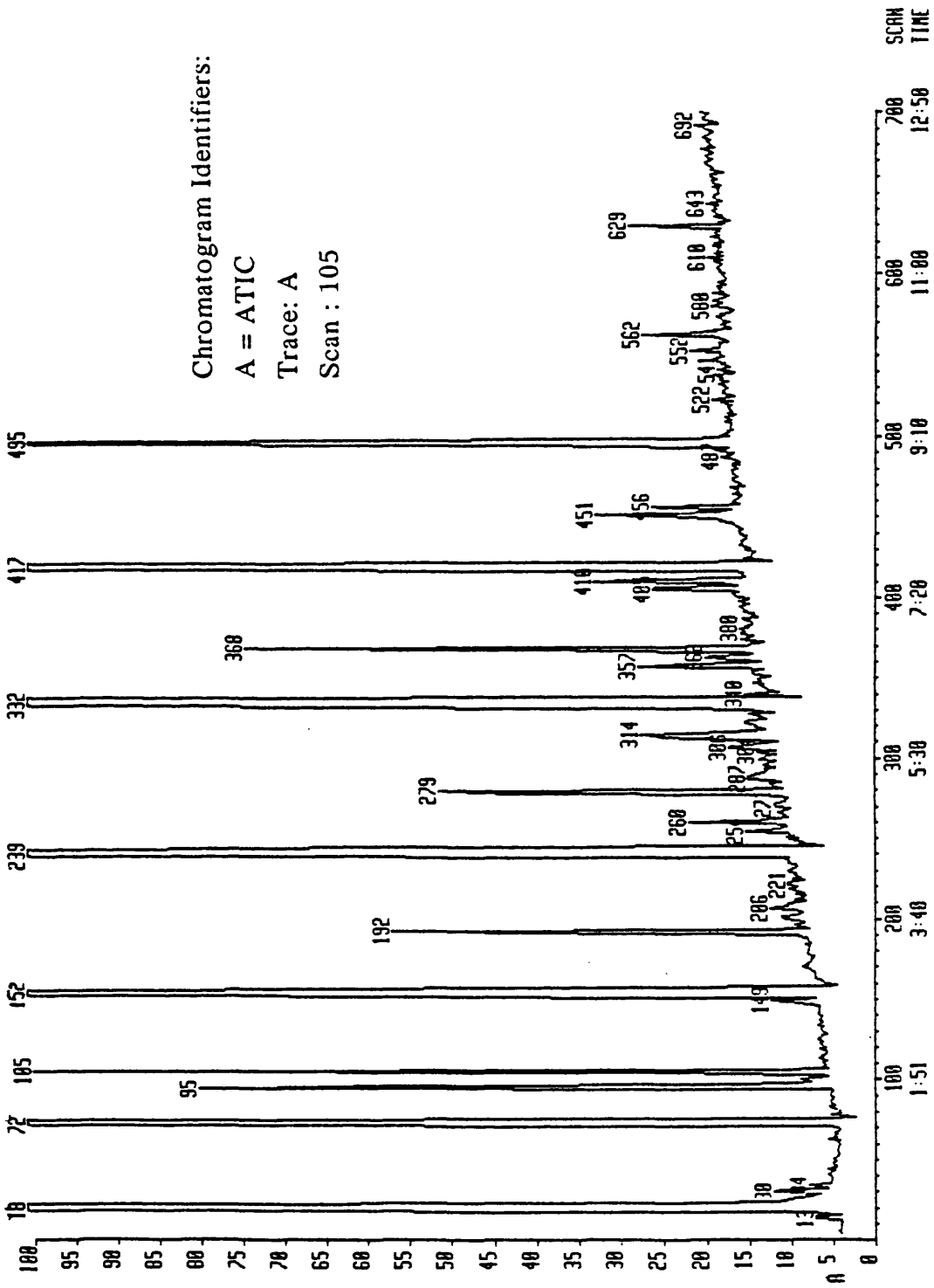


Fig. 7.68. GC trace for the liquid fraction in SATVA separation of products from the degradation of blend 48 (PDMS + 5% stearic acid).

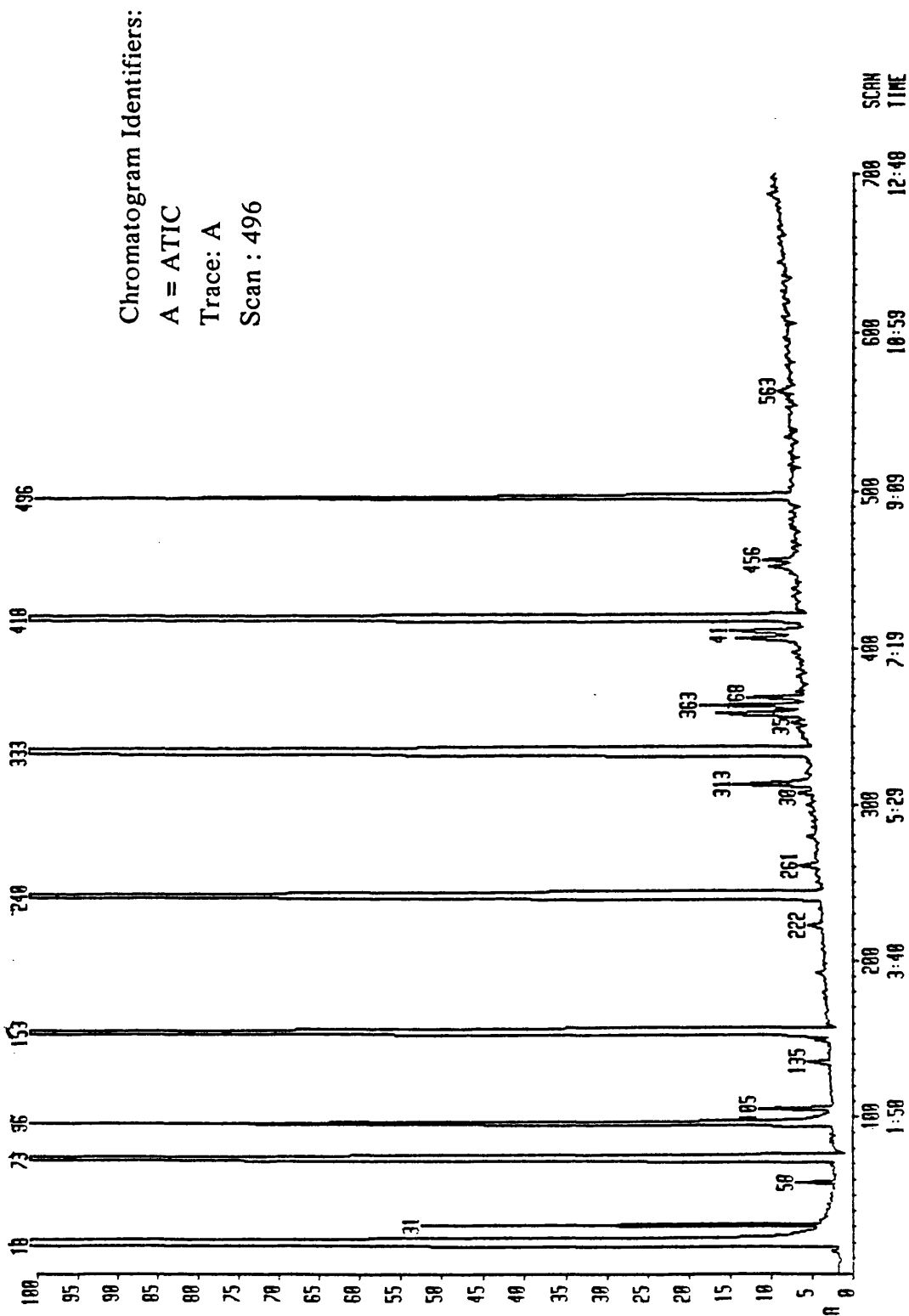


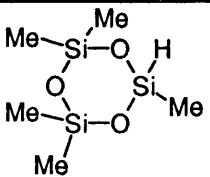
Fig. 7.69. GC trace for the liquid fraction in SATVA separation of products from the degradation of blend 50 (PDMS + 1% DHT-4A)

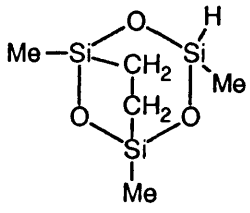
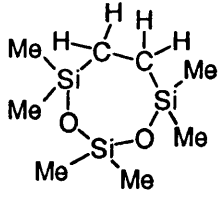
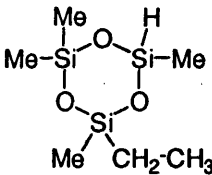
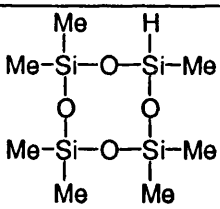
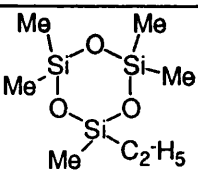
Table 7.6: Absorbance frequencies of Si-H groups in siloxane oligomers and their effects on Si-O-Si and O-SiMe¹⁵⁷.

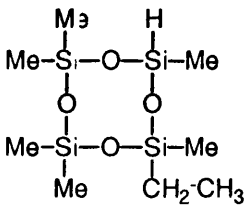
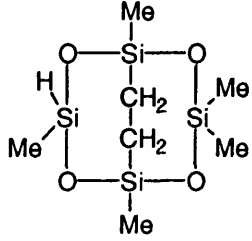
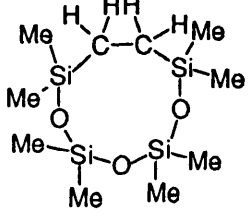
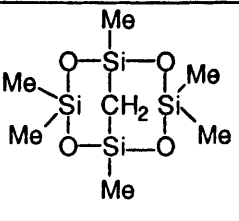
| Substance | Si-H (cm ⁻¹) | Si-O-Si (cm ⁻¹) | Si-Me |
|--|--------------------------|-----------------------------|---------------|
| D ₃ | | 1040 | 821 |
| D ₂ D ^H | 2174/2180 | 1044 | 817, 850 |
| DD ₂ ^H | 2177/2181 | 1048 | 811, 843, 886 |
| D ₄ | | 1090 (1080) | 818 |
| D ₃ D ^H | 2170 (2163) | 1097 | 818, 832 |
| D ₂ D ₂ ^H | 2169-2172 | 1100-1101 | 813, 840, 884 |

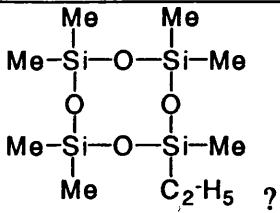
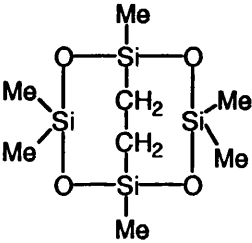
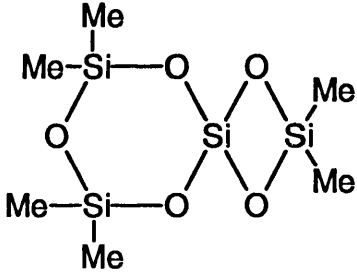
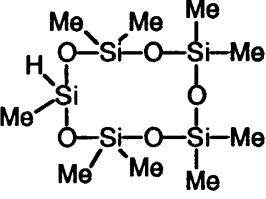
Note: Cyclic oligomers with one silicon atom substituted with one hydrogen are represented as D₂D^H, D₃D^H etc. while with two silicon with hydrogens are represented as DD₂^H, D₂D₂^H etc. Absorption values in brackets are from IR spectra in CCl₄ while others are from gas spectra.

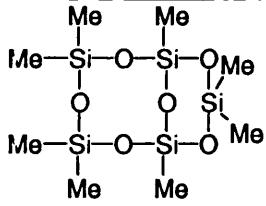
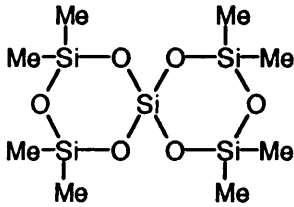
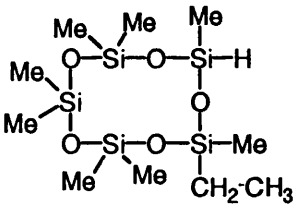
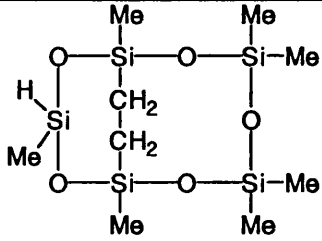
Table 7.7. Mass spectrum m/e data and assignments for fraction 3 from SATVA separation of condensable products of degradation of blend 26 after heating up to 600°C.

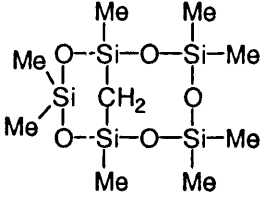
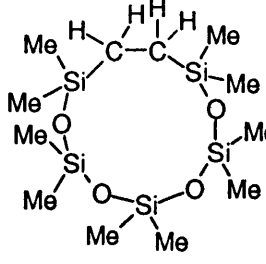
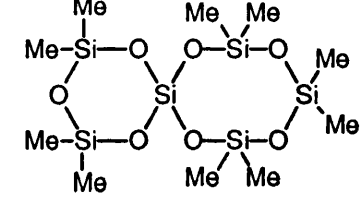
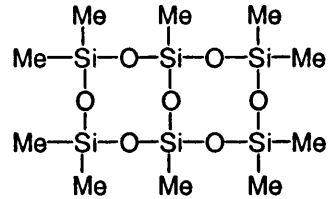
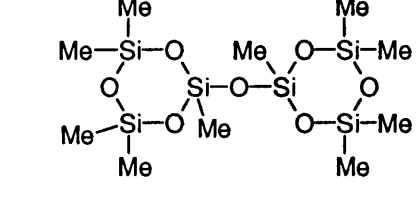
| Scan | m/e (% abundance) | Structure/Name and Boiling point ¹¹⁹ | Comments |
|------|--|--|----------|
| 30 | 97(100), 99(60), 61(50), 151(35), 117(10) | Unidentified | |
| 57 | 193(100), 194(20), 89(18), 133(15), 195(14), 207(10), 177(8), 163(6), 75(5), 103(3), 191(3), 208(1) |  (D ₂ D ^H); 1, 1, 3, 3, 5-Pentamethylcyclo-trisiloxane | Minor |
| 72 | | Hexamethylcyclo-trisiloxane (D ₃); BP = 135° | Major |

| | | | |
|-----|--|--|---|
| 98 | 205(100), 206(26), 95(25), 208(15), 189(10), 73(8), 131(5), 59(5), 220(<1) |  <p style="text-align: center;">? (D^HD₂C₂); 1, 3, 5-Trimethyl-1, 3, 5-trisila-2, 4, 6-trioxabicyclo[3.1.2]octane</p> | Trace |
| 105 | 219(100), 89(25), 220(20), 193(18), 44(18), 133(15), 207(13), 102(8), 163(5), 75(3), 234(0) |  <p style="text-align: center;">(D₃C₂); 1, 1, 3, 3, 5, 5-Hexamethyl-1, 3, 5-trisila-2, 4-dioxacycloheptane</p> | Minor in blends 45-48 but trace in others |
| 115 | 207(100), 193(30), 206(16), 208(12), 133(7), 96(6), 177(4), 221(3), 222(<1) |  <p style="text-align: center;">1, 1, 3, 5-Tetramethyl-3-ethyl, -1, 3, 5-trisila-2, 4, 6-trioxacyclohexane</p> | Trace |
| 134 | 267(100), 268(35), 193(20), 269(15), 73(10), 133(7), 281(6), 282(1) |  <p style="text-align: center;">BP = 66°/20, 165°/760; Heptamethylcyclotetrasiloxane</p> | Minor |
| 140 | 207(100), 208(25), 209(12), 147(8), 177(5), 103(5) |  <p style="text-align: center;">-C₂H₅ ? ; 1, 1, 3, 3, 5-Pentamethyl-5-ethyltricyclosiloxane</p> | Trace |
| 147 | 41(100), 43(80), 55(75), 56(60), 70(40), 83(22), 97(4) | Hydrocarbon | Trace |
| 152 | | Octamethylcyclotetrasiloxane (D ₄), BP = 175° | Major |

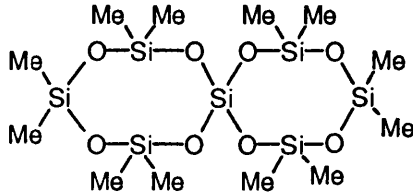
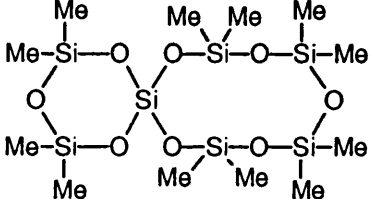
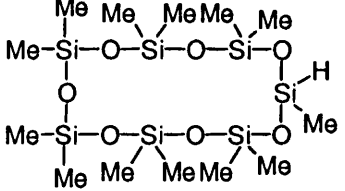
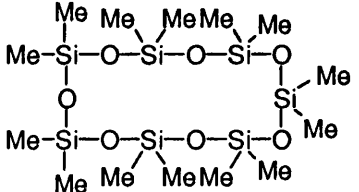
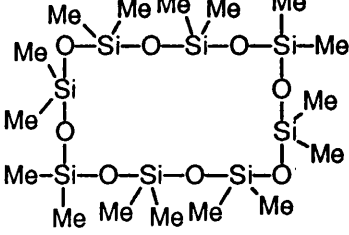
| | | | |
|-----|---|---|---|
| 163 | 281(100), 282(22), 283(11), 193(11), 73(8), 265(15), 133(13), 191(5), 249(5), 296(0) |  <p style="text-align: right;">1, 1, 3, 3, 5, 7- Hexamethyl, 5-ethyl-1, 3, 5, 7-tetrasilolane-2, 4, 6, 8-tetraoxacyclooctane</p> | Trace |
| 187 | 265(100), 266(30), 125(25), 267(16), 249(10), 191(8), 103(3), 280(0) |  <p style="text-align: right;">(D₂D₂DHC₂); 1, 3, 3, 5, 7-Pentamethyl-1, 3, 5, 7- tetrasilolane-2, 4, 6, 8- tetraoxabicyclo[3.3.2]decane</p> | Trace |
| 192 | 293(100), 294(30), 295(22), 193(20), 265(17), 73(11), 139(10), 281(8), 207(6), 59(5), 308(0) |  <p style="text-align: right;">(D₄C₂); 1, 1, 3, 3, 5, 5, 7, 7-Octamethyl-1, 3, 5, 7- tetrasilolane-2, 4, 6-trioxacyclononane</p> | Minor in blends 45- 48 but trace in others |
| 196 | 265(100), 266(20), 125(20), 207(10), 267(8), 249(5), 79(6), 191(5), 103(3), 280(0) |  <p style="text-align: right;">(D₂D₂C)¹⁵⁸; 1, 3, 3, 5, 7, 7-Hexamethyl-1, 3, 5, 7-tetrasilolane- 2, 4, 6, 8-tetraoxabicyclo[3.3.1]nonane</p> | Minor |

| | | | |
|-----|--|--|-------------------|
| 200 | 281(100), 295(85), 282(25), 193(23), 133(20), 295(18), 59(17), 233(12), 297(13), 126(10), 248(14), 251(10), 267(7). Plus 41(100), 43(80), 55(70), 69(40), 83(22), 97(4) |  <p>1, 1, 3, 3, 5, 5, 7-heptamethyl-7-ethylcyclotetrasiloxane plus Hydrocarbon</p> | Trace |
| 206 | 279(100), 280(30), 73(20), 282(18), 59(8), 191(7), 265(6), 124(6), 132(5), 133(4), 207(4), 294(0) |  <p>(D₂D₂C₂); 1, 3, 3, 5, 7, 7-Hexamethyl-1, 3, 5, 7-tetrasilolane-2, 4, 6, 8-tetraoxabicyclo[3.3.2]decane</p> | Trace |
| 210 | 267(100), 126(30), 268(28), 269(21), 193(20), 269(15), 251(14), 77(10), 134(7), 283(6), 284(4) |  <p>2, 2, 4, 4, 8, 8-Hexamethyl-2, 4, 6, 8-tetrasilolane-1, 3, 5, 7, 9-pentaoxaspiro [5.3]nonane</p> | Trace in blend 44 |
| 221 | 73(100), 267(45), 341(40), 59(25), 253(20), 193(12), 237(10), 355(5), 133(2), 356(1) |  <p>(D₄DH); Nonamethylcyclododecasiloxane</p> | Minor |

| | | | |
|------|--|--|----------------------|
| ~230 | 341(100), 73(85), 163(40), 342(30), 325(25), 155(20), 345(18), 126(10), 251(8), 59(5), 193(4), 356(0) |  <p style="text-align: center;">(D₃D₂); BP = 203°, mp = 118°; 1, 3, 3, 5, 5, 7, 9, 9-Octamethyl-1, 3, 5, 7, 9-pentasilolane-2, 4, 6, 8, 10, 11- hexaoxabicyclo[5.3.1]undecane</p> | Trace |
| 231 | 341(100), 342(32), 343(22), 73(21), 325(20), 163(18), 155(12), 251(8), 126(6), 193(4), 59(3), 356(0) |  <p style="text-align: center;">BP = 204°, mp = 121°; 2, 2, 4, 4, 8, 8, 10, 10-Octamethyl-2, 4, 6, 8, 10-pentasilolane-1, 3, 5, 7, 9, 11- hexaoxaspiro[5.5]undecane¹¹⁹</p> | Minor in blend 44 |
| 240 | | Decamethylcyclopentasiloxane (D ₅); BP = 210° | Major |
| 254 | 41(60), 43(80), 55(70), 69(40), 83(22), 97(4) | Hydrocarbon | Trace |
| 256 | 73(100), 267(18), 355(12), 325(5), 191(4), 193(2), 59(2), 291(2), 370(0) |  <p style="text-align: center;">1, 1, 3, 3, 5, 5, 7, 9-Octamethyl-7- ethylcyclopentasiloxane</p> | Trace |
| 260 | 339(100), 293(95), 265(70), 340(30), 125(28), 294(20), 267(18), 193(15), 249(12), 73(7), 354(0) |  <p style="text-align: center;">(D₂D₂D^HC₂); 1, 3, 3, 5, 5, 7, 9-Heptamethyl-1, 3, 5, 7, 9-pentasilolane-2, 4, 6, 8, 10- pentaoxabicyclo[5.3.2]dodecane</p> | Trace |

| | | | |
|-----|--|---|--|
| 265 | 339(100), 73(75), 340(30), 162(28), 153(15), 322(12), 59(8), 249(4), 193(3), 103(2), 125(2), 354(0) |  <p>(D₃D₂C)¹⁵⁸; 1, 3, 3, 5, 5, 7, 9, 9-Octaxamethyl-1, 3, 5, 7, 9- pentasila-2, 4, 6, 8, 10- pentaoxabicyclo[5.3.1]undecane</p> | Minor |
| 279 | 73(100), 85(50), 367(45), 267(26), 368(20), 269(16), 59(15), 279(15), 281(12), 249(10), 191(8), 207(4), |  <p>(D₅C₂); 1, 1, 3, 3, 5, 5, 7, 7, 9, 9-Decamethyl-1, 3, 5, 7, 9- pentasila-2, 4, 6, 8-tetraoxacycloundecane</p> | Minor in blends 45- 48 but trace in others |
| 290 | 327(100), 415(90) 73(68), 59(18), 416(38), 328(33), 417(28), 329(26), 399(13), 297(8), 192(6), 430(0) |  <p>2, 2, 4, 4, 6, 6, 10, 10, 12, 12-Decamethyl-1, 3, 5, 7, 9, 11, 13-hepta-oxa-2, 4, 6, 8, 10, 12- hexasilaspiro[7.5]tridecane¹¹⁹</p> | Trace in other blends but minor in blend 44 |
| 294 | 73(100), 327(32), 415(25), 59(3), 207(2), 193(2), 430(0) |  <p>1, 3, 3, 5, 5, 7, 9, 9, 11, 11-Decamethyl-1, 3, 5, 7, 9, 11- hexasila-2, 4, 6, 8, 10, 12, 13- hepta-oxabicyclo[5.5]tridecane¹¹⁹</p> | Trace |
| 306 | 73(100), 41(78), 43(75), 55(52), 69(38), 83(25), 97(15), 327(12), 415(10), 59(3), 207(2), 430(0) |  <p>1, 1- Bis(pentamethylcyclotrisiloxane)ether¹¹⁹ + Hydrocarbon compound</p> | Trace |

| | | | |
|-----|---|---|---|
| 314 | 73(100), 341(40), 327(22) 59(18), 325(16), 415(15), 147(8), 133(6), 207(3), 311(2), 429(1), 430(0) | <p style="text-align: right;">(D₅DH);</p> <p style="text-align: center;">Undecamethylcyclohexasiloxane</p> | Minor in others but trace in blend 44 |
| 332 | | <p style="text-align: center;">Dodecamethylcyclohexasiloxane (D₆);</p> <p style="text-align: center;">BP = 245°</p> | Major |
| 349 | 73(100), 325(50), 413(40), 414(15), 326(10), 147(2), 191(1), 193(1), 207(1), 428(0) | <p style="text-align: right;">(D₄D₂C)¹⁵⁸;</p> <p style="text-align: center;">1, 3, 3, 5, 5, 7, 9, 9, 11, 11-Decamethyl- 1, 3, 5, 7, 9, 11-hexasila-2, 4, 6, 8, 10, 12-hexaoxabicyclo[5.5.1]tridecane</p> | Trace |
| 357 | 43(100), 41(95), 55(70), 57(50), 69(40), 83(35), 97(20), 207(10) 111(5), | Hydrocarbon | Trace |
| 368 | 73(100), 85(36), 341(15), 59(12), 441(10), (147(7), 352(6), 442(4), 207(3), 456(0) | <p style="text-align: right;">(D₆C₂);</p> <p style="text-align: center;">1, 1, 3, 3, 5, 5, 7, 7, 9, 9, 11, 11- Dodecamethyl-1, 3, 5, 7, 9, 11-hexasila-2, 4, 6, 8, 10-pentaoxacyclotridecane</p> | Minor in blends 45- 48 but trace in others |

| | | | |
|-----|--|---|----------------------|
| 375 | 73(100), 401(85), 489(50), 402(40), 403(30), 385(22), 490(18), 327(15), 59(14), 147(12), 297(10), 163(8), 207(7), 504(0) |  <p>2, 2, 4, 4, 6, 6, 10, 10, 12, 12, 14, 14-Dodecamethyl-2, 4, 6, 8, 10, 12, 14-heptasila-1, 3, 5, 7, 9, 11, 13, 15-octaoxaspiro [7.7]pentadecane</p> | Minor in blend 44 |
| 385 | 73(100), 401(45), 489(30), 402(28), 341(20), 403(17), 441(16), 385(15), 491(13), 327(11), 353(11), 163(10), 147(9), 59(7), 207(7), 504(0) |  <p>2, 2, 4, 4, 6, 6, 8, 8, 12, 12, 14, 14-Dodecamethyl-2, 4, 6, 8, 10, 12, 14-heptasila-1, 3, 5, 7, 9, 11, 13, 15-octaoxaspiro[9.5]pentadecane</p> | Minor in blend 44 |
| 400 | 73(100), 147(25), 281(22), 327(20), 59(10), 133(8), 415(6), 207(5), 489(3), 504(0) |  <p>(D₆DH); Tridecamethylcycloheptasiloxane</p> | Trace |
| 418 | 73(100), 147(45), 281(40), 327(7), 415(4), 207(3), 503(2), 518(0) |  <p>(D₇); Tetradecamethylcycloheptasiloxane</p> | Major |
| 496 | 73(100), 44(58), 147(22), 355(10), 221(8), 281(7), 401(4), 207(3), 592(0) |  <p>(D₈); Hexadecamethylcyclooctasiloxane</p> | Major |

| | | | |
|-----|---|--|-------|
| 552 | 149(100), 41(20), 43(17), 57(15), 79(4), 207(3) | Some hydrocarbon + (D ₉); Octadecamethylcyclononasiloxane | Trace |
|-----|---|--|-------|

Note: Nomenclature of the compounds is based on the rules set out in reference 119.

The structures of the products were proposed after consideration of experimental evidence of various kinds as follows:

- the m/e values of parent ions minus methyl group.
- absorption peaks of the IR spectra
- homologous series could often be proposed from smooth plots of retention times or scan values against molecular weights or number of repeating units or atoms, as shown in Fig. 7.70 for the cyclic oligomers of the type (D₃, D₄ etc.)¹⁵⁹, while Figs. 7.71-7.74. represent (D₂D^H, D₃D^H etc.), (D₂D^HC₂, D₃D^HC₂ etc.), (D₃C₂, D₄C₂ etc) and (D₂D₂C, D₃D₂C etc.) types of compounds. The X axis represents the molecular weight while the y axis represents scan values.

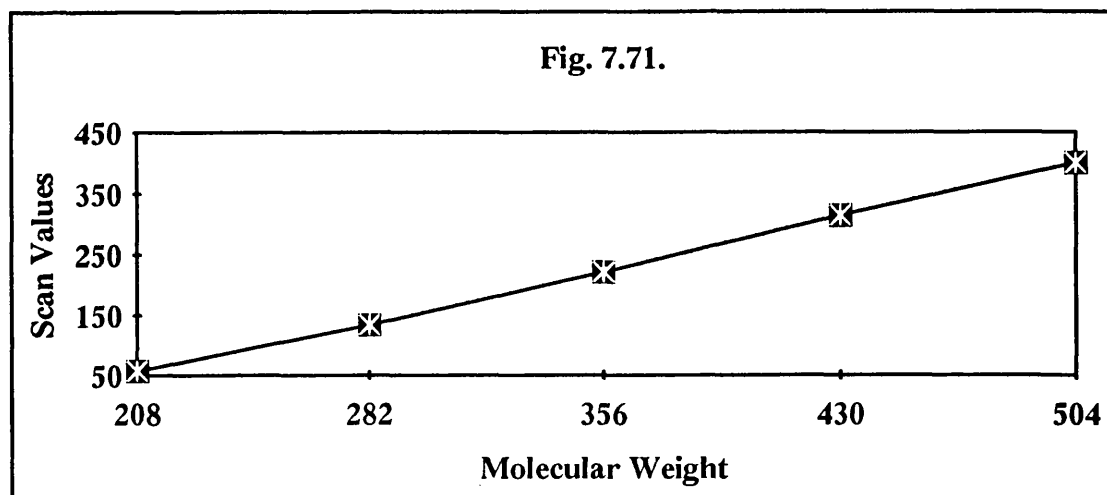
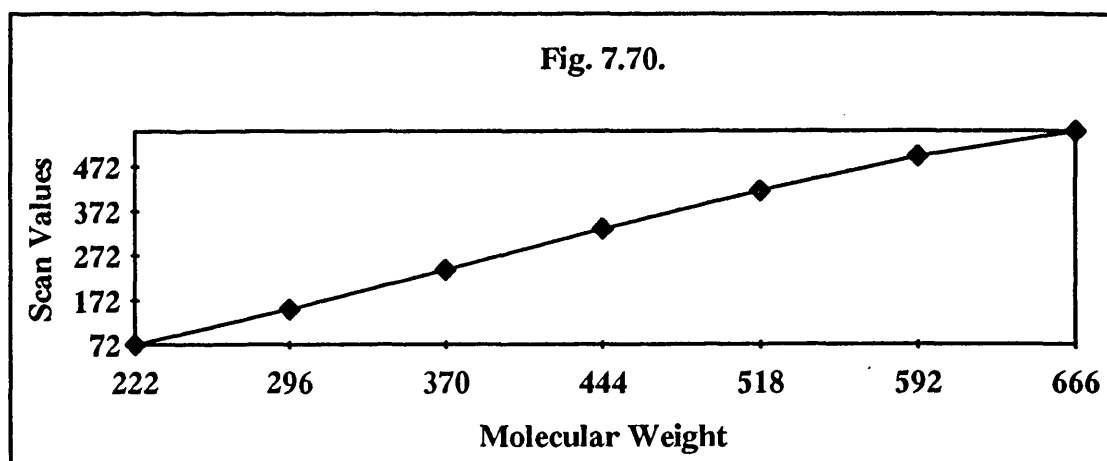


Fig. 7.72.

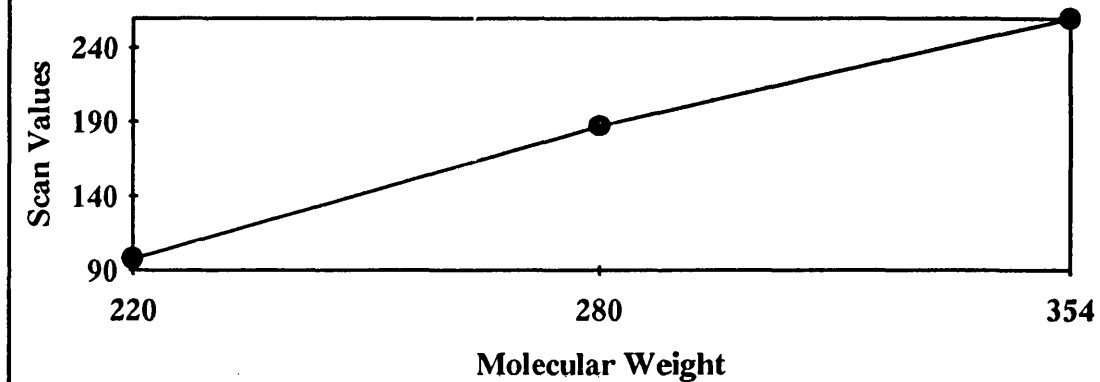


Fig. 7.73.

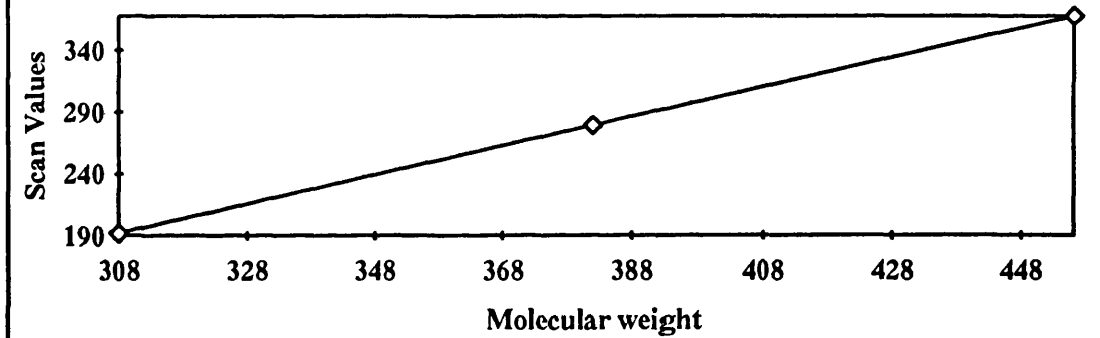
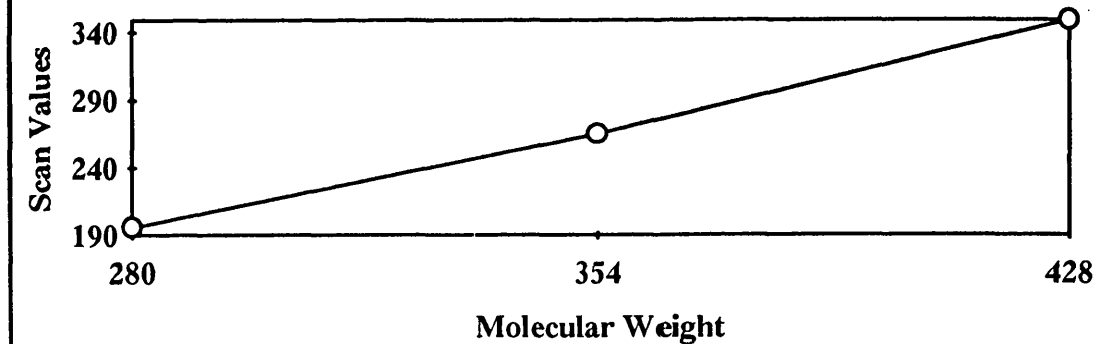


Fig. 7.74.



7.5. MECHANISMS OF FORMATION OF DEGRADATION PRODUCTS FROM PDMS AND INORGANIC FILLERS

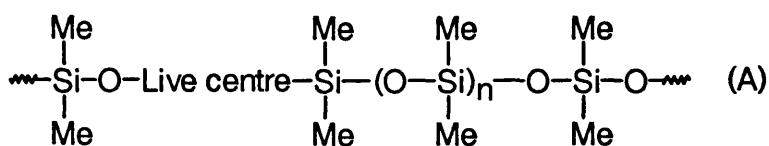
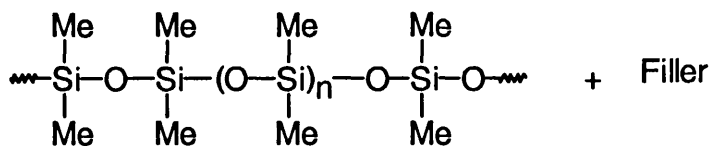
Blends of PDMS and Inorganic fillers

The fact that all blends were stabilised at least to some extent depending on the type of filler and percentage content, and formed insoluble, rubbery residues implies that the mechanism of formation of the degradation products has been changed in the presence of fillers/additives. This was also confirmed by the trace amounts of ketene, $\text{H}_2\text{C}=\text{C}=\text{O}$, which was not produced in the case when polymer was degraded alone. Most inorganic fillers caused the formation of methane, cyclic compounds with $-\text{CH}_2-\text{CH}_2-$ and $-\text{CH}_2-\text{CH}_2-\text{CH}_2-$ linkage and bicyclic compounds with methylene or $-\text{CH}_2-\text{CH}_2-$ linkage. The ability of the filler to stay intact with the polymer before complete degradation indicates that there was interaction between the components which made the systems stable.

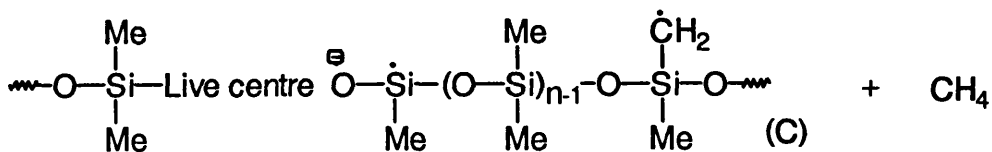
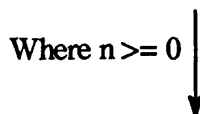
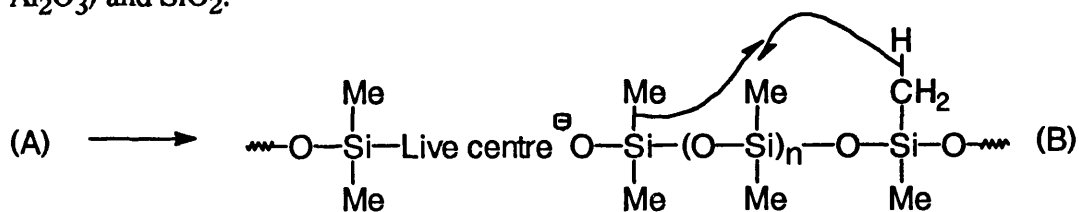
The initial stabilisation of the polymer in the presence of a filler can be due to the reduction in the flexibility of the PDMS chain which allows it to twist and change shape. The following factors lead to the restriction of the mobility of the polymer chains in filled PDMS: (i) the bonds due to polymer-filler adsorption and (ii) steric hindrance due to the presence of solid particles of the filler and their aggregation. Thus the formation of cyclic siloxane oligomers in the breakdown of PDMS, in which depolymerisation occurs by random elimination or from chain ends (if active) by cleavage of Si-O bond, is difficult, thus raising the threshold degradation temperature. However, stabilisation at higher temperatures is due to interaction occurring between the components in the temperature region 200-300°C. This results in the formation of polymer-filler and also polymer-polymer bonds due to crosslinking of the polymer radicals. There is the possibility for the formation of 'live' active centres, (where 'live centre' refers to centres of the type $-\text{Si}-\text{O}-\text{MCO}_3-\text{Si}-$ and $-\text{Si}-\text{O}-\text{M}-\text{O}-\text{Si}-$, $\text{M} = \text{Ca}, \text{Mg}, \text{Ti}$ etc.) permitting fixing of the filler to the polymer chain, which also explains the ability of the polymer to stay intact with the filler before complete degradation. The partial ionic nature of the Si^+-O^- bond in PDMS chain would not only be expected to assist adsorption at the surface of the active filler but also to facilitate reaction with it. Electron microscope prints confirm the interaction between the fillers and PDMS. Formation of cyclic siloxane oligomers then occurs at higher temperatures in siloxane segments in the same way as in PDMS, described in Chapter 4.

Formation of methane also indicates that there are some bonds in the polymer backbone other than the normal Si-O-Si bonds, which have a weakening effect on the neighbouring Si-CH₃ bonds and a strengthening effect on the Si-O bonds. 'Live' centres

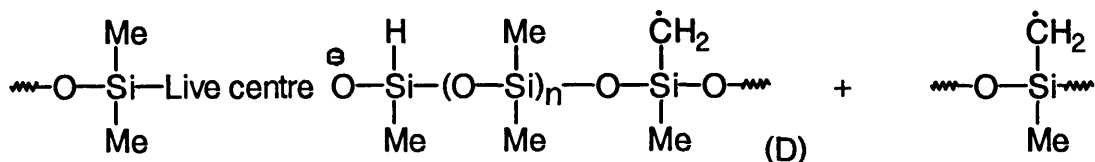
introduced in the polymer chain would cause this result due to their ability to withdraw electrons both by inductive effect and resonance. The following mechanism is proposed for the formation of active 'live' centres and then the formation of methane by a free radical mechanism seems more reasonable:



where 'live centre' refers to MCO_3 ($\text{M} = \text{Ca}$ or Mg), metal oxides (CaO , MgO , TiO_2 and Al_2O_3) and SiO_2 .

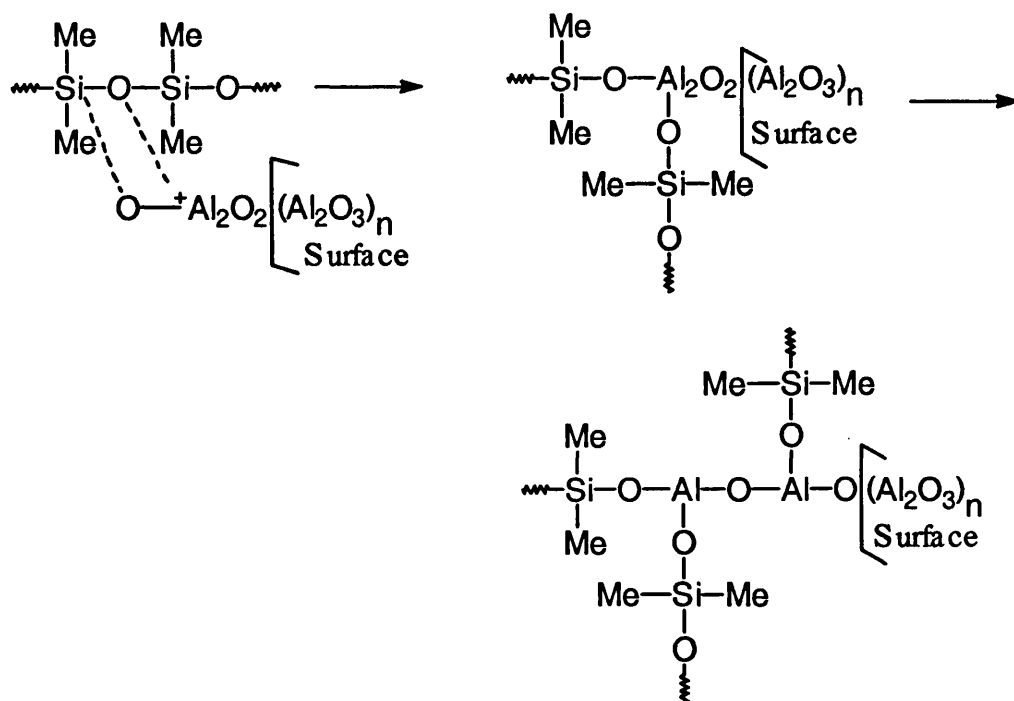


Abstraction of a hydrogen by silicon atom



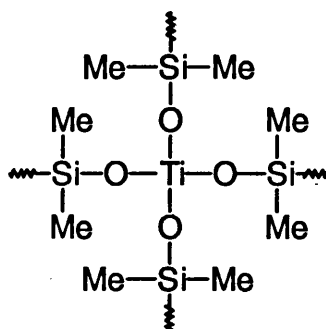
Bicyclic compounds with methylene links of the type shown above were revealed by GC-MS of most blends which produced methane (Table 7.7). There would be larger oligomers of these types but due to their involatility these would appear as CRF. Blend 44, however, did not form these bicyclic oligomers.

Most of the fillers formed methane from the chain (B) as shown above and formed most other compounds thereafter but Al_2O_3 was an exception which did not result in formation of methane while SiO_2 formed only trace amount of methane. It seems that more basic the filler, the more Si-C bond scission occurs. Since other fillers which reacted with the polymer and thus caused the breaking of Si-C bond are basic compounds while Al_2O_3 is amphoteric, this different chemical nature of Al_2O_3 is possibly the reason for the normal depolymerisation of the polymer which occurs resulting in the formation of cyclic siloxane oligomers by Si-O bond cleavage instead of the breaking of Si-C bonds. It also seems that fillers, especially metal oxides, which have NaCl type of structure result in formation of more methane possibly due to their easy interaction with the polymer while fillers which have complex structures such as the TiO_2 rutile structure, although they stabilise the polymer considerably by interaction, do not form large quantities of methane. However, it is clear that the polymer is chemically involved with the Al_2O_3 since its extraction from the filler at 400°C was not possible. The sponge like texture of the residue from blends containing Al_2O_3 and $\text{Al}(\text{OH})_3$ suggests that the polymer chains were rather branched so that possibly the filler eventually forms a structure of the type:



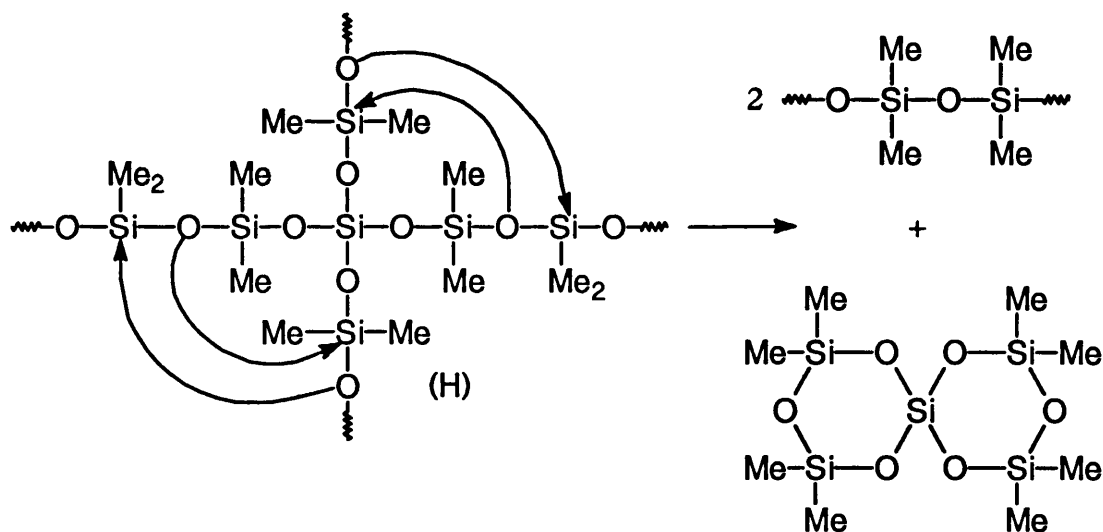
The degradation products are formed from the siloxane segments by depolymerisation as described in Chapter 4.

TiO₂ would be expected to form eventually a structure of the type:

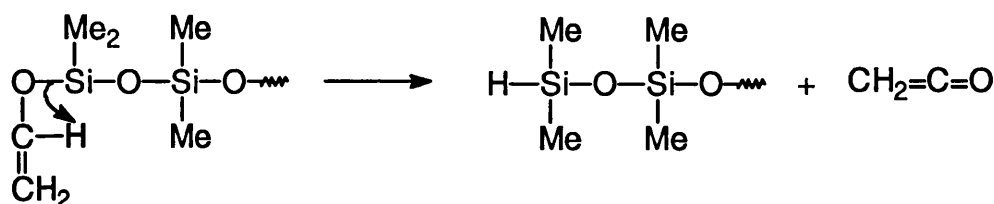


but the texture of the residue is more like the texture of the residues from the NaCl type fillers since above type of structure would result in a residue with sponge like structure.

Silica although is always tetrahedrally bound to four oxygen atoms, but the bonds have considerable ionic character and this possibly is the cause of formation of trace amounts of methane. SiO₂ would result in the formation of a structure of the type (H) as given below. This structure then depolymerises to form the corresponding compound as shown and larger oligomers. The GC-MS results are given in Table 7.7.

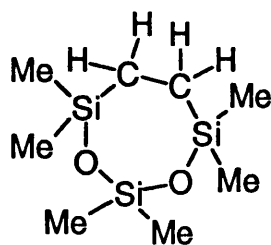


Formation of Ketene



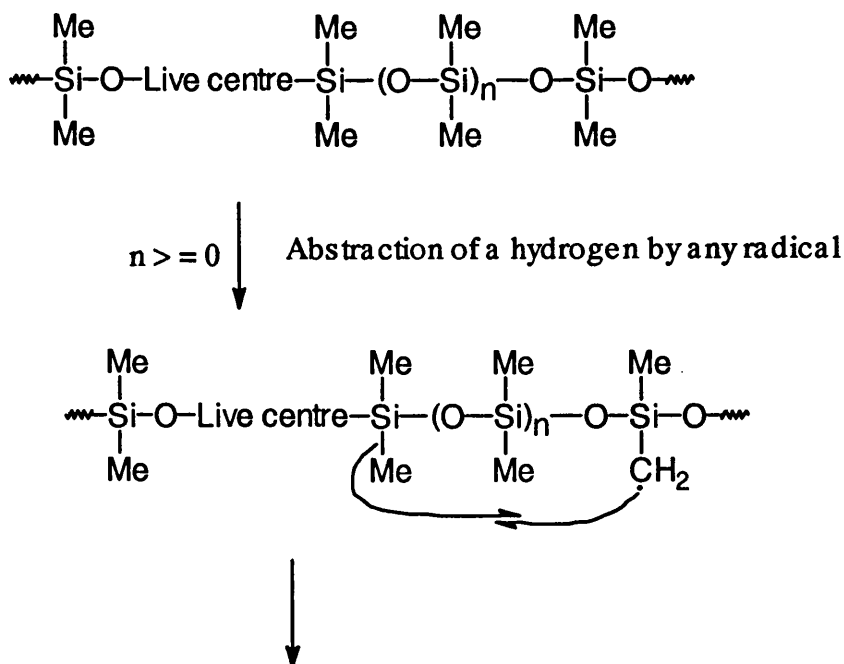
Formation of Other compounds

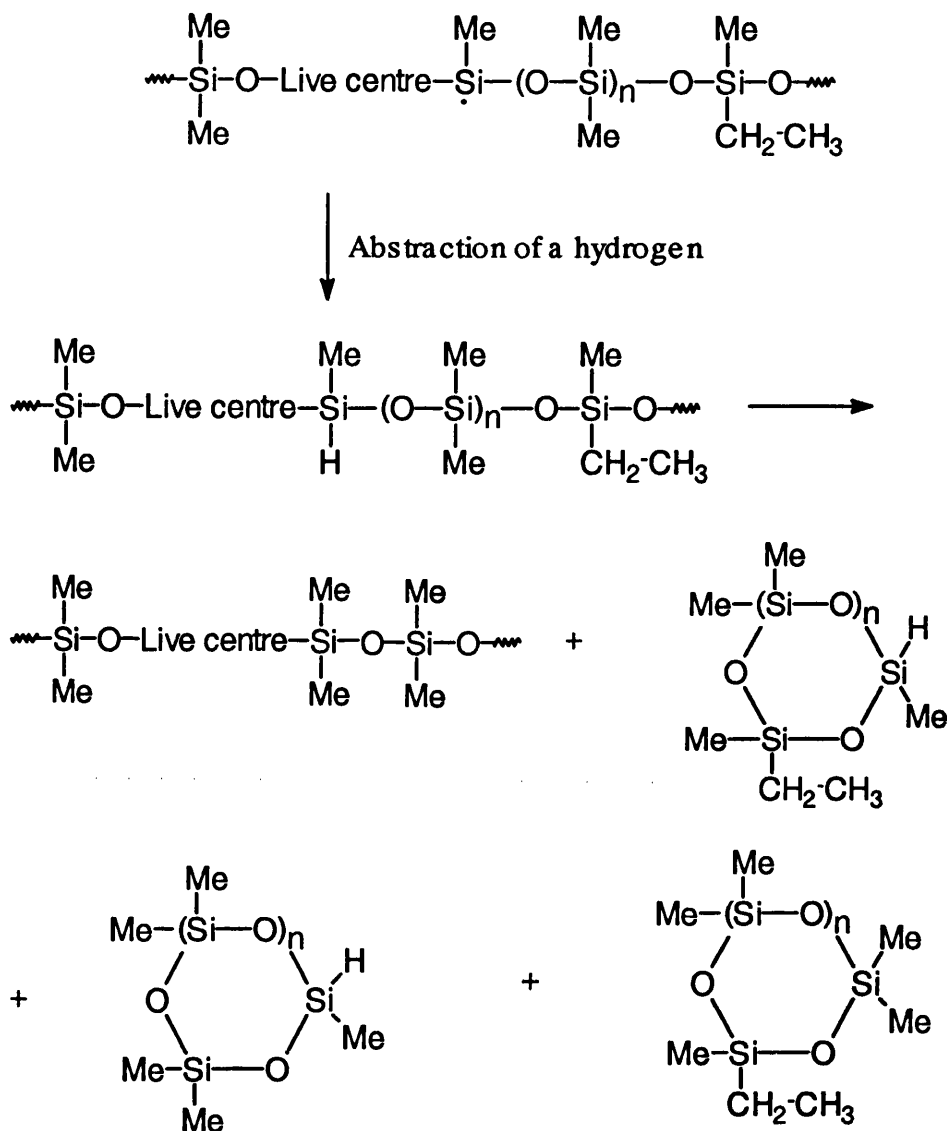
There were also trace amounts of cyclic compounds with $-(\text{CH}_2)_2-$ links instead of oxygen as in siloxanes from the blends with coated fillers, while they were second most dominant compounds after the cyclic siloxane oligomers in the blends with stearic acid and calcium stearate as additives. The proposed structure of one of these compounds is given below but there were larger molecular weight compounds in this series as well as given in Table 7.7.



The proposed mechanism for their formation is similar to that described in Chapter 6 but the reasonable explanation for such mechanism is difficult since the expected compounds should be bicyclic compounds with $-(\text{CH}_2)_2-$ links.

There were also compounds possibly with one silicon atom with one ethyl group substituted instead of both methyls. The following mechanism is proposed for their formation:





7.6. CONCLUSIONS

Most fillers/additives used stabilise PDMS by chemical interactions with the polymer and also by acting as heat sinks. In such cases an increase in the percentage content of the filler increased the stability of the polymer-additive system.

The fillers/additives have same stabilisation effects on polymer samples with different end groups.

The additives which have prolonged effects on stability of the polymer even with 1% content clearly are not acting as heat sinks but are interacting chemically. The degradation products were almost exclusively cyclic siloxane oligomers.

Basic inorganic fillers caused the scission of a Si-C bond near the point of filler-polymer interaction due to the electron-withdrawing effects caused by interaction. This resulted in the formation of methane by radical reactions. Si-C bond scission increased with increasing basicity of the filler while amphoteric metal oxides have no effect in weakening the Si-C bond.

The main degradation products from all blends investigated were still cyclic siloxane oligomers, D₃-D₂₄ as were found from the pure PDMS, with cyclic trimer, D₃, being the major product. However, cyclic and bicyclic products with methylene and -(CH₂)₂- links were also present in the case of blends which produced methane on degradation.

Blends which have a possible radical source either from an additive with a large alkyl group, or a coating on the filler, produced new products containing mainly -(CH₂)₂- links. Radical sources also cause crosslinking of the polymer.

Crosslinking follows hydrogen abstraction from the methyl groups on silicon atoms, thus making the polymer more stable and insoluble.

Interaction between the components occurs at temperatures lower than the true depolymerisation temperature of the polymer.

Small amounts of impurities affect the degradation behaviour and the stability of the polymer. The amount of stabilisation depends on the type of impurity and the percentage content.

Particle size, type and surface treatment of the filler also have great effects on the stabilisation of the polymer. Fillers with smaller particle size and highly surface treated for better dispersion, show most stabilisation.

Cyclic trimer and tetramer (possibly others as well) polymerise in the presence of a filler and this polymerisation is more in a closed system than under continuous vacuum conditions. The polymerisation from the degradation products possibly would be more important in the case of blends which form rubbery and bubble-like residues before complete degradation. PDMS with most additives forms a thick rubbery skin on the top of the sample. This forms a protective shield and prevents the degradation products from escaping. Polymerisation of degradation products in such cases to larger oligomers is likely.

Fillers which form chemical bonds with the polymer and decompose themselves at lower temperatures, initiate the degradation of the polymer at lower temperature as well but the overall effect may result in stabilisation of the polymer.

Metal hydroxides which have free hydrogens on the surface for interaction lead to the formation of great quantities of methane at their decomposition temperatures. Amphoteric metal hydroxides (show both basic and acidic properties e.g. $\text{Al}(\text{OH})_3$) are more effective in this reaction than basic hydroxides.

PDMS retards the decomposition of fillers at their true decomposition temperatures and this effect is more pronounced with metal carbonates.

Oxygen has a profound effect on the degradation of PDMS and in a limited supply of oxygen, there is evidence of cross-linking and oxidation of methyl groups.

Most blends investigated showed 25-50°C more stabilisation initially in inert atmosphere than in the air. However, the weight loss in air occurs in a long temperature range and in small steps thus making the degradation process slow and more complex while in inert atmosphere it occurs for most blends continuously. The overall effect for most blends represents more stabilisation in air than in inert atmosphere.

Stabilisation of blends, with different percentage content, increases in either atmosphere with increasing percentage content of the corresponding filler/additive if it is also acting as a heat sink.

CHAPTER 8

BLEND OF POLYOLEFINS, POLYDIMETHYLSILOXANE AND INORGANIC FILLER

8.1. INTRODUCTION

Many research workers have described the use of silicones in combination with other ingredients to provide a degree of fire retardance to some thermoplastics, including crosslinked polyethylene used for wire and cable applications, but these systems were found unsatisfactory to be used as fire retardants for uncrosslinked polyolefins^{37, 38, 42, 43}. These flame retardants were based on reactive silicone polymers, a linear silicone resin, soluble in the fluid, plus a metal soap. While a wide variety of metal soaps may be used, magnesium stearate was found to be the best of the many soaps considered as described in Chapter 1.

The objective of the current chapter was to study the thermal degradation properties of uncrosslinked polyolefins in the presence of coated CaCO_3 and PDMS in an inert atmosphere, to investigate if these ingredient combinations were effective fire retardants.

8.2. EXPERIMENTAL

8.2.1. Preparation and Composition of Blends

All blends were prepared as described in Chapter 2. The compositions of the PDMS and additives were based on percentage by weight and are given in Table 8.1.

Table 8.1. Characteristics of samples examined

| Sample | Polymer | Additive |
|----------|---------------|---------------------------------------|
| Blend 57 | LDPE:BP77 | 33.3% PDMS, 33.3% CaCO ₃ |
| Blend 58 | PEA | 5.0% PDMS, 30.0% CaCO ₃ |
| Blend 59 | EEA copolymer | 34.65% PDMS, 0.35% CaCO ₃ |
| Blend 60 | EEA copolymer | 34.30% PDMS, 0.70% CaCO ₃ |
| Blend 61 | EEA copolymer | 33.25% PDMS, 1.75% CaCO ₃ |
| Blend 62 | EEA copolymer | 31.50% PDMS, 3.50% CaCO ₃ |
| Blend 63 | EEA copolymer | 24.50% PDMS, 10.50% CaCO ₃ |
| Blend 64 | EEA copolymer | 17.50% PDMS, 17.50% CaCO ₃ |
| Blend 65 | EEA copolymer | 10.50% PDMS, 24.50% CaCO ₃ |
| Blend 66 | EEA copolymer | 5.0% PDMS, 30.00% CaCO ₃ |
| Blend 67 | EEA copolymer | 33.3% PDMS, 33.3% CaCO ₃ |

Note: Calcium carbonate used in all blends was a stearate coated whiting type with mean particle size of 1.5 microns, while the PDMS used was with vinyl end groups.

8.2.2. Analysis of Blends of Polyolefins with PDMS and CaCO₃

The thermal behaviour of these blends was investigated using TG-DTG (both in dynamic nitrogen and air), TVA and SATVA. The experimental procedure was as described in Chapter 2 unless indicated otherwise. The sample sizes for the TG experiments were approximately 5-10 mg while for the TVA experiments 100 mg samples were used. TG results in dynamic nitrogen and air are given in Table 8.2 (a) and (b), respectively. The behaviour of each blend predicted, assuming no interaction between the components, was calculated from the TG curves of the components and their relative amounts.

8.3. RESULTS AND DISCUSSION

8.3.1. Thermogravimetry

8.3.1.1. TG-DTG Under Nitrogen

Blends of Polyolefins, PDMS and CaCO₃

The TG curve obtained for blend 57 (Fig. 8.1) shows a trend towards higher temperature and stabilisation is shown throughout the degradation of up to 140°C. There are two main degradation stages shown, as expected, the second stage starting at 491°C when weight loss is 40%. It is obvious from the knowledge from chapters 5, 6 and 7 that the first stage of degradation is mainly due to the weight loss of LDPE while the second is due to PDMS. PDMS and LDPE both have been stabilised while there was no effect on the stabilisation of LDPE when it was degraded with CaCO₃. Nevertheless, LDPE maintained a stabilisation of 5-10°C in the presence of PDMS. It seems that the stabilisation of PDMS with CaCO₃ by interaction also has an effect on the stabilisation of LDPE. The only reasonable explanation for this behaviour is that radicals formed during degradation of LDPE introduce radical sites in PDMS chains by H-abstraction and crosslinking occurs between two polymers. This interaction results in the formation of a copolymer system (IR spectra of the insoluble CRF and residue show absorptions of both polymers, discussed in Chapter 6) which is more stable than either polymer alone. The small weight loss (3%) seen in the TG curve in the region 375-400°C is possibly due to initial decomposition of LDPE when radicals due to decomposition of LDPE are introduced in the system. The degradation process slows down since some of these alkyl radicals abstract hydrogens from the methyl groups substituted on the silicon atoms and introduce radicals in the PDMS chains and this results in the interaction between the radicals of two components.

Blend 58 starts to degrade 50°C later than expected (Fig. 8.2) but destabilisation starts after 16% weight loss and this destabilisation remains during the first stage of degradation, which from the knowledge of previous work carried out in chapters 5 and 6 is mainly due to the weight loss of PEA. The destabilisation is thought to be due to the filler and PEA interacting as discussed in Chapter 5, since it was found that PEA is stabilised in the presence of PDMS due to the interaction of the components, which has been attributed to the formation of copolymer systems.

The TG curves obtained for blends 59-67 (Figs. 8.3-8.11, respectively) show a trend towards higher temperatures, 125°C more initially than expected. Increasing percentage content of the filler does not have any further effect on the initial stabilisation

but stabilisation increases afterwards as the percentage content of the filler is increased. Stabilisation is shown throughout the degradation by up to 135°C, depending on the PDMS and filler content. It is observed that stabilisation of EEA copolymer increases if the content of PDMS is increased to about twice of CaCO₃. The stabilisation of PDMS, however, increases with increasing filler content, thus decreasing EEA copolymer content as seen in blend 67 which shows most stabilisation. These observations agree with the results shown by blends of EEA copolymer with PDMS and blends of PDMS with CaCO₃ with different percentage content, discussed in chapters 6 and 7, respectively. This again indicates that higher stabilisation of the EEA copolymer depends on the higher PDMS content rather than the filler.

8.3.1.2. *TG-DTG Under Air*

Thermogravimetric experiments were performed for some of the above blends under an atmosphere of air for the purpose of comparison with the results obtained under nitrogen.

The TG traces of blends 57 (Fig. 8.1), 59 (Fig. 8.3), 66 (Fig. 8.10) and 67 (Fig. 8.11), show a remarkable increase in stability, the rate maximum depending on the type of polymer/copolymer and additive content. This stability is maintained throughout the degradation for most of the blends mentioned above as seen from their TG curves. Blend 57 shows a stabilisation of 25-50°C initially which gradual increases to 150°C near the end of the degradation. Blend 67 starts to develop stability after 2.5% weight loss and develops a stabilisation of about 105°C throughout the degradation after 35% weight loss. The level of residues are much more than expected at the end of the degradation indicating the formation of inert residue. The reason for the high level of residues is due to the formation of silica which is inert as explained in previous chapters.

The TG-DTG traces show that the degradation processes for most blends are much more complicated than when degradation for these blends was carried out in an inert atmosphere since DTG curves of most of these blends show two main degradation stages accompanied by other small complex degradation stages.

The TG-DTG results (Table 8.2 (a) and (b)) show that all blends mentioned above show 25-80°C more stabilisation in an inert atmosphere than in air, while it was found that pure PDMS was 25-30°C more stable in air than in an inert atmosphere whereas LDPE and EEA copolymer were 147°C and 113°C, respectively, more stable initially in inert atmosphere. The explanation for the differences of these results is as given

previously, when these polyolefins were degraded alone (Chapter 3) and in the presence of additives chapters 5, 6 and 7).

Table 8.2. (a) TG results under nitrogen

Temperatures shown in brackets are calculated values assuming that there was no interaction between the components.

| Sample | T _{thresh} (°C) | T ₅₀ (°C) | T _{max} (°C) | T _{stop} (°C) | % residue at 600°C |
|----------|--------------------------|----------------------|-----------------------|------------------------|--------------------|
| Blend 57 | 375 (250) | 555 (461) | 387, 478, 598 | 650 (500) | 40.0 (33.8) |
| Blend 58 | 325 (250) | 405 (417) | 412, 475 | 575 (380) | 31.8 (31.3) |
| Blend 59 | 375 (250, 375) | 434 (430) | 441 | 600 (500) | 4.0 (1.3) |
| Blend 60 | 375 (250, 375) | 457 (430) | 460, 482 | 625 (500) | 3.0 (1.7) |
| Blend 61 | 375 (250, 375) | 461 (432) | 457, 478 | 635 (500) | 4.8 (2.7) |
| Blend 62 | 375 (250, 375) | 463 (435) | 455, 482 | 635 (500) | 8.0 (4.3) |
| Blend 63 | 375 (250, 375) | 471 (440) | 448, 483 | 650(500) | 16.0 (11.3) |
| Blend 64 | 375 (250, 375) | 474 (450) | 448, 485 | 620 (500) | 19.0 (18.1) |
| Blend 65 | 375 (250, 375) | 475 (450) | 435, 488 | 587 (500) | 25.0 (25.0) |
| Blend 66 | 375 (250, 375) | 457 (455) | 430, 463 | 525 (520) | 30.5 (30.4) |
| Blend 67 | 375 (250, 375) | 557 (448) | 473, 585 | 650 (500) | 40.0 (33.7) |

Table 8.2. (b) TG results under air

Temperatures shown in brackets are calculated values assuming that there was no interaction between the components.

| Sample | T _{thresh} (°C) | T ₅₀ (°C) | T _{max} (°C) | T _{stop} (°C) | % residue at 600°C |
|----------|--------------------------|----------------------|-----------------------|------------------------|--------------------|
| Blend 57 | 300, 375 (275) | 480 (352) | 392, 480, 499 | 515 (400) | 39.0 (34.5) |
| Blend 66 | 300, 400 (267) | 465 (393) | 382, 492 | 500 (550) | 29.5 (30.1) |
| Blend 67 | 325, 375 (275) | 478 (374) | 424, 476 | 510 (500) | 43.0 (34.5) |

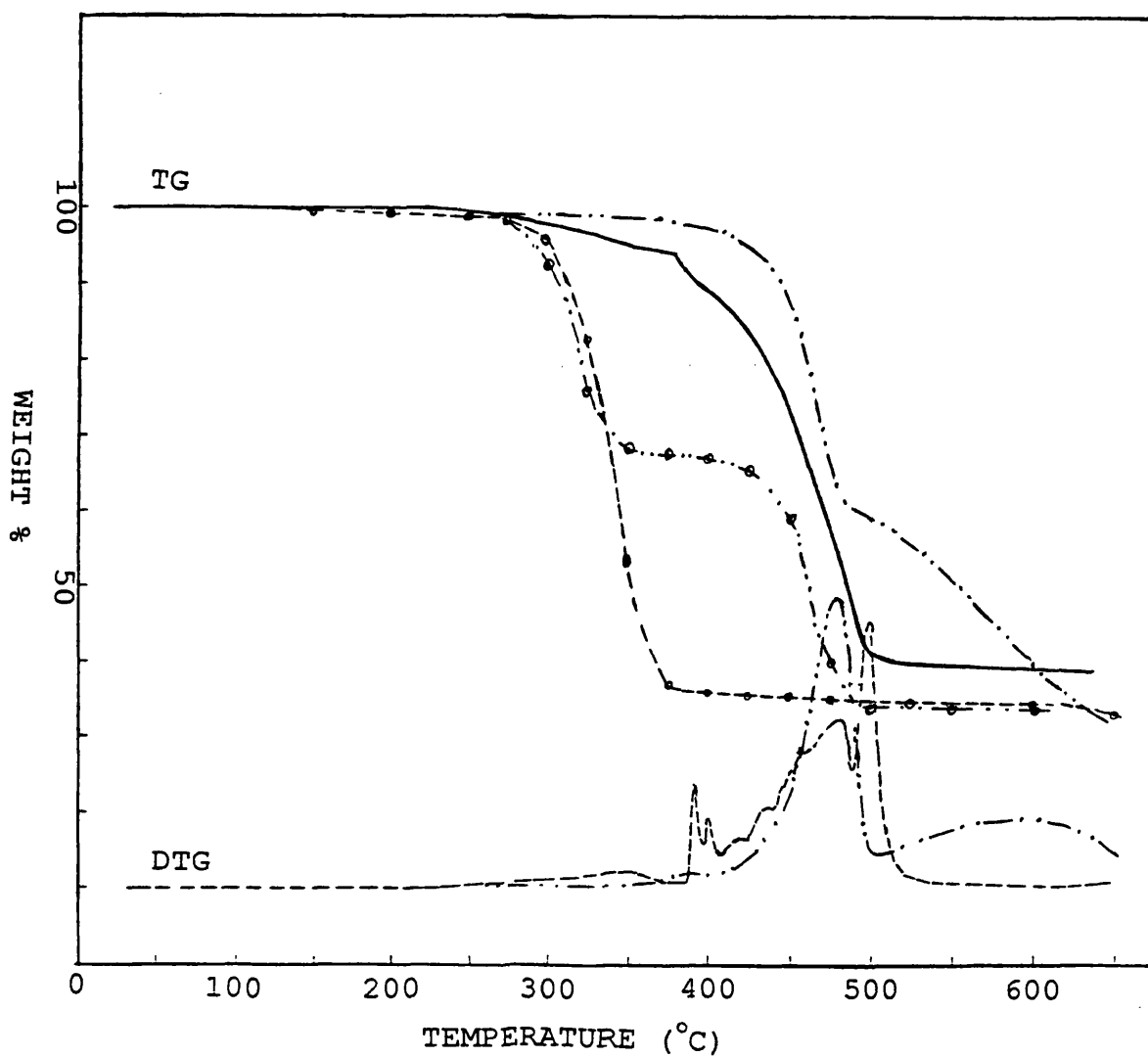


Fig. 8.1. TG-DTG traces for blend 57 (LDPE:PB77, 33.3% PDMS and 33.3% CaCO_3) under nitrogen: experimental (---) and calculated (-·-·-), and air: experimental (—; ----) and calculated (-·-·-).

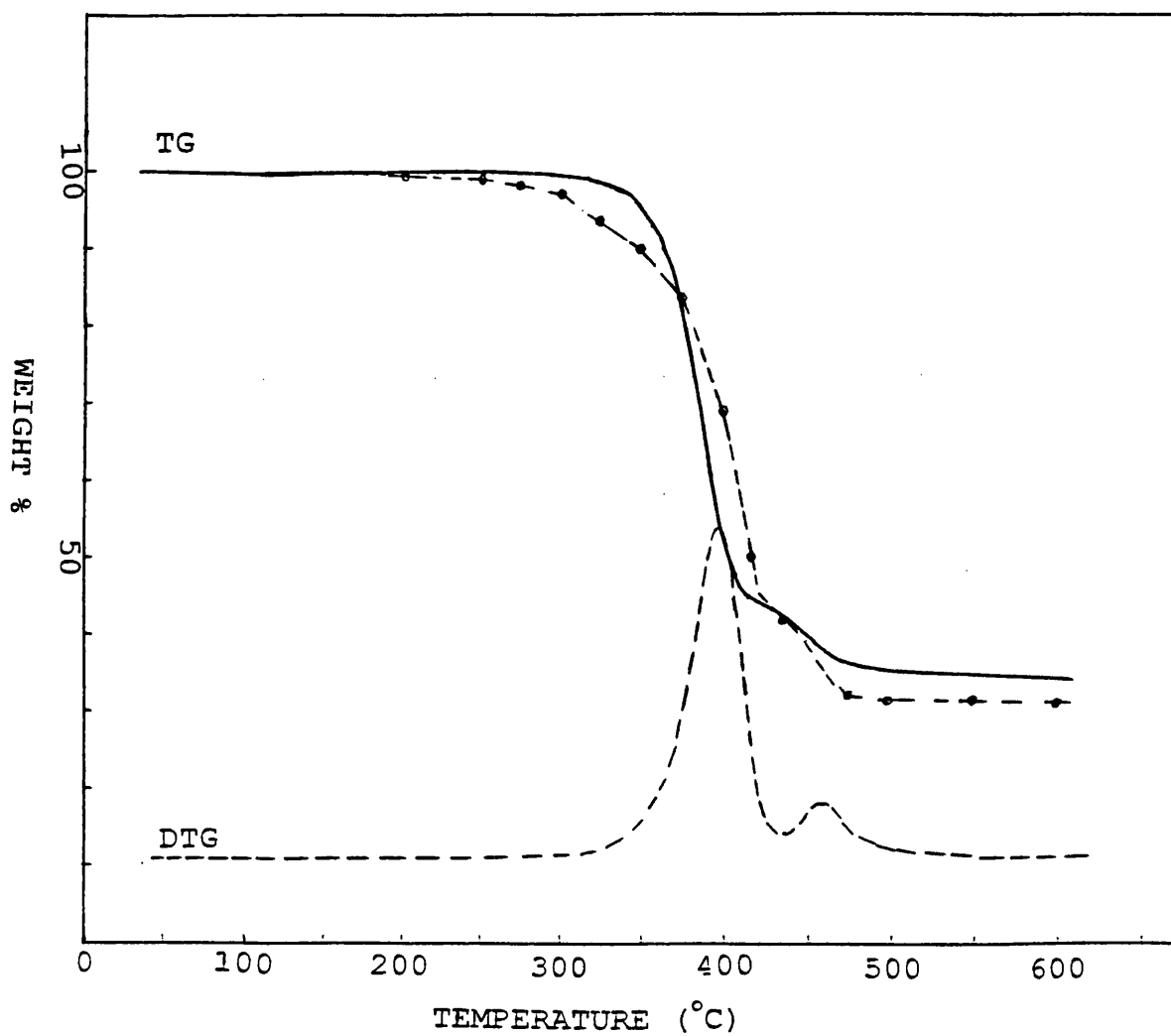


Fig. 8.2. TG-DTG traces for blend 58 (PEA, 5% PDMS and 30% CaCO_3) under nitrogen: experimental (—; ----) and calculated (---).

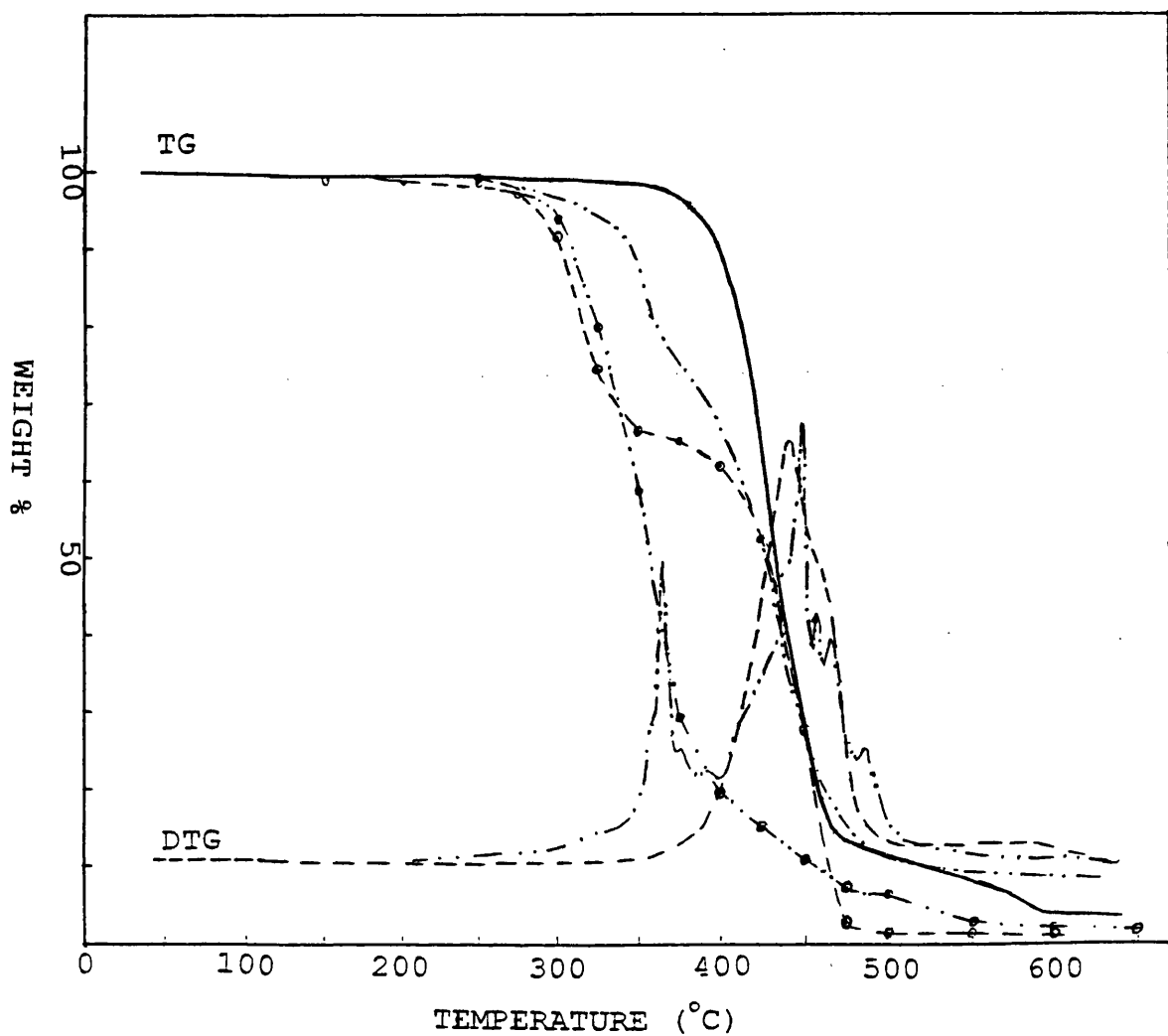


Fig. 8.3. TG-DTG traces for blend 59 (EEA copolymer, 34.65% PDMS and 0.35% CaCO_3) under nitrogen: experimental (—; ----) and calculated (- - -), and air: experimental (- · - ·) and calculated (- · · - ·).

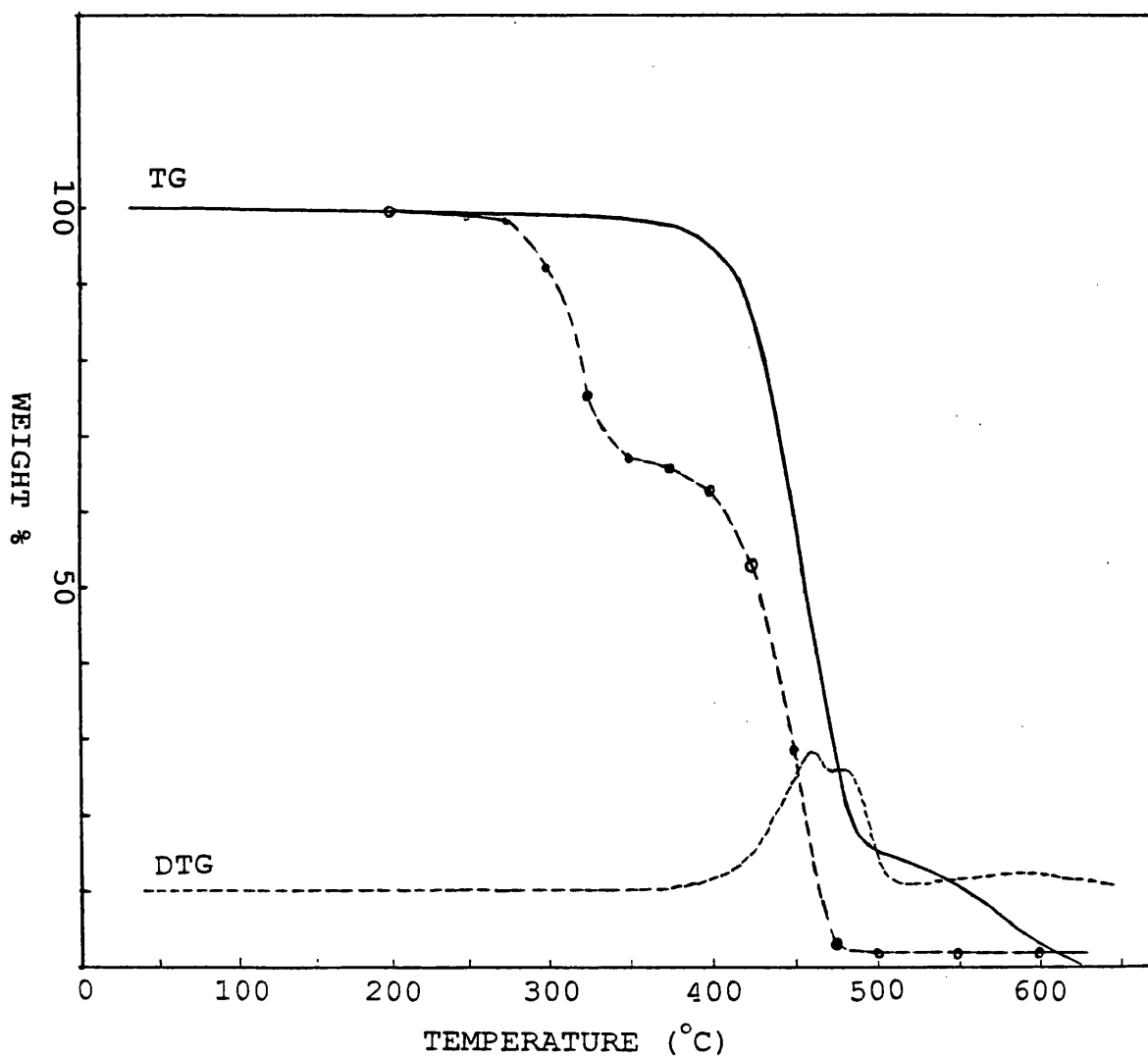


Fig. 8.4. TG-DTG traces for blend 60 (EEA copolymer, 34.30% PDMS and 0.70% CaCO_3) under nitrogen: experimental (—; —) and calculated (- - -).

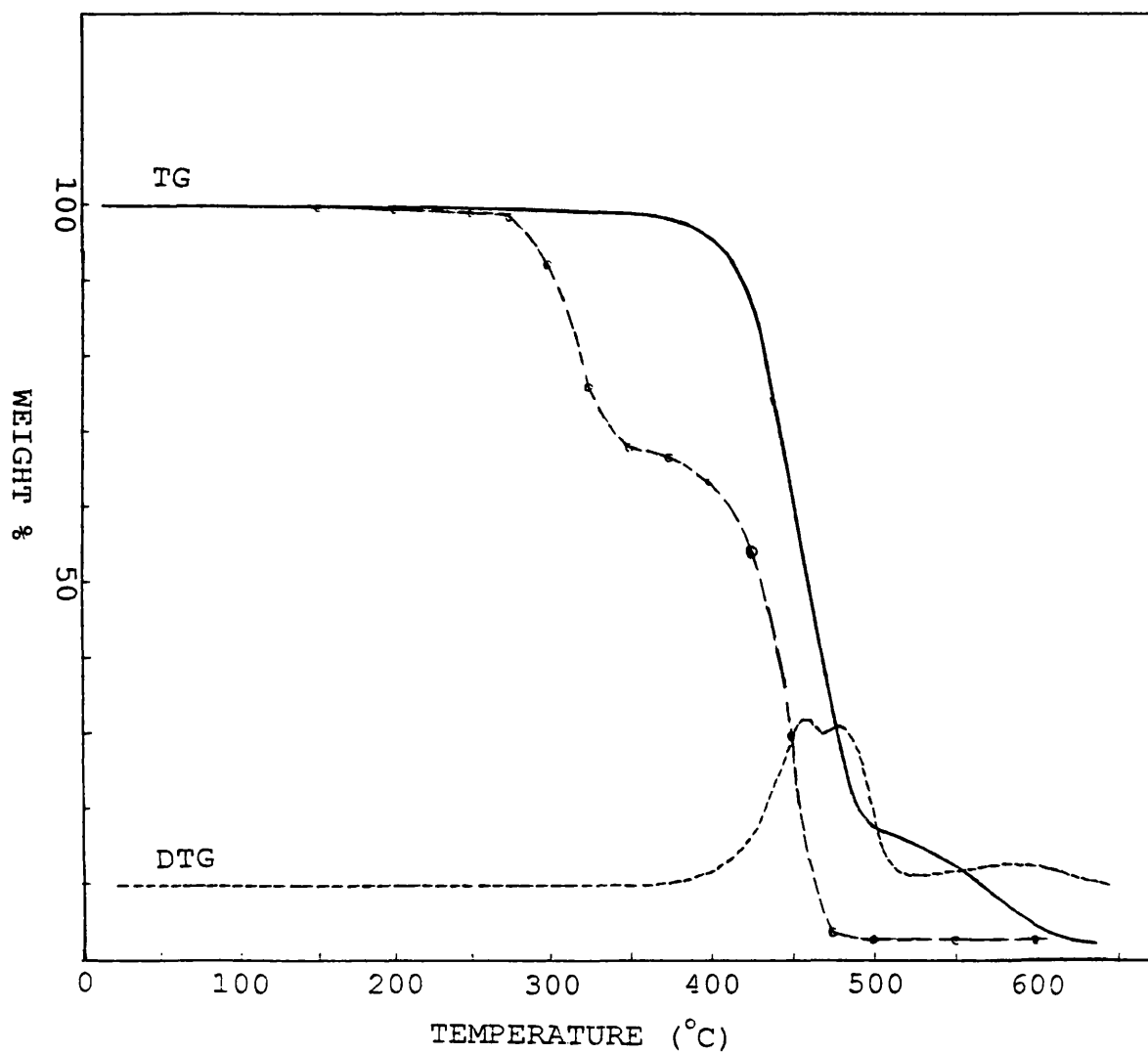


Fig. 8.5. TG-DTG traces for blend 61 (EEA copolymer, 33.25% PDMS and 1.75% CaCO_3) under nitrogen: experimental (—; ----) and calculated (-·-·-).

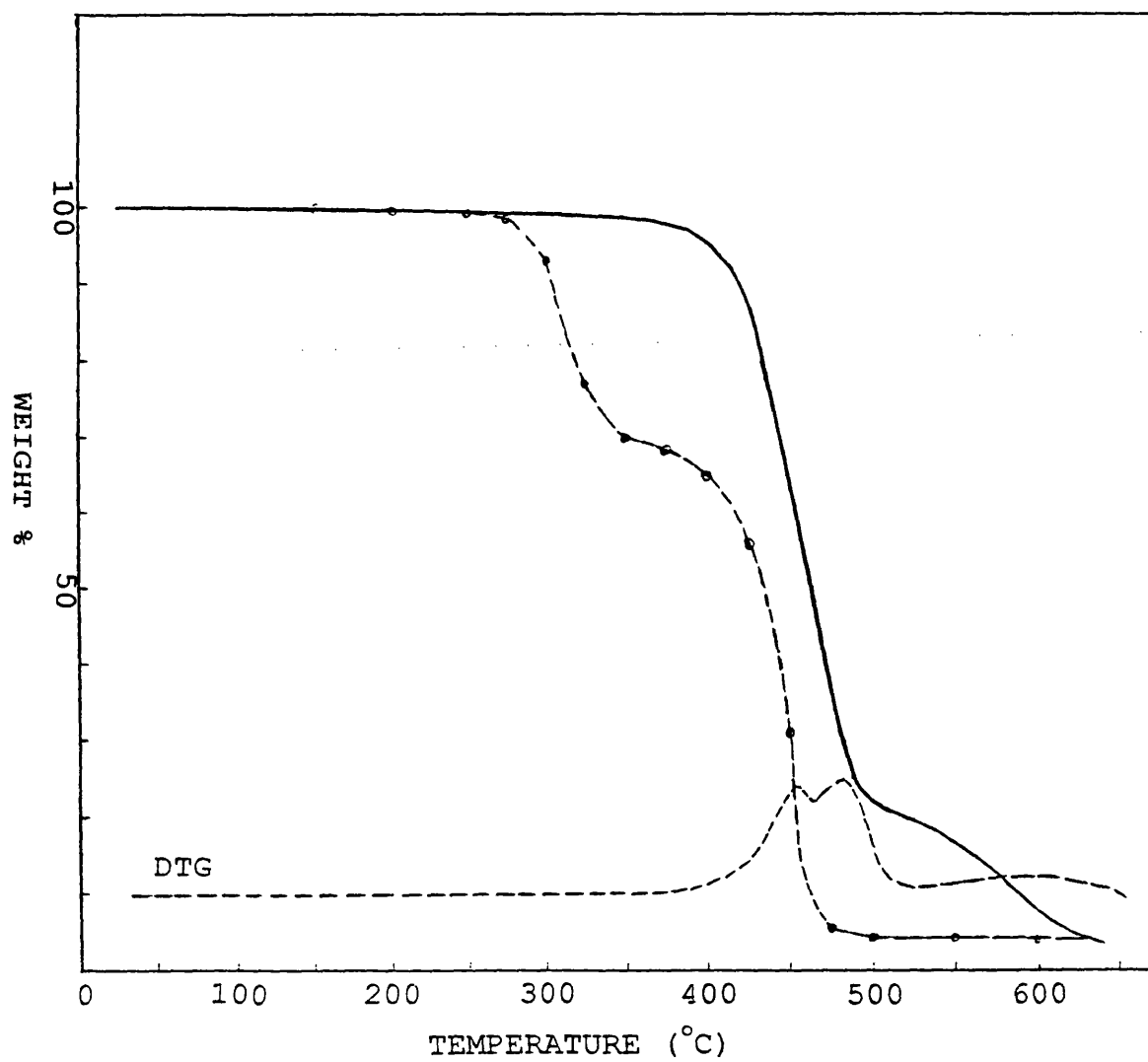


Fig. 8.6. TG-DTG traces for blend 62 (EEA copolymer, 31.50% PDMS and 3.50% CaCO_3) under nitrogen: experimental (—; ---) and calculated (- - ->).

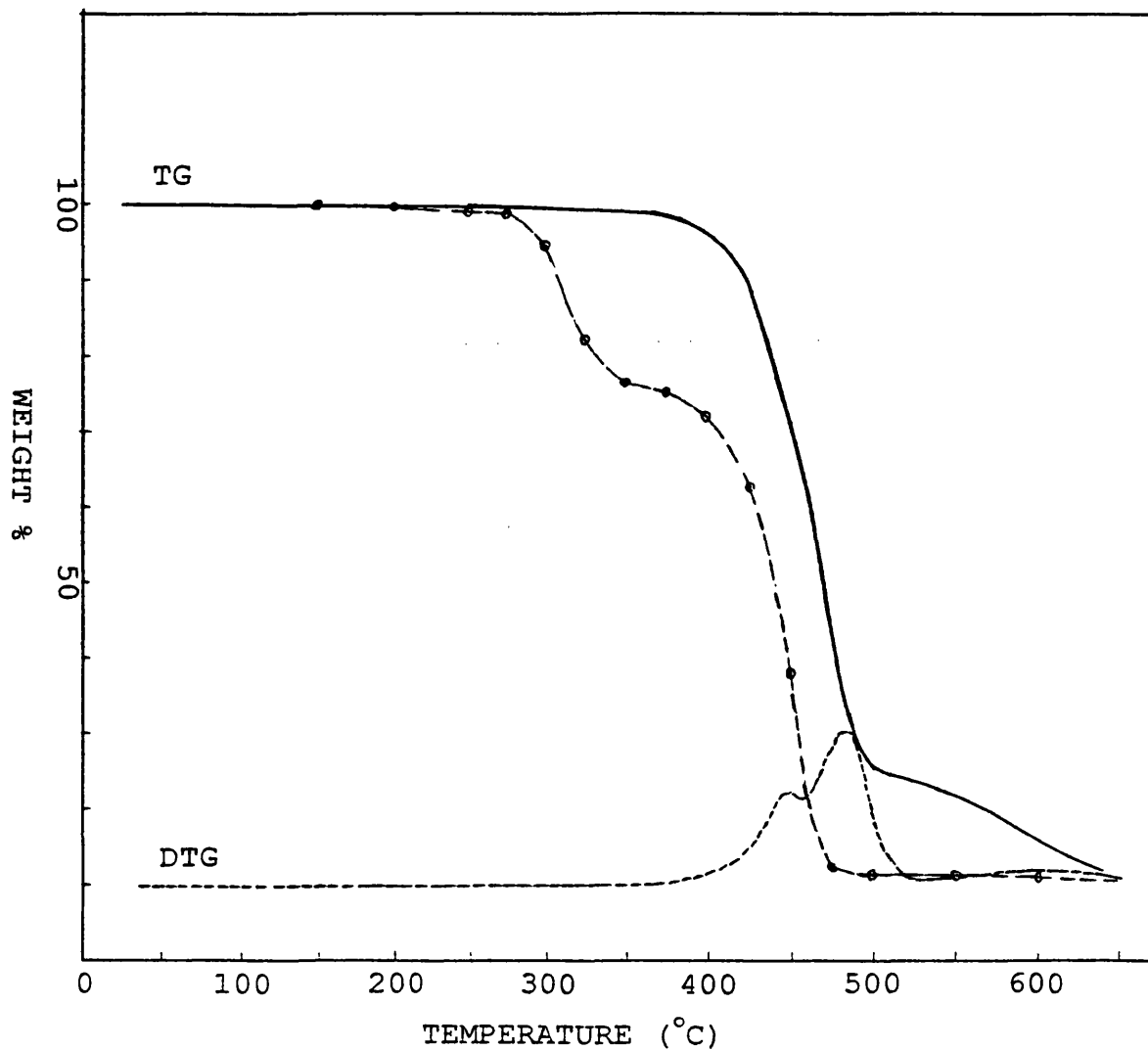


Fig. 8.7. TG-DTG traces for blend 63 (EEA copolymer, 24.50% PDMS and 10.50% CaCO_3) under nitrogen: experimental (—; ----) and calculated (- - -).

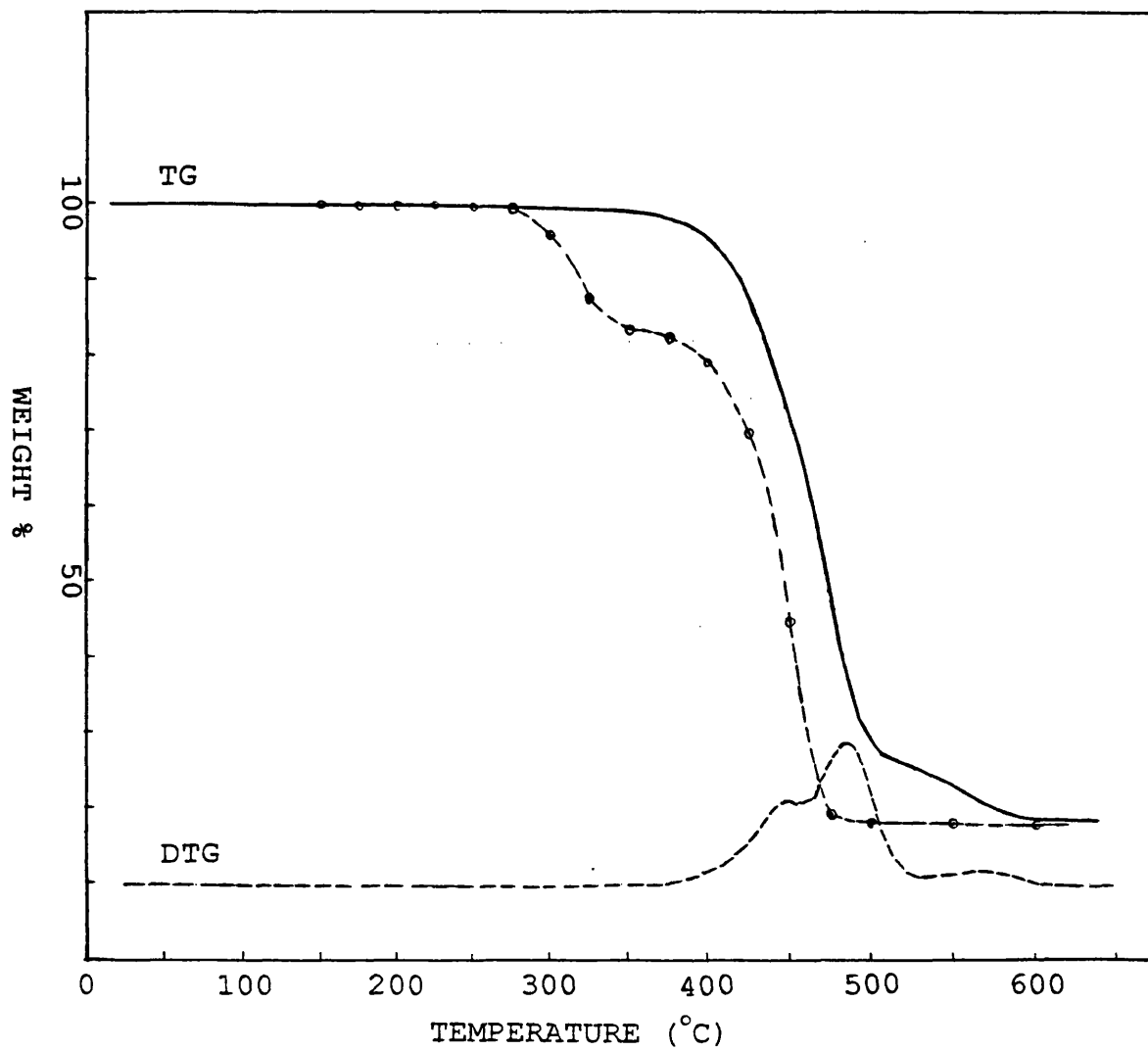


Fig. 8.8. TG-DTG traces for blend 64 (EEA copolymer, 17.50% PDMS and 17.50% CaCO_3) under nitrogen: experimental (—; ----) and calculated (- - -).

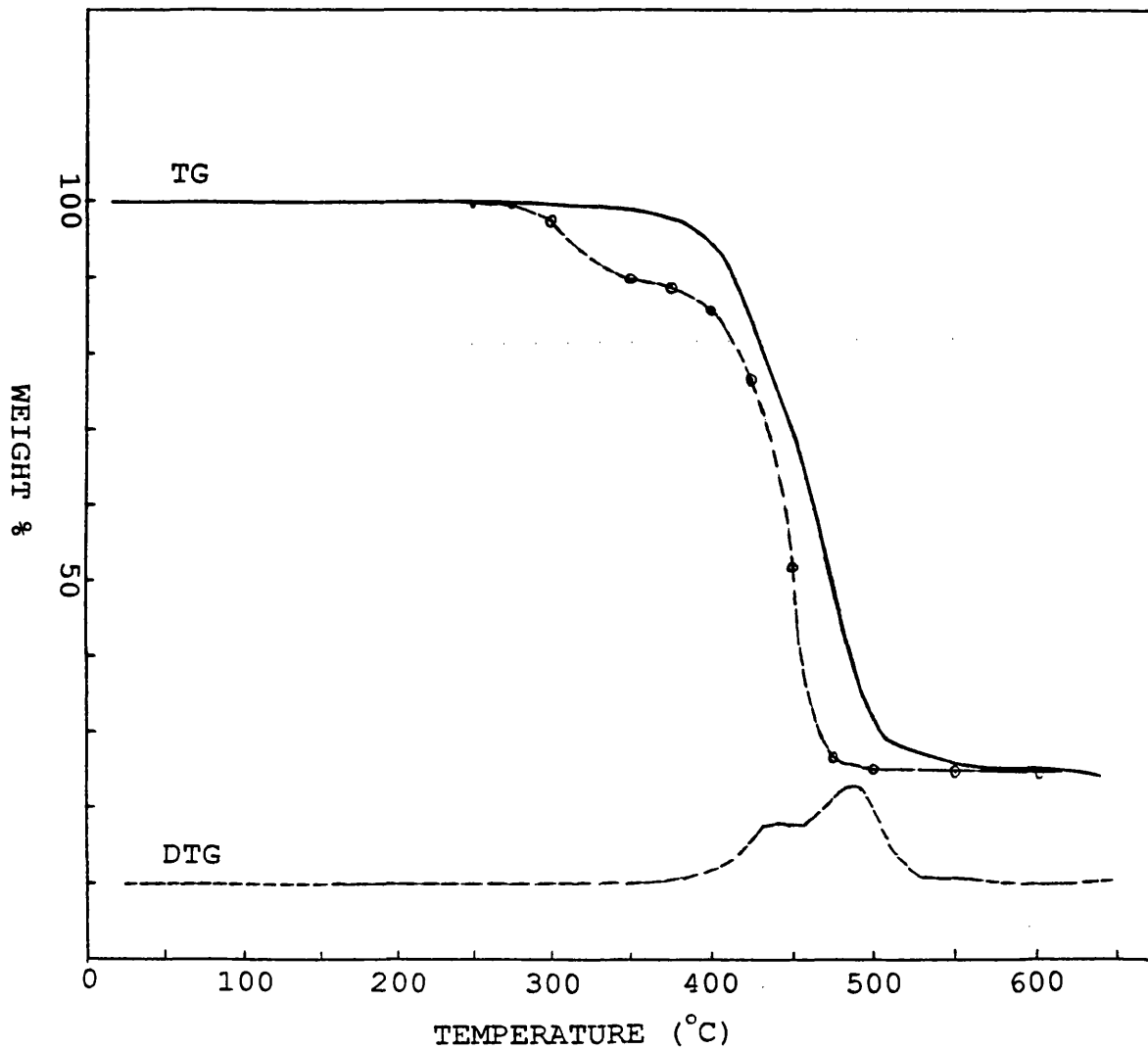


Fig. 8.9. TG-DTG traces for blend 65 (EEA copolymer, 10.50% PDMS and 24.50% CaCO_3) under nitrogen: experimental (—; ----) and calculated (-·-·-).

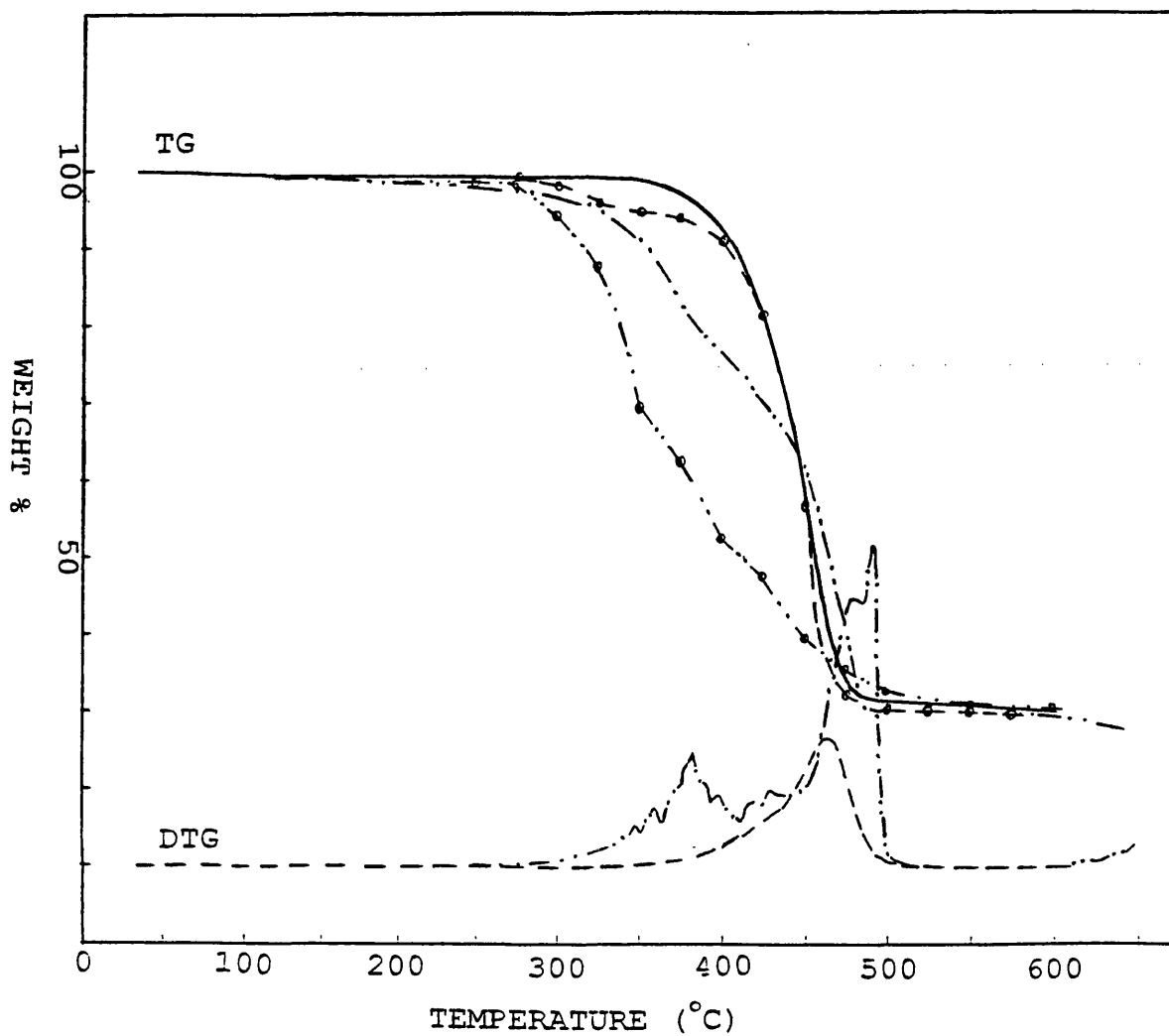


Fig. 8.10. TG-DTG traces for blend 66 (EEA copolymer, 5% PDMS and 30% CaCO₃) under nitrogen: experimental (—; ----) and calculated (- - - -), and air: experimental (- · - ·) and calculated (- · · · - ·).

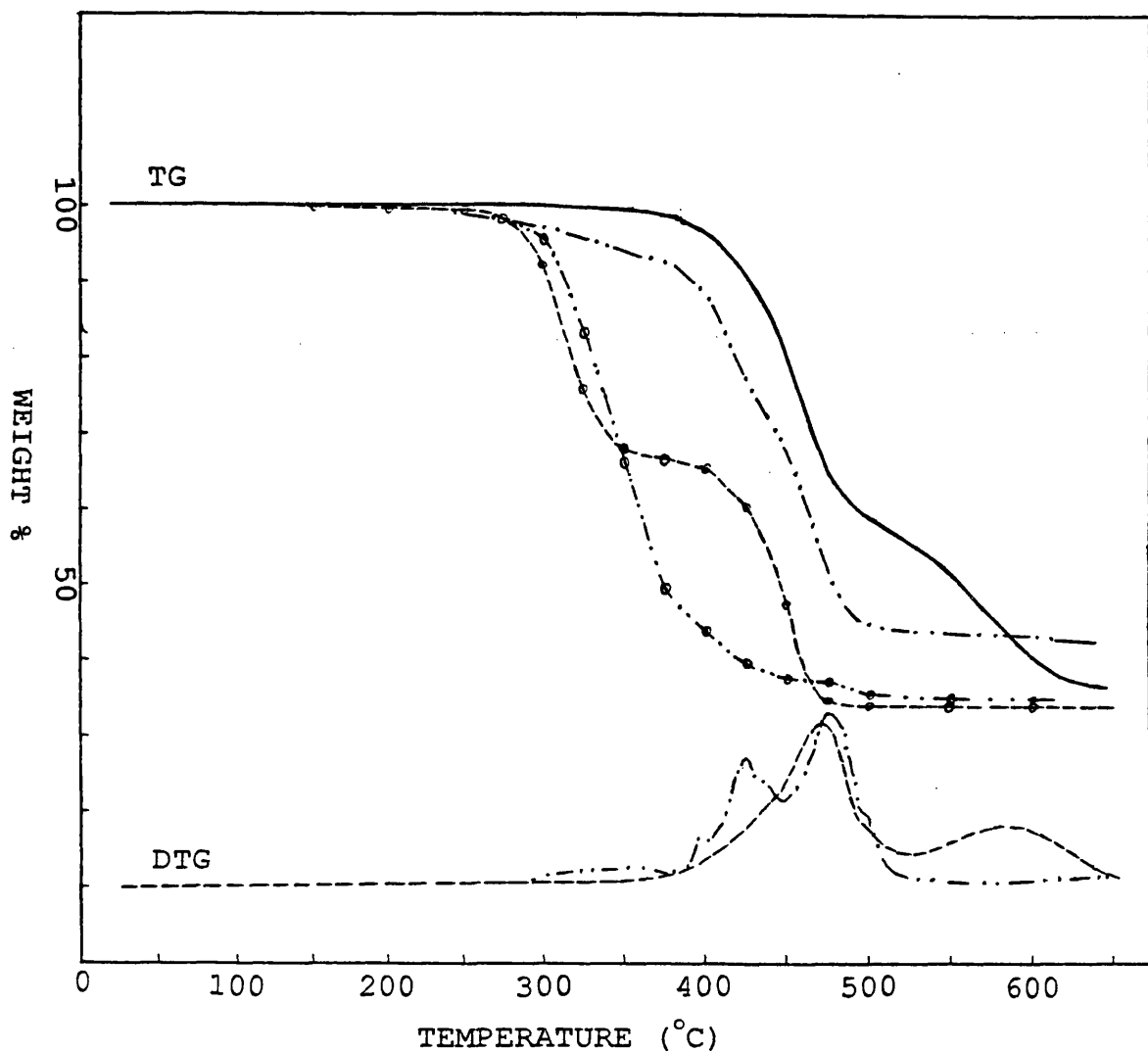


Fig. 8.11. TG-DTG traces for blend 67 (EEA copolymer, 33.3% PDMS and 33.3% CaCO_3) under nitrogen: experimental (—; ----) and calculated (- - - -), and air: experimental (- - - -) and calculated (- - - - - -).

8.3.2. Thermal Volatilisation Analysis (TVA) and SATVA Separation of Condensable Degradation Products

Blend of LDPE, CaCO₃ and PDMS

Volatilisation of degradation products from blend 57 (33.3% PDMS, 33.3% CaCO₃) started at the normal degradation temperature of LDPE but gradually a stabilisation of 10-20°C developed (Fig. 8.12 (a)). GC-MS results for the products from the first degradation stage showed the presence of degradation products from both polymers. There is a small rise for the -196°C trace indicating a very small amount of non-condensable gaseous products. The second stage of degradation which starts around 480°C shows volatilisation of silicone compounds as well as hydrocarbons. This result backs up the TG result which indicated that LDPE had been stabilised as well in the presence of PDMS and filler.

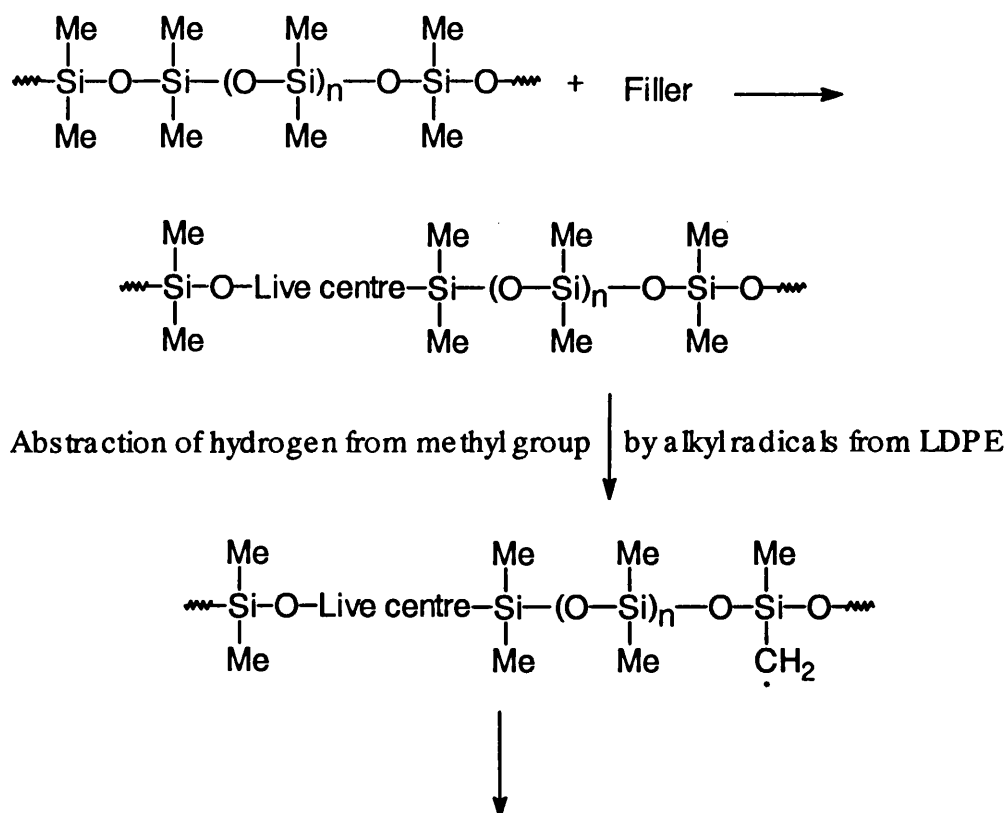
The SATVA trace (Fig. 8.13) for the separation of the condensable volatile degradation products of blend 57 was the sum of the SATVA traces from blends 13 (LDPE with 50% PDMS) and 26 (PDMS with 50% CaCO₃) and the degradation products were also found to be the sum of those of the two blends. There is no clear indication of any other new products formed but the GC trace is so complex that any new compound formed from the interactions would be difficult to detect unless formed in large quantities.

The CRF collected was a colourless material showing hard and soft patches on the TVA tube due to oligomers from both type of components. It was not dripping/running down the TVA tube on cooling as in the case of pure PDMS. The IR spectra of the CRF fractions separated into soluble and insoluble at room temperature, were similar to those of blend 13.

The residue was rubbery at 480°C, formed a bubble like the residue from blend 26, had shiny top surface and was more than expected. The IR spectrum of the soluble residue, at room temperature, was similar to the IR spectrum of the CRF from PDMS except that the absorptions for the asymmetric Si-O-Si stretching vibration for the siloxanes broadened indicating the different alkyl groups substituted on the silicon atoms. There were also weak absorptions similar to those in the LDPE spectrum. The IR spectrum of the residue insoluble at room temperature was also similar to that of blend 13 except there were also absorptions for the filler as well. The characteristic band for LDPE at 1465 cm⁻¹ was masked under the strong absorption due to carbonate ions

and was recognised from the rocking of methylene groups at 722 cm^{-1} and 732 cm^{-1} . The IR spectrum of the residue at 600°C was like that of the residue from blend 26 (PDMS with 50% CaCO_3) at this temperature and the IR spectrum was also similar to it showing absorptions due to filler and siloxane groups. It was difficult to see the presence of LDPE since it could only be recognised from the rocking of methylene groups at 722 cm^{-1} and 732 cm^{-1} but these were masked due to strong absorption at 715 cm^{-1} of the filler. However, it is clear that if it is present, it is in small amount. The interactions which result in stabilisation of LDPE are as follows in Scheme 8.1:

Scheme 8.1:



(i) Crosslinking occurs between two PDMS radicals

or (ii) An interaction occurs between the radicals of the two polymers resulting in a copolymer system.

Blend of PEA, PDMS and CaCO_3

Volatilisation of blend 58 (5% PDMS, 30% CaCO_3) started at the normal degradation temperature of PEA (Fig. 8.12 (b)). It is clear from the areas under peaks corresponding to the different cold traps that degradation products were as volatile as in

the case of pure PEA. A second degradation stage started at about 450°C due to the evolution of the degradation products from the decomposition of PDMS. There is evidence for non-condensable gaseous products at the first stage and small amount during the second stage.

Degradation products were found to be mainly similar to the sum of degradation products from pure PEA and blends 48 (PDMS with 5% stearic acid) and 14 (PEA with 7.1% PDMS) as were seen from the GC-MS results. There should also be degradation products resulting from the interaction of the filler and PDMS but were not detected possibly due to their negligible amounts or perhaps crosslinking by radicals from polyolefins is more favoured than crosslinking introduced from filler and PDMS interaction. The mechanisms for the formation of these compounds resulting from crosslinking are given in Chapter 6.

The CRF was a viscous yellowish brown liquid, without any noticeable presence of the less viscous liquid CRF from PDMS. The IR spectrum of the CRF, run in dichloromethane, was similar to the IR spectrum of the CRF from blend 14, Chapter 6.

The residue was dark brown with a shiny top layer and it was clear from the state of the residue that the polymers did not spread on melting but stayed intact as a lump. The IR spectrum showed mainly the presence of filler but there were weak absorptions for siloxane groups.

Blends of EEA Copolymer, PDMS and CaCO₃

The TVA traces for blends 59-67 were mainly similar in shape to that for blend 4 (EEA copolymer with CaCO₃, Chapter 5) up to 500°C but volatile degradation products including non-condensable gaseous products, seem to be more than for blend 4. Another degradation stage starts after 540°C as seen from Fig. 8.14 (b) of blend 67. The stabilisation trend is similar to that seen in the TG curves.

The SATVA curves for the separation of the condensable volatile products of degradation were similar to those of blends 18-20 (EEA copolymer with PDMS) showing three gaseous product peaks plus a fourth broad, poorly-resolved fraction indicating a number of different degradation products. The first peak, which was due to ethylene and ethane, decreased as the filler and PDMS content was becoming near to 1:1 and blend 67 showed only a small amount of ethylene (Fig. 8.15).

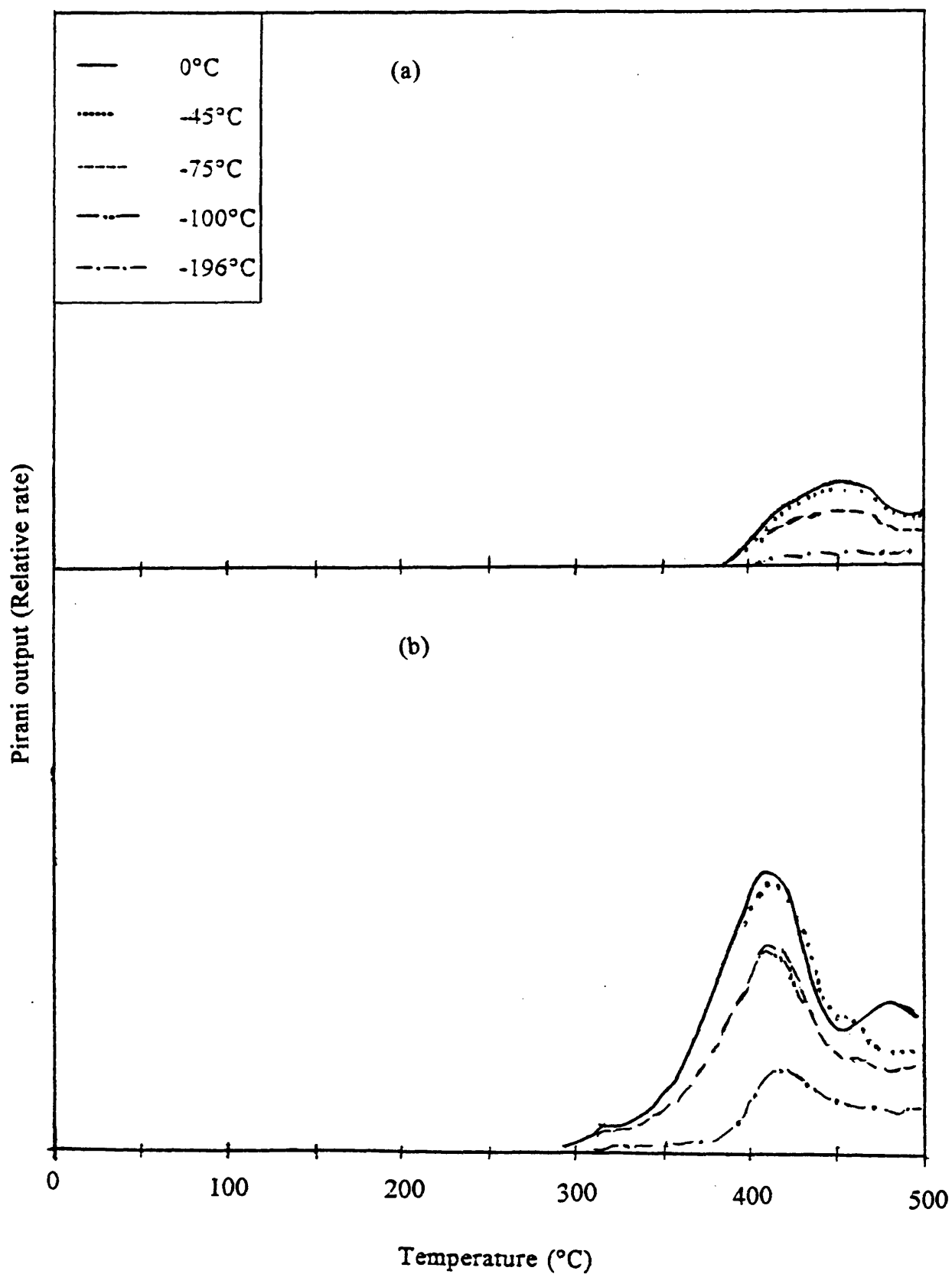


Fig. 8.12. TVA traces for blends: (a) blend 57 (LDPE:PB77, 33.3% PDMS and 33.3% CaCO_3) (b) 58 (PEA, 5% PDMS and 30% CaCO_3).

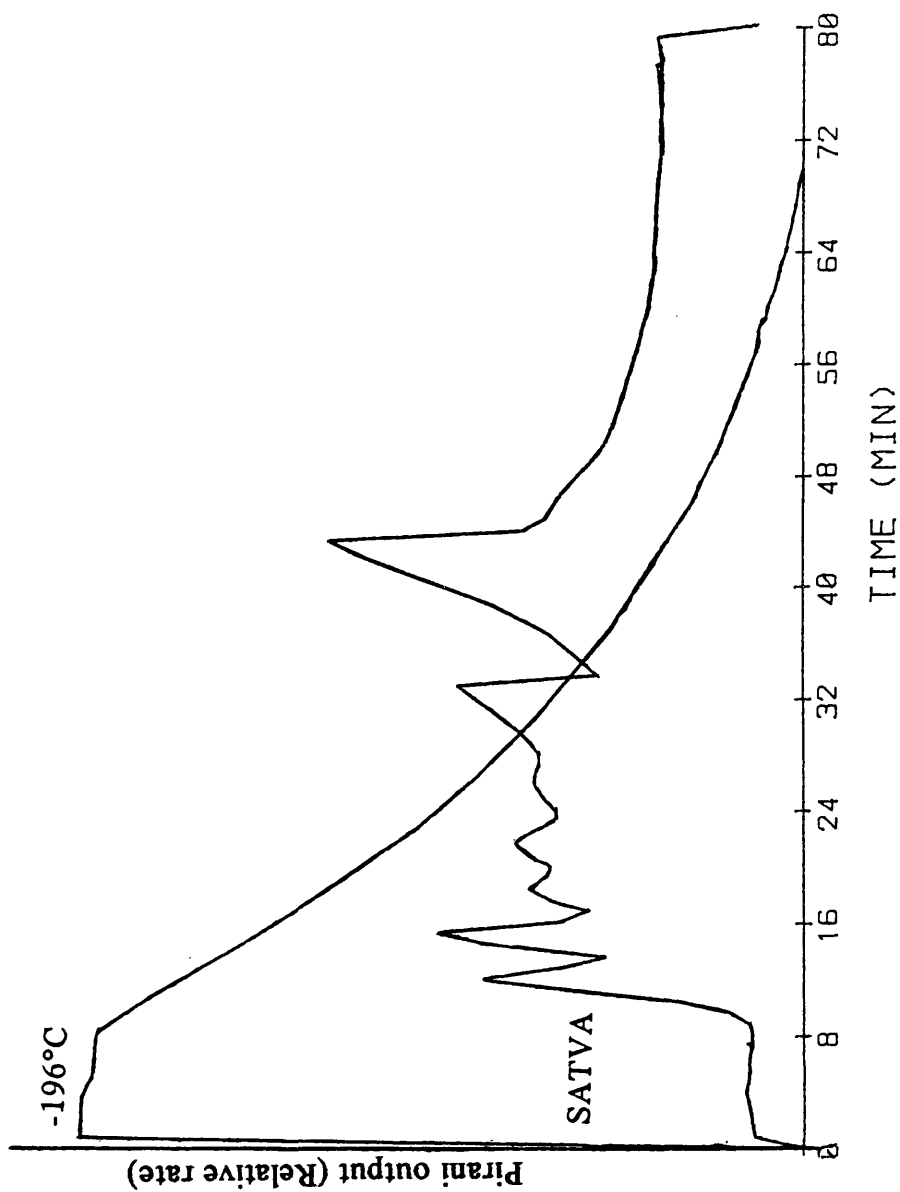


Fig. 8.13. SATVA trace for warm up from -196°C to ambient temperature of condensable volatile products from degradation for blend 57 (LDPE:BP77 + 33.3% PDMS + 33.3% CaCO_3).

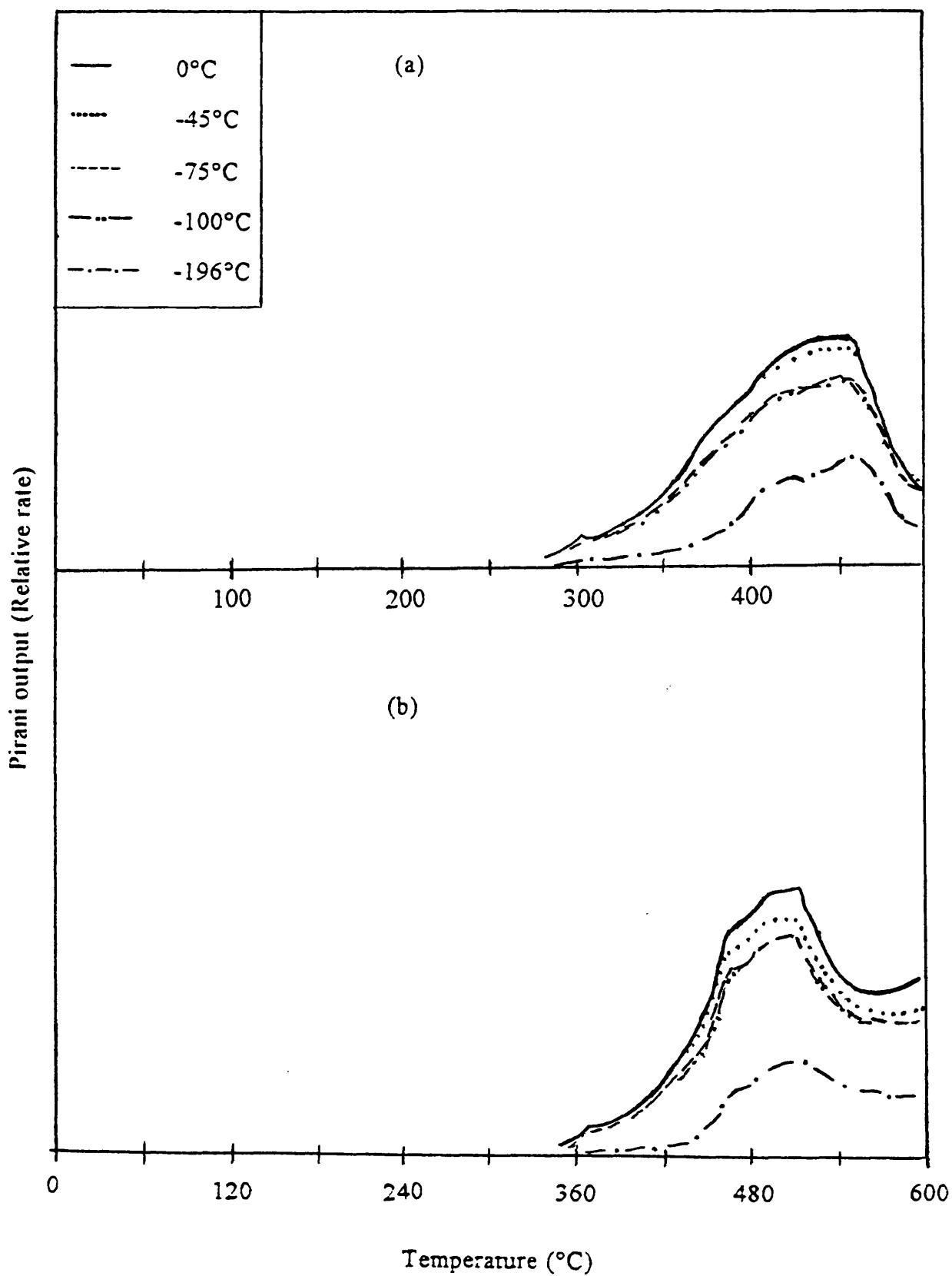


Fig. 8.14. TVA traces for blends: (a) blend 66 (EEA copolymer, 5% PDMS and 30% CaCO₃) (b) 67 (EEA copolymer, 33.3% PDMS and 33.3% CaCO₃).

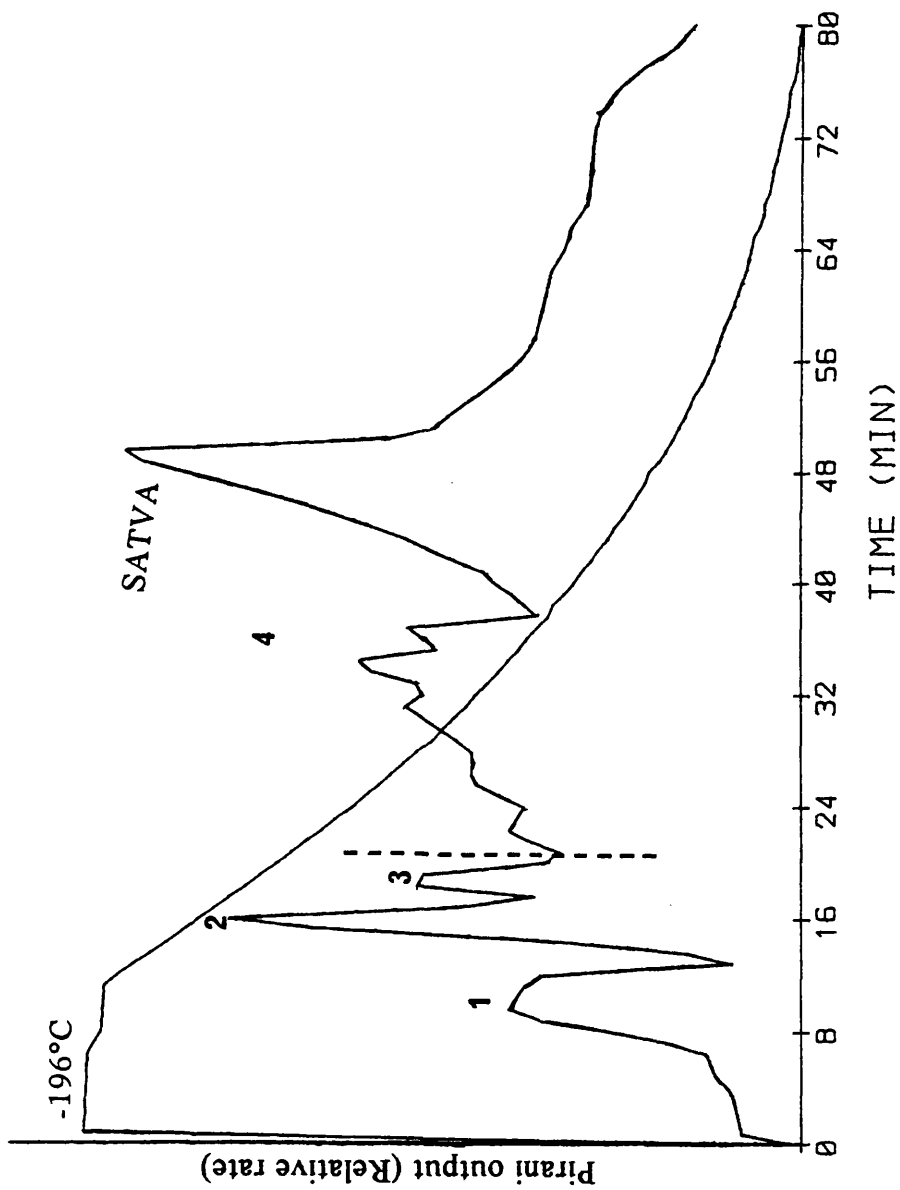


Fig. 8.15. SATVA trace for warm up from -196°C to ambient temperature of condensable volatile products from degradation for blend 67 (EEA copolymer + 33.3% PDMS + 33.3% CaCO₃).

The IR spectra of the volatile products of degradation in the fourth fraction from blends 59-67, in the gas phase, were similar to those from blends 18 and 20 (Chapter 6).

The GC-MS results showed the degradation products to be similar to those from blends 20 (Chapter 6) and 26 (Chapter 7). Again, as for blend 20, there is evidence for silicone compounds with large organic substituents, possibly large alkyl groups. Other new degradation products were not detected.

The residues from blends 59-67 were different in appearance since the residues with less PDMS content (e.g. blend 66 etc.) did not show the formation of a bubble, instead the residue was pale yellow at 480°C, had a shiny top layer and was difficult to break. Other blends showed bubbles at 480°C but these bubbles were not well defined. Blend 67, however, showed a well defined thin layered bubble. The residue (47.2%) from blend 67 was still rubbery at 600 °C

The mechanisms of formation of the degradation products from these blends are the combination of those described in chapters 5, 6 and 7 for the corresponding polymer-additive systems.

All above results show that PDMS combined with the filler stabilises the polymer/copolymer systems, including LDPE which so far was found to be unaffected by filler alone, and only showed slight stabilisation in the presence of PDMS. These results in combination with others described in previous chapters show that interaction of LDPE and PDMS radicals is important for the stabilisation of LDPE. It is important, therefore to use PDMS which does not decompose before the decomposition temperature of LDPE or use a combination of ingredients which would stabilise PDMS at least up to the decomposition temperature of LDPE.

Rubbery residues formed from blends with high PDMS content also contribute in stabilisation since the degradation products would be trapped in the bubble at least for some time and the reactions between the radicals are favoured in such an environment. These reactions may result in the formation of stable compounds.

The residues with shiny surfaces formed from the filler and PDMS interaction possibly also acts as a physical barrier to prevent the diffusion of the degradation products from the polymer-blend system.

8.4. CONCLUSIONS

All the polyolefins tested were stabilised in the presence of CaCO_3 and PDMS. The stabilisation of the polyolefins seems mainly due to interactions with PDMS, especially in the case of LDPE.

Stabilisation of polyolefins increases with increasing PDMS content; better results are obtained with all three components in equal ratios by weight.

Bubble-like residues are result of the interaction of PDMS and filler and their formation is favoured for blends with these two components in larger amounts.

REFERENCES

1. D. A. Purser, 'Modelling Toxic and Physical Hazards in Fire, Paper of FRCA Conference: International Progress in Fire Safety', U.S.A. (1987).
2. H.L. Kaplan, A.F. Grand and G.E. Hartzell, 'Combustion Technology, Technomic, Lancaster (1983).
3. Home Office report of the Technical Sub-committee on the fire risks of new materials, Central Fire Brigades Advisory Council (1978).
4. N. Grassie, "Chemistry Of High Polymer Degradation", Butterworths, London (1956).
5. N. Grassie, "Cleavage Reactions, Thermal Degradation" in "Chemical Reactions of Polymers", E.M. Fettes (ed.), Interscience, New York (1964).
6. N. Grassie, "Degradation of Polymers" in "Encyclopedia of Polymer Science and Technology", vol. 4, 647-716, Wiley-Interscience, New York (1966).
7. R.T. Conley, "Thermal Stability of Polymers", Dekker, New York, (1970).
8. T.L. Junod, "Gaseous Emissions and Toxic Hazards Associated with Plastics in Fire Situation" (1976). A literature review. National Aeronautics Space Administration Tech. Note TN-D8338.
9. C.F. Cullis and M.M. Hirschler, "The Combustion of Organic Polymers" The City University, London, Clarendon Pres, Oxford (1981).
10. W. Schnabel, "Polymer Degradation: Principles and Practical Applications", Hanser, New York (1983).
11. T. Kelen, "Polymer Degradation", van Nostrand Reinhold, New York (1983).
12. N. Grassie and G. Scott, "Polymer Degradation and Stabilisation", Cambridge University Press, Cambridge (1985).
13. N. Grassie and A Scotney, "Polymer Handbook", 2nd edition, J. Brandrup and E.H. Immergut (eds.), Wiley-Interscience, New Yark, 11473 (1975).
14. J. Heller, Biomaterials, 1, 51 (1980).
15. N. Grassie and H.W. Melville, Proc. Roy. Soc.London, A 199, 1, 14, 24 (1949).

16. N. Grassie in "Developments in Polymer Degradation-1", 137, N. Grassie (ed.), Applied Science, London (1977).
17. I.C McNeill and M. Zulfiqar, *J. Polymer Sci., Polym. Chem. Ed.*, **16**, 3201 (1978).
18. A. Tkáč , in "Developments in Polymer Stabilisation", G. Scott (ed.), Applied Science, London, vol. 5, 153 (1982).
19. M.M. Hirschler, in 'Developments in Polymer Stabilisation', G. Scott (ed.), Applied Science, London, vol. 5, 107 (1982).
20. A. H. Frazer, "High-temperature resistant polymers" Interscience, New York (1968).
21. J.J. Idris, *J. macromol. Sci., Rev. macromol. Chem.*, **C 2**, 303 (1968).
22. A. D. Delman, *J. macromol. Sci., Rev. macromol. Chem.*, **C 3**, 153 (1968).
23. A. D. Delman, *J. macromol. Sci., Rev. macromol. Chem.*, **C 3**, 281 (1969).
24. C. S. Marvel, *J. macromol. Sci., Rev. macromol. Chem.*, **C 13**, 219 (1975).
25. P. E. Cassidy and N.C. Fawcett, *J. macromol. Sci., Rev. macromol. Chem.*, **C 17**, 209 (1979).
26. D.W. Van Krevelen, *Polymer*, **16**, 617 (1975).
27. R.A. Dipert, M. J. Drews and R.G. Gann in "Encyclopedia of Polymer Science and Engineering", 2nd Edition, **7**, 185; N.M. Bikales, H.F. Mark, G. Menges and C.G. Overberger (eds), Wiley-Interscience, U.S.A. (1985).
28. G.L. Drake, Jr., in "Encyclopedia of Chemical Technology", 3rd edn., **10**, 363; H.F. Mark, D.F. Othmer, C.G. Overberger and G.T. Seaborg (eds.), Wiley-Interscience, U.S.A. (1978).
29. N. Grassie and M. Zulfiqar in "Developments in Polymer Stabilisation-1", 197, G. Scott (ed.), Applied Science, London (1979).
30. N. Grassie and G.A.P. Mendoza, *Poly. Deg. Stab.*, **11**, 145 (1985).
31. N. Grassie and D. Mackerron, *Poly. Deg. Stab.*, **5**, 43, 89 (1983).
32. N. Grassie and G.A.P. Mendoza, *Poly. Deg. Stab.*, **11**, 359 (1985).
33. E.D. Weil, in "Flame Retardancy of Polymeric Materials", **1**, 185, Kuryla and A.J. Papa (eds.), Marcel Dekker, New York (1975).

34. G. Camino, N. Grassie and I.C. McNeill, *J. Polymer Sci., Polym Chem. Ed.*, **16**, 95, (1978).
35. N. Grassie, "Thermal Degradation of Polymers", in "Chemical Reactions of Polymers", E. M. Fettes (ed.), 565-644, (1964).
36. I.C. McNeill, "The Thermal Degradation of Polymer Blends" in "Developments in Polymer Degradation-1", 171, N. Grassie (ed.), Ap. Pub., London (1977).
37. M.R. MacLaury, F.F. Holub, "Flame Retardant Compositions and Coated Article" U.S. Patent, 4,273,691 (1981).
38. A.G. Moody and R.J. Pennick, "Polymeric Blends Containing a Momoorganic Polysiloxane Resin", U.S. Patent 4,265,801 (1981).
39. G.F. Beekman, S. Petrie & L. Keating, Proceedings of the 44th Annual Technical Conference, Antec 86, Boston, 1167 (1986).
40. J. Rychlý, K. Veselý, E. Gál, M. Kummar. J. Jancár Jančář & L. Rychlá, *Poly. Deg. Stab.*, **30**, 57 (1990).
41. Shigeo Miyata, Takeshi Imahashi and Hitoshi Anabuki, *J. Appl. Polym. Sci.*, **25**, 415 (1980).
42. Kathleen R. Hartley, Donald L. Finney and Richard B. Bush, "New Silicone Technologies for Flam Retardant Wire Constructions" in 'International Wire & Cable Symposium Proceedings', 567 (1986).
43. C. Weise, D. Wolfer and J. Petzke, "Flame Resistant Molding Compositions" U.S. Patent 4,390,656 (1983).
44. B.S. Bernstein, *Polym. Eng. and Sci.*, **29**, 13 (1989).
45. A.K. Sen, B. Mukherjee, A.S. Bhattacharyya, L.K. Sanghi, P.P. De & A.K. Bhowmick, *Thermochimica Acta*, **157**, 45 (1990).
46. A.K. Sen, B. Mukherjee, A.S. Bhattacharyya, P.P. De & A.K. Bhowmick, *Poly. Deg. Stab.*, **36**, 281 (1992).
47. (a) J.E. Betts and F.F. Holub, Chem. Abstr. **90**, 138660e (1979); Ger. Offen. 2821807 (1979); (b) J.E. Betts and F.F. Holub, U.S. Pat. 4,123586 (1979).
48. "Plastics and Rubber Weekly", p.18 June 11 (1988).
49. I.C. McNeill, *J. Polym. Sci.*, A-1, **4**, 2479 (1966).

50. I.C. McNeill, *Europ. Polym. J.*, **3**, 409 (1967).
51. I.C. McNeill and D. Neil in "Thermal Analysis", R.F. Schwenker and P.D. Garn (eds.), Academic Press, New York p.353 (1969).
52. I.C. McNeill in "Thermal Analysis" p.417, R.F. Schwenker and P.D. Garn (eds.), Academic Press, New York (1969).
53. D.L. Gardner and I.C. McNeill, *J. Thermal Anal.* **1**, 389 (1969).
54. I.C. McNeill, *Europ. Polym. J.*, **6**, 373 (1970).
55. I.C. McNeill, in "Developments in Polymer Degradation", N. Grassie (ed.), Applied. Science, London, vol. **1**, p.43 (1977).
56. I.C. McNeill, L. Ackerman, S.N. Gupta, M. Zulfiqar and S. Zulfiqar, *J. Polym. Sci., Polym. Chem. Ed.*, **15**, 2381 (1977).
57. Interfacing TVA Apparatus to a BBC Microcomputer, designed in the Chemistry Department, University of Glsgow, as an undergraduate research project by Stuart W. Mackay under the supervision of Dr.I.C McNeill and Dr. J.K Tyler (1987/88).
58. L. Ackerman and W.J. McGill, *J. S. Afr. Chem. Inst.*, **26**, 82 (1973).
59. W.J. McGill, L. Payne and J. Fourie, *J. Appl. Polym. Sci.*, **22**, 269 (1978).
60. W.J. McGill, in "Developments in Polymer Degradation", N. Grassie (ed.), Applied. Science Publishers, London, vol. **5**, p.1 (1984).
61. I.C. McNeill, *J. Polym. Sci.*, **A4**, 2479 (1966).
62. N. Grassie and D.R. Bain, *Polym. Sci.*, **A1**, 2653, 2665, 2679 (1970).
63. "The Sadtler Handbook of Infrared Spectra", W.W. Simons (ed.), Sadtler-Heyden, London (1978).
64. "The Aldrich Libreray of Infrared Spectra", C.J. Pouchert (ed.), Aldrich, Chemical Co., Milwaukee (1981).
65. A.L. Smith, *Spectrochim, Acta*, **16**, 87 (1960).
66. W.A. Srowacka and T. Burnacka, *Chem. Anal. Warsaw*, **9**, 303 (1964).
67. N. Wright and M.J. Hunter, *J. Am. Chem.Soc.*, **69**, 803 (1947).
68. A.L. Smith and N.C. Angelotti, *Spectrochimica Acta*, **15**, 412 (1956).

69. W.S. Tatlock and E.G. Rochow, *J. Org. Chem.*, **17**, 1555 (1952).
70. "Infra-red Spectroscopy", R.T. Conley, Allyn and Bacon, Boston (1966).
71. V.A. Zeitler and C.A. Brown, *J. Am. Chem. Soc.*, **79**, 4616 (1957).
72. V.A. Zeitler and C.A. Brown, *J. Phys. Chem.*, **61**, 1174 (1957).
73. L.A. Wall, and S. Straus, *J. Polym. Sci.*, **44**, 313 (1960).
74. W.G. Oakes and R.B. Richards, *J. Chem. Soc.*, 2929 (1949).
75. N. Grassie and J.G. Speakman, *J. Polym. Sci. A-1*, **9**, 919 (1971).
76. D.M. Barrall II, R.S. Porter and J.F. Johnson, *Anal. Chem.*, **35**, 73 (1963).
77. K.J. Bombaugh, C.E. Cook and B.H. Clampitt, *Anal. Chem.*, **35**, 1834 (1963).
78. T. Otsu and L. Quach, *J. Polym. Sci. Polym. Chem. Ed.*, **19**, 2377 (1981).
79. Y. Uryu, H. Shiroki, M. Okada, K. Hosonuma and K. Matsuzaki, *J. Polymer Sci. A-1*, **9**, 2335 (1971).
80. E. Bortel, S. Hodorowicz and R. Lamont, *Makromol. Chem.*, **180**, 2491 (1979).
81. "CRC Hand Book of Chemistry and Physics", 69th edn., 1988-1989, R.C. Weast (edit.), CRC press, Inc., Florida (1988).
82. N. Grassie, J.G. Speakman and T.I. Davis, *J. Polymer Sci.*, **A-1**, **9**, 931 (1971).
83. G.G. Cameron and D.R. Kane, *J. Polym. Sci.*, **2 B**, 693 (1964).
84. G.G. Cameron and D.R. Kane, *Makromole. Chem.*, **109**, 194 (1967).
85. G.G. Cameron and D.R. Kane, *Makromole. Chem.*, **113**, 75 (1968).
86. E.A. Radell and H.C. Strutz, *Anal. Chem.*, **31**, 1890 (1959).
87. F.S. Kipping and L.L. Loyd, *J. Chem. Soc.*, **79**, 449 (1901).
88. U.S. Pat. 2,258,218 (Oct. 7, 1941), E. G. Rochow (to General Electrical Co.).
89. A.J. Barry and H.N. Beck, "Inorganic Polymers" F.G.A. Stone and W.A.G. Graham (eds.), Academic Press, New York (1962).

90. (i) "Chemistry of Organosilicon Compounds", Vladimír Bažant Václav Chvalovský and Jiří Rathouský (eds.), Translated by Arnošt Kotyk and Jiří salák, Academic press, New York and London (1965).
- (ii) J. Idris Jones, Chapter 8, "Polymetallosiloxanes II" in "Developments in Inorganic Polymer Chemistry", M.F. Lappert and G.J. Leigh (eds.), Elsevier Publishing Company, Amsterdam, London and New York (1962).
91. H.O. Pritchard and H.A. Skinner, *Chem. Rev.*, **55**, 745 (1955).
92. A.J. Smith, W. Adcock and W. Kitching, *J. Am. Chem. Soc.*, **92**, 6140 (1970).
93. E.A.V. Ebsworth, in "The Organometallic Compounds of Group IV Elements", vol. 1, Part 1, A. G. MacDiarmid, (ed.), Dekker (1968).
94. L. Pauling, "The Nature of the Chemical Bond", 3rd edn., Cornell University Press, N.Y. Ithaca (1960).
95. T.Cottrell, "The Strengths of Chemical Bonds", 2nd edn., Butterworths, London (1958).
96. A.L. Smith, "Analysis of Silicones", Willey, New York, (1974).
97. T.J. Barton and C.L. McIntosh, *J. Chem. Soc., Chem. Commun.*, 861 (1972).
98. A.C. Brook, F. Abdesaken, G. Gutekunst, and K. Kallury, *Chem. Eng. News* **59**, 18 (1981).
99. R. West, J.J. Fink, and J. Michl, *Chem. Eng. News* **59**, 89 (1981).
100. H. Sakurai, "Organosilicon and Bioorganosilicon Chemistry", John Wiley & Sons, Inc., New York (1984).
101. T.R. Hogness, T.L. Wilson and W.C. Johnson, *J. Am. Chem. Soc.*, **58**, 108 (1936).
102. H.J. Emeléus, A.G. Maddock and C. Reid, *J. Chem. Soc.*, 353 (1941).
103. V. Schomaker and D.P. Stevenson, *J. Am. Chem. Soc.*, **63**, 37 (1941).
104. J.E. Mark, *Macromolecules*, **11**, 627 (1978).
105. H.A. Liebhafsky, "Silicones under the Monogram", John Wiley & Sons, Inc., New York (1978).

106. R.H. Baney, C.E. Voight, and J.W. Mentele in "Structure-Solubility Relationships in Polymers" H. Seymour (ed.), Academic Press, Inc., New York (1977).
107. P.J. Flory, V. Crescenzi, and J.E. Mark, *J. Am. Chem. Soc.*, **86**, 146 (1964).
108. E.G. Rochow, "An Introduction to the Chemistry of the Silicones", John Wiley & Sons, Inc., New York (1951).
109. N. Grassie and I.G. MacFarlane, *Eur. Polym. J.*, **14**, 875 (1978).
110. W. Patnode and D. F. Wilcock, *J. Am. Chem. Soc.*, **68**, 358 (1946).
111. T.H. Thomson and T.C. Kendrick, *J. Polym. Sci.*, Part A-2, **7**, 537 (1969).
112. Yu. A. Aleksandrova, J. S. Nikitina and A.N. Pravednikov, *Polymer Sci. U.S.S.R.* MA10 1250 (1968).
113. V.V. Rodé, M.A. Verkhotin and S.R. Rafikov, *Výsokomolek. Soedin.*, **A 11**, 1529 (1969). [Translated in *Polymer Sci. U.S.S.R.* **11** : 3, 1733 (1969)].
114. K.A. Andrianov, V.S. Papkov, G.L. Slonimskii, A.A. Zhdanov and S. Ye Yakushkina, *Výsokomolek. Soedin.* **A 11**, 2030 (1969).
115. T.H. Thomson and T.C. Kendrick, *J. Polym. Sci.*, Part A-2, **8**, 1823 (1970).
116. M.A. Verkhotin, V.V. Rodé and S.R. Rafikov, *Výsokomolek. Soedin.*, **B.9**, 847 (1967).
117. C.M. Murphy, H. Ravner, and R.E. Kagarise, NRL, Report 6383, U.S. Naval Laboratory, Washington (1966).
118. G.J. Knight, *The British Polymer Journal*, **10**, 187 (1978).
119. Vladimír Bažant, Vladimír Václav Chvalovský and Jří Rothouský "Organosilicon Compounds", Parts 1 and 2, Translated by Arnošt Kotyk and Jří salák, Academic Press, New York and London (1965).
120. G.F. Beekman, S. Petrie & L. Keating, Antec 86, Plastics-Value through Technology, Proceedings of the 44th Annual Technical Conference, Boston, 1167 (1986).
121. L. Delfosse, C. Baillet, A. Brault, D. Brault, *Poly. Deg. Stab.*, **23**, 337-347 (1989).
122. L. Delfosse, C. Baillet, *Poly. Deg. Stab.*, **30**, 89 (1990).

123. J. Rychlý & J. Pavlinec, *Poly. Deg. Stab.*, **28**, 1, (1990).
124. J. Rychlý, L. Rychlá, *J. Thermal Anal.*, **35**, 77 (1989).
125. J.R. Falender, S.E. Lindsey, and J.C. Saam, *Polym. Eng. and Sci.*, **16**, No. 1 (1976).
126. A.L. Schroll and M.R. MacLaury, *J. Appl. Polym. Sci.*, **29**, 3883 (1984).
127. D.L. Finney, *Elastomerics*, **17** (1987).
128. R.F. Willis and R.F. Shaw, *Journal of Colloid and Interface Science*, **31**, No. 3, (1969).
129. C.C. Currie, *Ind. Eng. Chem.* **46**, 2331 (1954).
130. "Organic Peroxides" and "Free Radical Initiators" in Modern Plastics Encyclopedia, **62** (13), McGraw-Hill, New York (1985).
131. M.L. Dunham, D.L. Bailey, and R.M. Miner, *Ind. Eng. Chem.*, **49** (9), 1373 (1957).
132. W.J. Bobear, *Rubber Chem. Technol.*, **40**, 1560 (1967).
133. C.W. Lewis, *J. Polym. Sci.*, **33**, 153, (1958); *ibid.*, **37**, 425 (1959).
134. M. Kučera, M. Jelínek, J. Láníková, and K. Veselý, *J. Polym. Sci.*, **53**, 311 (1961).
135. M. Kučera, and J. Láníková, *J. Polym. Sci.*, **54**, 375 (1961).
136. M. Kučera, J. Láníková, and M. Jelínek, *J. Polym. Sci.*, **53**, 301 (1961).
137. M. Kučera, and J. Láníková, *J. Polym. Sci.*, **59**, 79 (1962).
138. R.C. Ochoff, A.M. Bueche and W.T. Grubb, *J. Am. Chem. Soc.*, **76**, 4659 (1954).
139. M. Kučera and M. Jelínek, *Czech. Pat.*, 89,809.
140. J.F. Hyde, *U.S. Pat.*, 2,542,333.
141. V.S. Osipchik, N.D. Rumyantseva, E.D. Lebedeva, N.I. Sokolova and M.S. Akutin, *Plasticheskie Massy* (Translated in English), No. 4, 33 (1987).
142. G.A. Zdorikova, A.A. Kolesnikov, T.A. Troitskaya, I.V. Surov and T.A. Rudakova, *Fire and Materials*, **14**, 125 (1989).

143. N.P. Kharitonov and V.V. Ostrovsky, "Thermal and Thermo-oxidative Degradation of Polyorganosiloxane", *Nauka* 185, 186, 160, 138, (1982).
144. M. Hatanka, R. Mahekawa, and H. Maruyama, *U.S. patent*, 3,862,082 (1975).
145. M. G. Noble and J.R. Browern, *U.S. patent*, 3,514,424 (1973).
146. R.A. Shingledecker, *U.S. patent*, 3,734,881 (1973).
147. C.W. Pfeifer, and W.J. Bobear, *U.S. patent*, 3,711,520 (1973).
148. B.D. Karstedt, *U.S. patent*, 3,539,530 (1970).
149. G. Christie, *U.S. patent*, 3,734,877 (1973).
150. K. Itoh, N. Harada, and T. Yoshida, *U.S. patent*, 3,862,081 (1975).
151. K. Itoh, N. Harada, and T. Yoshida, *Chem. Abstr.*, 81, 137409g (1974).
152. M. Hatanaka, R. Maekawa, and H. Maruyama, *Chem. Abstr.*, 82, 18352u (1975).
153. M. Hatanaka, R. Maekawa, and H. Maruyama, *Chem. Abstr.*, 82, 18357z (1975).
154. M. Hatanaka, R. Maekawa, and H. Maruyama, *Chem. Abstr.*, 82, 18356y (1975).
155. H.F. Lamereaux *U.S. patent*, 3,220,972 (1972).
156. D.T. Hurd, R.C. Osthoff and M.L. Corrin, *J. Am. Chem. Soc.*, 76, 243 (1954).
157. H. Kriegsmann, *Pure and Applied Chemistry*, 13, 203 (1966).
158. N. Grassie & K.F. Francy, *Poly. Deg. Stab.*, 2, 53, (1980).
159. N. Grassie & S.R. Beattie, *Poly. Deg. Stab.*, 7, 231, (1984).